



HAL
open science

Clinical and neuroimaging characterization of genetic frontotemporal lobar degeneration at the clinical and presymptomatic phase

Dario Saracino

► **To cite this version:**

Dario Saracino. Clinical and neuroimaging characterization of genetic frontotemporal lobar degeneration at the clinical and presymptomatic phase. Neuroscience. Sorbonne Université, 2022. English. NNT: 2022SORUS157 . tel-03891998v2

HAL Id: tel-03891998

<https://theses.hal.science/tel-03891998v2>

Submitted on 7 Jan 2023

HAL is a multi-disciplinary open access archive for the deposit and dissemination of scientific research documents, whether they are published or not. The documents may come from teaching and research institutions in France or abroad, or from public or private research centers.

L'archive ouverte pluridisciplinaire **HAL**, est destinée au dépôt et à la diffusion de documents scientifiques de niveau recherche, publiés ou non, émanant des établissements d'enseignement et de recherche français ou étrangers, des laboratoires publics ou privés.

Sorbonne Université

Ecole doctorale Cerveau Cognition Comportement (ED3C)

Institut du Cerveau / Equipes Basic to Translational Neurogenetics & ARAMIS

Caractérisation clinique et de neuroimagerie des Dégénérescences Lobaires Frontotemporales génétiques à la phase clinique et présymptomatique

Par Dario SARACINO

Thèse de doctorat de Neurosciences

Dirigée par Isabelle LE BER et Olivier COLLIOT

Présentée et soutenue publiquement le 06 juillet 2022

Devant un jury composé de :

Mme Florence PASQUIER (PU-PH)	Université de Lille	Rapporteur
Mme Mira DIDIC (PH-HDR)	Université d'Aix-Marseille	Rapporteur
Mme Claire Paquet (PU-PH)	Université de Paris	Examineur
Mr Richard LEVY (PU-PH)	Sorbonne Université	Examineur
Mme Isabelle LE BER (PH-HDR)	Sorbonne Université	Directeur de thèse
Mr Olivier COLLIOT (DR)	Sorbonne Université	Co-directeur de thèse



Aux patients et à leurs familles

Remerciements

Je tiens tout d'abord à exprimer ma gratitude aux professeurs Florence Pasquier et Mira Didic, qui m'ont fait l'honneur d'être rapporteurs de cette thèse, ainsi qu'aux professeurs Claire Paquet et Richard Levy qui ont accepté de faire partie des membres du jury. Je les remercie d'avoir évalué ce travail, et remercie le professeur Levy pour la confiance qu'il me témoigne.

Toute ma reconnaissance va ensuite à Isabelle Le Ber, qui m'a guidé dans ce parcours de thèse, et sans laquelle ce travail n'aurait pu jamais voir le jour. Sa façon d'appréhender la recherche clinique, mêlant une méthode rigoureuse, une véritable curiosité et une profonde humanité, a été une source d'inspiration inépuisable pour moi. Je la remercie de m'avoir fait confiance et d'avoir été toujours disponible et à l'écoute pendant ces années.

Je remercie vivement Olivier Colliot, qui a co-dirigé ces projets et qui m'a initié au monde de l'informatique et de la programmation. Grâce à son soutien, et à l'aide des co-équipiers d'Aramis, en particulier Alexandre, Simona, Alexis et Omar, mes connaissances se sont enrichies et diversifiées, me permettant d'acquérir des outils indispensables pour ce travail de thèse.

Je remercie les professeurs Alexis Brice, Alexandra Durr et Giovanni Stévanin de m'avoir accueilli dans l'équipe BTN, au sein de l'ICM. Un grand merci à l'ensemble des personnes du laboratoire avec qui j'ai eu la chance de partager du temps au cours de ces années, et en particulier à Agnès, Mathieu, Daisy, Claire, Morwena, Julie, Elena et bien d'autres. Ce parcours de thèse a été bien évidemment rendu plus agréable par leur amitié, leur soutien et tous les moments conviviaux passés ensemble.

Je remercie le professeur Bruno Dubois pour son accueil à l'IMMA, et toutes les personnes de l'équipe clinique et de recherche de l'IMMA avec qui j'ai été en contact. Un remerciement tout particulier à Aurélie, Sophie, Marie et Marion, qui ont été toujours très disponibles et enthousiastes et qui, chacune dans leur domaine, m'ont beaucoup appris. Je remercie également le professeur Jean-Christophe Corvol, le professeur David Grabli, le docteur Aurélie Méneret, ainsi que les collègues du DMU Neurosciences avec lesquels j'ai le plaisir de travailler actuellement.

Je tiens à remercier chaleureusement Marie-Odile, Lara et les collègues du FrontLab, Hugo, Maxime, Fouzia, Giorgia, Karim et Foudil, avec qui j'ai pu instaurer des collaborations riches et stimulantes.

Un grand merci à trois collègues et amis, Leila, Fábio et Lorenzo, dont le passage dans notre équipe a été marqué par des échanges fructueux et de très belles réalisations communes.

Je remercie particulièrement tous les cliniciens et chercheurs du réseau national français sur les DLFT, des protocoles PREV-DEMALS et Predict-PGRN. Ces projets alimentent la recherche sur les DLFT en France et constituent le socle des travaux réalisés dans cette thèse.

Je remercie mes parents, qui m'ont toujours soutenu dans mes choix professionnels et de vie, et qui même à distance ne m'ont jamais laissé sans leur appui et leurs bons conseils.

Enfin, je remercie Joanne avec qui j'ai la chance immense de partager ma vie.

Sommaire

Remerciements	3
Sommaire	4
Introduction	6
1. Les dégénérescences lobaires frontotemporales	7
1.1 Critères diagnostiques des DLFT et leur évolution.....	8
1.1.1 De la « maladie de Pick » à la DFTc : évolution nosographique et des critères diagnostiques	8
1.1.2 Les aphasies primaires progressives : un réseau, plusieurs syndromes	12
1.1.3 Le variant temporal droit.....	16
1.1.4 DLFT et sclérose latérale amyotrophique	17
1.1.5 PSP et SCB : du « complexe de Pick » à leurs définitions actuelles.....	18
1.1.6 Évolution des cadres nosographiques et des frontières cliniques des DLFT	19
1.2 Formes anatomopathologiques des DLFT	23
1.2.1 Protéinopathie TDP-43 dans les DLFT et SLA	23
1.2.2 Protéine TAU et pathologie DLFT-TAU	27
1.2.3 Formes anatomopathologiques rares de DLFT	29
1.3 Aspects génétiques des DLFT	31
1.3.1 Le gène <i>GRN</i>	31
1.3.2 Le gène <i>C9orf72</i>	34
1.3.3 Les autres gènes responsables de DLFT et SLA	37
1.4 Neuroimagerie des DLFT.....	39
1.5 Les enjeux de la recherche dans les formes génétiques de DLFT, à l'ère des premiers essais thérapeutiques	41
1.5.1 La phase présymptomatique des DLFT	42
1.5.2 Quels biomarqueurs pour suivre la trajectoire du processus pathologique à la phase présymptomatique de la DLFT ?.....	47
Articles de revue.....	54
2. Objectifs de cette thèse.....	77
3. Méthodes spécifiques utilisées dans ces travaux.....	81
4. Résultats	83
4.1 Partie 1 – Aspects cliniques, langagiers, cognitifs et de neuroimagerie des APP associées aux mutations des gènes <i>GRN</i> et <i>C9orf72</i> (articles 1 et 2).....	83
4.2 Partie 2 – Trajectoires des neurofilaments plasmatiques dans les formes génétiques <i>GRN</i> et <i>C9orf72</i> , de la phase présymptomatique à la phase clinique (article 3).....	150
4.3 Partie 3 – Profil évolutif du métabolisme cérébral chez les porteurs de mutations du gène <i>GRN</i> à la phase présymptomatique (article 4)	172
4.4 Partie 4 – Profil d'atrophie de la substance grise et modifications longitudinales chez les porteurs d'expansion <i>C9orf72</i> à la phase présymptomatique	225
5. Discussion générale	230
Bibliographie	240
Annexe 1 – Critères diagnostiques	293
Tableau A1. Critères diagnostiques de DFTc (<i>adapté de Rascovsky et al., 2011</i>)	293
Tableau A2. Critères diagnostiques des APP (<i>adapté de Gorno-Tempini et al., 2011</i>).....	295
Tableau A3. Critères diagnostiques de SLA (<i>adapté de Hardiman et al., 2011</i>)	297
Annexe 2 – Les autres gènes de DLFT et SLA	298
Annexe 3 – Synopsis des protocoles Predict-PGRN et PREV-DEMALS.....	299
Annexe 4 – Méthodes d'analyse d'IRM structurale	301

Table des illustrations.....	303
Table des tableaux.....	304

Introduction

La première description des dégénérescences frontotemporales remonte aux travaux du neuropsychiatre tchèque Arnold Pick qui, en 1892, rapporta les caractéristiques cliniques de six patients atteints d'une démence caractérisée par des changements progressifs du langage et de la personnalité, en association avec une atrophie focale des lobes frontaux et temporaux (Pick, 1892). La première caractérisation anatomopathologique fut réalisée par Alois Alzheimer qui décrivit, en 1911, des corps argyrophiles typiques appelés « corps de Pick ». Le nom de « maladie de Pick » a ensuite été utilisé pendant une grande partie du 20^{ème} siècle pour désigner ce type de démence. C'est dans les années 80 que Mesulam introduisit « l'aphasie primaire progressive (APP) » (Mesulam, 1982), et le groupe de Brun et Gustafson « la démence frontotemporale (DFT) » (Brun, 1987 ; Gustafson, 1987) dont les premiers critères de diagnostic furent établis quelques années plus tard (The Lund and Manchester Groups, 1994). Ces critères ont été révisés en 1998, afin de différencier les présentations comportementales et les formes langagières, et inclure les données neuropsychologiques dans chacune des formes (Neary et al., 1998). La paralysie supranucléaire progressive (PSP), le syndrome/dégénérescence corticobasale (SCB/DCB) et la sclérose latérale amyotrophique (SLA) furent intégrées plus tardivement dans le spectre de ces maladies, en particulier par Kertesz qui, en 2003, souligna les chevauchements cliniques et histopathologiques de ces affections avec les DFT et les APP. Il proposa de regrouper ces maladies sous le concept plus large de « complexe de Pick » pour désigner d'une façon unitaire l'ensemble de ces tableaux comportementaux, langagiers et moteurs (Kertesz, 2003). Une vision plus moderne de la maladie tenant compte de ces différentes présentations cliniques a été élaborée au cours des deux dernières décennies, incluant une révision de leurs critères diagnostiques (Rascovsky et al., 2011 ; Gorno-Tempini et al., 2011 ; Armstrong et al., 2013 ; Höglinger et al., 2017) et accompagnant une avancée majeure des connaissances sur leurs bases neuropathologiques, biologiques et moléculaires. Aujourd'hui, le terme de dégénérescence lobaire frontotemporale (DLFT) désigne un spectre de maladies dégénératives hétérogènes au plan clinique, pathologique et génétique. Initialement utilisé pour décrire les formes neuropathologiques de la maladie, ce terme est maintenant adopté plus largement et, dans ce manuscrit, nous l'utiliserons pour désigner l'ensemble des formes cliniques et pathologiques de la maladie.

1. Les dégénérescences lobaires frontotemporales

Les DLFT représentent la deuxième cause de démence de l'adulte jeune après la maladie d'Alzheimer (MA) (Hogan et al., 2016). L'incidence des DLFT est estimée à 1,6 nouveaux cas/100 000 individus/an, et leur prévalence à 15/100 000 individus âgés entre 45 et 65 ans, ces estimations variant cependant selon l'origine des populations étudiées (Onyike et al., 2013; Hogan et al., 2016 ; Olney et al., 2017). En France, l'incidence standardisée selon l'âge est évaluée à 2,9 cas/100 000 individus/an, les DLFT contribuant à 2,6 % de l'ensemble des démences (Leroy et al., 2021). Leurs symptômes débutent généralement entre 55 et 65 ans, avec des âges extrêmes allant de la deuxième à la neuvième décennie (Moore et al., 2020a).

Les différentes formes clinico-pathologiques regroupées sous ce terme ont en commun une altération progressive des fonctions cognitives, des troubles comportementaux, du langage et/ou moteurs liés à une atteinte des lobes frontaux et temporaux, variablement associée à une atteinte sous-corticale. Le phénotype le plus fréquent est le variant comportemental de démence frontotemporale (DFTc), caractérisé par des modifications du comportement et de la personnalité, associés à des troubles cognitifs touchant les fonctions exécutives et la cognition sociale (Rascovsky et al., 2011). Environ 15 % des patients atteints de DFTc développent une SLA (Lomen-Hoerth et al., 2002), raison pour laquelle des aspects spécifiques de la SLA seront aussi abordés dans certaines parties de ce manuscrit. Les variants langagiers de DLFT, collectivement dénommés APP, sont quatre fois moins fréquents (Hogan et al., 2016). Le variant non-fluent/agrammatique (vnfAPP) et le variant sémantique d'APP (vsAPP) entrent dans le spectre des DLFT, alors que le variant logopénique (vlAPP) est majoritairement associé à un processus pathologique de type MA (Leyton et al., 2011). Enfin, dans 15 % des cas le phénotype associe un syndrome parkinsonien qui représente parfois l'expression dominante de la maladie dans le cas de la paralysie supranucléaire progressive (PSP) et du syndrome cortico-basal (SCB). Des critères diagnostiques ont été formulés par des consortia internationaux pour chacun de ces syndromes. Actuellement, seules une confirmation pathologique *post mortem* ou la mise en évidence d'une mutation causale permettent de formuler un diagnostic de certitude. Les caractéristiques principales de ces différents variants, et leurs critères diagnostiques sont brièvement récapitulés dans les paragraphes qui suivent.

1.1 Critères diagnostiques des DLFT et leur évolution

1.1.1 De la « maladie de Pick » à la DFTc : évolution nosographique et des critères diagnostiques

Comme mentionné dans l'introduction, le terme de « maladie de Pick » a été utilisé pendant près d'un siècle, avant que Brun, et les équipes de Lund et de Manchester ne définissent les premiers critères diagnostiques de la maladie et ne recommandent l'utilisation du terme de DFT, reléguant définitivement l'utilisation du terme de « maladie de Pick » à une sous-entité anatomopathologique de DLFT (Brun, 1987 ; The Lund and Manchester Groups, 1994 ; Neary et al., 1998). Depuis 2011, le diagnostic clinique de DFTc repose sur des critères formulés par Rascovsky et collaborateurs (2011). Contrairement aux premiers critères, établis à partir d'études cliniques, ceux-ci sont basés sur les symptômes les plus fréquemment observés dans une cohorte clinico-pathologique de 176 patients dont le diagnostic de DLFT a été confirmé par un examen *post mortem*. Cette révision met l'accent sur la survenue précoce de certains troubles comportementaux, prioritaires pour poser un diagnostic, permettant d'en améliorer considérablement la sensibilité et la spécificité.

Selon les critères actuels, les manifestations clés d'une DFTc sont des modifications comportementales survenant de façon insidieuse, persistantes ou récurrentes durant les trois premières années de la maladie, incluant 1) une apathie ou inertie, 2) une désinhibition comportementale, 3) une perte de sympathie ou d'empathie, 4) des comportements persévératifs, répétitifs, stéréotypés, compulsifs/obsessionnels, 5) une hyperoralité et des changements des habitudes alimentaires, 6) un syndrome cognitif de nature frontale dominé par un dysfonctionnement exécutif en l'absence d'une atteinte massive de la mémoire et des fonctions visuo-spatiales (Rascovsky et al., 2011). Un diagnostic de DFTc « possible » est établi en présence d'au moins trois de ces six dimensions symptomatologiques. Le diagnostic est considéré comme « probable » quand, aux critères de DFT possible, s'ajoutent l'observation d'un déclin fonctionnel progressif, ainsi que la mise en évidence d'une atteinte (atrophie, hypoperfusion ou hypométabolisme) des régions frontales et/ou temporales antérolatérales par les examens de neuroimagerie structurelle ou métabolique. Une confirmation pathologique *post mortem* (ou par biopsie) ou la mise en évidence d'une mutation causale permettent de formuler un diagnostic de DFTc « définie ». Ces critères de diagnostic sont récapitulés en annexe 1 (Tableau A1), et les principaux troubles comportementaux et leurs corrélats neuroanatomiques

sont brièvement décrits ci-dessous. Une étude chez 315 patients atteints de DFTc montre que les troubles comportementaux (en particulier l'apathie et les manifestations émotionnelles et affectives) sont plus sévères chez les patients débutant la maladie plus précocement (Fieldhouse et al., 2021).

L'apathie est l'une des principales manifestations « négatives » de la DFT. Cliniquement, elle se caractérise chez les patients atteints de DFTc par une perte d'initiative, un manque de motivation, un désintérêt, un appauvrissement des activités quotidiennes. Elle a été initialement définie par Marin comme un trouble de la motivation, qui a distingué les sous-types cognitif, sensoriel, moteur et affectif (Marin, 1990). Selon une interprétation plus moderne, l'apathie est considérée comme une réduction quantitative des comportements volontaires dirigés vers un objectif déterminé (Levy et Dubois, 2006). Des modèles théoriques récents ont suggéré qu'elle peut être divisée en plusieurs dimensions : l'apathie exécutive (c'est-à-dire les déficits dans le maintien des objectifs et de l'organisation), l'apathie émotionnelle (c'est-à-dire l'émoussement émotionnel et l'indifférence) et l'apathie d'initiation (c'est-à-dire la réduction de l'auto-activation) (Levy et Dubois, 2006). La première est aussi appelée « inertie cognitive » et résulte du dysfonctionnement des processus cognitifs nécessaires à planifier et suivre les actions, tandis que l'apathie émotionnelle dérive d'une incapacité à attribuer une valence émotionnelle aux comportements, entraînant leur dévalorisation. La troisième dimension de l'apathie, celle de l'auto-activation, est la plus sévère, car associée à un « vide mental » qui appauvrit considérablement la génération spontanée de pensées et d'actions (Levy et Dubois, 2006). Un modèle conceptuel proche, dérivé d'une approche empirique d'évaluation de l'apathie dans les maladies neurodégénératives, distingue apathie d'initiation, exécutive et émotionnelle, mettant l'accent sur l'impact d'un déficit de métacognition dans toutes les dimensions de l'apathie (Radakovic et Abrahams, 2018). Après une première proposition de critères pour définir l'apathie dans le cadre des troubles cognitifs d'origine neurologique (Robert et al., 2009), une reformulation récente des critères a été proposée (Miller et al., 2021). Des critères actuels définissent l'apathie sur la base de trois dimensions différentes, incluant une diminution de l'initiative, des intérêts et de l'expression et/ou de la réponse aux émotions (Miller et al., 2021). Certains auteurs ont néanmoins souligné qu'une structuration tripartite de l'apathie peut s'avérer en partie dépendante des modalités d'évaluation adoptées, avec la possibilité que d'autres domaines (comme celui de l'apathie sociale) puissent en représenter des dimensions additionnelles (Dickson et al., 2022). Quoiqu'il en soit, le syndrome de DFTc récapitule toutes les dimensions

de l'apathie décrites, reflétant un dysfonctionnement global des circuits frontaux-sous-corticaux (Levy et Czernecki, 2006 ; Massimo et al., 2015 ; Radakovic et Abrahams, 2018). Des corrélats neuronaux distincts ont été identifiés pour chaque dimension de l'apathie dans la DFTc, les troubles d'initiation étant associés à une atteinte prédominante au niveau du cortex cingulaire antérieur, les difficultés de planification à une atteinte du cortex dorsolatéral préfrontal, et les déficits de la motivation à un retentissement prédominant au niveau du cortex orbitofrontal (Massimo et al., 2015). L'atrophie au niveau des aires motrices supplémentaires et du striatum est également associée à la sévérité de l'apathie (Zamboni et al., 2008 ; Massimo et al., 2009).

La désinhibition comportementale est une autre composante majeure des critères de la DFTc, qui traduit un déficit du contrôle inhibiteur. Elle se manifeste par une perte des convenances sociales, un trouble des conduites interpersonnelles, des comportements sociaux inappropriés, des actes impulsifs et irréfléchis, comme rapporté par Snowden et collaborateurs (2001). À côté de l'aspect comportemental, la désinhibition peut se manifester également au niveau cognitif (Aron et al., 2007). La composante cognitive de la désinhibition se traduit dans une incapacité à résister à des interférences externes ou internes, à inhiber les processus cognitifs précédemment activés et à supprimer des réponses hâtives, inappropriées ou non pertinentes (Migliaccio et al., 2020). Ainsi, l'impulsivité (définie comme une prédisposition à des réactions rapides, non planifiées, en réponse à un stimulus, avec une capacité réduite à évaluer les conséquences de ces réactions) est un symptôme de la DFTc qui peut être considéré comme résultant de la désinhibition cognitive et comportementale (Chamberlain et Sahakian, 2007). Les comportements de dépendance à l'environnement, d'utilisation d'objets et d'imitation, peuvent également être partiellement attribués à un défaut d'inhibition (Jarry et al., 2017). Des études neuroanatomiques relient la désinhibition cognitivo-comportementale de la DFTc à une atteinte des structures fronto-basales et temporo-limbiques (Massimo et al., 2009 ; Hornberger et al., 2011). Les régions principalement impliquées comprennent le cortex orbitofrontal médial, le cortex temporal latéral et les aires limbiques incluant l'insula antérieure, le gyrus parahippocampal, l'amygdale et le nucleus accumbens, principalement du côté droit (Zamboni et al., 2008; Sheelakumari et al., 2020).

Les modifications du comportement alimentaire et l'hyperoralité se manifestent par des changements des préférences et des conduites alimentaires, une précipitation sur la nourriture, une goinfrerie, une boulimie, jusqu'à la consommation d'objets non comestibles (Rascovsky et

al., 2011). On peut considérer quatre domaines distincts de dysfonctionnement concernant les habitudes alimentaires, les préférences alimentaires, les conduites à table et le comportement moteur (Azuar et al., 2015, communication AAIC 2015, non publié). Bien que non spécifiques, ces troubles sont plus fréquents dans la DFTc que dans d'autres démences dégénératives (Ahmed et al., 2016) et certains, comme les troubles des conduites à table, s'avèrent être très discriminants entre DFTc et MA (Azuar et al., 2015, communication AAIC 2015, non publié). Pour comprendre les bases physiopathologiques et biologiques des modifications du comportement alimentaire, l'équipe du Pr Hodges a étudié de façon approfondie le système neuroendocrinien de l'appétit, montrant un dérèglement de l'axe leptine-peptide apparenté à l'agouti (AgRP) chez les patients atteints de DFTc (Ahmed et al., 2016 ; Ahmed et al., 2021). La même équipe a mis en évidence que le support neuroanatomique de l'hyperphagie et des troubles des conduites alimentaires est un dysfonctionnement d'un ensemble de régions cérébrales comprenant l'hypothalamus postérieur, le cortex orbitofrontal et le cortex cingulaire bilatéral (Piguet et al., 2011 ; Ahmed et al., 2015 ; Ahmed et al., 2016).

Les troubles émotionnels et affectifs, la perte d'empathie et de sympathie font partie des caractéristiques centrales de la DFTc. Ces troubles se manifestent par une altération des relations interpersonnelles, un émoussement affectif, une incapacité à attribuer une valence émotionnelle aux stimuli extérieurs, une réponse diminuée aux besoins et sentiments d'autrui (Rascovsky et al., 2011). Le déficit de la théorie de l'esprit, comprenant la capacité à attribuer des émotions (théorie de l'esprit affective) ou des intentions (théorie de l'esprit cognitive) à autrui, est l'un des éléments à l'origine de ces réponses anormales chez les patients DFTc (Gregory et al., 2002 ; Adenzato et al., 2010 ; Bertoux et al., 2016). Le test des faux pas, le test de reconnaissance des émotions, le test des fausses croyances et le « *reading the mind in the eyes* » font partie des instruments de référence pour l'évaluation de la théorie de l'esprit et des déficits d'empathie (Samson et al., 2007 ; Funkiewiez et al., 2012 ; Schroeter et al., 2018 ; Delbeuck et al., 2022). Pour certains, le déficit de théorie de l'esprit dans le contexte d'une DFTc dépendrait plus d'une incapacité à inhiber ses propres perspectives mentales qu'à celle d'inférer les croyances d'autrui (Le Bouc et al., 2012), reliant le déficit de la théorie de l'esprit au trouble de l'inhibition cognitive qui caractérise la DFTc. Au niveau neuroanatomique, les déficits de théorie de l'esprit sont associés à une atteinte du réseau de saillance, comprenant le cortex cingulaire antérieur, l'insula, les régions orbitofrontales, préfrontal médiales et temporo-pariétales, l'amygdale et le striatum (Kumfor et Piguet, 2012 ; Day et al., 2013 ; Christidi et al., 2018). Plus spécifiquement, l'inférence des états mentaux d'autrui est corrélée à l'activation

métabolique et fonctionnelle du carrefour temporo-pariétal, tandis que la capacité à inhiber ses propres perspectives est associée à celle du gyrus frontal moyen droit (Le Bouc et al., 2012).

Enfin, les comportements persévératifs, stéréotypés et compulsifs se manifestent sous forme de mouvements répétitifs simples jusqu'à des comportements complexes et ritualisés, ou des stéréotypies verbales (Rascovsky et al., 2011). Des idées fixes, persévératives, des obsessions, une psychorigidité sont également observés chez les patients atteints de DFTc. Ils traduisent le déficit de flexibilité mentale de ces patients et leur incapacité à adapter de façon flexible leur pensée et leur comportement (Migliaccio et al., 2020). Les comportements compulsifs observés chez les patients atteints de DFTc sont des actions répétitives, non dirigées vers un but, et non adaptées à un contexte (Migliaccio et al., 2020). Au plan neuroanatomique, la présence d'éléments obsessionnels-compulsifs dans la DLFT est associée à une atteinte prédominante au niveau des régions temporales droites, du cortex ventromédial préfrontal et du striatum dorsal (Seeley et al., 2005 ; Josephs et al. 2009 ; Finenberg et al., 2014).

La présence de troubles cognitifs est considérée, à part entière, comme l'un des éléments du diagnostic dans les critères de Rascovsky et collaborateurs (2011). Le profil cognitif des patients atteints de DFTc est dominé par une altération des fonctions exécutives, incluant des troubles attentionnels, de la mémoire de travail, de la planification, de la flexibilité mentale, des capacités d'abstraction, de résolution de problèmes, du contrôle inhibiteur (Rascovsky et al., 2011 ; Snowden et al., 2015) ; et un déficit de la cognition sociale. Il faut noter que le critère cognitif pour le diagnostic de DFTc concerne « la présence d'un déficit de performance sur au moins un test évaluant les fonctions exécutives ». Le déficit de la cognition sociale et l'évaluation de la théorie de l'esprit (abordées précédemment) ne sont pas intégrées dans ces critères. Pour une revue des échelles principales et des batteries cognitives utilisées en France pour l'évaluation des troubles cognitivo-comportementaux, voir Thomas-Antérion, 2012, et Godefroy et al., 2018.

1.1.2 Les aphasies primaires progressives : un réseau, plusieurs syndromes

Selon la définition proposée par Mesulam (2001), les aphasies primaires progressives regroupent l'ensemble des syndromes dégénératifs focaux où l'atteinte langagière est isolée ou largement prédominante au cours des deux premières années de la maladie (Mesulam, 2001).

Initialement, les APP ont été considérées comme de formes rares de DLFT comprenant deux entités linguistiques : l'aphasie progressive non-fluente (APNF) et la démence sémantique (DS) (Neary et al., 1998). La classification établie en 2011 par Gorno-Tempini et collaborateurs est toujours utilisée, et définit trois variants anatomo-cliniques d'APP décrits ci-dessous, ainsi qu'en annexe (Tableau A2).

Le variant non-fluent/agrammatique (vnfAPP) est caractérisé par une production du langage perturbée et laborieuse, avec des troubles phono-articulatoires pouvant aller jusqu'à une apraxie de la parole (Gorno-Tempini et al., 2004). L'agrammatisme est la perte de la capacité à s'exprimer de manière grammaticalement et syntaxiquement correcte, ce qui conduit à des phrases « télégraphiques », à la structure extrêmement simplifiée. L'élocution est lente, hypofluente, dysprosodique et ponctuée de paraphasies phonologiques. Des troubles grammaticaux et syntaxiques peuvent aussi perturber la production écrite, mais souvent en moindre mesure que l'expression orale. La compréhension à l'oral et à l'écrit est normalement préservée, bien que la compréhension des phrases syntaxiquement complexes puisse être difficile (Rohrer et al., 2010a; Gorno-Tempini et al., 2011). Les altérations corticales structurales et métaboliques qui sous-tendent le vnfAPP sont localisées au niveau du gyrus frontal inférieur (pars opercularis et triangularis), des régions prémotrices et motrices supplémentaires de l'hémisphère gauche (Gorno-Tempini et al., 2004 ; Routier et al. 2018). La possible dissociation entre une forme purement agrammatique sous-tendue par une atrophie focale fronto-operculo-insulaire, et un profil associant agrammatisme et apraxie de la parole, caractérisé par une atteinte prémotrice surajoutée, soulève la question d'une dualité syndromique au sein du vnfAPP (Rohrer et al., 2010; Tetzloff et al., 2019). En outre, un phénotype d'apraxie de la parole progressive isolée, sans autre atteinte langagière, a aussi été décrit chez certains patients, justifiant la proposition d'une catégorie diagnostique supplémentaire (Botha et al., 2015).

Le variant sémantique d'APP (vsAPP) est défini par la présence d'une anomie et d'un déficit de la compréhension des mots isolés, dus à une atteinte prédominante du stock sémantique. Les troubles de la compréhension portent initialement sur les mots de basse fréquence et peu familiers (Mesulam et al., 2003). Rarement, le début est marqué par des troubles sémantiques spécifiques d'une catégorie donnée (Lambon Ralph et al., 2007). La mémoire sémantique est atteinte, avec une perte progressive des connaissances générales précédemment acquises et consolidées. Cette atteinte conduit à un discours qui, malgré une

fluence préservée voire parfois logorrhéique, est peu compréhensible et informatif, ponctué de paraphrasies sémantiques, verbales et de mots « fourre-tout », pouvant aller jusqu'à un véritable jargon. Une dyslexie et une dysgraphie de surface (difficultés de lecture et d'écriture pour les mots à la correspondance graphème-phonème irrégulière) peuvent aussi être notées (Wilson et al., 2009). La répétition de mots et de phrases est en revanche préservée. La diffusion du processus lésionnel vers des aires non-langagières étend le trouble sémantique à d'autres modalités, déterminant, par exemple, une prosopagnosie (Gainotti et al., 2007). L'atteinte neuroanatomique prédomine au niveau du lobe temporal antérieur allant jusqu'au pôle, de façon unilatérale au niveau de l'hémisphère dominant, ou bilatérale (Gorno-Tempini et al., 2004 ; Routier et al., 2018).

Contrairement aux deux formes précédentes, le variant logopénique d'APP (vlAPP) est, lui, le plus souvent associé à une pathologie de type amyloïde. Nous le décrivons néanmoins dans ce chapitre car plusieurs études récentes basées sur des cohortes anatomo-pathologiques (ou évaluées avec un PET-amyloïde, ou avec une analyse des biomarqueurs de la maladie d'Alzheimer dans le LCR), montrent que cette forme peut aussi être associée, dans 6 à 20 % des cas, à une pathologie non-amyloïde qui est le plus souvent une DLFT (Kim et al., 2016 ; Santos-Santos et al. 2018 ; Bergeron et al., 2018). De plus, le vlAPP représente l'un des phénotypes qui peut être associé aux formes génétiques de DLFT, notamment aux mutations du gène *GRN*, comme nous le montrons dans cette thèse (article 1, Saracino et al., 2021a). Cette forme est caractérisée par une atteinte prédominante de la mémoire de travail auditivo-verbale, entraînant au premier plan des troubles de la récupération des mots isolés et un déficit de répétition des phrases avec un « effet longueur ». Le discours spontané est haché, interrompu de pauses ce qui conduit à une fluence réduite (Gorno-Tempini et al., 2008 ; Gorno-Tempini et al., 2011). La présence d'erreurs phonologiques (inversions plus que distorsions des phonèmes) est l'une des caractéristiques les plus récurrentes de cette forme (Leyton et al., 2014). L'épargne des composantes motrices du langage différencie le vlAPP du vnfAPP, alors que le respect des compétences sémantiques le distingue du vsAPP. Bien que ce critère soit requis pour le diagnostic, le déficit de la répétition de phrases n'est pas toujours facile à mettre en évidence chez les patients atteints d'un vlAPP, au moins dans les phases initiales. Cette dissociation a conduit certains auteurs à proposer une révision des critères actuels pour distinguer des patients logopéniques avec répétition épargnée, d'une forme distincte se caractérisant par une anomie progressive isolée (Mesulam et Weintraub, 2014; Marshall et al., 2018). Les lésions responsables du vlAPP siègent au niveau du carrefour temporo-pariétal, comprenant la partie

postérieure du gyrus temporal supérieur et moyen, ainsi que le gyrus supramarginal et angulaire du lobe pariétal de l'hémisphère dominant (Gorno-Tempini et al., 2008).

Sur un plan fonctionnel, le réseau du langage peut être divisé en une composante dorsale, allant du carrefour temporo-pariétal au cortex frontal, impliquée dans la production phono-articulaire, et une composante ventrale, s'étendant du gyrus temporal supérieur au pôle temporal et au cortex frontal inférieur, responsable des représentations lexico-sémantiques (Saur et al., 2008). L'hétérogénéité clinique des trois variants d'APP reflète une vulnérabilité différente de ce réseau dans chacun de ces syndromes. Même si l'atteinte corticale est apparemment focale, les déficits langagiers des APP sont aussi liés à un dysfonctionnement à l'échelle de système, avec une altération de la connectivité entre les principaux nœuds fonctionnels du réseau du langage, chaque variant présentant une « signature fonctionnelle » caractéristique (Bonakdarpour et al., 2019).

Les critères diagnostiques actuels permettent non seulement d'établir un diagnostic précis, de distinguer les systèmes neuronaux impliqués dans le langage et de guider la rééducation, mais ils offrent aussi la possibilité de relier les principaux phénotypes langagiers à des formes pathologiques particulières. Ainsi, la majorité des patients avec une APP non fluente ou sémantique présentent une forme lésionnelle rentrant dans le spectre de la DLFT (Deramecourt et al., 2010) tandis que, comme mentionné précédemment, les formes logopéniques sont le plus souvent associées à une pathologie amyloïde, constituant le variant langagier de la MA (Chare et al., 2014 ; Spinelli et al., 2017 ; Bergeron et al., 2018). Néanmoins, cette critériologie rencontre des limites. Ces critères ne sont, par exemple, pas applicables chez 20 à 30 % des patients atteints d'APP qui ne rentrent dans aucun des variants décrits. En effet, certains patients présentent un syndrome langagier répondant, en même temps, aux critères de plusieurs formes d'APP (dites APP « mixtes »). D'autres ne remplissent les critères d'aucun variant au début de la maladie (APP « inclassables ») (Mesulam et al., 2014 ; Bergeron et al., 2018). Enfin, certains auteurs ont proposé d'inclure des variants supplémentaires dans cette classification, comme l'apraxie de la parole progressive et l'anomie pure progressive, déjà mentionnées plus haut, ou encore la dysprosodie progressive (Marshall et al., 2018), néanmoins cela ne fait pas actuellement l'objet d'un consensus international.

1.1.3 Le variant temporal droit

Différentes études ont souligné l'existence d'un variant syndromique additionnel affectant de façon isolée ou prédominante le pôle temporal de l'hémisphère non dominant (le plus souvent droit). Le variant temporal droit de DFT (DFTvtd) correspond, en termes anatomiques, à une atteinte focale initialement circonscrite au pôle temporal de l'hémisphère non spécialisé dans le langage, ne répondant donc pas aux critères d'APP en l'absence de syndrome aphasique. Nous intégrons ce variant dans ce chapitre car l'étude récente de Ulugut et collaborateurs (2021) montre que, bien qu'elles soient hétérogènes au plan lésionnel, ces formes rentrent néanmoins généralement dans le cadre d'une pathologie de type DLFT (Ulugut et al., 2021). Dans l'étude citée, la majorité des patients avec un diagnostic *post mortem* présentaient des lésions TDP-43-positives (3/5), et plus rarement des inclusions TAU (1/5) ou FUS (1/5) (Ulugut et al., 2021). Une revue de la littérature portant sur 44 cas de DFTvtd confirme la prédominance des lésions TDP-43, retrouvées chez 67 % des patients de cette étude (Ulugut et al., 2021).

Bien que les premières descriptions de cette forme particulière soient anciennes (Edwards-Lee et al. 1997 ; Thompson et al., 2003 ; Seeley et al., 2005 ; Joubert et al., 2006), ses caractéristiques clinico-pathologiques ont été assez peu étudiées jusqu'à récemment, raison pour laquelle un groupe d'étude international (*Neuropsychiatric International Consortium for Frontotemporal Dementia*) travaille actuellement à en définir des critères de diagnostic. L'étude de 619 patients atteints de DLFT montre que cette entité n'est pas exceptionnelle : sa fréquence est comparable à celle de la forme temporale gauche, représentant environ 10 % des cas (Ulugut Erkoyun et al., 2020). Il ressort des études existantes que le syndrome comportemental des formes temporales droites est particulier. Il est dominé par une désinhibition, une irascibilité et une psychorigidité, plus qu'une apathie. Des idées obsessionnelles, des conduites ritualisées, des comportements compulsifs sont fréquents, tout comme une dépression (Ulugut Erkoyun et al., 2020). Une hyper-religiosité, des hallucinations visuelles complexes et des déformations des perceptions somesthésiques sont notés chez 15 à 30 % des patients selon les études (Chan et al., 2009 ; Josephs et al., 2009 ; Ulugut et al., 2021). Sur le plan cognitif, le DFTvtd se caractérise par un dysfonctionnement exécutif, une prosopagnosie, un trouble de la mémoire épisodique et une désorientation spatiale. Les troubles du langage sont beaucoup moins fréquents et sévères que dans la forme temporale gauche et concernent surtout la dénomination (Josephs et al., 2009). L'atteinte

neuroanatomique est asymétrique, nettement prédominante à droite, et concerne le lobe temporal, les régions frontales ventrales et, dans une moindre mesure, les gyri temporaux supérieur, moyen et inférieur, les régions limbiques et pariétales inférieures, représentant l'atteinte en miroir du vsAPP (Ulugut Erkoyun et al., 2020). La prosopagnosie est liée à une atteinte des pôles temporaux et du gyrus fusiforme antérieur (Ulugut Erkoyun et al., 2020).

1.1.4 DLFT et sclérose latérale amyotrophique

Il existe des liens étroits entre DLFT et SLA, ces deux maladies appartenant à un même continuum clinique (DFT-SLA). Très brièvement, la sclérose latérale amyotrophique (SLA) ou maladie de Charcot est consécutive à une dégénérescence des neurones moteurs du cortex moteur, du tronc cérébral et de la moelle épinière, qui se manifeste cliniquement par une faiblesse musculaire, une spasticité, une amyotrophie, des crampes et des fasciculations (Brooks et al. 2000 ; Hardiman et al., 2011) (annexe 1, Tableau A3). La durée d'évolution dépasse rarement 5 ans, en particulier dans les formes bulbaires ou respiratoires (Chiò et al., 2011 ; Robberecht et Philips, 2013). Environ 15 % des patients avec une DLFT développent une atteinte du motoneurone ou une SLA, dès le début ou durant l'évolution de leur maladie (Lomen-Hoerth et al., 2002 ; Lillo et al., 2010). Cette association concerne plus fréquemment les patients présentant une forme comportementale de DLFT. Cependant, même si cela est moins connu, APP et SLA peuvent également être associées (Vinceti et al., 2019). Une étude récente de 130 patients atteints d'une APP révèle que 12 % ont secondairement développé une SLA (essentiellement une forme non fluente) (Tan et al., 2019). Inversement, environ 50 % des patients atteints de SLA développent des troubles cognitifs de nature frontale et/ou des troubles comportementaux de sévérité variable, qui répondent aux critères diagnostiques de DFTc chez 15 % des patients (Lomen-Hoerth et al., 2003 ; Gordon et al., 2011). Des outils d'évaluation cognitive comme l'Edinburgh Cognitive and Behavioural ALS Screen ont été spécifiquement développés pour permettre le dépistage systématique des troubles cognitifs, dont l'évaluation peut s'avérer délicate chez les patients atteints de SLA (Crockford et al., 2018).

1.1.5 PSP et SCB : du « complexe de Pick » à leurs définitions actuelles

Comme nous l'avons déjà mentionné, le spectre clinique de la DLFT ne se limite pas à des présentations cognitivo-comportementales mais inclut également des phénotypes moteurs, notamment le syndrome cortico-basal (SCB) et la paralysie supranucléaire progressive (PSP), qui ont été rattachés aux DFT initialement dans le cadre du « complexe de Pick » (Kertesz et al., 2003).

Les critères de SCB actuellement utilisés ont été établis en 2013 (Armstrong et al., 2013). Le tableau clinique associe un syndrome parkinsonien atypique, des myoclonies, des manifestations dystoniques, des symptômes cognitifs et comportementaux, liés à une atteinte sous-cortico-frontale (Armstrong et al. 2013). Un phénomène de membre étranger, une main capricieuse peuvent être présents (Armstrong et al., 2013 ; Tetreault et al., 2020). Une apraxie gestuelle (idéationnelle, idéo-motrice ou mélocinétique) unilatérale ou asymétrique, des troubles de la sensibilité d'origine corticale, des troubles visuo-constructifs reflètent le dysfonctionnement du lobe pariétal (Lee et al., 2011). Au niveau langagier, une apraxie de la parole isolée, avec ou sans apraxie oro-faciale, ou une altération d'allure agrammatique peuvent être des présentations inaugurales d'un SCB (Deramecourt et al., 2010). Au plan anatomique, sa forme caractéristique associe une atteinte asymétrique des aires préfrontales, péri-rolandiques et pariétales supérieures, ainsi que des noyaux gris centraux (Dickson et al., 2011 ; Armstrong et al., 2013). Le SCB est le terme correspondant à la forme clinique de la maladie, alors que l'on utilise plus volontiers le terme de dégénérescence cortico-basale pour désigner la forme anatomopathologique de la maladie, détaillée dans le chapitre 1.2.2. Le variant clinique du SCB, et la forme pathologique DCB présentent une double dissociation. D'une part, seulement 50 % des cas de SCB sont associés à une pathologie de DCB sous-jacente, les autres cas étant représentés par des tableaux pathologiques du spectre des DLFT, de la MA, ou des maladies à prions (Boeve et al., 1999 ; Whitwell et al., 2010). D'autre part, les cas avec diagnostic anatomopathologique de DCB peuvent se manifester par des présentations cliniques variables parfois éloignées d'un SCB typique, qui sont intégrées dans les critères diagnostiques actuels. Ces formes peuvent se présenter par des troubles langagiers prédominant, réalisant le plus souvent un vnfAPP, un « syndrome frontal comportemental-visuospatial » ou, enfin, par un phénotype mimant une PSP (Armstrong et al., 2013).

Les présentations cliniques de la PSP sont également multiples (Höglinger et al., 2017), allant bien au-delà du phénotype typique du syndrome de Steele-Richardson-Olszewski (ou

syndrome de Richardson) considéré dans la première formulation des critères cliniques (Litvan et al., 1996). La présentation typique de syndrome de Richardson associe un syndrome parkinsonien akinéto-rigide axial non ou peu sensible à la L-Dopa, une instabilité posturale entraînant des chutes en arrière, une dystonie axiale et une réduction de la vitesse des saccades verticales allant jusqu'à la paralysie supranucléaire du regard (Höglinger et al., 2017). Le profil cognitif est caractérisé par un dysfonctionnement exécutif, un ralentissement idéique marqué, une désinhibition cognitive et des persévérations (Kok et al., 2021). D'autres formes cliniques, moins typiques, comprennent : l'akinésie pure avec *freezing*, la forme parkinsonienne de PSP, ou des formes dominées par un syndrome frontal, par des troubles langagiers, ou ressemblant à un SCB (Höglinger et al., 2017). Au niveau anatomique, une atrophie du mésencéphale et des pédoncules cérébelleux supérieurs est fortement évocatrice du diagnostic de PSP, en particulier dans le syndrome de Richardson, tandis que l'atrophie est étendue aux régions frontotemporales bilatérales dans les présentations plus « corticales » de la maladie (Jabbari et al., 2020).

1.1.6 Évolution des cadres nosographiques et des frontières cliniques des DLFT

L'identification des formes génétiques de DLFT et la description des phénotypes associés aux mutations, l'accès aux biomarqueurs lésionnels de la maladie d'Alzheimer, et la description de cohortes anatomopathologiques mieux caractérisées ont récemment permis d'élargir les frontières des DLFT à des formes cliniques moins classiques. Les critères actuels présentent certaines limites, ne permettant pas de capturer ces formes les plus atypiques, comme celles observées en association avec certaines causes génétiques ou décrites ci-dessous.

1.1.6.1 Formes amnésiques de DLFT

La « préservation relative de la mémoire épisodique » est un élément des critères de diagnostic de DFTc (Rascovsky et al., 2011). Il existe pourtant de rares formes « amnésiques » de DLFT, caractérisées par une atteinte de la mémoire hippocampique dès les premières phases de la maladie (Graham et al., 2005 ; Hornberger et al., 2010 ; Bertoux et al., 2020). Ces formes représentent près de 11 % des cas dans une série de 71 patients atteints de DLFT avec confirmation pathologique (Graham et al., 2005). Dans cette forme, le syndrome amnésique est sévère dès le début, isolé ou parfois accompagné par des troubles du comportement. Il est associé à une atrophie marquée des hippocampes, au niveau desquels l'importance des lésions

TDP-43 ou TAU est comparable à celle observée dans les régions frontales (Graham et al., 2005). L'analyse détaillée du profil mnésique chez 44 patients présentant une DFTc a révélé que la moitié d'entre eux présentent un syndrome amnésique de type hippocampique en modalité verbale et visuelle, qui est quantitativement et qualitativement comparable à celui des patients atteints de MA (Bertoux et al., 2014). Ces observations doivent conduire à interpréter avec une certaine précaution le caractère prédictif d'un syndrome amnésique de type hippocampique à l'égard d'une MA sous-jacente, la nature lésionnelle nécessitant d'être confortée par l'analyse des biomarqueurs de la MA dans le LCR (ou TEP-amyloïde), et ce particulièrement chez les patients à profil « amnésique » avec des antécédents familiaux de DLFT (Bertoux et al., 2020).

1.1.6.2 DLFT et présentations psychiatriques

La présence d'une pathologie psychiatrique primaire (PPP) non dégénérative représente un critère d'exclusion pour le diagnostic de DFTc (Rascovsky et al., 2011). La frontière entre PPP et DFTc peut cependant être difficile à établir en raison de leurs chevauchements cliniques, de l'intrication possible des deux pathologies chez un même patient et, surtout, de la présence d'authentiques symptômes psychiatriques constituant des manifestations atypiques de la pathologie neurodégénérative chez certains patients atteints de DFTc (Krudop et al., 2017). Ainsi, des manifestations délirantes, paranoïaques, des hallucinations auditives ou visuelles sont présentes (à un moment de l'évolution) chez un tiers des 97 patients d'une cohorte clinico-pathologique dont le diagnostic de DLFT a été confirmé *post mortem* (Landqvist et al., 2015). Une revue de la littérature évalue que la présentation initiale est purement psychiatrique (psychose, délire, schizophrénie) chez 10 % des patients atteints DLFT (Shinagawa et al., 2014). Elle montre aussi que ces présentations sont plus fréquentes dans certaines formes anatomopathologiques (DLFT-FUS et DLFT-TDP type B) ou génétiques (*C9orf72* en particulier). En effet, 21 % à 56 % des patients porteurs d'expansion *C9orf72* présentent des troubles psychiatriques (Snowden et al., 2012 ; Galimberti et al., 2013 ; Kertesz et al., 2013 ; Ducharme et al., 2017). L'identification du gène *C9orf72* a, ainsi, contribué à l'étude des présentations et « formes psychiatriques » de DLFT. Il ressort des principales études sur cette forme génétique que les manifestations les plus fréquentes sont des troubles psychotiques avec des épisodes délirants et/ou des hallucinations multimodales (Ducharme et al., 2017). Le plus souvent, ces troubles précèdent de 1 à 5 ans ou coexistent avec la composante cognitivo-comportementale de la DFTc (Ducharme et al., 2017 ; Sellami et al., 2019). Parfois, des

épisodes délirants aigus surviennent bien plus précocement, plusieurs décennies avant les premiers symptômes de DLFT (Kertesz et al., 2013). L'imagerie cérébrale est souvent normale, ou montre une atteinte bifrontale discrète, peu caractéristique de DLFT (Ducharme et al., 2017). Finalement, le diagnostic entre DFTc et PPP peut rester longtemps incertain, dans les formes génétiques comme dans les formes non génétiques. Des recommandations ont récemment été élaborées par un consortium d'experts pour répondre à cette problématique (Ducharme et al., 2020). Pour guider le diagnostic en pratique clinique, elles suggèrent : 1) l'adoption d'échelles standardisées spécifiquement développées pour discriminer une PPP d'une DFTc, telles que la « *FTDvsPPD Checklist* » (Ducharme et al., 2019), 2) l'évaluation conjointe des patients par des psychiatres et neurologues experts, 3) la recherche systématique de signes neurologiques orientant vers une pathologie dégénérative, 4) la réalisation d'un bilan neuropsychologique extensif incluant au moins un test de cognition sociale, répété au cours du suivi, 5) l'évaluation quantitative du profil d'atrophie en IRM avec séquences 3D T1-pondérées et la réalisation d'une imagerie métabolique en TEP cérébrale au ¹⁸FDG (TEP-FDG), 6) le dosage de biomarqueurs biologiques incluant, si possible le dosage des neurofilaments (Ducharme et al., 2020), 7) la recherche d'expansion du gène *C9orf72*, recommandée chez tout patient présentant un phénotype psychiatrique et une histoire familiale de DLFT et/ou SLA ; elle est fortement recommandée aussi en présence d'une histoire familiale de troubles psychiatriques à début tardif et/ou présentant une détérioration neurologique progressive surajoutée (Ducharme et al., 2020).

1.1.6.3 Les formes lentement progressives de DLFT

Enfin, des formes évolutives particulières ont été décrites sous le terme de « *long lasting FTD* » (DFT lentement progressive) ou de « *phénocopie de DFTc* ». Alors que la durée d'évolution de la DFTc est généralement comprise entre 6 et 10 ans, certains patients dont la présentation clinique initiale est compatible avec une DFTvc restent relativement stables ou évoluent de façon extrêmement lente, sur plusieurs décennies (Hornberger et al., 2009 ; Khan et al., 2012 ; Devenney et al., 2018a ; Valente et al., 2019). L'atrophie et l'hypométabolisme cérébral sont peu marqués et également peu progressifs pendant plus d'une dizaine d'années (Khan et al., 2012 ; Valente et al., 2019). Ces formes, bien que rares, soulèvent le problème du diagnostic de DFTc « probable », difficile à établir dans ce contexte en l'absence de déclin cognitif ou fonctionnel notable pendant plusieurs années. Certains auteurs en font une entité spécifique (Devenney et al., 2018a). D'autres, au contraire, considèrent que cette entité n'est

pas unique puisque cette évolution lente peut être associée, ou non, à une expansion du gène *C9orf72* qui n'est en cause que chez une partie des patients (Khan et al., 2012).

1.2 Formes anatomopathologiques des DLFT

L'atteinte histologique des DLFT prédomine au niveau des lobes frontaux et temporaux, qui sont le siège d'une perte neuronale, d'une réaction microgliale et d'une vacuolisation des couches superficielles du cortex. La découverte de différentes protéines s'agréant sous forme d'inclusions dans les neurones et les cellules gliales de patients atteints de DLFT a contribué à mieux en comprendre les mécanismes biologiques et moléculaires et permet aujourd'hui de proposer une classification anatomopathologique basée sur l'anomalie protéique prédominante (Mackenzie et al., 2011a ; Forrest et al., 2018 ; Neumann et Mackenzie, 2019). Les études immunohistochimiques permettent de distinguer deux formes principales (comportant chacune différents sous-types) caractérisées par des inclusions de nature différente, décrites plus en détail dans ce chapitre.

1.2.1 Protéinopathie TDP-43 dans les DLFT et SLA

Dans 60 % des cas environ (appelés DLFT-TDP), les inclusions pathologiques sont composées de protéine TDP-43 (*transactive response DNA binding protein of 43 kDa*) (Neumann et al., 2006). TDP-43 est une ribonucléoprotéine de 414 acides aminés principalement localisée dans le noyau des neurones et des cellules gliales. Elle joue un rôle dans la régulation de l'épissage, la maturation et le transport des ARNs, ainsi que la biogénèse des micro-ARNs (Buratti et Baralle, 2001). Dans les processus dégénératifs, TDP-43 est relocalisée dans le cytoplasme, où elle s'agrège au sein d'inclusions, sous une forme clivée et hyperphosphorylée (Neumann et al., 2006).

Dans les DLFT, les lésions TDP-43-positives sont détectées dans les neurones, les astrocytes et les oligodendrocytes. Une classification des DLFT-TDP en cinq sous-types (A à E) est actuellement utilisée, reposant sur la localisation cellulaire, la densité et l'aspect des inclusions TDP-43-positives (Mackenzie et al., 2011a ; Lee et al., 2017a). Au niveau cellulaire, elles peuvent être présentes dans le cytoplasme, le noyau (où elles prennent souvent un aspect lenticulaire en « œil de chat ») et/ou dans les prolongations axonales en dégénérescence (« neurites dystrophiques »). Selon les sous-types, la présence de dépôts pathologiques peut concerner l'ensemble du cortex, ou se limiter aux couches les plus superficielles, comme illustré dans la Figure 1. Cette classification permet d'établir des corrélations entre chacun de ces sous-

types et des présentations clinico-génétiques particulières (Figure 1) (Mackenzie et al., 2011a ; Lee et al., 2017a). Brièvement, le type A est principalement associé à une DFTc ou un vnfAPP et, au niveau génétique, aux mutations des gènes *GRN* ou *C9orf72*. Le type B produit une DFTc et/ou SLA, et est associé, au plan génétique, aux expansions du gène *C9orf72*. Le type C est moins fréquent, et est identifié dans les formes temporales qu'elles soient à prédominance gauche (vsAPP) ou droite (DFTvtd). Le type D est beaucoup plus rare, et presque exclusivement associé aux mutations du gène *VCP*. Le type E, caractérisé par des inclusions cytoplasmiques à l'aspect granulo-filamenteux, a été décrit plus récemment (Lee et al., 2017a). Il est associé à une DFTc, d'évolution particulièrement rapide, parfois accompagnée d'une atteinte motoneuronale.

	Type A	Type B	Type C	Type D	Type E
I					
II					
III					
IV					
V					
VI					
White Matter					
Cortical Pathology	<ul style="list-style-type: none"> • NCI's including ring inclusions • Short DN's • +/- Lentiform NII's • +/- Oligo inclusions • Superficial 	<ul style="list-style-type: none"> • NCI's • Few DN's • +/- Oligo inclusions • Superficial and deep 	<ul style="list-style-type: none"> • Long DN's • Few NCI's • Superficial 	<ul style="list-style-type: none"> • Lentiform NII's • Few NCI's • Superficial and deep 	<ul style="list-style-type: none"> • GFNI's • Grains • Curvilinear oligodendroglial inclusions • Superficial and deep
Common Phenotype	bvFTD naPPA	bvFTD +/- MND	svPPA bvFTD	IBMPFD-ALS	bvFTD
Genetic Associations	<i>GRN</i> mutations	<i>C9orf72</i> mutations	None	<i>VCP</i> mutations	Uncertain

Figure 1. Classification des sous-types de DLFT-TDP

Une illustration schématique de l'aspect des lésions et de leur distribution dans les couches corticales et la substance blanche est proposée. ALS : sclérose latérale amyotrophique ; bvFTD : démence frontotemporale variant comportemental ; DN : neurites dystrophiques ; GFNI : inclusions neuronales granulo-filamenteuses ; IBMPFD : complexe myopathie à corps d'inclusion, maladie osseuse de Paget, démence frontotemporale ; naPPA : variant non-fluent/agrammatique d'aphasie primaire progressive ; MND : maladie des motoneurones ; NCI : inclusions neuronales cytoplasmiques ; NII : inclusions neuronales intranucléaires ; svPPA : variant sémantique d'aphasie primaire progressive. *Adapté de Lee et al., 2017.*

Par analogie avec le modèle de progression de la pathologie TAU dans la MA (Braak et al., 2006), différents stades anatomopathologiques séquentiels ont été décrits dans les DLFT-TDP (Brettschneider et al., 2014). Ils reflètent la propagation de la pathologie TDP-43 à travers les différentes aires corticales au cours de la maladie, qui débute dans les régions préfrontales antéro-basales et l'amygdale (stade I), touche ensuite l'ensemble du cortex préfrontal, le lobe temporal antérieur, l'hippocampe et le striatum (stade II), puis les aires sensori-motrices primaires, le cortex associatif pariéto-occipital, ainsi que les noyaux moteurs du tronc cérébral et la corne antérieure de la moelle épinière (stade III), avant de toucher les aires visuelles primaires quand la charge lésionnelle est maximale (stade IV) (Brettschneider et al. 2014). Le mécanisme de propagation des lésions n'est pas clairement établi. Cette progression suggère une diffusion des lésions selon un gradient antéro-postérieur par contiguïté, possiblement d'une cellule à l'autre, par un mécanisme dit « prion-like » similaire à celui décrit dans les maladies à prions (Nonaka et al., 2013) (Figure 2).

Les caractéristiques anatomopathologiques de la SLA sont moins hétérogènes que dans les DLFT. Elle est majoritairement associée à des lésions TDP-43-positives, présentes chez plus de 95% des patients (Neumann et al., 2006). Celles-ci forment des inclusions rondes ou enchevêtrées, localisées dans le cytoplasme et les axones des neurones moteurs ainsi que dans les cellules oligodendrogiales. Ce profil lésionnel est globalement comparable au type B des DLFT-TDP (Saber et al., 2015). Ces lésions sont associées aux corps de Bunina formant des dépôts éosinophiles arrondis quasiment pathognomoniques de la SLA (Bunina et al., 1962). Comme pour la DLFT, les stades anatomopathologiques proposés par Brettschneider et collaborateurs (2013) décrivent la topographie des lésions TDP-43 dans la SLA et leur progression avec l'évolution de la maladie. Les lésions sont initialement localisées au niveau du cortex moteur primaire et des motoneurones ponto-bulbaires et médullaires (stade I), pour ensuite s'étendre à la formation réticulée et aux noyaux pré-cérébelleux (stade II), à l'ensemble du cortex préfrontal et aux noyaux gris (stade III), et finalement aux hippocampes et aux lobes temporaux (stade IV) comme illustré dans la Figure 2 (Brettschneider et al., 2013 ; Verde et al., 2017).

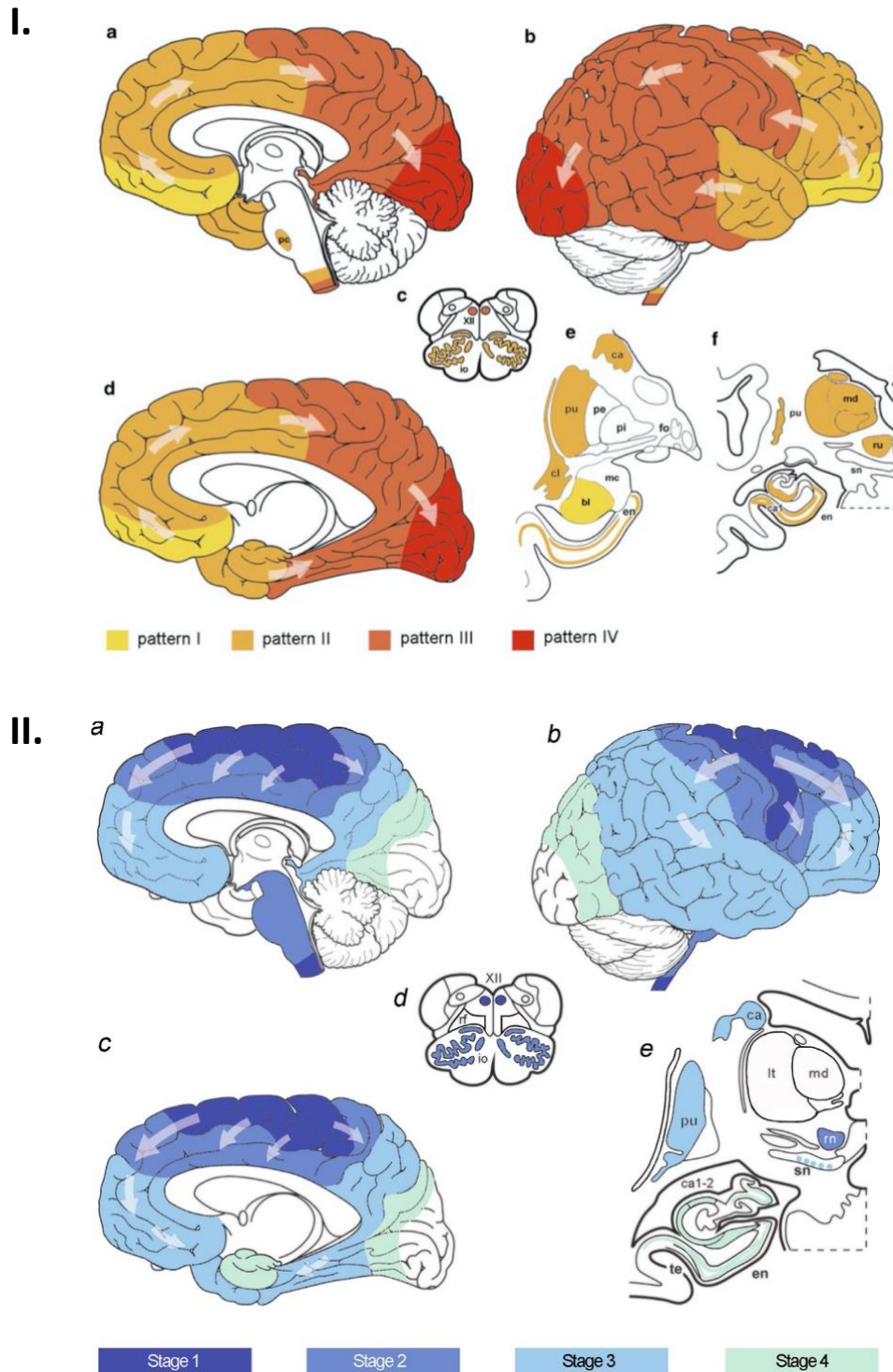


Figure 2. Représentation de la propagation de la pathologie TDP-43 dans la DFTc (I) et dans la SLA (II)
 bl : sous-noyaux basolatéraux de l'amygdale ; ca : noyau caudé ; ca1-2 : régions 1-2 du cornu Ammonis ; cl :
 claustrum ; en : cortex entorhinal ; fo : fornix ; io : noyau olivaire inférieur ; lt : thalamus latéral ; mc : sous-
 noyaux médiocentraux de l'amygdale ; md : thalamus médial ; pc : noyaux précérébelleux ; pe : pallidum
 externe ; pi : pallidum interne ; pu : putamen ; rf : formation réticulée ; rn : noyau rouge ; sn : substance noire ;
 te : cortex transentorhinal ; XII : noyau de l'hypoglosse.

Adapté de Brettschneider et al., 2013, Brettschneider et al., 2014, et de Verde et al., 2017.

Pour être complet, une pathologie de type TDP-43 caractérise aussi d'autres entités nosographiques externes au spectre des DLFT, et notamment la LATE (*Limbic-predominant Age-related TDP-43 Encephalopathy*) (Nelson et al., 2019). Dans la LATE, les inclusions TDP-43-positives ont un tropisme particulier pour les lobes temporaux médiaux et peuvent s'associer à une sclérose hippocampique (Josephs et al., 2014a ; Nelson et al., 2019). Des changements pathologiques compatibles avec une LATE peuvent concerner jusqu'à 50 % des individus de plus de 80 ans ; la présentation clinique principale est celle d'un syndrome amnésique de type hippocampique lentement progressif (Nelson et al., 2019). Enfin, il faut noter que des lésions TDP-43 sont occasionnellement associées aux plaques amyloïdes et aux dégénérescences neurofibrillaires dans la MA (Amador-Ortiz et al., 2007).

1.2.2 Protéine TAU et pathologie DLFT-TAU

Chez 30 % des patients environ, la présence d'inclusions neuronales et gliales positives pour la protéine TAU (*tubulin associated unit*) définit une DLFT-TAU (antérieurement appelée « tauopathie»). TAU est une protéine qui possède quatre domaines répétés permettant sa liaison aux microtubules. Elle est fortement exprimée dans les axones, où elle est associée au cytosquelette, contribuant à l'assemblage et à la stabilisation des microtubules. Cette protéine est codée par le gène *MAPT* (*microtubule associated protein tau*). Les exons 9 à 12 de ce gène codent pour les quatre domaines de liaison de TAU aux microtubules. L'épissage alternatif de l'exon 10 entraîne l'inclusion ou l'exclusion de l'un de ces domaines de liaison, produisant deux types d'isoformes protéiques contenant 3 (formes 3R) ou bien 4 (4R) domaines de liaison (Goedert et al., 1989 ; Goedert et Jakes, 1990). Les formes 3R et 4R sont normalement exprimées de façon équivalente dans le cerveau humain adulte (Goedert et al., 1989). Dans les DLFT-TAU, le ratio 3R/4R est souvent déséquilibré et la protéine TAU est anormalement phosphorylée, conduisant à son accumulation sous forme d'inclusions cytoplasmiques neuronales et/ou gliales avec une prédominance de la forme 3R ou de la forme 4R (Sergeant et al., 2005). Plusieurs types anatomopathologiques, caractérisés par des différentes formes de lésions TAU-positives, sont distingués (Forrest et al., 2018). La maladie de Pick (associée à des inclusions TAU-3R), la DCB et la PSP (toutes les deux associées à l'agrégation de protéine TAU-4R) représentent les principales formes de DLFT-TAU. Une méta-analyse portant sur 544 patients avec un diagnostic anatomopathologique de DLFT-TAU montre que la DCB est

légèrement plus fréquente (35 %) que la PSP (31 %) et la maladie de Pick (30 %), alors que d'autres entités sont bien plus rares (Josephs et al., 2011).

Brièvement, la DCB est caractérisée par la présence de neurones gonflés et achromiques au niveau cortical, ainsi que des noyaux gris centraux, du mésencéphale et du cervelet, justifiant l'appellation proposée par Rebeiz (Rebeiz et al., 1967). Les lésions gliales TAU-positives de la DCB forment des « plaques astrocytaires », ainsi que des corps spiralés dans le cytoplasme des oligodendrocytes (Dickson et al., 2002). Dans la PSP, les lésions TAU-positives neuronales ont un aspect globulaire, enchevêtré au niveau sous-cortical. Elles prennent une conformation allongée, en forme de flammèche au niveau cortical. La pathologie gliale est principalement représentée par des « touffes astrocytaires » et des corps spiralés dans les oligodendrocytes (Lee et Leugers, 2012). La maladie de Pick est, elle, caractérisée par la présence de « corps de Pick » qui sont des inclusions intra-neuronales argyrophiles, basophiles et arrondies, de « neurones de Pick » (neurones gonflés en dégénérescence), ainsi que des inclusions astrocytaires et oligodendrogiales (Mackenzie et Neumann, 2016). Cliniquement, la maladie de Pick se présente le plus souvent comme une DFTc, plus rarement comme un vnfAPP ou un SCB (Hodges et al., 2004).

En marge de ces trois formes principales, deux autres entités anatomopathologiques associées à des inclusions de protéine TAU 4R ont été plus récemment décrites. La « tauopathie gliale globulaire » est caractérisée par des lésions globulaires constituées de protéine TAU dans les astrocytes et les oligodendrocytes qui, en fonction de leur distribution, peuvent déterminer un phénotype de DFTc, un syndrome motoneuronal ou un syndrome parkinsonien atypique (Ahmed et al., 2013). La maladie à grains argyrophiles, probablement sous-diagnostiquée, est caractérisée par l'association de petites inclusions argyrophiles fusiformes constituées de protéine TAU dans le neuropile (« grains »), de neurones gonflés et de corps spiralés dans les oligodendrocytes argyrophiles (Ferrer et al., 2008). Ces lésions ont un tropisme préférentiel pour les régions hippocampiques, déterminant des phénotypes amnésiques lentement évolutifs. Elles coexistent fréquemment avec d'autres pathologies, en particulier avec des lésions de PSP, de DCB ou de MA (Irwin et al., 2015). Même si cela a été l'objet de controverses lors de leur description, elles sont actuellement considérées comme des entités appartenant au groupe des DLFT-TAU (Irwin et al., 2015 ; Giannini et al., 2020). Il faut également citer, parmi ces dernières, les rares formes liées aux mutations du gène *MAPT* qui peuvent être responsables de formes 3R, 4R ou de formes mixtes 3R/4R.

Enfin, il faut mentionner que des lésions TAU-positives sont présentes dans d'autres maladies hors de spectre des DLFT, telles que la MA, la maladie de Niemann-Pick type C, l'encéphalopathie traumatique chronique, ou encore dans deux formes de tauopathie primaire liée au vieillissement (Primary age-related tauopathy, PART, ou Aging-related tau astrogliopathy, ARTAG) (Crary et al., 2014 ; Kovacs et al., 2016). Une classification complète des maladies associées aux inclusions de protéine TAU est présentée dans la Figure 3 (Ganguly et Jog, 2020).

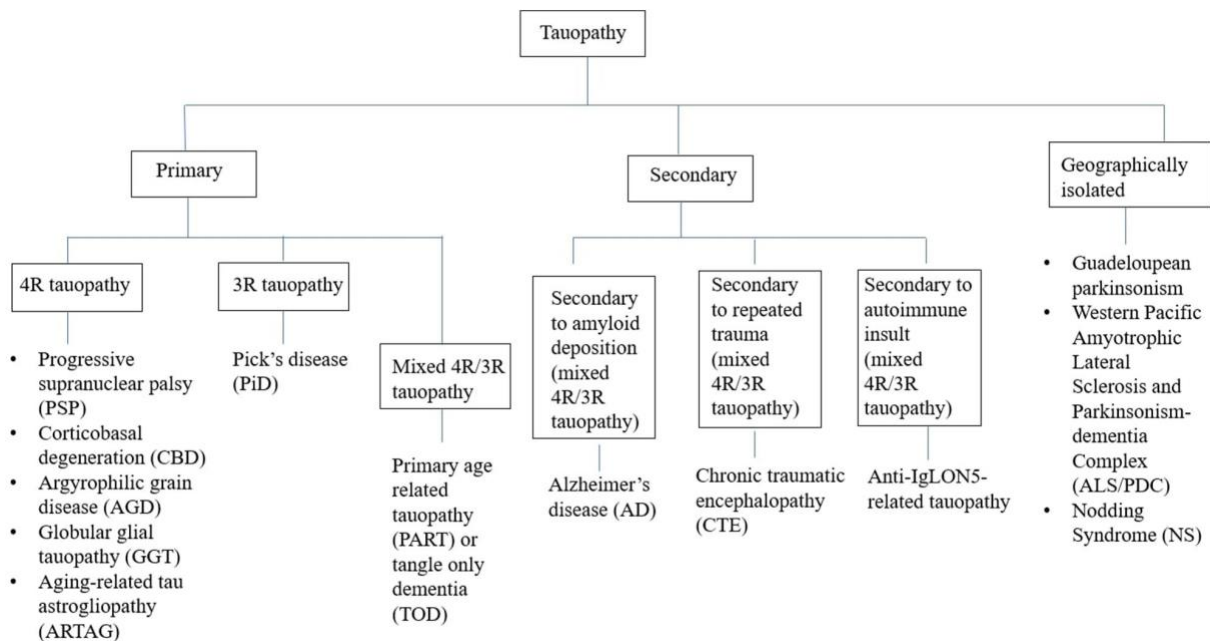


Figure 3. Classification des tauopathies
Adapté de Ganguly et Jog, 2020.

1.2.3 Formes anatomopathologiques rares de DLFT

Pour être complet, il convient de citer des formes anatomopathologiques beaucoup plus rares, observées chez 5 à 10 % des patients (Mackenzie et Neumann, 2016). L'une, initialement appelée DLFT-FUS, est caractérisée par des inclusions composées de protéine FUS (*Fused in sarcoma*) (Neumann et al., 2009). Cette entité a ensuite été redéfinie sous le terme de DLFT-FET après la découverte de protéines additionnelles, EWS (*Ewing's sarcoma*) et TAF15 (*TATA-binding protein associated factor 15*), formant un complexe moléculaire avec FUS dans les inclusions (Neumann et al., 2011). Trois sous-types pathologiques de DLFT FUS/FET sont

décrits. Le plus fréquent (dit « DLFT-U atypique ») se caractérise par des inclusions cytoplasmiques et nucléaires d'aspect globulaire et filamenteux au niveau du cortex, du striatum (notamment du noyau caudé) et de l'hippocampe (Neumann et al., 2009). Les deux autres sous-types, beaucoup plus rares, sont représentés par la maladie à inclusions neuronales de filaments intermédiaires (ou NIFID pour *Neuronal intermediate filament inclusion disease*) caractérisée par des inclusions neuronales composées de neurofilaments ou d'autres filaments intermédiaires comme l'alpha-internexine, et la maladie à corps basophiles (ou BIBD pour *basophilic inclusion body disease*) (Neumann et al., 2009). Généralement, les DLFT-FET se manifestent par une DFTc particulièrement précoce et d'évolution rapide, marquée par des conduites désinhibées, des comportements agressifs et antisociaux (Neumann et al., 2009), souvent en association avec une SLA (Mackenzie et al., 2011b ; Chornenka et al., 2020).

Il existe également des cas presque anecdotiques de DLFT se caractérisant par des inclusions cytoplasmiques positives à l'ubiquitine et à d'autres protéines du protéasome, en l'absence d'inclusions TDP-43, TAU ou FUS/FET, dénommée DLFT-UPS (*ubiquitine proteasome system*) (Mackenzie et al., 2010). Avec l'avancée remarquable des techniques immunohistochimiques et biochimiques, les DLFT sans aucune inclusion décelable (DLFT-ni, *no inclusions*) sont désormais exceptionnelles (Rademakers et al., 2012).

1.3 Aspects génétiques des DLFT

Une cause génétique est retrouvée chez un quart à un tiers des patients, qui en général ont une histoire familiale de DLFT, de démence ou de SLA, avec un mode de transmission majoritairement autosomique dominant (Goldman et al., 2005 ; Wood et al., 2013). Historiquement, c'est en 1998 que le premier gène, *MAPT*, a été cloné (Hutton et al., 1998). Depuis, un grand nombre de gènes ont été identifiés en partie grâce au développement des technologies de séquençage de haut débit au cours de la dernière décennie. Actuellement, plus de 20 gènes sont répertoriés comme responsables de DLFT et SLA, et expliquent environ 80 % des cas familiaux et 10 à 15 % des formes sporadiques (Le Ber, 2013 ; Pottier et al., 2016). Les deux formes génétiques les plus fréquentes sont causées par des mutations des gènes *GRN* (ou *PGRN*) et *C9orf72* (chromosome 9 open reading frame 72). Elles sont détaillées ci-dessous. Les causes génétiques plus rares et leurs caractéristiques sont résumées dans le Tableau 1. Les aspects génétiques des DLFT et les méthodes actuelles pour le diagnostic génétique ont été traités plus largement dans un article de revue de la littérature qui est joint à cette thèse (article de revue 1, Sellami et al., 2020a).

1.3.1 Le gène *GRN*

1.3.1.1 Fonctions physiologiques de la progranuline et implications dans la pathologie

Les mutations du gène *GRN*, situé sur le chromosome 17, ont été identifiées en 2006 dans des formes familiales de DLFT (Baker et al., 2006 ; Cruts et al., 2006). Elles sont responsables de 15 à 20 % des DLFT familiales et de 5 % des formes sporadiques (Rademakers et al., 2007 ; Le Ber et al. 2008). Le gène *GRN* code pour la progranuline, une protéine de 68,5 kDa. Les mutations du gène *GRN* sont principalement représentées par des mutations non-sens, des mutations des sites d'épissage ou des insertions/délétions provoquant un décalage du cadre de lecture, ou des délétions exoniques ou géniques (Cruts et al., 2006 ; Baker et al., 2006). La grande majorité des mutations entraînent un codon stop prématuré, conduisant à la dégradation de l'ARN mutant par un mécanisme de « *nonsense mediated RNA-decay* », et à une haploinsuffisance. Le niveau de progranuline fonctionnelle est ainsi réduit d'environ 50 %. La sécrétion lymphocytaire de la progranuline la rend détectable dans le plasma, et le taux de

progranuline plasmatique représente un bon indicateur d'une mutation causale quand il est abaissé (Ghidoni et al., 2012 ; Sellami et al., 2020b).

Dans le système nerveux central, la progranuline est fortement exprimée dans les neurones et la microglie (Daniel et al., 2000) où elle assure plusieurs fonctions biologiques (Ahmed et al., 2007). Elle favorise la prolifération cellulaire, la différenciation des neurones au cours du développement et est un facteur de survie neuronale. De plus, elle joue un rôle dans la modulation de la réponse inflammatoire via les récepteurs de la cytokine TNF- α et, par ce biais, est un acteur important de la neuroinflammation (Tang et al., 2011). Elle intervient également au niveau de la voie lysosomale. La progranuline est en effet internalisée dans le lysosome via son interaction avec le récepteur sortiline (Cenik et al., 2012), où elle est clivée en peptides de plus petite taille, les granules. Les granules ont des activités biologiques adverses à celles de la protéine native, incluant une action anti-proliférative et pro-inflammatoire (Paushter et al., 2018). La progranuline est aussi exprimée dans les tissus périphériques, principalement dans les cellules endothéliales et les lymphocytes, avec des fonctions pléiotropiques dans la cicatrisation tissulaire, la modulation de la réponse immunitaire, la tumorigenèse et l'homéostasie métabolique (Jian et al., 2020). Même si les mécanismes pathologiques de la maladie restent largement spéculatifs, il est probable que c'est à travers un déficit des différentes fonctions cellulaires de la progranuline (en particulier au niveau de la survie neuronale et la neuroinflammation) que les mutations du gène *GRN* sont pathogènes (Petkau et Leavitt, 2014). Par ailleurs, dans le compartiment lysosomal, la progranuline active la fonction d'enzymes lysosomales comme la cathepsine D et la glucocérébrosidase, et stimule la maturation de coactivateurs enzymatiques tels que les saposines (Paushter et al., 2018 ; Arrant et al., 2019 ; Tayebi et al., 2020). La pathophysiologie de la maladie pourrait aussi être liée à une dysfonction de son rôle dans le lysosome. En effet, des dépôts de lipofuscine, un marqueur de dysfonctionnement lysosomal, sont présents dans les neurones et cellules microgliales des modèles murins knock-out pour le gène *GRN* (Ahmed et al., 2010 ; Tanaka et al., 2014) et l'activité des enzymes lysosomales dont la fonction est stimulée par la progranuline est réduite chez les patients porteurs de mutation, appuyant le rôle d'un dysfonctionnement lysosomal dans la pathologie (Beel et al., 2017 ; Arrant et al., 2019).

1.3.1.2 Phénotypes associés aux mutations du gène GRN

Les phénotypes cliniques associés aux mutations du gène *GRN* et l'âge de début de la maladie sont hétérogènes. Les symptômes débutent vers l'âge de 60 ans, avec des âges extrêmes

allant de la troisième à la neuvième décennie, et évoluent en 7 à 10 ans (Le Ber et al., 2008 ; Moore et al., 2020a). Cette grande variabilité de l'âge de début chez des porteurs de mutations dont les effets biologiques sont similaires, n'est pas complètement expliquée. Elle suggère la contribution de facteurs modificateurs, environnementaux ou génétiques, dont les impacts se combinent à ceux de la mutation. Ainsi, certains polymorphismes des gènes *TMEM106B* et du gène *GFRA2* pourraient influencer l'âge de début ou la sévérité de la maladie (Gallagher et al., 2014 ; Lattante et al., 2014 ; Pottier et al., 2018).

La présentation clinique la plus fréquente est celle d'une DFTc. Un tableau d'APP est rapporté chez certains patients (Snowden et al., 2006 ; Mesulam et al., 2007 ; Rohrer et al., 2010b) et pourrait représenter le phénotype inaugural dans environ 15 % des cas (Le Ber et al., 2008 ; Chen-Plotkin et al., 2011 ; Moore et al., 2020a). Néanmoins, si l'on considère des séries de patients avec APP, les mutations du gène *GRN* sont globalement assez rares, comme l'ont montré deux études nord-américaines, l'une identifiant seulement 3 porteurs de *GRN* dans une population de 100 patients avec une APP (Flanagan et al., 2015), l'autre retrouvant une fréquence de mutations même inférieure, calculée à 1,2 %, dans une cohorte de 403 patients (Ramos et al., 2019). Les profils langagiers de ces patients n'ont pas été étudiés de façon détaillée, et ce sujet a fait l'objet d'une partie de ce travail de thèse (article 1, Saracino et al., 2021a). La moitié des patients développent un syndrome parkinsonien akinéto-rigide, en général au cours de l'évolution de la maladie (Gasca-Salas et al., 2016). Il peut être au premier plan dans des formes plus rares se manifestant par un SCB ou mimant une maladie à corps de Lewy (Le Ber et al., 2008 ; Coppola et al., 2017 ; Moore et al., 2020a). Des atypies cliniques caractérisent cette forme génétique. Un dysfonctionnement des aires associatives postérieures, se manifestant par une apraxie idéo-motrice, des troubles visuo-spatiaux et/ou des hallucinations visuelles, survient précocement et plus fréquemment (25 et 50 % des cas) chez les porteurs de mutations du gène *GRN* que dans les formes non génétiques de DFTc (Le Ber et al., 2008 ; Rohrer et al., 2009). De même, près de 20 % des patients présentent des troubles de mémoire épisodique, quelque fois inauguraux, dont le profil cognitif peut être compatible avec un dysfonctionnement hippocampique (Rademakers et al., 2007 ; Le Ber et al., 2008). Cette observation est à mettre en relation avec l'atrophie hippocampique sévère fréquemment démontrée à l'examen *post mortem* des patients avec mutations du gène *GRN*, parfois telle qu'elle a été qualifiée de « sclérose hippocampique » dans certaines études (Rademakers et al., 2007).

Pour finir, il faut aussi mentionner que de très rares mutations homozygotes du gène *GRN* conduisent à un tableau clinico-pathologique de céroïde-lipofuscinose neuronale de type 11 (CLN11). Il s'agit d'une maladie d'accumulation lysosomale débutant en général avant l'âge de 20 ans dont la présentation clinique associe une ataxie cérébelleuse, une épilepsie myoclonique, une rétinite pigmentaire et des troubles cognitifs (Smith et al., 2012 ; Huin et al., 2020).

1.3.2 Le gène *C9orf72*

*1.3.2.1 Mécanismes pathogéniques des expansions du gène *C9orf72**

En 2011, l'identification des expansions pathologiques du gène *C9orf72* dans des formes familiales de DLFT et de SLA a représenté une découverte majeure dans ces deux maladies (DeJesus-Hernandez et al., 2011 ; Renton et al., 2011). Les expansions du gène *C9orf72* représentent en effet la cause génétique la plus fréquente dans les formes familiales de DLFT (expliquant 30 % des cas environ), de SLA familiales (40%) et de DFT/SLA (80 % des cas) (Majounie et al., 2012 ; Le Ber et al., 2013a). Le premier intron du gène *C9orf72* contient une séquence répétée de 1 à 30 hexanucléotides GGGGCC (G₄C₂) (Renton et al., 2011 ; DeJesus-Hernandez et al., 2011 ; Beck et al., 2013). Les individus porteurs d'expansions pathogènes possèdent plusieurs centaines à plusieurs milliers de répétitions G₄C₂ (Renton et al., 2011 ; DeJesus-Hernandez et al., 2011). Il faut noter que, comme dans d'autres maladies à expansions, il existe un mosaïcisme tissulaire, c'est-à-dire que le nombre de répétitions G₄C₂ varie d'un tissu à l'autre chez un même patient, et d'une région à l'autre au sein du système nerveux central. Le nombre des répétitions, classiquement analysé à partir de l'ADN extrait des lymphocytes pour le diagnostic, n'est pas prédictif de la taille de l'expansion observée dans le cerveau (van Blitterswijk et al., 2013 ; McGoldrick et al., 2018). La taille de l'expansion dans les différentes régions du cerveau n'est pas non plus déterminante du phénotype clinique (DFT versus SLA) (Camuzat et al., poster RFMASA 2021, non publié).

Trois mécanismes pathologiques principaux, non mutuellement exclusifs, semblent impliqués dans la neurodégénérescence. Le gène *C9orf72* code pour la protéine C9ORF72, et son expansion entraîne une diminution de la transcription, conduisant à une réduction de la synthèse de la protéine C9ORF72. Les fonctions biologiques de cette protéine ne sont que

partiellement connues (DeJesus-Hernandez et al., 2011). Compte tenu de sa forte homologie de séquence avec les protéines DENN (*differentially expressed in normal and neoplastic cells*), et de l'interaction de celles-ci avec des petites protéines GTPases, C9ORF72 est supposée agir en tant que protéine GAP (*GTPase activating protein*) (Levine et al., 2013 ; Tang et al., 2020). Les protéines GAP interviennent dans plusieurs fonctions biologiques telles que l'activation de l'endocytose et de l'autophagie, la promotion du trafic vésiculaire, et la voie lysosomale, suggérant l'implication de C9ORF72 dans ces différentes voies et fonctions (Webster et al., 2016). La perte de fonction de C9ORF72 dans ces différents processus biologiques n'est cependant probablement pas suffisante pour expliquer, seule, la neurodégénérescence, car les modèles murins knock-out pour *C9orf72* ne développent pas de troubles moteurs ou cognitifs francs, ni de signes de dégénérescence neuronale (Koppers et al., 2015 ; Sellier et al., 2016). Deux autres mécanismes sont impliqués dans le processus pathologique. D'une part les ARNs mutants s'accumulent sous forme de *foci* dans le noyau (Mizielinska et al., 2013 ; Lagier-Tourenne et al., 2013). D'autre part, l'activation d'une traduction anormale (« non ATG dépendante ») entraîne la production non physiologique de dipeptides (ou DPR, *dipeptide repeat*) et leur agrégation dans le cytoplasme (Mackenzie et al., 2014). Ces *foci* d'ARNs et les lésions composées de DPR constituent des caractéristiques lésionnelles spécifiques des formes *C9orf72*. Elles sont associées à des inclusions p62-positives (en particulier dans le cervelet), ainsi qu'à des inclusions TDP-43-positives dont les caractéristiques sont détaillées dans la partie de ce manuscrit décrivant les aspects anatomopathologiques des DLFT.

1.3.2.2 Phénotypes associés aux mutations du gène *C9orf72*

Au plan clinique, l'âge des premiers signes de la maladie se situe aux alentours de 50 ans, avec une variabilité importante allant de moins de 30 à plus de 90 ans, y compris chez des sujets d'une même famille (Moore et al., 2020a). Contrairement à d'autres maladies à expansion, l'âge de début de la maladie n'est pas corrélé à la taille de l'expansion dans les lymphocytes, et il n'y a pas, à l'heure actuelle, d'argument solide en faveur d'un phénomène d'anticipation au plan clinique, ni au plan moléculaire (Fournier et al., 2019 ; Jackson et al., 2020). Les présentations cliniques sont également hétérogènes, mais globalement assez différentes de celles des mutations du gène *GRN*, suggérant des tropismes lésionnels distincts dans ces deux formes génétiques. Comme mentionné précédemment, les phénotypes classiquement associés aux expansions du gène *C9orf72* sont la DFTc, la SLA ou l'association de ces deux pathologies. Un début bulbaire est plus fréquemment observé que dans les formes

non génétiques de SLA (Millecamps et al., 2012). Seuls quelques rares cas d'APP associées à des expansions *C9orf72* (Boeve et al., 2012 ; Ramos et al., 2019 ; Moore et al., 2020a) ont été décrits, ainsi qu'un cas exceptionnel de phonagnosie progressive (Didic et al., 2020). Globalement, les formes langagières, impliquées chez 1 à 4 % seulement des patients porteurs d'expansion, sont beaucoup plus rares que dans les formes *GRN* (Le Ber et al., 2013a). De même, un syndrome parkinsonien atypique est très rarement une manifestation inaugurale de cette forme génétique (moins de 5 % des porteurs) (Gasca-Salas et al., 2016).

En marge des phénotypes de DLFT, et comme nous l'avons abordé dans le chapitre 1.1.6, les expansions du gène *C9orf72* peuvent être à l'origine de présentations psychiatriques telles que des manifestations délirantes, paranoïaques, des hallucinations multimodales ou, plus rarement, un trouble bipolaire (Floris et al., 2013), un trouble obsessionnel-compulsif (Calvo et al., 2012) ou une catatonie (Holm, 2014). Ces manifestations sont associées ou représentent des présentations prodromales, précédant de quelques années le tableau cognitivo-comportemental (Snowden et al., 2012 ; Le Ber et al., 2013a ; Galimberti et al., 2013 ; Kertesz et al., 2013 ; Ducharme et al., 2017). Une série italienne explorant les troubles psychiatriques chez 39 porteurs d'expansions montre que des symptômes psychotiques, survenant entre 48 et 70 ans, étaient inauguraux chez 10 d'entre eux (26 %) (Galimberti et al., 2013). De façon intéressante, des phénotypes purement psychiatriques, tels que des tableaux de psychoses atypiques, des troubles schizoïdes ou bipolaires, peuvent débiter plus précocement, vers l'âge de 40 ans, et rester isolés pendant plusieurs décennies (Ducharme et al., 2017 ; Sellami et al., 2019). Enfin, une étude sur 1 414 apparentés de premier et deuxième degré de patients porteurs d'expansions du gène *C9orf72* montre que la récurrence des troubles psychiatriques est environ 5 fois plus élevée chez ces individus comparés aux apparentés de patients atteints de DFT non génétique (Devenney et al., 2018b).

Au-delà, une étude récente a exploré certains traits de personnalité chez des individus porteurs d'expansion du gène *C9orf72* dès leur enfance (Gossink et al., 2022). Cette étude évalué les éléments biographiques principaux concernant le développement, l'adolescence, la vie sociale et relationnelle et l'éducation, à partir d'interviews semi-structurées en présence des patients et/ou conjoints et/ou fratrie. Dans cette étude, les traits tels qu'une diminution d'empathie dès l'adolescence, une psychorigidité avec des « schémas comportementaux fixes », une tendance à s'isoler et à se désintéresser des autres étaient plus représentés chez les porteurs d'expansion (Gossink et al., 2022). Si ces résultats suggèrent une vulnérabilité

psychopathologique et des dysfonctionnements cérébraux lents, survenant bien avant le début des troubles dégénératifs chez les porteurs de mutation, il faut néanmoins souligner que cette étude n'est basée que sur un nombre réduit de porteurs (n=20) et de contrôles non porteurs (n=23), évalués de façon rétrospective, avec des informants de parenté variable, et qu'elle nécessite donc d'être validée d'une façon plus large, robuste, et par des enquêtes spécifiques.

1.3.3 Les autres gènes responsables de DLFT et SLA

Le gène *MAPT*, localisé sur le chromosome 17, n'est responsable que d'environ 10 % des formes familiales de DLFT (Hutton et al., 1998). La fréquence des mutations de ce gène est relativement faible en France, alors qu'elle est comparable à celle des gènes *GRN* et *C9orf72* dans le nord de l'Europe, en raison d'un effet fondateur (Pickering-Brown et al., 2004). Selon leur localisation dans le gène, les mutations de *MAPT* peuvent modifier le ratio TAU 3R/4R ou diminuer sa capacité de liaison aux microtubules, les deux phénomènes aboutissant à l'accumulation de la protéine TAU sous forme hyperphosphorylée (Hutton et al., 1998 ; van Swieten et Spillantini, 2007). Les caractéristiques anatomopathologiques peuvent être celles d'une DLFT-TAU 3R, d'une forme 4R ou d'une forme mixte, dont les lésions sont superposables aux formes sporadiques (Forrest et al., 2018). Dans cette forme, l'âge de début est précoce, les premiers symptômes survenant aux alentours de 50 ans (Moore et al., 2020a). Le phénotype clinique le plus fréquemment associé est celui d'une DFTc. Moins souvent, la maladie se manifeste par un tableau de PSP ou un SCB (van Swieten et Spillantini, 2007). Les formes pures d'APP sémantiques ou non-fluents sont rares (Henz et al., 2015), même si des troubles sémantiques sont fréquemment associés aux troubles comportementaux dans les formes DFTc de la maladie (Pickering-Brown et al., 2008).

Les causes génétiques plus rares de DLFT avec ou sans SLA sont brièvement listées dans le tableau présenté en annexe 2 et sont présentées de façon plus détaillée dans un article de revue joint à cette thèse (article de revue 1, Sellami et al., 2020a). Il est intéressant de souligner que des APP sémantiques et non-fluents sont des phénotypes relativement souvent associés aux mutations des gènes *TBKI* et *TARDBP* (Caroppo et al., 2015a ; Caroppo et al., 2016 ; Swift et al., 2021a). En pratique clinique, l'ensemble de ces gènes peuvent être analysés dans un cadre de diagnostic, avec une stratégie qui repose sur le dosage plasmatique de la progranuline et l'analyse du gène *C9orf72* (non détectable par séquençage) proposés à tous les

patients, ensuite complétée par une analyse par séquençage d'un panel de gènes de DFT/SLA dans les formes familiales ou précoces (avant 55 ans).

1.4 Neuroimagerie des DLFT

Les examens de neuroimagerie, en particulier les séquences volumétriques T1-pondérées d'IRM, sont complémentaires du diagnostic clinique de DLFT, permettant de mettre en évidence des profils d'atteinte corticale fortement évocateurs. Le TEP-FDG démontre une diminution du métabolisme cérébral du glucose, qui peut être détectée plus précocement que les anomalies à l'imagerie morphologique, reflétant le dysfonctionnement neuronal et synaptique qui précède la perte de volume cérébral (Kerklaan et al., 2014). Les DLFT sont caractérisées par un profil d'atrophie ou de dysfonctionnement métabolique qui touche les lobes frontaux et temporaux antéro-latéraux de façon relativement circonscrite au début (Rosen et al., 2002 ; Whitwell et al., 2012). Cette atteinte peut cependant varier d'un patient à un autre, comme le montre une étude portant sur 66 sujets ayant une DLFTc définissant quatre profils selon la prédominance de l'atrophie au niveau des régions frontales, des régions temporales, fronto-temporales ou fronto-temporo-pariétales (Whitwell et al., 2009). Des retentissements corticaux distincts corrélient avec des manifestations comportementales différentes. Ainsi, l'atteinte prédomine dans les régions préfrontales médiales chez les patients présentant un profil comportemental apathique (Massimo et al., 2015), alors qu'elle touche préférentiellement les régions orbitofrontales et temporo-limbiques lorsque la désinhibition comportementale est au premier plan (Snowden et al., 2001 ; Santamaría-García et al., 2016). Dans les APP, l'hétérogénéité du retentissement du réseau langagier reflète la présentation clinique de chaque variant, avec une très forte concordance anatomo-clinique (Gorno-Tempini et al., 2011 ; Routier et al., 2018).

Les formes génétiques de DLFT présentent des caractéristiques de neuroimagerie propres à chaque génotype. Chez les patients avec mutation du gène *GRN*, l'atteinte corticale prédomine au niveau des aires frontotemporales et insulaires, souvent de façon nettement asymétrique, et s'étend rapidement aux régions pariétales et postérieures (Whitwell et al., 2012). Une atrophie sous-corticale, principalement striatale est associée (Whitwell et al., 2012). La présence d'hypersignaux de la substance blanche détectables en séquences T2-pondérées et FLAIR, considérées comme reflétant l'atteinte dégénérative axonale, est fréquente, surtout dans les phases avancées (Caroppo et al., 2014 ; Ameur et al., 2016 ; Sudre et al., 2019). Plusieurs études de connectivité fonctionnelle ont investigué les réseaux neuronaux impliqués dans la pathologie *GRN*, révélant des altérations des mesures de connectivité locale s'étendant du cortex préfrontal aux aires associatives pariétales postérieures (Premi et al., 2014). L'atteinte

précoce du cortex pariétal dans la pathologie *GRN* est renforcée par une étude évaluant la connectivité structurelle interhémisphérique, démontrant que la perte maximale de cohérence interhémisphérique touche d'abord les régions pariétales pour concerner ensuite d'une façon plus diffuse la plupart des nœuds frontotemporaux (Gazzina et al., 2022). Le thalamus est atteint d'une façon discrète et relativement tardive, touchant surtout le noyau dorsomédian et latérodorsal (Bocchetta et al., 2020).

Les DLFT associées aux expansions du gène *C9orf72* se caractérisent, elles, par une atteinte corticale étendue touchant en premier lieu le cortex frontal et les régions temporales latérales bilatéralement et, dans une moindre mesure, les régions associatives postérieures (Whitwell et al., 2012 ; Rohrer et al., 2015). L'atteinte thalamique est particulièrement précoce dans la pathologie *C9orf72* et généralisée à tous les noyaux, avec un effet qui prédomine au niveau du pulvinar, alors que cette structure est généralement épargnée dans les autres formes génétiques (Bocchetta et al., 2020). L'atrophie touche également les hippocampes et le cervelet, surtout au niveau de son lobe postérieur et du noyau dentelé (Whitwell et al., 2012 ; Bocchetta et al., 2020). Le profil d'atrophie chez les patients porteurs de mutations du gène *MAPT* est plutôt symétrique, touchant davantage le cortex préfrontal orbital et mésial, ainsi que les régions temporales internes et antérieures, et le striatum (Whitwell et al., 2012 ; Rohrer et al., 2015).

1.5 Les enjeux de la recherche dans les formes génétiques de DLFT, à l'ère des premiers essais thérapeutiques

Comme nous l'avons montré précédemment, les trois dernières décennies ont connu des avancées cliniques et scientifiques considérables dans le domaine des DLFT, avec la définition des critères diagnostiques actuellement utilisés, l'identification des protéinopathies sous-jacentes, la découverte de leurs causes génétiques, permettant une meilleure compréhension de leurs mécanismes physiopathologiques. Cependant, dans le même temps, les avancées dans le domaine de la thérapeutique sont longtemps restées modestes. Aujourd'hui, il n'existe toujours pas de traitement curatif dans ces affections. La prise en charge repose essentiellement sur des interventions pharmacologiques (basées, entre autres, sur les antidépresseurs sérotoninergiques) et non-pharmacologiques (stimulation cognitive, ergothérapie etc.) visant à limiter la sévérité des symptômes, en particulier celle des troubles comportementaux (pour une revue : Khoury et al., 2021).

La découverte des principales formes génétiques de DLFT a néanmoins permis d'identifier des mécanismes physiopathologiques susceptibles d'être modifiés par des interventions ciblées, dans le but de ralentir ou d'arrêter le processus lésionnel. Comme nous l'avons mentionné dans le chapitre dédié, les mutations du gène *GRN* entraînent une perte de fonction partielle de la progranuline. Les stratégies thérapeutiques en cours de développement visent à restaurer l'expression de la progranuline à des niveaux proches des valeurs physiologiques (Arrant et al., 2017 ; Demarais et al., 2019). Le premier essai (FRM-0334) a évalué l'effet d'un inhibiteur d'une histone désacétylase. Même s'il n'a pas montré de bénéfice, cet essai a ouvert la voie des premières thérapeutiques dans cette forme génétique (Ljubenkov et al., 2021). Actuellement, plusieurs essais de phases 1 à 3 sont en cours et certains sont cités ici à titre d'exemple. Ils reposent principalement sur des stratégies de thérapie génique visant à supplémer une copie fonctionnelle du gène *GRN* (PR006/PRV-FTD101, phase 1/2 ; PBFT02, phase 1/2), sur l'administration d'une forme recombinante de la progranuline (DNL593, Phase 1/2) ou sur l'administration d'un anticorps monoclonal anti-sortiline qui bloque le récepteur lysosomal de la progranuline pour en limiter la dégradation (AL001, Phase 3).

D'autres approches sont en développement dans les formes génétiques *C9orf72*. En particulier, certaines sont basées sur l'administration d'oligonucléotides anti-sens (*antisense*

oligonucleotides, ASO). Brièvement, les ASOs sont des séquences d'ARN synthétisées qui peuvent se lier par complémentarité à un ARN messager cible, entraînant la dégradation ou la répression de ce dernier. Les ASOs ont montré leur efficacité dans l'atrophie musculaire spinale (Finkel et al., 2017) et sont aussi évalués dans d'autres maladies à expansions, comme la maladie de Huntington (Tabrizi et al., 2019). Un essai de phase 1/2 est actuellement en cours chez les patients porteurs d'expansion du gène *C9orf72* atteints de SLA ou de DFT (WVE-004). L'essai de phase 1 BIIB078 (IONIS-C9Rx) a été récemment interrompu pour manque d'efficacité. Des résultats précliniques encourageants ont été publiés pour un autre ASOs (afinersen), ayant fait l'objet d'une étude pilote sur un seul patient (Tran et al., 2022). Des approches alternatives font également l'objet d'essais de phase 2 (TPN-101 et LAM-002A).

La recherche thérapeutique est moins avancée dans les formes génétiques plus rares et dans les formes non-génétiques. De nombreuses stratégies ciblent la protéinopathie TAU dans la MA, avec des champs d'application envisagés dans les DLFT-TAU. Ces approches incluent inhibition de l'expression, des modifications post-traductionnelles, de l'agrégation, immunothérapie active et passive, mais aucune n'a fait preuve d'efficacité jusqu'à présent, dans les DLFT associées aux mutations du gène *MAPT* ou dans les DLFT-TAU sporadiques comme les PSP (essais LMT/TRx0237, BIIB092 et ABBV-8E12) (Imbimbo et al., 2021). Dans les formes non génétiques, un essai de phase 1 (Veri-T) est actuellement en cours avec l'inhibiteur de la myéloperoxydase verdiperstat, ciblant la réponse inflammatoire associée à la pathologie TDP-43.

1.5.1 La phase présymptomatique des DLFT

1.5.1.1 Le modèle des formes génétiques et mise au point sur les définitions actuelles

Le développement de thérapeutiques ciblant les formes génétiques laisse entrevoir la possibilité d'intervenir précocement chez les sujets porteurs de mutation, durant la phase présymptomatique de la maladie. Cette phase, correspondant au stade lésionnel le plus précoce et le moins sévère, représente donc la meilleure « fenêtre thérapeutique » de la maladie. Le modèle conceptuel de la MA, en particulier dans ses formes monogéniques, a largement contribué à définir la notion d'un stade présymptomatique de cette maladie, caractérisé par l'accumulation silencieuse et progressive de lésions pathologiques, jusqu'à un stade prodromal

de trouble cognitif léger (Bateman et al., 2012 ; Selkoe et Hardy, 2016 ; Dubois et al., 2016 ; Petersen et al., 2018), et à définir la séquence des modifications des biomarqueurs précédant la maladie clinique. La cascade des marqueurs dans la MA débute par une diminution du peptide A β 42 dans le LCR environ 25 ans avant les symptômes, suivie par la détection des modifications des PET amyloïde et FDG, avant que les anomalies structurelles (en particulier une atrophie hippocampique) et les premiers changements cognitifs n'apparaissent, environ 2-3 ans avant le début clinique (McDade et al., 2018).

Les études de la phase présymptomatique des DLFT et de la SLA génétiques sont plus récentes, et les modifications des marqueurs durant cette phase, et à proximité de la conversion clinique, sont encore largement méconnues. Au cours des dernières années, plusieurs consortia ont étudié la phase présymptomatique des formes génétiques de DLFT/SLA, en particulier chez les porteurs asymptomatiques issus des familles concernées par *GRN* et *C9orf72*, les deux formes génétiques les plus fréquentes. On peut citer, entre autres, les travaux du consortium Européen et Canadien GENFI (*Genetic Frontotemporal Initiative*), ceux des consortia nord-américains ALLFTD et Pre-fALS (*Presymptomatic familial ALS*) (Benatar et Wu, 2012). En France, deux études impliquant plusieurs centres experts nationaux ont les mêmes objectifs. Ces deux études ont permis d'inclure et de suivre dans le temps environ 200 participants à risque d'être porteurs de mutations du gène *GRN* (suivis depuis 2010 dans le cadre du PHRC national Predict-PGRN) et d'expansions du gène *C9orf72* (suivis depuis 2015 dans le cadre du projet ANR-PRTS PREV-DEMALS). L'objectif commun de ces initiatives est de mieux caractériser la phase présymptomatique et d'identifier des biomarqueurs utiles, en particulier, pour la mise en place et le suivi des essais thérapeutiques.

Ces études soulèvent la question de la définition des différents stades qui constituent la phase présymptomatique et de leurs frontières. Des recommandations ont été publiées récemment pour utiliser une nomenclature consensuelle distinguant trois stades en fonction de la proximité du début clinique (Figure 4) (Benussi et al., 2021 ; Benatar et al., 2022). Le stade « *no disease* » précède l'accumulation de toute lésion pathologique. Il ne peut être démontré formellement que ce stade existe bien dans toutes les formes génétiques en l'absence d'un traceur/marqueur lésion-spécifique actuellement disponible dans les DLFT (Benussi et al., 2021). Le stade « préclinique » désigne la période suivant le début du processus neurodégénératif, et précédant l'apparition des premiers signes de la maladie. Le stade « prodromal » débute quand les premiers signes d'atteinte cognitive, comportementale ou

motrice se manifestent, jusqu'à ce que l'expression clinique ne remplisse les critères de la maladie. Le stade « clinique » est défini sur les critères diagnostiques de DFTvc, APP, SLA ou d'autres syndromes associés. Une adaptation est proposée chez les patients porteurs d'une mutation présentant des symptômes qui ne répondent pas strictement aux critères établis mais ont un impact significatif sur les activités sociales/professionnelles sans perte d'autonomie (par exemple, en raison de déficits langagiers ou d'un comportement socialement inapproprié), ou avec perte d'autonomie (Benussi et al., 2021). Une synthèse des concepts actuels au sujet de la phase présymptomatique dans les DLFT/SLA génétiques a fait l'objet d'un article de revue de la littérature joint à cette thèse (article de revue 2, Saracino et al., 2022).

Actuellement, l'échelle de référence utilisée de façon consensuelle pour définir les stades de la DLFT, de sa phase présymptomatique à sa phase clinique, est la CDR+NACC FTLD (*Clinical Dementia Rating scale plus National Alzheimer's Disease Coordinating Center for Frontotemporal Lobar Degeneration*) (Miyagawa et al., 2020a ; Peakman et al., 2022). Cette version modifiée de la CDR comporte un item comportemental et un item langagier adaptés pour l'évaluation des patients atteints de DLFT. Globalement, cette échelle mesure l'impact de la maladie sur différents domaines dont la mémoire, l'orientation, le langage, les soins personnels, les sorties et le comportement, générant un score global de 0 à 3 qui reflète la gravité clinique. Par consensus, les individus ayant un score global de la CDR+NACC FTLD à 0 sont considérés au stade préclinique, ceux au stade prodromal ont un score global à 0,5. La phénoconversion est définie par un score CDR+NACC FTLD supérieur ou égal à 1 (Miyagawa et al., 2020b ; Peakman et al., 2022).

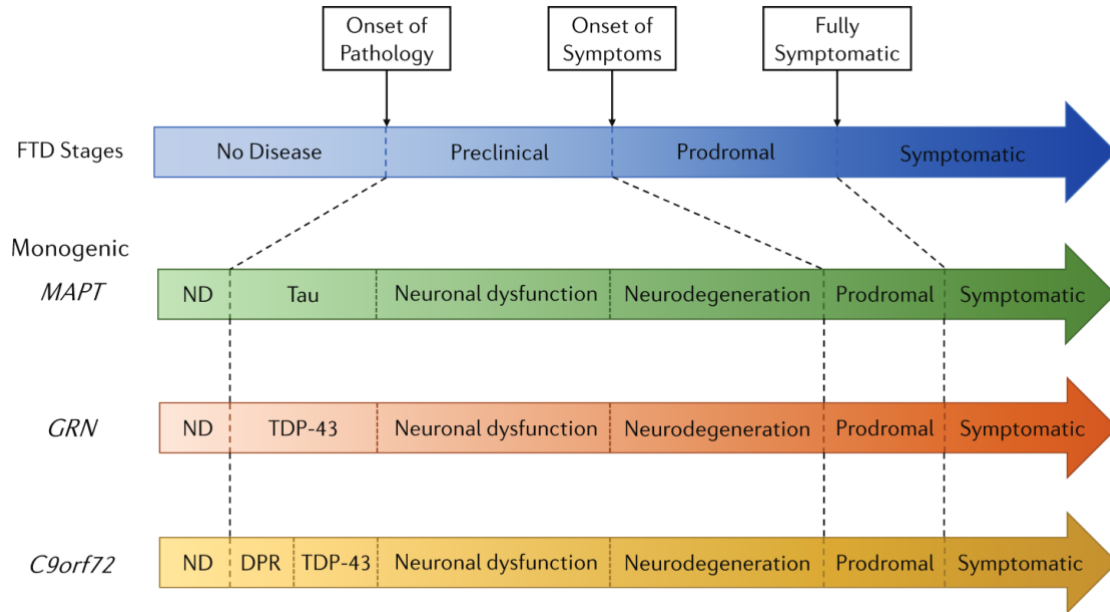


Figure 4. Modèle conceptuel de la répartition en stades de la phase présymptomatique des DLFT génétiques
 DPR : inclusions de dipeptides répétés ; ND : *no disease*, absence de lésions pathologiques.
Adapté de Benussi et al., 2021.

1.5.1.2 Le stade prodromal

Définir le stade prodromal de la maladie reste un challenge difficile à ce jour (Staffaroni et al., 2020a ; Tavares et al., 2020 ; Malpetti et al., 2021a). Selon les recommandations citées précédemment, il est défini par « la survenue de modifications comportementales subtiles, de changements graduels de la cognition sociale, des fonctions exécutives ou du langage de sévérité modérée, permettant une préservation globale de l'autonomie dans la vie quotidienne, même si un impact léger sur la qualité des relations interpersonnelles ou dans l'exécution de tâches complexes est toléré », correspondant à un score global de CDR+NACC FTLD à 0,5 (Benussi et al., 2021). Néanmoins, la plupart des symptômes et déficits cognitifs observés au début de la DFTc sont peu spécifiques, en particulier quand ils surviennent de façon isolée, et sont variables d'un patient à l'autre, ou selon le génotype, rendant cette définition relativement imprécise. Ainsi, dans les formes *GRN*, les premiers dysfonctionnements cognitifs portent sur l'attention, la vitesse de traitement de l'information, les fonctions exécutives et les fluences verbales, et sont détectables 2 à 4 ans avant que la symptomatologie ne remplisse les critères d'une DLFT (Jiskoot et al., 2018 ; Panman et al., 2021). Chez les porteurs d'expansions *C9orf72*, les modifications cognitives précoces sont détectées 5 à 10 ans avant l'âge de début

estimé et portent sur la cognition sociale, l'inhibition cognitive, les connaissances sémantiques et la mémoire épisodique verbale, dans ses composantes de rappel immédiat et rappel libre différé (Russell et al., 2020 ; Montembeault et al., 2020 ; Moore et al., 2020b ; Poos et al., 2021). Sur la base de ces observations, des échelles composites spécifiques à chacune des formes génétiques principales, regroupant les tests cognitifs les plus pertinents, ont été élaborées pour évaluer le stade prodromal de façon plus fine (Poos et al., 2022).

Des critères plus précis ont été récemment proposés par le consortium ALLFTD pour définir la « DFTc prodromale » basés sur l'étude de 72 porteurs de mutations au stade prodromal (Barker et al., 2022). Ce groupe propose le terme de « déficit cognitif et/ou comportemental léger » pour définir ce stade (*mild behavioural and/or cognitive impairment in bvFTD*, MBCI-FTD) par analogie avec le terme usuel de « déficit cognitif léger » (« *mild cognitive impairment* », MCI) utilisé dans la MA. Les critères, proposés pour la recherche, sont relativement calqués sur les critères de diagnostic de Rascovsky et collaborateurs (2011), incluant des critères principaux (une apathie sans dysphorie majeure, une désinhibition comportementale, une irritabilité, une perte d'empathie, des comportements répétitifs simples ou complexes, une jovialité excessive et des changements des conduites alimentaires) et des critères additionnels (déficit des fonctions exécutives, de la dénomination, la cognition sociale et la métacognition) (Barker et al., 2022). Trois critères principaux, ou deux critères principaux et un critère additionnel sont requis pour un diagnostic de MBCI-FTD (Figure 5).

Le stade prodromal de la SLA est, lui, défini par des plaintes motrices légères (crampes, fatigue précoce) et/ou des signes mineurs à l'examen neurologique (fasciculations, modifications des réflexes, mais sans faiblesse musculaire décelable) (Benatar et al., 2022). Des signes isolés de dénervation à l'EMG reflétant une souffrance des neurones moteurs inférieurs, et une augmentation de l'excitabilité corticale à la stimulation magnétique transcranienne liée à l'atteinte des neurones moteurs supérieurs, peuvent également supporter un dysfonctionnement motoneuronal au stade prodromal (Geevasinga et al., 2015 ; Benatar et al., 2022 ; Querin et al., 2022). La communauté SLA utilise le terme de « phénotransition » pour désigner le passage du stade préclinique au stade prodromal de SLA (Benatar et al., 2022). Le terme de « phénoconversion » est, lui, utilisé pour désigner la phase de transition entre le stade prodromal et la phase clinique avérée (selon les critères internationaux). Globalement, le stade prodromal correspond donc à une phase transitionnelle de trouble cognitif, comportemental

et/ou moteur léger, avant que la condition pathologique ne réponde aux critères d'un syndrome clinique défini.

Definition of MSCI-FTD
<p>A clinical syndrome defined by the presence of persistent and progressive decline in behavior and/or cognition for more than six months based on observation or history provided by knowledgeable informant.</p> <p>1. Must be present to diagnose MSCI-FTD</p> <ul style="list-style-type: none">A. Concern regarding behavioural and/or cognitive change from previous functioning, per informant, clinician, or patientB. Preserved instrumental activities of daily living (unless due to physical impairment, e.g. motor neuron disease or parkinsonism)C. > 18 years old <p>2. Possible MSCI-FTD</p> <p>At least three of the following core features (A–G) are sufficient, and must represent a change from previous behaviour, to diagnose possible MSCI-FTD</p> <ul style="list-style-type: none">A. Apathy without moderate-severe dysphoriaB. Behavioural disinhibitionC. Irritability or agitationD. Loss of empathy or sympathyE. Repetitive behaviours (either E1 or E2)<ul style="list-style-type: none">E1. Simple: Aberrant motor behaviour, or restlessness (e.g. pacing, fidgeting, tapping)E2. Complex: Perseverative, compulsive or ritualistic behaviour (e.g. rigidity, rituals, hoarding)F. Joviality or gregariousnessG. Appetite changes/hyperorality <p>If only two of the above core features (A–G) are present, then at least one of the following (H or I or J) must also be present to diagnose Possible MSCI-FTD:</p> <ul style="list-style-type: none">H. Neuropsychological deficits in context of intact or relatively preserved time/place orientation and visuospatial skills (one of H1–H2 must be present)<ul style="list-style-type: none">H1. Clinical impairment or clinically significant decline on executive tasks (e.g. verbal generation, set-shifting, etc.)H2. Clinical impairment or clinically significant decline on naming testsI. Reduced insight for at least one aspect of behavioural or cognitive changeJ. Impairments on standardized measures of social cognition (one of J1–J2 must be present)<ul style="list-style-type: none">J1. Reduced understanding or awareness of social expectationsJ2. Low socioemotional sensitivity <p>3. Probable MSCI-FTD</p> <p>Both of the following (A–B) must be present to diagnose Probable MSCI-FTD:</p> <ul style="list-style-type: none">A. Meets criteria for Possible MSCI-FTDB. Genetic or biomarker evidence of FTLT (at least one of B1–B3 must be present)<ul style="list-style-type: none">B1. Presence of a known pathogenic mutationB2. Imaging evidence of FTLT<ul style="list-style-type: none">B2.1 Frontal and/or anterior temporal atrophy on MRI or CTB2.2 Frontal and/or anterior temporal hypoperfusion or hypometabolism on PET or SPECTB3. Other plasma/CSF biomarkers indicative of FTLT pathology <p>4. Exclusionary criteria for MSCI-FTD</p> <ul style="list-style-type: none">A. History of sudden onset or other medical conditions severe enough to account for symptoms (e.g. cerebrovascular, infectious, toxic, inflammatory, or metabolic disorders, traumatic brain injury or brain tumour)B. Plasma or CSF or molecular imaging biomarkers more consistent with Alzheimer's disease than FTLTC. Meets diagnostic criteria for Probable bvFTD

Figure 5. Critères de recherche proposés pour le trouble cognitif et / ou comportemental léger de la démence frontotemporale
Adapté de Barker et al., 2022.

1.5.2 Quels biomarqueurs pour suivre la trajectoire du processus pathologique à la phase présymptomatique de la DLFT ?

Un biomarqueur est une caractéristique observable et mesurable dont les niveaux servent d'indicateurs objectifs de différents états physiologiques ou pathologiques, ou sont associés à la réponse aux interventions thérapeutiques (Hendrix et al., 2021). Depuis quelques années, de nombreuses études cherchent à identifier des marqueurs biologiques et de

neuroimagerie, à définir la cascade de ces marqueurs, pour suivre la progression des formes génétiques de DLFT de la phase présymptomatique à la phase clinique, et définir des critères de mise en place et de suivi des essais thérapeutiques (Swift et al., 2021b ; Querin et al., 2022). Nous citons ici quelques-unes de ces études et quelques marqueurs d'intérêt.

1.5.2.1 Les neurofilaments dans les biofluides

Parmi les différents marqueurs biologiques étudiés, le taux des neurofilaments dans les fluides, bien que non spécifique, s'avère particulièrement prometteur. Les neurofilaments sont des protéines structurales constituant le cytosquelette et des axones, qui se composent de trois sous-unités principales : les chaînes lourdes (NfH), intermédiaires et légères (NfL, *neurofilament light chain*). Leur relargage dans le LCR, puis dans le sang, est consécutif à une perte neuronale. Au cours des dernières années, de nombreuses études ont démontré que le taux des NfL, et de façon moins constante des NfH phosphorylés (pNfH), augmente dans le LCR dans nombreuses affections neurologiques, notamment dans les maladies neurodégénératives (Khalil et al., 2018 ; Bridel et al., 2019 ; Gaetani et al., 2019). Le développement récent de techniques de dosage en ELISA digitale de haute sensibilité comme le single molecule array (SiMoA®) rend possible l'analyse moins invasive des taux de NfL et pNfH dans le sérum et le plasma, où leurs concentrations sont sensiblement inférieures, mais fortement corrélées, à celles du LCR (Meeter et al., 2016 ; Alirezai et al., 2020). Dans le contexte des DLFT et SLA, les NfL plasmatiques représentent un biomarqueur utile pour suivre la progression de la maladie. Les niveaux sont plus élevés chez les patients que chez les témoins sains (Meeter et al., 2016 ; Weydt et al., 2016). Dans les formes génétiques, en particulier dans les formes *GRN* et *C9orf72*, leurs taux augmentent avec la progression de la maladie, des niveaux plus élevés prédisant une survie plus courte et un phénotype plus sévère (Gendron et al., 2017a ; Benatar et al., 2019 ; Wilke et al., 2022). En outre, à la phase présymptomatique, les taux de NfL augmentent 2 à 5 ans avant la phénoconversion (Meeter et al., 2016 ; Benatar et al., 2019 ; van der Ende et al., 2019 ; Rojas et al., 2021), avec une élévation plus rapide 12 mois environ avant l'apparition des symptômes (Poesen et Van Damme, 2019). Toutes ces caractéristiques font des NfL un biomarqueur fiable, utile pour la stratification des patients, pour l'identification des sujets proches de la phénoconversion et pour le suivi de la réponse au traitement dans les essais cliniques. Néanmoins, son utilisation reste actuellement limitée dans les DLFT/SLA, en particulier à cause de l'absence de seuils pathologiques clairement définis, consensuels, pour l'interprétation des taux mesurés dans ces maladies. Cela est en partie dû au fait que la majorité

des études portent sur des populations aux caractéristiques hétérogènes. L'étude de Rojas et collaborateurs (2021) analyse ainsi les taux des NfL chez 385 porteurs de mutations *GRN*, *C9orf72* et *MAPT* issus pour moitié du consortium ALLFTD, et pour moitié du consortium GENFI. Le seuil optimal pour stratifier les porteurs par rapport à leur proximité de la phénoconversion diffère significativement entre les deux cohortes (respectivement 13,6 et 19,8 pg/mL) (Rojas et al., 2021). Cette discordance importante pourrait être due à des questions méthodologiques, mais est aussi très probablement liée à l'hétérogénéité des deux populations comparées dans cette étude (en termes de proportion des différentes formes génétiques, et d'âge) soulignant la nécessité de stratifier les porteurs de mutations selon le génotype et selon l'âge, sur la base de seuils définis de façon consensuelle.

1.5.2.2 Les autres marqueurs d'intérêt dans les biofluides

D'autres biomarqueurs fluidiques, reflets de la fonction synaptique (pentaxine neuronale 2, NPTX2), de la cascade inflammatoire ou de l'activation astrogliale (protéine gliale fibrillaire acide, GFAP) semblent également se modifier durant la phase présymptomatique. Ainsi, une diminution de la NPTX2 dans le LCR, une augmentation de la GFAP circulante et des protéines du complément C3b et C1q dans le LCR semblent survenir séquentiellement, à proximité de la conversion clinique (Heller et al., 2020 ; van der Ende et al., 2020 ; Swift et al., 2021b). Une étude récente du consortium GENFI dans une cohorte de près de 400 individus porteurs de mutations *GRN*, *C9orf72* ou *MAPT* montre que, parmi les biomarqueurs cités, le premier qui se modifie est le taux de NPTX2, suivi des taux de NfL, puis de pNfH, de GFAP et enfin des C3b et C1q, et ce en particulier chez les porteurs de mutations *GRN* (van der Ende et al., 2021).

Comme cela a été mentionné, les expansions GGGGCC du gène *C9orf72* entraînent la production pathologique et l'accumulation cytoplasmique de peptides DPR dont il existe 5 espèces (dépendant du cadre de lecture de la traduction non ATG dépendante, et du brin sens ou du brin antisens). Parmi celles-ci, les poly(GP) sont abondamment exprimés dans le tissu cérébral des patients, et leur sévérité est corrélée à celle d'autres marqueurs lésionnels, tels que la densité des *foci* ARNs. De façon intéressante, les poly(GP) sont dosables dans le LCR des patients (Lehmer et al., 2017 ; Gendron et al., 2017b ; Meeter et al., 2018 ; Wilson et al., 2022), et leur dosage en SiMoA montre une excellente spécificité (100%) et sensibilité (100%) (Wilson et al., 2022). Ils sont également détectables dans le LCR au stade présymptomatique, même en l'absence de tout autre marqueur de dégénérescence, constituant potentiellement un

marqueur précoce et spécifique de cette forme génétique (Lehmer et al., 2017). Enfin, mentionnons que notre équipe, en collaboration avec les équipes ARAMIS (O. Colliot, ICM) et DYLISS (E. Becker, INRIA Rennes) a identifié quatre micro-ARNs (miR-34a-5p, miR345-5p, miR-200c-3p et miR-10a-3p) constituant une « signature » plasmatique chez les porteurs d'expansion *C9orf72*. Leur profil d'expression est dynamiquement altéré au cours de la progression, de la phase présymptomatique à la phase clinique, apportant un outil potentiel supplémentaire de prédiction de la progression et de la proximité de la phénoconversion (Kmetzsch et al., 2020). Les principaux biomarqueurs fluidiques étudiés durant la phase présymptomatique sont récapitulés dans le Tableau 1.

Biomarqueur	Relevance	Références
Protéines poly(GP) (LCR)	Élevées dès les premiers stades de la pathologie <i>C9orf72</i>	Lehmer et al., 2017 Meeter et al., 2018
NfL et NfH (LCR et sérum/plasma)	Augmentation dans le stade prodromal, dans les ~5 ans avant la phénoconversion	Benatar et al., 2019 van der Ende et al., 2019 Rojas et al., 2021 Saracino et al., 2021c Wilke et al., 2022
NPTX2 et NPTXR (LCR)	Diminution dans la phase présymptomatique tardive	van der Ende et al., 2020 van der Ende et al., 2021
GFAP (plasma)	Augmentation dans le stade prodromal et clinique de la pathologie <i>GRN</i>	Heller et al., 2020 van der Ende et al., 2021
Protéines du complément C3b et C1q (plasma)	Augmentation chez les patients <i>GRN</i>	van der Ende et al., 2021
sTREM2 (LCR)	Augmentation chez les patients <i>GRN</i>	Woollacott et al., 2018
YKL-40 (LCR)	Augmentation chez les patients <i>GRN</i>	Woollacott et al., 2020
CHIT1 (LCR)	Augmentation chez les patients <i>C9orf72</i> et <i>GRN</i>	Barschke et al., 2020
Cytokines (IL-1, IL-6, IL-8, IL-11, IL-12, IL-15, TNF- α) (principalement LCR)	Profil altéré à la phase clinique de la pathologie <i>GRN</i>	Swift et al., 2021
Micro-ARNs (plasma)	Profil dynamiquement altéré chez les porteurs <i>C9orf72</i> , en particulier dans le stade prodromal	Kmetzsch et al., 2020

Tableau 1. Principaux biomarqueurs fluidiques étudiés dans les DLFT génétiques
 CHIT1 : chitotriosidase 1 ; GFAP : protéine gliale fibrillaire acide ; NfH : chaîne lourde des neurofilaments ;
 NfL : chaîne légère des neurofilaments ; NPTX2 : pentraxine neuronale type 2 ; NPTXR : récepteur de la
 pentraxine neuronale ; sTREM2 : *soluble triggering receptor expressed on myeloid cells 2* ; YKL-40 : *chitinase
 3-like 1 glycoprotein*.

1.5.2.3 Les marqueurs de neuroimagerie structurale et microstructurale

Plusieurs travaux basés sur la neuroimagerie structurale et microstructurale ont étudié les atteintes neuroanatomiques observables au cours du stade préclinique des DLFT. Chez les porteurs de mutations du gène *GRN*, la perte de volume cortical survient, à l'échelle de groupe, entre 15 et 10 ans avant l'âge estimé de début de la maladie. Elle touche d'une façon asymétrique les régions insulaires, temporales externes, temporo-pariétales et frontales supérieures (Rohrer et al., 2015). Les porteurs à la phase présymptomatique présentent un déclin accéléré de l'épaisseur corticale au niveau du gyrus temporal supérieur et moyen, incluant le sillon temporal supérieur (Moreno et al., 2013 ; Borrego-Ecjia et al., 2021). Ces résultats, initialement obtenus dans une étude restreinte de 13 porteurs (Moreno et al., 2013), ont été confirmés dans une étude de réplique sur 100 porteurs de la cohorte GENFI (Borrego-Ecjia et al., 2021), retrouvant également un effet significatif au niveau du gyrus frontal supérieur. Des altérations tractographiques au niveau du faisceau unciné et des radiations thalamiques précèdent d'environ 2 ans les changements au niveau de la substance grise (Panman et al., 2021).

Chez les porteurs d'expansion *C9orf72*, des modifications du volume cortical sont identifiables en IRM structurale, 25 à 20 ans avant le début estimé de maladie. Elles concernent principalement les aires frontales, temporo-insulaires, les régions associatives pariéto-temporales et les hippocampes (Rohrer et al., 2015 ; Lee et al., 2017b ; Bertrand et al., 2018 ; Wen et al., 2018 ; Panman et al., 2019 ; Le Blanc et al., 2020). Une atteinte sous-corticale, notamment thalamique en particulier au niveau du pulvinar et des noyaux latéraux, est également observée précocement dans les formes *C9orf72* (Bertrand et al., 2018 ; Bocchetta et al., 2021). Malgré cette distribution large du profil d'atrophie, une étude basée sur le suivi longitudinal de 83 porteurs à la phase présymptomatique de la cohorte GENFI ne retrouvait pas de progression significative du déclin de l'épaisseur corticale comparativement aux contrôles (Le Blanc et al., 2020). La caractérisation microstructurale de la substance blanche en imagerie à tension de diffusion (DTI) montre une atteinte également précoce, contemporaine de l'atrophie corticale, touchant les faisceaux fronto-temporaux, cortico-spinaux, les radiations thalamiques et le corps calleux (Lee et al., 2017b ; Bertrand et al., 2018 ; Wen et al., 2018 ; Panman et al., 2019). Là encore, ces altérations n'ont pas montré de progression significative sur 2 ans de suivi, même si l'étude en question était basée uniquement sur 12 porteurs (Panman et al., 2019).

Au niveau médullaire, les porteurs d'expansion *C9orf72* présentent une atrophie de la substance blanche au niveau cervical, et des altérations structurelles au niveau des faisceaux cortico-spinaux chez les sujets présymptomatiques de plus de 40 ans. Ces observations suggèrent la possibilité d'une détection précoce de la dégénérescence motoneuronale, avant toute altération électromyographique (Geevasinga et al., 2015 ; Querin et al., 2019).

1.5.2.4 Les altérations précoces en neuroimagerie fonctionnelle

Pour aller plus loin, un certain nombre d'études en IRM fonctionnelle (IRMf) ont évalué si ces altérations structurelles précoces, liées au processus dégénératif, sont accompagnées voire précédées par des remaniements de la connectivité fonctionnelle entre les réseaux qu'elles constituent. Une altération des mesures de connectivité locale dans les régions pariétales et une augmentation compensatrice au niveau préfrontal sont notées durant la phase présymptomatique de la pathologie *GRN*, précédant une perte de connectivité touchant l'ensemble des aires fronto-temporo-pariétales à la phase clinique (Premi et al., 2014). Une analyse d'IRMf de repos chez 15 porteurs d'expansion *C9orf72* a mis en évidence une altération du réseau de saillance et de la connectivité au niveau du pulvinar (Lee et al., 2017b). D'autres auteurs ont démontré une altération du réseau somato-moteur à la phase présymptomatique (Waugh et al., 2021), avec une topographie comparable à ce qui est observé chez les porteurs présentant une SLA (Agosta et al., 2017).

1.5.2.5 Les marqueurs en imagerie métabolique et de perfusion

Les changements de la perfusion et du métabolisme cérébral, explorés respectivement par des séquences ASL (*arterial spin labeling*) en IRM ou en TEP-FDG sont aussi observés durant la phase préclinique précoce (Jacova et al., 2013 ; Caroppo et al., 2015b ; Mutsaerts et al., 2019 ; De Vocht et al., 2020). Dans la pathologie *GRN*, ces études sont rares et la plupart portent sur des populations hétérogènes ou de petits effectifs (Jacova et al., 2013 ; Caroppo et al., 2015b). Dans le cas de *C9orf72*, seulement quelques études ont abordé cette question. L'une portant sur une petite série de 17 porteurs a révélé un hypométabolisme s'étendant aux aires frontales, temporales et insulaires, ainsi qu'au thalamus (De Vocht et al., 2020). Une atteinte légèrement plus étendue, touchant également les régions cingulaires et pariétales, a été mise en évidence dans une étude plus récente sur un effectif comparable (n=15) (Popuri et al., 2021). Une distribution similaire de l'hypoperfusion corticale avait été retrouvée dans une étude basée sur l'analyse des séquences d'ASL (Mutsaerts et al., 2019). La définition d'un profil propre à

chaque forme génétique et leurs changements longitudinaux au stade préclinique nécessite des investigations complémentaires.

Articles de revue

Article de revue 1. Sellami L, Saracino D, Le Ber I. Genetic forms of frontotemporal lobar degeneration: Current diagnostic approach and new directions in therapeutic strategies. *Rev. Neurol. (Paris)*. 2020; 176: 571-581.

Article de revue 2. Saracino D, Le Ber I. How can we define the presymptomatic C9orf72 disease in 2022? An overview on the current definitions of preclinical and prodromal phases. *Rev. Neurol. (Paris)*. 2022; 178: 426-436.



Available online at
ScienceDirect
www.sciencedirect.com

Elsevier Masson France
EM|consulte
www.em-consulte.com



General review

Genetic forms of frontotemporal lobar degeneration: Current diagnostic approach and new directions in therapeutic strategies



L. Sellami ^{a,b,1}, D. Saracino ^{a,b,1}, I. Le Ber ^{a,b,c,*}

^a Inserm U1127, CNRS UMR 7225, Institut du cerveau et de la moelle épinière (ICM), Sorbonne université, hôpital Pitié-Salpêtrière, AP-HP, Paris, France

^b Département de neurologie, centre de référence des démences rares ou précoces, IM2A, hôpital Pitié-Salpêtrière, AP-HP, Paris, France

^c Institut du cerveau et de la moelle épinière (ICM), FrontLab, hôpital Pitié-Salpêtrière, AP-HP, 47-83, boulevard de l'Hôpital, CS21414, 75646 Paris cedex, France

INFO ARTICLE

Article history:

Received 13 January 2020
 Received in revised form
 11 February 2020
 Accepted 12 February 2020
 Available online 17 April 2020

Keywords:

Frontotemporal lobar degeneration
 Frontotemporal dementia
 Next-generation sequencing
 Progranulin (GRN)
 C9orf72
 Clinical trial.

ABSTRACT

Recent advances in the genetics of neurodegenerative diseases have substantially improved our knowledge about the genetic causes of frontotemporal lobar degeneration (FTLD). Three major genes, namely progranulin (GRN), C9orf72 and MAPT, as well as several less common genes, are responsible for the majority of familial cases and for a significant proportion of sporadic forms, including FTLD with or without associated amyotrophic lateral sclerosis and some rarer clinical presentations. Plasma progranulin dosage and next-generation sequencing are currently available tools which allow the detection of a genetic cause in a more rapid and efficient way. This has important consequences for clinical practice and genetic counseling for patients and families. The ongoing investigations on some therapeutic candidates targeting different biological pathways involved in the most frequent genetic forms of FTLD, as well as a better understanding of the early pathophysiological modifications occurring during the presymptomatic phase of the disease could hopefully contribute to develop effective disease-modifying therapies. The identification of a causal mutation in a family is of utmost importance indeed to propose to presymptomatic carriers their inclusion in clinical trials with the aim to prevent or delay the onset of disease.

© 2020 Elsevier Masson SAS. All rights reserved.

* Corresponding author. Institut du cerveau et de la moelle épinière (ICM), FrontLab, hôpital Pitié-Salpêtrière, AP-HP, 47-83, boulevard de l'Hôpital, CS21414, 75646 Paris cedex, France.

E-mail address: isabelle.leber@upmc.fr (I. Le Ber).

¹ These authors equally contributed to the manuscript.

<https://doi.org/10.1016/j.neurol.2020.02.008>

0035-3787/© 2020 Elsevier Masson SAS. All rights reserved.

1. Introduction

Frontotemporal lobar degeneration (FTLD) designates a spectrum of degenerative dementias with remarkable heterogeneity from a clinical, pathological and genetic point of view. FTLD is considered the second cause of adult-onset dementia after Alzheimer's Disease (AD). Its estimated incidence is 1.6 new cases/100,000 subjects/year and its prevalence is as high as 10–15/100,000 subjects between 45 and 65 years [1,2].

The most frequent clinical phenotype is the behavioral variant of frontotemporal dementia (bvFTD), characterized by predominant frontal lobe dysfunction which manifests as behavioral changes, social cognition deficits and dysexecutive syndrome [3]. Predominant expressive and/or receptive language deficits at onset define the primary progressive aphasia (PPAs) [4]. PPA is further distinguished into a nonfluent/agrammatic variant (nfvPPA, previously known as progressive non-fluent aphasia, PNFA) and a semantic variant (svPPA, previously known as semantic dementia, SD). A third presentation, the logopenic variant (lvPPA) is more often associated with underlying AD pathology [5].

Other syndromes mainly characterized by atypical parkinsonism are included in the FTLD spectrum: Richardson's syndrome, which is predictive of underlying progressive supranuclear palsy (PSP) pathology (as well as other clinical syndromes associated with underlying PSP, such as progressive gait freezing) [6], and corticobasal syndrome (CBS), which may be due to underlying corticobasal degeneration (CBD) but also other pathological substrates (e.g. AD) [7]. Finally, amyotrophic lateral sclerosis (ALS) can be present in up to 15% of FTLD patients—mostly in those with bvFTD phenotype—or their relatives [8].

Similar to other neurodegenerative conditions, the pathological substrate of FTLD is the aggregation of insoluble proteins forming pathological inclusions within the neurons. A pathological classification of FTLD is based on the immunohistochemical identification of those proteins. The majority (50–60%) of FTLD cases are characterized by the accumulation of a 43 kDa TAR DNA-binding protein (TDP-43), and are designated as FTLD-TDP. Four different subtypes of FTLD-TDP (from A to D) have been established mainly depending on the relative abundance of TDP-43 deposits within the various cortical layers, on the shape of the stained neurites and on the presence of intranuclear inclusions [9]. The existence of a fifth subtype (FTLD-TDP type E) with distinctive pathological features and associated with a more severe clinical course has been recently proposed [10]. The accumulation of cleaved and hyperphosphorylated Tau protein characterizes FTLD-TAU, the second most common pathological variant (30–40% of cases) [11]. In FTLD-FET/FUS (< 10% of cases), other proteins including FUS, EWS and/or TAF15 are present. These proteins, like TDP-43, are located within the nuclei and play a role in RNA metabolism under physiological conditions [12]. In very rare cases, the accumulations are solely composed of ubiquitin and other proteasomal components (FTLD-UPS) (Fig. 1).

Genetic factors play a crucial role in the FTLD-ALS continuum. A family history is present in 30–40% of patients, with evidence of autosomal dominant transmission in the

majority of them. This has to be intended in the broadest sense, because, for instance, the presence of one or more cases of ALS in the pedigree of a patient affected by bvFTD should still raise the suspicion of a genetic etiology. An impressive amount of knowledge on FTLD genetics has developed during the past two decades. Twenty-two genes are currently associated with FTLD-ALS and a causative mutation is nowadays identifiable in more than 80% of familial cases and in 10–15% of sporadic forms approximately [8,13] (Fig. 2). In this vast genetic landscape, three genes appear by far the most relevant ones due to their frequency in genetic FTLD: progranulin (GRN), chromosome 9 open reading frame 72 (C9orf72) and microtubule associated protein tau (MAPT) [14–18].

In this review, we will focus on the major FTLD genes, their associated phenotypes and disease mechanisms, and propose an updated diagnostic algorithm to include the less common genes, in order to define a paradigm for the optimal use of genetic analyses. We will also give an overview on the ongoing clinical trials involving pathology-specific disease-modifying approaches in FTLD-related genetic mutations and highlight some promising therapeutic strategies that target the underlying pathology.

2. The major FTLD genes

2.1. Progranulin gene

GRN gene (formerly known as PGRN) mutations were identified in 2006 as responsible for autosomal dominant FTLD [14,15]. They cause approximately 15–20% of familial FTLD and up to 5% of sporadic cases worldwide [19]. GRN encodes progranulin, a glycosylated secretory protein. Progranulin is highly localized within the lysosomes, where it is cleaved into smaller peptides called granulins with complementary biological activities [20]. Its functions in the brain, though not completely elucidated, relate to neuronal proliferation and survival, axonal growth and neuroinflammation [21]. Progranulin is also expressed in peripheral tissues, mostly in epithelial cells and lymphocytes, and its pleiotropic functions include major roles in wound repair, tumorigenesis and metabolic homeostasis [22].

Heterozygous GRN mutations cause FTLD via haploinsufficiency, but the exact disease mechanism remains largely speculative. Currently, more than 70 pathogenic null mutations are known, mainly consisting in non-sense variations, exon deletions or small insertions/deletions causing frameshifts (www.molgen.ua.ac.be/FTDMutations/) [23]. Most lead to a truncated mRNA which is rapidly degraded, thus reducing the level of functional progranulin by about 50% [14,15]. Polymorphisms in TMEM106B gene, encoding another lysosomal protein, have been shown to modulate progranulin levels, likely altering the susceptibility to the disease [24]. Of note, GRN mutations when present at the homozygous state lead to neuronal ceroid-lipofuscinosis type 11 (CLN11), a multi-systemic lysosomal storage disorder [25,26].

GRN-associated FTLD displays remarkable inter- and intra-familial variability of age at onset and clinical phenotype. Age at onset ranges from the late fourth to the ninth decade, with a

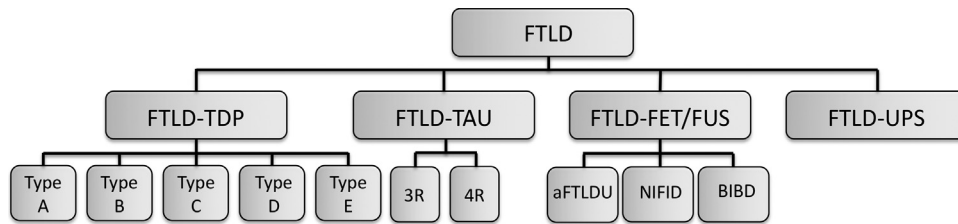


Fig. 1 – Pathological classification of frontotemporal lobar degeneration. TDP: transactive response (TAR) DNA binding protein; 3R: 3-repeat Tau inclusions; 4R: 4-repeat Tau inclusions; FET: Fused in sarcoma (FUS), Ewing’s sarcoma, TATA-binding protein associated factor (TAF) 15; aFTLDU: atypical frontotemporal lobar degeneration with ubiquitin-positive inclusions; NIFID: neuronal intermediate filament inclusion disease; BIBD: basophilic inclusion body disease; FTLD-UPS: frontotemporal lobar degeneration with inclusions positive for ubiquitin and proteasome system markers.

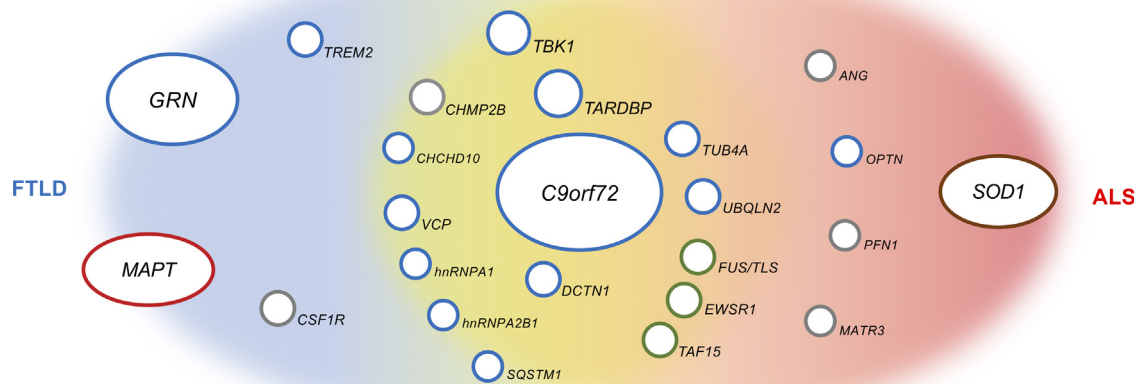


Fig. 2 – Landscape of the genes associated with the FTLN-ALS continuum. Major genes are represented as larger balloons. The list of ALS-associated genes is not exhaustive. Different pathological substrates are represented by different colors of the balloons’ lines (red: FTLD-TAU; blue: FTLD-TDP; green: FTLD-FET/FUS; brown: SOD1-positive inclusions; grey: other or unknown pathology). ALS: amyotrophic lateral sclerosis; FTLN: frontotemporal lobar degeneration; SOD1: superoxide dismutase 1.

peak between 60 and 65 years [27,28]. The main clinical presentation is bvFTD, in which apathy commonly prevails over disinhibition among the behavioral manifestations. Besides, 15-20% of patients develop a language disorder at onset, characterized by expressive deficits with reduced verbal output, resulting in *nvPPA*, *lvPPA* or a mixed *PPA* variant [29,30]. Parkinsonism can be associated with these syndromes or can be found in the context of a CBS, another clinical presentation of *GRN* mutations [27]. Up to half of the patients show apraxia, dyscalculia and other parietal lobe dysfunctions, about 25% present visual hallucinations and 10-30% display an episodic memory deficit at the neuropsychological assessment [27].

Neuroimaging studies reveal mostly asymmetric brain atrophy and/or hypometabolism involving frontal, insular, temporal and parietal regions. Subcortical and periventricular white matter hyperintensities of likely degenerative nature are visible in T2-weighted MRI sequences [31]. The neuropathological substrate is FTLD-TDP type A, with characteristic intranuclear “cat’s-eye” inclusions [9].

Due to its secretion, progranulin can be measured in the plasma, and a reduction of plasma progranulin levels is highly predictive of *GRN* mutations [32]. Progranulin dosage is performed in symptomatic patients as part of the diagnostic work-up (see below), while it has no indications for their at-risk relatives.

2.2. *C9orf72* repeat expansion

One of the major advances in the genetics of the FTLN-ALS continuum has been the identification, in 2011, of the GGGGCC hexanucleotide repeat expansion in the first intron of *C9orf72* gene in families concerned by FTLN, ALS or a combination of both [16,17]. This mutation explains approximately 25% of familial FTLNs and up to 80% of cases with the FTLN-ALS association [33]. Moreover, it is the first genetic cause of ALS, being responsible for 40% of familial and 6% of sporadic cases [34].

The protein encoded by *C9orf72* is a guanine nucleotide exchange factor (GEF) interacting with various GTPases which

is involved in several cellular functions including vesicular trafficking and phagosome formation [35]. Most individuals in control populations harbor less than 23 GGGGCC repeats, and most often only 2 to 8 repeats, in the first intron of the gene. An expansion above 30 is considered pathological, even if the majority of patients have many hundreds or thousands of repeats. Three different pathogenic mechanisms, not mutually exclusive, have been proposed: a) loss of physiological functions of the C9orf72 protein; b) toxicity of mutant RNA that aggregates into nuclear foci; c) accumulation of dipeptide repeats proteins (DPR) generated by repeat-associated non-ATG (RAN) translation [36].

The mean age at onset in C9orf72 carriers is around 59 years, but it can vary, even in the same family, from 30 to more than 80 years [28]. The most common cognitive phenotype is bvFTD, characterized by remarkably slow progression of behavioral alterations and executive deficits in a subset of the mutation carriers. Rarer clinical presentations include PPA (nfvPPA or svPPA) or parkinsonian syndrome [33,37]. In ALS patients, the disease has no particular distinguishing features; bulbar onset and co-occurring cognitive deterioration are overall more frequent with respect to non-mutated cases. The appearance of ALS drastically shortens the disease course [33]. Interestingly, psychiatric symptoms and syndromes (such as auditory hallucinations, delusions, obsessive-compulsive disorder, bipolar disorder and schizophrenia) may be present in up to around 50% of C9orf72 patients [38]. They can coexist with the neurological deficits or even appear years or decades before their onset [39]. In C9orf72 disease frontal and temporal atrophy is almost bilateral and symmetrical [40].

A mosaicism consisting of different sizes of the GGGGCC expansion amongst the different tissues, and among different central nervous system (CNS) regions, has been evidenced in C9orf72 carriers [41]. Additionally, the number of GGGGCC repeats in peripheral lymphocytes appears to unpredictably vary over time in subjects with multiple blood samples, as well as through generations in parents-offspring pairs [42]. Consequently, no reliable correlations can be established between the size of the expansion in lymphocytes and the severity of the disease or its age of onset, differently from some other repeat expansion disorders [42]. The role of short expansions (e.g. a few dozen hexanucleotides) is even more controversial, as they have been found in symptomatic patients as well as in some old unaffected first-degree relatives [41]. Research on putative genetic modifiers, including but not limited to TMEM106B, is currently underway [24,43].

The underlying pathological substrate is FTLT-DTP type A or occasionally type B. Widespread p62-positive inclusions, most notably in the cerebellum where TDP-43 pathology is absent, has been reported in C9orf72 patients, especially with predominant motor phenotypes [44]. Additionally, intranuclear RNA foci and cytoplasmic DPR inclusions are present in the pyramidal cells of the hippocampus, the granular layer of the cerebellum and in several neocortical regions [45].

2.3. MAPT gene mutations

MAPT was the first gene identified in families affected by FTLT, in 1998, and the frequent occurrence of parkinsonism

together with cognitive and behavioral manifestations in those kindreds led to the descriptive term of “frontotemporal dementia and parkinsonism linked to chromosome 17” (FTDP-17) [18]. This acronym should be avoided however, considering the frequency of parkinsonism in other genetic forms of FTLT, and the absence of homogeneity in pathological subtypes of FTLT-TAU [46].

In France, the frequency of MAPT mutations is 5–10% in familial forms and about 3% in sporadic cases, but it can be as high as 20% in some countries, as in northern Europe, due to founder effects [47].

The tau (tubulin-associated unit) protein encoded by MAPT exists in two different splice variants, 3R and 4R, and is involved in microtubule assembly, cytoskeleton stabilization and axonal transport. Currently more than 50 pathogenic mutations are known, mainly consisting of missense or non-sense base changes, which act by altering the physiological balance of tau isoforms, impairing its binding to axonal cytoskeleton and eventually leading to tau hyperphosphorylation and accumulation [48,49].

The age at onset ranges between the third and the seventh decade, with a peak around 50 years, thus earlier than in the other principal genetic forms. The main clinical phenotype is bvFTD with prevailing disinhibition, at times associated with obsessive-compulsive symptoms, episodic memory disturbances and semantic impairment [50]. svPPA (without any behavioral troubles), as well as nfvPPA with prominent apraxia of speech, are rarer presentations [50,51]. In addition to the atypical parkinsonism associated with bvFTD, other motor phenotypes include CBS and PSP [50].

Neuroimaging studies show predominant bilateral frontal and anterior temporal involvement [40]. The neuropathology associated with MAPT mutations is FTLT-TAU. Neuronal tau accumulations mainly consist of fibrillary tangles, straight filaments and Pick body-like inclusions. A glial pathology in the form of tufted astrocytes, astrocytic plaques or oligodendroglial coiled bodies (somewhat reminiscent of PSP or CBS) often coexists [46,49,50].

3. Other rare FTLT genes

3.1. Rare genes involved in FTLT-ALS association

TARDBP gene, coding the TDP-43 protein, is responsible for ~1% of FTLT and ~3% of ALS cases, and is the most common genetic cause of FTLT-ALS after C9orf72. Almost all pathogenic mutations are located in exon 6 [52]. TANK-binding kinase 1 (TBK1) loss-of-function mutations are associated with late-onset familial ALS, with or without associated FTLT [53]. It is worth noticing that nfvPPA and svPPA are relatively frequent cognitive phenotypes for both TARDBP and TBK1 mutations [54,55]. Other genes occurring in < 1% of familial FTLT-ALS cases each include TUB4A and CHMP2B [56,57]. Both have been associated with ALS, bvFTD and late-onset atypical parkinsonian syndromes. Notably, the pathology underlying CHMP2B mutations is the rare FTLT-UPS, with ubiquitin- and p62-positive inclusions, in absence of TDP-43 accumulation. Additionally, mutations in ANG, OPTN, PFN1, UBQLN1 and MATR3 genes have been mainly reported in ALS families, with

or without associated cognitive impairment. FUS/TLS, EWSR1 and TAF15 genes, encoding for three RNA-binding proteins of the FET (Fused in sarcoma (FUS), Ewing's sarcoma, TATA-binding protein associated factor (TAF) 15) family, are all associated with ALS (very rarely co-occurring with dementia), and are characterized by a distinctive underlying pathological substrate (FTLD-FET/FUS) [58].

3.2. Rare genes involved in complex phenotypes

In some families, symptoms of FTLD or ALS are integrated in a more complex phenotypic association including other neurological, musculoskeletal or extra-neurological diseases. This emphasizes the importance of investigating associated features in the family during a thorough clinical interview [59].

A variable association of FTLD, inclusion body myopathy (IBM), Paget's disease of bone (PDB) and, rarely, ALS was initially described in some North American families and designated with the acronym IBMPPD (Inclusion-Body Myopathy with Paget's disease of bone and Frontotemporal Dementia) or "multisystem proteinopathy" (MSP) [60]. VCP is the main gene involved in this complex phenotype. It is responsible for up to 3% of familial FTLD cases, with FTLD-TDP type D as the pathological substrate [9]. Approximately 90% of VCP mutation carriers present IBM, 60% PDB and 30% bvFTD [59]. Rarer genes leading to MSP include SQSTM1, encoding the p62 protein, and two genes coding for heterogeneous ribonucleoproteins, hnRNPA1 and hnRNPA2B1 [61,62].

Mutations in CSF1R (colony stimulating factor receptor 1) gene cause a white-matter disorder initially known as hereditary diffuse leukoencephalopathy with spheroids (HDLS) [63], and currently designated as adult-onset leukoencephalopathy with axonal spheroids and pigmented glia (ALSP), to encompass all its pathological features [64]. The onset of symptoms occurs during the fourth decade (range 18-78 years). CSF1R mutations have been found in individuals showing bvFTD or CBS phenotypes [65,66] but the clinical presentations also variably include seizures, parkinsonism, cerebellar ataxia, spasticity and depression [65]. Extensive white-matter T2-hyperintensities and thinning of corpus callosum are distinctive MRI findings [64,67]. A rapid clinical deterioration, the appearance of (mostly generalized) seizures and diffuse white-matter involvement with bifrontal atrophy at MRI are important clues for this genetic form. Although rare, CSF1R mutations should be investigated in cases with autosomal dominant disease but also in "apparently sporadic" cases, as the frequency of de novo mutations can be as high as 40% [64].

CHCHD10 gene mutations lead to another complex syndrome associating FTLD-ALS with cerebellar ataxia, mitochondrial myopathy and hearing impairment [56,68]. The mutations of DCTN1 gene, encoding the p150^{Glued} subunit of dynactin, are associated with ALS, FTLD, parkinsonism and Perry syndrome [69]. Finally, homozygous and compound heterozygous TREM2 mutations cause polycystic lipomembranous osteodysplasia with sclerosing leukoencephalopathy (PLOS), also known as Nasu-Hakola syndrome), but have also been reported in association with an FTLD-like syndrome, without associated bone changes [70].

4. Genetic diagnosis in FTLD: new challenges and recommendations

The growing complexity of the genetic landscape of FTLD-ALS, with 22 genes involved thus far, represents an obvious difficulty in identifying the causal mutations. The analysis of all responsible genes with the standard sequencing techniques is time-consuming and expensive. The development of next generation sequencing (NGS) in the past decade has considerably eased the identification of a causal mutation in FTLD patients and it is nowadays possible to analyze most FTLD genes [71]. However, not all genes undergo mutations diagnosable by means of NGS. This is the case for the *C9orf72* gene, whose repeat expansions should be looked for separately with repeat primed-PCR or Southern blot, the gold standard methods for repeat expansion detection. Moreover, the interpretation of the huge load of data and the considerable number of variants of uncertain significance (VUS) generated by NGS are new challenges for genetic diagnosis [72]. Significant diagnostic difficulties arise, for instance, in the presence of missense mutations in FTLD causative genes, such as GRN or TBK1, as they have a variable impact on protein synthesis and their pathogenic role is still unclear in the majority of cases [73]. Therefore, caution must be taken when interpreting uncertain results and a good expertise in the genotypes underlying FTLD phenotypes is needed. In this context, studies of familial segregation and additional evidence of pathogenicity (from *in silico* and/or *in vitro* models) may be of paramount importance to validate the pathogenicity of genetic variants. A higher level of complexity in the interpretation of NGS data and in the identification of the causal mutation comes from the identification of double mutations—especially involving the rarest FTLD genes—in few FTLD patients [74]. Therefore, the extensive analysis of all FTLD genes might be warranted in selected cases, as the identification of a first mutation does not rule out the possibility of a digenic etiology.

To maximize the efficacy of the NGS approach, recommendations for genetic diagnosis in FTLD-ALS patients and families should be proposed. In most genetic forms of FTLD, the core features display a remarkable intra- and interfamilial variability, hence the importance of investigating not only cognitive-behavioral symptoms, but also the existence of ALS, other neurological, musculoskeletal or extra-neurological (e.g. Paget's disease of bone) diseases in the proband or the proband's family during a thorough clinical interview. The clinical phenotypes of the proband and affected relatives should be carefully detailed, paying special attention to the heterogeneity in age at onset and clinical presentation.

An algorithm for genetic diagnosis in FTLD-ALS, considering the role of the major genes and the additional contribution from NGS, is presented in Fig. 3. Briefly, plasma progranulin dosage should be performed in all FTLD patients (with or without positive family history), and low levels should prompt immediate GRN gene analysis. The association of FTLD with ALS in the same individual or within the family is most often due to the *C9orf72* repeat expansion. The research of *C9orf72* repeat expansion should be carried out in all subjects with FTLD and FTLD-ALS (both non-familial and familial forms,

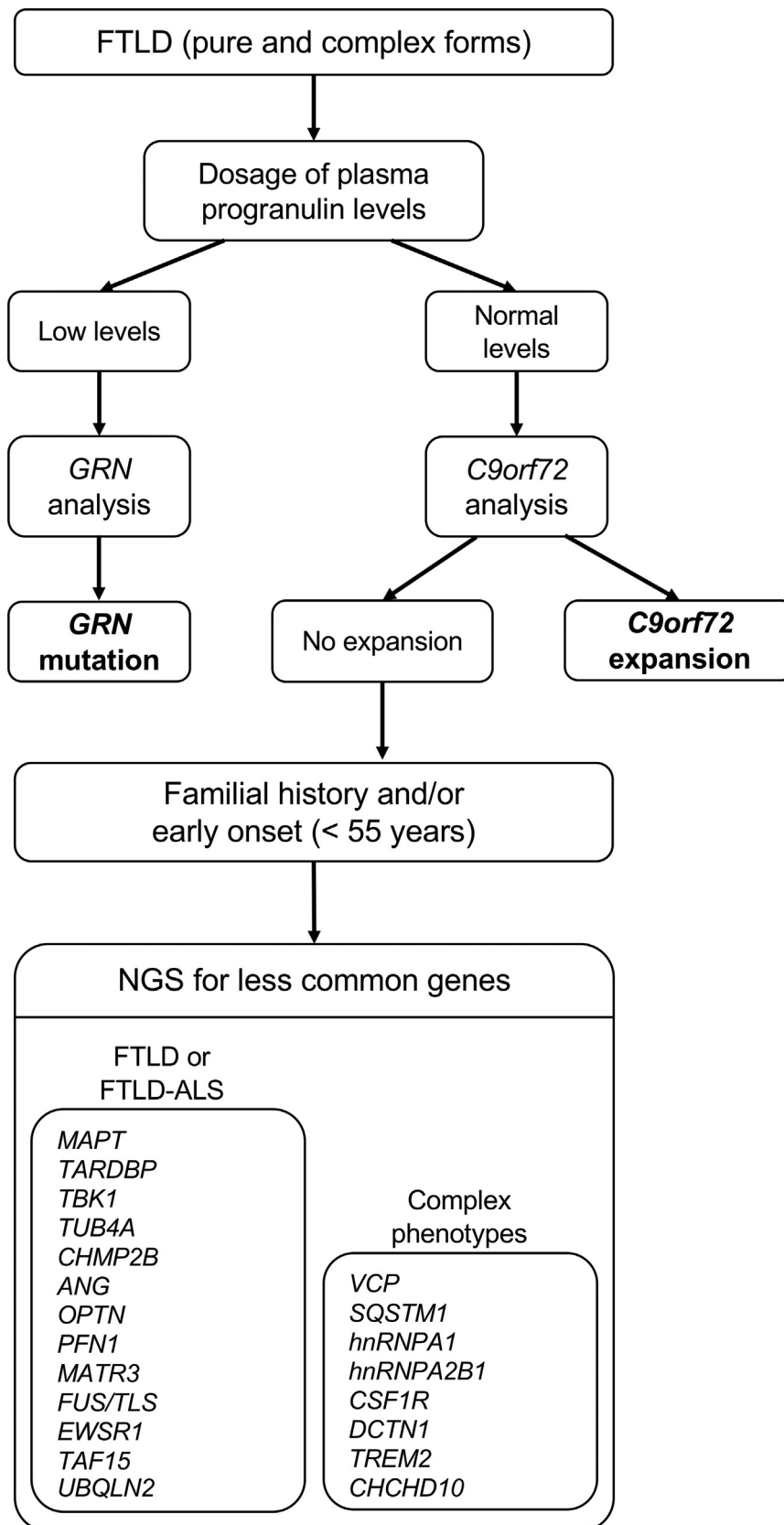


Fig. 3 – Optimal diagnostic algorithm for genetic diagnosis in FTLT, including major and less common genes. ALS: amyotrophic lateral sclerosis; FTLT: frontotemporal lobar degeneration; NGS: next-generation sequencing.

considering the presence of ALS not only in the proband but also the proband's family as well). If *GRN* and *C9orf72* mutations are absent, FTLN-ALS NGS is a second-level approach to genetic diagnosis. Atypical FTLN clinical presentations or unusual phenotypic associations should raise the suspicion of the involvement of different, rare genes, possibly prioritizing those more closely associated with the specific clinical context.

5. Targeted therapies for FTD genetic mutations

Considerable advances in the genetics of FTLN have paved the way to new therapeutic perspectives. Several novel therapies to delay the outbreak and progression of genetic FTD are emerging and some examples of molecules currently being tested are discussed below.

5.1. Therapeutic approaches for *GRN* gene mutations

The main pathogenic mechanism of *GRN* mutations arises from a loss of functional progranulin, and strategies to restore progranulin haploinsufficiency have emerged as promising avenues of research for *GRN*-related FTLN. A targeted intervention in *GRN* mutations might be the replacement of progranulin haploinsufficiency by upregulating expression of the nonmutant *GRN* allele. Histone deacetylase (HDAC) inhibitors were shown to promote progranulin expression through epigenetic regulation in human neuronal cells [75]. A phase II randomized, double-blind, placebo-controlled trial has tested HDAC inhibitors (FRM-0334) (<https://www.clinicaltrials.gov/>, NCT02149160), for which results are still pending. Another avenue of research has focused on the sortilin (SORT1)-progranulin axis. SORT1 is a clearance neuronal receptor via an endocytosis mechanism [76]. An open-label phase 2 study in human carriers is currently ongoing (<https://www.clinicaltrials.gov/>, NCT03987295). Other therapeutic approaches to rescue progranulin haploinsufficiency failed to demonstrate efficacy. An 8-week phase 1 clinical trial of nimodipine, a blood-brain barrier-penetrating calcium channel blocker, did not show any significant effect on the concentrations of progranulin in plasma and CSF [77]. Similarly, a small phase 2 clinical trial of amiodarone led to inconclusive results [78]. Other therapeutic approaches stemming from promising preclinical data in animal models, including oral small molecules, gene therapy and cell-based strategies are currently under development.

5.2. Therapeutic approaches for *C9orf72* repeat expansion

Since 2011, substantial advances have been achieved in our knowledge regarding *C9orf72*-mediated disease and its underlying pathogenesis. Toxic gain of function from *C9orf72* repeat RNA and DPR proteins have been proposed as a crucial disease mechanism [36]. Hence, main drug discovery efforts aimed at reducing the gain of toxicity caused by the repeat-containing *C9orf72* transcripts. Potential therapies based on this approach consist of antisense oligonucleotides (ASOs). ASOs are short DNA or RNA segments binding a complementary RNA

sequence that are already used to modulate gene expression in several neurological diseases. A recent phase 2 clinical trial of ASO therapy targeting RNA-mediated toxicity in human has been conducted in Huntington disease (HTT_{RK}) another repeat expansions disease. This trial showed its safety and tolerability, and a dose-dependent reduction in levels of the harmful mutant protein in the nervous system [79]. The most important breakthrough in the field of ASO therapy is undoubtedly the recent Food and Drug Administration approval for nusinersen, an antisense drug for the treatment of spinal muscular atrophy [80]. All these studies pave the way for the development of ASO therapies in neurodegenerative disorders and hold a great promise for the discovery of effective disease-modifying therapies for *C9orf72*-associated disease. In vivo studies in *C9orf72* mice showed a significant reduction of RNA foci, DPR proteins and the development of behavioral deficits after a single dose of ASO therapy [81]. A phase 1 first-in-human study (BIIB078) assessing the safety and tolerability of ASO-mediated therapy administered intrathecally is currently underway in subjects with *C9orf72*-associated ALS (<https://www.clinicaltrials.gov/>, NCT03626012). Several other approaches including therapies based on small molecules and targeting DPR are also under development [13].

5.3. Therapeutic approaches for *MAPT* gene mutations

Several strategies targeting different aspects of tau-related pathogenesis are currently being investigated, including protein kinases inhibitors for modulating tau phosphorylation, Microtubule stabilizers, tau aggregation inhibitors and anti-tau immunotherapy. Potentially relevant clinical trials for different tauopathies include a phase 3 trial of LMTX (TRx0237), a modified derivative of the tau aggregation inhibitor methylthionine chloride in subjects with bvFTD (<https://www.clinicaltrials.gov/>, NCT01626378) and a phase 2 trial of anti-tau immunotherapy, ABBV-8E12, a humanized recombinant anti-tau antibody, in patients with PSP (<https://www.clinicaltrials.gov/>, NCT03391765). These studies were completed in 2018, though their results have not been published yet. Gosuranemab (BIIB092), another tau-directed monoclonal antibody, demonstrated good tolerability in PSP patients in a phase 1b trial [82]. So far, these trials have mostly included PSP patients, but it is likely that some of these molecules will be tested in FTLN patients carrying *MAPT* mutations as well.

6. At the dawn of a new therapeutic era: the presymptomatic phase as a target window in genetic FTLN

The study of presymptomatic stage in mutation carriers is of utmost importance in light of the advent of promising preventive trials in genetic FTLN families. The presymptomatic phase indeed represents the optimal window for testing therapeutic molecules that target the FTLN-related neurobiological abnormalities at the earliest stage of the disease, before the occurrence of clinical symptoms. The identification of imaging and fluid biomarkers become crucial to monitor

therapeutic trials at this stage, and research studies focusing on the presymptomatic phase of genetic FTLT have become of increasing interest over the past few years [83,84]. Emerging data from several studies of well-characterised presymptomatic genetic cohorts, such as GENFI (Genetic Frontotemporal dementia Initiative) [84], LEFFTDS (Longitudinal Evaluation of Familial Frontotemporal Dementia Subjects) [85], Predict-PGRN [86] and PREV-DEMALS [87], suggested that the first pathological alterations associated with FTLT gene mutations can be detected 15-10 years before onset of overt clinical symptoms. Accumulating results across these studies have identified early biomarkers in mutation carriers, encompassing neuropsychological, biological and multimodal neuroimaging changes (i.e. structural and functional MRI and PET imaging) [84,87-91], but these markers still remain to be validated at the individual level. Once validated, the panel of early biomarkers identified at the presymptomatic stage could be used as efficacy endpoints in clinical trials. The significant advances that have been achieved in the understanding of the biomarkers cascade throughout the presymptomatic stage of genetic FTLT provide insight into the measurement of early disease progression and potential effects of disease-modifying therapies.

7. Conclusion

In the last few years, a major breakthrough has been achieved in the understanding of the genetics and molecular biology of FTLT. A remaining challenge is translating this substantial knowledge into therapeutic opportunities. Whilst much remains to be done in the field of drug discovery, it is noteworthy that we are now reaching a turning point as regards the development of early biomarkers and preventive therapeutic approaches targeting the prodromal stage of genetic FTLT, before the onset of overt clinical symptoms in causative mutations carriers. The current investigations target different aspects of FTLT pathophysiology and several appealing potential therapeutic candidates are currently being tested in the setting of clinical trials. These studies will hopefully expand the scope of potentially interesting disease-modifying therapies in FTLT.

Disclosure of interest

I.L.B. is principal investigator for Alector in France and scientific consultant for Prevail Therapeutics. L.S. was supported by a grant from the Société Française de Neurologie - Revue Neurologique.

REFERENCES

- [1] Onyike CU, Diehl-Schmid J. The epidemiology of frontotemporal dementia. *Int Rev Psychiatry* 2013;25:130-7. <http://dx.doi.org/10.3109/09540261.2013.776523>.
- [2] Olney NT, Spina S, Miller BL. Frontotemporal Dementia. *Neurol Clin* 2017;35:339-74. <http://dx.doi.org/10.1016/j.ncl.2017.01.008>.
- [3] Rascovsky K, Hodges JR, Knopman D, Mendez MF, Kramer JH, Neuhaus J, et al. Sensitivity of revised diagnostic criteria for the behavioural variant of frontotemporal dementia. *Brain* 2011;134:2456-77. <http://dx.doi.org/10.1093/brain/awr179>.
- [4] Gorno-Tempini ML, Hillis AE, Weintraub S, Kertesz A, Mendez M, Cappa SF, et al. Classification of primary progressive aphasia and its variants. *Neurology* 2011;76:1006-14. <http://dx.doi.org/10.1212/WNL.0b013e31821103e6>.
- [5] Rogalski E, Sridhar J, Rader B, Martersteck A, Chen K, Cobia D, et al. Aphasie variant of Alzheimer disease: clinical, anatomic, and genetic features. *Neurology* 2016;87:1337-43. <http://dx.doi.org/10.1212/WNL.0000000000003165>.
- [6] Höglinger GU, Respondek G, Stamelou M, Kurz C, Josephs KA, Lang AE, et al. Clinical diagnosis of progressive supranuclear palsy: The movement disorder society criteria: MDS clinical diagnostic criteria for PSP. *Mov Disord* 2017;32:853-64. <http://dx.doi.org/10.1002/mds.26987>.
- [7] Armstrong MJ, Litvan I, Lang AE, Bak TH, Bhatia KP, Borroni B, et al. Criteria for the diagnosis of corticobasal degeneration. *Neurology* 2013;80:496-503. <http://dx.doi.org/10.1212/WNL.0b013e31827f0fd1>.
- [8] Pottier C, Ravenscroft TA, Sanchez-Contreras M, Rademakers R. Genetics of FTLT: overview and what else we can expect from genetic studies. *J Neurochem* 2016;138:32-53. <http://dx.doi.org/10.1111/jnc.13622>.
- [9] Mackenzie IRA, Neumann M, Baborie A, Sampathu DM, Du Plessis D, Jaros E, et al. A harmonized classification system for FTLT-TDP pathology. *Acta Neuropathol* 2011;122:111-3. <http://dx.doi.org/10.1007/s00401-011-0845-8>.
- [10] Lee EB, Porta S, Michael Baer G, Xu Y, Suh E, Kwong LK, et al. Expansion of the classification of FTLT-TDP: distinct pathology associated with rapidly progressive frontotemporal degeneration. *Acta Neuropathol* 2017;134:65-78. <http://dx.doi.org/10.1007/s00401-017-1679-9>.
- [11] Irwin DJ, Cairns NJ, Grossman M, McMillan CT, Lee EB, Van Deerlin VM, et al. Frontotemporal lobar degeneration: defining phenotypic diversity through personalized medicine. *Acta Neuropathol* 2015;129:469-91. <http://dx.doi.org/10.1007/s00401-014-1380-1>.
- [12] Neumann M, Bentmann E, Dormann D, Jawaid A, DeJesus-Hernandez M, Ansorge O, et al. FET proteins TAF15 and EWS are selective markers that distinguish FTLT with FUS pathology from amyotrophic lateral sclerosis with FUS mutations. *Brain* 2011;134:2595-609. <http://dx.doi.org/10.1093/brain/awr201>.
- [13] Desmarais P, Rohrer JD, Nguyen QD, Herrmann N, Stuss DT, Lang AE, et al. Therapeutic trial design for frontotemporal dementia and related disorders. *J Neurol Neurosurg Psychiatry* 2019;90:412-23. <http://dx.doi.org/10.1136/jnnp-2018-318603>.
- [14] Cruts M, Gijssels I, van der Zee J, Engelborghs S, Wils H, Pirici D, et al. Null mutations in progranulin cause ubiquitin-positive frontotemporal dementia linked to chromosome 17q21. *Nature* 2006;442:920-4. <http://dx.doi.org/10.1038/nature05017>.
- [15] Baker M, Mackenzie IR, Pickering-Brown SM, Gass J, Rademakers R, Lindholm C, et al. Mutations in progranulin cause tau-negative frontotemporal dementia linked to chromosome 17. *Nature* 2006;442:916-9. <http://dx.doi.org/10.1038/nature05016>.
- [16] DeJesus-Hernandez M, Mackenzie IR, Boeve BF, Boxer AL, Baker M, Rutherford NJ, et al. Hexanucleotide Repeat in Noncoding Region of C9ORF72 Causes Chromosome 9p-Linked FTD and ALS. *Neuron* 2011;72:245-56. <http://dx.doi.org/10.1016/j.neuron.2011.09.011>.
- [17] Renton AE, Majounie E, Waite A, Simón-Sánchez J, Rollinson S, Gibbs JR, et al. A hexanucleotide repeat expansion in C9ORF72 is the cause of chromosome 9p21-

- Linked ALS-FTD. *Neuron* 2011;72:257–68. <http://dx.doi.org/10.1016/j.neuron.2011.09.010>.
- [18] Hutton M, Lendon CL, Rizzu P, Baker M, Froelich S, Houlden H, et al. Association of missense and 5'-splice-site mutations in tau with the inherited dementia FTDP-17. *Nature* 1998;393:4.
- [19] Rademakers R, Neumann M, Mackenzie IR. Recent advances in the molecular basis of frontotemporal dementia. *Nat Rev Neurol* 2012;8:423–34. <http://dx.doi.org/10.1038/nrneurol.2012.117>.
- [20] Paushter DH, Du H, Feng T, Hu F. The lysosomal function of progranulin, a guardian against neurodegeneration. *Acta Neuropathol* 2018;136:1–17. <http://dx.doi.org/10.1007/s00401-018-1861-8>.
- [21] Ahmed Z, Mackenzie IR, Hutton ML, Dickson DW. Progranulin in frontotemporal lobar degeneration and neuroinflammation. *Journal of Neuroinflammation* 2007;4:7. <http://dx.doi.org/10.1186/1742-2094-4-7>.
- [22] Cenik B, Sephton CF, Kutluk Cenik B, Herz J, Yu G, Progranulin. A proteolytically processed protein at the crossroads of inflammation and neurodegeneration. *J Biol Chem* 2012;287:32298–306. <http://dx.doi.org/10.1074/jbc.R112.399170>.
- [23] Cruts M, Theuns J, Van Broeckhoven C. Locus-specific mutation databases for neurodegenerative brain diseases. *Hum Mutat* 2012;33:1340–4. <http://dx.doi.org/10.1002/humu.22117>.
- [24] Lattante S, Le Ber I, Galimberti D, Serpente M, Rivaud-Péchoux S, Camuzat A, et al. Defining the association of TMEM106B variants among frontotemporal lobar degeneration patients with GRN mutations and C9orf72 repeat expansions. *Neurobiol Aging* 2014;35. <http://dx.doi.org/10.1016/j.neurobiolaging.2014.06.023> [2658.e1–2658.e5].
- [25] Smith KR, Damiano J, Franceschetti S, Carpenter S, Canafoglia L, Morbin M, et al. Strikingly different clinicopathological phenotypes determined by progranulin-mutation dosage. *Am J Hum Genet* 2012;90:1102–7. <http://dx.doi.org/10.1016/j.ajhg.2012.04.021>.
- [26] Huin V, Barbier M, Bottani A, Lohrinus JA, Clot F, Lamari F, et al. Homozygous GRN mutations: new phenotypes and new insights into pathological and molecular mechanisms. *Brain* 2020;143:303–19. <http://dx.doi.org/10.1093/brain/awz377>.
- [27] Le Ber I, Camuzat A, Hannequin D, Pasquier F, Guedj E, Rovelet-Lecrux A, et al. Phenotype variability in progranulin mutation carriers: a clinical, neuropsychological, imaging and genetic study. *Brain* 2008;131:732–46. <http://dx.doi.org/10.1093/brain/awn012>.
- [28] Moore KM, Nicholas J, Grossman M, McMillan CT, Irwin DJ, Massimo L, et al. Age at symptom onset and death and disease duration in genetic frontotemporal dementia: an international retrospective cohort study. *Lancet Neurol* 2020;19. [http://dx.doi.org/10.1016/S1474-4422\(19\)30394-1](http://dx.doi.org/10.1016/S1474-4422(19)30394-1).
- [29] Rohrer JD, Crutch SJ, Warrington EK, Warren JD. Progranulin-associated primary progressive aphasia: a distinct phenotype? *Neuropsychologia* 2010;48:288–97. <http://dx.doi.org/10.1016/j.neuropsychologia.2009.09.017>.
- [30] Kim G, Ahmadian SS, Peterson M, Parton Z, Memon R, Weintraub S, et al. Asymmetric pathology in primary progressive aphasia with progranulin mutations and TDP inclusions. *Neurology* 2016;86:627–36. <http://dx.doi.org/10.1212/WNL.0000000000002375>.
- [31] Caroppo P, Le Ber I, Camuzat A, Clot F, Naccache L, Lamari F, et al. Extensive white matter involvement in patients with frontotemporal lobar degeneration: think progranulin. *JAMA Neurol* 2014;71:1562. <http://dx.doi.org/10.1001/jamaneurol.2014.1316>.
- [32] Ghidoni R, Stoppani E, Rossi G, Piccoli E, Albertini V, Paterlini A, et al. Optimal plasma progranulin cutoff value for predicting null progranulin mutations in neurodegenerative diseases: a multicenter Italian study. *Neurodegenerative Diseases* 2012;9:121–7. <http://dx.doi.org/10.1159/000333132>.
- [33] Le Ber I, Guillot-Noel L, Hannequin D, Lacomblez L, Golfier V, Puel M, et al. C9ORF72 repeat expansions in the frontotemporal dementias spectrum of diseases: a flow-chart for genetic testing. *JAD* 2013;34:485–99. <http://dx.doi.org/10.3233/JAD-121456>.
- [34] Majounie E, Renton AE, Mok K, Dopper EG, Waite A, Rollinson S, et al. Frequency of the C9orf72 hexanucleotide repeat expansion in patients with amyotrophic lateral sclerosis and frontotemporal dementia: a cross-sectional study. *Lancet Neurol* 2012;11:323–30. [http://dx.doi.org/10.1016/S1474-4422\(12\)70043-1](http://dx.doi.org/10.1016/S1474-4422(12)70043-1).
- [35] Webster CP, Smith EF, Bauer CS, Moller A, Hautbergue GM, Ferraiuolo L, et al. The C9orf72 protein interacts with Rab1a and the ULK1 complex to regulate initiation of autophagy. *EMBO J* 2016;35:1656–76. <http://dx.doi.org/10.15252/emboj.201694401>.
- [36] Cruts M, Gijssels I, Van Langenhove T, van der Zee J, Van Broeckhoven C. Current insights into the C9orf72 repeat expansion diseases of the FTLD/ALS spectrum. *Trends in Neurosci* 2013;36:450–9. <http://dx.doi.org/10.1016/j.tins.2013.04.010>.
- [37] Snowden JS, Adams J, Harris J, Thompson JC, Rollinson S, Richardson A, et al. Distinct clinical and pathological phenotypes in frontotemporal dementia associated with MAPT, PGRN and C9orf72 mutations. *Amyotroph Lateral Scler Frontotemporal Degener* 2015;16:497–505. <http://dx.doi.org/10.3109/21678421.2015.1074700>.
- [38] Snowden JS, Rollinson S, Thompson JC, Harris JM, Stopford CL, Richardson AMT, et al. Distinct clinical and pathological characteristics of frontotemporal dementia associated with C9ORF72 mutations. *Brain* 2012;135:693–708. <http://dx.doi.org/10.1093/brain/awr355>.
- [39] Devenney EM, Ahmed RM, Halliday G, Piguet O, Kiernan MC, Hodges JR. Psychiatric disorders in C9orf72 kindreds: study of 1,414 family members. *Neurology* 2018;1. <http://dx.doi.org/10.1212/WNL.0000000000006344>.
- [40] Whitwell JL, Weigand SD, Boeve BF, Senjem ML, Gunter JL, DeJesus-Hernandez M, et al. Neuroimaging signatures of frontotemporal dementia genetics: C9ORF72, tau, progranulin and sporadic. *Brain* 2012;135:794–806. <http://dx.doi.org/10.1093/brain/awz001>.
- [41] McGoldrick P, Zhang M, van Blitterswijk M, Sato C, Moreno D, Xiao S, et al. Unaffected mosaic C9orf72 case: RNA foci, dipeptide proteins, but upregulated C9orf72 expression. *Neurology* 2018;90:e323–31. <http://dx.doi.org/10.1212/WNL.0000000000004865>.
- [42] Fournier C, Barbier M, Camuzat A, Anquetil V, Lattante S, Clot F, et al. Relations between C9orf72 expansion size in blood, age at onset, age at collection and transmission across generations in patients and presymptomatic carriers. *Neurobiol Aging* 2019;74:234. <http://dx.doi.org/10.1016/j.neurobiolaging.2018.09.010> [e1–234.e8].
- [43] Barbier M, Camuzat A, Houot M, Clot F, Caroppo P, Fournier C, et al. Factors influencing the age at onset in familial frontotemporal lobar dementia: Important weight of genetics. *Neurol Genet* 2017;3:e203. <http://dx.doi.org/10.1212/NXG.000000000000203>.
- [44] Troakes C, Maekawa S, Wijesekera L, Rogelj B, Siklós L, Bell C, et al. An MND/ALS phenotype associated with C9orf72 repeat expansion: Abundant p62-positive, TDP-43-negative inclusions in cerebral cortex, hippocampus and cerebellum but without associated cognitive decline: p62

- proteinopathy. *Neuropathology* 2012;32:505-14. <http://dx.doi.org/10.1111/j.1440-1789.2011.01286.x>.
- [45] Mackenzie IRA, Frick P, Neumann M. The neuropathology associated with repeat expansions in the C9ORF72 gene. *Acta Neuropathol* 2014;127:347-57. <http://dx.doi.org/10.1007/s00401-013-1232-4>.
- [46] Forrest SL, Kril JJ, Stevens CH, Kwok JB, Hallupp M, Kim WS, et al. Retiring the term FTDP-17 as MAPT mutations are genetic forms of sporadic frontotemporal tauopathies. *Brain* 2018;141:521-34. <http://dx.doi.org/10.1093/brain/awx328>.
- [47] Pickering-Brown S, Baker M, Bird T, Trojanowski J, Lee V, Morris H, et al. Evidence of a founder effect in families with frontotemporal dementia that harbor the tau + 16 splice mutation. *Am J Med Genet* 2004;125B:79-82. <http://dx.doi.org/10.1002/ajmg.b.20083>.
- [48] Pickering-Brown SM. The complex aetiology of frontotemporal lobar degeneration. *Exp Neurol* 2007;206:1-10. <http://dx.doi.org/10.1016/j.expneurol.2007.03.017>.
- [49] Ghetti B, Oblak AL, Boeve BF, Johnson KA, Dickerson BC, Goedert M. Invited review: frontotemporal dementia caused by microtubule-associated protein tau gene (MAPT) mutations: a chameleon for neuropathology and neuroimaging. *Neuropathol Appl Neurobiol* 2015;41:24-46. <http://dx.doi.org/10.1111/nan.12213>.
- [50] van Swieten J, Spillantini MG. Hereditary frontotemporal dementia caused by tau gene mutations. *Brain Pathology* 2007;17:63-73. <http://dx.doi.org/10.1111/j.1750-3639.2007.00052.x>.
- [51] Henz S, Ackl N, Knels C, Rominger A, Flatz W, Teipel S, et al. A pair of siblings with a rare R5H-Mutation in Exon 1 of the MAPT-Gene. *Fortschr Neurol Psychiatr* 2015;83:397-401. <http://dx.doi.org/10.1055/s-0035-1553236>.
- [52] Benajiba L, Le Ber I, Camuzat A, Lacoste M, Thomas-Anterion C, Couratier P, et al. TARDBP mutations in motoneuron disease with frontotemporal lobar degeneration. *Ann Neurol* 2009;65:470-3. <http://dx.doi.org/10.1002/ana.21612>.
- [53] Freischmidt A, Wieland T, Richter B, Ruf W, Schaeffer V, Müller K, et al. Haploinsufficiency of TBK1 causes familial ALS and fronto-temporal dementia. *Nat Neurosci* 2015;18:631-6. <http://dx.doi.org/10.1038/nn.4000>.
- [54] Caroppo P, Camuzat A, Guillot-Noel L, Thomas-Anterion C, Couratier P, Wong TH, et al. Defining the spectrum of frontotemporal dementias associated with TARDBP mutations. *Neurol Genet* 2016;2:e80. <http://dx.doi.org/10.1212/NXG.000000000000080>.
- [55] Caroppo P, Camuzat A, De Septenville A, Couratier P, Lacomblez L, Auriacombe S, et al. Semantic and nonfluent aphasic variants, secondarily associated with amyotrophic lateral sclerosis, are predominant frontotemporal lobar degeneration phenotypes in TBK1 carriers. *Alzheimer Dement* 2015;1:481-6. <http://dx.doi.org/10.1016/j.dadm.2015.10.002>.
- [56] Perrone F, Nguyen HP, Van Mossevelde S, Moisse M, Sieben A, Santens P, et al. Investigating the role of ALS genes CHCHD10 and TUBA4A in Belgian FTD-ALS spectrum patients. *Neurobiol Aging* 2017;51:177.e9-177.e16. <http://dx.doi.org/10.1016/j.neurobiolaging.2016.12.008>.
- [57] Skibinski G, Parkinson NJ, Brown JM, Chakrabarti L, Lloyd SL, Hummerich H, et al. Mutations in the endosomal ESCRTIII-complex subunit CHMP2B in frontotemporal dementia. *Nat Genet* 2005;37:806-8. <http://dx.doi.org/10.1038/ng1609>.
- [58] Svetoni F, Frisone P, Paronetto MP. Role of FET proteins in neurodegenerative disorders. *RNA Biol* 2016;13:1089-102. <http://dx.doi.org/10.1080/15476286.2016.1211225>.
- [59] Al-Obeidi E, Al-Tahan S, Surampalli A, Goyal N, Wang AK, Hermann A, et al. Genotype-phenotype study in patients with valosin-containing protein mutations associated with multisystem proteinopathy. *Clin Genet* 2018;93:119-25. <http://dx.doi.org/10.1111/cge.13095>.
- [60] Watts GDJ, Wymer J, Kovach MJ, Mehta SG, Mumm S, Darvish D, et al. Inclusion body myopathy associated with Paget disease of bone and frontotemporal dementia is caused by mutant valosin-containing protein. *Nat Genet* 2004;36:377-81. <http://dx.doi.org/10.1038/ng1332>.
- [61] Le Ber I. SQSTM1 Mutations in French Patients With Frontotemporal Dementia or Frontotemporal Dementia With Amyotrophic Lateral Sclerosis. *JAMA Neurol* 2013. <http://dx.doi.org/10.1001/jamaneurol.2013.3849>.
- [62] Kim HJ, Kim NC, Wang Y-D, Scarborough EA, Moore J, Diaz Z, et al. Mutations in prion-like domains in hnRNPA2B1 and hnRNPA1 cause multisystem proteinopathy and ALS. *Nature* 2013;495:467-73. <http://dx.doi.org/10.1038/nature11922>.
- [63] Rademakers R, Baker, Matt, Nicholson, Alexandra M, Rutherford, et al. Mutations in the colony stimulating factor 1 receptor (CSF1R) gene cause hereditary diffuse leukoencephalopathy with spheroids. *Nature Genetics* 2012;44:8. <http://dx.doi.org/10.1038/ng.1027>.
- [64] Konno T, Yoshida K, Mizuno T, Kawarai T, Tada M, Nozaki H, et al. Clinical and genetic characterization of adult-onset leukoencephalopathy with axonal spheroids and pigmented glia associated with CSF1R mutation. *Eur J Neurol* 2017;24:37-45. <http://dx.doi.org/10.1111/ene.13125>.
- [65] Guerreiro R, Kara E, Le Ber I, Bras J, Rohrer JD, Taipa R, et al. Genetic Analysis of Inherited Leukodystrophies: Genotype-Phenotype Correlations in the CSF1R Gene. *JAMA Neurol* 2013;70:875. <http://dx.doi.org/10.1001/jamaneurol.2013.698>.
- [66] Kim E-J, Kim Y-E, Jang J-H, Cho E-H, Na DL, Seo SW, et al. Analysis of frontotemporal dementia, amyotrophic lateral sclerosis, and other dementia-related genes in 107 Korean patients with frontotemporal dementia. *Neurobiol Aging* 2018;72:186. <http://dx.doi.org/10.1016/j.neurobiolaging.2018.06.031> [e1-186.e7].
- [67] Codjia P, Ayrygnac X, Mochel F, Mouzat K, Carra-Dalliere C, Castelnuovo G, et al. Adult-Onset Leukoencephalopathy with Axonal Spheroids and Pigmented Glia: An MRI Study of 16 French Cases. *AJNR Am J Neuroradiol* 2018;39:1657-61. <http://dx.doi.org/10.3174/ajnr.A5744>.
- [68] Chausseant A, Le Ber I, Ait-El-Mkadem S, Camuzat A, de Septenville A, Bannwarth S, et al. Screening of CHCHD10 in a French cohort confirms the involvement of this gene in frontotemporal dementia with amyotrophic lateral sclerosis patients. *Neurobiol Aging* 2014;35:2884. <http://dx.doi.org/10.1016/j.neurobiolaging.2014.07.022> [e1-2884.e4].
- [69] Wider C, Dachsel JC, Farrer MJ, Dickson DW, Tsuboi Y, Wszolek ZK. Elucidating the genetics and pathology of Perry syndrome. *J Neurol Sci* 2010;289:149-54. <http://dx.doi.org/10.1016/j.jns.2009.08.044>.
- [70] Peplonska B, Berdyski M, Mandecka M, Barczak A, Kuzma-Kozakiewicz M, Barcikowska M, et al. TREM2 variants in neurodegenerative disorders in the Polish population. Homozygosity and compound heterozygosity in FTD patients. *Amyotro Later Scler and Frontotemp Degen* 2018;19:407-12. <http://dx.doi.org/10.1080/21678421.2018.1451894>.
- [71] Goldman JS, Van Deerlin VM. Alzheimer's disease and frontotemporal dementia: the current state of genetics and genetic testing since the advent of next-generation sequencing. *Mol Diagn Ther* 2018;22:505-13. <http://dx.doi.org/10.1007/s40291-018-0347-7>.
- [72] Richards S, Aziz N, Bale S, Bick D, Das S, Gastier-Foster J, et al. Standards and guidelines for the interpretation of sequence variants: a joint consensus recommendation of the American College of Medical Genetics and Genomics and the Association for Molecular Pathology. *Genet Med* 2015;17:405-23. <http://dx.doi.org/10.1038/gim.2015.30>.

- [73] Saracino D, Sellami L, Clot F, Camuzat A, Lamari F, Rucheton B, et al. The missense p.Trp7Arg mutation in GRN gene leads to progranulin haploinsufficiency. *Neurobiology of Aging* 2020;85:154.e9–154.e11. <http://dx.doi.org/10.1016/j.neurobiolaging.2019.06.002>.
- [74] Pottier C, Bieniek KF, Finch N, van de Vorst M, Baker M, Perkersen R, et al. Whole-genome sequencing reveals important role for TBK1 and OPTN mutations in frontotemporal lobar degeneration without motor neuron disease. *Acta Neuropathol* 2015;130:77–92. <http://dx.doi.org/10.1007/s00401-015-1436-x>.
- [75] She A, Kurtser I, Reis SA, Hennig K, Lai J, Lang A, et al. Selectivity and Kinetic Requirements of HDAC inhibitors as progranulin enhancers for treating frontotemporal dementia. *Cell Chem Biol* 2017;24:892–906. <http://dx.doi.org/10.1016/j.chembiol.2017.06.010> [e5].
- [76] Lee WC, Almeida S, Prudencio M, Caulfield TR, Zhang Y-J, Tay WM, et al. Targeted manipulation of the sortilin–progranulin axis rescues progranulin haploinsufficiency. *Hum Mol Genet* 2014;23:1467–78. <http://dx.doi.org/10.1093/hmg/ddt534>.
- [77] Sha SJ, Miller ZA, Min S, Zhou Y, Brown J, Mitic LL, et al. An 8-week, open-label, dose-finding study of nimodipine for the treatment of progranulin insufficiency from GRN gene mutations. *Alzheimer Dement* 2017;3:507–12. <http://dx.doi.org/10.1016/j.trci.2017.08.002>.
- [78] Alberici A, Archetti S, Pilotto A, Premi E, Cosseddu M, Bianchetti A, et al. Results from a pilot study on amiodarone administration in monogenic frontotemporal dementia with granulin mutation. *Neurol Sci* 2014;35:1215–9. <http://dx.doi.org/10.1007/s10072-014-1683-y>.
- [79] Tabrizi SJ, Leavitt BR, Landwehrmeyer GB, Wild EJ, Saft C, Barker RA, et al. Targeting huntingtin expression in patients with Huntington’s disease. *N Engl J Med* 2019;380:2307–16. <http://dx.doi.org/10.1056/NEJMoa1900907>.
- [80] Finkel RS, Mercuri E, Darras BT, Connolly AM, Kuntz NL, Kirschner J, et al. Nusinersen versus sham control in infantile-onset spinal muscular atrophy. *N Engl J Med* 2017;377:1723–32. <http://dx.doi.org/10.1056/NEJMoa1702752>.
- [81] Jiang J, Zhu Q, Gendron TF, Saberi S, McAlonis-Downes M, Seelman A, et al. Gain of toxicity from ALS/FTD-linked repeat expansions in C9ORF72 is alleviated by antisense oligonucleotides targeting GGGGCC-containing RNAs. *Neuron* 2016;90:535–50. <http://dx.doi.org/10.1016/j.neuron.2016.04.006>.
- [82] Boxer AL, Qureshi I, Ahljanian M, Grundman M, Golbe LI, Litvan I, et al. Safety of the tau-directed monoclonal antibody BIIB092 in progressive supranuclear palsy: a randomised, placebo-controlled, multiple ascending dose phase 1b trial. *Lancet Neurol* 2019;18:549–58. [http://dx.doi.org/10.1016/S1474-4422\(19\)30139-5](http://dx.doi.org/10.1016/S1474-4422(19)30139-5).
- [83] Bateman RJ, Xiong C, Benzinger TLS, Fagan AM, Goate A, Fox NC, et al. Clinical and biomarker changes in dominantly inherited Alzheimer’s disease. *N Engl J Med* 2012;367:795–804. <http://dx.doi.org/10.1056/NEJMoa1202753>.
- [84] Rohrer JD, Nicholas JM, Cash DM, van Swieten J, Dopper E, Jiskoot L, et al. Presymptomatic cognitive and neuroanatomical changes in genetic frontotemporal dementia in the Genetic Frontotemporal dementia Initiative (GENFI) study: a cross-sectional analysis. *Lancet Neurol* 2015;14:253–62. [http://dx.doi.org/10.1016/S1474-4422\(14\)70324-2](http://dx.doi.org/10.1016/S1474-4422(14)70324-2).
- [85] Boeve B, Bove J, Brannelly P, Brushaber D, Coppola G, Dever R, et al. The longitudinal evaluation of familial frontotemporal dementia subjects protocol: Framework and methodology. *Alzheimer Dement* 2020;16:22–36. <http://dx.doi.org/10.1016/j.jalz.2019.06.4947>.
- [86] Caroppo P, Habert M-O, Durrleman S, Funkiewiez A, Perlberg V, Hahn V, et al. Lateral temporal lobe: an early imaging marker of the presymptomatic GRN disease? *J Alzheimers Dis* 2015;47:751–9. <http://dx.doi.org/10.3233/JAD-150270>.
- [87] Bertrand A, Wen J, Rinaldi D, Houot M, Sayah S, Camuzat A, et al. Early cognitive, structural, and microstructural changes in presymptomatic C9orf72 carriers younger than 40 years. *JAMA Neurol* 2018;75:236. <http://dx.doi.org/10.1001/jamaneurol.2017.4266>.
- [88] Jiskoot LC, Panman JL, van Asseldonk L, Franzen S, Meeter LHH, Donker Kaat L, et al. Longitudinal cognitive biomarkers predicting symptom onset in presymptomatic frontotemporal dementia. *J Neurol* 2018;265:1381–92. <http://dx.doi.org/10.1007/s00415-018-8850-7>.
- [89] Jiskoot LC, Panman JL, Meeter LH, Dopper EGP, Donker Kaat L, Franzen S, et al. Longitudinal multimodal MRI as prognostic and diagnostic biomarker in presymptomatic familial frontotemporal dementia. *Brain* 2019;142:193–208. <http://dx.doi.org/10.1093/brain/awy288>.
- [90] van der Ende EL, Meeter LH, Poos JM, Panman JL, Jiskoot LC, Dopper EGP, et al. Serum neurofilament light chain in genetic frontotemporal dementia: a longitudinal, multicentre cohort study. *Lancet Neurol* 2019;18:1103–11. [http://dx.doi.org/10.1016/S1474-4422\(19\)30354-0](http://dx.doi.org/10.1016/S1474-4422(19)30354-0).
- [91] Galimberti D, Fumagalli GG, Fenoglio C, Cioffi SMG, Arighi A, Serpente M, et al. Progranulin plasma levels predict the presence of GRN mutations in asymptomatic subjects and do not correlate with brain atrophy: results from the GENFI study. *Neurobiol Aging* 2018;62:245. <http://dx.doi.org/10.1016/j.neurobiolaging.2017.10.016> [e9-245.e12].



Available online at
ScienceDirect
www.sciencedirect.com

Elsevier Masson France
EM|consulte
www.em-consulte.com



International meeting of the French society of neurology 2022

How can we define the presymptomatic C9orf72 disease in 2022? An overview on the current definitions of preclinical and prodromal phases

D. Saracino ^{a,b,c,*}, I. Le Ber ^{a,b}

^a Sorbonne Université, Paris Brain Institute–Institut du Cerveau–ICM, Inserm U1127, CNRS UMR 7225, AP-HP - Hôpital Pitié-Salpêtrière, Paris, France

^b Reference Centre for Rare or Early Dementias, IM2A, Département de Neurologie, AP-HP–Hôpital Pitié-Salpêtrière, Paris, France

^c Aramis Project Team, Inria Research Center of Paris, Paris, France

INFO ARTICLE

Article history:

Received 20 January 2022

Accepted 8 March 2022

Available online 5 May 2022

Keywords:

Frontotemporal dementia

Frontotemporal lobar degeneration

Amyotrophic lateral sclerosis

C9orf72

Biomarker

Presymptomatic disease

ABSTRACT

Repeat expansions in C9orf72 gene are the main genetic cause of frontotemporal dementia, amyotrophic lateral sclerosis and related phenotypes. With the advent of disease-modifying treatments, the presymptomatic disease phase is getting increasing interest as an ideal time window in which innovant therapeutic approaches could be administered. Recommendations issued from international study groups distinguish between a preclinical disease stage, during which lesions accumulate in absence of any symptoms or signs, and a prodromal stage, marked by the appearance the first subtle cognitive, behavioral, psychiatric and motor signs, before the full-blown disease. This paper summarizes the current definitions and criteria for these stages, in particular focusing on how fluid-based, neuroimaging and cognitive biomarkers can be useful to monitor disease trajectory across the presymptomatic phase, as well as to detect the earliest signs of clinical conversion. Continuous advances in the knowledge of C9orf72 pathophysiology, and the integration of biomarkers in the clinical evaluation of mutation carriers will allow a better diagnostic definition of C9orf72 disease spectrum from the earliest stages, with relevant impact on the possibility of disease prevention.

© 2022 Elsevier Masson SAS. All rights reserved.

* Corresponding author. Paris Brain Institute - Institut du Cerveau (ICM), AP-HP - Hôpital Pitié-Salpêtrière, 47-83 boulevard de l'Hôpital, 75013 Paris, France.

E-mail address: dario.saracino@icm-institute.org (D. Saracino).

<https://doi.org/10.1016/j.neurol.2022.03.007>

0035-3787/© 2022 Elsevier Masson SAS. All rights reserved.

1. Introduction

Frontotemporal dementia (FTD) and amyotrophic lateral sclerosis (ALS) are neurodegenerative diseases lying along a clinical continuum and sharing common pathophysiological and genetic mechanisms. One of the most relevant advances in the understanding of how these two diseases are related has been the identification, in 2011, of a hexanucleotide repeat expansion in *C9orf72* in families concerned by FTD, ALS, or the combination of the two [1,2].

C9orf72 expansions turned out to be the most frequent cause of genetic FTD and ALS in most countries, explaining up to 25% of familial FTD cases and around 40% of familial ALS cases [3–5]. When both disorders coexist, *C9orf72* expansions can be found in up to 80% of cases [3,4]. Besides, they can occur also in FTD or ALS patients without overt family history of neurodegenerative diseases, at a frequency estimated between 6% and 20% [5,6] thus underscoring the importance of genetic testing even in apparently sporadic cases. Notably, no such overlap exists with other relatively frequent genes after *C9orf72*, such as progranulin gene (*GRN*) and microtubule associated protein tau gene (*MAPT*), identified in FTD phenotypes, or superoxide dismutase 1 (*SOD1*), responsible of pure ALS. Less common disease-causing genes can be involved in both cognitive, motor, or complex phenotypes [7].

The age at onset in *C9orf72* disease is extremely variable, ranging between the 2nd and the 9th decade, with a peak at 58 years [8]. There is increasing evidence about the heterogeneity of clinical phenotypes, encompassing cognitive, behavioral and motor syndromes. In addition to the behavioral variant of FTD (bvFTD), ALS and the association FTD/ALS, *C9orf72* patients may occasionally present with psychiatric phenotypes, mainly qualifying as atypical, late-onset psychoses [9–11]. Less common presentations, identifiable in less than 5% of carriers, include primary progressive aphasia (PPA) variants [8,12], and parkinsonian syndromes (corticobasal syndrome, progressive supranuclear palsy, and, rarely, typical parkinsonism) [13–15].

Knowledge about the implications of *C9orf72* repeat expansion in disease pathophysiology has been continuously increasing since the discovery of the gene. The first intron of *C9orf72* contains a G₄C₂ sequence which in healthy individuals mostly ranges between two and eight repeats, and in any case below 30, which has been conventionally fixed as a pathogenic threshold [2,16]. The majority of affected individuals carry a pathologic expansion in the range of hundreds or thousands of repeats [9]; interestingly, the repeat length does not significantly affect the disease phenotype or the age at onset [17]. In addition, expansions of intermediate length (between 20 and 30 repeats), have been suggested to increase the risk of developing parkinsonian syndromes or ALS [18,19]. The biological functions of the C9ORF72 protein are not completely understood, but it has been determined to act as a GTPase activating protein (GAP), in partnership with two other subunits [20].

Three main pathogenic mechanisms have been hypothesized in *C9orf72*-associated disease, including loss of physiological role of C9ORF72 protein, accumulation of RNA foci in the nuclei and toxicity from dipeptide repeat proteins (DPR)

generated from repeat-associated non-ATG (RAN) translation [21]. Hence, RNA foci and cytoplasmic DPRs accumulations coupled with p62-positive inclusions represent pathological hallmarks specific to *C9orf72* disease, in addition to diffuse neuronal and oligodendroglial TDP-43 positive inclusions [22,23].

Insights in the disease mechanisms have paved the way to the development of disease-modifying treatments, mainly acting to contrast the deleterious effect of the *C9orf72* expansion. Among them, one of the most developed so far consists of antisense oligonucleotides (ASOs), small DNA or RNA molecules binding to a complementary RNA sequence and leading to its degradation, thus modulating gene expression [24]. Phase I and II trials targeting *C9orf72*-associated FTD and ALS have started in recent years (www.clinicaltrials.gov NCT03626012, NCT04288856, NCT04931862, NCT04993755). These interventions should be eventually developed to block the pathological cascade and, ideally, prevent or significantly delay the occurrence of clinical symptoms. Therefore, the presymptomatic disease phase is getting more and more interest as an ideal time window in which innovant therapeutic – or rather preventive – approaches should be tested. At present, the definitions and the time references of the presymptomatic phase, as well as the tools of choice for the longitudinal monitoring of the disease trajectory are a matter of intensive research. This review provides an overview on the current knowledge about the presymptomatic phase of the *C9orf72* disease, particularly focusing on: i) the proposed classification of presymptomatic stages; ii) the contribution of biomarkers to trace preclinical disease trajectory; and iii) the earliest clinically relevant changes associated with disease onset, and their interest in ongoing and future clinical trials tackling *C9orf72*-associated pathology.

2. Current framework for defining the presymptomatic disease stages

At present there is limited information about the sequential ordering of events occurring in FTD and ALS before clinical onset. In the field of neurodegenerative diseases, studies focusing on Alzheimer's disease (AD), particularly in its monogenic forms, have substantially contributed to define the concept of a presymptomatic disease stage, characterized by progressive lesion accumulation [25–27], up to a prodromal, oligosymptomatic stage defined as mild cognitive impairment (MCI) [28]. In Huntington's disease (HD), longitudinal studies on presymptomatic carriers allowed to depict the progressive changes occurring during the pre-manifest phase, with the useful contribution of repeat length and other genetic modifiers in the prediction of the age at onset [29–31].

In the case of FTD and ALS, a privileged point of view to study the presymptomatic phase is offered by carriers of disease-causative mutations, identified among first-degrees relatives of genetic patients. Over the recent years, international consortia have been built to assemble and study large cohorts of presymptomatic carriers in a standardized manner, to increase our knowledge on presymptomatic stage. The Genetic Frontotemporal Initiative (GENFI), has been developed

in Europe and Canada (www.genfi.org), and the ARTFL (Advancing Research and Treatment in Frontotemporal Lobar degeneration) and LEFFTDS (Longitudinal Evaluation of Familial FrontoTemporal Dementia Subjects) (www.allftd.org), as well as the presymptomatic familial ALS (Pre-fALS) study [32], have been initiated in US. Besides, multiple national initiatives have assembled country-based cohorts, such as the Australian DINAD (Dominantly Inherited Non-Alzheimer Dementias, www.ecdc.org.au/genetic-ftd-trials); the New Zealand Genetic FTD (FTDGeNZ) [33], the French PREV-DEMALS and Predict-PGRN [34,35] cohorts, the Belgian presymptomatic *C9orf72* cohort [36], and the Multi-partner Consortium to expand Dementia Research in Latin America (ReDLat) [37]. All these initiatives highlight the important challenge and critical need to better characterize this stage of the disease.

Overall, research results coming from the abovementioned initiatives contributed to generate a conceptual framework useful to define and further classify the presymptomatic phases of FTD and ALS, which could be thus employed in the context of *C9orf72* expansions, responsible for both of these diseases. Key recommendations have been recently defined in the works by Benussi et al. (2021) [38] and Benatar et al. (2021) [39], and are summarized below (Fig. 1).

The **preclinical disease stage** defines the period between the start of the neurodegenerative process and the appearance of the first signs and symptoms of disease. Theoretically, with *C9orf72* expansions this phase should correspond to progressive accumulation of DPR proteins, RNA foci and, sequentially, TDP-43 pathology [40,41]. However, the limited information obtainable from pathological biomarkers in vivo does not allow to determine how early these degenerative changes occur. Therefore, it is currently unclear whether a “no disease” stage, characterized by the absence of any pathological lesions exists, and the boundary between this latter and the subsequent preclinical phase is particularly hard to identify [38]. During the preclinical stage, clinical symptoms are completely absent, and no ongoing denervation changes should be found on electromyography (EMG) [39]. Different

biomarkers can variably contribute to inform on preclinical disease trajectory, as it will be discussed further [36,42].

The **prodromal disease stage** is defined by the appearance of the first subtle cognitive, behavioral and motor signs, and lasts up to the onset of full-blown disease. Prodromal FTD is characterized by gradual changes affecting social cognition, executive functions or language, as well as recent behavioral modifications including reduced initiative, diminished empathy, change in dietary habits, repetitive or ritualized actions or behaviors [38]. These changes from the individual’s baseline status should be of such intensity as to preserve independence in daily living, albeit a mild impact on close relationships or highly demanding professional tasks cannot be excluded [38]. From a quantitative approach, the Clinical Dementia Rating (CDR) plus National Alzheimer’s Disease Coordinating Center (NACC) Frontotemporal Lobar Degeneration (FTLD) rating scale (CDR + NACC FTLD) is one of the tools of choice to score the severity of symptoms in FTD patients [43,44]. Preclinical, asymptomatic stage is defined by a CDR + NACC FTLD global score equal to 0, whereas prodromal subjects should present a score of 0.5. Prodromal ALS is characterized by mild motor complaints (cramps, early fatigue), subtle signs at neurological examination (fasciculations, changes in reflexes) or isolated EMG signs of ongoing denervation, without overt muscular weakness. Phenotransition is the term proposed by the ALS community to indicate the passage from the preclinical to the prodromal stage [39].

Overall, to account for the heterogeneity of the cognitive/clinical manifestations of the prodromal stage, especially with the occurrence of *C9orf72* expansions, the unifying concept of mild cognitive/behavioral/motor impairment (MCBMI) has been proposed [38]. However, several confounding factors should be ruled out before affirming that a MCBMI is due to underlying FTD or ALS. Cognitive impairment, especially affecting domains which are atypical for FTD, could result from degenerative processes unrelated to mutational status, as well as from non-degenerative conditions (cerebrovascular lesions or sleep disturbances among many others). Subtle changes in behavior or personality are not specific for FTD, and

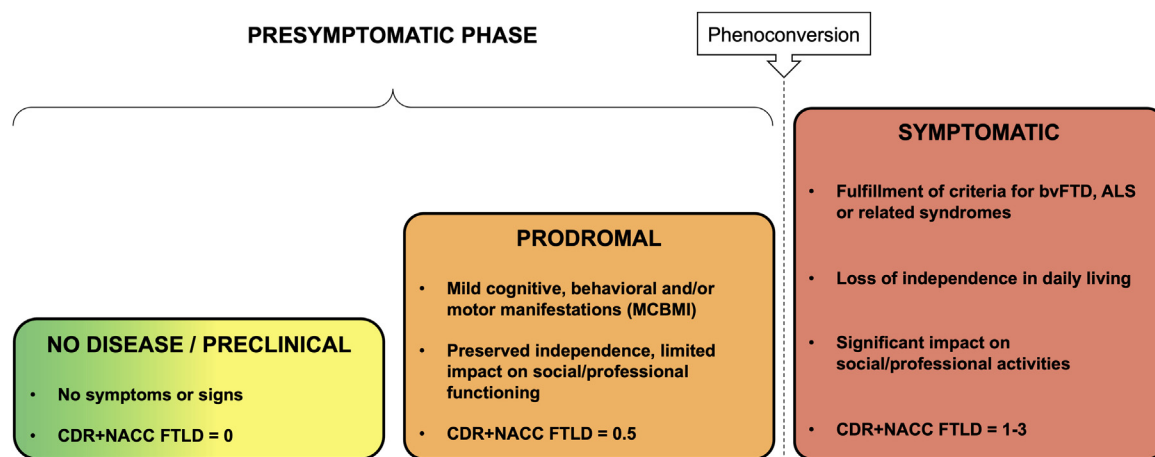


Fig. 1 – Overview on the presymptomatic and symptomatic stages in *C9orf72* disease. ALS: amyotrophic lateral sclerosis; bvFTD: behavioral variant of frontotemporal dementia; CDR + NACC FTLD: Clinical Dementia Rating plus National Alzheimer’s Disease Coordinating Center Frontotemporal Lobar Degeneration (FTLD) rating scale, global score; MCBMI: mild cognitive/behavioral/motor impairment.

could derive from unrelated psychiatric conditions or substance abuse. When evaluating motor signs and symptoms, common confounding conditions such as radiculopathies should be carefully looked for. Moreover, *C9orf72* disease offers another source of uncertainty, due to the existence of long-standing psychiatric phenotypes, hardly distinguishable from primary psychiatric disorders, which could precede the onset of FTD or ALS by years or decades [45,46].

The term “phenoconversion” indicates the transition from the prodromal to the full-blown clinical stage. Clear boundaries between the two stages are barely definable, therefore some operational criteria for phenoconversion have been proposed, including: i) fulfillment of diagnostic criteria for bvFTD, PPA, ALS or other associated syndromes; ii) CDR + NACC FTL score equal or greater than 1; iii) loss of independence in daily living; iv) significant impact on social/professional activities despite preserved autonomy (e.g., because of language deficits or inappropriate social behavior) [38].

It should be kept in mind, however, that some inconsistencies may emerge when applying this general framework to individual disease carriers, because of the differences in the temporal course across distinct genotypes [8,47], the inter-individual variability in presymptomatic trajectories and the role of disease modifiers whose role is only partially understood [48,49].

3. The role of biomarkers across the presymptomatic phases

3.1. Definition and types of biomarkers

The term “biomarker” indicates an observable and measurable feature whose levels serve as objective indicators of

different physiological or pathological states, or are associated with response to therapeutic interventions [50]. In the context of presymptomatic *C9orf72* carriers, biomarkers are intended to monitor disease evolution from the presymptomatic to the full-blown stages, to predict the proximity to phenoconversion and, eventually, to serve as outcome measures in therapeutic trials [51,52]. It has to be kept in mind that the analytical variability of a biomarker should be appropriate for its context of use. For instance, during the preclinical phase an optimal disease-tracking biomarker should be sensitive enough to capture the evolution of the underlying pathophysiological cascade, which could last several years or decades. On the other hand, a valuable biomarker to predict clinical onset should stay as stable as possible in non-progressing carriers, and display clear and sustained changes close to phenoconversion. Different approaches can be used to provide biomarkers, and those which contribute the most to monitor presymptomatic *C9orf72* disease are summarized in Table 1.

3.2. Biomarkers to define the preclinical disease trajectory

As already stated, it is hard to define the beginning of lesion accumulation in most neurodegenerative diseases. However, *C9orf72* pathophysiology offers a privileged point of view, as DPR proteins, and in particular poly(GP) proteins (originated from both sense and antisense expanded transcripts) can be detectable in the cerebrospinal fluid (CSF) of asymptomatic carriers [53,54], without being associated with biomarkers of ongoing degeneration. There is a modest but significant increase of poly(GP) over time, and overall their levels are higher in patients than in presymptomatic carriers [54,55]. Autoptical studies have shown that accumulation of RNA foci and DPR-positive inclusions precede TDP-43 nuclear delocalization and cytoplasmic deposition, underscoring that these

Table 1 – Main biomarkers studied to monitor *C9orf72* disease.

Type of biomarker	Measure	Relevance	References
Fluid-based	Poly(GP) proteins (CSF)	High levels since the earliest stages	[53,54]
	NfL and NfH (CSF and plasma)	Increase in prodromal phase, ≤ 5 years before phenoconversion	[47,77–80]
	MiRNA	Altered profile, mostly in prodromal carriers	[90]
	CHIT1 (CSF)	Increase in patients	[87]
Neuroimaging	Cortical thickness, brain volumes, WM microstructure	Altered from 20–25 years before onset, slowly progressive	[35,58,62–66]
	Functional connectivity	Early salience and thalamic-seeded network dysregulation	[58,59]
	Cerebral blood flow (ASL)	Decreased from 12.5 years before onset	[104]
	Gyrification index	Congenitally reduced in <i>C9orf72</i> carriers	[109]
	Cervical spinal cord WM volume and FA	Altered metrics mostly in carriers >40 years	[73]
	FDG PET uptake	Hypometabolism consistent with structural changes	[36]
	UCB-J PET uptake	Reduced synaptic density in preclinical phase	[102]
Neuropsychological	Verbal fluencies	Reduced scores since young age	[91]
	Episodic memory	Preclinical changes reflecting executive dysfunction	[92]
	Social cognition	Deficits in late presymptomatic phase	[93]
	Cognitive inhibition	Deficits mostly in > 40 years	[94]
	Semantic knowledge	Deficits in late presymptomatic phase	[98]
	Gestural praxis	Impaired before 40 years	[35]
Neurophysiological	Cortical excitability	Increase in ALS patients	[74]

ASL: arterial spin labeling; CHIT1: chitotriosidase; FA: fractional anisotropy; FDG: fluorodeoxyglucose; miRNA: micro-RNA; NfH: neurofilament heavy chain; NfL: neurofilament light chain; UCB-J: synaptic vesicle glycoprotein 2A PET tracer; WM: white matter.

changes are more closely related to the expansion itself, than to downstream degenerative events [56].

The preclinical cascade model in AD suggests that brain metabolic changes may antedate structural modifications [26,57]. A limited number of studies have explored the role of fluorodeoxyglucose (FDG) positron emission tomography (PET) in the preclinical phase of genetic FTD; for what concerns *C9orf72* carriers, clusters of significant hypometabolism have been found in frontotemporal cortices, basal ganglia and thalami, at a time in which volume loss is already detectable [36]. However, information about temporal dynamics of these alterations is currently lacking. Similarly, few studies have investigated the potential of functional magnetic resonance imaging (fMRI) to detect functionally compensated network dysregulations in asymptomatic carriers [58,59]. Salience network and thalamic-seeded network alterations are identifiable early, and are somewhat reminiscent of what observed in *C9orf72*-associated bvFTD [58,60]. The profile of connectivity changes extends over time, spreading towards the areas mostly affected in the symptomatic phase, which could herald impending neurodegeneration [59,61].

A number of structural MRI studies elegantly depicted the profile of brain changes identifiable at different points of the preclinical phase and, more recently, investigated their rate of change over time [35,58,62–66]. Overall, *C9orf72* carriers display significant and widespread cortical volume loss compared to non-carriers, including frontal areas, temporoparietal cortices, associative parietotemporal regions, and hippocampi approximately 20 to 25 years before their estimated disease onset [35,58,62,64,66]. At the subcortical level, there is a diffuse and massive volume loss in the thalamus, with prominent involvement of the pulvinar subnucleus [65], a profile which is coherent with what observed in the clinical phase [67]. Early cerebellar involvement has been also evidenced, in particular in lobules VIIa-Crus II and VIIb, connected to the dorsolateral prefrontal cortex via the thalamus [65]. Notably, the precocity of gray matter alterations and the degree of subcortical involvement are more important in *C9orf72* carriers compared to *MAPT* or *GRN* carriers [62,65]. Individual baseline atrophy at the asymptomatic phase ($CDR + NACC\ FTDL = 0$) may be implemented in predictive models of progression towards the prodromal and clinical disease stages [68].

Gray matter changes are associated with, and often preceded by, white matter tracts degeneration. In *C9orf72* carriers, diffusion tensor imaging (DTI) analyses identified reduced fractional anisotropy (FA), a marker of microstructural integrity, in thalamic radiation, corpus callosum, frontotemporal and corticospinal tracts (CST) [35,58,63,66,69], which are critically involved in the development of FTD and ALS.

Structural changes predictably appear more pronounced and diffuse among the older carriers, namely over 40 years of age [35,66]. However, a greater progression compared to non-carriers is barely detectable [63], and only one longitudinal study found a trend towards accelerated cortical thinning in presymptomatic carriers, though not reaching statistical significance [64]. This is in line with the modest rates of atrophy observed during the clinical phase of *C9orf72* disease [70].

Spinal cord imaging features have been proposed as biomarkers for the development of ALS treatments [71], with

measurable progression throughout the disease course [72]. Presymptomatic *C9orf72* carriers display white matter atrophy at the cervical level, with progressive reduction of FA in CST occurring in individuals over 40 years old [73]. This is particularly relevant taking into account that no neurophysiological measures proved usefulness to detect motor neuron degeneration in asymptomatic *C9orf72* carriers [74].

In summary, the preclinical phase of *C9orf72* disease is marked by diffuse changes, mostly identifiable by means of neuroimaging approaches, which appear early and progress smoothly over the years. However, there is no sufficient evidence to ascertain if and how these changes could predict the subsequent clinical phenotype an individual carrier will manifest.

3.3. Biomarkers to support proximity to clinical onset

In neurodegenerative disorders, one of the most relevant contribution of biomarkers is the aid to identify those individuals who are going to develop the first symptoms and signs of the disease, hence predicting phenocconversion [26,42,75]. This information could enhance the stratification of carriers for clinical trials, and possibly provide outcome measures for treatment response [76].

Among the fluid-based biomarkers investigated for this purpose, neurofilaments turned out to be particularly useful [77–80]. Neurofilaments are structural proteins highly expressed in axons, composed of three main subunits, heavy (NfH), medium and light chain (NfL). Both NfL and NfH are released in extracellular fluids in proportion to neuronal loss in several neurological disorders, including neurodegenerative conditions [81–83]. With the development of the highly sensitive Simoa technique, neurofilament dosage can be easily performed in plasma or serum, whose levels are extremely correlated to CSF levels, thus allowing less invasive, repeatable dosages [84,85]. NfL levels in preclinical *C9orf72* carriers are comparable to controls at a group level [77,84], with steady, low-amplitude increases over the years [79,80]. NfL levels and their annualized rates of change increase during or just before the prodromal phase [47,77,79], thus allowing to identify those who are at risk of short-term progression to clinical disease, in the subsequent two to five years [78]. NfH are particularly stable during the presymptomatic phase, while mostly increasing at the moment of the phenocconversion and during the symptomatic stage [80]. Their changes occur earlier and are more pronounced in individuals displaying a phenotype of ALS [47,75].

Other proteomic biomarkers have been investigated in the presymptomatic phase of genetic FTD, including those linked to synaptic function, astrogliosis, inflammation, and complement activation [42,52,86]. Overall, levels of neuronal pentraxin 2 (NPTX2) decrease, while glial fibrillary acidic protein (GFAP) and complement proteins C3b and C1q sequentially increase, along with NfL and NfH, at the transition between presymptomatic and symptomatic FTD associated with *GRN* mutations, whereas their trajectory is much less clear for *C9orf72* expansions [42]. Preliminary evidence on novel putative biomarkers identified in the CSF of *C9orf72* patients such as chitotriosidase (CHIT1) has not been validated yet in the presymptomatic phase [87].

The expression profile of circulating miRNAs has been found to be altered in several neurodegenerative conditions [88,89]. In particular, a signature of four miRNA is dynamically altered throughout the presymptomatic and clinical phase of *C9orf72* disease, yielding an added value in the prediction of phenoconversion [90].

The transition towards the prodromal and clinical disease stage is marked by progressive cognitive and behavioral modifications, and the identification of the most appropriate neuropsychological/behavioral measures is the subject of active research. Longitudinal assessments of cognitive functions in presymptomatic cohorts of FTD mutation carriers provided information about the cognitive trajectories occurring in the main genetic groups [62]. One study showed that *C9orf72* carriers display worse scores in verbal fluencies since young age, without relevant changes over time, thus pointing towards a general neurodevelopmental disorder [91]. Episodic memory deficits have been also identified in the presymptomatic phase of *C9orf72* disease, with features more closely reflecting a profile of executive impairment rather than a true amnesic syndrome of hippocampal type [66,92].

Among the cognitive functions most closely related to FTD spectrum, social cognition and cognitive inhibition deficits mostly occur in the late presymptomatic phase and are potential predictive biomarkers of phenoconversion [93–95]. This underscores the usefulness of the Social Cognition and Emotional Assessment, shortened version, (mini-SEA) [96] and the Hayling test [97] to capture relevant, prodromal cognitive changes in *C9orf72* carriers. Additional changes observed in presymptomatic carriers include deficits in the praxis scores [35], and impairment in semantic knowledge occurring more closely to onset [98], in line with a profile of semantic dysfunction observed in some *C9orf72* patients [9,12].

As for cognitive changes, the earliest, subtle behavioral alterations, far from fulfilling bvFTD criteria, are remarkably difficult to identify. A commonly encountered difficulty is to discriminate between true new-onset behavioral changes and personality traits or attitudes which are typical of the individual and have been present for a long time. When feasible, repeated assessments with appropriate and sensitive tools, such as the Cambridge Behavioral Inventory (CBI-R) [99], could aid to provide quantitative assessments of this often elusive constellation of symptoms [62]. Among the behavioral dimensions investigated in presymptomatic *C9orf72* carriers, apathy scores are higher than controls and increase over time, predicting subsequent cognitive impairment [100].

Overall, core criteria to define the thresholds of cognitive and/or behavioral impairments that comply with a diagnosis of MCBMI due to FTD have not been defined yet, apart from a global score of CDR + NACC FTLD equal to 0.5 [38]. This useful tool presents some limitations, however, as it may not reliably identify the core symptoms attributable to prodromal FTD, and discrete cognitive and behavioral impairments (such as those found in a depressed individual showing attentional deficits) are a possible source of bias.

For carriers developing an ALS phenotype, neurophysiological biomarkers support the identification of early signs of motor neuron dysfunction. Isolated denervation signs at EMG, such as positive sharp waves in a single limb muscle or in paraspinous muscles, can indicate early lower motor neuron

degeneration, in absence of confounding factors [39]. On the other hand, increased cortical excitability at transcranial magnetic stimulation points towards upper motor neuron involvement [74]. Quantitative measures of motor unit loss, such as Motor Unit Number Index (MUNIX) at EMG, only investigated at the clinical stage so far [101], could represent a promising approach to better define prodromal ALS.

Finally, other biomarker modalities have contributed to illustrate different pathophysiological changes occurring in the presymptomatic phase of *C9orf72* disease, and it is possible that their use will be extended to investigational protocols in the upcoming years. These include a reduction of synaptic density in thalamic and frontotemporal regions observed with UCB-J PET [102], executive oculomotor abnormalities at video-oculographic examination [103], and progressive changes in cerebral blood flow measured by arterial spin labeling (ASL) MRI sequences [104].

4. Long-standing psychopathological and personality features in *C9orf72* carriers blur the definition of prodromal stage

One of the difficulties in defining the prodromal stage in *C9orf72* carriers is due to the frequent presence of a prominent psychopathological, rather than cognitive, symptomatology at disease onset. Patients with *C9orf72*-associated bvFTD often show a constellation of psychiatric symptoms and syndromes [4,105–107], which can be inaugural of the cognitive disorder. Even more noteworthy, a subset of *C9orf72* carriers may present with isolated psychiatric phenotypes preceding dementia onset by several years or decades [46]. These are usually young adult individuals displaying psychotic syndromes, starting usually at a later age compared to primary psychiatric disorders [10,45,46]. The usually long disease history, in the absence of patent biomarkers of neuronal loss [45,79], favors the hypothesis of a dysfunctional brain disorder, eventually resulting in a degenerative syndrome. Other psychiatric disturbances display increased frequency among the presymptomatic *C9orf72* carriers, including mania [45], depression, substance abuse/dependence, and post-traumatic stress disorder [108]. Collectively, these findings point to life-long psychiatric vulnerability in the presence of the *C9orf72* expansion.

This susceptibility could also translate into several atypical behavioral and personality features present since early life, including fixed behavioral patterns, reduced empathy, tendency to hoarding and excessive sporting [107]. The importance of recognizing these traits in presymptomatic carriers is two-fold: first, it provides a baseline behavioral assessment to be accounted for when evaluating the occurrence of relevant behavioral changes in the prodromal or manifest disease stage; second, it draws attention on the impact *C9orf72* expansion may have on brain development and maturation. This is of fundamental importance to correctly define the age of disease onset in patients.

The presence of long-standing structural signatures in the brains of *C9orf72* carriers, changing little over the years [58,91,109,110], provides additional evidence in favor of a neurodevelopmental hypothesis. The identification of low

gyrification, index of immature cortical development, in the regions which are commonly atrophied during the disease also suggests that these abnormalities might confer vulnerability to future degeneration [109]. This is in line with the proposed role for C9ORF72 protein in nervous system maturation and synaptic modeling [111,112].

Overall, several lines of evidence support an influence of C9orf72 repeat expansion on the brain which extends beyond the promotion of neurodegeneration, and the boundaries between developmental and degenerative manifestations appear to be quite blurred. The existence of international initiatives such as the Neuropsychiatric International Consortium on FTD (NIC-FTD) will hopefully expand the knowledge on these dimensions of the disease and raise clinicians' awareness of atypical presentations occurring with C9orf72.

5. Conclusion

Research on genetic FTD and ALS is progressing at an impressive pace. In particular, major advances have been made in the understanding of the pathophysiology of C9orf72 disease since the discovery of the gene, and the events occurring in the presymptomatic phase have been partially elucidated. A shared conceptual framework, and the major acquisitions on the use of biomarkers, are undoubtedly helpful for clinicians and researchers to stratify presymptomatic carriers according to their presumed proximity to disease onset. Some unresolved issues still remain, notably for what concerns the translation of evidence collected from large cohort studies to the individual level for clinical purposes. The implementation of those concepts in current practice could hopefully contribute to overcome these obstacles. Additionally, a revision of the currently adopted diagnostic criteria shall be considered, aiming to capture also earlier and milder forms, with obvious impact on disease prevention.

Disclosure of interests

I.L.B. served as a member of advisory boards for Prevail Therapeutics, Denali Therapeutics and Alector, and received research grants from ANR, DGOS, Vaincre Alzheimer Association, ARSla Association, Fondation Plan Alzheimer, JPND outside of the present work.

REFERENCES

- [1] DeJesus-Hernandez M, Mackenzie IR, Boeve BF, Boxer AL, Baker M, Rutherford NJ, et al. Expanded GGGGCC hexanucleotide repeat in noncoding region of C9ORF72 causes chromosome 9p-Linked FTD and ALS. *Neuron* 2011;72:245–56. <http://dx.doi.org/10.1016/j.neuron.2011.09.011>.
- [2] Renton AE, Majounie E, Waite A, Simón-Sánchez J, Rollinson S, Gibbs JR, et al. A hexanucleotide repeat expansion in C9ORF72 is the cause of chromosome 9p21-linked ALS-FTD. *Neuron* 2011;72:257–68. <http://dx.doi.org/10.1016/j.neuron.2011.09.010>.
- [3] Majounie E, Renton AE, Mok K, Doppler EG, Waite A, Rollinson S, et al. Frequency of the C9orf72 hexanucleotide repeat expansion in patients with amyotrophic lateral sclerosis and frontotemporal dementia: a cross-sectional study. *Lancet Neurol* 2012;11:323–30. [http://dx.doi.org/10.1016/S1474-4422\(12\)70043-1](http://dx.doi.org/10.1016/S1474-4422(12)70043-1).
- [4] Le Ber, Guillot-Noel L, Hannequin D, Lacomblez L, Golfier V, Puel M, et al. C9ORF72 repeat expansions in the frontotemporal dementias spectrum of diseases: a flow-chart for genetic testing. *J Alzheimers Dis* 2013;34:485–99. <http://dx.doi.org/10.3233/JAD-121456>.
- [5] Cammack AJ, Atassi N, Hyman T, van den Berg LH, Harms M, Baloh RH, et al. Prospective natural history study of C9orf72 ALS clinical characteristics and biomarkers. *Neurology* 2019. <http://dx.doi.org/10.1212/WNL.0000000000008359>.
- [6] Mahoney CJ, Beck J, Rohrer JD, Lashley T, Mok K, Shakespeare T, et al. Frontotemporal dementia with the C9ORF72 hexanucleotide repeat expansion: clinical, neuroanatomical and neuropathological features. *Brain* 2012;135:736–50. <http://dx.doi.org/10.1093/brain/awr361>.
- [7] Sellami L, Saracino D, Le Ber I. Genetic forms of frontotemporal lobar degeneration: current diagnostic approach and new directions in therapeutic strategies. *Rev Neurol (Paris)* 2020;2020. <http://dx.doi.org/10.1016/j.neurol.2020.02.008>. S0035378720305105.
- [8] Moore KM, Nicholas J, Grossman M, McMillan CT, Irwin DJ, Massimo L, et al. Age at symptom onset and death and disease duration in genetic frontotemporal dementia: an international retrospective cohort study. *Lancet Neurol* 2020;19:145–56. [http://dx.doi.org/10.1016/S1474-4422\(19\)30394-1](http://dx.doi.org/10.1016/S1474-4422(19)30394-1).
- [9] Snowden JS, Rollinson S, Thompson JC, Harris JM, Stopford CL, Richardson AMT, et al. Distinct clinical and pathological characteristics of frontotemporal dementia associated with C9ORF72 mutations. *Brain* 2012;135:693–708. <http://dx.doi.org/10.1093/brain/awr355>.
- [10] Galimberti D, Fenoglio C, Serpente M, Villa C, Bonsi R, Arighi A, et al. Autosomal dominant frontotemporal lobar degeneration due to the C9ORF72 hexanucleotide repeat expansion: late-onset psychotic clinical presentation. *Biol Psychiatry* 2013;74:384–91. <http://dx.doi.org/10.1016/j.biopsych.2013.01.031>.
- [11] Devenney EM, Ahmed RM, Halliday G, Piguat O, Kiernan MC, Hodges JR. Psychiatric disorders in C9orf72 kindreds: study of 1,414 family members. *Neurology* 2018;91:e1498–507. <http://dx.doi.org/10.1212/WNL.0000000000006344>.
- [12] Saracino D, Géraudie A, Remes AM, Ferrieux S, Noguès-Lassialle M, Bottani S, et al. Primary progressive aphasia associated with C9orf72 expansions: another side of the story. *Cortex* 2021;145:145–59. <http://dx.doi.org/10.1016/j.cortex.2021.09.005>.
- [13] Boeve BF, Boylan KB, Graff-Radford NR, DeJesus-Hernandez M, Knopman DS, Pedraza O, et al. Characterization of frontotemporal dementia and/or amyotrophic lateral sclerosis associated with the GGGGCC repeat expansion in C9ORF72. *Brain* 2012;135:765–83. <http://dx.doi.org/10.1093/brain/aww004>.
- [14] Gasca-Salas C, Masellis M, Khoo E, Shah BB, Fisman D, Lang AE, et al. Characterization of movement disorder phenomenology in genetically proven, familial frontotemporal lobar degeneration: a systematic review and meta-analysis. *PLoS ONE* 2016;11. <http://dx.doi.org/10.1371/journal.pone.0153852>. e0153852.
- [15] Carneiro F, Saracino D, Huin V, Clot F, Delorme C, Méneret A, et al. Isolated parkinsonism is an atypical presentation of GRN and C9orf72 gene mutations. *Parkinsonism Relat Disord* 2020;80:73–81. <http://dx.doi.org/10.1016/j.parkreldis.2020.09.019>.

- [16] Beck J, Poulter M, Hensman D, Rohrer JD, Mahoney CJ, Adamson G, et al. Large C9orf72 hexanucleotide repeat expansions are seen in multiple neurodegenerative syndromes and are more frequent than expected in the UK population. *Am J Hum Genet* 2013;92:345–53. <http://dx.doi.org/10.1016/j.ajhg.2013.01.011>.
- [17] Fournier C, Barbier M, Camuzat A, Anquetil V, Lattante S, Clot F, et al. Relations between C9orf72 expansion size in blood, age at onset, age at collection and transmission across generations in patients and presymptomatic carriers. *Neurobiol Aging* 2019;74. <http://dx.doi.org/10.1016/j.neurobiolaging.2018.09.010>. 234.e1–234.e8.
- [18] Nuytemans K, Bademci G, Kohli MM, Beecham GW, Wang L, Young JJ, et al. C9ORF72 intermediate repeat copies are a significant risk factor for Parkinson disease. *Ann Hum Genet* 2013;77:351–63. <http://dx.doi.org/10.1111/ahg.12033>.
- [19] Iacoangeli A, Al Khleifat A, Jones AR, Sproviero W, Shatunov A, Opie-Martin S, et al. C9orf72 intermediate expansions of 24–30 repeats are associated with ALS. *Acta Neuropathol Commun* 2019;7:115. <http://dx.doi.org/10.1186/s40478-019-0724-4>.
- [20] Tang D, Sheng J, Xu L, Yan C, Qi S. The C9orf72-SMCR8-WDR41 complex is a GAP for small GTPases. *Autophagy* 2020;16:1542–3. <http://dx.doi.org/10.1080/15548627.2020.1779473>.
- [21] Lagier-Tourenne C, Baughn M, Rigo F, Sun S, Liu P, Li H-R, et al. Targeted degradation of sense and antisense C9orf72 RNA foci as therapy for ALS and frontotemporal degeneration. *Proc Natl Acad Sci U S A* 2013;110:E4530–9. <http://dx.doi.org/10.1073/pnas.1318835110>.
- [22] Mizielinska S, Lashley T, Norona FE, Clayton EL, Ridler CE, Fratta P, et al. C9orf72 frontotemporal lobar degeneration is characterised by frequent neuronal sense and antisense RNA foci. *Acta Neuropathol* 2013;126:845–57. <http://dx.doi.org/10.1007/s00401-013-1200-z>.
- [23] Mackenzie IRA, Frick P, Neumann M. The neuropathology associated with repeat expansions in the C9ORF72 gene. *Acta Neuropathol* 2014;127:347–57. <http://dx.doi.org/10.1007/s00401-013-1232-4>.
- [24] Jiang J, Zhu Q, Gendron TF, Saberi S, McAlonis-Downes M, Seelman A, et al. Gain of toxicity from ALS/FTD-linked repeat expansions in C9ORF72 is alleviated by antisense oligonucleotides targeting GGGGCC-containing RNAs. *Neuron* 2016;90:535–50. <http://dx.doi.org/10.1016/j.neuron.2016.04.006>.
- [25] Selkoe DJ, Hardy J. The amyloid hypothesis of Alzheimer's disease at 25 years. *EMBO Mol Med* 2016;8:595–608. <http://dx.doi.org/10.15252/emmm.201606210>.
- [26] Jack CR, Bennett DA, Blennow K, Carrillo MC, Dunn B, Haeberlein SB, et al. NIA-AA research framework: toward a biological definition of Alzheimer's disease. *Alzheimers Dement* 2018;14:535–62. <http://dx.doi.org/10.1016/j.jalz.2018.02.018>.
- [27] Dubois B, Villain N, Frisoni GB, Rabinovici GD, Sabbagh M, Cappa S, et al. Clinical diagnosis of Alzheimer's disease: recommendations of the International Working Group. *Lancet Neurol* 2021;20:484–96. [http://dx.doi.org/10.1016/S1474-4422\(21\)00066-1](http://dx.doi.org/10.1016/S1474-4422(21)00066-1).
- [28] Petersen RC, Lopez O, Armstrong MJ, Getchius TSD, Ganguli M, Gloss D, et al. Practice guideline update summary: mild cognitive impairment: report of the Guideline development, dissemination, and implementation subcommittee of the American Academy of Neurology. *Neurology* 2018;90:126–35. <http://dx.doi.org/10.1212/WNL.0000000000004826>.
- [29] Langbehn D, Brinkman R, Falush D, Paulsen J, Hayden M. on behalf of an International Huntington's Disease Collaborative Group. A new model for prediction of the age of onset and penetrance for Huntington's disease based on CAG length: prediction of the age of onset and penetrance for HD. *Clin Genet* 2004;65:267–77. <http://dx.doi.org/10.1111/j.1399-0004.2004.00241.x>.
- [30] Biglan KM, Ross CA, Langbehn DR, Aylward EH, Stout JC, Queller S, et al. Motor abnormalities in premanifest persons with Huntington's disease: the PREDICT-HD study: motor abnormalities in premanifest HD. *Mov Disord* 2009;24:1763–72. <http://dx.doi.org/10.1002/mds.22601>.
- [31] Lee J-M, Wheeler VC, Chao MJ, Vonsattel JPG, Pinto RM, Lucente D, et al. Identification of genetic factors that modify clinical onset of Huntington's disease. *Cell* 2015;162:516–26. <http://dx.doi.org/10.1016/j.cell.2015.07.003>.
- [32] Benatar M, Wu J. Presymptomatic studies in ALS: rationale, challenges, and approach. *Neurology* 2012;79:1732–9. <http://dx.doi.org/10.1212/WNL.0b013e31826e9b1d>.
- [33] Ryan B, Baker A, Ilse C, Brickell KL, Kersten HM, Danesh-Meyer HV, et al. Diagnosing pre-clinical dementia: the NZ genetic frontotemporal dementia study (FTDGeNZ). *N Z Med J* 2018;131:88–91.
- [34] Caroppo P, Habert M-O, Durrleman S, Funkiewiez A, Perlberg V, Hahn V, et al. Lateral temporal lobe: an early imaging marker of the presymptomatic GRN disease? *J Alzheimers Dis* 2015;47:751–9. <http://dx.doi.org/10.3233/JAD-150270>.
- [35] Bertrand A, Wen J, Rinaldi D, Houot M, Sayah S, Camuzat A, et al. Early cognitive, structural, and microstructural changes in presymptomatic C9orf72 carriers younger than 40 years. *JAMA Neurol* 2018;75:236. <http://dx.doi.org/10.1001/jamaneurol.2017.4266>.
- [36] De Vocht J, Blommaert J, Devrome M, Radwan A, Van Weehaeghe D, De Schaepdryver M, et al. Use of multimodal imaging and clinical biomarkers in presymptomatic carriers of C9orf72 repeat expansion. *JAMA Neurol* 2020;77:1008. <http://dx.doi.org/10.1001/jamaneurol.2020.1087>.
- [37] Ibanez A, Yokoyama JS, Possin KL, Matallana D, Lopera F, Nitrini R, et al. The multi-partner consortium to expand dementia research in Latin America (ReDLat): driving multicentric research and implementation science. *Front Neurol* 2021;12:631722. <http://dx.doi.org/10.3389/fneur.2021.631722>.
- [38] Benussi A, Alberici A, Samra K, Russell LL, Greaves CV, Bocchetta M, et al. Conceptual framework for the definition of preclinical and prodromal frontotemporal dementia. *Alzheimers Dement* 2021. <http://dx.doi.org/10.1002/alz.12485>.
- [39] Benatar M, Wu J, McHutchison C, Postuma RB, Boeve BF, Petersen R, et al. Preventing amyotrophic lateral sclerosis: insights from pre-symptomatic neurodegenerative diseases. *Brain* 2021. <http://dx.doi.org/10.1093/brain/awab404>.
- [40] Troakes C, Maekawa S, Wijesekera L, Rogelj B, Siklós L, Bell C, et al. An MND/ALS phenotype associated with C9orf72 repeat expansion: abundant p62-positive, TDP-43-negative inclusions in cerebral cortex, hippocampus and cerebellum but without associated cognitive decline: p62 proteinopathy. *Neuropathology* 2012;32:505–14. <http://dx.doi.org/10.1111/j.1440-1789.2011.01286.x>.
- [41] Mackenzie IR, Neumann M. Subcortical TDP-43 pathology patterns validate cortical FTLD-TDP subtypes and demonstrate unique aspects of C9orf72 mutation cases. *Acta Neuropathol* 2020;139:83–98. <http://dx.doi.org/10.1007/s00401-019-02070-4>.
- [42] van der Ende EL, Bron EE, Poos JM, Jiskoot LC, Panman JL, Papma JM, et al. A data-driven disease progression model of fluid biomarkers in genetic frontotemporal dementia. *Brain* 2021. <http://dx.doi.org/10.1093/brain/awab382>.

- [43] Miyagawa T, Brushaber D, Syrjanen J, Kremers W, Fields J, Forsberg LK, et al. Use of the CDR® plus NACC FTLD in mild FTLD: data from the ARTFL/LEFFTDS consortium. *Alzheimers Dement* 2020;16:79–90. <http://dx.doi.org/10.1016/j.jalz.2019.05.013>.
- [44] Peakman G, Russell LL, Convery RS, Nicholas JM, Van Swieten JC, Jiskoot LC, et al. Comparison of clinical rating scales in genetic frontotemporal dementia within the GENFI cohort. *J Neurol Neurosurg Psychiatry* 2022;93:158–68. <http://dx.doi.org/10.1136/jnnp-2021-326868>.
- [45] Ducharme S, Bajestan S, Dickerson BC, Voon V. Psychiatric presentations of C9orf72 mutation: what are the diagnostic implications for clinicians? *J Neuropsychiatry Clin Neurosci* 2017;29:195–205. <http://dx.doi.org/10.1176/appi.neuropsych.16090168>.
- [46] Sellami L, St-Onge F, Poulin S, Laforce R. Schizophrenia phenotype preceding behavioral variant frontotemporal dementia related to C9orf72 repeat expansion: cognitive and behavioral neurology. *Cogn Behav Neurol* 2019;32:120–3. <http://dx.doi.org/10.1097/WNN.000000000000189>.
- [47] Benatar M, Wu J, Lombardi V, Jeromin A, Bowser R, Andersen PM, et al. Neurofilaments in pre-symptomatic ALS and the impact of genotype. *Amyotroph Lateral Scler Frontotemporal Degener* 2019;20:538–48. <http://dx.doi.org/10.1080/21678421.2019.1646769>.
- [48] Zhang M, Ferrari R, Tartaglia MC, Keith J, Surace EI, Wolf U, et al. A C6orf10/LOC101929163 locus is associated with age of onset in C9orf72 carriers. *Brain* 2018;141:2895–907. <http://dx.doi.org/10.1093/brain/awy238>.
- [49] Barbier M, Camuzat A, El Hachimi K, Guegan J, Rinaldi D, Lattante S, et al. SLITRK2, an X-linked modifier of the age at onset in C9orf72 frontotemporal lobar degeneration. *Brain* 2021;144:2798–811. <http://dx.doi.org/10.1093/brain/awab171>.
- [50] Hendrix SB, Mogg R, Wang SJ, Chakravarty A, Romero K, Dickson SP, et al. Perspectives on statistical strategies for the regulatory biomarker qualification process. *Biomark Med* 2021;15:669–84. <http://dx.doi.org/10.2217/bmm-2020-0523>.
- [51] Taga A, Maragakis NJ. Current and emerging ALS biomarkers: utility and potential in clinical trials. *Expert Rev Neurother* 2018;18:871–86. <http://dx.doi.org/10.1080/14737175.2018.1530987>.
- [52] Swift IJ, Sogorb-Esteve A, Heller C, Synofzik M, Otto M, Graff C, et al. Fluid biomarkers in frontotemporal dementia: past, present and future. *J Neurol Neurosurg Psychiatry* 2021;92:204–15. <http://dx.doi.org/10.1136/jnnp-2020-323520>.
- [53] Lehmer C, Oeckl P, Weishaupt JH, Volk AE, Diehl-Schmid J, Schroeter ML, et al. Poly-GP in cerebrospinal fluid links C9orf72-associated dipeptide repeat expression to the asymptomatic phase of ALS/FTD. *EMBO Mol Med* 2017;9:859–68. <http://dx.doi.org/10.15252/emmm.201607486>.
- [54] Meeter LHH, Gendron TF, Sias AC, Jiskoot LC, Russo SP, Donker Kaat L, et al. Poly(GP), neurofilament and grey matter deficits in C9orf72 expansion carriers. *Ann Clin Transl Neurol* 2018;5:583–97. <http://dx.doi.org/10.1002/acn3.559>.
- [55] Gendron TF, Chew J, Stankowski JN, Hayes LR, Zhang Y-J, Prudencio M, et al. Poly(GP) proteins are a useful pharmacodynamic marker for C9ORF72-associated amyotrophic lateral sclerosis. *Sci Transl Med* 2017;9. <http://dx.doi.org/10.1126/scitranslmed.aai7866>. eai7866.
- [56] Vatsavayai SC, Yoon SJ, Gardner RC, Gendron TF, Vargas JNS, Trujillo A, et al. Timing and significance of pathological features in C9orf72 expansion-associated frontotemporal dementia. *Brain* 2016;139:3202–16. <http://dx.doi.org/10.1093/brain/aww250>.
- [57] Dubois B, Hampel H, Feldman HH, Scheltens P, Aisen P, Andrieu S, et al. Preclinical Alzheimer's disease: definition, natural history, and diagnostic criteria. *Alzheimers Dement* 2016;12:292–323. <http://dx.doi.org/10.1016/j.jalz.2016.02.002>.
- [58] Lee SE, Sias AC, Mandelli ML, Brown JA, Brown AB, Khazenzon AM, et al. Network degeneration and dysfunction in presymptomatic C9ORF72 expansion carriers. *Neuroimage Clin* 2017;14:286–97. <http://dx.doi.org/10.1016/j.nicl.2016.12.006>.
- [59] Waugh RE, Danielian LE, Shoukry RFS, Floeter MK. Longitudinal changes in network homogeneity in presymptomatic C9orf72 mutation carriers. *Neurobiol Aging* 2021;99:1–10. <http://dx.doi.org/10.1016/j.neurobiolaging.2020.11.014>.
- [60] Smallwood Shoukry RF, Clark MG, Floeter MK. Resting state functional connectivity is decreased globally across the C9orf72 mutation spectrum. *Front Neurol* 2020;11:598474. <http://dx.doi.org/10.3389/fneur.2020.598474>.
- [61] Agosta F, Ferraro PM, Riva N, Spinelli EG, Domi T, Carrera P, et al. Structural and functional brain signatures of C9orf72 in motor neuron disease. *Neurobiol Aging* 2017;57:206–19. <http://dx.doi.org/10.1016/j.neurobiolaging.2017.05.024>.
- [62] Rohrer JD, Nicholas JM, Cash DM, van Swieten J, Dopfer E, Jiskoot L, et al. Presymptomatic cognitive and neuroanatomical changes in genetic frontotemporal dementia in the Genetic Frontotemporal Dementia Initiative (GENFI) study: a cross-sectional analysis. *Lancet Neurol* 2015;14:253–62. [http://dx.doi.org/10.1016/S1474-4422\(14\)70324-2](http://dx.doi.org/10.1016/S1474-4422(14)70324-2).
- [63] Panman JL, Jiskoot LC, Bouts MJRJ, Meeter LHH, van der Ende EL, Poos JM, et al. Gray and white matter changes in presymptomatic genetic frontotemporal dementia: a longitudinal MRI study. *Neurobiol Aging* 2019;76:115–24. <http://dx.doi.org/10.1016/j.neurobiolaging.2018.12.017>.
- [64] Le Blanc G, Jetté Pomerleau V, McCarthy J, Borroni B, van Swieten J, Galimberti D, et al. Faster cortical thinning and surface area loss in presymptomatic and symptomatic C9orf72 repeat expansion adult carriers. *Ann Neurol* 2020;88:113–22. <http://dx.doi.org/10.1002/ana.25748>.
- [65] Bocchetta M, Todd EG, Peakman G, Cash DM, Convery RS, Russell LL, et al. Differential early subcortical involvement in genetic FTD within the GENFI cohort. *Neuroimage Clin* 2021;30:102646. <http://dx.doi.org/10.1016/j.nicl.2021.102646>.
- [66] Pappa JM, Jiskoot LC, Panman JL, Dopfer EG, den Heijer T, Donker Kaat L, et al. Cognition and gray and white matter characteristics of presymptomatic C9orf72 repeat expansion. *Neurology* 2017;89:1256–64. <http://dx.doi.org/10.1212/WNL.0000000000004393>.
- [67] Bocchetta M, Iglesias JE, Neason M, Cash DM, Warren JD, Rohrer JD. Thalamic nuclei in frontotemporal dementia: Mediodorsal nucleus involvement is universal but pulvinar atrophy is unique to C9orf72. *Hum Brain Mapp* 2020;41:1006–16. <http://dx.doi.org/10.1002/hbm.24856>.
- [68] Staffaroni AM, Cobigo Y, Goh S-YM, Kornak J, Bajorek L, Chiang K, et al. Individualized atrophy scores predict dementia onset in familial frontotemporal lobar degeneration. *Alzheimers Dement* 2020;16:37–48. <http://dx.doi.org/10.1016/j.jalz.2019.04.007>.
- [69] Wen J, Zhang H, Alexander DC, Durrleman S, Routier A, Rinaldi D, et al. Neurite density is reduced in the presymptomatic phase of C9orf72 disease. *J Neurol Neurosurg Psychiatry* 2018. <http://dx.doi.org/10.1136/jnnp-2018-318994>. jnnp-2018-318994.
- [70] Staffaroni AM, Goh S-YM, Cobigo Y, Ong E, Lee SE, Casaletto KB, et al. Rates of brain atrophy across disease

- stages in familial frontotemporal dementia associated with MAPT, GRN, and C9orf72 pathogenic variants. *JAMA Netw Open* 2020;3:e2022847. <http://dx.doi.org/10.1001/jamanetworkopen.2020.22847>.
- [71] El Mendili M-M, Cohen-Adad J, Pelegrini-Issac M, Rossignol S, Morizot-Koutlidis R, Marchand-Pauvert V, et al. Multi-parametric spinal cord MRI as potential progression marker in amyotrophic lateral sclerosis. *PLoS ONE* 2014;9:e95516. <http://dx.doi.org/10.1371/journal.pone.0095516>.
- [72] van der Burgh HK, Westeneng H-J, Meier JM, van Es MA, Veldink JH, Hendrikse J, et al. Cross-sectional and longitudinal assessment of the upper cervical spinal cord in motor neuron disease. *Neuroimage Clin* 2019;24:101984. <http://dx.doi.org/10.1016/j.nicl.2019.101984>.
- [73] Querin G, Bede P, El Mendili MM, Li M, Péligrini-Issac M, Rinaldi D, et al. Presymptomatic spinal cord pathology in c9orf72 mutation carriers: a longitudinal neuroimaging study. *Ann Neurol* 2019;86:158–67. <http://dx.doi.org/10.1002/ana.25520>.
- [74] Geevasinga N, Menon P, Nicholson GA, Ng K, Howells J, Kril JJ, et al. Cortical function in asymptomatic carriers and patients with C9orf72 amyotrophic lateral sclerosis. *JAMA Neurol* 2015;72:1268. <http://dx.doi.org/10.1001/jamaneurol.2015.1872>.
- [75] Benatar M, Zhang L, Wang L, Granit V, Statland J, Barohn R, et al. Validation of serum neurofilaments as prognostic and potential pharmacodynamic biomarkers for ALS. *Neurology* 2020;95:e59–69. <http://dx.doi.org/10.1212/WNL.00000000000009559>.
- [76] Boxer AL, Gold M, Feldman H, Boeve BF, Dickinson SL-J, Fillit H, et al. New directions in clinical trials for frontotemporal lobar degeneration: methods and outcome measures. *Alzheimers Dement* 2020;16:131–43. <http://dx.doi.org/10.1016/j.jalz.2019.06.4956>.
- [77] van der Ende EL, Meeter LH, Poos JM, Panman JL, Jiskoot LC, Doppler EGP, et al. Serum neurofilament light chain in genetic frontotemporal dementia: a longitudinal, multicentre cohort study. *Lancet Neurol* 2019;18:1103–11. [http://dx.doi.org/10.1016/S1474-4422\(19\)30354-0](http://dx.doi.org/10.1016/S1474-4422(19)30354-0).
- [78] Rojas JC, Wang P, Staffaroni AM, Heller C, Cobigo Y, Wolf A, et al. Plasma neurofilament light for prediction of disease progression in familial frontotemporal lobar degeneration. *Neurology* 2021;96:e2296–2312. <http://dx.doi.org/10.1212/WNL.00000000000011848>.
- [79] Saracino D, Dorgham K, Camuzat A, Rinaldi D, Rametti-Lacroux A, Houot M, et al. Plasma NFL levels and longitudinal change rates in C9orf72 and GRN-associated diseases: from tailored references to clinical applications. *J Neurol Neurosurg Psychiatry* 2021;92:1278–88. <http://dx.doi.org/10.1136/jnnp-2021-326914>.
- [80] Wilke C, Reich S, Swieten JC, Borroni B, Sanchez-Valle R, Moreno F, et al. Stratifying the presymptomatic phase of genetic frontotemporal dementia by serum NfL and pNfH: a longitudinal multicentre study. *Ann Neurol* 2022;91:33–47. <http://dx.doi.org/10.1002/ana.26265>.
- [81] Khalil M, Teunissen CE, Otto M, Piehl F, Sormani MP, Gatringer T, et al. Neurofilaments as biomarkers in neurological disorders. *Nat Rev Neurol* 2018;14:577–89. <http://dx.doi.org/10.1038/s41582-018-0058-z>.
- [82] Bridel C, van Wieringen WN, Zetterberg H, Tijms BM, Teunissen CE, the NFL Group, et al. Diagnostic value of cerebrospinal fluid neurofilament light protein in neurology: a systematic review and meta-analysis. *JAMA Neurol* 2019;76:1035. <http://dx.doi.org/10.1001/jamaneurol.2019.1534>.
- [83] Wilke C, Haas E, Reetz K, Faber J, Garcia-Moreno H, Santana MM, et al. Neurofilaments in spinocerebellar ataxia type 3: blood biomarkers at the preataxic and ataxic stage in humans and mice. *EMBO Mol Med* 2020;12. <http://dx.doi.org/10.15252/emmm.201911803>.
- [84] Meeter LH, Doppler EG, Jiskoot LC, Sanchez-Valle R, Graff C, Benussi L, et al. Neurofilament light chain: a biomarker for genetic frontotemporal dementia. *Ann Clin Transl Neurol* 2016;3:623–36. <http://dx.doi.org/10.1002/acn3.325>.
- [85] Alirezaei Z, Pourhanifeh MH, Borran S, Nejati M, Mirzaei H, Hamblin MR. Neurofilament light chain as a biomarker, and correlation with magnetic resonance imaging in diagnosis of CNS-related disorders. *Mol Neurobiol* 2020;57:469–91. <http://dx.doi.org/10.1007/s12035-019-01698-3>.
- [86] Heller C, Foiani MS, Moore K, Convery R, Bocchetta M, Neason M, et al. Plasma glial fibrillary acidic protein is raised in progranulin-associated frontotemporal dementia. *J Neurol Neurosurg Psychiatry* 2020;91:263–70. <http://dx.doi.org/10.1136/jnnp-2019-321954>.
- [87] Barschke P, Oeckl P, Steinacker P, Al Shweiki MR, Weishaupt JH, Landwehrmeyer GB, et al. Different CSF protein profiles in amyotrophic lateral sclerosis and frontotemporal dementia with C9orf72 hexanucleotide repeat expansion. *J Neurol Neurosurg Psychiatry* 2020;91:503–11. <http://dx.doi.org/10.1136/jnnp-2019-322476>.
- [88] Grasso M, Piscopo P, Confaloni A, Denti M. Circulating miRNAs as biomarkers for neurodegenerative disorders. *Molecules* 2014;19:6891–910. <http://dx.doi.org/10.3390/molecules19056891>.
- [89] Schneider R, McKeever P, Kim T, Graff C, van Swieten JC, Karydas A, et al. Downregulation of exosomal miR-204-5p and miR-632 as a biomarker for FTD: a GENFI study. *J Neurol Neurosurg Psychiatry* 2018;89:851–8. <http://dx.doi.org/10.1136/jnnp-2017-317492>.
- [90] Kmetzsch V, Anquetil V, Saracino D, Rinaldi D, Camuzat A, Gareau T, et al. Plasma microRNA signature in presymptomatic and symptomatic subjects with C9orf72-associated frontotemporal dementia and amyotrophic lateral sclerosis. *J Neurol Neurosurg Psychiatry* 2021;92:485–93. <http://dx.doi.org/10.1136/jnnp-2020-324647>.
- [91] Lulé DE, Müller H-P, Finsel J, Weydt P, Knehr A, Winroth I, et al. Deficits in verbal fluency in presymptomatic C9orf72 mutation gene carriers—a developmental disorder. *J Neurol Neurosurg Psychiatry* 2020;91:1195–200. <http://dx.doi.org/10.1136/jnnp-2020-323671>.
- [92] Poos JM, Russell LL, Peakman G, Bocchetta M, Greaves CV, Jiskoot LC, et al. Impairment of episodic memory in genetic frontotemporal dementia: a GENFI study. *Alz Dem Diag Ass Dis Mo* 2021;13. <http://dx.doi.org/10.1002/dad2.12185>.
- [93] Russell LL, Greaves CV, Bocchetta M, Nicholas J, Convery RS, Moore K, et al. Social cognition impairment in genetic frontotemporal dementia within the GENFI cohort. *Cortex* 2020;133:384–98. <http://dx.doi.org/10.1016/j.cortex.2020.08.023>.
- [94] Montembeault M, Sayah S, Rinaldi D, Le Toullec B, Bertrand A, Funkiewiez A, et al. Cognitive inhibition impairments in presymptomatic C9orf72 carriers. *J Neurol Neurosurg Psychiatry* 2020;91:366–72. <http://dx.doi.org/10.1136/jnnp-2019-322242>.
- [95] Franklin HD, Russell LL, Peakman G, Greaves CV, Bocchetta M, Nicholas J, et al. The Revised Self-Monitoring Scale detects early impairment of social cognition in genetic frontotemporal dementia within the GENFI cohort. *Alz Res Ther* 2021;13:127. <http://dx.doi.org/10.1186/s13195-021-00865-w>.
- [96] Funkiewiez A, Bertoux M, de Souza LC, Lévy R, Dubois B. The SEA (Social cognition and Emotional Assessment): a clinical neuropsychological tool for early diagnosis of

- frontal variant of frontotemporal lobar degeneration. *Neuropsychology* 2012;26:81-90. <http://dx.doi.org/10.1037/a0025318>.
- [97] Burgess P, Shallice T. *The Hayling and Brixton Tests*. Bury St Edmunds: Thames Valley Test Company; 1997.
- [98] Moore K, Convery R, Bocchetta M, Neason M, Cash DM, Greaves C, et al. A modified Camel and Cactus Test detects presymptomatic semantic impairment in genetic frontotemporal dementia within the GENFI cohort. *Appl Neuropsychol Adult* 2020;1-8. <http://dx.doi.org/10.1080/23279095.2020.1716357>.
- [99] Wear HJ, Wedderburn CJ, Mioshi E, Williams-Gray CH, Mason SL, Barker RA, et al. The Cambridge Behavioural Inventory revised. *Dement Neuropsychol* 2008;2:102-7. <http://dx.doi.org/10.1590/S1980-57642009DN20200005>.
- [100] Malpetti M, Jones PS, Tsvetanov KA, Rittman T, Swieten JC, Borroni B, et al. Apathy in presymptomatic genetic frontotemporal dementia predicts cognitive decline and is driven by structural brain changes. *Alzheimers Dement* 2021;17:969-83. <http://dx.doi.org/10.1002/alz.12252>.
- [101] Querin G, Biferi MG, Pradat P-F. Biomarkers for C9orf72-ALS in symptomatic and pre-symptomatic patients: state-of-the-art in the new era of clinical trials. *J Neuromuscul Dis* 2022;9:25-37. <http://dx.doi.org/10.3233/JND-210754>.
- [102] Malpetti M, Holland N, Jones PS, Ye R, Cope TE, Fryer TD, et al. Synaptic density in carriers of C9orf72 mutations: a [11C]UCB-J PET study. *Ann Clin Transl Neurol* 2021;8:1515-23. <http://dx.doi.org/10.1002/acn3.51407>.
- [103] Behler A, Knehr A, Finsel J, Kunz MS, Lang C, Müller K, et al. Eye movement alterations in presymptomatic C9orf72 expansion gene carriers. *J Neurol* 2021;268:3390-9. <http://dx.doi.org/10.1007/s00415-021-10510-z>.
- [104] Mutsaerts HJMM, Mirza SS, Petr J, Thomas DL, Cash DM, Bocchetta M, et al. Cerebral perfusion changes in presymptomatic genetic frontotemporal dementia: a GENFI study. *Brain* 2019;142:1108-20. <http://dx.doi.org/10.1093/brain/awz039>.
- [105] Snowden, Adams J, Harris J, Thompson JC, Rollinson S, Richardson A, et al. Distinct clinical and pathological phenotypes in frontotemporal dementia associated with MAPT, PGRN and C9orf72 mutations. *Amyotroph Lateral Scler Frontotemporal Degener* 2015;16:497-505. <http://dx.doi.org/10.3109/21678421.2015.1074700>.
- [106] Ducharme S, Dols A, Laforce R, Devenney E, Kumfor F, van den Stock J, et al. Recommendations to distinguish behavioural variant frontotemporal dementia from psychiatric disorders. *Brain* 2020;143:1632-50. <http://dx.doi.org/10.1093/brain/awaa018>.
- [107] Gossink F, Dols A, Stek ML, Scheltens P, Nijmeijer B, Cohn Hokke P, et al. Early life involvement in C9orf72 repeat expansion carriers. *J Neurol Neurosurg Psychiatry* 2022;93:93-100. <http://dx.doi.org/10.1136/jnnp-2020-325994>.
- [108] De Vocht J, Stam D, Nicolini M, Lamaire N, Laroy M, Vande Castele T, et al. Psychopathology in premanifest C9orf72 repeat expansion carriers. *J Neurol Neurosurg Psychiatry* 2022;93:565-7. <http://dx.doi.org/10.1136/jnnp-2021-327774>.
- [109] Caverzasi E, Battistella G, Chu SA, Rosen H, Zanto TP, Karydas A, et al. Gyrification abnormalities in presymptomatic c9orf72 expansion carriers. *J Neurol Neurosurg Psychiatry* 2019;90:1005-10. <http://dx.doi.org/10.1136/jnnp-2018-320265>.
- [110] Bede P, Siah WF, McKenna MC, Li Hi Shing S. Consideration of C9orf72-associated ALS-FTD as a neurodevelopmental disorder: insights from neuroimaging. *J Neurol Neurosurg Psychiatry* 2020;91:1138. <http://dx.doi.org/10.1136/jnnp-2020-324416>.
- [111] Xu W, Xu J. C9orf72 dipeptide repeats cause selective neurodegeneration and cell-autonomous excitotoxicity in drosophila glutamatergic neurons. *J Neurosci* 2018;38:7741-52. <http://dx.doi.org/10.1523/JNEUROSCI.0908-18.2018>.
- [112] Yeh T-H, Liu H-F, Li Y-W, Lu C-S, Shih H-Y, Chiu C-C, et al. C9orf72 is essential for neurodevelopment and motility mediated by Cyclin G1. *Exp Neurol* 2018;304:114-24. <http://dx.doi.org/10.1016/j.expneurol.2018.03.002>.

2. Objectifs de cette thèse

Cette thèse porte sur la caractérisation clinique et en neuroimagerie des DLFT associées aux mutations du gène *GRN* et aux expansions du gène *C9orf72*, au cours des phases cliniques et présymptomatiques de la maladie.

Ce travail a été rendu possible grâce à la collecte de données cliniques et échantillons biologiques effectuée depuis 1998 par les membres du « réseau national de recherche clinique et génétique sur les DLFT/DLFT-SLA » (réseau Inserm RBM 02-59). Ce réseau de recherche réunit des cliniciens experts sur ces pathologies, des généticiens et neuropathologistes de 17 centres hospitaliers universitaires français. Cette collaboration nationale a permis de constituer une cohorte de près de 3 000 patients atteints de DLFT et/ou SLA dont les données clinico-biologiques sont disponibles pour la recherche. Elle a été la base de plusieurs travaux présentés dans cette thèse.

Ces travaux de thèse sont aussi basés sur les données issues de deux protocoles nationaux multicentriques prospectifs, le PHRC Predict-PGRN et l'étude PREV-DEMALS, auxquels ont participé les centres de Paris, Lille, Limoges, Rouen, Marseille, Nantes et Toulouse. Ces deux études visent à analyser la phase présymptomatique de sujets asymptomatiques porteurs d'une mutation *GRN* (PHRC Predict-PGRN, initié en 2010) ou *C9orf72* (ANR-PRTS PREV-DEMALS, initié en 2015). Le protocole de ces deux études est assez similaire incluant, outre des prélèvements sanguins génétiques et plasmatiques, une évaluation clinique, un bilan neuropsychologique, une évaluation comportementale, une IRM cérébrale et une TEP cérébrale au ¹⁸FDG (TEP-FDG). Globalement, environ 200 apparentés de premier degré de patients porteurs d'une mutation des gènes *GRN* ou *C9orf72* ont été inclus dans ces deux études. Les participants de ces deux protocoles ont été suivis de façon longitudinale pendant 3 à 5 ans au cours de 3 visites (pour le détail complet des deux protocoles, voir annexe 3).

La première partie de cette thèse est consacrée à la caractérisation clinico-linguistique des aphasies primaires progressives associées aux mutations des gènes *GRN* et *C9orf72*, ou « APP génétiques ». Bien que les causes moléculaires de DFTc soient multiples, et maintenant bien connues, les formes génétiques d'APP restent encore relativement peu étudiées. Des phénotypes d'APP ont été décrits en association avec des mutations des gènes *GRN* (Snowden

et al., 2006 ; Mesulam et al., 2007 ; Le Ber et al., 2008 ; Rohrer et al., 2010b ; Kim et al., 2016), du gène *C9orf72* (Le Ber et al., 2013a ; Saint-Aubert et al., 2014 ; Haapanen et al., 2020 ; Moore et al., 2020a), ou d'autres gènes moins fréquents (Henz et al., 2015 ; Caroppo et al., 2015a ; Caroppo et al., 2016 ; Swift et al., 2021a ; Mol et al., 2021). Cependant, à ce jour, aucune étude n'a été conduite sur des séries relativement larges de patients avec « APP génétique » pour en déterminer les caractéristiques spécifiques. Étudier les phénotypes langagiers associés aux mutations des gènes de DLFT est pourtant important pour préciser les dysfonctionnements des systèmes neuroanatomiques dans ces processus pathologiques, pour adapter les recommandations du diagnostic génétique en tenant compte en particulier des phénotypes plus rares et, finalement, pour permettre la prise en compte de ces patients dans les essais thérapeutiques. Seuls quelques cas isolés d'APP associée aux mutations du gène *GRN* ou *C9orf72* ont été décrits de manière détaillée jusqu'à récemment. Ces descriptions ont suggéré que les formes génétiques d'APP pourraient présenter des caractéristiques cliniques relativement spécifiques (Deramecourt et al., 2010 ; Rohrer et al., 2010b ; Josephs et al., 2014b). Le premier objectif de cette thèse fut de caractériser les aspects cliniques, langagiers et cognitifs, ainsi que le profil d'atrophie de la substance grise, dans des cohortes relativement importantes de patients avec une APP liée à une mutation du gène *GRN* (article 1, Saracino et al., 2021a) ou *C9orf72* (article 2, Saracino et al., 2021b).

La suite de cette thèse a porté sur l'étude de marqueurs de la trajectoire des formes génétiques de DLFT, de leur phase présymptomatique à leur phase symptomatique, dans le cadre des études Predict-PGRN et PREV-DEMALS. Notre objectif vise à développer ou valider des outils biologiques, d'imagerie structurelle et métabolique permettant d'évaluer et de mesurer la réponse thérapeutique, particulièrement durant la phase présymptomatique des DLFT génétiques.

Nous avons tout d'abord étudié les taux de NfL plasmatiques dans une importante population de porteurs symptomatiques et présymptomatiques de mutations des gènes *GRN* et *C9orf72*. Bien que plusieurs études aient analysé les taux de NfL dans les DLFT et SLA génétiques (Meeter et al., 2016 ; van der Ende et al., 2019 ; Benatar et al., 2019) et montré leur pertinence dans la prédiction de la phénoconversion (Rojas et al., 2021), certains prérequis manquent pour permettre l'utilisation du dosage et l'interprétation des taux dans les essais thérapeutiques et la pratique clinique. En particulier, la variabilité des NfL dans des conditions physiologiques, en fonction de l'âge a été peu étudiée. Il n'y a pour le moment pas de consensus

sur les seuils pathologiques à considérer dans les essais thérapeutiques pour identifier la proximité de la phénoconversion. De même, les connaissances concernant les variations des taux des NfL en fonction du génotype, de l'âge, du stade de la maladie, des caractéristiques cliniques sont incomplètes. Notre étude (article 3, Saracino et al., 2021c) a visé à définir des valeurs de référence pour les taux de NfL, et leurs changements longitudinaux chez des contrôles, à établir la trajectoire gène-spécifique des NfL au cours de la maladie pour *GRN* et pour *C9orf72* séparément, et à proposer de seuils appropriés en fonction de l'âge et du gène responsable, afin de fournir des outils concrets pour suivre la maladie et les essais thérapeutiques à la phase clinique et présymptomatique.

Nous avons ensuite eu pour objectif de caractériser les altérations structurelles et métaboliques précoces, et leur progression longitudinale, durant la phase présymptomatique des formes *C9orf72* et *GRN*. Ces travaux ont intégré l'étude des données de cognition et l'information relative aux dosages des NfL, permettant une meilleure stratification des porteurs. Ils font l'objet d'un article soumis (article 4) et d'un article en préparation. Comme mentionné dans l'introduction, ces dernières années ont été marquées par une accélération des recherches autour de biomarqueurs de la progression des DLFT génétiques durant la phase présymptomatique. La caractérisation de leurs profils d'évolution dans le temps, de manière différentielle selon la mutation causale, est un prérequis indispensable à leur emploi à l'échelle individuelle, dans le cadre de la recherche ainsi que dans la pratique clinique.

Chez les porteurs de mutations de *GRN*, des altérations structurelles et une atrophie cérébrale sont détectables à l'échelle individuelle 2 à 4 ans avant la phénoconversion (Jiskoot et al., 2019 ; Panman et al., 2021 ; Bocchetta et al., 2021). Des changements du métabolisme cérébral ou de la perfusion cérébrale pourraient précéder les modifications structurelles, comme c'est le cas dans les formes génétiques de MA (Bateman et al., 2012). Des études précédentes – dont une issue de la même cohorte Predict-PGRN – ont analysé les modifications métaboliques ou de perfusion cérébrale pendant la phase présymptomatique des mutations de *GRN*, mais leurs conclusions sont restées limitées en raison d'effectifs réduits, de l'hétérogénéité des populations étudiées ou de l'absence de suivi longitudinal (Jacova et al., 2013 ; Caroppo et al., 2015b ; Mutsaerts et al., 2019). Le but de notre étude (article 4, soumis) est d'analyser le profil dynamique du métabolisme cérébral mesuré par TEP-FDG chez les porteurs présymptomatiques de mutations du gène *GRN* qui ont été suivis pendant 5 ans. Il est aussi d'évaluer la séquence temporelle des modifications précliniques intégrant également les

modifications en IRM structurelle, biologiques (NfL) et cognitives. Enfin l'objectif est de fournir un indicateur quantitatif pour suivre, à l'échelle individuelle, l'évolution de la phase préclinique, bien avant la phénoconversion.

La phase présymptomatique des expansions *C9orf72* est marquée par des changements volumétriques détectables, à l'échelle de groupe, environ 25 ans avant l'âge estimé du début clinique (Rohrer et al., 2015 ; Lee et al., 2017b ; Bertrand et al., 2018 ; Panman et al., 2019 ; Bocchetta et al., 2021). Leur progression au cours de la phase préclinique est peu étudiée (Le Blanc et al., 2020). A partir de la cohorte PREV-DEMALS, nous avons cherché à caractériser le profil régional d'atrophie de la substance grise et sa progression longitudinale sur une période de 3 ans, selon la proximité à la conversion clinique. L'un des objectifs de cette étude est aussi d'établir des taux de progression régionaux significativement différents entre porteurs de l'expansion *C9orf72* et contrôles, comme marqueur quantitatif de progression du processus neurodégénératif durant la phase présymptomatique.

Dans leur ensemble, les études longitudinales conduites dans cette thèse ont un double objectif : d'un point de vue scientifique, elles visent à une meilleure compréhension des mécanismes pathophysiologiques des DLFT, associant les premières modifications cognitives observées dans la maladie aux premières altérations cérébrales qui en sont responsables. D'autre part, elles ont pour objectif de contribuer à mieux tracer la phase présymptomatique, et de proposer des outils utilisables en pratique dans les essais thérapeutiques.

3. Méthodes spécifiques utilisées dans ces travaux

Dans ce projet de thèse, des méthodes spécifiques d'analyse ont été utilisées, comprenant le prétraitement et l'analyse d'exams de neuroimagerie, ainsi que des dosages biochimiques. Certaines de ces techniques sont communes à la plupart des études réalisées. Leurs aspects principaux sont brièvement abordés ci-dessous, et les aspects particuliers de certaines analyses, moins classiques (PET-PAC) ou récemment développées (SiMoA), sont détaillés.

Analyses d'imagerie structurelle. L'étude du profil d'atrophie de la substance grise a été réalisée avec deux approches complémentaires, habituellement utilisées en recherche : l'analyse de l'épaisseur corticale et l'approche de VBM, cette dernière s'étendant aussi aux analyses de l'étage sous-cortical. Pour la première approche, le logiciel FreeSurfer version 6.0 (Fischl et al., 2012) a été utilisé par l'intermédiaire du pipeline dédié « *t1-freesurfer* » de la plateforme Clinica (Routier et al., 2021). L'approche basée sur la VBM a été réalisée avec le logiciel SPM (*Statistical Parametric Mapping*) version 12 (<http://www.fil.ion.ucl.ac.uk/spm/software/spm12>), là encore par l'intermédiaire d'un pipeline de Clinica, « *t1-volume* » et ses différentes composantes (Routier et al., 2021), ainsi que, pour certaines analyses, du *toolbox* CAT12 (*Computational Anatomy Toolbox*, <http://www.neuro.uni-jena.de/cat>), remplaçant le traitement standard par SPM12. Ces approches sont détaillées dans l'annexe 4.

Analyse d'imagerie métabolique par PET-PAC. Les analyses des changements longitudinaux du métabolisme cortical posent des difficultés techniques notables, en raison d'un certain degré de variabilité entre les acquisitions et de la petite taille des variations attendues. C'est pour cela que, en plus des comparaisons longitudinales avec une méthode de référence, c'est-à-dire des comparaisons au niveau de voxel avec tests *T* appariés dans SPM12, une approche complémentaire a été implémentée dans cette thèse, basée sur le calcul du pourcentage de changement annualisé (PET-PAC, *metabolic percent annual changes*) (Fouquet et al., 2009). Brièvement, des cartes affichant le pourcentage de changement métabolique annuel au niveau de voxel peuvent être obtenues à l'aide d'un pipeline automatisé intégré dans le logiciel BrainVISA (<http://brainvisa.info/web/index.html>) par la plate-forme CATI (Centre d'Acquisition et Traitement des Images ; <https://cati-neuroimaging.com>). Dans un premier temps, l'IRM de base et celle de suivi sont co-registrées, afin d'obtenir une moyenne à partir

de laquelle les paramètres optimaux de transformation dans l'espace MNI sont calculés. Ensuite, les images TEP de base et de suivi sont alignées aux images anatomiques, corrigées pour les effets de volume partiel et lissées. Finalement, dans les voxels communs aux deux volumes TEP, le calcul du changement métabolique entre la valeur de base et de suivi, exprimé en pourcentage de changement annualisé, est réalisé tenant en compte l'intervalle temporel entre les deux acquisitions (Fouquet et al., 2009).

Dosages plasmatiques en SiMoA. Les concentrations plasmatiques de la chaîne légère des neurofilaments, de l'ordre des pg/mL, sont trop faibles pour être mesurées avec des techniques immuno-enzymatiques conventionnelles comme l'ELISA, dont la sensibilité est située autour du ng/mL. La technique de dosage ultrasensible SiMoA® (Rissin et al., 2010) permet d'améliorer significativement le seuil de détection, atteignant des sensibilités de l'ordre de 10^{-13} g/mL avec le kit commercial communément utilisé pour les NfL (Quanterix, Billerica, MS, USA). Brièvement, des billes de capture recouvertes d'anticorps sont combinées avec le plasma et l'anticorps détecteur biotinylé. Les étapes suivantes comprennent un premier lavage, l'ajout de la streptavidine- β -galactosidase (SBG) pour marquer les complexes immuns capturés, un deuxième lavage, et l'ajout du substrat résorufine β -Dgalactopyranoside (RGP). Les billes sont ensuite remises en suspension et capturées individuellement dans les puits d'un disque SiMoA, où le signal fluorescent produit par l'hydrolyse du RGP par l'action de la SBG est détecté par une caméra. Lorsque l'analyte est présent en quantité faible, sa concentration est proportionnelle à la quantité de puits activés (mesure numérique) ; lorsque les quantités deviennent plus importantes et que la plupart des puits sont saturés, la concentration d'analyte est déterminée à partir du signal fluorescent total (mesure analogique).

4. Résultats

4.1 Partie 1 – Aspects cliniques, langagiers, cognitifs et de neuroimagerie des APP associées aux mutations des gènes *GRN* et *C9orf72* (articles 1 et 2)

Article 1. Saracino D, Ferrieux S, Noguès-Lassiaille M, Houot M, Funkiewiez A, Sellami L, Deramecourt V, Pasquier F, Couratier P, Pariente J, Géraudie A, Epelbaum S, Wallon D, Hannequin D, Martinaud O, Clot F, Camuzat A, Bottani S, Rinaldi D, Auriacombe S, Sarazin M, Didic M, Boutoleau-Bretonnière C, Thauvin-Robinet C, Lagarde J, Roué-Jagot C, Sellal F, Gabelle A, Etcharry-Bouyx F, Morin A, Coppola C, Levy R, Dubois B, Brice A, Colliot O, Gorno-Tempini ML, Teichmann M, Migliaccio R, Le Ber I; French Research Network on FTD/FTD-ALS. Primary Progressive Aphasia Associated With GRN Mutations: New Insights Into the Nonamyloid Logopenic Variant. *Neurology*. 2021; 97: e88-e102.

Article 2. Saracino D, Géraudie A, Remes AM, Ferrieux S, Noguès-Lassiaille M, Bottani S, Cipriano L, Houot M, Funkiewiez A, Camuzat A, Rinaldi D, Teichmann M, Pariente J, Couratier P, Boutoleau-Bretonnière C, Auriacombe S, Etcharry-Bouyx F, Levy R, Migliaccio R, Solje E, Le Ber I; French research network on FTD/FTD-ALS and PREV-DEMALS study groups. Primary progressive aphasia associated with C9orf72 expansions: Another side of the story. *Cortex*. 2021; 145: 145-159.

Résumé

Le premier objectif de ma thèse fut de caractériser les aspects langagiers, cognitifs, et les systèmes neuroanatomiques impliqués dans les formes génétiques d'APP avec mutation du gène *GRN* et avec expansion du gène *C9orf72*. Les principaux résultats de ces deux articles sont brièvement résumés ci-dessous.

La première partie du travail (article 1, Saracino et al., 2021a) a porté sur l'étude de 32 patients répondant aux critères diagnostiques d'APP et porteurs de mutation du gène *GRN* (« APP-*GRN* »). Cette cohorte a été sélectionnée à partir de 162 patients ayant une mutation *GRN* recrutés dans le cadre du réseau français de recherche sur les DLFT/DLFT-SLA. Environ 20 % des porteurs de mutation *GRN* dans cette cohorte nationale présentaient donc un phénotype d'APP (32/162). Ces 32 patients « APP-*GRN* » ont été retenus dans l'étude après application des critères d'inclusion et d'exclusion (article 1). En particulier, aucun n'avait un profil de biomarqueurs dans le LCR compatible avec une co-pathologie de type MA.

Les évaluations des patients ont été effectuées après une durée médiane de la maladie de 2 ans (1,5–2,5). Brièvement, la parole et le langage ont été évalués avec la version française de la Boston Diagnostic Aphasia Examination (BDAE/HDAE-F) (Mazaux et Orgogozo, 1982) et/ou avec le protocole Montréal-Toulouse d'examen linguistique de l'aphasie (MT-86) (Nespoulous et al., 1992) selon les centres. Cette évaluation a été complétée par des épreuves de fluence verbale (lettre P et animaux sur 2 minutes), de dénomination (DO 80), de compétences sémantiques (*pyramids and palm trees test* ou batterie d'évaluation des connaissances sémantiques du GRECO), une évaluation de l'apraxie bucco-faciale et de la parole (Teichmann et al., 2013). Les autres domaines cognitifs ont été évalués avec un protocole relativement standardisé composé de tests communément utilisés par les centres du réseau, détaillés dans les articles 1 et 2. Les critères diagnostiques des différents variants d'APP (non-fluent/agrammatique, sémantique, logopénique, mixte ou inclassable) ont été appliqués (Gorno-Tempini et al., 2011 ; Mesulam et al., 2014 ; Bergeron et al., 2018) et les diagnostics validés avec chaque neurologue expert référent, pour retenir un diagnostic consensuel. La fréquence des différents variants et leurs caractéristiques linguistiques ont été étudiés à l'aide d'analyses descriptives. Les études d'imagerie ont été effectuées à partir des séquences d'IRM réalisées en routine clinique. Une analyse de VBM a été effectuée pour comparer les profils d'atrophie de la substance grise avec ceux de patients APP sans mutation aux caractéristiques démographiques et cliniques similaires.

De façon intéressante, et inattendue, la forme logopénique d'APP (habituellement sous-tendue par une pathologie amyloïde) s'est révélée être le variant le plus représenté dans cette série. Ce diagnostic concernait en effet près de 41 % des patients (13/32 patients), avec un profil caractérisé principalement par une production langagière spontanée réduite, un manque du mot, de longues pauses, des difficultés de répétition et de compréhension de phrases longueur-dépendantes. Des erreurs phonologiques étaient fréquentes (10/13 cas), sans atteinte majeure des composantes phono-articulatoires du langage. Au sein de ce groupe, nous avons proposé une distinction plus fine entre patients présentant un « vlAPP pure », sans aucun autre déficit associé (7/13), et ceux ayant une forme qualifiée de « vlAPP+ » (6/13), en raison de difficultés additionnelles subtiles (telles qu'une simplification syntaxique ou un pseudo-bégaiement ou une très légère difficulté d'articulation, ou encore des erreurs d'appariement sémantique). Ces déficits, très discrets, étaient perçus essentiellement en situation de test, et ces patients ne répondaient pas aux critères de forme mixte tels que définis par Bergeron et collaborateurs (2018), justifiant ainsi leur classement diagnostique en vlAPP+. Globalement le profil d'atrophie caractérisé en VBM était strictement comparable à celui des patients ayant une forme logopénique de MA (confirmée par les biomarqueurs). Néanmoins un cluster additionnel d'atrophie dans le cortex orbital postérieur a été identifié dans la comparaison avec les contrôles.

De plus, un quart des patients présentaient une forme mixte d'APP (8/32, 25 %) associant, dans tous les cas, des troubles d'allure logopénique associés à des troubles sémantiques (5/8) et/ou des déficits d'élaboration grammaticale (6/8). Cette observation renforce le résultat précédent, positionnant les troubles logopéniques selon un gradient allant de la forme pure, à la forme vlAPP+, jusqu'à des formes mixtes. Il faut noter que les différences entre ces trois groupes ne sont expliquées ni par la durée, ni par la sévérité de la maladie (qui étaient globalement comparables entre les groupes au moment de l'évaluation), mais plus probablement par une atteinte lésionnelle et une distribution de l'atrophie d'emblée plus étendues dans les formes mixtes que dans les formes pures.

Près d'un tiers des patients présentaient un vnfAPP (9/32 patients, 28 %). Leur profil langagier était, dans la grande majorité des cas, dominé par un agrammatisme. Seul un patient présentait une apraxie de la parole sans trouble syntaxique majeur. Cette observation est cohérente avec la dichotomie proposée au sein des vnfAPP, distinguant une forme purement « agrammatique » et une forme plutôt « motrice » (Tetzloff et al., 2019). Ce résultat souligne

que les mutations du gène *GRN* impactent principalement les composantes grammaticales/syntaxiques du langage, plus que ses aspects articulatoires. Il renforce l'hypothèse d'une dissociation des réseaux impliqués dans ces deux composantes, l'un s'étendant du cortex préfrontal aux régions temporales latérales, l'autre plus limité aux aires prémotrices (Tetzloff et al., 2019). Les formes sémantiques pures se sont avérées beaucoup plus rares, concernant seulement 2 patients de cette série.

Dans l'article 2 (Saracino et al., 2021b), un travail descriptif similaire a été conduit pour caractériser les présentations langagières des APP associées aux expansions du gène *C9orf72*. Cet objectif est plus difficile à mener, en raison de la rareté des phénotypes APP dans cette forme génétique. Ainsi, sur 330 porteurs d'expansions *C9orf72* recrutés par les collaborateurs du réseau national, seuls 11 avaient un diagnostic initial d'APP, soit environ 3 % des porteurs d'expansion. Six ont pu être inclus dans l'étude après application des critères d'exclusion. Nous avons inclus cinq autres patients d'origine finlandaise dans le cadre d'une collaboration avec l'équipe du Pr Solje (Université de Kuopio). Ces 5 patients ont été suivis entre 1996 et 2016, et évalués avec des tests langagiers et de cognition validés internationalement (Kaivorinne et al., 2013 ; Haapanen et al., 2020). Enfin, après une revue exhaustive de la littérature, trois cas précédemment publiés avec une caractérisation langagière approfondie (Cerami et al., 2013 ; Hsiung et al., 2012 ; Snowden et al., 2012) ont été inclus, permettant l'étude d'une petite série de 16 patients « APP-*C9orf72* » au total.

Parmi eux, 56 % (9/16) présentaient un vnfAPP, dominé par une apraxie de la parole, 19 % (3/16) avaient un vsAPP, et 25 % avaient une forme mixte (2/16) ou une APP inclassable (2/16). Aucun ne présentait un variant logopénique. De façon intéressante, les 2 patients avec une APP mixte présentaient le même tableau langagier, initialement dominé par une réduction de la fluence et des troubles syntaxiques, et évoluant de façon similaire avec l'apparition de difficultés de type sémantique dès la deuxième année de maladie. Les analyses de VBM dans le groupe des patients avec un vnfAPP montraient une atteinte du gyrus frontal moyen et inférieur de gauche, concordant avec le profil clinique. L'étude longitudinale chez un individu présentant un vsAPP a démontré une atrophie s'étendant du pôle temporal gauche au cortex orbitofrontal et temporo-polaire droit au cours du suivi, de façon contemporaine à l'apparition de comportements répétitifs-obsessionnels. Globalement, cette caractérisation langagière, complétée par l'étude des corrélats neuroanatomiques au niveau individuel et de groupe, met en évidence une atteinte plus focalisée sur les composantes antérieures du réseau du langage

dans le cadre de la pathologie *C9orf72*. L'atteinte de lobe temporal antérieur, retrouvée dans les formes sémantiques pures, mais aussi dans les APP mixtes, semble représenter un élément récurrent dans les formes *C9orf72*, alors qu'il est très inhabituel dans les mutations du gène *GRN*.

Globalement, ces deux études montrent une atteinte des réseaux du langage plutôt postérieure dans le cas des mutations *GRN*, et plus antérieure dans le cas des mutations *C9orf72*. Ceci suggère une vulnérabilité différente selon le processus pathologique, avec un tropisme lésionnel particulier dans chacune de ces deux causes génétiques. Elles posent les bases neuroanatomiques des formes langagières associées à ces deux génotypes, qui pourraient être explorées à un stade plus précoce, chez les porteurs de mutations à la phase présymptomatique.

Pratiquement, dans le cadre de ces deux publications, j'ai contribué à la validation des phénotypes langagiers des patients inclus dans les papiers, j'ai effectué les analyses statistiques permettant les comparaisons cliniques, cognitives et langagières, et j'ai réalisé les analyses d'imagerie incluant le pré-traitement des images et les analyses statistiques pour comparer les groupes.

Primary Progressive Aphasia Associated With *GRN* Mutations

New Insights Into the Nonamyloid Logopenic Variant

Dario Saracino, MD, Sophie Ferrieux, Marie Noguès-Lassaille, Marion Houot, MSc, Aurélie Funkiewiez, PhD, Leila Sellami, MD, Vincent Deramecourt, MD, PhD, Florence Pasquier, MD, PhD, Philippe Couratier, MD, PhD, Jérémie Pariente, MD, PhD, Amandine Géraudie, MSc, Stéphane Epelbaum, MD, PhD, David Wallon, MD, PhD, Didier Hannequin, MD, PhD, Olivier Martinaud, MD, PhD, Fabienne Clot, PhD, Agnès Camuzat, MSc, Simona Bottani, MSc, Daisy Rinaldi, PhD, Sophie Auriacombe, MD, Marie Sarazin, MD, PhD, Mira Didic, MD, PhD, Claire Boutoleau-Brettonnière, MD, PhD, Christel Thauvin-Robinet, MD, Julien Lagarde, MD, Carole Roué-Jagot, MD, François Sellal, MD, PhD, Audrey Gabelle, MD, PhD, Frédérique Etcharry-Bouyx, MD, PhD, Alexandre Morin, MD, Cinzia Coppola, MD, PhD, Richard Levy, MD, PhD, Bruno Dubois, MD, Alexis Brice, MD, PhD, Olivier Colliot, PhD, Maria Luisa Gorno-Tempini, MD, PhD, Marc Teichmann, MD, PhD, Raffaella Migliaccio, MD, PhD, and Isabelle Le Ber, MD, PhD, on behalf of the French Research Network on FTD/FTD-ALS

Correspondence

Dr. Le Ber
isabelle.leber@upmc.fr

Neurology® 2021;97:e88-e102. doi:10.1212/WNL.00000000000012174

Abstract

Objective

To determine relative frequencies and linguistic profiles of primary progressive aphasia (PPA) variants associated with *GRN* (progranulin) mutations and to study their neuroanatomic correlates.

Methods

Patients with PPA carrying *GRN* mutations (PPA-*GRN*) were selected among a national prospective research cohort of 1,696 patients with frontotemporal dementia, including 235 patients with PPA. All patients with amyloid-positive CSF biomarkers were excluded. In this cross-sectional study, speech/language and cognitive profiles were characterized with standardized evaluations, and gray matter (GM) atrophy patterns using voxel-based morphometry. Comparisons were performed with controls and patients with sporadic PPA.

Results

Among the 235 patients with PPA, 45 (19%) carried *GRN* mutations, and we studied 32 of these. We showed that logopenic PPA (lvPPA) was the most frequent linguistic variant ($n = 13$, 41%), followed by nonfluent/agrammatic (nfvPPA; $n = 9$, 28%) and mixed forms ($n = 8$, 25%). Semantic variant was rather rare ($n = 2$, 6%). Patients with lvPPA, qualified as nonamyloid lvPPA, presented canonical logopenic deficit. Seven of 13 had a pure form; 6 showed subtle additional linguistic deficits not fitting criteria for mixed PPA and hence were labeled as

From Sorbonne Université (D.S., M.H., L.S., S.E., A.C., S.B., D.R., A.M., R.L., B.D., A.B., O.C., M.T., R.M., I.L.B.), Paris Brain Institute-Institut du Cerveau (ICM), Inserm U1127, CNRS UMR 7225, AP-HP-Hôpital Pitié-Salpêtrière; Reference Centre for Rare or Early Dementias (D.S., S.F., M.N.-L., M.H., A.F., L.S., S.E., D.R., A.M., R.L., B.D., M.T., R.M., I.L.B.), IM2A, Département de Neurologie, AP-HP-Hôpital Pitié-Salpêtrière; Aramis Project Team (D.S., S.E., S.B., A.M., O.C.), Inria Research Center of Paris; Centre of Excellence of Neurodegenerative Disease (CoEN) (M.H.), ICM, CIC Neurosciences, Département de Neurologie, AP-HP-Hôpital Pitié-Salpêtrière, Sorbonne Université; FrontLab (A.F., R.L., B.D., M.T., R.M., I.L.B.), Paris Brain Institute-Institut du Cerveau (ICM); Université Lille (V.D., F.P.), Inserm U1171, CHU Lille, DistAlz, LICEND, CNR-MAJ; CMRR Service de Neurologie (P.C.), CHU de Limoges; Department of Neurology (J.P., A.G.), Toulouse University Hospital; ToNIC (J.P., A.G.), Toulouse Neuroimaging Centre, Inserm, UPS, University of Toulouse; Normandie Université (D.W., D.H.), UNIROUEN, Inserm U1245 and Rouen University Hospital, Department of Neurology and CNR-MAJ, Normandy Center for Genomic and Personalized Medicine; Rouen University Hospital (O.M.), Department of Neurology; Normandie Université (O.M.), UNICAEN, PSL Research University, EPHE, INSERM, U1077, CHU de Caen Normandie, Neuropsychologie et Imagerie de la Mémoire Humaine, Caen; UF de Neurogénétique Moléculaire et Cellulaire (F.C.), Département de Génétique, AP-HP, Hôpitaux Universitaires La Pitié Salpêtrière-Charles Foix; EPHE (A.C.), PSL Research University, Paris; CMRR Nouvelle Aquitaine/Institut des Maladies Neurodégénératives clinique (IMNc) (S.A.), CHU de Bordeaux Hôpital Pellegrin; Unit of Neurology of Memory and Language (M.S., J.L., C.R.-J.), GHU Paris Psychiatry and Neurosciences, University of Paris, Hôpital Sainte Anne; Université Paris-Saclay (M.S., J.L., C.R.-J.), CEA, CNRS, Inserm, BioMaps, Orsay; Aix Marseille Université (M.D.), INSERM, Institut de Neurosciences des Systèmes, Marseille; APHM (M.D.), Timone, Service de Neurologie et Neuropsychologie, APHM Hôpital Timone Adultes, Marseille; CHU Nantes (C.B.-B.), Inserm CIC04, Department of Neurology, Centre Mémoire de Ressources et Recherche, Nantes; Centre de génétique (C.T.-R.), Hôpital d'Enfants, CHU Dijon Bourgogne; CMRR Département de Neurologie (F.S.), Hôpitaux Civils, Colmar, INSERM U1118, Université de Strasbourg, Faculté de Médecine, 67085 Strasbourg; CMRR (A.G.), Département de Neurologie, CHU de Montpellier, Inserm U1061, Université de Montpellier i-site MUSE; Department of Neurology (F.E.-B.), CMRR Angers University Hospital, Angers, France; Department of Advanced Medical and Surgical Sciences (C.C.), University of Campania Luigi Vanvitelli, Naples, Italy; and Department of Neurology (M.L.G.-T.), Memory and Aging Center, University of California, San Francisco.

Go to [Neurology.org/N](https://www.neurology.org/N) for full disclosures. Funding information and disclosures deemed relevant by the authors, if any, are provided at the end of the article.

Coinvestigators are listed in appendix 2 at the end of the article.

Glossary

A β = β -amyloid; AD = Alzheimer disease; AOS = apraxia of speech; BDAE = Boston Diagnostic Aphasia Examination–French version; bvFTD = behavioral variant of FTD; CBS = corticobasal syndrome; DD = disease duration; FTD = frontotemporal dementia; FTLN = frontotemporal lobar degeneration; GM = gray matter; lvPPA = logopenic variant of PPA; MNI = Montreal Neurological Institute; MT = middle temporal; nfvPPA = nonfluent/agrammatic variant of PPA; PNFA = progressive nonfluent aphasia; PPA = primary progressive aphasia; svPPA = semantic variant of PPA; TDP-43 = TAR DNA-binding protein 43.

logopenic-spectrum variant. GM atrophy involved primarily left posterior temporal gyrus, mirroring neuroanatomic changes of amyloid-positive-lvPPA. Patients with nfvPPA presented agrammatism (89%) rather than apraxia of speech (11%).

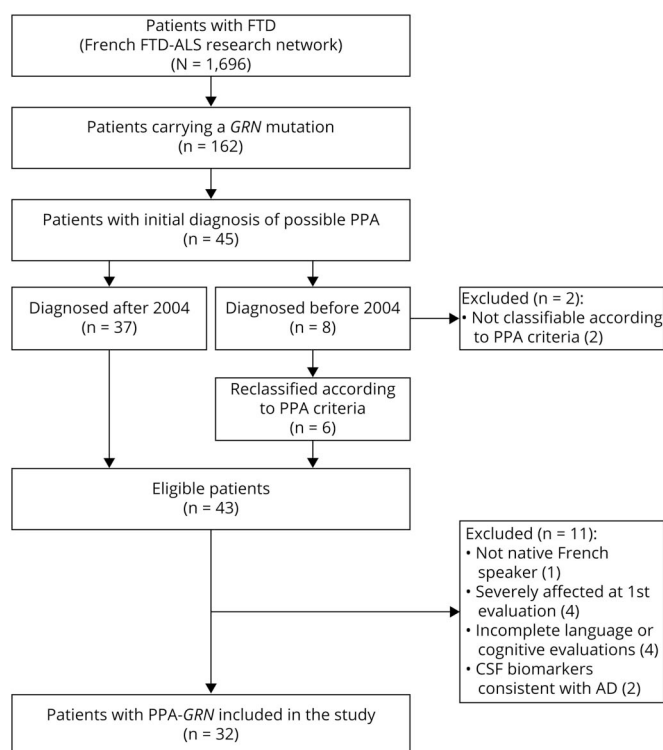
Conclusions

This study shows that the most frequent PPA variant associated with GRN mutations is nonamyloid lvPPA, preceding nfvPPA and mixed forms, and illustrates that the language network may be affected at different levels. GRN testing is indicated for patients with PPA, whether familial or sporadic. This finding is important for upcoming GRN gene-specific therapies.

Primary progressive aphasia (PPAs) are rare neurodegenerative disorders divided into 3 main clinical variants.^{1,2} The nonfluent/agrammatic variant (nfvPPA; formerly progressive nonfluent aphasia [PNFA]) is characterized by disrupted, effortful language production, with agrammatism and apraxia of speech (AOS). The semantic variant (svPPA; formerly semantic dementia) is dominated by anomia, conceptual knowledge, and language comprehension

deficits. Patients with logopenic variant (lvPPA) feature impairment of phonologic working memory with single-word retrieval, sentence repetition deficits, and phonologic errors. Those variants show characteristic neuroanatomic profiles involving left inferior frontal gyrus in nfvPPA, anterior temporal lobe in svPPA, and temporoparietal junction in lvPPA.³ nfvPPA and svPPA are associated predominantly with frontotemporal lobar degeneration (FTLD) with tau or

Figure 1 Flowchart of the Inclusion Process



AD = Alzheimer disease; ALS = amyotrophic lateral sclerosis; FTD = frontotemporal dementia; PPA = primary progressive aphasia.

TAR DNA-binding protein 43 (TDP-43) neuronal inclusions.^{4,5} Most lvPPA cases are reported to be associated with amyloid pathology.⁵⁻¹²

GRN and *C9orf72*, the most prevalent frontotemporal dementia (FTD) genes, are associated predominantly with behavioral variant of FTD (bvFTD) and, much more rarely, with a PPA phenotype.¹³⁻¹⁸ The description of case reports suggested that genetic PPA might have specific language and cognitive profiles.^{16,19-21} Moreover, defining their linguistic spectrum in large cohorts and depicting specific profiles that may deserve appropriate genetic testing would be of utmost importance in light of upcoming therapies. For this purpose, we aimed to comprehensively characterize the linguistic and cognitive profiles and the patterns of gray matter (GM) atrophy of PPA associated with *GRN* mutations in a series of 32 patients, offering the opportunity to analyze homogeneous groups with highly predictable pathology and potentially link specific molecular dysfunctions with clinical phenotypes.

Methods

Selection of Patients

The patients included in this study were prospectively enrolled in a clinico-genetic research cohort from 1996 to 2018 by neurologists of tertiary referral centers for neurodegenerative dementias, FTD, and PPA from 12 French university hospitals contributing to a national research network (Inserm RBM 02-59). All centers applied similar standardized evaluations and diagnostic procedures. Behavioral changes were evaluated with a scale derived from the Frontal Behavioral Scale, the Frontal Behavioral Inventory, and the Neuropsychiatric Inventory integrating the main elements of frontal syndrome (including apathy, disinhibition, hyperorality, stereotyped/ritualistic behaviors, emotion/affects) with the main caregiver and the patient.^{15,22,23} Cognitive and speech/language deficits were evaluated with semistandardized protocols, the scales of which are described below, by neuropsychologists and speech-language pathologists specialized in neurodegenerative dementias and PPA. Patients were also evaluated by neuroimaging procedures (brain MRI, SPECT, and/or fluorodeoxyglucose-PET) and by CSF biomarkers in more recent cases. Biological samples were collected for genetic analyses and progranulin plasma dosage. Diagnoses were based on international diagnostic criteria.^{2,23}

During this period, a total of 1,696 patients with FTD or PPA were evaluated with these procedures, including 1,103 (65.0%) patients presenting bvFTD, 292 (17.2%) presenting bvFTD associated with amyotrophic lateral sclerosis, 235 (13.8%) presenting PPA, 39 (2.4%) presenting progressive supranuclear palsy, and 27 (1.6%) presenting corticobasal syndrome (CBS). Among the 1,696 patients, 162 carried pathogenic *GRN* mutations, 45 of whom received a diagnosis of PPA (PPA-*GRN*) based on investigations detailed below

(figure 1). Of note, 330 of 1,696 patients carried a *C9orf72* expansion, but only 7 received a diagnosis of PPA.

In the context of the present investigation, a team of neurologists (R.M., L.S., D.S.), speech-language pathologists (S.F., M.N.L.), and a neuropsychologist (A.F.) from the French reference center on FTD and PPA reviewed the clinical data and scales of the 45 patients with PPA-*GRN*. They independently validated the final diagnosis and variant classification based on current international criteria.² MRI and functional neuroimaging were visually reviewed to confirm the PPA-consistent neuroimaging pattern. Notably, 8 patients investigated before the definition of lvPPA³ were reclassified according to current criteria when possible (n = 6) or excluded when not possible as a result of insufficient data to establish the variant (n = 2). Other exclusion criteria were CSF biomarkers consistent with Alzheimer disease (AD) copathology (n = 2), non-French native language (n = 1), language that was too severely compromised at the first evaluation (n = 4), or incomplete language/cognitive evaluations (n = 4) to formally diagnose a PPA variant at onset. CSF biomarkers were considered in favor of AD according to the following cutoffs: β -amyloid ($A\beta_{1-42}$) peptide <500 pg/mL, total tau protein >450 pg/mL, and phosphorylated tau >60 pg/mL. In case of discordant results, the following cutoffs were applied: $\tau/A\beta_{1-42} \geq 1.15$ and phosphorylated $\tau/A\beta_{1-42} \geq 0.21$, according to manufacturer's instructions (ELISA kit, Innogenetics, Ghent, Belgium).

At the end of this selection process, 32 patients with *GRN*-related PPA were included in this study. Notably, AD pathology was excluded for 24 of 32 (75%) by CSF biomarkers. CSF was not obtained for 8 carriers, among whom only 3 had lvPPA. The 32 patients with PPA were kept in the study because demographic and clinical characteristics were similar in both groups (with or without CSF), especially for executive functions and episodic memory (supplemental data available from Dryad, table e-1, doi.org/10.5061/dryad.x3ffbg7hr). The list of *GRN* mutations is provided in table e-2. After their inclusion, the patients were clinically evaluated in the context of their usual neurologic follow-up.

Speech/Language Assessments

Speech and Language Evaluations

Speech/language deficits in the 32 patients with PPA were assessed by speech-language pathologists with expertise in neurodegenerative dementias. The performed tests are shown in table e-3 (doi.org/10.5061/dryad.x3ffbg7hr). Detailed speech/language evaluations were based on the Boston Diagnostic Aphasia Examination–French version (BDAE)²⁴ (n = 26 patients) and/or the Montreal-Toulouse protocol for examination of aphasia²⁵ (n = 18). Twelve had both batteries. Briefly, these scales evaluate motor speech production, grammar, single-word and sentence comprehension, repetition of words and sentences of increasing length and grammatical complexity, knowledge of objects/people, reading,

Table 1 Demographic, Linguistic, and Clinical Characteristics of Patients With PPA Carrying *GRN* Mutations at First Evaluation

	All Patients	lvPPA	nfvPPA	svPPA	Mixed PPA
Patients, n (%)	32	13 (41)	9 (28)	2 (6)	8 (25)
Demographic data					
F/M, n	20/12	8/5	7/2	1/1	4/4
Handedness (R/L/Adx), n	29/2/1	10/2/1	9/0/0	2/0/0	8/0/0
Family history, n (%)^a	26 (81)	10 (77)	9 (100)	2 (100)	5 (63)
Education level, y	9.0 [8.8, 13.3]	9.0 [6.0, 15.0]	9.0 [9.0, 12.0]	7.0 [6.0, 8.0]	10.5 [9.0, 11.5]
Age at onset, y	62.0 [59.0, 63.3]	62.0 [59.0, 63.0]	62.0 [56.0, 63.0]	63.5 [60.3, 66.8]	63.0 [61.5, 64.8]
Age at first evaluation, y	64.0 [60.0, 66.0]	63.0 [62.0, 65.0]	63.0 [58.0, 65.0]	66.0 [63.0, 69.0]	65.0 [63.3, 66.8]
Disease duration at first evaluation, y	2.0 [1.5, 2.5]	1.5 [1.5, 2.5]	1.5 [1.0, 2.0]	2.8 [2.6, 2.9]	2.2 [1.9, 2.5]
Speech and language assessment					
Global Aphasia Severity score (of 5)^b	3.0 [2.0, 3.0]	3.0 [2.3, 3.0]	3.0 [3.0, 4.0]	1.0 [1.0, 1.0]	3.0 [2.0, 3.0]
Agrammatism (discrete to severe), n (%)^c	14 (44)	0	8 (89)	0	6 (75)
Semantic fluency in 2 min	10 [5, 16]	11 [6, 18]	13 [9, 16]	4 [2, 6]	5 [4, 11]
Phonologic (F) fluency in 2 min	5 [2, 9]	9 [2, 10]	4 [3, 7]	3 [1, 4]	7 [5, 7]
Confrontation naming, %	79 [50, 91]	76 [59, 89]	88 [83, 94]	1 [1, 1]	64 [25, 86]
Oral single-word comprehension, n (%)^c	9 (28)	3 (23)	1 (11)	2 (100)	3 (38)
Oral sentence comprehension, %	66 [34, 82]	77 [53, 86]	69 [66, 88]	19 [10, 29]	33 [16, 67]
Repetition of sentences, %	56 [50, 69]	50 [38, 69]	63 [56, 100]	50 [50, 50]	31 [0, 69]
Written sentence comprehension, %	77 [63, 85]	74 [70, 80]	68 [43, 89]	38 [30, 46]	80 [77, 85]
Disease progression					
Median disease duration at death, y (n of deceased)	7.5 [6.8, 8.0] (8)	7.5 [7.3, 7.8] (2)	6.5 [5.9, 7.3] (4)	— (0)	8.5 [8.3, 8.8] (2)
Frontal lobe dysfunction, n (%)	32 (100)	13 (100)	9 (100)	2 (100)	8 (100)
Executive dysfunction, n (%)	31 (97)	13 (100)	8 (89)	2 (100)	8 (100)
Behavioral symptoms, n (%)	18 (56)	8 (62)	2 (22)	2 (100)	6 (75)
Amnesic syndrome, n (%)	12 (38)	6 (46)	2 (22)	2 (100)	2 (25)
Parietal syndrome, n (%)	18 (56)	8 (62)	5 (56)	1 (50)	4 (50)
Parkinsonism, n (%)	11 (34)	3 (23)	5 (56)	0	3 (38)
Psychiatric disorders, n (%)^d	5 (16)	1 (8)	1 (11)	1 (50)	2 (25)

Abbreviations: Adx = ambidextrous; FTLT = frontotemporal lobar degeneration; lvPPA = logopenic variant of PPA; nfvPPA = nonfluent/agrammatic variant of PPA; PPA = primary progressive aphasia; svPPA = semantic variant of PPA. Numbers are presented for categorical measures with percentages in parentheses. Medians are presented for numerical measures with first and third quartiles within brackets.

^a Family history of FTLT spectrum disorders.

^b Aphasia severity rating score evaluates the global severity of impairment of spontaneous speech and conversation following Boston Diagnostic Aphasia Examination–French version recommendations.

^c Number (percentage) of patients with impaired performance.

^d Delusions, depression, or bipolar disorder.

spelling, and writing skills. Speech/language assessment also evaluated oral confrontation naming with the DO80 Picture-Naming Test,²⁶ buccofacial praxis,¹¹ and phonologic and semantic fluencies.²⁷ The Pyramid and Palm-Tree Test or La batterie d'évaluation des connaissances sémantiques du

GRECO semantic battery²⁸ was performed in the patients who showed semantic impairment in previous batteries.

Spontaneous speech was elicited by means of a semistructured interview, followed by the Cookie Theft picture description from

Table 2 Cognitive Characteristics of Patients With PPA Carrying *GRN* Mutations at First Evaluation

Scores	All Patients	lvPPA	nvPPA	svPPA	Mixed PPA
MMSE (of 30)	20.0 [15.0, 24.5]	20.5 [15.8, 24.8]	23.0 [19.0, 25.0]	9.5 [7.3, 11.8]	16.5 [11.0, 22.8]
MDRS (of 144)	110.0 [91.5, 115.3]	112.5 [102.2, 115.2]	113.0 [109.0, 121.0]	72.0	102.0 [77.0, 108.0]
Attention (of 37)	33.5 [32.0, 34.8]	33.0 [32.0, 35.0]	34.0 [34.0, 34.0]	30.0	32.0 [32.0, 35.0]
Initiation (of 37)	23.0 [15.8, 30.3]	26.0 [18.0, 33.0]	28.0 [25.5, 29.5]	9.0	21.0 [13.0, 23.0]
Construction (of 6), n (%) ^a	4 (29)	0	2 (67)	1 (100)	1 (20)
Conceptualization (of 39)	26.5 [21.0, 30.5]	29.0 [29.0, 31.0]	27.0 [25.5, 32.0]	19.0	25.0 [15.0, 26.0]
Memory (of 25)	16.5 [11.3, 19.0]	19.0 [15.0, 25.0]	19.0 [17.5, 21.5]	9.0	12.0 [11.0, 17.0]
FAB (of 18)	10.5 [7.8, 13.0]	12.0 [8.5, 13.5]	11.0 [9.5, 14.8]	3.5 [2.3, 4.8]	8.5 [7.0, 12.3]
Forward digit span	4.0 [3.0, 5.0]	4.0 [3.0, 4.0]	5.0 [3.0, 5.5]	5.0 [4.5, 5.5]	4.0 [3.0, 4.3]
Backward digit span	3.0 [2.0, 3.0]	3.0 [2.0, 3.0]	3.0 [3.0, 3.0]	1.0 [1.0, 1.0]	2.5 [2.0, 3.0]
TMT-A	62.0 [54.0, 74.0]	62.0 [48.0, 73.0]	61.5 [53.5, 65.0]	NA	65.0 [59.5, 78.5]
TMT-B	263.0 [180.5, 329.5]	188.0 [178.2, 245.0]	263.0 [186.0, 313.0]	NA	439.5 [372.8, 506.2]
TMT (B-A)	190.0 [122.5, 237.5]	132.5 [122.2, 178.0]	201.0 [139.5, 251.5]	NA	380.0 [310.5, 449.5]
FCSRT: free recall (of 48)	21.0 [14.3, 26.8]	23.5 [19.5, 30.0]	21.0 [16.0, 26.0]	NA	12 [8.0, 13.0]
FCSRT: total recall (of 48)	39.0 [27.0, 46.0]	40.0 [34.3, 46.8]	43.0 [40.0, 46.0]	NA	25.0 [24.0, 31.5]
FCSRT: sensitivity to cueing, %	75 [43, 92]	71 [42, 93]	85 [77, 92]	NA	43 [40, 57]
ROCF recall (of 36)	15.0 [12.0, 19.0]	17.0 [11.8, 19.0]	12.0 [12.0, 14.3]	15.0 [15.0, 15.0]	15.8 [14.5, 17.4]
ROCF copy (of 36)	33.0 [28.5, 36.0]	31.0 [27.3, 35.0]	33.0 [31.5, 35.3]	33.0 [32.0, 34.0]	36.0 [30.0, 36.0]
Ideo-motor apraxia (of 63)	57.5 [46.0, 60.3]	58.0 [55.0, 60.0]	58.0 [34.0, 59.0]	33.0 [30.0, 36.0]	47.0 [43.0, 63.0]

Abbreviations: FAB = Frontal Assessment Battery; FCSRT = Free and Cued Selective Reminding Test; lvPPA = logopenic variant of PPA; MDRS = Mattis Dementia Rating Scale; MMSE = Mini Mental Status Examination; NA = not available or unable to test; nvPPA = nonfluent/agrammatic variant of PPA; PPA = primary progressive aphasia; ROCF = Rey-Osterrieth Complex Figure; svPPA = semantic variant of PPA; TMT = Trail Making Test. Results are expressed as the median values with the first and third quartiles within brackets for numerical measures. Maximal scores of each test are indicated in parentheses.

^a Absolute count (percentage) of patients with impaired performance with respect to the total number of individuals who underwent the test.

BDAE. The patient's speech was scored at the time of the test by the speech-language pathologists. Written transcriptions were available for all patients. The verbal output was analyzed with respect to its production rate and the possible presence of word-finding pauses, phonologic errors, and *conduites d'approche* (i.e., repetitive effortful production of syllables and phonemes to approximate the target word).²⁹ The dissociation between single-word retrieval difficulties in spontaneous speech and naming (DO80 confrontation naming test) was signaled whenever present. Phonologic errors in spontaneous speech and naming tasks were transcribed. In addition, the rate of phonologic errors in the confrontation naming task was calculated (as well as for other types of errors such as verbal and semantic paraphasias, neologisms, periphrases, lack of response).

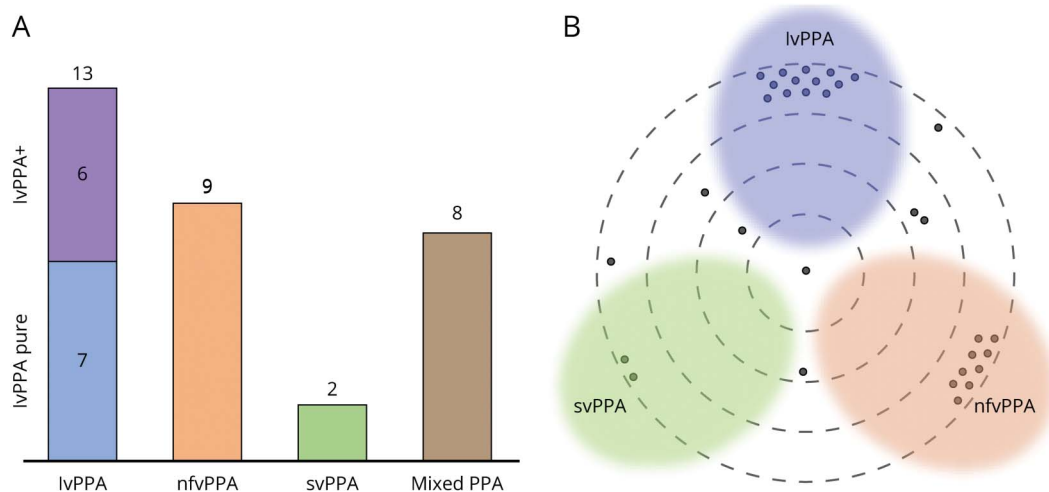
Grammaticality was evaluated by assessing the appropriateness of syntactic elaboration during spontaneous speech, referring to a validated scale.¹⁰ Agrammatism was defined by

the presence of a "frank" impairment in grammar/syntax (corresponding to definite or severe grade). To assess grammaticality in language reception, we referred to the performances in sentence comprehension tasks in the BDAE or Montreal-Toulouse protocol for examination of aphasia. AOS was diagnosed in the presence of effortful, groping speech with inconsistent phonemic substitutions or distortions due to inaccurate articulation and difficulty with initiating utterances, as previously defined.² Auditory-verbal working memory was evaluated with forward and backward digit span tests (see below). Finally, the global severity of deficits in spontaneous/conversational speech was scored from 0 (no useable speech or auditory comprehension) to 5 (subjective difficulties not apparent to the listener) following BDAE recommendations (table e-4, doi.org/10.5061/dryad.x3ffbg7hr).

Criteria Fulfillment and Aphasia Classification

The diagnosis of nvPPA, svPPA, or lvPPA was validated in patients strictly fulfilling the current criteria for 1 of these

Figure 2 Schematic Description of the PPA-GRN Cohort



(A) Number of patients diagnosed with each of the clinical variants. (B) Distribution of the cohort with respect to the linguistic deficits. Each patient is represented by a dot; the position of the dot mirrors the predominant linguistic deficits. lvPPA = logopenic variant of PPA; nfvPPA = nonfluent/agrammatic variant of PPA; PPA = primary progressive aphasia; svPPA = semantic variant of PPA.

variants but not the others.² The patients were diagnosed as having mixed PPA when the criteria for >1 variant were met and as having unclassifiable PPA when not meeting criteria for any specific PPA variants.^{6,7} To thoroughly describe the linguistic spectrum of lvPPA in GRN patients, we labeled those without any additional signs of other variants as having pure lvPPA, and some meeting canonical lvPPA criteria with very mild additional signs as having lvPPA+. Patients with lvPPA+ presented all the elements for lvPPA diagnosis with other mild features not allowing them to be classified as having mixed PPA.

Neuropsychological Evaluations

All cognitive domains other than language were evaluated with a semistandardized battery²² to investigate the presence of additional cognitive impairments (table e-3, doi.org/10.5061/dryad.x3ffbg7hr).

Comparisons Between Patients With PPA-GRN and Patients With Sporadic PPA

We compared patients with PPA-GRN with 2 groups of patients with sporadic PPA (11 with lvPPA and 9 with nfvPPA) who did not carry any FTD-causative mutations and underwent the same diagnostic workup. The 11 patients with lvPPA had a CSF profile in favor of underlying AD (lvPPA-AD). We compared demographic characteristics, speech/language, neuropsychological scores, and clinical symptoms between groups according to their PPA variant using Fisher exact test for categorical variables because of small frequencies. The Wilcoxon rank-sum test was used for numerical variables, because the continuous variables were not gaussian. Correction for multiple testing was handled with the Benjamini-Hochberg method. Statistical analyses were performed with R4.0.3 (R Foundation for Statistical Computing, Vienna, Austria).

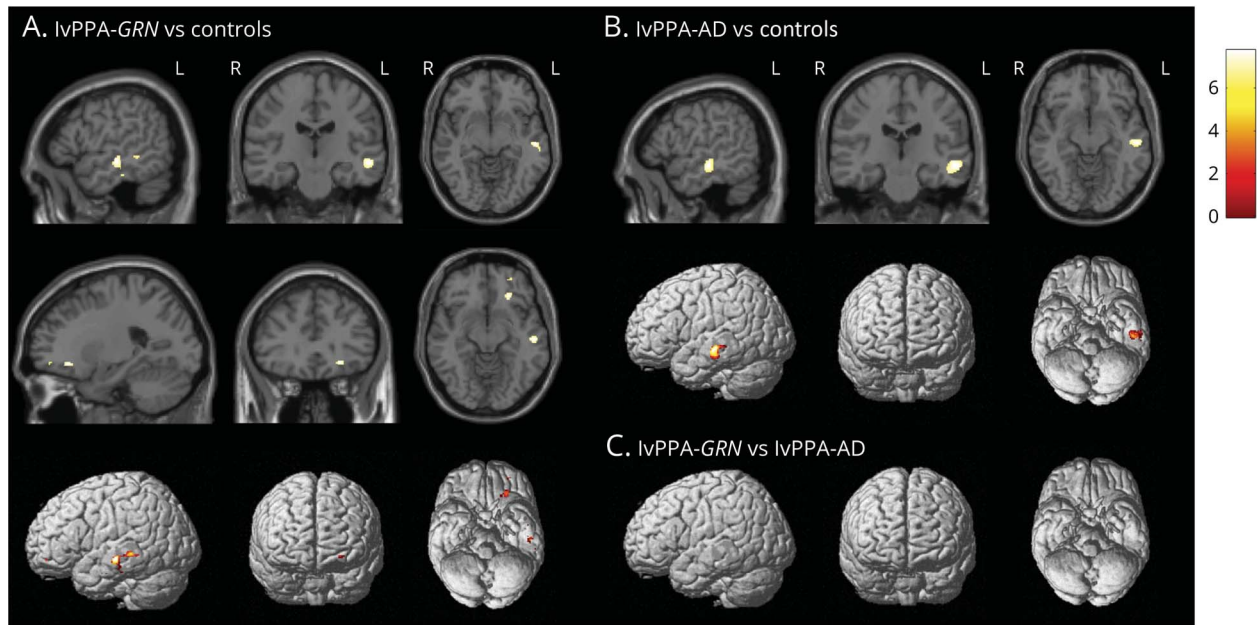
GM Atrophy in Patients With lvPPA-GRN

We analyzed brain 3-dimensional T1-weighted MRI sequences available for 8 patients with lvPPA-GRN. The mean delay between the clinical evaluation and brain MRI was ≤ 6 months. Their demographic and clinical data were similar to those of all patients with lvPPA-GRN of this study to ensure that they were representative of the entire group (table e-5, doi.org/10.5061/dryad.x3ffbg7hr). They were compared to 20 controls with similar demographic characteristics and to 11 patients with lvPPA-AD.

Voxel-based morphometry analyses were performed using the t1-volume pipeline of Clinica (www.clinica.run), a wrapper of the segmentation, run Dartel, and normalize to Montreal Neurological Institute (MNI) space routines implemented in Statistical Parametrical Mapping. After the unified segmentation procedure, a group template was created using Dartel, and the Dartel-to-MNI method was then applied, incorporating the native space images into the MNI space. For group analyses, we used 2-sample *t* tests with age at MRI and sex as confounding covariates. The following set of contrasts was applied: lvPPA-GRN vs controls, lvPPA-AD vs controls, and lvPPA-GRN vs lvPPA-AD. The statistical threshold was set at $p < 0.05$, corrected at the peak level for family-wise error. The Neuromorphometrics atlas (www.neuromorphometrics.com) was used to identify anatomic regions with significant differences. To validate our findings by means of a complementary approach, we also analyzed cortical thickness profiles in patients with lvPPA-GRN with the FreeSurfer software (supplemental data, available in Dryad).

Literature Review

Finally, to place our study in the context of the existing literature and to gain further insights in previously published



(A) Comparison between IvPPA-GRN and controls; 2 main clusters of atrophy are present at the level of the left middle temporal gyrus and the left posterior orbital gyrus. (B) Comparison between IvPPA-AD and controls; isolated cluster of atrophy at the level of the left middle temporal gyrus. (C) Comparison between IvPPA-GRN and IvPPA-AD; no significant differences between the 2 groups of patients were found. Color bar refers to the *t* values (table e-9, doi.org/10.5061/dryad.x3ffb7hr). IvPPA-AD = logopenic variant of primary progressive aphasia associated with Alzheimer disease; IvPPA-GRN = logopenic variant of primary progressive aphasia associated with *GRN* mutations; VBM = voxel-based morphometry.

PPA-GRN phenotypes, we performed an extensive review of the literature (D.S. and I.L.B.). Our PubMed search used the following terms: (*GRN* or *PGRN* or progranulin) or (frontotemporal lobar degeneration and genetics) and (PPA or Primary Progressive Aphasia). A total of 190 articles published between 2006 (year of *GRN* identification) and 2020 were found. To determine PPA-GRN frequencies within PPA or *GRN* patient cohorts, we selected cohort studies using the following inclusion criteria: (1) identification of *GRN* mutations with validated pathogenicity, (2) PPA diagnosis based on fulfillment of consensus criteria, and (3) cohort including at least 30 patients with PPA or *GRN* carriers. This led to the inclusion of 8 cohort studies, from which we extracted essential measures of frequency (number of cases of PPA-GRN in the total number of patients). To characterize the phenotypes of previously published cases of PPA-GRN, we selected case reports and small case series fulfilling the following criteria: (1) identification of *GRN* mutations of proven pathogenicity, (2) accurate descriptions of individual PPA phenotypes at onset and during follow-up, and (3) availability of the scores of formal speech/language evaluations. Notably, patients with mixed bvFTD-PPA phenotype at onset were excluded. We therefore encompassed 12 studies (including 1 published in 2003 identified through cross-referencing), comprehensively describing 23 patients with PPA-GRN. For each of them, we extracted essential clinical information and verified the fulfillment of criteria of each PPA variant.

Standard Protocol Approvals, Registrations and Patient Consents

The ethics committee of Paris-Necker Hospital approved the research study (project RBM 02–59). All patients provided written informed consent before their inclusion.

Data Availability

All relevant data are reported in the article. The raw data supporting the findings of this study are available from the corresponding author on reasonable request.

Results

Description of the PPA-GRN Population

Among the overall population of 235 patients with PPA, 45 (19%) carried *GRN* mutations, of whom 32 (14%) were included in this study. On the other hand, the frequency of PPA phenotype among the 162 *GRN* carriers was estimated at 20% (32 of 162) or at 28% (45 of 162).

The demographic, clinical, linguistic, and cognitive characteristics of the 32 patients are presented in tables 1 and 2 and table e-6 (doi.org/10.5061/dryad.x3ffb7hr). All were White. Their median age at onset was 62 years (interquartile range 59.0–63.3 years). Notably, only 26 (81%) had a positive family history (table 1). Patients were at an early stage of the disease, as reflected by the short median disease duration (DD) (2.0 years, interquartile range 1.5–2.5 years) and the median aphasia severity

score of 3.0 at the first evaluation. All signs/symptoms occurring afterward, during disease progression, are detailed in table 1.

Linguistic Characteristics in Patients With PPA-GRN

A canonical PPA variant was diagnosed in 24 patients at their first evaluation (figure 2). Overall, lvPPA was the most frequent variant (41%, 13 of 32 cases), followed by nfvPPA (28%, 9 of 32) and mixed PPA (25%, 8 of 32). svPPA was much less frequent (6%, 2 of 32). None had unclassifiable PPA. The 8 patients diagnosed with mixed PPA fulfilled the criteria of >1 variant. Nevertheless, the complexity of their phenotype was not due to a longer DD (2 ± 0.8 years), which was similar to that of the entire cohort (2.2 ± 0.5 years).

Specific profiles emerged from in-depth analysis of the linguistic deficits of each patient, presented in table e-6 (doi.org/10.5061/dryad.x3ffbg7hr). Patients with lvPPA-GRN presented sparse spontaneous speech, marked by word-finding difficulties, incomplete sentences, and prolonged pauses without motor speech deficit. Most patients exhibited sentence-level processing deficit (repetition and comprehension of long sentences), contrasting with preserved processing at the single-word level. Seven (22%) had pure lvPPA, while 6 had lvPPA+ with co-occurrence of a mild articulatory disorder ($n = 1$ case) and/or syntax oversimplification ($n = 3$) and/or semantic impairment ($n = 5$). Illustrative case reports of pure lvPPA (patient 25) and lvPPA+ (patient 02) are given in supplemental data (doi.org/10.5061/dryad.x3ffbg7hr). At the group level, the profile of lvPPA-GRN was indistinguishable from that of the patients with sporadic lvPPA-AD (table e-7).

Agrammatism prevailed in most (8 of 9) patients with nfvPPA, whereas AOS was the predominant presentation in only 1 case (patient 04). Notably, patients with nfvPPA had slightly better performances in overall cognitive functioning and verbal memory than the global cohort (table 2). Language and cognitive scores did not differ significantly between patients with nfvPPA-GRN and those with sporadic nfvPPA (table e-8, doi.org/10.5061/dryad.x3ffbg7hr). As the disease progressed, 22% of patients with nfvPPA-GRN evolved to a CBS.

Eight patients with mixed PPA presented varying degrees of reduced speech output and word-finding difficulties with pauses. Confrontation naming and repetition of long sentences were impaired in all, and almost all exhibited phonologic errors in spontaneous speech/naming. These logopenic/phonologic impairments co-occurred with semantic deficits (5 of 8 patients) and/or grammar production and reception deficits (6 of 8).

Progression of PPA-GRN

All the patients have been clinically followed up in the context of their usual neurologic care. Twelve patients also underwent 1 to 3 complete standardized speech/language assessments during their clinical follow-up.

Disease progression in patients with PPA-GRN was remarkably severe and rapid (table 1). The mean DD at

complete mutism was 5.0 ± 1.3 years. Eight patients died after a mean DD of 7.3 ± 1.2 years, in line with the short survival of patients with GRN mutations. Fourteen were lost to follow-up after a mean DD of 3.9 ± 1.4 years, and 10 were still being followed up at the time of the study (5.6 ± 1.7 years).

During disease progression, all patients secondarily developed overt frontal disturbances. A cognitive executive syndrome was present in almost all patients at follow-up (31 of 32) and prevailed over behavioral impairment (18 of 32). More than half of patients subsequently developed a parietal syndrome. This could likely be related to the fast propagation of lesions to anterior frontotemporal and posterior parietal regions in GRN disease. A paradigmatic case description from our series exemplifies this progression pattern (supplemental data). The broadening of the clinical syndrome during disease evolution led to the formulation of secondary diagnoses, later fulfilling criteria for bvFTD ($n = 16$) or for CBS ($n = 3$) (table e-6, doi.org/10.5061/dryad.x3ffbg7hr).

Neuroanatomic Changes in lvPPA-GRN

Patients with lvPPA-GRN showed significant atrophy in the left middle temporal (MT) and posterior orbital gyri compared to controls ($p < 0.05$, family-wise error correction), as illustrated in figure 3A. Cortical thickness analyses were concordant with these results despite showing more extended prefrontal and left temporoparietal junction involvement, likely due to the less stringent correction adopted (figure e-1, doi.org/10.5061/dryad.x3ffbg7hr).

Patients with lvPPA-AD showed significant atrophy only in the left MT gyrus compared to controls (figure 3B). When directly compared, no significant differences emerged between the lvPPA-GRN and the lvPPA-AD groups (figure 3C). A detailed list of coordinates with local maximum atrophy for each comparison is provided in table e-9 (doi.org/10.5061/dryad.x3ffbg7hr).

PPA-GRN Cases in the Literature

In the literature, the frequency of PPA phenotypes in GRN carriers ranged from 12% to 38% according to cohort studies^{15,18,30-32} (table e-10, doi.org/10.5061/dryad.x3ffbg7hr). The frequency of GRN mutation carriers within PPA cohorts ranged from 2% to 10%^{18,33-35} (table e-11).

Descriptions of 23 patients carrying GRN mutations with in-depth linguistic characterization are summarized in table 3. Fourteen were reported up to 2011, the year of the definition of the current diagnostic criteria. They were diagnosed with PPA ($n = 4$), PNFA ($n = 8$), nfvPPA ($n = 1$), or progressive anomia ($n = 1$). It is noteworthy that the most recurrent linguistic deficits were impaired naming (13 of 14), reduced speech output (12 of 14), word-retrieval difficulties in spontaneous speech (11 of 14), and phonologic errors (10 of 14). Frank agrammatism was seldom present, as well as AOS, which characterized 4 cases of PNFA/nfvPPA.

Table 3 Description of Previously Published PPA Cases With *GRN* Mutations

	Krefft et al., ⁴⁹ 2003 Mesulam et al., ¹⁴ 2007			Snowden et al., ¹³ 2006		Snowden et al., ¹⁹ 2007	Beck et al., ⁵⁰ 2008					Rohrer et al., ¹⁶ 2010
Patient	PPA1: A	PPA1: C	PPA1: D	III-5	III-1	N.	240-4	255-9	255-10	430-2	431-3	SC
Diagnosis	PPA	PPA	PPA	PNFA	PNFA	Progressive anomia	PNFA	PNFA/ CBS	PNFA	PNFA	PNFA/ SD	PPA
AAO, y	60	61	65	63	65	66	NA	NA	NA	NA	NA	62
DD at evaluation, y	5	1	3	2	2	3	4	1	3	4	1	3
Reduced speech output	—	+	+	+	+	+	+	+	+	+	—	+
Impaired naming	+	+	+	+	+	+	—	+	+	+	+	+
Word-retrieval difficulties	+	+	+	+	+	+	—	—	+	—	+	+
Impaired word repetition	—	NA	NA	+ ^a	+ ^a	—	NA	NA	NA	NA	NA	+
Impaired sentences repetition	—	NA	NA	+ ^a	+ ^a	—	NA	NA	NA	NA	NA	+
Phonologic paraphasias	—	—	+	+	+	—	+	—	+	+	+	+
Agrammatism	—	—	—	—	+	(+)	—	—	—	—	—	+
AOS	—	—	—	+ ^b	—	—	— ^c	+	— ^c	+	—	—
Impaired sentences comprehension	—	+	+	—	+	—	NA	NA	NA	NA	NA	+ ^e
Impaired word comprehension	+	+	NA	—	—	—	NA	—	—	+	—	+
Impaired object knowledge	—	—	NA	—	—	—	—	—	—	—	+	—
Impaired reading	NA	+	NA	+ ^a	—	—	—	+	—	+	+ ^d	+
Verbal/semantic paraphasias	+	+	+	(+)	—	—	NA	NA	NA	NA	NA	+

Continued

When the 9 most recent cases described after 2011 were split according to their diagnoses, lvPPA was the most frequent variant (5 of 9) even if mild comprehension deficits emerged in 2 of them.^{17,21} The cause of this is possibly to be ascribed to increasing sentence complexity or latent semantic impairment. The diagnoses of nfvPPA relied mainly on the presence of agrammatism, whereas AOS was a rare occurrence (1 of 9). Overall, sentence-level processing deficits, when investigated, were a common finding among cases of PPA-GRN from the literature.

Discussion

The first evidence that FTD genes could produce PPA phenotypes was provided by Snowden et al.¹³ and Mesulam et al.¹⁴ after discovery of the *GRN* gene. They described patients with “nonfluent” aphasia who had phonologic deficits, namely progressive anomia, without overt motor speech impairment, and subsequent repetition and reading deficits. Circumscribed,

profound anomia was remarkably predominant in 1 of them who received a diagnosis of progressive anomia.¹⁹ A few *GRN* carriers with PNFA or nfvPPA have since been reported, but most were characterized according to the dichotomization of PPA in semantic dementia and PNFA, before the definition of the lvPPA. More recently, it emerged that not only agrammatism but also phonologic/logopenic deficits may be predominant in some cases. However, few underwent extensive linguistic characterization, and specific characteristics of genetic PPA have not yet been investigated in large series of patients. Here, we describe the linguistic, cognitive, and neuroimaging characteristics of 32 patients with PPA who carried *GRN* mutations, representing a large cohort for a rare genetic disease, thus providing the first in-depth characterization of PPA-GRN.

The first important finding of the study is the high frequency of PPA among *GRN* carriers, as high as 20% or even 28% when we consider all 45 patients with PPA-GRN (including also those with insufficient clinical data to be in the study). This is in line with the frequencies of PPA in other *GRN*

Table 3 Description of Previously Published PPA Cases With *GRN* Mutations (*continued*)

	Deramecourt et al., ²⁰ 2010	Cerami et al., ⁵¹ 2011	Caso et al., ⁵² 2014	Josephs et al., ²¹ 2014			Mesulam et al., ¹⁴ 2007 Mesulam et al., ⁶ 2014 Kim et al., ¹⁷ 2016				
Patient	7	2	SC	1	2	3	PPA3: 1 A	P22/2	3	PPA3:B/ P21/4	
Diagnosis	nvPPA	PNFA	nvPPA	lvPPA	lvPPA	lvPPA	PPA	nvPPA	nvPPA	lvPPA	lvPPA
AAO, y	60	NA	60	56	61	56	65	56	50	53	62
DD at evaluation, y	1	1	3	2	3	2	1	2 (5 at death)	2 (6 at death)	8 at death	2 (6 at death)
Reduced speech output	+	+	+	+	+	+	+	+	+	+	+
Impaired naming	+	+	+	—	+	+	+	—	—	+	+
Word-retrieval difficulties	+	+	+	+	+	+	+	+	—	+	+
Impaired word repetition	—	—	(+) ^f	NA	NA	NA	—	NA	NA	NA	—
Impaired sentences repetition	+	+	+	+	+	+	+ ^c	NA	(+)	NA	NA
Phonologic paraphasias	+	+	+	+	+	+	+	NA	+	NA	—
Agrammatism	+	+	+	—	—	—	+	+	+	—	—
AOS	(+)	— ^c	+	—	—	—	—	—	—	—	—
Impaired sentences comprehension	+	+	+	+ ^g	+ ^g	+	+ ^g	NA	(+)	NA	— ^h
Impaired word comprehension	—	—	—	—	—	+	—	NA	—	NA	— ^h
Impaired object knowledge	—	NA	NA	—	—	+	—	NA	NA	NA	—
Impaired reading	—	+	NA	—	—	+	+ ^g	NA	NA	NA	NA
Verbal/semantic paraphasias	+	NA	—	NA	NA	NA	—	NA	—	NA	—

Abbreviations: AAO = age at onset; AOS = apraxia of speech; CBS = corticobasal syndrome; DD = disease duration; lvPPA = logopenic variant of PPA; NA = not available; nvPPA = nonfluent/agrammatic variant of PPA; PNFA = progressive non-fluent aphasia; PPA = primary progressive aphasia; SC = single case; SD = semantic dementia. + indicates presence; — indicates absence; and (+) indicates occasional or mild difficulties.

^a Phonologic errors.

^b Stuttering.

^c Buccofacial apraxia.

^d Phonologic dyslexia.

^e Worse for passive, reversible, and complex sentences.

^f With word length effect.

^g For complex sentences.

^h Intermittent comprehension deficits.

cohorts varying from 12% to 38% (table e-10, doi.org/10.5061/dryad.x3ffbg7hr). Some discrepancies between these studies might reflect distinct geographic origins and genetic backgrounds among populations or different proportions of each PPA variant (especially lvPPA) within these cohorts. Some cohorts, like ours, may also be enriched in familial and genetic cases (table e-11). Of note, only 7 of 330 (2%) *C9orf72* expansion carriers in the overall cohort received a diagnosis of PPA, not allowing us to describe and compare them as a group. The markedly different frequency of *GRN* and *C9orf72* mutations in patients with PPA suggests that gene-specific biological defects lead to distinct brain

structures and language networks vulnerability and highlights the importance of conducting separate studies of each genotype.

Another major finding is the high prevalence of logopenic variants, representing the main PPA phenotype associated with *GRN* mutations. The consensus criteria for lvPPA require impaired single-word retrieval in spontaneous speech and naming and impaired repetition of sentences/phrases with 3 of the following deficits: phonologic errors, spared single-word comprehension, spared motor speech, and absence of frank agrammatism.² All our patients with lvPPA fit these criteria.

Seven of them had no other linguistic deficits (pure lvPPA), whereas 6 (lvPPA+) had an obvious predominant logopenic deficit but a broader mild deficit in semantics, grammar, or articulation not fitting criteria for mixed PPA. Overall, these subtle variabilities in lvPPA phenotypes could be better gathered under the umbrella term logopenic-spectrum variant.

By itself, the former group, defining lvPPA in its strictest sense, encompassed 22% of the *GRN* carriers. This high prevalence was unexpected because lvPPA typically results from amyloid pathology suggestive of AD.⁴ However, recent studies have reported amyloid-negative cases of lvPPA that could represent as many as 14% of patients with lvPPA⁷ based on negative AD biomarkers in CSF,¹¹ negative Pittsburgh compound B-PET,^{10,12,21} or nonamyloid pathology at autopsy.⁶⁻⁸ In the literature, no major linguistic differences distinguish amyloid-negative and amyloid-positive lvPPA except for worse sentence repetition, naming, and word comprehension in amyloid-negative patients.^{12,36}

The coincidental association of *GRN* mutations with comorbid amyloid pathology responsible for lvPPA is unlikely in our patients because AD biomarkers were negative for all patients for whom CSF was available (10 of 10, not available in 3). A direct role of *GRN* mutations in the emergence of the phonologic/logopenic deficit is much more likely. This is supported by the report of a number of patients with *GRN* mutations displaying predominant logopenic deficit^{16,34,35} and by prior descriptions of 6 patients with nonamyloid lvPPA, among whom 3 carried *GRN* mutations.²¹ The frequency of logopenic spectrum in our study is also concordant with a pathological study on 4 patients with PPA-*GRN*, half of whom presented a logopenic variant.¹⁷ Last, strong evidence linked amyloid-negative lvPPA with TDP-43 pathology, mostly type A,⁷ which is also the major pathological type underlying *GRN* mutations.

The diagnosis of lvPPA according to the consensus criteria remains challenging, partially due to the intrinsic difficulties in assessing key features and the possible overlap between variants. Most studies have demonstrated the good predictability of svPPA criteria, but the separation of lvPPA from nfvPPA is more elusive. The features defining lvPPA are still a matter of debate. Some groups have proposed adaptations to consensus criteria, suggesting the replacement of impaired repetition by absence of definite grammar and comprehension impairment as a core feature of lvPPA.³⁷ Others have proposed less strict criteria, tolerating moderate impairment of single-word comprehension “as long as it doesn’t exceed that of complex sentence comprehension.”³⁸ The importance of considering phonologic errors among the main criteria has also been underlined.³⁹ Finally, some studies showed that the most discriminative features to correctly classify patients were single-word comprehension deficit, agrammatism, impaired sentence repetition, and motor speech disorders.^{6,10,29}

The diagnostic complexity and criteria inconsistencies for lvPPA might possibly explain its unexpected frequency in our

series, especially because the criteria were applied retrospectively for some patients (2 with lvPPA) evaluated before 2004. However, this is unlikely to explain all our cases, and the application of the most discriminative features cited above also categorized most of these patients as having lvPPA, thus validating the robustness of the diagnoses. In addition, our patients with lvPPA-*GRN* showed significant GM atrophy in the left posterior MT gyrus, a part of the left temporoparietal junction shown to be critically involved in phonologic processing and verbal short-term memory and predominantly altered in lvPPA.⁴⁰⁻⁴³ Consistent with our neuroanatomic results, pathological studies demonstrated predominant TDP-43 inclusions in the left posterior temporal gyri and inferior parietal lobule in 2 patients with lvPPA-*GRN*.¹⁷ More generally, the posterior lateral temporal lobe appears to be a crucial area particularly vulnerable in *GRN* disease, even at the earliest stages of the pathologic process.⁴⁴ The neuroimaging pattern in our patients was also comparable to that of lvPPA-AD in our study except for additional atrophy in fronto-orbital areas. That likely mirrored the mild impairment in frontal functions in patients with lvPPA-*GRN*, both of which are not unexpected in a cohort of *GRN* carriers.

Plasma progranulin dosage, predicting *GRN* mutations when low, has been used routinely by French centers since 2009 for all patients with bvFTD and PPA, including those with lvPPA when AD biomarkers are negative. This provides another possible explanation for the high prevalence of lvPPA in our study. lvPPA is also possibly underdiagnosed because of the lack of molecular investigations in amyloid-negative lvPPA cases and of detailed linguistic explorations in large *GRN* cohorts. Overall, our study confirms that different molecular and pathologic processes may underlie the clinical and topographic syndrome of lvPPA and provides strong evidence that *GRN* mutations may be involved in a part of amyloid-negative lvPPA. Genetic screening in cohorts of amyloid-negative lvPPA will be needed to confirm this hypothesis and eventually to clarify their etiology.

Two different forms of nfvPPA, dominated by agrammatism or AOS, have emerged from the description of their linguistic characteristics, patterns of atrophy, and underlying pathology.^{20,45,46} Prevailing AOS is associated with focal atrophy in premotor cortex and rather predictive of FTLD-TAU, whereas patients with agrammatism had more widespread atrophy, extending to premotor, prefrontal, and temporoparietal regions, and were more likely to harbor TDP-43 inclusions.^{45,47} The more diffuse pattern of atrophy evidenced in the latter group has been associated with more severe language deficits during disease progression and a worse outcome.⁴⁷

The relatively large number of patients in our study allowed us to depict the most recurrent linguistic profile characterizing nfvPPA-*GRN*. Nearly all our patients had frank agrammatism, whereas the phenotype dominated by AOS was rare in this study, as in the literature. This study thus provides an additional piece of evidence for a clinicopathologic duality among

patients with *nvPPA* and for a privileged link between the agrammatic subtype of *nvPPA* and TDP-43 pathology, which is the pathologic substrate of *GRN* mutations.

Multiple levels of language elaboration (auditory-verbal short-term memory, grammar processing, semantic access, and, occasionally, semantic storage) may all be simultaneously altered in *PPA-GRN*. Anatomic regions associated with these functions include left posterior inferior frontal, anterior inferior parietal, temporopolar, posterior superior, and MT cortices.^{11,48} The most prevalent linguistic deficits in our patients with mixed *PPA* almost always included core features of *lvPPA* associated with moderate grammatical and word-comprehension deficits and deep/phonologic dyslexia, similar to some reported *GRN* carriers.^{13,16,21,35}

The multifaceted presentation of *PPA* phenotypes, particularly in their mixed forms, offers an interesting opportunity to consider the degenerative conditions associated with progranulin deficiency from a network perspective. According to the current model of language processing, a ventral stream involved in word meaning links the superior temporal gyrus to the middle/inferior temporal gyri, temporal pole, and inferior frontal cortices. A dorsal pathway involved in sound articulation connects the superior temporal gyrus with inferior parietal and frontal cortices. Our results and previous studies suggest that the temporal lobe and temporoparietal junction are key regions in the *GRN*-mediated pathologic process^{43,44} and that both the dorsal and ventral language pathways may be altered to varying degrees in *PPA-GRN*. We can speculate that the resulting predominant phenotype depends largely on which parts of the network are affected and to what extent.

This study provides important information for clinical practice. On the basis of the literature and our results, we propose some recommendations for genetic testing according to the *PPA* variant. The remarkably high frequency of patients with *PPA* without family history of *FTD* in our series (up to 19%) indicates that genetic studies should not be limited to familial cases. Overall, *PPA* is more often associated with *GRN* than with *C9orf72* mutations. We suggest measuring plasma progranulin levels in all patients with *nvPPA* and those with amyloid-negative *lvPPA* (even without family history) before analyzing the *GRN* gene when levels are decreased. Moreover, considering both the patients with *lvPPA+* and those with mixed forms, an important proportion of our *GRN* cohort (14 of 32, 44%) escaped a strict classification, indicating that *GRN* mutations should also be considered primarily in patients displaying atypical/mixed *PPA* variants. *AOS* is rarely associated with *GRN* and is generally predictive of *FTLD-TAU* pathology,^{45,46} supporting the *MAPT* gene analysis as the first indication in this phenotype, particularly in patients with a family history of *FTD*. *svPPA* is also rarely associated with *GRN* mutations and, more broadly, with *FTD* gene mutations.

This study contributes to a better description of the linguistic spectrum in a large cohort of patients with *PPA* related to

GRN mutations, with major clinical impact due to upcoming *GRN*-targeted therapies. The heterogeneous phenotypes in our patients suggest that *GRN* mutations may exert a noxious effect on distinct neocortical networks, with partial overlap in some key linguistic areas. The most prevalent *PPA-GRN* phenotype determines logopenic/phonologic deficits correlated with left posterior temporal atrophy. In clinical practice, this study highlights that *GRN* should be investigated in the emerging group of logopenic variants with negative *AD* biomarkers and emphasizes the usefulness of measuring plasma progranulin levels in this indication.

Our study had some limitations. Due to the rarity of genetically determined *PPA*, cases were recruited over a long time lapse and required some data harmonization to compare linguistic and cognitive impairments. However, the rigorous evaluation and selection process of the patients ensured the reliability of the diagnoses and the classification of *PPA* variants. Conversely, our inclusion procedure, based on fulfillment of international criteria for *PPA*, may have prevented us from capturing milder and unclassifiable phenotypes in this study. Last, some subgroups such as those with *svPPA* were presented in only a descriptive way because they were too small to perform statistical analyses.

The prediction of the trajectory of neurodegenerative diseases, in particular *PPA*, at the individual level is still very challenging. Our study shows that mutations in *GRN* gene, all resulting in progranulin deficiency, can lead to different *PPA* variants. It seems to indicate that the causal mechanism may be more complex than the gene alone, and still unknown patient-specific factors might interact with causal mutations, resulting in variable clinical phenotypes. Further studies addressing the earliest disease stages in gene carriers will likely provide insights into which factors affect the severity of the linguistic and extralinguistic deficits and preferentially drive the phenotype to *PPA*. More specifically, the study of genetic modifiers, especially those connected to language-learning disabilities, might clarify the biological determinants of selective lesion tropism for the language networks in patients displaying genetic *PPA*. Advances in these domains could enhance our understanding of the disease trajectory in *FTLD*, provide new evidence supporting different degenerative pathways, link specific molecular dysfunctions with clinical phenotypes, and finally facilitate the correct classification of these still elusive cognitive phenotypes.

Acknowledgment

The authors thank the DNA and cell bank of the ICM (ICM, Paris), Kathy Larcher (UF de Neurogénétique, Pitié-Salpêtrière Hospital, Paris), Sandrine Noël (UF de Neurogénétique, Pitié-Salpêtrière Hospital, Paris), and Isabelle David (UF de Neurogénétique, Pitié-Salpêtrière Hospital, Paris) for their technical assistance. The authors also thank Valerio Gargiulo for his support in the final editing of the manuscript.

Study Funding

The research leading to these results received funding from the Investissement d'avenir ANR-11-INBS-0011. This work

was funded by the Programme Hospitalier de Recherche Clinique (PHRC) FTLD-exome (to I.L.B., promotion by Assistance Publique Hôpitaux de Paris), PHRC Predict-PGRN (to I.L.B., promotion by Assistance Publique Hôpitaux de Paris).

Disclosure

The authors report no disclosures relevant to the manuscript. Go to [Neurology.org/N](https://www.neurology.org/N) for full disclosures.

Publication History

Received by *Neurology* October 23, 2020. Accepted in final form March 26, 2021.

Appendix 1 Authors

Name	Location	Contribution
Dario Saracino, MD	Hôpital Pitié-Salpêtrière, Paris, France	Designed and conceptualized the study; analyzed and interpreted the data; performed statistical analysis; drafted the manuscript for intellectual content
Sophie Ferrieux	Hôpital Pitié-Salpêtrière, Paris, France	Major role in the acquisition of data; analyzed the data
Marie Noguès-Lassaille	Hôpital Pitié-Salpêtrière, Paris, France	Major role in the acquisition of data; analyzed the data
Marion Houot, MSc	Hôpital Pitié-Salpêtrière, Paris, France	Analyzed the data; performed statistical analysis
Aurélie Funkiewiez, PhD	Hôpital Pitié-Salpêtrière, Paris, France	Major role in the acquisition of data; analyzed the data
Leila Sellami, MD	Hôpital Pitié-Salpêtrière, Paris, France	Analyzed and interpreted the data; revised the manuscript for intellectual content
Vincent Deramecourt, MD, PhD	Lille University Hospital, France	Major role in the acquisition of data; revised the manuscript for intellectual content
Florence Pasquier, MD, PhD	Lille University Hospital, France	Major role in the acquisition of data; revised the manuscript for intellectual content
Philippe Couratier, MD, PhD	Limoges University Hospital, France	Major role in the acquisition of data; revised the manuscript for intellectual content
Jérémie Pariente, MD, PhD	Toulouse University Hospital, France	Major role in the acquisition of data; revised the manuscript for intellectual content
Amandine Géraudie, MSc	Toulouse University Hospital, France	Major role in the acquisition of data; revised the manuscript for intellectual content
Stéphane Epelbaum, MD, PhD	Hôpital Pitié-Salpêtrière, Paris, France	Major role in the acquisition of data; revised the manuscript for intellectual content

Appendix 1 (continued)

Name	Location	Contribution
David Wallon, MD, PhD	Rouen University Hospital, France	Major role in the acquisition of data; revised the manuscript for intellectual content
Didier Hannequin, MD, PhD	Rouen University Hospital, France	Major role in the acquisition of data; revised the manuscript for intellectual content
Olivier Martinaud, MD, PhD	Caen University Hospital, France	Major role in the acquisition of data; revised the manuscript for intellectual content
Fabienne Clot, PhD	Hôpital Pitié-Salpêtrière, Paris, France	Analyzed the data; revised the manuscript for intellectual content
Agnès Camuzat, MSc	Hôpital Pitié-Salpêtrière, Paris, France	Interpreted the data; revised the manuscript for intellectual content
Simona Bottani, MSc	Hôpital Pitié-Salpêtrière, Paris, France	Analyzed the data; revised the manuscript for intellectual content
Daisy Rinaldi, PhD	Hôpital Pitié-Salpêtrière, Paris, France	Major role in the acquisition of data; revised the manuscript for intellectual content
Sophie Auriacombe, MD	Bordeaux University Hospital, France	Major role in the acquisition of data; revised the manuscript for intellectual content
Marie Sarazin, MD, PhD	Hôpital Sainte Anne, Paris, France	Major role in the acquisition of data; revised the manuscript for intellectual content
Mira Didic, MD, PhD	Aix-Marseille University Hospital, Marseille, France	Major role in the acquisition of data; revised the manuscript for intellectual content
Claire Boutoleau-Bretonnière, MD, PhD	Nantes University Hospital, France	Major role in the acquisition of data; revised the manuscript for intellectual content
Christel Chauvin-Robinet, MD, PhD	Dijon-Bourgogne University Hospital, Dijon, France	Major role in the acquisition of data; revised the manuscript for intellectual content
Julien Lagarde, MD	Hôpital Sainte Anne, Paris, France	Major role in the acquisition of data; revised the manuscript for intellectual content
Carole Roué-Jagot, MD	Hôpital Sainte Anne, Paris, France	Major role in the acquisition of data; revised the manuscript for intellectual content
François Sellal, MD, PhD	Strasbourg-Colmar University Hospital, Strasbourg, France	Major role in the acquisition of data; revised the manuscript for intellectual content
Audrey Gabelle, MD, PhD	Montpellier University Hospital, France	Major role in the acquisition of data; revised the manuscript for intellectual content

Appendix 1 (continued)

Name	Location	Contribution
Frédérique Etchary-Bouyx, MD, PhD	Angers University Hospital, France	Major role in the acquisition of data; revised the manuscript for intellectual content
Alexandre Morin, MD	Hôpital Pitié-Salpêtrière, Paris, France	Major role in the acquisition of data; revised the manuscript for intellectual content
Cinzia Coppola, MD, PhD	Naples University Hospital, Italy	Revised the manuscript for intellectual content
Richard Levy, MD, PhD	Hôpital Pitié-Salpêtrière, Paris, France	Revised the manuscript for intellectual content
Bruno Dubois, MD	Hôpital Pitié-Salpêtrière, Paris, France	Revised the manuscript for intellectual content
Alexis Brice, MD, PhD	Hôpital Pitié-Salpêtrière, Paris, France	Revised the manuscript for intellectual content
Olivier Colliot, PhD	Hôpital Pitié-Salpêtrière, Paris, France	Interpreted the data; revised the manuscript for intellectual content
Maria Luisa Gorno-Tempini, MD, PhD	University of California, San Francisco	Interpreted the data; revised the manuscript for intellectual content
Marc Teichmann, MD, PhD	Hôpital Pitié-Salpêtrière, Paris, France	Revised the manuscript for intellectual content
Raffaella Migliaccio, MD, PhD	Hôpital Pitié-Salpêtrière, Paris, France	Analyzed and interpreted the data; revised the manuscript for intellectual content
Isabelle Le Ber, MD, PhD	Hôpital Pitié-Salpêtrière, Paris, France	Designed and conceptualized the study; analyzed and interpreted the data; drafted the manuscript for intellectual content

Appendix 2 Coinvestigators

Name	Location	Role	Contribution
Serge Belliard, MD	Rennes University Hospital, France	Site investigator	Coordinated communication among sites
Frédéric Blanc, MD	Hôpitaux Civils, Strasbourg, France	Site investigator	Coordinated communication among sites
Mathieu Ceccaldi, MD, PhD	University Hospital La Timone, Marseille, France	Site investigator	Coordinated communication among sites
Charles Duyckaerts, MD, PhD	Hôpital Pitié-Salpêtrière, Paris, France	Site investigator	Coordinated neuropathology for site
Maité Formaglio, MD	Lyon University Hospital, France	Site investigator	Coordinated communication among sites
Véronique Golfier, MD	Rennes University Hospital, France	Site investigator	Coordinated communication among sites

Appendix 2 (continued)

Name	Location	Role	Contribution
Lucette Lacomblez, MD	Hôpital Pitié-Salpêtrière, Paris, France	Site investigator	Coordinated communication among sites
Bernard-François Michel, MD	Hôpital Sainte-Marguerite, Marseille, France	Site investigator	Coordinated communication among sites
Catherine Thomas-Anterion, MD	Plein-Ciel Hospital, Lyon, France	Site investigator	Coordinated communication among sites
Martine Vercelletto, MD	Nantes University Hospital, France	Site investigator	Coordinated communication among sites

References

- Mesulam M-M. Primary progressive aphasia. *Ann Neurol*. 2001;49(4):425-432.
- Gorno-Tempini ML, Hillis AE, Weintraub S, et al. Classification of primary progressive aphasia and its variants. *Neurology*. 2011;76(11):1006-1014.
- Gorno-Tempini ML, Dronkers NF, Rankin KP, et al. Cognition and anatomy in three variants of primary progressive aphasia. *Ann Neurol*. 2004;55(3):335-346.
- Mesulam M, Wicklund A, Johnson N, et al. Alzheimer and frontotemporal pathology in subsets of primary progressive aphasia. *Ann Neurol*. 2008;63(6):709-719.
- Spinelli EG, Mandelli ML, Miller ZA, et al. Typical and atypical pathology in primary progressive aphasia variants. *Ann Neurol*. 2017;81(13):430-443.
- Mesulam M-M, Weintraub S, Rogalski EJ, Wieneke C, Geula C, Bigio EH. Asymmetry and heterogeneity of Alzheimer's and frontotemporal pathology in primary progressive aphasia. *Brain*. 2014;137(pt 4):1176-1192.
- Bergeron D, Gorno-Tempini ML, Rabinovici GD, et al. Prevalence of amyloid- β pathology in distinct variants of primary progressive aphasia. *Ann Neurol*. 2018;84(5):729-740.
- Chare L, Hodges JR, Leyton CE, et al. New criteria for frontotemporal dementia syndromes: clinical and pathological diagnostic implications. *J Neurol Neurosurg Psychiatry*. 2014;85(8):865-870.
- Hu WT, McMillan C, Libon D, et al. Multimodal predictors for Alzheimer disease in nonfluent primary progressive aphasia. *Neurology*. 2010;75(7):595-602.
- Leyton CE, Villemagne VL, Savage S, et al. Subtypes of progressive aphasia: application of the international consensus criteria and validation using β -amyloid imaging. *Brain*. 2011;134(pt 10):3030-3043.
- Teichmann M, Kas A, Boutet C, et al. Deciphering logopenic primary progressive aphasia: a clinical, imaging and biomarker investigation. *Brain*. 2013;136(pt 11):3474-3488.
- Santos-Santos MA, Rabinovici GD, Iaccarino L, et al. Rates of amyloid imaging positivity in patients with primary progressive aphasia. *JAMA Neurol*. 2018;75(3):342.
- Snowden JS, Pickering-Brown SM, Mackenzie IR, et al. Progranulin gene mutations associated with frontotemporal dementia and progressive non-fluent aphasia. *Brain*. 2006;129(pt 11):3091-3102.
- Mesulam M, Johnson N, Krefft TA, et al. Progranulin mutations in primary progressive aphasia: the PPA1 and PPA3 families. *Arch Neurol*. 2007;64(1):43-47.
- Le Ber I, Camuzat A, Hannequin D, et al. Phenotype variability in progranulin mutation carriers: a clinical, neuropsychological, imaging and genetic study. *Brain*. 2008;131(pt 3):732-746.
- Rohrer JD, Crutch SJ, Warrington EK, Warren JD. Progranulin-associated primary progressive aphasia: a distinct phenotype? *Neuropsychologia*. 2010;48(1):288-297.
- Kim G, Ahmadian SS, Peterson M, et al. Asymmetric pathology in primary progressive aphasia with progranulin mutations and TDP inclusions. *Neurology*. 2016;86(7):627-636.
- Le Ber I, Guillot-Noel L, Hannequin D, et al. C9ORF72 repeat expansions in the frontotemporal dementias spectrum of diseases: a flow-chart for genetic testing. *J Alzheimers Dis*. 2013;34(2):485-499.
- Snowden JS, Pickering-Brown SM, du Plessis D, et al. Progressive anomia revisited: focal degeneration associated with progranulin gene mutation. *Neurocase*. 2007;13(5):366-377.
- Deramecourt V, Lebert F, Debachy B, et al. Prediction of pathology in primary progressive language and speech disorders. *Neurology*. 2010;74(1):42-49.
- Josephs KA, Duffy JR, Strand EA, et al. Progranulin-associated PiB-negative logopenic primary progressive aphasia. *J Neurol*. 2014;261(3):604-614.
- Le Ber I, Guedj E, Verpillat P, et al. Demographic, neurological and behavioural characteristics and brain perfusion SPECT in frontal variant of frontotemporal dementia. *Brain*. 2006;129(pt 11):3051-3065.
- Rascovsky K, Hodges JR, Knopman D, et al. Sensitivity of revised diagnostic criteria for the behavioural variant of frontotemporal dementia. *Brain*. 2011;134(pt 9):2456-2477.

24. Mazaux J, Orgogozo J. *HDAE (BDAE): Echelle d'évaluation de l'aphasie*. ECPA (Editions du Centre de Psychologie Appliquée); 1982.
25. Nespoulos J, Lecours A, Lafond D, et al. *Protocole Montréal-Toulouse d'examen linguistique de l'aphasie MT-86*. Ortho Edition; 1992.
26. Deloche G, Hannequin D. *DO 80: Epreuve de dénomination orale d'image*. ECPA (Editions du Centre de Psychologie Appliquée); 1997.
27. Godefroy O. *GREFEX. Fonctions exécutives et pathologies neurologiques et psychiatriques: Evaluation en pratique clinique*. Solal; 2008.
28. Merck C, Charnallet A, Auriacombe S, et al. La batterie d'évaluation des connaissances sémantiques du GRECO (BECS-GRECO): validation et données normatives. *Revue de Neuropsychologie*. 2011;3(4):235.
29. Marshall CR, Hardy CJD, Volkmer A, et al. Primary progressive aphasia: a clinical approach. *J Neurol*. 2018;265(6):1474-1490.
30. Chen-Plotkin AS, Martinez-Lage M, Sleiman PMA, et al. Genetic and clinical features of progranulin-associated frontotemporal lobar degeneration. *Arch Neurol*. 2011;68(4):488-497.
31. Van Mossevelde S, van der Zee J, Gijssels I, et al. Clinical features of TBK1 carriers compared with C9orf72, GRN and non-mutation carriers in a Belgian cohort. *Brain*. 2016;139(pt 2):452-467.
32. Moore KM, Nicholas J, Grossman M, et al. Age at symptom onset and death and disease duration in genetic frontotemporal dementia: an international retrospective cohort study. *Lancet Neurol*. 2020;19(2):145-156.
33. Gil-Navarro S, Lladó A, Rami L, et al. Neuroimaging and biochemical markers in the three variants of primary progressive aphasia. *Demen Geriatr Cogn Disord*. 2013;35(1-2):106-117.
34. Flanagan EP, Baker MC, Perkerson RB, et al. Dominant frontotemporal dementia mutations in 140 cases of primary progressive aphasia and speech apraxia. *Demen Geriatr Cogn Disord*. 2015;39(5-6):281-286.
35. Ramos EM, Dokuru DR, Van Berlo V, et al. Genetic screen in a large series of patients with primary progressive aphasia. *Alzheimers Dement*. 2019;15(4):553-560.
36. Whitwell JL, Duffy JR, Strand EA, et al. Clinical and neuroimaging biomarkers of amyloid-negative logopenic primary progressive aphasia. *Brain Lang*. 2015;142:45-53.
37. Mesulam M-M, Weintraub S. Is it time to revisit the classification guidelines for primary progressive aphasia? *Neurology*. 2014;82(13):1108-1109.
38. Botha H, Duffy JR, Whitwell JL, et al. Classification and clinicoradiologic features of primary progressive aphasia (PPA) and apraxia of speech. *Cortex*. 2015;69:220-236.
39. Leyton CE, Ballard KJ, Pigué O, Hodges JR. Phonologic errors as a clinical marker of the logopenic variant of PPA. *Neurology*. 2014;82(18):1620-1627.
40. Gorno-Tempini ML, Brambati SM, Ginex V, et al. The logopenic/phonological variant of primary progressive aphasia. *Neurology*. 2008;71(16):1227-1234.
41. Rohrer JD, Caso F, Mahoney C, et al. Patterns of longitudinal brain atrophy in the logopenic variant of primary progressive aphasia. *Brain Lang*. 2013;127(2):121-126.
42. Rogalski E, Cobia D, Martersteck A, et al. Asymmetry of cortical decline in subtypes of primary progressive aphasia. *Neurology*. 2014;83(13):1184-1191.
43. Bonakdarpour B, Hurley RS, Wang AR, et al. Perturbations of language network connectivity in primary progressive aphasia. *Cortex*. 2019;121:468-480.
44. Whitwell JL, Weigand SD, Boeve BF, et al. Neuroimaging signatures of frontotemporal dementia genetics: C9ORF72, tau, progranulin and sporadics. *Brain*. 2012;135(pt 3):794-806.
45. Josephs KA, Duffy JR, Strand EA, et al. Clinicopathological and imaging correlates of progressive aphasia and apraxia of speech. *Brain*. 2006;129(pt 6):1385-1398.
46. Rohrer JD, Rossor MN, Warren JD. Syndromes of nonfluent primary progressive aphasia: a clinical and neurolinguistic analysis. *Neurology*. 2010;75(7):603-610.
47. Tetzloff KA, Duffy JR, Clark HM, et al. Progressive agrammatic aphasia without apraxia of speech as a distinct syndrome. *Brain*. 2019;142(8):2466-2482.
48. Rohrer JD, Ridgway GR, Crutch SJ, et al. Progressive logopenic/phonological aphasia: erosion of the language network. *NeuroImage*. 2010;49(1):984-993.
49. Krefft TA, Graff-Radford NR, Dickson DW, Baker M, Castellani RJ. Familial primary progressive aphasia. *Alzheimer Dis Assoc Disord*. 2003;17(2):106-112.
50. Beck J, Rohrer JD, Campbell T, et al. A distinct clinical, neuropsychological and radiological phenotype is associated with progranulin gene mutations in a large UK series. *Brain*. 2008;131(pt 3):706-720.
51. Cerami C, Marcone A, Galimberti D, Villa C, Scarpini E, Cappa SF. From genotype to phenotype: two cases of genetic frontotemporal lobar degeneration with premorbid bipolar disorder. *JAD*. 2011;27(4):791-797.
52. Caso F, Agosta F, Magnani G, et al. Clinical and MRI correlates of disease progression in a case of nonfluent/agrammatic variant of primary progressive aphasia due to progranulin (GRN) Cys157LysfsX97 mutation. *J Neurol Sci*. 2014;342(1-2):167-172.

SUPPLEMENTAL DATA

	Negative AD biomarkers	AD biomarkers not available	<i>p</i> -value
Number of patients (%)	24 (75%)	8 (25%)	
Demographic data			
Gender (F/M)	13/11	7/1	0.205
Handedness (R/L/Adx), n	23/0/1	6/2/0	0.056
Education, y	9.0 [9.0, 11.5]	8.5 [5.0, 14.0]	0.466
Age at onset, y	62.5 [59.0, 64.0]	59.5 [56.5, 60.8]	0.142
Age at evaluation, y	64.0 [62.0, 66.3]	60.5 [57.8, 63.5]	0.102
Duration at evaluation, y	2.0 [1.4, 2.5]	1.8 [1.5, 2.1]	0.877
Duration of follow-up, y	5.3 [4.0, 6.3]	6.0 [5.8, 7.3]	0.116
PPA variants			
nfvPPA	6 (25%)	3 (38%)	0.673
svPPA	1 (4%)	1 (12%)	
lvPPA	10 (42%)	3 (38%)	
Mixed PPA	7 (29%)	1 (12%)	
Aphasia Severity Rating Scale	3.0 [2.0, 4.0]	3.0 [2.5, 3.0]	0.957
Cognitive evaluation			
MMSE Total score	19.0 [14.8, 24.3]	22.0 [20.5, 24.5]	0.507
MDRS Total score	105.0 [88.0, 113.0]	118.5 [113.3, 123.7]	0.350
Attention	32.5 [32.0, 34.3]	35.0 [34.5, 35.5]	0.193
Initiation	22.0 [14.5, 31.5]	25.5 [24.3, 26.8]	0.715
Construction	6.0 [5.0, 6.0]	6.0 [6.0, 6.0]	0.078
Conceptualization	26.5 [19.8, 29.5]	31.0 [28.0, 34.0]	0.522
Memory	15.5 [10.8, 19.0]	21.0 [19.5, 22.5]	0.314
FAB Total score	9.5 [7.3, 12.8]	15.5 [14.3, 16.8]	0.089
TMT-A	65.0 [54.0, 74.0]	58.0 [48.3, 64.8]	0.335
TMT-B	306.0 [188.0, 358.0]	219.5 [159.3, 263.0]	0.218
TMT (B-A)	234.0 [132.5, 271.5]	156.0 [111.0, 192.8]	0.230
FCSRT Free recall	17.5 [12.3, 24.3]	25.5 [22.0, 26.8]	0.223
Total recall	39.0 [21.5, 46.0]	40.5 [34.3, 46.0]	0.672
Sensitivity of cueing, %	75.0 [54.0, 90.5]	70.0 [42.8, 88.3]	0.841

Table e-1. Comparison of PPA-GRN patients with negative AD biomarkers in CSF with PPA-GRN patients with undetermined AD biomarker status (CSF not available). There were no differences in demographics, linguistic characteristics, severity of aphasia, or cognitive performances between both groups (with and without available CSF). Results are expressed as median values with the first and third quartiles within brackets, or as counts with percentages indicated in parentheses. Statistical comparisons were performed with Fisher's exact test for categorical variables and Wilcoxon's rank-sum test for numerical variables. AD: Alzheimer disease; Adx: ambidextrous; CSF: cerebro-spinal fluid; F: female; FAB: Frontal Assessment Battery; FCSRT: Free and Cued Selective Reminding Test; L: left-handed; lvPPA: logopenic variant of PPA; M: male; MDRS: Mattis Dementia Rating Scale; MMSE: Mini Mental State Examination; nfvPPA: non-fluent/agrammatic variant of PPA; PPA: primary progressive aphasia; R: right-handed; svPPA: semantic variant of PPA; TMT: Trail Making Test; y: years.

c.DNA	Protein	Number of patients in this study	Plasma progranulin dosage ($\mu\text{g/L}$) ^a	Reference
Whole gene deletion	p.0	1	na	Cruts <i>et al.</i> , 2012
c.1A>G	p.?	1	32	Cruts <i>et al.</i> , 2012
c.-7_138del	p.0?	1	26	Cruts <i>et al.</i> , 2012
c.255delC	p.Phe86Serfs*170	1	na	Cruts <i>et al.</i> , 2012
c.380_381delCT	p.Pro127Argfs*2	3	30; na; 26	Cruts <i>et al.</i> , 2012
c.460C>T	p.Gln154*	1	45	New mutation
c.463-1G>T	p.?	1	33	New mutation
c.512del	p.Cys171Serfs*85	1	28	New mutation
c.592_593delAG	p.Arg198Glyfs*19	2	55; 30	Cruts <i>et al.</i> , 2012
c.607del	p.Ser203Profs*53	1	51	Pottier <i>et al.</i> , 2018
c.619dup	p.Met207Asnfs*11	1	na	Pottier <i>et al.</i> , 2018
c.709-1G>A	p.?	1	52	Pottier <i>et al.</i> , 2018
c.745C>T	p.Gln249*	1	26	Pottier <i>et al.</i> , 2018
c.759_760delTG	p.Cys253*	2	46; 41	Cruts <i>et al.</i> , 2012
c.813_816delCACT	p.Thr272Serfs*10	2	na; 45	Cruts <i>et al.</i> , 2012
c.988_989del	p.Thr330Alafs*6	3	70; 54; 45	Pottier <i>et al.</i> , 2018
c.1072C>T	p.Gln358*	2	35; 34	Cruts <i>et al.</i> , 2012
c.1201C>T	p.Gln401*	3	23; na; 37	Cruts <i>et al.</i> , 2012
c.1494_1498delAGTGG	p.Glu498Aspfs*12	4	48; na; na; na	Cruts <i>et al.</i> , 2012

Table e-2. List of the GRN mutations carried by PPA patients included in this study. ^aThreshold: 71 $\mu\text{g/L}$. na: not available, PPA: primary progressive aphasia. References: Cruts M, Theuns J, Van Broeckhoven C. Locus-specific mutation databases for neurodegenerative brain diseases. *Human Mutation* 2012;33:1340–4; Pottier C, Zhou X, Perkerson RB, et al. Potential genetic modifiers of disease risk and age at onset in patients with frontotemporal lobar degeneration and GRN mutations: a genome-wide association study. *The Lancet Neurology* 2018;17:548–58.

<u>Language evaluation</u>	N= (Total = 32)
Global language evaluation^a	32^a
<i>BDAE/HDAE-F</i>	26
<i>MT86</i>	18
Confrontation naming	32
<i>DO80</i>	32
Buccofacial praxis	32
Fluencies (in 2 minutes)	30
<i>Phonological fluencies (letter F)</i>	30
<i>Semantic fluencies (animals)</i>	30
Additional semantic batteries^b	18^b
<i>BECS-GRECO</i>	5
<i>PPTT</i>	4
<u>Cognitive evaluation</u>	N= (Total = 32)
Global cognitive efficiency	32
<i>MMSE</i>	32
<i>MDRS</i>	18
Executive functions^c	32^c
<i>Digit spans</i>	26
<i>FAB</i>	20
<i>Trail making test</i>	18
<i>WCST</i>	9
Memory	32
Verbal memory – <i>FCSRT</i> ^d	26^d
Visual memory ^e	32^e
<i>Rey Figure recall</i>	14
<i>Baddeley's doors test</i>	9
<i>DMS48</i>	11
Visuo-constructive abilities^f	32
<i>Rey Figure copy</i>	24
<i>Pentagon drawing (from MMSE)</i>	32
Limb apraxia^f	26
<i>Ideo-motor apraxia</i>	25
<i>Limb-kinetic</i>	11

Table e-3. Language and neuropsychological protocols. N: number of patients who underwent each test. ^aFor the 13 patients who were evaluated using both scales, we used BDAE performance for statistical analyses. ^bAdditional semantic batteries (PPTT or BECS-GRECO) were performed for the subset of patients who displayed semantic impairment in other language batteries. ^cAt least three tests evaluating executive functions were performed for each patient. ^dNot possible to evaluate verbal memory in a subset of patients because of the language disorder. ^eAt least one visual memory test was performed for each patient. The Z-score for the DMS48 and the percentiles for ROCF recall and doors test were calculated to obtain a homogeneous scoring system for all visual memory tests. ^fParietal syndrome was diagnosed when praxis, visuo-constructive abilities, or both were impaired (no patients had Gerstmann syndrome). BDAE/HDAE-F: Boston Diagnostic Aphasia Examination–French version; FAB: Frontal Assessment Battery; FCSRT: Free and Cued Selective Reminding Test; MDRS: Mattis Dementia Rating Scale; MMSE: Mini Mental Status Examination; MT86: Montreal-Toulouse protocol for linguistic examination of aphasia; PPTT: Pyramid and Palm Tree Test; WCST: Wisconsin Card Sorting Test.

Score	Description
0	No usable speech or auditory comprehension
1	All communication is through fragmentary expression; great need for inference, questioning, and guessing by the listener. The range of information that can be exchanged is limited and the listener carries the burden of communication
2	Conversation about familiar subjects is possible with help from the listener. There are frequent failures to convey the idea, but the patient shares the burden of communication with the examiner
3	The patient can discuss almost all everyday problems with little or no assistance. Reduction of speech and/or comprehension, however, makes conversation about certain material difficult or impossible
4	Some obvious loss of fluency in speech or facility of comprehension, without significant limitation on ideas expressed or form of expression
5	Minimal discernible speech handicaps; the patient may have subjective difficulties that are not apparent to the listener

Table e-4. Description of the scores of the global aphasia severity rating scale. This scoring system is integrated in the BDAE battery (Mazeaux et Orgogozo, HDAE (BDAE): Echelle d'évaluation de l'aphasie. Paris: ECPA (Editions du Centre de Psychologie Appliquée); 1982).

	lvPPA-GRN (VBM)	Controls	<i>p</i> -value	lvPPA-GRN (all)	<i>p</i> -value
Number of patients	8	20		13	
Demographic data					
Age at MRI, y	63.5 [62.8, 66.0]	64.0 [58.0, 71.3]	0.721	-	-
Gender (F/M)	3/5	15/5	0.061	8/5	0.387
Handedness (R/L/Adx)	8/0/0	20/0	1	10/2/1	0.687
Education, y	10.0 [8.3, 15.3]	11.0 [9.0, 12.0]	0.377	9.0 [6.0, 15.0]	0.826
Age at onset, y	62.0 [59.0, 63.0]	-	-	62.0 [59.0, 63.0]	0.883
Duration at evaluation and MRI, y	2.5 [1.5, 2.6]	-	-	1.5 [1.5, 2.5]	0.527
Duration of follow-up, y	5.0 [4.0, 6.0]	-	-	6.0 [5.0, 6.8]	0.421
Speech and language assessment					
Aphasia Severity Rating Scale	3 [2.3, 3.8]	-	-	3 [2.3, 3]	0.864
Agrammatism (discrete to severe) ^a	0 (0%)	-	-	0 (0%)	-
Semantic fluency in 2 minutes	10.0 [7.5, 12.0]	-	-	10.5 [6.3, 18.3]	0.658
Phonological (F) fluency in 2 minutes	5.5 [2.0, 9.8]	-	-	9.0 [2.0, 10.0]	0.765
Confrontation naming, %	74 [68, 85]	-	-	76 [59, 89]	0.942
Oral single-word comprehension ^a	1 (12.5%)	-	-	4 (30.8%)	0.524
Oral sentence comprehension, %	79 [59, 86]	-	-	77 [53, 86]	0.785
Repetition of sentences, %	59 [48, 72]	-	-	53 [45, 66]	0.666
Written sentence comprehension, %	77 [70, 90]	-	-	73 [70, 80]	0.603
Neuropsychological evaluation					
MMSE	19.5 [15.8, 23.3]	-	-	20.5 [15.8, 24.8]	0.938
MDRS	113.0 [112.0, 116.0]	-	-	113.0 [112.0, 116.0]	1
FAB	10.5 [8.3, 13.5]	-	-	12.0 [8.5, 13.5]	0.885
Forward digit span	4.0 [3.0, 4.5]	-	-	4.0 [3.0, 4.0]	0.913
Backward digit span	3.0 [2.0, 3.0]	-	-	3.0 [2.0, 3.0]	0.547
TMT-A	55.0 [45.3, 71.0]	-	-	62.0 [48.0, 73.0]	0.811
TMT-B	185.0 [178.5, 269.0]	-	-	188.0 [178.3, 245.0]	0.896
TMT(B-A)	142.0 [126.0, 188.0]	-	-	132.5 [122.3, 178.0]	0.896
FCSRT: free recall	20.5 [10.0, 28.8]	-	-	23.5 [19.5, 30.0]	0.586
FCSRT: total recall	40.0 [22.3, 45.0]	-	-	40.0 [34.3, 46.8]	0.743
FCSRT: sensitivity to cueing, %	71.0 [34.3, 85.3]	-	-	71.0 [42.0, 93.3]	0.785
ROCF recall	15.0 [8.5, 17.0]	-	-	17.0 [11.8, 19.0]	0.708
ROCF copy	30.0 [27.0, 35.0]	-	-	31.0 [27.3, 35.0]	0.844
Ideo-motor apraxia	57.0 [52.5, 59.0]	-	-	58.0 [55.0, 60.0]	0.593

Table e-5. Comparison of demographic data, speech/language and cognitive scores between the lvPPA-GRN patients included in the VBM analysis, controls, and the entire group of lvPPA-GRN patients. Statistical comparisons were performed with Fisher's exact test for categorial variables and Wilcoxon's rank-sum test for numerical variables. There were no differences between the groups. Median values are indicated, with the first and third quartiles in brackets. ^aAbsolute count and percentage of patients with impaired performance. Adx: ambidextrous; F: female; FAB: Frontal Assessment Battery; FCSRT: Free and Cued Selective Reminding Test; L: left-handed; lvPPA-GRN: logopenic variant of primary progressive aphasia associated with GRN mutations; M: male; MDRS: Mattis Dementia Rating Scale; MMSE: Mini Mental Status Examination; R: right-handed; ROCF: Rey-Osterrieth Complex Figure; TMT: Trail Making Test; VBM: voxel-based morphometry; y: years.

Case	A A O	Symptom at onset	Agram matism	AOS	Sentence comprehension deficit		Impaired single-word retrieval in spontaneous speech	Impaired repetition of sentences		Phonological errors	Impaired phonological working memory ^a	Impaired confrontation naming	Impaired single- word comprehension		Impaired object knowledge	Surface dyslexia / dysgraphia	Disease progression		
					SSy	L/CSy		SS	LS				HF	LF			Duration at last follow-up	Other relevant impairments	Diagnosis at last follow-up
<i>NfvPPA</i>																			
#04	52	ES	-	+	-	+	+	-	-	+	-	-	-	-	-	-	6	Park., PLD, FCSd	PPA/CBS
#05	52	WFD	+	+	-	+	+	-	+	-	-	-	-	-	-	-	5	FCSd	-
#09	59	SD	+	-	-	+	+	-	-	+	-	-	-	-	-	-	5.5	BvD, FCSd, PLD	PPA/FTD
#18	56	ES	+	(+)	-	+	-	-	+	-	+	-	-	-	-	-	5	FCSd, Park.	-
#22	63	ES	+	+	-	+	-	-	+	+	+	+	-	+	-	-	6	FCSd, Park., PLD	-
#24	64	NA	+	-	-	+	+	-	+	+	+	-	-	-	-	-	7	PLD, FCSd, Park.	PPA/CBS
#27	62	WFD	+	-	-	+	+	-	-	+	-	+	-	-	-	-	3	PLD, FCSd	-
#28	69	ES	+	+	-	+	+	-	+	+	+	-	-	-	-	-	5	FCSd, Park.	-
#29	63	ES	+	-	-	+	+	-	+	-	-	-	-	-	-	-	6	BvD	PPA/FTD
<i>“Pure lvPPA”</i>																			
#08	63	WFD	-	-	-	+	+	-	+	+	+	+	-	-	-	-	8	FCSd	Mixed PPA
#13	64	SR	-	-	-	+	+	+	+	+	+	+	-	-	-	-	4	BvD, FCSd, Park.	PPA/FTD
#17	63	WFD	-	-	-	+	+	+	+	-	+	+	-	-	-	-	7	BvD, FCSd, PLD	PPA/FTD
#19	59	RD	-	-	-	+	+	+	+	+	+	+	-	-	-	-	5	PLD, FCSd	Mixed PPA
#21	59	WFD	-	-	-	+	+	-	+	+	+	+	-	-	-	-	8	PLD, FCSd, Park.	PPA/CBS
#25	62	WFD	-	-	-	-	+	-	+	+	+	-	-	-	-	-	6	FCSd	Mixed PPA
#30	59	WFD	-	-	-	-	+	-	+	-	(+)	+	-	-	-	-	4	BvD, FCSd, PLD	PPA/FTD
<i>LvPPA+</i>																			
#02	62	WFD	-	(+)	-	+	+	+	+	-	+	+	-	-	-	-	6	BvD, FCSd	PPA/FTD
#10	54	WFD	(+)	-	-	+	+	-	+	+	+	+	-	-	(+)	-	6	BvD, FCSd, PLD	PPA/FTD
#16	60	WFD	-	-	-	+	+	-	+	+	+	+	-	(+)	-	-	8	FCSd, PLD	-
#23	69	WFD	(+)	-	-	+	+	-	+	+	+	+	-	-	(+)	-	6	BvD, FCSd, PLD	PPA/FTD
#26	58	WFD	(+)	-	-	+	+	-	+	+	+	+	-	(+)	-	-	6	BvD, FCSd, PLD, Park.	PPA/FTD
#31	66	WFD	-	-	+	+	+	+	+	+	+	+	-	-	(+)	-	3	(BvD) ^b , FCSd	-

Case	A A O	Symptom at onset	Agram matism	AOS	Sentence comprehension deficit		Impaired single-word retrieval in spontaneous speech	Impaired sentences repetition		Phonological errors	Impaired phonological working memory ^a	Impaired confrontation naming	Impaired single- word comprehension		Impaired object knowledge	Surface dyslexia / dysgraphia	Disease progression		
					SSy	L/CSy		SS	LS				HF	LF			Duration at last follow-up	Other relevant impairments	Diagnosis at last follow-up
<i>SvPPA</i>																			
#06	57	CD	-	-	+	+	+	NA	NA	-	-	+	+	+	+	+	7	(BvD) ^b , FCSd	-
#11	70	NA	-	-	+	+	+	-	+	-	+	+	+	+	+	+	5	BvD, FCSd, PLD	PPA/FTD
<i>Mixed PPA</i>																			
#01 S>L	60	WFD	-	-	+	+	+	-	+	+	+	+	+	+	+	+	7	BvD, FCSd	PPA/FTD
#03 L>S	63	WFD	-	-	-	+	+	-	+	+	(+)	+	-	+	-	-	7	BvD, FCSd, Park.	PPA/FTD
#07 L=A	67	NA	+	-	+	+	+	-	+	-	+	+	+	+	+	-	4	FCSd, Park.	-
#12 L=S>A	56	WFD	+	-	+	+	+	+	+	+	+	+	-	+	+	+	5	BvD, FCSd, PLD, Park.	PPA/FTD
#14 A>L	63	WFD	+	-	-	+	+	+	+	+	+	+	-	-	(+)	-	5	BvD, FCSd, PLD	PPA/FTD
#15 L=S=A	64	NA	+	-	+	+	+	+	+	+	+	+	+	+	+	-	9	BvD, FCSd	PPA/FTD
#20 A>S>L	68	WFD	+	-	+	+	+	+	+	+	+	+	+	+	+	+	4	BvD, FCSd, PLD	PPA/FTD
#32 L>A	62	WFD	+	+	-	+	+	-	+	+	+	+	-	+	-	+	4	FCSd, PLD	-

Table e-6. Detailed linguistic description of the cohort at first evaluation and syndromic progression. +: present; -: absent; (+): borderline or mild impairment, defined by a “questionable” grade for agrammatism and apraxia of speech in the scale proposed by Leyton et al. (2011), and by a score just below the threshold of the corresponding tests for the other items. A: agrammatic/non-fluent phenotype; AAO: age at onset; AOS: apraxia of speech; BvD: Behavioral disorders; CBS: corticobasal syndrome; CD: comprehension deficits; ES: effortful speech; FCSd: frontal cognitive syndrome; FTD: frontotemporal dementia; HF: high frequency; L: logopenic phenotype; L/CS: long or syntactically complex sentences; LF: low frequency; lvPPA: logopenic variant of primary progressive aphasia; NA: not available; nfvPPA: non-fluent/agrammatic variant of primary progressive aphasia; Park.: parkinsonism; PLD: parietal lobe dysfunction; PPA: primary progressive aphasia; RD: reading difficulties; S: semantic phenotype; SD: syntactic difficulties; SR: speech reduction; SS: short sentences; SSy: simple syntax; svPPA: semantic variant of primary progressive aphasia; WFD: word-finding difficulties. ^aDigit span. ^bIrritability, obsessions or ritualistic behaviors.

	lvPPA-GRN	lvPPA-AD	p-value	corrected p-value
Number of patients	13	11		
Demographic data				
Gender (F/M)	8/5	6/5	1.000	-
Handedness (R/L/Adx), n	10/2/1	9/1/1	1.000	-
Family history, n ^a	10 (77%)	0	<0.001*	-
Education level, y	9.0 [6.0, 15.0]	12.0 [11.0, 15.0]	0.501	-
Age at onset, y	62.0 [59.0, 63.0]	64.0 [60.0, 66.0]	0.308	-
Age at first evaluation, y	63.0 [62.0, 65.0]	66.0 [62.0, 69.0]	0.383	-
Disease duration at first evaluation, y	1.5 [1.5, 2.5]	2.0 [1.3, 3.3]	0.638	-
Speech and language assessment				
Aphasia Severity Rating Scale (/5) ^b	3.0 [2.3, 3.0]	3.0 [3.0, 4.0]	0.148	0.861
Agrammatism (discrete to severe), n ^c	0	0	1.000	1.000
Semantic fluency in 2 minutes	11 [6, 18]	12 [11, 13]	0.697	0.941
Phonological (F) fluency in 2 minutes	9 [2, 10]	11 [7, 14]	0.129	0.861
Confrontation naming, %	76 [59, 89]	86 [81, 89]	0.258	0.902
Oral single-word comprehension, n ^c	3 (23%)	1 (9%)	0.596	0.941
Oral sentence comprehension, %	77 [53, 86]	92 [88, 99]	0.039*	0.534
Repetition of sentences, %	50 [38, 69]	60 [52, 68]	0.486	0.941
Written sentence comprehension, %	74 [70, 80]	80 [78, 87]	0.245	0.902
Cognitive evaluation				
MMSE (/30)	20.5 [15.8, 24.8]	24.0 [19.5, 24.0]	0.535	0.941
MDRS (/144)	112.5 [102.2, 115.2]	121.0 [117.8, 127.0]	0.059	0.534
Attention (/37)	33.0 [32.0, 35.0]	34.0 [33.0, 35.5]	0.622	0.941
Initiation (/37)	26.0 [18.0, 33.0]	30.0 [29.5, 31.0]	0.623	0.941
Construction (/6) ^d	0	1 (14%)	1.000	1.000
Conceptualization (/39)	29.0 [29.0, 31.0]	34.0 [32.5, 35.5]	0.288	0.916
Memory (/25)	19.0 [15.0, 25.0]	19.0 [18.0, 21.5]	0.934	1.000
FAB (/18)	12.0 [8.5, 13.5]	13.0 [11.3, 14.5]	0.350	0.941
Forward digit span	4.0 [3.0, 4.0]	4.0 [4.0, 5.0]	0.546	0.941
Backward digit span	3.0 [2.0, 3.0]	3.0 [2.0, 3.0]	0.744	0.960
TMT-A	62.0 [48.0, 73.0]	75.0 [58.5, 95.0]	0.254	0.902
TMT-B	188.0 [178.2, 245.0]	252.5 [148.0, 330.8]	0.818	0.986
TMT(B-A)	132.5 [122.2, 178.0]	179.0 [110.5, 252.8]	0.699	0.941
FCSRT: free recall (/48)	23.5 [19.5, 30.0]	21.0 [11.5, 24.5]	0.558	0.941
FCSRT: total recall (/48)	40.0 [34.3, 46.8]	41.0 [23.5, 44.5]	0.768	0.960
FCSRT: sensitivity to cueing, %	71 [42, 93]	77 [66, 86]	0.845	0.986
ROCF recall (/36)	17.0 [11.8, 19.0]	13.5 [9.8, 15.5]	0.559	0.941
ROCF copy (/36)	31.0 [27.3, 35.0]	33.0 [32.0, 34.0]	0.681	0.941
Ideo-motor apraxia (/63)	58.0 [55.0, 60.0]	60.0 [53.8, 60.5]	0.698	0.941

Disease progression				
Median disease duration at last follow-up, y	6.0 [5.0, 7.0]	4.0 [3.0, 7.0]	0.159	-
Frontal lobe dysfunction, n	13 (100%)	11 (100%)	1.000	1.000
Executive dysfunction, n	13 (100%)	11 (100%)	1.000	1.000
And/or behavioral symptoms, n	8 (62%)	2 (18%)	0.047*	0.534
Amnesic syndrome, n	6 (46%)	8 (73%)	0.240	0.902
Parietal syndrome, n	8 (62%)	6 (55%)	1.000	1.000
Parkinsonism, n	3 (23%)	1 (9%)	0.596	0.941
Psychiatric disorders, n ^e	1 (8%)	5 (45%)	0.061	0.534

Table e-7. Comparison of lvPPA-GRN patients with lvPPA associated with underlying Alzheimer’s disease. Numbers are presented for categorical measures, with percentages in parentheses. Medians are presented for numerical measures, with first and third quartiles within brackets. Corrections for multiple comparisons were handled with the Benjamini-Hochberg method. ^aFamily history of FTLD spectrum disorders. ^bAphasia severity rating score evaluates the global severity of impairment of spontaneous speech and conversation following BDAE recommendations. ^cNumber (and percentage) of patients with impaired performance. ^dAbsolute count and percentage of patients with any degree of impairment, with respect to the total number of those who underwent the test. ^eDelusions, depression or bipolar disorder. AD: Alzheimer’s disease; Adx: ambidextrous; F: female; FAB: Frontal Assessment Battery; FCSRT: Free and Cued Selective Reminding Test; FTLD: frontotemporal lobar degeneration; L: left-handed; lvPPA: logopenic variant of PPA; M: male; MDRS: Mattis Dementia Rating Scale; MMSE: Mini Mental Status Examination; PPA: primary progressive aphasia; R: right-handed; ROCF: Rey-Osterrieth Complex Figure; TMT: Trail Making Test; y: years.

	nfvPPA-GRN	sporadic nfvPPA	p-value	corrected p-value
Number of patients	9	9		
Demographic data				
Gender (F/M)	7/2	3/6	0.153	-
Handedness (R/L), n	9/0	7/2	0.471	-
Family history, n ^a	9 (100%)	0	<0.001*	-
Education level, y	9.0 [9.0, 12.0]	14.0 [9.0, 15.0]	0.245	-
Age at onset, y	62.0 [56.0, 63.0]	67.0 [67.0, 70.0]	0.092	-
Age at first evaluation, y	63.0 [58.0, 65.0]	70.0 [68.0, 72.0]	0.069	-
Disease duration at first evaluation, y	1.5 [1.0, 2.0]	2.0 [1.0, 3.0]	0.469	-
Speech and language assessment				
Global Aphasia Severity score (/5) ^b	3.0 [3.0, 4.0]	4.0 [3.0, 4.0]	0.224	0.949
Agrammatism (discrete to severe), n ^c	8 (89%)	6 (67%)	0.577	0.949
Apraxia of speech, n ^c	4 (44%)	6 (67%)	0.637	0.949
Semantic fluency in 2 minutes	13 [9, 16]	13 [9, 16]	0.915	1.000
Phonological (F) fluency in 2 minutes	4 [3, 7]	4 [3, 10]	0.683	0.949
Confrontation naming, %	88 [83, 94]	96 [89, 96]	0.425	0.949
Oral single-word comprehension, n ^c	1 (11%)	2 (22%)	1.000	1.000
Oral sentence comprehension, %	69 [66, 88]	89 [78, 100]	0.102	0.949
Repetition of sentences, %	63 [56, 100]	85 [72, 91]	0.766	0.963
Written sentence comprehension, %	68 [43, 89]	77 [62, 93]	0.669	0.949
Cognitive evaluation				
MMSE (/30)	23.0 [19.0, 25.0]	25.0 [23.5, 25.5]	0.143	0.949
MDRS (/144)	113.0 [109.0, 121.0]	127.0 [120.0, 131.0]	0.267	0.949
Attention (/37)	34.0 [34.0, 34.0]	36.0 [35.5, 36.5]	0.101	0.949
Initiation (/37)	28.0 [25.5, 29.5]	30.0 [26.0, 31.5]	0.647	0.949
Construction (/6) ^d	2 (67%)	0	0.067	0.949
Conceptualization (/39)	27.0 [25.5, 32.0]	32.0 [31.5, 36.5]	0.358	0.949
Memory (/25)	19.0 [17.5, 21.5]	21.0 [19.5, 23.0]	0.647	0.949
FAB (/18)	11.0 [9.5, 14.8]	10.0 [8.5, 14.0]	0.648	0.949
Forward digit span	5.0 [3.0, 5.5]	4.0 [4.0, 5.3]	0.677	0.949
Backward digit span	3.0 [3.0, 3.0]	3.0 [3.0, 4.3]	0.228	0.949
TMT-A	61.5 [53.5, 65.0]	78.0 [49.0, 96.5]	0.412	0.949
TMT-B	263.0 [186.0, 313.0]	150.0 [110.0, 245.5]	0.700	0.949
TMT(B-A)	201.0 [139.5, 251.5]	108.0 [73.0, 196.5]	0.700	0.949
FCSRT: free recall (/48)	21.0 [16.0, 26.0]	23.0 [18.0, 26.5]	1.000	1.000
FCSRT: total recall (/48)	43.0 [40.0, 46.0]	45.0 [41.5, 46.5]	0.625	0.949
FCSRT: sensitivity to cueing, %	85 [77, 92]	81 [78, 93]	0.776	0.963
ROCF recall (/36)	12.0 [12.0, 14.3]	9.0 [8.0, 11.5]	0.171	0.949
ROCF copy (/36)	33.0 [31.5, 35.3]	33.0 [32.8, 34.5]	0.841	1.000
Ideomotor apraxia (/63)	58.0 [34.0, 59.0]	55.5 [51.5, 61.8]	0.712	0.949

Disease progression				
Median disease duration at last follow-up, y	5.5 [5.0, 6.0]	5.0 [5.0, 6.0]	0.714	-
Frontal lobe dysfunction, n	9 (100%)	7 (78%)	0.471	0.949
Executive dysfunction, n	8 (89%)	7 (78%)	1.000	1.000
And/or behavioral symptoms, n	2 (22%)	6 (67%)	0.153	0.949
Amnesic syndrome, n	2 (22%)	3 (33%)	1.000	1.000
Parietal syndrome, n	5 (56%)	2 (22%)	0.335	0.949
Parkinsonism, n	5 (56%)	4 (44%)	1.000	1.000
Psychiatric disorders, n ^e	1 (11%)	3 (33%)	0.577	0.949

Table e-8. Comparison of nfvPPA-GRN patients with sporadic nfvPPA patients. Numbers are presented for categorical measures, with percentages in parentheses. Medians are presented for numerical measures, with first and third quartiles within brackets. Corrections for multiple comparisons were handled with the Benjamini-Hochberg method. ^aFamily history of FTLN spectrum disorders. ^bAphasia severity rating score evaluates the global severity of impairment of spontaneous speech and conversation following BDAE recommendations. ^cNumber (and percentage) of patients with impaired performance. ^dAbsolute count and percentage of patients with any degree of impairment, with respect to the total number of those who underwent the test. ^eDelusions, depression or bipolar disorder. F: female; FAB: Frontal Assessment Battery; FCSRT: Free and Cued Selective Reminding Test; FTLN: frontotemporal lobar degeneration; L: left-handed; M: male; MDRS: Mattis Dementia Rating Scale; MMSE: Mini Mental Status Examination; nfvPPA: non-fluent/agrammatic variant of PPA; PPA: primary progressive aphasia; R: right-handed; ROCF: Rey-Osterrieth Complex Figure; TMT: Trail Making Test; y: years.

Cluster-level p _{FWE-corr}	k _E	Voxel-level p _{FWE-corr}	T	(Z)	MNI coordinates (x, y, z)			Region (Neuromorphometrics)
					mm	mm	mm	
lvPPA-GRN vs controls								
<0.001	296	0.004	7.78	5.44	-52	-20	-9	Left middle temporal gyrus
0.002	79	0.007	7.48	5.32	-22	32	-10	Left posterior orbital gyrus
0.017	15	0.021	6.92	5.08	-27	51	-9	Left anterior orbital gyrus
lvPPA-AD vs controls								
<0.001	416	0.002	7.91	5.64	-54	-21	-10	Left middle temporal gyrus
lvPPA-GRN vs lvPPA-AD								
NS								

Table e-9. VBM analyses in lvPPA patients. The analyses were performed using SPM12 adopting a family-wise error rate correction at the peak-level of $p < 0.05$, and a height threshold for $T = 6.472$ (lvPPA-GRN vs controls) and $T = 6.238$ (lvPPA-AD vs controls). The comparison between lvPPA-GRN and lvPPA-AD produced no significant results. No cluster extent correction was adopted. K_E : extent coefficient; lvPPA-AD: logopenic variant of primary progressive aphasia associated with Alzheimer’s disease; lvPPA-GRN: logopenic variant of primary progressive aphasia associated with GRN mutations; MNI: Montreal Neurological Institute; NS: not significant; p_{FWE-corr}: family-wise error-corrected p value; T: result of T test; VBM: voxel-based morphometry; (Z): result of Z test.

	This study	Le Ber <i>et al.</i> , 2008	Chen-Plotkin <i>et al.</i> , 2011	Le Ber <i>et al.</i> , 2013	Van Mossevelde <i>et al.</i> , 2016	Moore <i>et al.</i> , 2020
Origin of patients	France	France	Europe, USA, Australia	France	Belgium	International
Number of <i>GRN</i> patients	162	32	94	59	52	1179
% of PPA cases (n=)	20% (32) – 28% (45)	16% (5)	15% (14)	12% (7)	38% (20)	14% (160)

Table e-10. Frequency of patients with PPA variants in various *GRN* cohorts. The number of patients is indicated in parentheses. The frequency in the present study is estimated at 20% (when considering only patients with accurate clinical data who were included in the study cohort) or at 28% (when considering all patients with an initial diagnosis of PPA). References: Le Ber I, Camuzat A, Hannequin D, et al. Phenotype variability in progranulin mutation carriers: a clinical, neuropsychological, imaging and genetic study. *Brain*. 2008;131:732–746; Chen-Plotkin AS, Martinez-Lage M, Sleiman PMA, et al. Genetic and clinical features of progranulin-associated frontotemporal lobar degeneration. *Arch Neurol*. 2011;68:488–497; Le Ber I, Guillot-Noel L, Hannequin D, et al. C9ORF72 Repeat Expansions in the Frontotemporal Dementias Spectrum of Diseases: A Flow-chart for Genetic Testing. *Journal of Alzheimer’s Disease*. 2013;34:485–499; Van Mossevelde S, van der Zee J, Gijssels I, et al. Clinical features of TBK1 carriers compared with C9orf72, GRN and non-mutation carriers in a Belgian cohort. *Brain*. 2016;139:452–467; Moore KM, Nicholas J, Grossman M, et al. Age at symptom onset and death and disease duration in genetic frontotemporal dementia: an international retrospective cohort study. *Lancet Neurol*. 2020;19:145–156.

	This study	Le Ber <i>et al.</i> , 2013	Gil-Navarro <i>et al.</i> , 2013	Flanagan <i>et al.</i> , 2015	Ramos <i>et al.</i> , 2019
Origin of patients	France	France	Spain	USA	USA
Number of PPA patients	235	73	32	100	403
% <i>GRN</i> (n=)	14% (32) – 19% (45)	10% (7)	6% (2)	3% (3)	2.3% (9)

Table e-11. Frequency of *GRN* mutation carriers in PPA cohorts. The number of patients is indicated in parentheses. The frequency in the present study is estimated at 14% (when considering only patients with accurate clinical data who were included in the study cohort) or at 19% (when considering all patients with an initial diagnosis of PPA). References: Le Ber I, Guillot-Noel L, Hannequin D, et al. C9ORF72 Repeat Expansions in the Frontotemporal Dementias Spectrum of Diseases: A Flow-chart for Genetic Testing. *Journal of Alzheimer’s Disease*. 2013;34:485–499; Gil-Navarro S, Lladó A, Rami L, et al. Neuroimaging and Biochemical Markers in the Three Variants of Primary Progressive Aphasia. *Dementia and Geriatric Cognitive Disorders*. 2013;35:106–117; Flanagan EP, Baker MC, Perkerson RB, et al. Dominant Frontotemporal Dementia Mutations in 140 Cases of Primary Progressive Aphasia and Speech Apraxia. *Dementia and Geriatric Cognitive Disorders*. 2015;39:281–286; Ramos EM, Dokuru DR, Van Berlo V, et al. Genetic screen in a large series of patients with primary progressive aphasia. *Alzheimer’s & Dementia*. 2019;15:553–560.

Cortical thickness analysis in lvPPA-GRN patients

Methods

We performed a complementary study of the pattern of grey matter (GM) atrophy in lvPPA-GRN patients compared to controls by means of cortical thickness analysis. This study was performed using the *t1-freesurfer* and the *statistics-surface* pipelines of Clinica (<http://www.clinica.run>). The FreeSurfer processing (<http://surfer.nmr.mgh.harvard.edu/>) includes segmentation of subcortical structures, extraction of cortical surfaces, cortical thickness estimation, spatial normalization onto the FreeSurfer surface template, and parcellation of cortical regions. Subsequently, a point-wise, vertex-to-vertex model based on the Matlab SurfStat toolbox (<http://www.math.mcgill.ca/keith/surfstat/>) was used to conduct a group comparison of whole brain cortical thickness. Data were smoothed using a Gaussian kernel with a full width at half maximum set to 8 mm. Age and gender were included in the general linear model. Statistics were corrected for multiple comparisons using the random field theory for non-isotropic images. We applied a statistical threshold of $p < 0.001$ (height threshold), and an extent threshold of $p < 0.05$ corrected for multiple comparisons at cluster level.

Results

LvPPA-GRN patients showed significant GMA in the left parieto-temporal junction including supramarginal gyrus and middle temporal (MT) gyrus compared to controls. Additionally, cortical thickness was locally reduced in the left frontal lobe, namely in the orbital regions and in the superior frontal gyrus (Figure e-1).

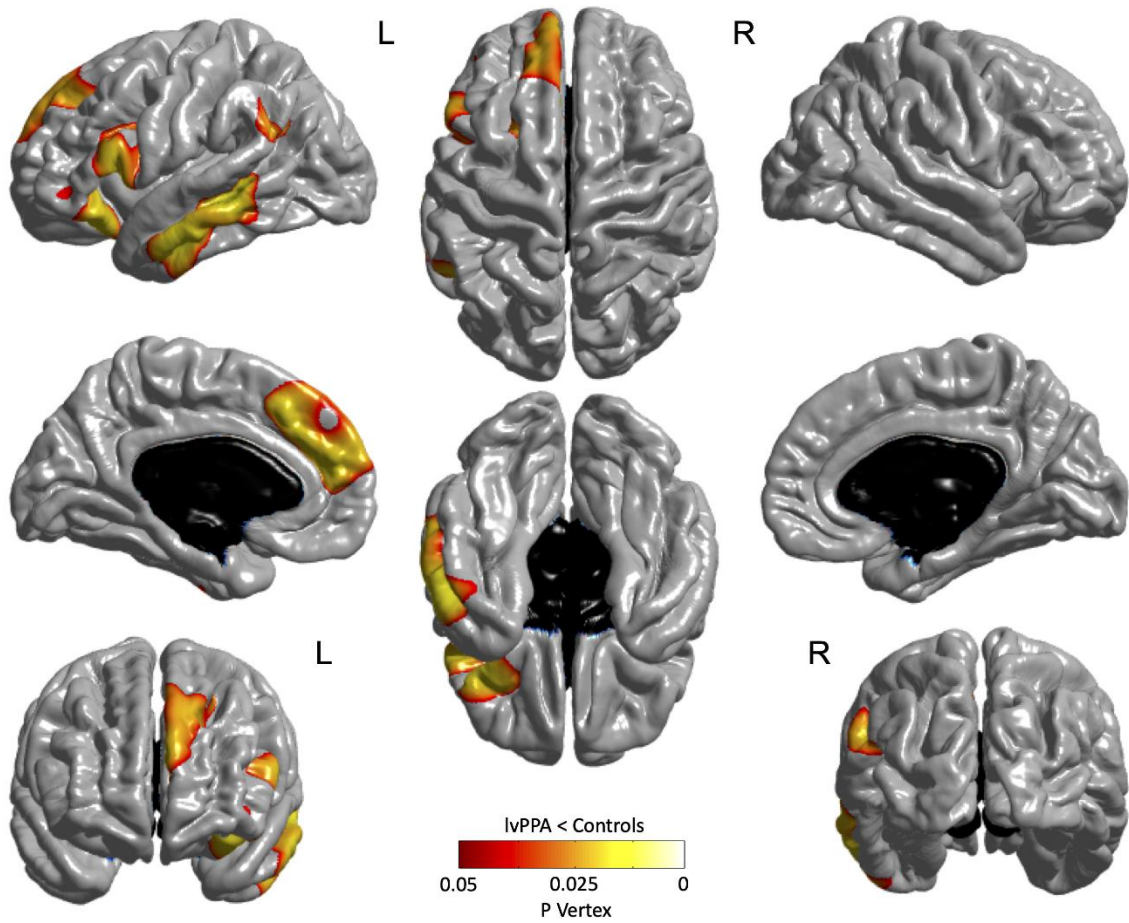


Figure e-1. Cortical thickness analysis of lvPPA-GRN patients compared to controls. Regions of significant reduction of cortical thickness in lvPPA-GRN compared to controls are shown with their respective color-coded corrected p -values at the vertex level. LvPPA-GRN: logopenic variant of primary progressive aphasia associated with *GRN* mutations.

Illustrative case descriptions

Patient #25: “pure lvPPA”

Patient #25 is a right-handed patient who presented with progressive word-finding difficulties in oral and written expression at 62 years of age. His propositional speech was interspersed with frequent pauses, without circumlocutions or word substitutions, but remained fully intelligible. He had no difficulties in language comprehension, neither oral nor written. The patient underwent his first speech/language evaluation at the age of 63 years, one year after the onset of symptoms. Aphasia severity was rated 4/5 on the BDAE scale. Confrontational naming was preserved for nouns and only mildly impaired for verbs with a frequency effect (2 errors). Single-word repetition was normal, whereas sentence repetition was impaired, with several omissions in the longest sentences. Writing showed some graphemic and verbal paraphasias. No motor speech or syntactic deficits were evidenced. Single-word comprehension and object knowledge were intact. Brain MRI at age 63 already showed mild left superior temporal and parietal atrophy (Figure e-2A).

Two-and-half years after disease onset, mild worsening of single-word retrieval and phonological errors in spontaneous speech appeared. The speech/language assessment showed a significant deficit in sentence repetition with length effect (11/16 for the BDAE subtest) and borderline impaired sentence comprehension (35/38 for the MT86 subtest). The MMSE was 29/30 and MDRS 138/144, with prevailing deficits in the attention subtest (33/37). Moderate executive dysfunction and auditory-verbal working memory deficits were also present (forward digit span: 4, backward digit span: 3, 5/6 categories for the WCST, 3 errors for the TMT-B).

Significant progression was evident at four years from onset (66 years). Spontaneous speech was reduced, sentences were telegraphic and often incomplete. Articulatory troubles and buccofacial apraxia had become established. Naming was impaired (DO80: 51/80) and repetition was altered for both short and long sentences in the BDAE subtest (3/16). Oral and written comprehension were still within normal limits. By that time, the MMSE decreased to 25/30, the MDRS was

129/144 and the FAB 15/18. The forward digit span was 3 and at the WCST 4/6 categories were identified, with 17 errors. There were no behavioral disturbances, visuospatial deficits, or ideomotor or constructional apraxia.

At 66 years of age (four years from disease onset), brain MRI showed widespread cortical atrophy involving the superior and middle temporal and parietal regions on the left side, as well as the prefrontal region (Figure e-2B). Oral expression became almost impossible at six years of follow-up.

There was a family history of dementia in one parent and two cousins. The plasma progranulin level was 37 µg/L. *GRN* analysis disclosed the c.1201C>T, p.Gln401* mutation.

Patient #02: “lvPPA+”

Patient #02, a right-handed individual, manifested word-finding difficulties, reduced fluency, and mildly effortful speech at the age of 62 years. He was only partially aware of his language difficulties. One year after the onset of symptoms (63 years), the severity of aphasia was rated 3/5 on the BDAE scale. Speech output was reduced, characterized by phonological errors and frequent pauses which often prevented full intelligibility. Naming was mildly impaired (DO80: 77/80). Additionally, some rare semantic paraphasias on low-frequency items were identified. However, single word comprehension and object knowledge were completely spared. Repetition was normal for single words and impaired for sentences (9/16). Comprehension of both the longest and syntactically complex sentences was impaired. At that time, the MMSE was 28/30. Auditory-verbal working memory was impaired (forward digit span: 4; backward digit span: 4). The FAB score was 13/15 (one subtest was not possible because of language disorders). There was also mild deficit in cognitive flexibility (TMT B-A: 123”). Brain MRI at age 64 years showed left-predominant fronto-temporo-parietal atrophy. Cerebral SPECT showed a significant

hypoperfusion in the left perisylvian and temporo-parietal cortices, extending towards the temporal pole and the prefrontal cortex.

Four years from onset, the patient progressively developed behavioral disturbances with apathy, loss of empathy, hyperorality, and binge eating with a gain in body weight. At six years of follow-up, he became totally dependent, neglecting personal care and spending all day in repetitive, purposeless activities.

The family history was unremarkable. The plasma progranulin level was 33 µg/L. *GRN* analysis revealed a splice site mutation c.463-1G>T.

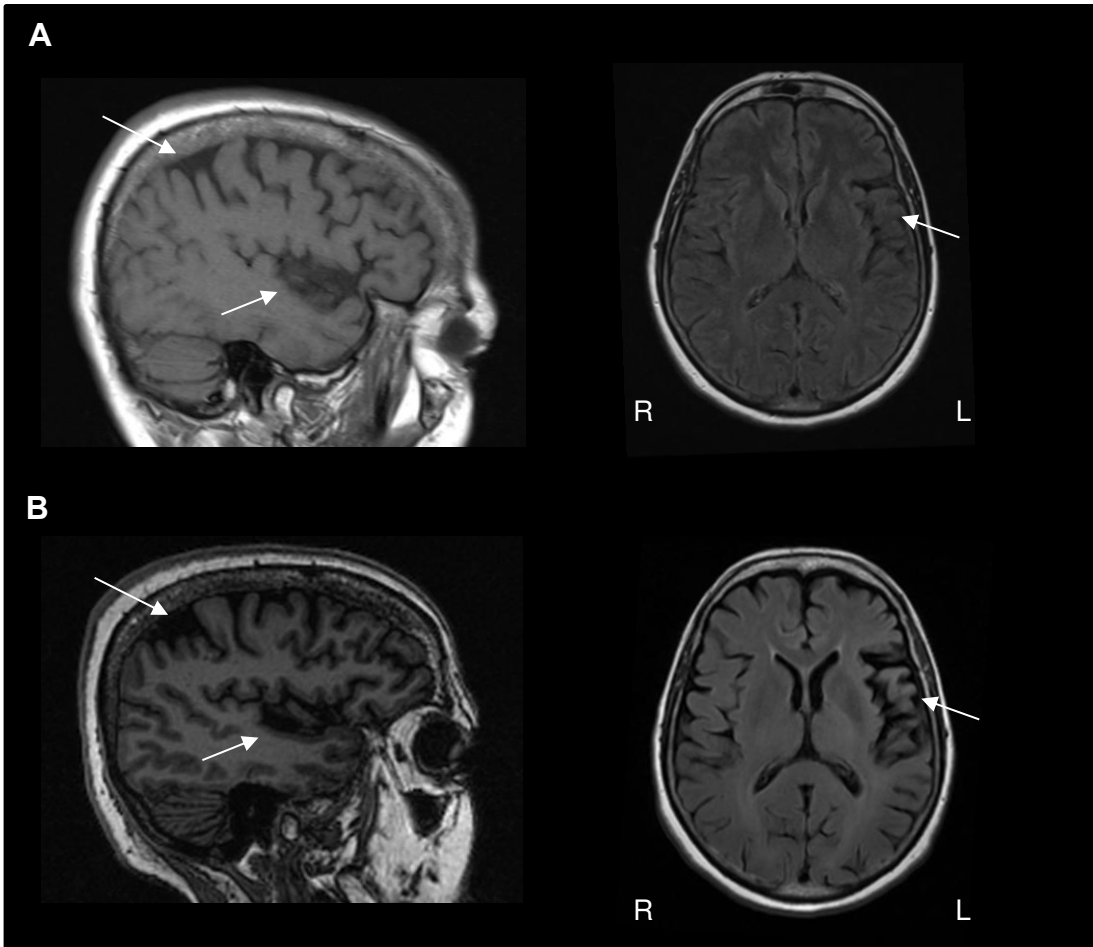


Figure e-2. Baseline and follow-up brain MRI of a patient with pure lvPPA. A: patient #25 at age 63, one year from onset (sagittal T1 and axial FLAIR sequences). B: patient #25 at age 66, four years from onset (sagittal T1 and axial FLAIR sequences). Progression of atrophy in left parietal and superior temporal cortex (arrows).



Single Case Report

Primary progressive aphasia associated with C9orf72 expansions: Another side of the story

Dario Saracino ^{a,b,c}, Amandine Géraudie ^{d,e}, Anne M. Remes ^{f,g},
 Sophie Ferrieux ^b, Marie Noguès-Lassaille ^b, Simona Bottani ^{a,c},
 Lorenzo Cipriano ^{a,h}, Marion Houot ^{a,b,i}, Aurélie Funkiewiez ^{b,j},
 Agnès Camuzat ^{a,k}, Daisy Rinaldi ^{a,b}, Marc Teichmann ^{a,b,j},
 Jérémie Pariente ^{d,e}, Philippe Couratier ^l, Claire Boutoleau-Bretonnière ^m,
 Sophie Auriacombe ⁿ, Frédérique Etcharry-Bouyx ^o, Richard Levy ^{a,b,j},
 Raffaella Migliaccio ^{a,b,j}, Eino Solje ^{p,q} and Isabelle Le Ber ^{a,b,j,*}, The French
 research network on FTD/FTD-ALS and PREV-DEMALS study groups

^a Sorbonne Université, Paris Brain Institute – Institut Du Cerveau – ICM, Inserm U1127, CNRS UMR 7225, AP-HP - Hôpital Pitié-Salpêtrière, Paris, France

^b Reference Centre for Rare or Early-Onset Dementias, IM2A, Département de Neurologie, AP-HP - Hôpital Pitié-Salpêtrière, Paris, France

^c Aramis Project Team, Inria Research Center of Paris, Paris, France

^d Department of Neurology, Toulouse University Hospital, Toulouse, France

^e ToNIC, Toulouse NeuroImaging Centre, Inserm, UPS, University of Toulouse, Toulouse, France

^f Research Unit of Clinical Neuroscience, Neurology, University of Oulu, Oulu, Finland

^g MRC Oulu, Oulu University Hospital, Oulu, Finland

^h Department of Advanced Medical and Surgical Sciences, University of Campania “L. Vanvitelli” – Naples, Italy

ⁱ Center of Excellence of Neurodegenerative Disease (CoEN), ICM, CIC Neurosciences, Département de Neurologie, AP-HP - Hôpital Pitié-Salpêtrière, Sorbonne Université, Paris, France

^j Paris Brain Institute – Institut Du Cerveau (ICM), FrontLab, Paris, France

^k EPHE, PSL Research University, Paris, France

^l CMRR Service de Neurologie, CHU de Limoges, Limoges, France

^m CHU Nantes, Inserm CIC04, Department of Neurology, Centre Mémoire de Ressources et Recherche, Nantes, France

ⁿ CMRR Nouvelle Aquitaine / Institut des Maladies Neurodégénératives Clinique (IMNC), CHU de Bordeaux Hôpital Pellegrin, Bordeaux, France

^o Department of Neurology, CMRR Angers University Hospital, Angers, France

^p Institute of Clinical Medicine - Neurology, University of Eastern Finland, Kuopio, Finland

^q Neuro Center, Neurology, Kuopio University Hospital, Kuopio, Finland

ARTICLE INFO

Article history:

Received 3 June 2021

Reviewed: 29 June 2021

ABSTRACT

C9orf72 repeat expansions are rarely associated with primary progressive aphasia (PPA). In-depth characterization of the linguistic deficits, and the underlying patterns of grey-matter atrophy in PPA associated with the C9orf72 expansions (PPA-C9orf72) are currently

* Corresponding author. Institut du Cerveau (ICM) – Paris Brain Institute, AP-HP - Hôpital Pitié-Salpêtrière, Paris, France.

E-mail address: isabelle.leber@upmc.fr (I. Le Ber).

<https://doi.org/10.1016/j.cortex.2021.09.005>

0010-9452/© 2021 Elsevier Ltd. All rights reserved.

Revised 4 August 2021

Accepted 15 September 2021

Action editor Stefano Cappa

Published online 1 October 2021

Keywords:

Primary progressive aphasia

Frontotemporal dementia

Frontotemporal lobar degeneration

C9orf72

Progranulin (GRN)

lacking. In this study, we comprehensively analyzed a unique series of 16 patients affected by PPA-*C9orf72*. Eleven patients were issued from two independent French and Finnish cohorts, and five were identified by means of literature review. Voxel-based morphometry (VBM) studies were performed on three of them.

This study depicts the spectrum of *C9orf72*-related aphasic phenotypes, and illustrates their linguistic presentation. The non-fluent/agrammatic variant was the most frequent phenotype in our series (9/16 patients, 56%), with apraxia of speech being the main defining feature. Left frontal lobe atrophy was present in these subjects, peaking in inferior frontal gyrus. Three patients (19%) showed the semantic variant, with progression of atrophy in temporo-polar regions, later involving orbitofrontal cortex. Anterior temporal lobe dysfunction was also particularly relevant in two patients (12.5%) with mixed forms of PPA. Lastly, two patients (12.5%) had unclassifiable PPA with predominating word-finding difficulties. No PPA-*C9orf72* patients in our series fulfilled the criteria of the logopenic variant.

Importantly, this study underlines the role of *C9orf72* mutation in the disruption of the most anterior parts of the language network, including prefrontal and temporo-polar areas. It provides guidelines for *C9orf72* testing in PPA patients, with important clinical impact as gene-specific therapies are upcoming.

© 2021 Elsevier Ltd. All rights reserved.

1. Introduction

Primary progressive aphasias (PPAs) are rare neurodegenerative diseases initially presenting with speech and language disorders (Gorno-Tempini et al., 2011). The non-fluent/agrammatic variant (nfvPPA) is associated with effortful language production, agrammatism and apraxia of speech, related to involvement of inferior frontal gyrus of the dominant hemisphere. The semantic variant (svPPA) is dominated by conceptual knowledge and language comprehension deficits, associated with anterior temporal lobe atrophy. The logopenic variant (lvPPA) is characterized by phonological working memory impairment with single-word retrieval and sentence repetition deficits, and predominant temporal–parietal junction involvement in the hemisphere specialized into language. However, this classification may not be applied to all cases, some of them not meeting criteria for any of the abovementioned variants (unclassifiable PPA, uPPA), or fulfilling criteria for more than one variant (mixed PPA, mPPA) (Bergeron et al., 2018).

In some patients, PPA phenotypes are caused by mutations in genes responsible for autosomal dominant frontotemporal dementias (FTD). Gene-specific lesion tropism leads to the neuroanatomical profile of cortical atrophy and, hence, in some cases to the resulting predominant linguistic deficits. As such, PPAs are associated with GRN mutations in ~15–20% of carriers (Moore et al., 2020; Saracino et al., 2021) and their phenotypes are dominated by non-amyloid lvPPA and nfvPPA linguistic variants (Le Ber et al., 2008; Moore et al., 2020; Saracino et al., 2021). Conversely, MAPT (Henz et al., 2015), TARDBP (Caroppo et al., 2015; Gelpi et al., 2014; González-Sánchez et al., 2018; Mol et al., 2021), and TBK1 mutations (Caroppo et al., 2015; Hirsch-Reinshagen et al., 2019; Pottier et al., 2015; Swift et al., 2021; van der Zee et al., 2017) much more rarely cause a PPA syndrome; in those rare instances, linguistic impairment usually meets criteria of svPPA, and less frequently nfvPPA.

C9orf72 repeat expansions are the most frequent genetic cause of FTD and amyotrophic lateral sclerosis (ALS). PPA

variants are rather exceptional *C9orf72*-associated phenotypes (Boeve et al., 2012; Majounie et al., 2012; Moore et al., 2020). Therefore, their main linguistic deficits, and the underlying patterns of grey-matter atrophy are not well characterized. To fill this gap, we analyzed the linguistic and neuroanatomical profiles of a unique series of 16 PPA patients carrying *C9orf72* expansions (PPA-*C9orf72*), including 11 patients coming from two independent French and Finnish study cohorts, and five additional patients with in-depth clinical descriptions identified in the literature.

2. Materials and methods

2.1. Study design and patients

The patients analyzed in the French cohort of this study were prospectively included in the context of a national clinical and research network on FTD and ALS between 1996 and 2020 (Research project RBM02-59), as well as PREV-DEMALS study (ClinicalTrials.gov Identifier: NCT02590276). All participating centers employed comparable diagnostic protocols and clinical evaluations (Le Ber et al., 2006; Saracino et al., 2021). Molecular analyses were performed in all patients to search for FTD disease-causing mutations. The ethics committee of Paris-Necker Hospital approved the study. All patients provided written informed consent. No part of the study procedures and analyses was pre-registered prior to the research being conducted. We report how we determined our sample size, all data exclusions, all inclusion/exclusion criteria, whether inclusion/exclusion criteria were established prior to data analysis, all manipulations, and all measures in the study. During this time interval, 330 patients carrying *C9orf72* expansions (at least >30 repeats) were included, 11 (3.3%) of whom received an initial diagnosis of PPA (PPA-*C9orf72*). Five were excluded because of severely compromised language/cognitive functions at first evaluation ($n = 3$), or CSF biomarkers consistent with Alzheimer disease (AD) co-pathology ($n = 2$, one with svPPA and one with lvPPA phenotype).

Here, we report the linguistic and clinical characteristics of the remaining six PPA-C9orf72 patients, among which CSF biomarkers were negative in four (not analyzed in two: #2 and #3). They did not carry mutations in all known FTD-causative genes, and had plasma progranulin levels within normal limits. The standardized speech/language evaluation protocol was carried out with the Boston Diagnostic Aphasia Examination–French version (BDAE/HDAE-F) (Mazaux & Orgogozo, 1982) ($n = 5$) and/or the Montreal-Toulouse protocol for examination of aphasia (MT86) (Nespolous et al., 1992) ($n = 3$). Two patients were tested with both batteries. All underwent more extensive language evaluations also including oral confrontation naming (Deloche & Hannequin, 1997), buccofacial praxis (Teichmann et al., 2013), phonological and semantic fluencies (Godefroy & GREFEX, 2008), the Pyramid and Palm–Tree Test (PPTT) (Howard & Patterson, 1992) or the BECS-GRECO semantic battery (Merck et al., 2011). Other cognitive domains were evaluated with a semi-standardized battery (Saracino et al., 2021).

Additionally, five patients belonging to a Finnish cohort, that have been partially described in a prior study (Haapanen et al., 2020), were included for a more detailed linguistic analysis in the current work. They were diagnosed at the Kuopio University Hospital between 1996 and 2016. They were all of Finnish descent and were not tested for other FTD-causative mutations, which are, however, extremely rare in the Finnish population, likely due to genetic isolation (Haapanen et al., 2020). Their speech/language evaluation relied on the Western Aphasia Battery (WAB) (Shewan & Kertesz, 1980), whereas the other cognitive domains were tested in neuropsychological assessment including the Consortium to Establish a Registry for Alzheimer's disease neuropsychological battery (CERAD-NB). Legal copyright restrictions prevent public archiving of the various assessment instruments and test batteries used in this study, which can be obtained from the copyright holders in the cited references.

The diagnosis of PPA variant was based on international criteria (Gorno-Tempini et al., 2011). Patients were labelled as mPPA when criteria for more than one variant co-occurred in a relatively early disease stage (Bergeron et al., 2018), and as uPPA when their linguistic impairment did not meet the criteria for any of the variants.

After the first evaluation, patients were periodically evaluated for usual clinical care. The median disease duration at the last follow-up was 4.0 years [IQR: 2.6, 5.0]. Some patients secondarily developed additional neurological or cognitive symptoms leading to secondary diagnoses (Table 1).

2.2. Voxel-based morphometry (VBM) analysis

We performed VBM analyses to characterize the neuroanatomical features in two PPA-C9orf72 patients with the nfvPPA phenotype (nfvPPA-C9orf72), and in a third patient with the svPPA phenotype (svPPA-C9orf72). This latter individual was evaluated multiple times. Their 3D T1-weighted MRI scans were all performed ≤ 6 months before or after clinical evaluation. They were compared with 35 controls selected to match each patient based on their demographic characteristics.

We employed a VBM-based approach with the T1-volume pipeline of Clinica (<http://www.clinica.run>), a wrapper of the segmentation, run Dartel, and normalize to Montreal Neurological Institute (MNI) space routines implemented in Statistical Parametrical Mapping (SPM). After the unified segmentation procedure, a group template was created using Dartel, and the Dartel-to-MNI method was then applied, incorporating the native space images into the MNI space.

We used two-sample t-tests for the group analysis, applying the contrast PPA-C9orf72 vs controls, with age at MRI and gender as nuisance covariates. In order to capture the full extent of brain atrophy, we generated false discovery rate (FDR)-corrected maps at cluster level, because of the well-known limited statistical power of single-subject VBM. We used the AAL3.1 atlas to label cortical and subcortical regions harboring significant differences (Rolls et al., 2020).

2.3. Literature review

We performed an extensive literature review to get deeper insights in linguistic characteristics of previously reported PPA-C9orf72 patients (AG, DS). A PubMed search employed the following search terms ((C9orf72) OR (chromosome 9 open reading frame 72) OR (c9)) AND ((primary progressive aphasia) OR (PPA)) OR frontotemporal* from 2011 (year of C9orf72 identification) to 2021. A total of 874 articles were found, 53 of which were initially selected for full-text review after a first screening of research studies on PPA and C9orf72 written in English. We subsequently reviewed the 31 more relevant papers specifically focusing on genetic screening in PPA cohorts, or on phenotypic characterization of C9orf72 cohorts or cases, to eventually focus only on those dealing with PPA-C9orf72 patients. We excluded the papers without detailed clinical/linguistic descriptions ($n = 26$) or in which the causative role of C9orf72 expansion was not unequivocal (e.g., CSF biomarker profile in favor of AD pathology or presence of a second FTD or AD-disease causing mutation, $n = 2$) (Supplementary Table 1). Finally, only five PPA-C9orf72 patients had in-depth linguistic evaluation and could be kept in the study (Cerami et al., 2013; Hsiung et al., 2012; Snowden et al., 2012).

3. Results

3.1. Clinical phenotypes

Overall, 16 PPA-C9orf72 patients including our six novel French patients, five Finnish patients and five cases from the literature, were described and analyzed in this study. Their median age at onset was 63 (range: 39–78). Patients were at an early stage of the disease, as reflected by the short median disease duration (DD) (2.0 years; interquartile range, IQR: 1.5, 2.5). Their demographic, clinical and linguistic features are summarized in Table 1. In order to better illustrate the heterogeneity of clinical phenotypes, we described in detail the clinical histories and the linguistic characteristics of three paradigmatic cases, each presenting a different PPA variant. The conditions of our ethics approval do not permit public archiving of the individual patient clinical, behavioral and linguistic data supporting this study. Readers seeking access

Table 1 – Clinical and linguistic features of the 16 PPA-C9orf72 patients. + indicates presence, – absence, and (+) partial or mild difficulties. §: appeared during disease evolution; †: disease duration at death. AAO: age at onset; ALS: amyotrophic lateral sclerosis; AOS: apraxia of speech; BD: Behavioral disorders; bvFTD: behavioral variant of frontotemporal dementia; CS: complex sentences; DD: disease duration; FCSd: frontal cognitive syndrome; mPPA: mixed primary progressive aphasia; NA: not available; nfvPPA: non-fluent/agrammatic variant of PPA; Park: parkinsonism; PLD: parietal lobe dysfunction; PNFA: progressive non-fluent aphasia; PPA: primary progressive aphasia; SS: simple sentences; svPPA: semantic variant of PPA; uPPA: unclassifiable PPA; y: years. An overall description of the Finnish cohort without detail on individual phenotypes was provided in [Haapanen et al., 2020](#).

	This study						Snowden et al. (2012)					Cerami et al. (2013)	Hsiung et al. (2012)			
	French cohort			Finnish cohort												
Patient	#01	#02	#03	#04	#05	#06	Case 1	Case 2	Case 3	Case 4	Case 5	Case 30	Case 31	Case 32	Case 2	C2
Diagnosis	svPPA	svPPA	nfvPPA	nfvPPA	mPPA	mPPA	uPPA	uPPA	nfvPPA	nfvPPA	nfvPPA	PNFA	PNFA	PNFA	svPPA	PNFA
AAO (y)	39	55	63	57	74	68	63	65	70	78	62	52	62	58	68	67
DD at evaluation (y)	3	4	1	1	2	2	.5	2	2	2	3	1	2	4	4	1
Reduced speech output	–	–	+	+	+	+	–	–	–	+	+	+	+	+	–	+
Impaired naming	+	+	–	+	+	+	–	+	+	+	+	+	+	+	+	+
Word-retrieval difficulties	–	+	–	+	+	+	+	+	+	+	+	NA	NA	NA	+	+
Impaired word repetition	–	–	–	–	–	–	–	–	–	–	–	NA	NA	NA	–	NA
Impaired sentences repetition	–	–	–	–	–	–	–	–	–	–	–	NA	NA	NA	–	NA
Phonological paraphasias	–	–	+	–	–	+	–	–	–	–	–	+	–	+	–	NA
Agrammatism	–	–	–	(+)	+	(+)	–	–	–	–	+	+	+	+	–	–
AOS	–	–	+	+	–	+	–	–	+	+	–	–	–	–	–	+
Impaired sentences comprehension	+(CS)	+(SS, CS)	–	+(CS)	+(CS)	+(CS)	+(CS)	+(CS)	+	+	+	–	–	–	+	+
Impaired word comprehension	+	+	–	–	+§	+§	–	–	–	–	–	–	–	–	+	–
Impaired object knowledge	+	+	–	–	+§	+§	–	–	–	–	–	–	–	–	+	–
Impaired reading	+	NA	–	–	–	NA	–	–	–	–	+	NA	NA	NA	NA	+
Verbal/semantic paraphasias	+	+	–	–	–	+	–	–	–	–	–	–	–	–	NA	NA
Duration at last follow-up	10	10	2	2.5	4	5	4	4†	1	3†	5†	4	4	NA	5	2
Other relevant impairments at follow-up	BD, FCSd	BD, FCSd, PLD	ALS	BD, FCSd, Park	FCSd	FCSd, (PLD)	FCSd, BD, Park	FCSd	FCSd, Park	FCSd, Park	FCSd	FCSd, Park	–	FCSd, Park	BD	BD
Diagnosis at last follow up	svPPA	svPPA	PPA/ALS	PPA/bvFTD	mPPA	mPPA	uPPA	uPPA	nfvPPA	nfvPPA	nfvPPA	PNFA	PNFA	PNFA	svPPA/bvFTD	PNFA/bvFTD

Patients in bold are analyzed in the current study.

to the data should contact the corresponding author (Dr Isabelle Le Ber). Data will be shared with named individuals following completion of a data sharing agreement and approval by the local ethics committee.

3.1.1. Patient #01: svPPA

At the age of 39, this right-handed patient with high-grade education (20 years of formal education) started to complain of insidious language difficulties. They mainly consisted of loss of word meaning, anomia, and difficulties in oral comprehension, especially with some idiomatic expressions. Notably, he had difficulties with his professional vocabulary (he worked as a veterinarian but could not define words such as “hippopotamus” or “chick”), mistook the names of his colleagues, and became unable to completely understand scientific articles.

Speech/language evaluation (BDAE) at 3 years from onset showed fluent, moderately informative language, with anomia, semantic/verbal paraphasias, and circumlocutions. The severity of aphasia was rated 3/5. Naming was impaired

(DO80: 52/80, below 2.5 SD), as well as single-word comprehension (56/72 for the BDAE subtest, normal value (n.v.) >68/72) and object knowledge (visual version of the PPTT: 33/52; n.v. >47/52). At the sentence level, comprehension was mildly affected in both the oral (14/15 for the BDAE commands subtest, n.v. >12/15) and written modalities (8/10 for the BDAE sentences and paragraphs comprehension subtest, n.v. >8/10). Surface dyslexia and dysgraphia were present. Repetition, motor speech and syntactic skills were unaffected. The Mini-Mental State Examination (MMSE) was 27/30. There was no evidence of dysexecutive disorders, episodic memory impairment, or visuo-spatial or visuo-constructive dysfunction (forward and backward digit span: 7 and 7, Rey–Osterrieth Complex Figure copy and recall: 36/36 and 22.5/36). Brain MRI at age 43 showed left temporal pole atrophy (Fig. 1A), with corresponding hypometabolism on cerebral ^{18}F FDG-PET (Fig. 1B).

At 4.5 years from onset, the patient presented further deterioration of naming (DO80: 47/80) and semantic skills (PPTT: 25/52), along with increasing difficulties in reading and

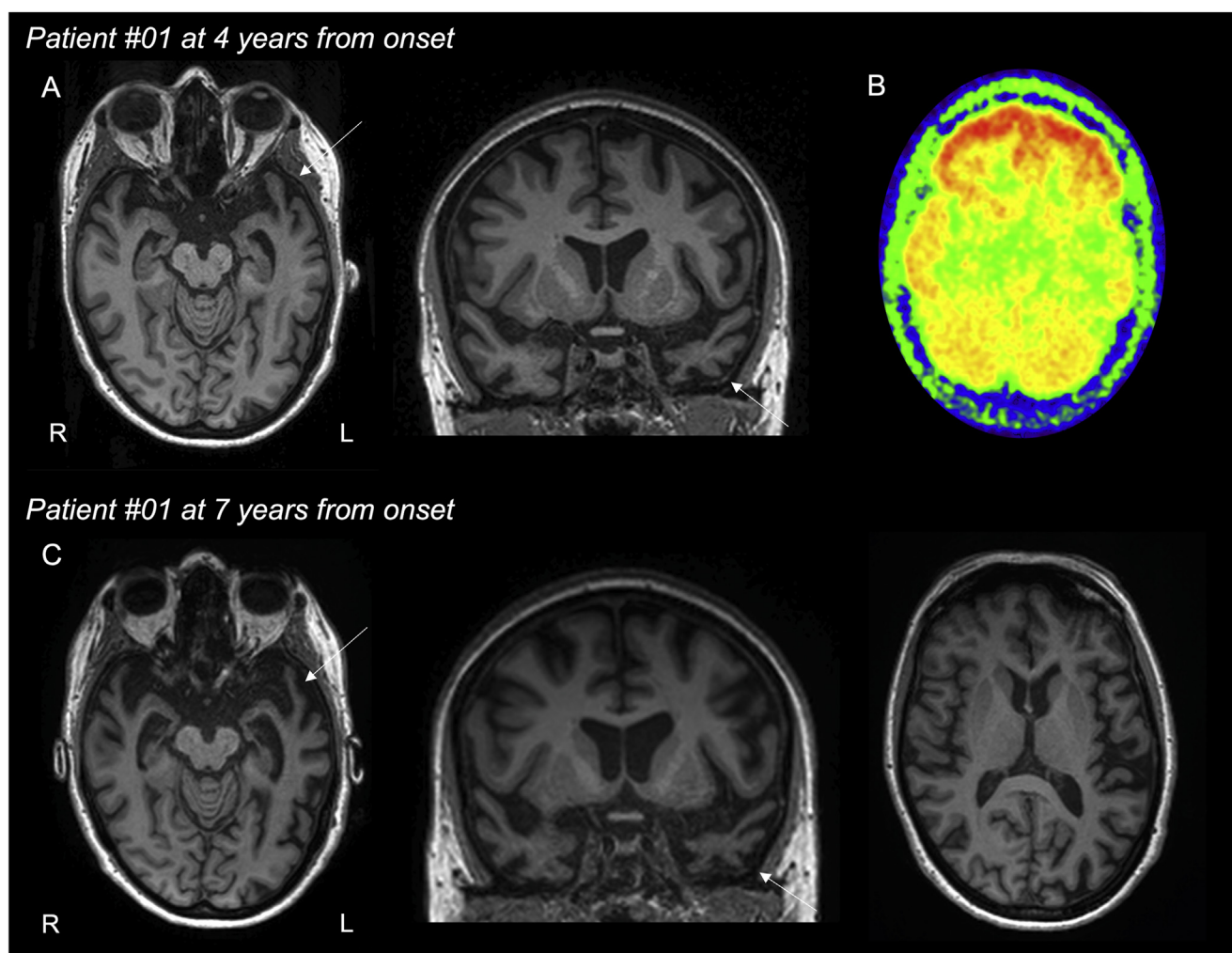


Fig. 1 – MRI and ^{18}F FDG-PET studies in patient #01. **A:** cortical atrophy prevailing in the left anterior temporal lobe (arrows) at age 43, 4 years after onset. **B:** asymmetric temporo-polar hypometabolism, prevailing on the left side, at the same age. **C:** progression of atrophy in left temporal regions (arrows), and extension to the contralateral side and frontal cortex at age 46, 7 years after onset.

writing irregular words. Global cognitive efficiency remained stable and there was no evidence of additional cognitive deficits. After six years of follow-up (45 years), the patient manifested severe difficulties in understanding conversational speech, while his verbal output was almost not understandable due to word-finding difficulties and circumlocutions. He also displayed some repetitive, ritualistic-obsessive behaviors and behavioral disinhibition. Initial impairment in executive functions was noticed at cognitive testing (Frontal Assessment Battery, FAB: 15/18). Left temporal atrophy became more extensive in a follow-up brain MRI performed at age 46, along with subtle prefrontal atrophy (Fig. 1C).

Comprehension difficulties became so severe as to no longer allow oral or written communication by the age of 47, eight years from onset. There was a family history of psychosis in one of the patient's cousins.

3.1.2. Patient #04: *nfvPPA*

Patient #04, a right-handed person with 9 years of formal education, complained of difficulties in speech production with articulatory troubles at age 57, progressively leading to reduction of speech output. Moreover, he displayed mild personality changes with impulsiveness, reduced initiative and unawareness of risks. Speech/language evaluation (MT86) at age 58 revealed apraxia of speech, reduced fluency and loss of prosody, with moderately affected intelligibility (aphasia severity score 4/5). Syntactic difficulties were evident in speech production and perception, with impaired comprehension of complex sentences (30/38 for the syntactic MT86 subtest, *n.v.* >34/38). Morphosyntactic troubles were present also in sentence writing tasks (18/34 for the MT86 word and sentence writing subtest, *n.v.* >29/34). Phonological and semantic fluencies were reduced (13 words in 2 min for both:

between 2.5 and 1.5 SD for phonological, and below 2.5 SD for semantic fluency). Repetition and semantic knowledge were unaffected. His MMSE was 27/30. Some elements of executive dysfunction were evident at neuropsychological testing (FAB 12/18; forward digit span: 5; backward digit span: 3). Episodic memory, praxis and visuospatial functions were unimpaired. Neurological examination did not reveal bulbar or pseudo-bulbar signs, and there was no dysphagia; muscle atrophy and fasciculations were absent, and there were no pyramidal signs. At age 58 brain MRI revealed bilateral cortico-subcortical fronto-temporal atrophy, prevailing in left perisylvian areas (Fig. 2A). Bilateral prefrontal, left fronto-opercular and anterior temporal hypometabolism was found in ¹⁸FDG-PET (Fig. 2B). CSF biomarkers were not in favor of AD.

At 2.5 years from onset, a mild right-predominant akinetic-rigid syndrome was present at neurological examination; pyramidal or motor neuron signs did not appear during follow-up, and EMG testing was persistently negative. The family history was positive for dementia in the patient's mother, who deceased at 72 years.

3.1.3. Patient #06: *mPPA*

This right-handed patient with 11 years of education complained of initial difficulties in language production at age 68, with reduced fluency and troubles in word-finding, without comprehension impairment. His first speech/language evaluation at age 70, two years from onset, revealed non-fluent, slowed utterances with apraxia of speech (aphasia severity rating 3/5). Buccofacial apraxia was noticed too, with major impact on tongue movements. Aside from his articulatory disorder, he presented impairment in naming (DO80: 54/80, below 2.5 SD), due to a combination of semantic and phonemic paraphasias. Occasional paragraphic errors (inversion

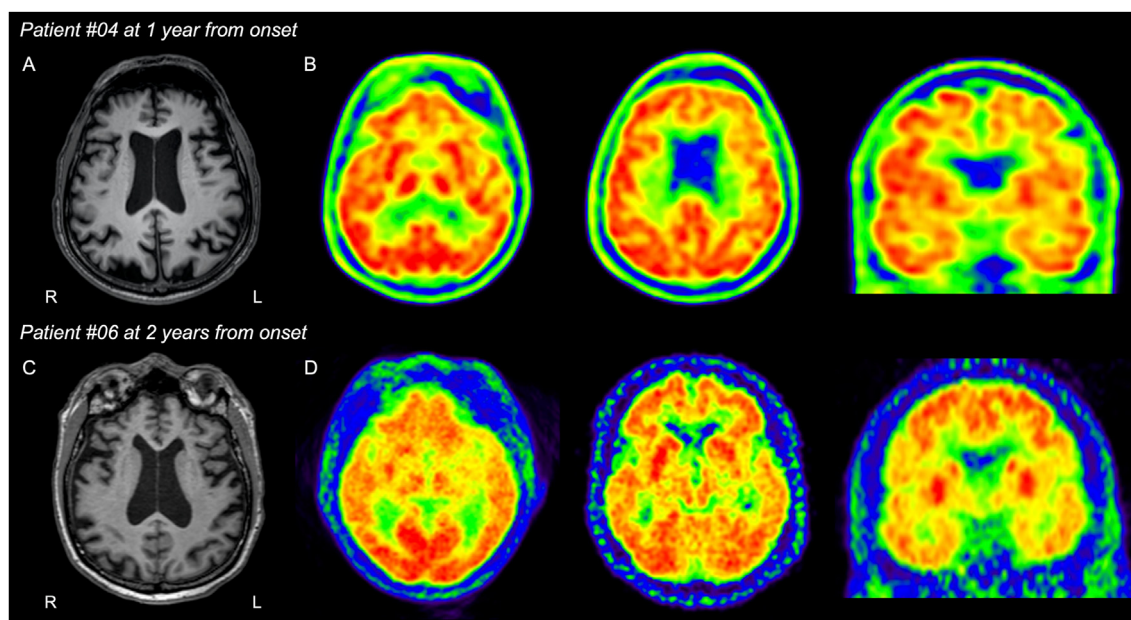


Fig. 2 – MRI and ¹⁸FDG-PET studies in patients #04 and #06. **A:** bilateral fronto-temporal atrophy prevailing in left perisylvian areas. **B:** asymmetric left-predominant fronto-temporal hypometabolism with involvement of fronto-opercular cortex. **C:** bilateral peri-sylvian atrophy with slight predominance on the left side. **D:** bitemporal hypometabolism, prevailing in the left temporal pole.

or substitution of syllables) were noticed in writing tasks. His MMSE was 27/30 and Mattis Dementia Rating Scale (MDRS) 122/144, with prevailing deficit in the initiation subtask (23/37), which is a proxy of categorial verbal fluency. Executive impairment was present (FAB 14/18; TMT below 10th percentile), whereas episodic memory was relatively spared. Brain MRI evidenced bilateral fronto-temporal atrophy, with slight predominance on the left perisylvian areas (Fig. 2C). Cerebral ^{18}F FDG-PET showed a discrete left-predominant temporal hypometabolism (Fig. 2D). Notably, EMG excluded motor neuron involvement. CSF biomarkers were not in favor of AD.

During disease evolution his communication skills further worsened, mainly because of increasing anomia. Evaluation at 3 years from onset evidenced markedly impaired naming (Boston naming test: 9/34, <1st percentile) and semantics skills (PPTT, verbal version: 36/52). His motor speech difficulties remained quite stable. The other cognitive domains did not get significantly worse, with except for initial ideo-motor apraxia for intransitive limb gestures. His motor testing was persistently normal. His mother was affected by ALS, one sibling had bvFTD and another had both FTD and ALS.

3.2. Characteristics of PPA-C9orf72 patients in this study and the literature

The most prevalent PPA variant among C9orf72 patients was nfvPPA in our series (5/11, 45%), and even more so when considering the overall dataset including this series and previously reported cases diagnosed as “PNFA” (9/16, 56%) (Table 1).

Notably, the defining feature was apraxia of speech in 80% of our nfvPPA cases, isolated agrammatism being present in only one patient. The other main features were slowed, hypofluent speech (4/5), impairment in naming (4/5), and difficulties in comprehension of (mainly complex) sentences (4/5); evidence of clear phonological disruption was seldom present (1/5). These characteristics were also common in PNFA cases from the literature, with the only remarkable exception of agrammatism prevailing over apraxia of speech among the core clinical features.

All reported svPPA patients (2/11 in our series, 18%; 3/16 in the overall dataset, 19%) had fluent, logorrheic speech, with massive impairment in naming and in comprehension in conversational speech. The two svPPA we reported had the longest disease course (10 years at last follow-up in both cases). Behavioral changes reminiscent of anterior temporal disruption (ritualistic, stereotyped or compulsive behaviors, loss of mental flexibility) appeared during disease course. Earlier and more severe frontal behavioral impairments were described in the previously reported svPPA patient (Cerami et al., 2013).

The two mixed PPA-C9orf72 patients (#05 and #06) showed a similar profile, with grammar-syntactical deficits and reduced fluency prevailing during the first year of the disease (apraxia of speech was clearly present in #06), associated with moderate verbal and visual semantic deficits at onset (comprehension and object-knowledge difficulties). The syndromic progression followed a similar time-course in both patients, semantic deficit becoming predominant after three years from onset.

Lastly, the linguistic profile of the two patients diagnosed as uPPA included word-finding difficulties and impairment in the comprehension of syntactically complex sentences, without frank agrammatism, motor speech disturbances, repetition impairment, phonological or semantic disruption. They showed discrete asymmetric, left-predominant fronto-temporal atrophy, peaking in the perisylvian areas (Supplementary Figure 1). Both developed mutism relatively quickly after the diagnosis. Notably, no patients from our cohort showed a linguistic profile compatible with lvPPA.

Overall, the majority of PPA-C9orf72 patients eventually displayed at least a moderate degree of impairment in executive functions during follow-up (12/16, 75%), whereas clinically relevant behavioral troubles were reported in 6/16 cases (38%). In three patients (2 nfvPPA and 1 svPPA) the final diagnosis was PPA associated with bvFTD.

Concerning the intercurrent motor features, only one patient from the overall series (#03) developed (bulbar-onset) ALS, between 1 and 2 years from the onset of linguistic deficits. Atypical parkinsonism was more frequent during the disease course (6/16, 38%).

3.3. Grey matter atrophy profile in PPA-C9orf72 patients

VBM analysis in the svPPA-C9orf72 patient (#01) initially showed isolated left superior temporal pole atrophy at age 43, 4 years after disease onset. At 47 years, 7 years from disease onset, there was progression of left anterior temporal lobe atrophy, along with right temporopolar and orbitofrontal involvement (Supplementary Figure 2, Supplementary Table 2).

VBM study in nfvPPA-C9orf72 patients compared with controls displayed a cluster of significant frontal atrophy in the left frontal lobe, peaking at the level of inferior and middle frontal gyri (Supplementary Figure 3, Supplementary Table 3).

4. Discussion

A first contribution of the present study is the definition of a remarkably low frequency of PPA with C9orf72 expansions, representing only 3% of carriers. This frequency is fairly concordant with those estimated in the largest cohorts of C9orf72 carriers, PPA being the presenting phenotype in only 1–3% of C9orf72 carriers (Majounie et al., 2012; Le Ber et al., 2013; Moore et al., 2020) (Table 2). On the other hand, the prevalence of C9orf72 repeat expansion in cohorts of PPA patients ranges from 1% to 8% (Table 2), with the remarkable exception of small Finnish cohorts where it reaches ~28% (Haapanen et al., 2020; Kaivorinne et al., 2013). This finding, stemming from observations conducted on a limited number of PPA patients (<30 cases), is possibly related to the founder effect and high prevalence of C9orf72 repeat expansion in Finland, making it a very relevant genetic cause of FTD in this country (Haapanen et al., 2020; Majounie et al., 2012). Aside from that, due to the rarity of PPA-C9orf72 patients, only single cases or small series have been described in detail (Cerami et al., 2013; Hsiung et al., 2012; Snowden et al., 2012), and comprehensive characterization of their linguistic and

Table 2 – Summary of the most important revised papers contributing to determine the frequency of PPA in C9orf72 cohorts, and of C9orf72 expansion in PPA cohorts. The largest study cohorts, contributing to a better estimation of frequencies, are shown first. FTLD: frontotemporal lobar degeneration; lvPPA: logopenic variant of PPA; mPPA: mixed PPA; na: not available; nfvPPA: non-fluent/agrammatic variant of PPA; NOS: not otherwise specified; PPA: primary progressive aphasia; PNFA: progressive non-fluent aphasia; SD: semantic dementia; svPPA: semantic variant of PPA. *Some patients may be duplicated among two or more cohorts.

Reference (origin of the cohort)	Cohort of PPA patients	Cohort of C9orf72 carriers	Frequency of C9orf72 carriers in PPA cohort (%)	Frequency of PPA patients in C9orf72 cohort (%)	PPA variants
Largest C9orf72 cohorts					
Boeve et al. (2012) (USA)	141 PPA 76 nfvPPA 65 svPPA	103 C9orf72	0%	0%	–
(Majounie et al., 2012)* (Europe, USA)	378 PPA 176 PNFA 202 SD	625 C9orf72	5%	3%	18 PPA-C9orf72*: 11 PNFA 7 SD
Le Ber et al. (2013) (France)	73 PPA 62 PNFA 11 SD	202 C9orf72	7%	2%	5 PPA-C9orf72: 3 PNFA 2 SD
Ramos et al. (2020) (USA)	85 PPA 36 nfvPPA 45 svPPA 4 lvPPA	95 C9orf72	1%	1%	1 PPA-C9orf72 1 svPPA
(Moore et al., 2020)* (International)	–	1433 C9orf72	–	3%	46 PPA-C9orf72* 26 nfvPPA 13 svPPA 3 lvPPA 4 PPA-NOS
Largest PPA cohorts					
Mahoney et al. (2012) (UK)	102 PPA 49 PNFA 53 SD	19 C9orf72	1%	5%	1 PPA-C9orf72: 1 PNFA
Simón-Sánchez et al. (2012) (The Netherlands)	101 PPA	42 C9orf72	8%	19%	8 PPA-C9orf72: 2 svPPA 6 PPA-NOS
Snowden et al. (2012) (UK)	118 PPA 66 PNFA 53 SD	32 C9orf72	3%	10%	3 PPA-C9orf72: 3 nfvPPA
Galimberti et al. (2013) (Italy)	98 PPA 64 PNFA 34 SD	39 C9orf72	2%	5%	2 PPA-C9orf72: 2 SD
Flanagan et al. (2015) (USA)	100 PPA 17 nfvPPA 16 svPPA 54 lvPPA 13 uPPA	–	2%	–	2 PPA-C9orf72: 1 svPPA 1 uPPA
Bocchetta et al. (2018) (UK)	193 PPA 103 PNFA 76 SD	28 C9orf72	1%	7%	2 PPA-C9orf72 14 PPA-NOS 2 nfvPPA
Ramos et al. (2019) (USA)	403 PPA 125 nfvPPA 122 svPPA 89 lvPPA 5 mPPA 18 uPPA 44 PPA-NOS	–	1%	–	4 PPA-C9orf72 3 nfvPPA 1 svPPA
Costa et al. (2020) (International)	495 PPA	56 C9orf72	1%	2%	4 PPA-C9orf72
Additional study cohorts					
Hsiung et al. (2012) (Canada)	–	30 C9orf72	–	17%	5 PPA-C9orf72: 5 PNFA
Cerami et al. (2013) (Italy)	86 FTLD	–	–	–	1 PPA-C9orf72: 1 svPPA

Table 2 – (continued)

Reference (origin of the cohort)	Cohort of PPA patients	Cohort of C9orf72 carriers	Frequency of C9orf72 carriers in PPA cohort (%)	Frequency of PPA patients in C9orf72 cohort (%)	PPA variants
Gil-Navarro et al. (2013) (Spain)	32 PPA 15 nfvPPA 5 svPPA 7 lvPPA 5 uPPA	–	6%	–	2 PPA-C9orf72: 2 nfvPPA
Irwin et al. (2013) (USA)	–	64 C9orf72	–	8%	5 PPA-C9orf72: 4 nfvPPA 1 svPPA
Kaivorinne et al. (2013) (Finland)	27 PPA 20 PNFA 7 SD	22 C9orf72	22%	27%	6 PPA-C9orf72: 6 PNFA
Van Langenhove et al. (2013) (Belgium)	–	26 C9orf72	–	12%	3 PPA-C9orf72: 2 PNFA 1 SD
Benussi et al. (2014) (Italy)	82 PPA	26 C9orf72	1%	4%	1 PPA-C9orf72
(Fletcher et al., 2015a)* (UK)	37 PPA 20 PNFA 17 SD	–	3%	–	1 PPA-C9orf72*: 1 PNFA
(Fletcher et al., 2015b)* (UK)	34 PPA 15 PNFA 19 SD	–	3%	–	1 PPA-C9orf72*: 1 PNFA
Snowden et al. (2015) (UK)	–	42 C9orf72	–	10%	4 PPA-C9orf72: 4 PNFA
(Hardy et al., 2016)* (UK)	32 PPA 18 nfvPPA 14 svPPA	–	3%	–	1 PPA-C9orf72*: 1 nfvPPA
Rohrer et al. (2016) (UK)	37 PPA 13 nfvPPA 10 svPPA 7 lvPPA 7 uPPA	–	3%	–	1 PPA-C9orf72 1 nfvPPA
Van Mossevelde et al. (2016) (Belgium)	79 PPA 43 PNFA 33 SD 2 lvPPA 1 uPPA	65 C9orf72	10%	12%	8 PPA-C9orf72: 5 PNFA 3 SD
Öijerstedt et al. (2019) (Sweden)	132 FTLD	35 C9orf72	–	3%	1 PPA-C9orf72 1 PPA-NOS
Cajanus et al. (2020) (Finland)	-	26 C9orf72	–	19%	5 PPA-C9orf72
Haapanen et al. (2020) (Finland)	18 PPA: 16 nfvPPA 2 PPA-NOS	–	28%	–	5 PPA-C9orf72 3 nfvPPA 2 PPA-NOS

cognitive profiles is currently lacking. Our study describes the linguistic features and the neuroimaging profiles of a series of 16 PPA-C9orf72 patients, including cases issued from French and Finnish cohorts, and five additional individuals described in detail in the literature.

In this cohort, 56% (9/16) of PPA-C9orf72 patients presented the nfvPPA phenotype, before svPPA (3/16, 19%), mPPA (2/16, 12.5%) and uPPA (2/16, 12.5%). Interestingly, the most prominent linguistic feature in the majority of nfvPPA-C9orf72 cases was apraxia of speech, whereas patients in our series less frequently presented with progressive agrammatic aphasia. Prior neuroimaging studies in nfvPPA patients supported the duality of its clinical presentation. Apraxia of speech is associated with bilateral, left-predominant superior frontal

atrophy, including premotor and supplementary motor areas, while agrammatic PPA with more widespread prefrontal involvement, extending to middle and inferior frontal gyri, clearly lateralized on the left ([Botha et al., 2015](#); [Cordella et al., 2019](#); [Tetzloff et al., 2019](#)). These phenotypes are not unexpected in C9orf72 carriers, in which prefrontal atrophy has been reported long before symptom onset ([Bertrand et al., 2018](#); [Bocchetta et al., 2021](#); [Le Blanc et al., 2020](#); [Lee et al., 2017](#); [Rohrer et al., 2015](#)). A selective lesion tropism predominating on the left side, mainly centered on inferior frontal gyrus and/or fronto-opercular cortices may potentially drive the clinical presentation to nfvPPA in some patients, as observed in our cohort. From the neuropathological point of view, apraxia of speech and, more largely, nfvPPA are usually

associated with tau protein deposition when occurring sporadically (Bergeron et al., 2018). The presence of the *C9orf72* expansion thus qualifies as one of the causes of nfvPPA with underlying frontotemporal lobar degeneration (FTLD) with TAR DNA-binding protein of 43 kDa (FTLD-TDP) pathological substrate, as in the case of GRN mutations.

This study also highlights that svPPA could be a possible clinical phenotype in the *C9orf72* expansion carriers, although with lesser frequency than nfvPPA. Interestingly, both the svPPA-*C9orf72* patients from our series presented with an isolated, progressive disruption of the semantic system, and both showed a particularly long disease course, with 10 years of disease duration at last follow-up. Notably, slowly progressive FTD cases could be occasionally due to *C9orf72* repeat expansions, and they reflect the major clinical heterogeneity associated with this genetic cause in terms of disease phenotype and progression (Khan et al., 2012; Suhonen et al., 2015). These patients during their disease course exhibited behavioral changes which were mainly characterized by ritualistic, compulsive and stereotyped actions with loss of mental flexibility, rather than prevailing disinhibited or apathetic conducts, consistent with bilateral anterior temporal pathology. Accordingly, the progression of atrophy seen in one case study was greater in anterior temporal lobe, with later and less relevant involvement of orbitofrontal cortex.

Additional evidence for anterior temporal lobe disruption in the *C9orf72* patients is provided by the two mPPA cases described in this study, in whom semantic disturbances took over the predominantly non-fluent/agrammatic disturbances shortly after disease onset. Similarly, semantic disturbances have been already reported in association with frontal behavioral disturbances in previous *C9orf72* cases (Snowden et al., 2012). Furthermore, the relevance of anterior temporal lobe dysfunction in the *C9orf72* expansion carriers has been recently highlighted in two patients presenting temporal-variant FTD (tv-FTD), with object recognition and language difficulties being part of the clinical picture during disease evolution (Caso et al., 2020). Altogether, besides the svPPA phenotype, the *C9orf72* expansion can trigger anterior temporal lobe degeneration, producing semantic deficits also in patients initially presenting with different linguistic variants or behavioral syndromes.

The linguistic spectrum of the *C9orf72* repeat expansion appears in striking contrast with those observed in other FTD-causing mutations. The main presentations of PPA associated with GRN mutations (PPA-GRN) are logopenic variants, followed by nfvPPA syndrome in which agrammatism clearly predominates over apraxia of speech (Moore et al., 2020; Saracino et al., 2021). Semantic deficits rarely occur in isolation, though they can add up to logopenic or agrammatic impairment in the mixed forms. Overall, sentence-level processing deficits, naming difficulties, and phonological disturbances are the main linguistic features of GRN-associated PPA (Rohrer, Crutch, et al., 2010; Saracino et al., 2021). On the other hand, lvPPA has been exceptionally if ever reported in the *C9orf72* repeat expansion carriers (Moore et al., 2020). This phenotype requires the coexistence of word-finding difficulties and sentence repetition deficits to be diagnosed (Gorno-Tempini et al., 2011), and this latter impairment is remarkably rare in PPA-*C9orf72* (Table 1). Therefore, it is not

surprising that the atrophy pattern involves quite distinct, more posterior regions within the language network in PPA-GRN, namely posterior temporal lobe, temporo-parietal junction and posterior frontal areas (Rohrer, Ridgway, et al., 2010; Saracino et al., 2021; Whitwell et al., 2015).

Less common FTD/ALS genes may also produce PPA phenotypes, and the available information stems from the description of single cases or very small series. *MAPT* mutations may produce both nfvPPA and svPPA phenotypes, in association with underlying FTLD with tau pathology (FTLD-tau) (Moore et al., 2020). However, pure svPPA cases are rather rare, whereas bvFTD associated with anomia and profound semantic deficits is a more common occurrence (Henz et al., 2015; Pickering-Brown et al., 2002; Roncero et al., 2021). *TARDBP* carriers may also display important bilateral temporal atrophy, and the corresponding linguistic phenotype is more commonly svPPA (Caroppo et al., 2016; Gelpi et al., 2014; González-Sánchez et al., 2018; Mol et al., 2021). Somatic mutations of *TARDBP* in the lateral and medial temporal cortices of patients with sporadic svPPA also highlight the role of *TARDBP* in temporal lobe pathology (van Rooij et al., 2020). Linguistic presentations associated with *TBK1* mutations are more heterogeneous and almost equally represented by nfvPPA and svPPA (Caroppo et al., 2015; Hirsch-Reinshagen et al., 2019; Pottier et al., 2015; Swift et al., 2021; van der Zee et al., 2017). Overall, these findings suggest that the degenerative process resulting from distinct FTD gene mutations displays a differential lesional tropism in patients with PPA phenotypes. Involvement of frontal areas among the *C9orf72* carriers is quite heterogeneous in terms of lateralization and peak of atrophy, thus giving rise to different nfvPPA subphenotypes. The temporo-polar cortex is predominantly involved in the context of *C9orf72*, as well as *MAPT*, *TARDBP* and *TBK1* mutations, whereas it is rather atypical in the GRN carriers, who frequently display a quite distinct pattern involving the posterior language areas.

Anyway, the rarity of PPA-*C9orf72*, and more largely of genetic PPA, may preclude the generalizability of our findings and the resulting genotype–phenotype correlations. Moreover, the speech/language batteries we used, though allowing a homogeneous description of patients observed across a wide time span, did not undergo validation studies in the PPA population and are not based on a cognitive approach to language dysfunction, thus lacking diagnostic accuracy to capture the most subtle linguistic deficits, especially for unclassifiable and mixed cases (Ivanova & Hallowell, 2013; Macoir et al., 2021). A more exhaustive linguistic evaluation based on the most recently validated tests would represent an added value for future works in this field. Additionally, the limited number of patients available in our series (even if rather important for such a rare phenotype in a rare genetic form) may have led to statistically underpowered VBM studies. Nevertheless, cluster-level corrected VBM analyses have proven their usefulness in elucidating significant patterns of atrophy even in single subjects or small-sized groups (Josephs et al., 2014; Khan et al., 2012). Furthermore, our neuroimaging results are well concordant with the linguistic and clinical phenotypes, and closely mirror the profiles of cortical involvement seen in the native acquisitions (Supplementary Figures 2 and 3).

In spite of the abovementioned limitations, this study offers an overview on the clinical progression of a relatively large series of PPA-C9orf72 cases. Interestingly, the frequency of patients developing ALS (6%, 1/16) was far below what it is expected in the C9orf72 carriers, approximately half of whom presenting motor neuron dysfunction during the disease course (Le Ber et al., 2013; Majounie et al., 2012; Snowden et al., 2012). Therefore, ALS seems a less common occurrence in patients initially displaying a PPA, rather than a bvFTD phenotype. Even if behavioral and executive disturbances were quite common during progression, the frequency of bvFTD as secondary diagnosis was indeed low, and specifically lower than what observed in a series of PPA-GRN recently reported (Saracino et al., 2021).

In conclusion, the current findings provide some important information for genetic testing in clinical practice, showing that C9orf72 gene should be analyzed in PPA patients with nfvPPA phenotype, notably when manifesting with apraxia of speech, and in those with predominant semantic impairment, especially when family history is positive for FTD/ALS. Non-amyloid lvPPA variants are not associated with the C9orf72 expansion in our series, even if some exceptions may occur. Finally, this study comprehensively describes the linguistic spectrum in a large cohort of patients with PPA related to C9orf72 expansion, and to refine the indications for molecular analyses in PPA patients, according to their phenotypes, with major clinical impact as targeted disease-modifying therapies are upcoming.

Funding

The research leading to these results received funding from the “Investissements d’avenir” ANR-11-INBS-0011, the Academy of Finland (no315460), and the University of Oulu Scholarship Foundation. This work was partially funded by the PHRC FTLN-exome (to ILB, promotion by Assistance Publique – Hôpitaux de Paris), the ANR-PRTS PREV-DEMALS project (to ILB, grant number ANR-14-CE15-0016-07, promotion by Assistance Publique – Hôpitaux de Paris), the Finnish Brain Foundation (to ES), the Orion Research Foundation (to ES), the Instrumentarium Science Foundation (to ES), and the Sigrid Jusélius Foundation (to ES). The funding source had no role in study design, data analysis or interpretation, writing or decision to submit the report for publication.

CRedit author statement

Dario Saracino: Conceptualization, Investigation, Formal analysis, Writing – Original Draft; **Amandine Géraudie:** Data Curation, Writing – Review & Editing; **Anne M Remes:** Ressources, Data Curation; **Sophie Ferrieux:** Formal analysis; **Marie Noguès-Laissaille:** Formal analysis; **Simona Bottani:** Formal analysis; **Lorenzo Cipriano:** Formal analysis; **Marion Houot:** Formal analysis; **Aurélie Funkiewiez:** Formal analysis; **Agnès Camuzat:** Data Curation, Formal analysis; **Daisy Rinaldi:** Data Curation; **Marc Teichmann:** Ressources, Writing – Review & Editing; **Jérémy Pariente:** Ressources; **Philippe Couratier:** Ressources; **Claire Boutoleau-Bretonnière:** Ressources; **Sophie Auriacombe:** Ressources; **Frédérique Etcharry-Bouyx:** Ressources; **the French research network on FTD/FTD-ALS and**

PREV-DEMALS study groups: Ressources; **Richard Levy:** Ressources; **Raffaella Migliaccio:** Formal analysis, Writing – Review & Editing; **Eino Solje:** Ressources, Validation, Writing – Review & Editing, Funding acquisition; **Isabelle Le Ber:** Conceptualization, Supervision, Writing – Review & Editing, Funding acquisition.

Declaration of competing interest

Disclosure of interests related to the present article: The authors declare no conflicts of interest.

Disclosure of interests unrelated to the present article: ILB served as a member of advisory boards for Prevail Therapeutic and Alector, and received research grants from ANR, DGOS, Vaincre Alzheimer Association, ARSla Association, Fondation Plan Alzheimer, JPND outside of the present work.

Acknowledgments

We are grateful to the DNA and cell bank of the ICM for the technical assistance (DNA and cell bank, ICM, Pitié-Salpêtrière hospital, Paris, France). We also thank Fabienne Clot for carrying out the genetic analyses. The study was partially conducted with the support of the Centre d’Investigation Clinique Neurosciences (CIC 1422), Pitié-Salpêtrière Hospital, Paris. This work is generated within the European Reference Network for Rare Neurological Diseases—Project ID No 739510.

Supplementary data

Supplementary data to this article can be found online at <https://doi.org/10.1016/j.cortex.2021.09.005>.

REFERENCES

- Benussi, L., Rossi, G., Glionna, M., Tonoli, E., Piccoli, E., Fostinelli, S., Paterlini, A., Flocco, R., Albani, D., Pantieri, R., Cereda, C., Forloni, G., Tagliavini, F., Binetti, G., & Ghidoni, R. (2014). C9ORF72 hexanucleotide repeat number in frontotemporal lobar degeneration: A genotype-phenotype correlation study. *J Alzheimers Dis*, 38, 799–808. <https://doi.org/10.3233/JAD-131028>
- Bergeron, D., Gorno-Tempini, M. L., Rabinovici, G. D., Santos-Santos, M. A., Seeley, W., Miller, B. L., Pijnenburg, Y., Keulen, M. A., Groot, C., van Berckel, B. N. M., van der Flier, W. M., Scheltens, P., Rohrer, J. D., Warren, J. D., Schott, J. M., Fox, N. C., Sanchez-Valle, R., Grau-Rivera, O., Gelpi, E., ... Ossenkoppele, R. (2018). Prevalence of amyloid- β pathology in distinct variants of primary progressive aphasia. *Annals of Neurology*, 84, 729–740. <https://doi.org/10.1002/ana.25333>
- Bertrand, A., Wen, J., Rinaldi, D., Houot, M., Sayah, S., Camuzat, A., Fournier, C., Fontanella, S., Routier, A., Couratier, P., Pasquier, F., Habert, M.-O., Hannequin, D., Martinaud, O., Caroppo, P., Levy, R., Dubois, B., Brice, A., Durrleman, S., Colliot, O., & Le Ber, I., for the Predict to Prevent Frontotemporal Lobar Degeneration and Amyotrophic Lateral Sclerosis (PREV-DEMALS) Study Group. (2018). Early cognitive, structural, and microstructural changes in presymptomatic C9orf72 carriers younger than 40 years. *JAMA Neurol*, 75, 236. <https://doi.org/10.1001/jamaneurol.2017.4266>

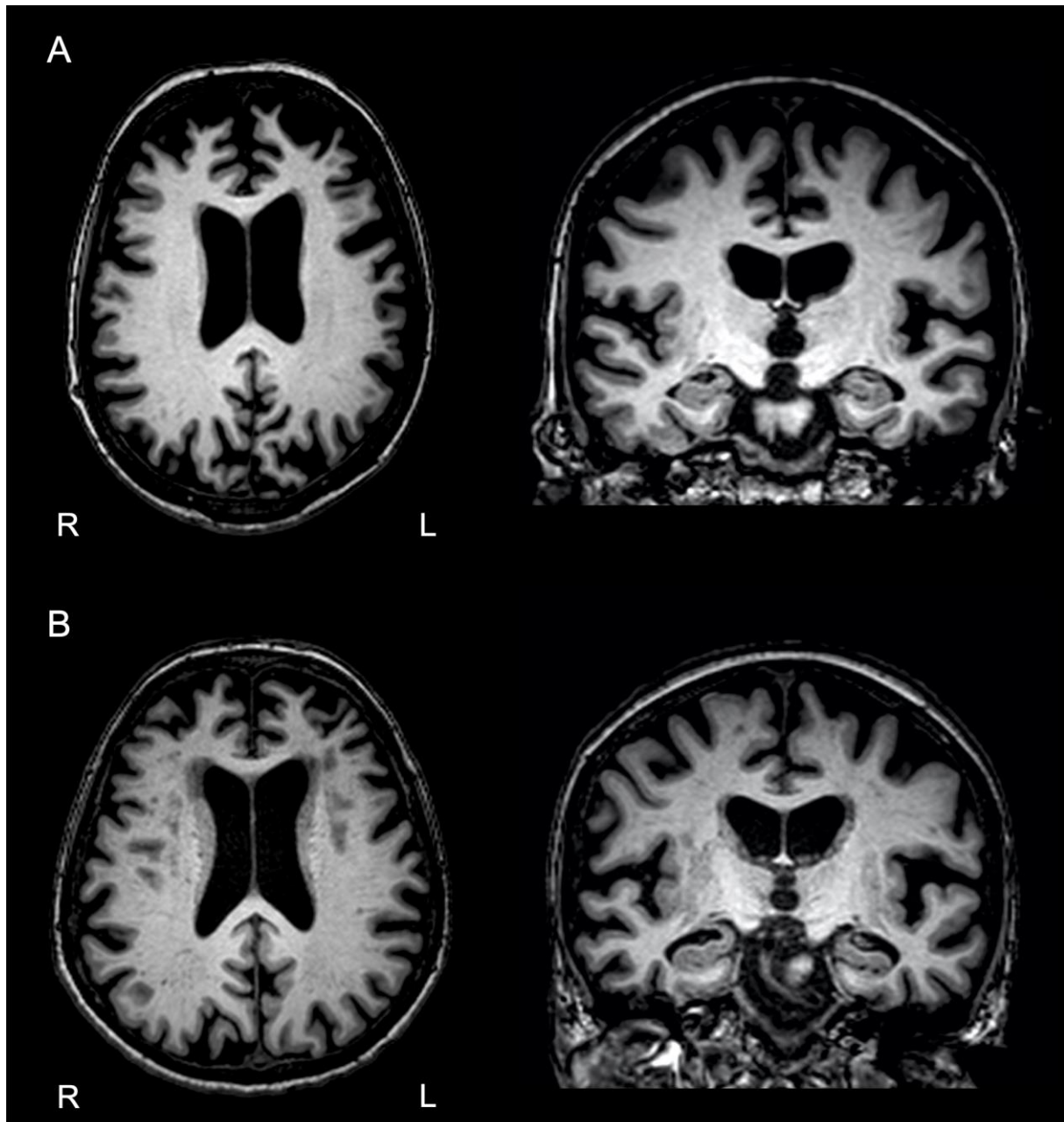
- Bocchetta, M., Gordon, E., Cardoso, M. J., Modat, M., Ourselin, S., Warren, J. D., & Rohrer, J. D. (2018). Thalamic atrophy in frontotemporal dementia — not just a C9orf72 problem. *NeuroImage: Clinical*, 18, 675–681. <https://doi.org/10.1016/j.nicl.2018.02.019>
- Bocchetta, M., Todd, E. G., Peakman, G., Cash, D. M., Convery, R. S., Russell, L. L., Thomas, D. L., Iglesias, J. E., van Swieten, J. C., Jiskoot, L. C., Seelaar, H., Borroni, B., Galimberti, D., Sanchez-Valle, R., Laforce, R., Jr., Moreno, F., Synofzik, M., Graff, C., Masellis, M., ... Zulaica, M. (2021). Differential early subcortical involvement in genetic FTD within the GENFI cohort. *NeuroImage Clin*, 30(102646). <https://doi.org/10.1016/j.nicl.2021.102646>
- Boeve, B. F., Boylan, K. B., Graff-Radford, N. R., DeJesus-Hernandez, M., Knopman, D. S., Pedraza, O., Vemuri, P., Jones, D., Lowe, V., Murray, M. E., Dickson, D. W., Josephs, K. A., Rush, B. K., Machulda, M. M., Fields, J. A., Ferman, T. J., Baker, M., Rutherford, N. J., Adamson, J., ... Rademakers, R. (2012). Characterization of frontotemporal dementia and/or amyotrophic lateral sclerosis associated with the GGGGCC repeat expansion in C9ORF72. *Brain: a Journal of Neurology*, 135, 765–783. <https://doi.org/10.1093/brain/aws004>
- Botha, H., Duffy, J. R., Whitwell, J. L., Strand, E. A., Machulda, M. M., Schwarz, C. G., Reid, R. I., Spychalla, A. J., Senjem, M. L., Jones, D. T., Lowe, V., Jack, C. R., & Josephs, K. A. (2015). Classification and clinicoradiologic features of primary progressive aphasia (PPA) and apraxia of speech. *Cortex; a Journal Devoted To the Study of the Nervous System and Behavior*, 69, 220–236. <https://doi.org/10.1016/j.cortex.2015.05.013>
- Cajanus, A., Katisko, K., Kontkanen, A., Ja, O., Haapasalo, A., Herukka, S.-K., Vanninen, R., Solje, E., Hall, A., & Remes, A. M. (2020). Serum neurofilament light chain in FTL D: Association with C9orf72, clinical phenotype, and prognosis. *Ann Clin Transl Neurol*, 7, 903–910. <https://doi.org/10.1002/acn3.51041>
- Caroppo, P., Camuzat, A., De Septenville, A., Couratier, P., Lacomblez, L., Auriacombe, S., Flabeau, O., Jornéa, L., Blanc, F., Sellal, F., Cretin, B., Meininger, V., Fleury, M.-C., Couarch, P., Dubois, B., Brice, A., & Le Ber, I. (2015). Semantic and nonfluent aphasic variants, secondarily associated with amyotrophic lateral sclerosis, are predominant frontotemporal lobar degeneration phenotypes in TBK1 carriers. *Alzheimer's & Dementia: Diagnosis, Assessment & Disease Monitoring*, 1, 481–486. <https://doi.org/10.1016/j.dadm.2015.10.002>
- Caroppo, P., Camuzat, A., Guillot-Noel, L., Thomas-Antérion, C., Couratier, P., Wong, T. H., Teichmann, M., Golfier, V., Auriacombe, S., Belliard, S., Laurent, B., Lattante, S., Millecamps, S., Clot, F., Dubois, B., van Swieten, J. C., Brice, A., & Le Ber, I. (2016). Defining the spectrum of frontotemporal dementias associated with TARDBP mutations. *Nature Genetics*, 2, e80. <https://doi.org/10.1212/NXG.0000000000000080>
- Caso, F., Agosta, F., Magnani, G., Cardamone, R., Borghesani, V., Miller, Z., Riva, N., La Joie, R., Coppola, G., Grinberg, L. T., Seeley, W. W., Miller, B. L., Gorno-Tempini, M. L., & Filippi, M. (2020). Temporal variant of frontotemporal dementia in C9orf72 repeat expansion carriers: Two case studies. *Brain Imaging and Behavior*, 14, 336–345. <https://doi.org/10.1007/s11682-019-00253-x>
- Cerami, C., Marcone, A., Galimberti, D., Zamboni, M., Fenoglio, C., Serpente, M., Scarpini, E., & Cappa, S. F. (2013). Novel evidence of phenotypical variability in the hexanucleotide repeat expansion in chromosome 9. *J Alzheimers Dis*, 35, 455–462. <https://doi.org/10.3233/JAD-122302>
- Cordella, C., Quimby, M., Touroutoglou, A., Brickhouse, M., Dickerson, B. C., & Green, J. R. (2019). Quantification of motor speech impairment and its anatomic basis in primary progressive aphasia. *Neurology*, 92, e1992–e2004. <https://doi.org/10.1212/WNL.0000000000007367>
- Costa, B., Manzoni, C., Bernal-Quiros, M., Kia, D. A., Aguilar, M., Alvarez, I., Alvarez, V., Andreassen, O., Anfossi, M., Bagnoli, S., Benussi, L., Bernardi, L., Binetti, G., Blackburn, D., Boada, M., Borroni, B., Bowns, L., Bråthen, G., Bruni, A. C., & ... Ferrari, R., for the International FTD-Genetics Consortium. (2020). C9orf72, age at onset, and ancestry help discriminate behavioral from language variants in FTL D cohorts. *Neurology*, 95, e3288–e3302. <https://doi.org/10.1212/WNL.0000000000010914>
- Deloche, G., & Hannequin, D. (1997). *DO 80: Epreuve de dénomination orale d'image*. Paris: ECPA (Editions du Centre de Psychologie Appliquée).
- Flanagan, E. P., Baker, M. C., Perkerson, R. B., Duffy, J. R., Strand, E. A., Whitwell, J. L., Machulda, M. M., Rademakers, R., & Josephs, K. A. (2015). Dominant frontotemporal dementia mutations in 140 cases of primary progressive aphasia and speech apraxia. *Dementia and Geriatric Cognitive Disorders*, 39, 281–286. <https://doi.org/10.1159/000375299>
- Fletcher, P. D., Downey, L. E., Golden, H. L., Clark, C. N., Slattery, C. F., Paterson, R. W., Rohrer, J. D., Schott, J. M., Rossor, M. N., & Warren, J. D. (2015a). Pain and temperature processing in dementia: A clinical and neuroanatomical analysis. *Brain: a Journal of Neurology*, 138, 3360–3372. <https://doi.org/10.1093/brain/awv276>
- Fletcher, P. D., Downey, L. E., Golden, H. L., Clark, C. N., Slattery, C. F., Paterson, R. W., Schott, J. M., Rohrer, J. D., Rossor, M. N., & Warren, J. D. (2015b). Auditory hedonic phenotypes in dementia: A behavioural and neuroanatomical analysis. *Cortex; a Journal Devoted To the Study of the Nervous System and Behavior*, 67, 95–105. <https://doi.org/10.1016/j.cortex.2015.03.021>
- Galimberti, D., Fenoglio, C., Serpente, M., Villa, C., Bonsi, R., Arighi, A., Fumagalli, G. G., Del Bo, R., Bruni, A. C., Anfossi, M., Clodomiro, A., Cupidi, C., Nacmias, B., Sorbi, S., Piaceri, I., Bagnoli, S., Bessi, V., Marcone, A., Cerami, C., ... Scarpini, E. (2013). Autosomal dominant frontotemporal lobar degeneration due to the C9ORF72 hexanucleotide repeat expansion: Late-onset psychotic clinical presentation. *Biological Psychiatry*, 74, 384–391. <https://doi.org/10.1016/j.biopsych.2013.01.031>
- Gelpi, E., van der Zee, J., Turon Estrada, A., Van Broeckhoven, C., & Sanchez-Valle, R. (2014). TARDBP mutation p.Ile383Val associated with semantic dementia and complex proteinopathy. *Neuropathology and Applied Neurobiology*, 40, 225–230. <https://doi.org/10.1111/nan.12063>
- Gil-Navarro, S., Lladó, A., Rami, L., Castellví, M., Bosch, B., Bargallo, N., Lomeña, F., Reñé, R., Montagut, N., Antonell, A., Molinuevo, J. L., & Sánchez-Valle, R. (2013). Neuroimaging and biochemical markers in the three variants of primary progressive aphasia. *Dementia and Geriatric Cognitive Disorders*, 35, 106–117. <https://doi.org/10.1159/000346289>
- Godefroy, O., & Grefex. (2008). *Fonctions exécutives et pathologies neurologiques et psychiatriques. Evaluation en pratique clinique*. Marseille: Solal.
- González-Sánchez, M., Puertas-Martín, V., Esteban-Pérez, J., García-Redondo, A., Borrego-Hernández, D., Méndez-Guerrero, A., Llamas-Velasco, S., Herrero-San Martín, A., Cordero-Vázquez, P., Herrero-Manso, M. C., Pérez-Martínez, D. A., & Villarejo-Galende, A. (2018). TARDBP mutation associated with semantic variant primary progressive aphasia, case report and review of the literature. *Neurocase*, 24, 301–305. <https://doi.org/10.1080/13554794.2019.1581225>
- Gorno-Tempini, M. L., Hillis, A. E., Weintraub, S., Kertesz, A., Mendez, M., Cappa, S. F., Ogar, J. M., Rohrer, J. D., Black, S., Boeve, B. F., Manes, F., Dronkers, N. F., Vandenberghe, R., Rascovsky, K., Patterson, K., Miller, B. L., Knopman, D. S., Hodges, J. R., Mesulam, M. M., & Grossman, M. (2011).

- Classification of primary progressive aphasia and its variants. *Neurology*, 76, 1006–1014. <https://doi.org/10.1212/WNL.0b013e31821103e6>
- Haapanen, M., Katisko, K., Hänninen, T., Krüger, J., Hartikainen, P., Haapasalo, A., Remes, A. M., & Solje, E. (2020). C9orf72 repeat expansion does not affect the phenotype in primary progressive aphasia. *J Alzheimers Dis*, 78, 919–925. <https://doi.org/10.3233/JAD-200795>
- Hardy, C. J. D., Buckley, A. H., Downey, L. E., Lehmann, M., Zimmerman, V. C., Varley, R. A., Crutch, S. J., Rohrer, J. D., Warrington, E. K., & Warren, J. D. (2016). The language profile of behavioral variant frontotemporal dementia. *J Alzheimers Dis*, 50, 359–371. <https://doi.org/10.3233/JAD-150806>
- Henz, S., Ackl, N., Knels, C., Rominger, A., Flatz, W., Teipel, S., Huppertz, H., Roeber, S., Neumann, M., & Danek, A. (2015). A pair of siblings with a rare R5H-mutation in exon 1 of the MAPT-gene. *Fortschr Neurol Psychiatr*, 83, 397–401. <https://doi.org/10.1055/s-0035-1553236>
- Hirsch-Reinshagen, V., Alfaify, O. A., Hsiung, G.-Y. R., Pottier, C., Baker, M., Perkerson, R. B., Rademakers, R., Briemberg, H., Foti, D. J., & Mackenzie, I. R. (2019). Clinicopathologic correlations in a family with a TBK1 mutation presenting as primary progressive aphasia and primary lateral sclerosis. *Amyotrophic Lateral Sclerosis & Frontotemporal Degeneration*, 20, 568–575. <https://doi.org/10.1080/21678421.2019.1632347>
- Howard, D., & Patterson, K. (1992). *The pyramids and palm trees test: A test of semantic access from words and pictures*. Bury St Edmunds: Thames Valley Test Company.
- Hsiung, G.-Y. R., DeJesus-Hernandez, M., Feldman, H. H., Sengdy, P., Bouchard-Kerr, P., Dwosh, E., Butler, R., Leung, B., Fok, A., Rutherford, N. J., Baker, M., Rademakers, R., & Mackenzie, I. R. A. (2012). Clinical and pathological features of familial frontotemporal dementia caused by C9ORF72 mutation on chromosome 9p. *Brain: a Journal of Neurology*, 135, 709–722. <https://doi.org/10.1093/brain/awr354>
- Irwin, D. J., McMillan, C. T., Brettschneider, J., Libon, D. J., Powers, J., Rascovsky, K., Toledo, J. B., Boller, A., Bekisz, J., Chandrasekaran, K., Wood, E. M., Shaw, L. M., Woo, J. H., Cook, P. A., Wolk, D. A., Arnold, S. E., Van Deerlin, V. M., McCluskey, L. F., Elman, L., ... Grossman, M. (2013). Cognitive decline and reduced survival in C9orf72 expansion frontotemporal degeneration and amyotrophic lateral sclerosis. *Neurologia I Neurochirurgia Polska*, 84, 163–169. <https://doi.org/10.1136/jnnp-2012-303507>
- Ivanova, M. V., & Hallowell, B. (2013). A tutorial on aphasia test development in any language: Key substantive and psychometric considerations. *Aphasiology*, 27, 891–920. <https://doi.org/10.1080/02687038.2013.805728>
- Josephs, K. A., Duffy, J. R., Strand, E. A., Machulda, M. M., Vemuri, P., Senjem, M. L., Perkerson, R. B., Baker, M. C., Lowe, V., Jack, C. R., Rademakers, R., & Whitwell, J. L. (2014). Progranulin-associated PiB-negative logopenic primary progressive aphasia. *Journal of Neurology*, 261, 604–614. <https://doi.org/10.1007/s00415-014-7243-9>
- Kaivorinne, A.-L., Bode, M. K., Paavola, L., Tuominen, H., Kallio, M., Renton, A. E., Traynor, B. J., Moilanen, V., & Remes, A. M. (2013). Clinical characteristics of C9ORF72-linked frontotemporal lobar degeneration. *Dement Geriatr Cogn Disord Extra*, 3, 251–262. <https://doi.org/10.1159/000351859>
- Khan, B. K., Yokoyama, J. S., Takada, L. T., Sha, S. J., Rutherford, N. J., Fong, J. C., Karydas, A. M., Wu, T., Ketelle, R. S., Baker, M. C., Hernandez, M.-D., Coppola, G., Geschwind, D. H., Rademakers, R., Lee, S. E., Rosen, H. J., Rabinovici, G. D., Seeley, W. W., Rankin, K. P., Boxer, A. L., & Miller, B. L. (2012). Atypical, slowly progressive behavioural variant frontotemporal dementia associated with C9ORF72 hexanucleotide expansion. *Neurologia I Neurochirurgia Polska*, 83, 358–364. <https://doi.org/10.1136/jnnp-2011-301883>
- Le Ber, I., Camuzat, A., Hannequin, D., Pasquier, F., Guedj, E., Rovelet-Lecrux, A., Hahn-Barma, V., van der Zee, J., Clot, F., Bakchine, S., Puel, M., Ghanim, M., Lacomblez, L., Mikol, J., Deramecourt, V., Lejeune, P., de la Sayette, V., Belliard, S., Vercelletto, M., ... Brice, A. (2008). Phenotype variability in progranulin mutation carriers: A clinical, neuropsychological, imaging and genetic study. *Brain: a Journal of Neurology*, 131, 732–746. <https://doi.org/10.1093/brain/awn012>
- Le Ber, Guedj, E., Verpillat, P., Volteau, M., Thomas-Anterion, C., Decousus, M., Hannequin, D., Vera, P., Lacomblez, L., Camuzat, A., Didic, M., Puel, M., Lotterie, J.-A., Golfier, V., Bernard, A.-M., Vercelletto, M., Magne, C., Sellal, F., Namer, I., ... Dubois, B. (2006). Demographic, neurological and behavioural characteristics and brain perfusion SPECT in frontal variant of frontotemporal dementia. *Brain: a Journal of Neurology*, 129, 3051–3065. <https://doi.org/10.1093/brain/awl288>
- Le Ber, Guillot-Noel, L., Hannequin, D., Lacomblez, L., Golfier, V., Puel, M., Martinaud, O., Deramecourt, V., Rivaud-Pechoux, S., Millecamps, S., Vercelletto, M., Couratier, P., Sellal, F., Pasquier, F., Salachas, F., Thomas-Anterion, C., Didic, M., Pariente, J., Seilhean, D., ... Brice, A., & The French research network on FTL/FTLD-ALS. (2013). C9ORF72 repeat expansions in the frontotemporal dementias spectrum of diseases: A flow-chart for genetic testing. *Jcls: Journal of the Society of Laparoendoscopic Surgeons*, 34, 485–499. <https://doi.org/10.3233/JAD-121456>
- Le Blanc, G., Jetté Pomerleau, V., McCarthy, J., Borroni, B., van Swieten, J., Galimberti, D., Sanchez-Valle, R., LaForce, R., Moreno, F., Synofzik, M., Graff, C., Masellis, M., Tartaglia, M. C., Rowe, J. B., Vandenberghe, R., Finger, E., Tagliavini, F., Mendonça, A., Santana, I., ... Ducharme, S., & the Genetic Frontotemporal Dementia Initiative (GENFI). (2020). Faster cortical thinning and surface area loss in presymptomatic and symptomatic C9orf72 repeat expansion adult carriers. *Annals of Neurology*, 88, 113–122. <https://doi.org/10.1002/ana.25748>
- Lee, S. E., Sias, A. C., Mandelli, M. L., Brown, J. A., Brown, A. B., Khazenzon, A. M., Vidovszky, A. A., Zanto, T. P., Karydas, A. M., Pribadi, M., Dokuru, D., Coppola, G., Geschwind, D. H., Rademakers, R., Gorno-Tempini, M. L., Rosen, H. J., Miller, B. L., & Seeley, W. W. (2017). Network degeneration and dysfunction in presymptomatic C9ORF72 expansion carriers. *Neuroimage Clin*, 14, 286–297. <https://doi.org/10.1016/j.nicl.2016.12.006>
- Macoir, J., Légaré, A., & Lavoie, M. (2021). Contribution of the cognitive approach to language assessment to the differential diagnosis of primary progressive aphasia. *Brain Sciences*, 11, 815. <https://doi.org/10.3390/brainsci11060815>
- Mahoney, C. J., Beck, J., Rohrer, J. D., Lashley, T., Mok, K., Shakespeare, T., Yeatman, T., Warrington, E. K., Schott, J. M., Fox, N. C., Rossor, M. N., Hardy, J., Collinge, J., Revesz, T., Mead, S., & Warren, J. D. (2012). Frontotemporal dementia with the C9ORF72 hexanucleotide repeat expansion: Clinical, neuroanatomical and neuropathological features. *Brain: a Journal of Neurology*, 135, 736–750. <https://doi.org/10.1093/brain/awr361>
- Majounie, E., Renton, A. E., Mok, K., Dopper, E. G., Waite, A., Rollinson, S., Chiò, A., Restagno, G., Nicolaou, N., Simon-Sanchez, J., van Swieten, J. C., Abramzon, Y., Johnson, J. O., Sendtner, M., Pamphlett, R., Orrell, R. W., Mead, S., Sidle, K. C., Houlden, H., ... Traynor, B. J. (2012). Frequency of the C9orf72 hexanucleotide repeat expansion in patients with amyotrophic lateral sclerosis and frontotemporal dementia: A cross-sectional study. *Lancet Neurology*, 11, 323–330. [https://doi.org/10.1016/S1474-4422\(12\)70043-1](https://doi.org/10.1016/S1474-4422(12)70043-1)
- Mazaux, J., & Orgogozo, J. (1982). *Hdae (BDAE): Echelle d'évaluation de l'aphasie*. Paris: ECPA (Editions du Centre de Psychologie Appliquée).

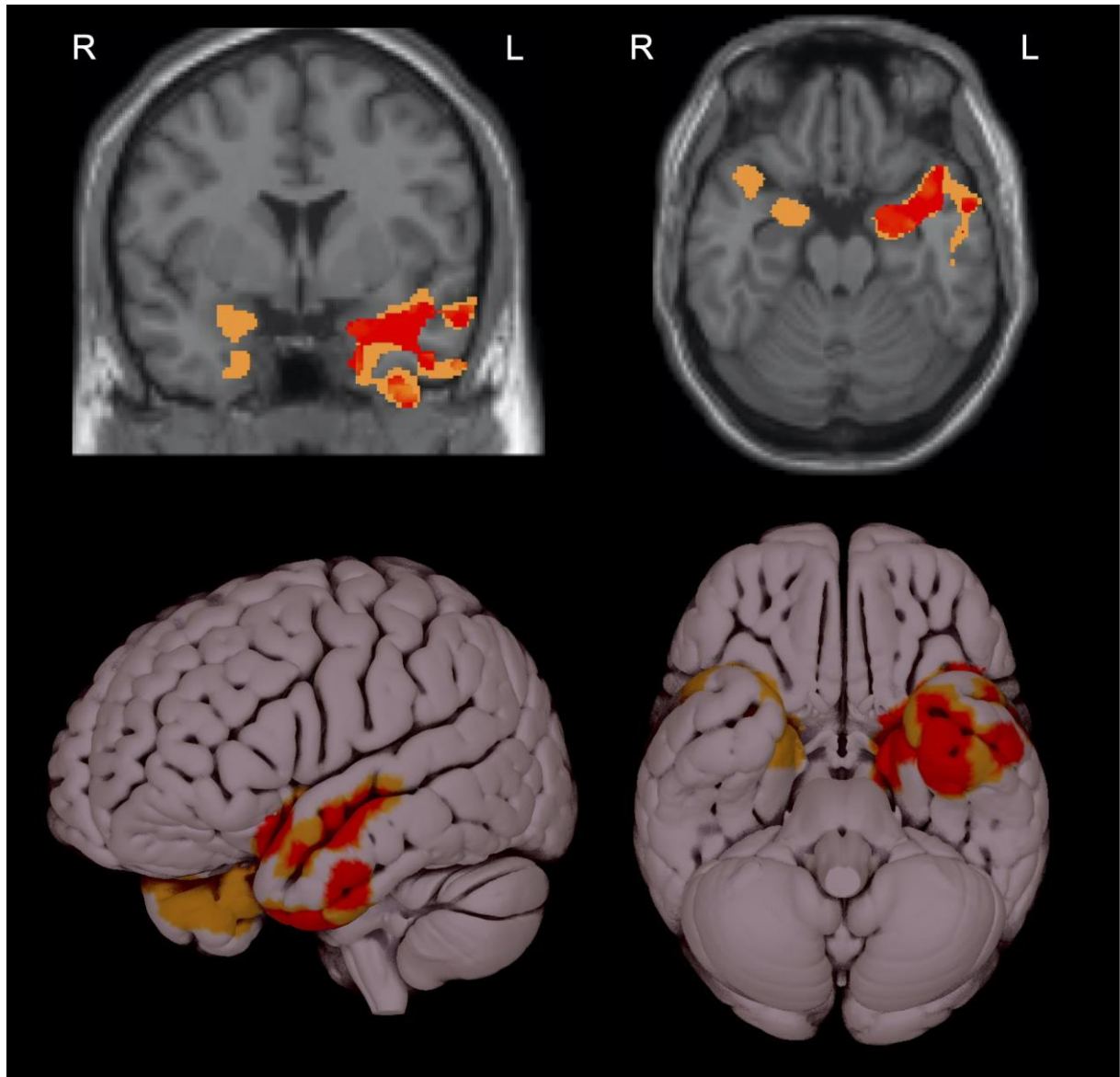
- Merck, C., Charnallet, A., Auriacombe, S., Belliard, S., Hahn-Barma, V., Kremin, H., Lemesle, B., Mahieux, F., Moreaud, O., Palisson, D. P., Roussel, M., Sellal, F., & Siegwart, H. (2011). La batterie d'évaluation des connaissances sémantiques du GRECO (BECS-GRECO) : Validation et données normatives. *Revue de neuropsychologie*, 3, 235. <https://doi.org/10.3917/rne.034.0235>
- Mol, M. O., Nijmeijer, S. W. R., van Rooij, J. G. J., van Spaendonk, R. M. L., Pijnenburg, Y. A. L., van der Lee, S. J., van Minkelen, R., Donker Kaat, L., Rozemuller, A. J. M., Janse van Mantgem, M. R., van Rheeën, W., van Es, M. A., Veldink, J. H., Hennekam, F. A. M., Vernooij, M., van Swieten, J. C., Cohn-Hokke, P. E., Seelaar, H., & Dopper, E. G. P. (2021). Distinctive pattern of temporal atrophy in patients with frontotemporal dementia and the I383V variant in TARDBP. *Neurologia I Neurochirurgia Polska*. <https://doi.org/10.1136/jnnp-2020-325150>. jnnp-2020-325150.
- Moore, K. M., Nicholas, J., Grossman, M., McMillan, C. T., Irwin, D. J., Massimo, L., Van Deerlin, V. M., Warren, J. D., Fox, N. C., Rossor, M. N., Mead, S., Bocchetta, M., Boeve, B. F., Knopman, D. S., Graff-Radford, N. R., Forsberg, L. K., Rademakers, R., Wszolek, Z. K., van Swieten, J. C., ... Geschwind, D. (2020). Age at symptom onset and death and disease duration in genetic frontotemporal dementia: An international retrospective cohort study. *Lancet Neurology*, 19, 145–156. [https://doi.org/10.1016/S1474-4422\(19\)30394-1](https://doi.org/10.1016/S1474-4422(19)30394-1)
- Nespolous, J., Lecours, A., Lafond, D., Lemay, M., Puel, M., Joannette, Y., Cot, F., & Rascol, A. (1992). *Protocole Montréal-Toulouse d'examen linguistique de l'aphasie MT-86 (Ortho Edition)*. Isbergues.
- Öjjerstedt, L., Chiang, H.-H., Björkström, J., Forsell, C., Lilius, L., Lindström, A.-K., Thonberg, H., & Graff, C. (2019). Confirmation of high frequency of C9orf72 mutations in patients with frontotemporal dementia from Sweden. *Neurobiology of Aging*, 84, 241.e21–241.e25. <https://doi.org/10.1016/j.neurobiolaging.2019.03.009>
- Pickering-Brown, S. M., Richardson, A. M. T., Snowden, J. S., McDonagh, A. M., Burns, A., Braude, W., Baker, M., Liu, W.-K., Yen, S.-H., Hardy, J., Hutton, M., Davies, Y., Allsop, D., Craufurd, D., Neary, D., & Mann, D. M. A. (2002). Inherited frontotemporal dementia in nine British families associated with intronic mutations in the tau gene. *Brain: a Journal of Neurology*, 125, 732–751. <https://doi.org/10.1093/brain/awf069>
- Pottier, C., Bieniek, K. F., Finch, N., van de Vorst, M., Baker, M., Perkersen, R., Brown, P., Ravenscroft, T., van Blitterswijk, M., Nicholson, A. M., DeTure, M., Knopman, D. S., Josephs, K. A., Parisi, J. E., Petersen, R. C., Boylan, K. B., Boeve, B. F., Graff-Radford, N. R., Veltman, J. A., ... Rademakers, R. (2015). Whole-genome sequencing reveals important role for TBK1 and OPTN mutations in frontotemporal lobar degeneration without motor neuron disease. *Acta Neuropathologica*, 130, 77–92. <https://doi.org/10.1007/s00401-015-1436-x>
- Ramos, E. M., Dokuru, D. R., Van Berlo, V., Wojta, K., Wang, Q., Huang, A. Y., Deverasetty, S., Qin, Y., van Blitterswijk, M., Jackson, J., Appleby, B., Bordelon, Y., Brannelly, P., Brushaber, D. E., Dickerson, B., Dickinson, S., Domoto-Reilly, K., Faber, K., Fields, J., ... on behalf of the ARTFL/LEFFTDS consortium, Coppola, G. (2020). Genetic screening of a large series of North American sporadic and familial frontotemporal dementia cases. *Alzheimer's & Dementia: the Journal of the Alzheimer's Association*, 16, 118–130. <https://doi.org/10.1002/alz.12011>
- Ramos, E. M., Dokuru, D. R., Van Berlo, V., Wojta, K., Wang, Q., Huang, A. Y., Miller, Z. A., Karydas, A. M., Bigio, E. H., Rogalski, E., Weintraub, S., Rader, B., Miller, B. L., Gorno-Tempini, M. L., Mesulam, M.-M., & Coppola, G. (2019). Genetic screen in a large series of patients with primary progressive aphasia. *Alzheimer's & Dementia*, 15, 553–560. <https://doi.org/10.1016/j.jalz.2018.10.009>
- Rohrer, J. D., Crutch, S. J., Warrington, E. K., & Warren, J. D. (2010). Progranulin-associated primary progressive aphasia: A distinct phenotype? *Neuropsychologia*, 48, 288–297. <https://doi.org/10.1016/j.neuropsychologia.2009.09.017>
- Rohrer, J. D., Nicholas, J. M., Cash, D. M., van Swieten, J., Dopper, E., Jiskoot, L., van Minkelen, R., Rombouts, S. A., Cardoso, M. J., Clegg, S., Espak, M., Mead, S., Thomas, D. L., De Vita, E., Masellis, M., Black, S. E., Freedman, M., Keren, R., MacIntosh, B. J., ... Rossor, M. N. (2015). Presymptomatic cognitive and neuroanatomical changes in genetic frontotemporal dementia in the genetic frontotemporal dementia initiative (GENFI) study: A cross-sectional analysis. *Lancet Neurology*, 14, 253–262. [https://doi.org/10.1016/S1474-4422\(14\)70324-2](https://doi.org/10.1016/S1474-4422(14)70324-2)
- Rohrer, J. D., Ridgway, G. R., Crutch, S. J., Hailstone, J., Goll, J. C., Clarkson, M. J., Mead, S., Beck, J., Mummery, C., Ourselin, S., Warrington, E. K., Rossor, M. N., & Warren, J. D. (2010). Progressive logopenic/phonological aphasia: Erosion of the language network. *Neuroimage*, 49, 984–993. <https://doi.org/10.1016/j.neuroimage.2009.08.002>
- Rohrer, J. D., Woollacott, I. O. C., Dick, K. M., Brotherhood, E., Gordon, E., Fellows, A., Toombs, J., Drueyeh, R., Cardoso, M. J., Ourselin, S., Nicholas, J. M., Norgren, N., Mead, S., Andreasson, U., Blennow, K., Schott, J. M., Fox, N. C., Warren, J. D., & Zetterberg, H. (2016). Serum neurofilament light chain protein is a measure of disease intensity in frontotemporal dementia. *Neurology*, 87, 1329–1336. <https://doi.org/10.1212/WNL.0000000000003154>
- Rolls, E. T., Huang, C.-C., Lin, C.-P., Feng, J., & Joliot, M. (2020). Automated anatomical labelling atlas 3. *Neuroimage*, 206, 116189. <https://doi.org/10.1016/j.neuroimage.2019.116189>
- Roncero, C., Popov, A., & Chertkow, H. (2021). Multiple high dose tDCS sessions produces perceived improvement and stabilisation in a person with a MAPT gene, presenting clinically as semantic variant primary progressive aphasia with severe cognitive impairment. *Brain Stimulation*, 14, 358–360. <https://doi.org/10.1016/j.brs.2021.02.001>
- van Rooij, J., Mol, M. O., Melhem, S., van der Wal, P., Arp, P., Paron, F., Donker Kaat, L., Seelaar, H., Netherlands Brain Bank, Miedema, S. S. M., Oshima, T., Eggen, B. J. L., Uitterlinden, A., van Meurs, J., van Kesteren, R. E., Smit, A. B., Buratti, E., & van Swieten, J. C. (2020). Somatic TARDBP variants as a cause of semantic dementia. *Brain: a Journal of Neurology*, 143, 3827–3841. <https://doi.org/10.1093/brain/awaa317>
- Saracino, D., Ferrieux, S., Noguès-Lassaille, M., Houot, M., Funkiewiez, A., Sellami, L., Deramecourt, V., Pasquier, F., Couratier, P., Pariente, J., Géraudie, A., Epelbaum, S., Wallon, D., Hannequin, D., Martinaud, O., Clot, F., Camuzat, A., Bottani, S., Rinaldi, D., ... Le Ber, I., & French research network on FTD/FTD-ALS. (2021). Primary progressive aphasia associated with GRN mutations: New insights into the non-amyloid logopenic variant. *Neurology*. <https://doi.org/10.1212/WNL.0000000000012174>. <https://doi.org/10.1212/WNL.0000000000012174>
- Shewan, C. M., & Kertesz, A. (1980). Reliability and validity characteristics of the western aphasia battery (WAB). *J Speech Hear Disord*, 45, 308–324. <https://doi.org/10.1044/jshd.4503.308>
- Simón-Sánchez, J., Dopper, E. G. P., Cohn-Hokke, P. E., Hukema, R. K., Nicolaou, N., Seelaar, H., de Graaf, J. R. A., de Koning, I., van Schoor, N. M., Deeg, D. J. H., Smits, M., Raaphorst, J., van den Berg, L. H., Schelhaas, H. J., De Die-Smulders, C. E. M., Majoor-Krakauer, D., Rozemuller, A. J. M., Willemsen, R., Pijnenburg, Y. A. L., Heutink, P., & van Swieten, J. C. (2012). The clinical and pathological phenotype of C9ORF72 hexanucleotide repeat expansions. *Brain: a Journal*

- of *Neurology*, 135, 723–735. <https://doi.org/10.1093/brain/awr353>
- Snowden, Adams, J., Harris, J., Thompson, J. C., Rollinson, S., Richardson, A., Jones, M., Neary, D., Mann, D. M., & Pickering-Brown, S. (2015). Distinct clinical and pathological phenotypes in frontotemporal dementia associated with MAPT, PGRN and C9orf72 mutations. *Amyotrophic Lateral Sclerosis & Frontotemporal Degeneration*, 16, 497–505. <https://doi.org/10.3109/21678421.2015.1074700>
- Snowden, J. S., Rollinson, S., Thompson, J. C., Harris, J. M., Stopford, C. L., Richardson, A. M. T., Jones, M., Gerhard, A., Davidson, Y. S., Robinson, A., Gibbons, L., Hu, Q., DuPlessis, D., Neary, D., Mann, D. M. A., & Pickering-Brown, S. M. (2012). Distinct clinical and pathological characteristics of frontotemporal dementia associated with C9ORF72 mutations. *Brain: a Journal of Neurology*, 135, 693–708. <https://doi.org/10.1093/brain/awr355>
- Suhonen, N.-M., Kaivorinne, A.-L., Moilanen, V., Bode, M., Takalo, R., Hänninen, T., & Remes, A. M. (2015). Slowly progressive frontotemporal lobar degeneration caused by the C9ORF72 repeat expansion: A 20-year follow-up study. *Neurocase*, 21, 85–89. <https://doi.org/10.1080/13554794.2013.873057>
- Swift, I. J., Bocchetta, M., Benotmane, H., Woollacott, I. O. C., Shafei, R., & Rohrer, J. D. (2021). Variable clinical phenotype in TBK1 mutations: Case report of a novel mutation causing primary progressive aphasia and review of the literature. *Neurobiology of Aging*, 99, 100. <https://doi.org/10.1016/j.neurobiolaging.2020.08.014>. e9-100.e15.
- Teichmann, M., Kas, A., Boutet, C., Ferrieux, S., Nogues, M., Samri, D., Rogan, C., Dormont, D., Dubois, B., & Migliaccio, R. (2013). Deciphering logopenic primary progressive aphasia: A clinical, imaging and biomarker investigation. *Brain: a Journal of Neurology*, 136, 3474–3488. <https://doi.org/10.1093/brain/awt266>
- Tetzloff, K. A., Duffy, J. R., Clark, H. M., Utianski, R. L., Strand, E. A., Machulda, M. M., Botha, H., Martin, P. R., Schwarz, C. G., Senjem, M. L., Reid, R. I., Gunter, J. L., Spychalla, A. J., Knopman, D. S., Petersen, R. C., Jack, C. R., Lowe, V. J., Josephs, K. A., & Whitwell, J. L. (2019). Progressive agrammatic aphasia without apraxia of speech as a distinct syndrome. *Brain: a Journal of Neurology*, 142, 2466–2482. <https://doi.org/10.1093/brain/awz157>
- Van Langenhove, T., van der Zee, J., Gijssels, I., Engelborghs, S., Vandenbergh, R., Vandenbulcke, M., De Bleecker, J., Sieben, A., Versijpt, J., Ivanoiu, A., Deryck, O., Willems, C., Dillen, L., Philtjens, S., Maes, G., Bäumer, V., Van Den Broeck, M., Mattheijssens, M., Peeters, K., ... Van Broeckhoven, C. (2013). Distinct clinical characteristics of C9orf72 expansion carriers compared with GRN, MAPT, and nonmutation carriers in a flanders-Belgian FTLT cohort. *JAMA Neurol*, 70, 365. <https://doi.org/10.1001/2013.jamaneurol.181>
- Van Mossevelde, S., van der Zee, J., Gijssels, I., Engelborghs, S., Sieben, A., Van Langenhove, T., De Bleecker, J., Baets, J., Vandenbulcke, M., Van Laere, K., Ceysens, S., Van den Broeck, M., Peeters, K., Mattheijssens, M., Cras, P., Vandenbergh, R., De Jonghe, P., Martin, J.-J., De Deyn, P. P., Cruts, M., & Van Broeckhoven, C. (2016). Clinical features of TBK1 carriers compared with C9orf72, GRN and non-mutation carriers in a Belgian cohort. *Brain: a Journal of Neurology*, 139, 452–467. <https://doi.org/10.1093/brain/awv358>
- Whitwell, J. L., Duffy, J. R., Strand, E. A., Machulda, M. M., Senjem, M. L., Schwarz, C. G., Reid, R., Baker, M. C., Perkerson, R. B., Lowe, V. J., Rademakers, R., Jack, C. R., & Josephs, K. A. (2015). Clinical and neuroimaging biomarkers of amyloid-negative logopenic primary progressive aphasia. *Brain and Language*, 142, 45–53. <https://doi.org/10.1016/j.bandl.2015.01.009>
- van der Zee, J., Gijssels, I., Van Mossevelde, S., Perrone, F., Dillen, L., Heeman, B., Bäumer, V., Engelborghs, S., De Bleecker, J., Baets, J., Gelpi, E., Rojas-García, R., Clarimón, J., Lleó, A., Diehl-Schmid, J., Alexopoulos, P., Perneczky, R., Synofzik, M., Just, J., ... Testi, S. (2017). TBK1 mutation spectrum in an extended European patient cohort with frontotemporal dementia and amyotrophic lateral sclerosis. *Hum Mutat*, 38, 297–309. <https://doi.org/10.1002/humu.23161>

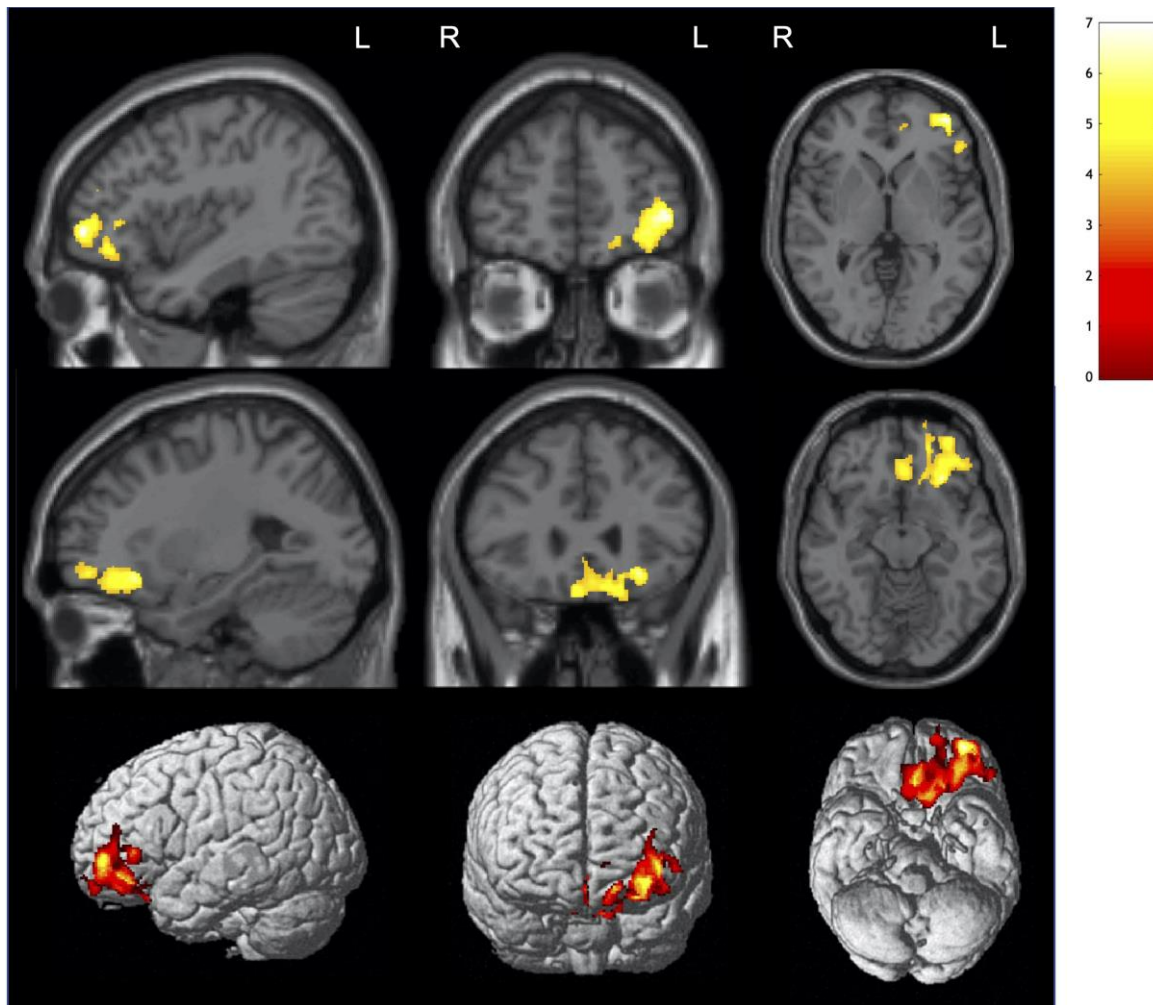
SUPPLEMENTARY MATERIALS



Supplementary Figure 1. MRI studies in Case 1 (A) and Case 2 (B) from the Finnish cohort. These patients, both presenting an unclassifiable primary progressive aphasia phenotype, displayed asymmetric, left-predominant frontotemporal atrophy prevailing in the perisylvian regions.



Supplementary Figure 2. Sequential VBM analyses in patient #01. VBM studies analyzed the pattern of atrophy of patient #01 at age 43 and its progression at age 46, compared to controls. Voxels which were already significantly atrophic at age 43 are represented in red, and those who became significant in the second study are represented in orange. VBM: voxel-based morphometry. For further details, see Supplementary Table 2.



Supplementary Figure 3. VBM analysis in nfvPPA-*C9orf72* patients compared to controls. A main cluster of atrophy is extended throughout the left inferior and middle frontal gyrus. NfvPPA-*C9orf72*: semantic variant of primary progressive aphasia associated with *C9orf72* expansion; VBM: voxel-based morphometry. For further details, see Supplementary Table 3.

Included papers	N=	References
1) Detailed clinical descriptions of PPA- <i>C9orf72</i> phenotypes	3	(Hsiung et al., 2012), (Snowden et al., 2012), (Cerami et al., 2013)
Excluded papers	N=	References
2) Insufficient clinical descriptions	26	(Boeve et al., 2012), (Mahoney et al., 2012), (Majounie et al., 2012), (Simón-Sánchez et al., 2012), (Galimberti et al., 2013), (Gil-Navarro et al., 2013), (Irwin et al., 2013), (Kaivorinne et al., 2013), (Le Ber et al., 2013), (Van Langenhove et al., 2013), (Benussi et al., 2014), (Flanagan et al., 2015), (Fletcher et al., 2015a), (Fletcher et al., 2015b), (Snowden et al., 2015), (Hardy et al., 2016), (Rohrer et al., 2016), (Van Mossevelde et al., 2016), (Bocchetta et al., 2018), (Öijerstedt et al., 2019), (Ramos et al., 2019), (Cajanus et al., 2020), (Costa et al., 2020), (Haapanen et al., 2020), (Moore et al., 2020), (Ramos et al., 2020)
3) Uncertain causative role of <i>C9orf72</i> expansion	2	(Mignarri et al., 2014), (Saint-Aubert et al., 2014)

Supplementary Table 1. Summary of included and excluded articles. PPA-*C9orf72*:
primary progressive aphasia associated with *C9orf72* expansion.

Cluster-level $p_{\text{FDR-corr}}$	k_E	Voxel-level $p_{\text{FDR-corr}}$	T	(Z)	MNI coordinates (x, y, z)			Region (AAL3.1)
					mm	mm	mm	
Patient #01 (svPPA-C9orf72) at age 43 vs controls								
<0.001	3485	0.601	5.42	3.85	-40	16	-22	Left superior temporal pole
Patient #01 (svPPA-C9orf72) at age 46 vs controls								
<0.001	6054	0.650	6.22	4.17	-40	16	-22	Left superior temporal pole
<0.001	6054	0.650	6.06	4.10	-58	-6	-14	Left middle temporal lobe
0.006	1537	0.650	6.12	4.13	42	15	-18	Right posterior orbital frontal gyrus
0.006	1537	0.728	4.73	3.54	28	18	-32	Right superior temporal pole

Supplementary Table 2. VBM analyses in one svPPA-C9orf72 patient at two different time points compared with controls. The analyses were performed using SPM12 adopting a false discovery rate correction at the cluster level of $p < 0.001$, and a threshold of $k_E = 3485$ (for age 43) and $k_E = 1537$ (for age 46). FDR: false discovery rate; K_E : extent coefficient; MNI: Montreal Neurological Institute; $p_{\text{FDR-corr}}$: false discovery rate-corrected p value; svPPA-C9orf72: semantic variant of primary progressive aphasia associated with C9orf72 expansion; T: result of T test; VBM: voxel-based morphometry; (Z): result of Z test.

Cluster-level $p_{\text{FDR-corr}}$	k_E	Voxel-level $p_{\text{FDR-corr}}$	T	(Z)	MNI coordinates (x, y, z)			Region (AAL3.1)
					mm	mm	mm	
nfvPPA-<i>C9orf72</i> patients vs controls								
<0.001	4872	0.678	6.31	4.20	-26	27	-12	Left inferior frontal gyrus – pars orbitalis
<0.001	4872	0.678	6.95	4.42	-39	52	0	Left middle frontal gyrus

Supplementary Table 3. VBM analyses in nfvPPA-*C9orf72* patients compared with controls. The analyses were performed using SPM12 adopting a false discovery rate correction at the cluster level of $p < 0.001$, and a threshold of $k_E = 4872$. FDR: false discovery rate; k_E : extent coefficient; MNI: Montreal Neurological Institute; nfvPPA-*C9orf72*: semantic variant of primary progressive aphasia associated with *C9orf72* expansion; $p_{\text{FDR-corr}}$: false discovery rate-corrected p value; T: result of T test; VBM: voxel-based morphometry; (Z): result of Z test.

SUPPLEMENTARY REFERENCES

- Benussi, L., Rossi, G., Glionna, M., Tonoli, E., Piccoli, E., Fostinelli, S., Paterlini, A., Flocco, R., Albani, D., Pantieri, R., Cereda, C., Forloni, G., Tagliavini, F., Binetti, G., Ghidoni, R., 2014. C9ORF72 Hexanucleotide Repeat Number in Frontotemporal Lobar Degeneration: A Genotype-Phenotype Correlation Study. *J Alzheimers Dis* 38, 799–808. <https://doi.org/10.3233/JAD-131028>
- Bocchetta, M., Gordon, E., Cardoso, M.J., Modat, M., Ourselin, S., Warren, J.D., Rohrer, J.D., 2018. Thalamic atrophy in frontotemporal dementia — Not just a C9orf72 problem. *NeuroImage: Clinical* 18, 675–681. <https://doi.org/10.1016/j.nicl.2018.02.019>
- Boeve, B.F., Boylan, K.B., Graff-Radford, N.R., DeJesus-Hernandez, M., Knopman, D.S., Pedraza, O., Vemuri, P., Jones, D., Lowe, V., Murray, M.E., Dickson, D.W., Josephs, K.A., Rush, B.K., Machulda, M.M., Fields, J.A., Ferman, T.J., Baker, M., Rutherford, N.J., Adamson, J., Wszolek, Z.K., Adeli, A., Savica, R., Boot, B., Kuntz, K.M., Gavriloa, R., Reeves, A., Whitwell, J., Kantarci, K., Jack, C.R., Parisi, J.E., Lucas, J.A., Petersen, R.C., Rademakers, R., 2012. Characterization of frontotemporal dementia and/or amyotrophic lateral sclerosis associated with the GGGGCC repeat expansion in C9ORF72. *Brain* 135, 765–783. <https://doi.org/10.1093/brain/aws004>
- Cajanus, A., Katisko, K., Kontkanen, A., Ja, O., Haapasalo, A., Herukka, S.-K., Vanninen, R., Solje, E., Hall, A., Remes, A.M., 2020. Serum neurofilament light chain in FTL D: association with C9orf72, clinical phenotype, and prognosis. *Ann Clin Transl Neurol* 7, 903–910. <https://doi.org/10.1002/acn3.51041>
- Cerami, C., Marcone, A., Galimberti, D., Zamboni, M., Fenoglio, C., Serpente, M., Scarpini, E., Cappa, S.F., 2013. Novel Evidence of Phenotypical Variability in the Hexanucleotide Repeat Expansion in Chromosome 9. *J Alzheimers Dis* 35, 455–462. <https://doi.org/10.3233/JAD-122302>
- Costa, B., Manzoni, C., Bernal-Quiros, M., Kia, D.A., Aguilar, M., Alvarez, I., Alvarez, V., Andreassen, O., Anfossi, M., Bagnoli, S., Benussi, L., Bernardi, L., Binetti, G., Blackburn, D., Boada, M., Borroni, B., Bowns, L., Bråthen, G., Bruni, A.C., Chiang, H.-H., Clarimon, J., Colville, S., Conidi, M.E., Cope, T.E., Cruchaga, C., Cupidi, C., Di Battista, M.E., Diehl-Schmid, J., Diez-Fairen, M., Dols-Icardo, O., Durante, E., Flisar, D., Frangipane, F., Galimberti, D., Gallo, M., Gallucci, M., Ghidoni, R., Graff, C., Grafman, J.H., Grossman, M., Hardy, J., Hernández, I., Holloway, G.J.T., Huey, E.D., Illán-Gala, I., Karydas, A., Khoshnood, B., Kramerberger, M.G., Kristiansen, M., Lewis, P.A., Lleó, A., Madhan, G.K., Maletta, R., Maver, A., Menendez-Gonzalez, M., Milan, G., Miller, B., Mol, M.O., Momeni, P., Moreno-Grau, S., Morris, C.M., Nacmias, B., Nilsson, C., Novelli, V., Öijerstedt, L., Padovani, A., Pal, S., Panchbhaya, Y., Pastor, P., Peterlin, B., Piaceri, I., Pickering-Brown, S., Pijnenburg, Y.A.L., Puca, A.A., Rainero, I., Rendina, A., Richardson, A.M.T., Rogaeva, E., Rogelj, B., Rollinson, S., Rossi, G., Rossmeier, C., Rowe, J.B., Rubino, E., Ruiz, A., Sanchez-Valle, R., Sando, S.B., Santillo, A.F., Saxon, J., Scarpini, E., Serpente, M., Smirne, N., Sorbi, S., Suh, E., Tagliavini, F., Thompson, J.C., Trojanowski, J.Q., Van Deerlin, V.M., Van der Zee, J., Van Broeckhoven, C., van Rooij, J., Van Swieten, J.C., Veronesi, A., Vitale, E., Waldö, M.L., Woodward, C., Yokoyama, J., Escott-Price, V., Polke, J.M., Ferrari, R.,

- for the International FTD-Genetics Consortium, 2020. C9orf72, age at onset, and ancestry help discriminate behavioral from language variants in FTLD cohorts. *Neurology* 95, e3288–e3302. <https://doi.org/10.1212/WNL.0000000000010914>
- Flanagan, E.P., Baker, M.C., Perkerson, R.B., Duffy, J.R., Strand, E.A., Whitwell, J.L., Machulda, M.M., Rademakers, R., Josephs, K.A., 2015. Dominant Frontotemporal Dementia Mutations in 140 Cases of Primary Progressive Aphasia and Speech Apraxia. *Dementia and Geriatric Cognitive Disorders* 39, 281–286. <https://doi.org/10.1159/000375299>
- Fletcher, P.D., Downey, L.E., Golden, H.L., Clark, C.N., Slattery, C.F., Paterson, R.W., Rohrer, J.D., Schott, J.M., Rossor, M.N., Warren, J.D., 2015a. Pain and temperature processing in dementia: a clinical and neuroanatomical analysis. *Brain* 138, 3360–3372. <https://doi.org/10.1093/brain/awv276>
- Fletcher, P.D., Downey, L.E., Golden, H.L., Clark, C.N., Slattery, C.F., Paterson, R.W., Schott, J.M., Rohrer, J.D., Rossor, M.N., Warren, J.D., 2015b. Auditory hedonic phenotypes in dementia: A behavioural and neuroanatomical analysis. *Cortex* 67, 95–105. <https://doi.org/10.1016/j.cortex.2015.03.021>
- Galimberti, D., Fenoglio, C., Serpente, M., Villa, C., Bonsi, R., Arighi, A., Fumagalli, G.G., Del Bo, R., Bruni, A.C., Anfossi, M., Clodomi, A., Cupidi, C., Nacmias, B., Sorbi, S., Piaceri, I., Bagnoli, S., Bessi, V., Marcone, A., Cerami, C., Cappa, S.F., Filippi, M., Agosta, F., Magnani, G., Comi, G., Franceschi, M., Rainero, I., Giordana, M.T., Rubino, E., Ferrero, P., Rogaeva, E., Xi, Z., Confaloni, A., Piscopo, P., Bruno, G., Talarico, G., Cagnin, A., Clerici, F., Dell’Osso, B., Comi, G.P., Altamura, A.C., Mariani, C., Scarpini, E., 2013. Autosomal Dominant Frontotemporal Lobar Degeneration Due to the C9ORF72 Hexanucleotide Repeat Expansion: Late-Onset Psychotic Clinical Presentation. *Biol Psychiatry* 74, 384–391. <https://doi.org/10.1016/j.biopsych.2013.01.031>
- Gil-Navarro, S., Lladó, A., Rami, L., Castellví, M., Bosch, B., Bargalló, N., Lomeña, F., Reñé, R., Montagut, N., Antonell, A., Molinuevo, J.L., Sánchez-Valle, R., 2013. Neuroimaging and Biochemical Markers in the Three Variants of Primary Progressive Aphasia. *Dementia and Geriatric Cognitive Disorders* 35, 106–117. <https://doi.org/10.1159/000346289>
- Haapanen, M., Katisko, K., Hänninen, T., Krüger, J., Hartikainen, P., Haapasalo, A., Remes, A.M., Solje, E., 2020. C9orf72 Repeat Expansion Does Not Affect the Phenotype in Primary Progressive Aphasia. *J Alzheimers Dis* 78, 919–925. <https://doi.org/10.3233/JAD-200795>
- Hardy, C.J.D., Buckley, A.H., Downey, L.E., Lehmann, M., Zimmerer, V.C., Varley, R.A., Crutch, S.J., Rohrer, J.D., Warrington, E.K., Warren, J.D., 2016. The Language Profile of Behavioral Variant Frontotemporal Dementia. *J Alzheimers Dis* 50, 359–371. <https://doi.org/10.3233/JAD-150806>
- Hsiung, G.-Y.R., DeJesus-Hernandez, M., Feldman, H.H., Sengdy, P., Bouchard-Kerr, P., Dwosh, E., Butler, R., Leung, B., Fok, A., Rutherford, N.J., Baker, M., Rademakers, R., Mackenzie, I.R.A., 2012. Clinical and pathological features of familial frontotemporal dementia caused by C9ORF72 mutation on chromosome 9p. *Brain* 135, 709–722. <https://doi.org/10.1093/brain/awr354>

- Irwin, D.J., McMillan, C.T., Brettschneider, J., Libon, D.J., Powers, J., Rascovsky, K., Toledo, J.B., Boller, A., Bekisz, J., Chandrasekaran, K., Wood, E.M., Shaw, L.M., Woo, J.H., Cook, P.A., Wolk, D.A., Arnold, S.E., Van Deerlin, V.M., McCluskey, L.F., Elman, L., Lee, V.M.-Y., Trojanowski, J.Q., Grossman, M., 2013. Cognitive decline and reduced survival in C9orf72 expansion frontotemporal degeneration and amyotrophic lateral sclerosis. *J Neurol Neurosurg Psychiatry* 84, 163–169. <https://doi.org/10.1136/jnnp-2012-303507>
- Kaivorinne, A.-L., Bode, M.K., Paavola, L., Tuominen, H., Kallio, M., Renton, A.E., Traynor, B.J., Moilanen, V., Remes, A.M., 2013. Clinical Characteristics of C9ORF72-Linked Frontotemporal Lobar Degeneration. *Dement Geriatr Cogn Disord Extra* 3, 251–262. <https://doi.org/10.1159/000351859>
- Le Ber, Guillot-Noel, L., Hannequin, D., Lacomblez, L., Golfier, V., Puel, M., Martinaud, O., Deramecourt, V., Rivaud-Pechoux, S., Millicamps, S., Vercelletto, M., Couratier, P., Sellal, F., Pasquier, F., Salachas, F., Thomas-Antérion, C., Didic, M., Pariente, J., Seilhean, D., Ruberg, M., Wargon, I., Blanc, F., Camu, W., Michel, B.-F., Berger, E., Sauvée, M., Thauvin-Robinet, C., Mondon, K., Tournier-Lasserre, E., Goizet, C., Fleury, M., Viennet, G., Verpillat, P., Meininger, V., Duyckaerts, C., Dubois, B., Brice, A., The French research network on FTL/FTLD-ALS, 2013. C9ORF72 Repeat Expansions in the Frontotemporal Dementias Spectrum of Diseases: A Flow-chart for Genetic Testing. *JAD* 34, 485–499. <https://doi.org/10.3233/JAD-121456>
- Mahoney, C.J., Beck, J., Rohrer, J.D., Lashley, T., Mok, K., Shakespeare, T., Yeatman, T., Warrington, E.K., Schott, J.M., Fox, N.C., Rossor, M.N., Hardy, J., Collinge, J., Revesz, T., Mead, S., Warren, J.D., 2012. Frontotemporal dementia with the C9ORF72 hexanucleotide repeat expansion: clinical, neuroanatomical and neuropathological features. *Brain* 135, 736–750. <https://doi.org/10.1093/brain/awr361>
- Majounie, E., Renton, A.E., Mok, K., Dopper, E.G., Waite, A., Rollinson, S., Chiò, A., Restagno, G., Nicolaou, N., Simon-Sanchez, J., van Swieten, J.C., Abramzon, Y., Johnson, J.O., Sendtner, M., Pamphlett, R., Orrell, R.W., Mead, S., Sidle, K.C., Houlden, H., Rohrer, J.D., Morrison, K.E., Pall, H., Talbot, K., Ansorge, O., Hernandez, D.G., Arepalli, S., Sabatelli, M., Mora, G., Corbo, M., Giannini, F., Calvo, A., Englund, E., Borghero, G., Floris, G.L., Remes, A.M., Laaksovirta, H., McCluskey, L., Trojanowski, J.Q., Van Deerlin, V.M., Schellenberg, G.D., Nalls, M.A., Drory, V.E., Lu, C.-S., Yeh, T.-H., Ishiura, H., Takahashi, Y., Tsuji, S., Le Ber, I., Brice, A., Drepper, C., Williams, N., Kirby, J., Shaw, P., Hardy, J., Tienari, P.J., Heutink, P., Morris, H.R., Pickering-Brown, S., Traynor, B.J., 2012. Frequency of the C9orf72 hexanucleotide repeat expansion in patients with amyotrophic lateral sclerosis and frontotemporal dementia: a cross-sectional study. *The Lancet Neurology* 11, 323–330. [https://doi.org/10.1016/S1474-4422\(12\)70043-1](https://doi.org/10.1016/S1474-4422(12)70043-1)
- Mignarri, A., Battistini, S., Tomai Pitinca, M.L., Monti, L., Burrioni, L., Ginanneschi, F., Ricci, C., Bavazzano, A., Federico, A., Restagno, G., Dotti, M.T., 2014. Double trouble? Progranulin mutation and C9ORF72 repeat expansion in a case of primary non-fluent aphasia. *J Neurol Sci* 341, 176–178. <https://doi.org/10.1016/j.jns.2014.03.030>
- Moore, K.M., Nicholas, J., Grossman, M., McMillan, C.T., Irwin, D.J., Massimo, L., Van Deerlin, V.M., Warren, J.D., Fox, N.C., Rossor, M.N., Mead, S., Bocchetta, M., Boeve, B.F.,

Knopman, D.S., Graff-Radford, N.R., Forsberg, L.K., Rademakers, R., Wszolek, Z.K., van Swieten, J.C., Jiskoot, L.C., Meeter, L.H., Dopfer, E.G., Papma, J.M., Snowden, J.S., Saxon, J., Jones, M., Pickering-Brown, S., Le Ber, I., Camuzat, A., Brice, A., Caroppo, P., Ghidoni, R., Pievani, M., Benussi, L., Binetti, G., Dickerson, B.C., Lucente, D., Krivensky, S., Graff, C., Öijerstedt, L., Fallström, M., Thonberg, H., Ghoshal, N., Morris, J.C., Borroni, B., Benussi, A., Padovani, A., Galimberti, D., Scarpini, E., Fumagalli, G.G., Mackenzie, I.R., Hsiung, G.-Y.R., Sengdy, P., Boxer, A.L., Rosen, H., Taylor, J.B., Synofzik, M., Wilke, C., Sulzer, P., Hodges, J.R., Halliday, G., Kwok, J., Sanchez-Valle, R., Lladó, A., Borrego-Ecija, S., Santana, I., Almeida, M.R., Tábuas-Pereira, M., Moreno, F., Barandiaran, M., Indakoetxea, B., Levin, J., Danek, A., Rowe, J.B., Cope, T.E., Otto, M., Anderl-Straub, S., de Mendonça, A., Maruta, C., Masellis, M., Black, S.E., Couratier, P., Lautrette, G., Huey, E.D., Sorbi, S., Nacmias, B., Laforce, R., Tremblay, M.-P.L., Vandenberghe, R., Damme, P.V., Rogalski, E.J., Weintraub, S., Gerhard, A., Onyike, C.U., Ducharme, S., Papageorgiou, S.G., Lyn, A.S., Brodtmann, A., Finger, E., Guerreiro, R., Bras, J., Rohrer, J.D., Heller, C., Convery, R.S., Woollacott, I.O., Shafei, R.M., Graff-Radford, J., Jones, D.T., Dheel, C.M., Savica, R., Lapid, M.I., Baker, M., Fields, J.A., Gavriloiva, R., Domoto-Reilly, K., Poos, J.M., Van der Ende, E.L., Panman, J.L., Donker Kaat, L., Seelaar, H., Richardson, A., Frisoni, G., Mega, A., Fostinelli, S., Chiang, H.-H., Alberici, A., Arighi, A., Fenoglio, C., Heuer, H., Miller, B., Karydas, A., Fong, J., João Leitão, M., Santiago, B., Duro, D., Ferreira, Carlos, Gabilondo, A., De Arriba, M., Tainta, M., Zulaica, M., Ferreira, Catarina, Semler, E., Ludolph, A., Landwehrmeyer, B., Volk, A.E., Miltenberger, G., Verdelho, A., Afonso, S., Tartaglia, M.C., Freedman, M., Rogaeva, E., Ferrari, C., Piaceri, I., Bessi, V., Lombardi, G., St-Onge, F., Doré, M.-C., Bruffaerts, R., Vandenbulcke, M., Van den Stock, J., Mesulam, M.M., Bigio, E., Koros, C., Papatriantafyllou, J., Kroupis, C., Stefanis, L., Shoesmith, C., Robertson, E., Coppola, G., Da Silva Ramos, E.M., Geschwind, D., 2020. Age at symptom onset and death and disease duration in genetic frontotemporal dementia: an international retrospective cohort study. *Lancet Neurol* 19, 145–156. [https://doi.org/10.1016/S1474-4422\(19\)30394-1](https://doi.org/10.1016/S1474-4422(19)30394-1)

Öijerstedt, L., Chiang, H.-H., Björkström, J., Forsell, C., Lilius, L., Lindström, A.-K., Thonberg, H., Graff, C., 2019. Confirmation of high frequency of C9orf72 mutations in patients with frontotemporal dementia from Sweden. *Neurobiol Aging* 84, 241.e21-241.e25. <https://doi.org/10.1016/j.neurobiolaging.2019.03.009>

Ramos, E.M., Dokuru, D.R., Van Berlo, V., Wojta, K., Wang, Q., Huang, A.Y., Deverasetty, S., Qin, Y., van Blitterswijk, M., Jackson, J., Appleby, B., Bordelon, Y., Brannelly, P., Brushaber, D.E., Dickerson, B., Dickinson, S., Domoto-Reilly, K., Faber, K., Fields, J., Fong, J., Foroud, T., Forsberg, L.K., Gavriloiva, R., Ghoshal, N., Goldman, J., Graff-Radford, J., Graff-Radford, N., Grant, I., Grossman, M., Heuer, H.W., Hsiung, G.-Y.R., Huey, E., Irwin, D., Kantarci, K., Karydas, A., Kaufer, D., Kerwin, D., Knopman, D., Kornak, J., Kramer, J.H., Kremers, W., Kukull, W., Litvan, I., Ljubenkova, P., Lungu, C., Mackenzie, I., Mendez, M.F., Miller, B.L., Onyike, C., Pantelyat, A., Pearlman, R., Petrucelli, L., Potter, M., Rankin, K.P., Rascovsky, K., Roberson, E.D., Rogalski, E., Shaw, L., Syrjanen, J., Tartaglia, M.C., Tatton, N., Taylor, J., Toga, A., Trojanowski, J.Q., Weintraub, S., Wong, B., Wszolek, Z., Rademakers, R., Boeve, B.F., Rosen, H.J., Boxer,

- A.L., on behalf of the ARTFL/LEFFTDS consortium, Coppola, G., 2020. Genetic screening of a large series of North American sporadic and familial frontotemporal dementia cases. *Alzheimer's Dement.* 16, 118–130. <https://doi.org/10.1002/alz.12011>
- Ramos, E.M., Dokuru, D.R., Van Berlo, V., Wojta, K., Wang, Q., Huang, A.Y., Miller, Z.A., Karydas, A.M., Bigio, E.H., Rogalski, E., Weintraub, S., Rader, B., Miller, B.L., Gorno-Tempini, M.L., Mesulam, M.-M., Coppola, G., 2019. Genetic screen in a large series of patients with primary progressive aphasia. *Alzheimer's & Dementia* 15, 553–560. <https://doi.org/10.1016/j.jalz.2018.10.009>
- Rohrer, J.D., Woollacott, I.O.C., Dick, K.M., Brotherhood, E., Gordon, E., Fellows, A., Toombs, J., Druyeh, R., Cardoso, M.J., Ourselin, S., Nicholas, J.M., Norgren, N., Mead, S., Andreasson, U., Blennow, K., Schott, J.M., Fox, N.C., Warren, J.D., Zetterberg, H., 2016. Serum neurofilament light chain protein is a measure of disease intensity in frontotemporal dementia. *Neurology* 87, 1329–1336. <https://doi.org/10.1212/WNL.0000000000003154>
- Saint-Aubert, L., Sagot, C., Wallon, D., Hannequin, D., Payoux, P., Nemmi, F., Bezy, C., Chauveau, N., Campion, D., Puel, M., Chollet, F., Pariente, J., 2014. A Case of Logopenic Primary Progressive Aphasia with C9ORF72 Expansion and Cortical Florbetapir Binding. *JAD* 42, 413–420. <https://doi.org/10.3233/JAD-140222>
- Simón-Sánchez, J., Dopper, E.G.P., Cohn-Hokke, P.E., Hukema, R.K., Nicolaou, N., Seelaar, H., de Graaf, J.R.A., de Koning, I., van Schoor, N.M., Deeg, D.J.H., Smits, M., Raaphorst, J., van den Berg, L.H., Schelhaas, H.J., De Die-Smulders, C.E.M., Majoor-Krakauer, D., Rozemuller, A.J.M., Willemsen, R., Pijnenburg, Y.A.L., Heutink, P., van Swieten, J.C., 2012. The clinical and pathological phenotype of C9ORF72 hexanucleotide repeat expansions. *Brain* 135, 723–735. <https://doi.org/10.1093/brain/awr353>
- Snowden, Adams, J., Harris, J., Thompson, J.C., Rollinson, S., Richardson, A., Jones, M., Neary, D., Mann, D.M., Pickering-Brown, S., 2015. Distinct clinical and pathological phenotypes in frontotemporal dementia associated with MAPT, PGRN and C9orf72 mutations. *Amyotroph Lateral Scler Frontotemporal Degener* 16, 497–505. <https://doi.org/10.3109/21678421.2015.1074700>
- Snowden, J.S., Rollinson, S., Thompson, J.C., Harris, J.M., Stopford, C.L., Richardson, A.M.T., Jones, M., Gerhard, A., Davidson, Y.S., Robinson, A., Gibbons, L., Hu, Q., DuPlessis, D., Neary, D., Mann, D.M.A., Pickering-Brown, S.M., 2012. Distinct clinical and pathological characteristics of frontotemporal dementia associated with C9ORF72 mutations. *Brain* 135, 693–708. <https://doi.org/10.1093/brain/awr355>
- Van Langenhove, T., van der Zee, J., Gijselinck, I., Engelborghs, S., Vandenberghe, R., Vandebulcke, M., De Bleecker, J., Sieben, A., Versijpt, J., Ivanoiu, A., Deryck, O., Willems, C., Dillen, L., Philtjens, S., Maes, G., Bäumer, V., Van Den Broeck, M., Mattheijssens, M., Peeters, K., Martin, J.-J., Michotte, A., Santens, P., De Jonghe, P., Cras, P., De Deyn, P.P., Cruts, M., Van Broeckhoven, C., 2013. Distinct Clinical Characteristics of C9orf72 Expansion Carriers Compared With GRN, MAPT, and Nonmutation Carriers in a Flanders-Belgian FTL D Cohort. *JAMA Neurol* 70, 365. <https://doi.org/10.1001/2013.jamaneurol.181>

Van Mossevelde, S., van der Zee, J., Gijssels, I., Engelborghs, S., Sieben, A., Van Langenhove, T., De Bleecker, J., Baets, J., Vandenbulcke, M., Van Laere, K., Ceysens, S., Van den Broeck, M., Peeters, K., Mattheijssens, M., Cras, P., Vandenberghe, R., De Jonghe, P., Martin, J.-J., De Deyn, P.P., Cruts, M., Van Broeckhoven, C., 2016. Clinical features of TBK1 carriers compared with C9orf72, GRN and non-mutation carriers in a Belgian cohort. *Brain* 139, 452–467. <https://doi.org/10.1093/brain/awv358>

4.2 Partie 2 – Trajectoires des neurofilaments plasmatiques dans les formes génétiques *GRN* et *C9orf72*, de la phase présymptomatique à la phase clinique (article 3)

Article 3. Saracino D, Dorgham K, Camuzat A, Rinaldi D, Rametti-Lacroux A, Houot M, Clot F, Martin-Hardy P, Jornea L, Azuar C, Migliaccio R, Pasquier F, Couratier P, Auriacombe S, Sauvée M, Boutoleau-Bretonnière C, Pariente J, Didic M, Hannequin D, Wallon D; French Research Network on FTD/FTD-ALS; PREV-DEMALS and Predict-PGRN study groups, Colliot O, Dubois B, Brice A, Levy R, Forlani S, Le Ber I. Plasma NfL levels and longitudinal change rates in *C9orf72* and *GRN*-associated diseases: from tailored references to clinical applications. *J. Neurol. Neurosurg. Psychiatry*. 2021; 92: 1278-1288.

Résumé

Comme nous l'avons déjà mentionné, la chaîne légère des neurofilaments (NfL) est un marqueur de dégénérescence neuronale dont les taux augmentent dans les biofluides dans un grand nombre d'affections neurologiques (Khalil et al., 2018 ; Gateani et al., 2019). Ce marqueur trouve un intérêt tout particulier dans les formes génétiques de DFT/SLA, car les taux augmentent dès la phase présymptomatique, environ 5 ans avant la phénoconversion (van der Ende et al., 2019). L'analyse des NfL est donc un paramètre à prendre en compte dans les recherches portant sur la phase présymptomatique des DLFT génétiques. Ce marqueur est également largement utilisé dans les essais thérapeutiques, en particulier pour stratifier les participants en fonction de leur proximité à la conversion clinique.

Les taux de NfL ont donc été analysés dans nos cohortes génétiques et présymptomatiques Predict-PGRN et PREV-DEMALS, afin d'être utilisés dans les études d'imagerie qui constituent la dernière partie de ma thèse. Les résultats des dosages de NfL dans ces cohortes ont néanmoins pu faire l'objet d'une publication indépendante ciblée sur ces résultats biologiques (article 3, Saracino et al., 2021c). Même si ce marqueur devient plus largement utilisé, l'interprétation des valeurs de NfL reste délicate en l'absence de valeurs de référence dans des populations contrôles, et d'une définition consensuelle des seuils pathologiques en fonction du phénotype et de la forme génétique. Dans ce travail, nous avons évalué les valeurs de référence dans des populations contrôles, comme prérequis indispensable à une interprétation de ce biomarqueur dans un contexte pathologique, et établi des seuils pathologiques dans nos populations génétiques.

Les NfL ont été dosés dans le plasma de 352 individus incluant des sujets contrôles (n=165), des individus porteurs de mutations des gènes *GRN* (n=86) et d'expansion *C9orf72* (n=101) au stade clinique (n=102) ou présymptomatique (n=85). Les 48 patients avec mutation *GRN* avaient tous un phénotype de DFTc ; les 54 patients porteurs d'une expansion *C9orf72* présentaient une DFTc (n = 27), une SLA (n = 16), ou un phénotype psychiatrique (n = 11). Une partie de la cohorte (n=175) a été évaluée longitudinalement avec des prélèvements répétés sur une durée moyenne de 3 ans. Brièvement, les dosages ont été effectués avec la technique de dosage ultrasensible SiMoA® en dupliquât, avec une médiane des coefficients de variation à 3,8 %. Les analyses en SiMoA® ont été faites en collaboration avec le Dr K. Dorgham (Centre d'Immunologie et Maladie Infectieuses, AP-HP Hôpital Pitié-Salpêtrière).

Dans une première étape, nous avons évalué les taux de NfL chez 165 contrôles âgés de 21 à 83 ans afin d'établir des valeurs normales dans des conditions physiologiques, et l'impact sur les taux de NfL de paramètres démographiques tels que le sexe et l'âge. La valeur médiane de NfL dans ce groupe était de 9,88 pg/mL (7,42–14,36) sans différence selon le sexe. L'âge a, par contre, un impact majeur, des valeurs plus élevées de NfL étant observées chez les individus plus âgés ($p=0,766$, $p<0,0001$). Globalement, l'augmentation des taux des NfL avec l'âge est quasiment linéaire jusqu'à 60 ans, et suivie par une hausse plus marquée au-delà de 60 ans. Nous avons ainsi déterminé des valeurs de référence par décennies, variant de ~5 pg/mL chez les plus jeunes (<30 ans) à ~18 pg/mL chez les plus âgés (≥ 70 ans). Le taux annualisé de changement chez les contrôles est d'environ +4 %, sans impact de l'âge au moment du prélèvement. Ce taux a été considéré comme le taux annualisé de référence dans des conditions physiologiques dans la suite de ce travail.

Les taux de NfL se sont révélés bien plus élevés chez les 102 patients étudiés, comparativement aux contrôles ($p<0,0001$), avec un effet majeur du génotype. En effet, les porteurs des mutations *GRN* avaient un taux médian environ deux fois plus élevé (86,21 pg/mL) que les patients *C9orf72* (37,16 pg/mL, $p=0,007$). Le taux annualisé de changement était aussi plus élevé chez les patients *GRN* (+29,3 % par an) que chez les porteurs d'expansions *C9orf72* (+24,7 % par an), ces deux taux étant globalement largement supérieurs à celui des contrôles (+4 % par an, $p<0,0001$). Les facteurs impactant les taux de NfL ont ensuite été étudiés dans le sous-groupe de patients *C9orf72*, qui est plus hétérogène au niveau clinique. De façon notable, le phénotype clinique a un impact majeur, les valeurs médianes de NfL étant plus élevées chez les patients SLA (71,76 pg/mL) que chez ceux ayant une DFTc (37,16 pg/mL, $p=0,008$). Ils étaient beaucoup plus faibles chez ceux ayant une présentation psychiatrique (15,3 pg/mL, $p=0,003$). De même, la progression de la maladie impacte le taux de NfL. Douze patients *C9orf72* avec une durée d'évolution remarquablement longue (DFTc de durée > à 14 ans, SLA >7 ans) avaient des taux bien plus bas (24,11 pg/mL, $p=0,005$), et une augmentation annuelle bien plus faible (+2,5 % par an) que les patients avec une durée de progression habituelle.

Sur la base des précédents résultats, obtenus chez les patients et les contrôles, nous avons calculé les seuils pathologiques optimaux en fonction du gène causal et de la classe d'âge considérée, selon la méthode visant à maximiser l'index de Youden. Ces valeurs seuil étaient remarquablement différentes selon les tranches d'âges. A titre d'exemple, les valeurs variaient

de façon croissante, de 9,74 à 26,74 pg/mL, entre les classes d'âges les plus jeunes et les plus âgées dans le groupe *C9orf72*.

Finalement, nous avons analysé les trajectoires des NfL chez 85 individus présymptomatiques porteurs de mutations *C9orf72* (n=48) et *GRN* (n=37). A l'échelle de groupe, les valeurs des NfL (8,08 pg/mL) et des taux annualisés de changement (+3,2 % par an) étaient comparables à celles des contrôles. Un effet gène-spécifique était néanmoins observé, les porteurs d'expansion du gène *C9orf72* présentant des valeurs discrètement plus élevées (8,48 pg/mL vs 7,70 pg/mL, $p=0.004$) et une corrélation plus forte avec l'âge que les porteurs de mutations du gène *GRN*. Quatre porteurs d'expansions *C9orf72*, présymptomatiques au moment de leur inclusion (CDR+NACC FTLD = 0), ont développé des signes cognitivo-comportementaux ou moteurs subtils durant leur suivi longitudinal, suggérant leur entrée dans le stade prodromal de la maladie selon la définition actuellement admise (CDR+NACC FTLD = 0,5). Les symptômes inauguraux observés chez ces individus incluaient variablement une discrète apathie, une jovialité excessive, une psychorigidité, des troubles attentionnels, des persévérations, un déficit de cognition sociale, des crampes et des fasciculations. L'un a développé une SLA, 6 ans après l'inclusion. De façon concordante, les NfL ont augmenté chez ces individus, avec des valeurs supérieures aux seuils pathologiques et au 95^{ème} percentile des classes d'âges correspondantes au cours du suivi, dans les 3 ans précédant les premières manifestations prodromales.

De façon plus intrigante, les taux de NfL de 4 autres sujets présymptomatiques (1 *C9orf72*, 3 *GRN*) ont augmenté pendant le suivi longitudinal, pouvant atteindre +15 % par an dans le cas de *C9orf72* et +62 % par an dans le cas de *GRN*, sans que leur suivi ne permette d'objectiver de signes de phénoconversion. Ces individus nécessitent un suivi plus prolongé.

Des résultats additionnels qui ne sont pas présentés dans la publication concernent l'association entre taux de NfL et lésions de la substance blanche, qui sont fréquentes chez les patients porteurs de mutation du gène *GRN*. Les patients *GRN* présentant une leucopathie de degré modéré ou sévère (selon la cotation visuelle utilisée par Ameur et collaborateurs, 2016), en l'absence de facteurs de risque vasculaire, avaient des valeurs de NfL plus élevées comparativement aux patients avec une leucopathie légère ou sans lésions ($p=0,013$). Par ailleurs, indépendamment de la cause génétique, les taux de NfL étaient positivement corrélés au score de la CDR+NACC FTLD ($\rho=0,52$, $p<0,0001$), reflétant ainsi la sévérité des symptômes de DFTc.

Globalement, cette étude propose des seuils pour l'analyse des taux de NfL en pratique clinique. Elle confirme que les taux plasmatiques de NfL sont significativement plus élevés chez les patients que chez les contrôles, mais révèle que ce profil d'augmentation des NfL dépend de façon importante du gène impliqué, nécessitant de considérer les seuils établis pour chaque population indépendamment, selon son génotype. Elle montre enfin que les NfL augmentent avec la progression dès le stade prodromal, des niveaux plus élevés prédisant un phénotype plus agressif. Fait intéressant, le taux plasmatique est moins élevé chez les patients présentant des phénotypes à progression lente et des formes psychiatriques de la maladie, ce qui suggère qu'ils pourraient être utilisés comme un prédicteur fiable de l'agressivité et de la rapidité de progression de la maladie. Ces analyses de NfL ont ensuite été utilisées dans les études d'imagerie de la dernière partie de ma thèse pour stratifier les participants et établir des corrélations avec les paramètres d'imagerie et cognitifs.





Pratiquement, dans le cadre de ce travail, j'ai réalisé le dosage SiMoA des NfL plasmatiques dans l'ensemble des échantillons (sous l'encadrement du Dr. Karim Dorgham), incluant les analyses biologiques, et j'ai également effectué les analyses statistiques des résultats.



OPEN ACCESS

Original research

Plasma NfL levels and longitudinal change rates in *C9orf72* and *GRN*-associated diseases: from tailored references to clinical applications

Dario Saracino ^{1,2,3}, Karim Dorgham ⁴, Agnès Camuzat,^{1,5} Daisy Rinaldi,^{1,2} Armelle Rametti-Lacroux,⁶ Marion Houot,^{1,2,7} Fabienne Clot,⁸ Philippe Martin-Hardy,¹ Ludmila Jornea,¹ Carole Azuar,^{1,2,6} Raffaella Migliaccio ^{1,2,6} Florence Pasquier,⁹ Philippe Couratier,¹⁰ Sophie Auriacombe,¹¹ Mathilde Sauvée,¹² Claire Boutoleau-Bretonnière,¹³ Jérémie Pariente,^{14,15} Mira Didic,^{16,17} Didier Hannequin,¹⁸ David Wallon,¹⁸ the French Research Network on FTD/FTD-ALS, the PREV-DEMALS and Predict-PGRN study groups, Olivier Colliot,^{1,3} Bruno Dubois,^{1,2,6} Alexis Brice,¹ Richard Levy,^{1,2,6} Sylvie Forlani,¹ Isabelle Le Ber ^{1,2,6}

► Additional supplemental material is published online only. To view, please visit the journal online (<http://dx.doi.org/10.1136/jnnp-2021-326914>).

For numbered affiliations see end of article.

Correspondence to

Dr Isabelle Le Ber, Sorbonne Université, Paris Brain Institute—Institut du Cerveau (ICM), Inserm U1127, CNRS UMR 7225; Reference Centre for Rare or Early Dementias, IM2A, Département de Neurologie, Hôpital Universitaire Pitié Salpêtrière, Paris, France; isabelle.leber@upmc.fr

Received 19 April 2021

Accepted 13 July 2021

Published Online First 4 August 2021



© Author(s) (or their employer(s)) 2021. Re-use permitted under CC BY-NC. No commercial re-use. See rights and permissions. Published by BMJ.

To cite: Saracino D, Dorgham K, Camuzat A, et al. *J Neurol Neurosurg Psychiatry* 2021;**92**:1278–1288.

ABSTRACT

Objective Neurofilament light chain (NfL) is a promising biomarker in genetic frontotemporal dementia (FTD) and amyotrophic lateral sclerosis (ALS). We evaluated plasma neurofilament light chain (pNfL) levels in controls, and their longitudinal trajectories in *C9orf72* and *GRN* cohorts from presymptomatic to clinical stages.

Methods We analysed pNfL using Single Molecule Array (SiMoA) in 668 samples (352 baseline and 316 follow-up) of *C9orf72* and *GRN* patients, presymptomatic carriers (PS) and controls aged between 21 and 83. They were longitudinally evaluated over a period of >2 years, during which four PS became prodromal/symptomatic. Associations between pNfL and clinical-genetic variables, and longitudinal NfL changes, were investigated using generalised and linear mixed-effects models. Optimal cut-offs were determined using the Youden Index.

Results pNfL levels increased with age in controls, from ~5 to ~18 pg/mL ($p < 0.0001$), progressing over time (mean annualised rate of change (ARC): +3.9%/year, $p < 0.0001$). Patients displayed higher levels and greater longitudinal progression (ARC: +26.7%, $p < 0.0001$), with gene-specific trajectories. *GRN* patients had higher levels than *C9orf72* (86.21 vs 39.49 pg/mL, $p = 0.014$), and greater progression rates (ARC: +29.3% vs +24.7%; $p = 0.016$). In *C9orf72* patients, levels were associated with the phenotype (ALS: 71.76 pg/mL, FTD: 37.16, psychiatric: 15.3; $p = 0.003$) and remarkably lower in slowly progressive patients (24.11, ARC: +2.5%; $p = 0.05$). Mean ARC was +3.2% in PS and +7.3% in prodromal carriers. We proposed gene-specific cut-offs differentiating patients from controls by decades.

Conclusions This study highlights the importance of gene-specific and age-specific references for clinical and therapeutic trials in genetic FTD/ALS. It supports the usefulness of repeating pNfL measurements and considering ARC as a prognostic marker of disease progression.

Trial registration numbers NCT02590276 and NCT04014673.

INTRODUCTION

GRN and *C9orf72* gene mutations are the main genetic causes of frontotemporal dementia (FTD) and/or amyotrophic lateral sclerosis (ALS).^{1–4} *GRN*-associated phenotypes are dominated by the behavioural variant of FTD (bvFTD),⁵ whereas *C9orf72* expansions lead to bvFTD, ALS or a combination of both.^{3,5} Less typical *C9orf72*-related phenotypes are characterised by psychiatric disorders⁶ or by a very slowly progressive disease in a subset of carriers.^{7,8}

A new era is emerging in genetic FTD and ALS, with the development of *GRN* and *C9orf72* disease-modifying therapies. The presymptomatic or prodromal phases appear to be the ideal time to deliver preventive treatments, before emergence of overt clinical manifestations. In this fast-moving context, detecting progression since disease beginning, at the biological level, up to full-blown clinical phase by means of circulating biomarkers is a major challenge. Neurofilament light chain (NfL) is highly expressed in axons. Accumulating evidence shows that elevated NfL reflects axonal damage and that levels in body fluids increase in proportion to neuronal loss in many neurodegenerative diseases.^{9–11} In particular, serum/plasma neurofilament light chain (pNfL) levels are elevated in FTD^{12–16} and ALS^{17–19} and appear to be efficient disease-tracking biomarkers at the clinical stage of genetic FTD/ALS. Additionally, relevant studies have demonstrated that NfL levels change in presymptomatic carriers (PS) of FTD/ALS-associated mutations, ~2–5 years before the fully symptomatic disease.^{14,20,21} They suggest NfL is also a valuable predictor of clinical proximity in PS, though an in-depth analysis by stratifying phenotypic converters according to their genotype would be useful.

Despite a growing number of studies, some fundamental prerequisites for translating pNfL dosage from research to therapeutic trials and clinical settings are missing. In particular, further insights in

Table 1 Descriptive data of the studied population

	Controls	Patients			PS		
		Overall	<i>C9orf72</i>	<i>GRN</i>	Overall	<i>C9orf72</i>	<i>GRN</i>
N	165	102	54	48	85	48	37
Gender (F/M)	96/69	46/56	24/30	22/26	52/33	30/18	22/15
Disease phenotype							
FTD (N)	–	75	27*	48	–	–	–
ALS (N)	–	6	6†	–	–	–	–
FTD/ALS (N)	–	10	10‡	–	–	–	–
Psychiatric (N)	–	11	11§	–	–	–	–
Age at disease onset (years)	–	58.0 (53.0–64.8)	58.0 (50.3–67.0)	58.0 (54.8–63.0)	–	–	–
Age at baseline sampling (years)	56.5 (45.9–66.3)	62.9 (58.3–69.6)	64.4 (58.0–71.5)	62.1 (58.5–66.2)	41.2 (34.2–47.5)	42.0 (34.4–47.4)	40.9 (33.2–48.8)
Age at baseline, range (years)	21.1–83.5	35.5–79.9	39.8–79.9	35.5–76.2	20.4–79.4	24.0–79.4	20.4–68.8
Disease duration at sampling (years)	–	3.5 (2.3–5.9)	5.1 (2.9–9.0)¶	2.9 (2.2–3.5)¶	–	–	–
pNfL at baseline (pg/mL)	9.88 (7.42–14.36)**	66.25 (33.74–98.86)**	39.49 (23.89–74.42)††	86.21 (58.17–118.13)††	8.08 (6.08–10.10)**	8.48 (6.71–11.52)	7.70 (5.59–9.23)
Mean (±SD) pNfL at baseline	12.08 (±7.57)**	81.21 (±75.99)**	64.52 (±63.92)††	99.99 (±84.40)††	8.79 (±4.02)**	9.76 (±4.69)‡‡	7.52 (±2.44)‡‡
Individuals with follow-up (N)	65	44	29	15	66	43	23
Mean (±SD) follow-up duration (years)	2.96 (±1.16)	2.00 (±1.21)	1.95 (±1.26)	2.08 (±1.13)	2.99 (±1.30)	2.83 (±0.65)	3.29 (±2.01)
Mean ARC (%)	+3.9**	+26.7**	+24.7††	+29.3††	+3.2**	+3.2	+3.3

Values are indicated as median and IQR, except where differently specified. There were no statistically significant differences between the groups, apart from specific occurrences, as follows.

*3/27 patients with FTD had SP course.

†2/6 patients with ALS had SP course.

‡3/10 patients with FTD/ALS had SP course.

§4/11 patients with psychiatric presentations had SP course.

¶Different disease duration at baseline between *C9orf72* and *GRN* patients ($p=0.0001$).

**Higher values in patients compared with controls ($p<0.0001$) and PS ($p<0.0001$).

††Higher values in *GRN* patients compared with *C9orf72* patients ($p<0.05$).

‡‡Higher values in *C9orf72* PS compared with *GRN* PS ($p<0.01$).

ALS, amyotrophic lateral sclerosis; ARC, annualised rate of change; F, female; FTD, frontotemporal dementia; M, male; pNfL, plasma neurofilament light chain; PS, presymptomatic carriers; SP, slowly progressive.

the variability of NfL levels in the healthy are needed to establish appropriate references and cut-offs to be used in neurodegenerative diseases. Determining NfL values and change rates in FTD/ALS patients according to their genotypes, as well as during the preclinical stage, is also a cornerstone for clinical studies.

Hereby, we first assessed physiological variations of pNfL and their longitudinal changes in healthy controls to propose reference values during life span across age classes. Next, we determined NfL levels in two cohorts of *GRN* and *C9orf72* carriers, separately, and delineated gene-specific trajectories from the presymptomatic to the clinical stage. Lastly, we established age-specific thresholds and annualised rates of change (ARCs) for each genetic form, in different disease stages, providing reference values to monitor clinical and therapeutic trials, and biological tools to predict disease progression.

MATERIALS AND METHODS

Participants

Our cohort consisted of 352 individuals whose characteristics are summarised in [table 1](#).

We evaluated the variability of pNfL levels under physiological conditions, in 165 neurologically healthy controls recruited in research context (online supplemental appendix A1). Sixty-five underwent longitudinal pNfL assessments over a mean interval of 3.0 ± 1.2 years (range: 1.3–6.3).

We also evaluated 101 *C9orf72* and 86 *GRN* mutation carriers. The *C9orf72* cohort consisted of 54 patients and 47 presymptomatic carriers (PS). The *GRN* cohort included 48 patients and 38 PS. They were recruited through a French research network

on FTD/ALS (Inserm RBM 02-59), and Predict to Prevent Frontotemporal Lobar Degeneration and Amyotrophic Lateral Sclerosis (PREV-DEMALS) and Natural History Characterization in Symptomatic and Asymptomatic Progranulin Gene Mutation Carriers (Predict-PGRN) national prospective studies.^{22–25} Individuals who had concurrent neurological conditions, other than FTD or ALS, were excluded.

In the patients' groups, the median age at disease onset (AAO) was 58.0 years, and disease duration at baseline sampling was 3.5 years (4.9 for *C9orf72* and 2.9 for *GRN* carriers). All *GRN* patients had FTD. Twenty-seven *C9orf72* patients presented with bvFTD; 16 had ALS; and 11 had a *C9orf72*-associated atypical psychosis as described in prior studies.^{6,26} Patients have been followed up until death ($n=37$), loss to follow-up ($n=58$) or are still followed up ($n=7$) in a research context or a clinical setting. Twelve *C9orf72* patients had slowly progressive course defined by disease duration of FTD of ≥ 14 years or ALS of ≥ 7 years, which corresponds to a significantly longer disease duration than commonly observed in each of the phenotypes.^{5,7,8,27,28} Forty-four patients underwent several plasma samplings over a mean of 2.0 ± 1.2 years (range: 0.7–6.1).

The 85 PS (47 *C9orf72* and 38 *GRN*) displayed no clinical symptoms and scored 0 on Clinical Dementia Rating (CDR) instrument plus National Alzheimer's Coordinating Center (NACC) frontotemporal lobar degeneration (FTLD) Behavior and Language Domains (CDR+NACC-FTLD). Sixty-six (43 *C9orf72*, 23 *GRN*) underwent longitudinal follow-up and plasma samplings in a research context over a mean of 3.0 ± 1.7 years (range: 0.9–7.8). Four *C9orf72* moved to prodromal stage during

the follow-up as they developed subtle cognitive/behavioural and/or motor symptoms, and reached CDR+NACC-FTLD=0.5 (online supplemental table A1).

For a subgroup analysis in *C9orf72* patients, we included five patients with primary psychiatric disorders whose demographic data were comparable to the former.

Laboratory methods

Plasma sampling

All blood samples were collected in EDTA tubes with similar standardised collection and handling procedures. They were centralised and processed using the same protocol at the DNA/cell bank Paris Brain Institute, Pitié-Salpêtrière Hospital (Biological Resource Centre, NF S96-900). Plasma was extracted at room temperature, after centrifugation at 2500 rpm during 10 min at +4°C. Aliquots were stored in polypropylene tubes at -80°C.

pNfL measurements

We analysed pNfL levels in 668 samples (352 baseline and 316 follow-up) of patients, PS and controls. Measurements were performed in the same facility, blinded to clinical-genetic status, using Single Molecule Array (SiMoA) technology in 13 runs, according to the manufacturer's instructions (Quanterix, USA). Calibrators were run in duplicate in each experiment, and fit with a four-parameter logistic regression, with $1/y^2$ weighting. Samples were assessed at a 1:4 dilution in duplicate. Those with a coefficient of variation (CV) of $\geq 15\%$ were reanalysed.¹² NfL concentration was interpolated from standard curves. The median intra-assay CV was 3.8% (range: 0%–14.7%). Three internal control plasmas of different NfL concentrations were analysed in each run, demonstrating satisfactory run-to-run variability (mean interassay CVs: 13%, 11% and 9%).

Statistical analyses

Statistical analyses were performed using the software R V.4.0.3 (Vienna, Austria). A two-sided p value of <0.05 was considered significant. As the investigated variables were not Gaussian, we reported them as median and first and third quartiles. We compared demographic and clinical variables between the groups using Fisher's exact test for categorical variables, and Mann-Whitney-Wilcoxon, Kruskal-Wallis and Dunn's test for continuous variables. Corrections for multiple comparisons were handled with the Benjamini-Hochberg method. Correlation analyses were performed with Spearman's test.

We used generalised linear models (GLMs) to investigate the association between pNfL levels, their log-transformed value, or their change rate (used as dependent variables) and genetic status, gender, phenotype, AAO, age at sampling, disease duration and baseline pNfL levels (independent variables). We used linear mixed-effects models (LMEMs) to test for significant differences in pNfL levels between time points.²⁹ We employed the following terms as fixed effects: time point (from T_0 up to T_3), baseline age, gender, genetic status and interaction terms between time point and age, and between time point and genetic status. Random intercept terms for participants were included in the model. For each of the models, type II Wald χ^2 tests were used. The normality of the residuals as well as heteroscedasticity were checked visually. Cook's distances and hat values were calculated to identify influential data. R-squared (R^2) was calculated to evaluate the goodness of fit in GLM, as well as conditional R^2 (R^2_c) in LMEM.

To perform unbiased longitudinal analyses in patients and in PS, we selected separate subgroups of controls based on demographic features and follow-up duration (online supplemental tables A2 and A3).

All groups were split to separately analyse 10-year discrete age classes, from <30 to ≥ 70 years. The sixth and seventh decades, in which FTLD and ALS usually begin, were further stratified into 5-year classes. We used receiver operating characteristic curve and Youden Index to establish the optimal cut-offs to separate patients from controls for each decade. We selected the method maximising Youden Index across all age classes and validated it through 10 000 bootstrap runs. In each age class, we analysed outliers with respect to pNfL baseline levels or progression rate (online supplemental appendix A2).

RESULTS

Demographic, clinical characteristics of participants and pNfL levels are shown in table 1. Variables were comparable between *C9orf72* and *GRN* patients, except for disease duration at baseline. Overall, disease duration was rather homogeneous among *GRN* patients and much more heterogeneous in the *C9orf72* group due to a handful of slowly progressive carriers.

pNfL levels in controls: effect of demographic factors, longitudinal changes and progression rate

At baseline, age at sampling in controls ranged between 21.1 and 83.5 years (table 1). Their pNfL levels (median: 9.88 pg/mL, IQR: 7.42–14.36) were comparable between men and women.

Median pNfL levels increased with age ($r=0.766$, $p<0.0001$) (figure 1 and table 2), ranging from 5.01 pg/mL in the youngest to 17.52 pg/mL in the oldest individuals. Therefore, we split the controls into discrete age-classes to define references for each decade. Levels significantly differed between age-classes ($p<0.0001$), and gradually increased up to 60 years, with steeper progression thereafter. Gender had no effect in any age-classes, and was not considered in further analyses. Two individuals had unexpectedly high values for their age-class. One had elevated levels at age 59 (59.61 pg/mL), but normal measures at 61 (10 pg/mL). In another 82-year-old participant pNfL levels were 50.97 pg/mL, without follow-up. The inclusion or exclusion of these two individuals in the subsequent analyses led to comparable results.

Next, we evaluated the rate of annual increase in 65 controls with longitudinal samplings, over a 3 year interval. Levels increased over time ($p<0.0001$, $R^2_c=0.93$) regardless of the age at baseline sampling, and at a comparable rate throughout all age-classes. The mean increase per year was 0.366 pg/mL, corresponding to mean ARC of +3.9%. This rate was constant across ages ($p=0.196$), and only moderately associated with baseline levels ($p=0.013$, $R^2=0.10$).

pNfL levels in *C9orf72* and *GRN* patients

Patients displayed higher levels than controls ($p<0.0001$) (figure 2). Unlike controls, values did not vary with the age at sampling in the overall patients' group ($p=0.261$, $R^2=0.07$), nor with gender ($p=0.274$). Nevertheless, age at sampling and pNfL levels were moderately correlated in *C9orf72* patients ($r=0.284$, $p=0.037$) (online supplemental figure A1).

The genotype had a major effect on pNfL: levels were much higher, and less variable, in *GRN* (86.21 pg/mL) than *C9orf72* patients (39.49 pg/mL, $p=0.014$). This finding was unbiased by disease duration, slightly shorter in *GRN* patients, or by clinical phenotypes. Indeed, the same effect was evidenced when

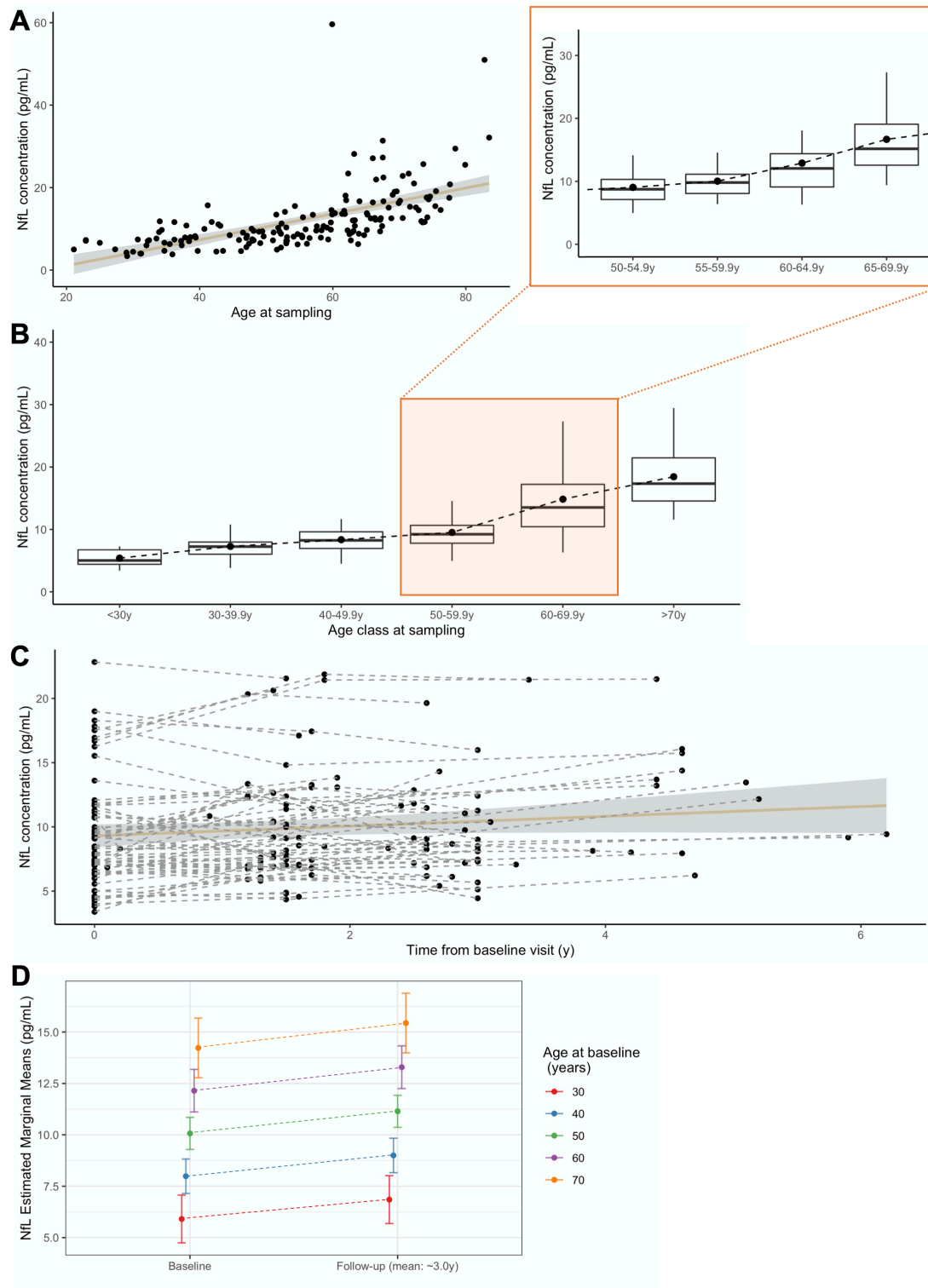


Figure 1 pNfL levels in controls. (A) Association of pNfL levels with the age at sampling ($r=0.766$, $p<0.0001$). (B) pNfL levels in discrete age classes, each representing a decade, with greater detail on the period in which disease usually manifests, 50.0–69.9 years, split in four classes (insert). Boxes represent median values and first and third quartiles; whiskers extend up to the lowest and highest values no further than 1.5*IQR; dots represent mean values. (C) Spaghetti plot representing pNfL variations across all the analysed time points, for controls undergoing longitudinal sampling, at the individual (dashed lines) and group (continuous line, CI 99%) levels. (D) Prediction of pNfL increase, from baseline to last follow-up, for a given age at baseline. CI: confidence interval; NFL, neurofilament light chain; pNfL, plasma neurofilament light chain.

analysing only *GRN* and *C9orf72* patients with FTD (excluding ALS and other phenotypes) (86.21 vs 37.16 pg/mL, $p=0.007$). The two genetic groups were then described separately.

C9orf72 patients

In *C9orf72* patients, a later AAO was associated with higher pNfL levels ($r=0.389$, $p=0.004$). Median values were lower in

Table 2 Plasma neurofilament light chain levels in each of the age classes in controls

Age class (years)	N	5th P	25th P	Median (50th percentile)	75th P	95th P
<30	8	3.69	4.40	5.01	6.73	7.22
30.0–39.9	25	4.00	6.02	7.26	7.99	11.47
40.0–49.9	24	4.61	6.96	8.25	9.62	11.60
50.0–54.4	19	5.42	7.10	8.73	10.29	14.26
55.0–59.9	20	7.20	8.11	9.84	11.86	16.80
60.0–64.9	21	7.38	9.09	12.03	14.36	23.41
65.0–69.9	23	9.82	12.55	15.14	19.05	27.27
≥70	25	11.70	14.57	17.52	22.83	31.60

Values are indicated in pg/mL.

early-onset patients (≤ 50 years: 22.49 pg/mL) than those with AAO between 50–65 years (48.57 pg/mL) and late-onset patients (≥ 65 : 68.00 pg/mL; $p=0.002$) (figure 2).

pNfL levels negatively correlated with disease duration ($r=-0.311$, $p=0.021$). Additionally, values were two-fold lower in patients with slowly progressive course (24.11 pg/mL, $n=12$) compared with the others (52.47 pg/mL, $n=42$; $p=0.05$). This was even more significant when comparing them with 11 patients deceased after a median disease duration of 6.0 years (77.24 pg/mL; $p=0.01$).

Values also varied according to the phenotype. ALS patients had higher levels (71.76 pg/mL) than those with isolated FTD (37.16 pg/mL, $p=0.008$). Interestingly, patients with psychiatric presentation had unexpectedly lower levels (15.3 pg/mL, IQR: 11.48–21.75) than those with FTD or ALS ($p=0.003$, age-corrected). Their values were not different from those of patients with primary psychiatric disorders with comparable demographic features (21.03 pg/mL, IQR: 10.75–25.09; $p=0.844$).

GRN patients

pNfL levels did not correlate with AAO and age at sampling in GRN patients (figure 2). There were no differences between patients with early, intermediate or late onset, and no association between pNfL values and disease duration at baseline, possibly because disease duration was much less variable in GRN than in *C9orf72* patients.

Longitudinal progression and ARC in patients

Forty-four patients (29 *C9orf72* and 15 GRN) underwent follow-up plasma samples over 2.0 ± 1.2 years (table 1). pNfL levels increased over time in both genotypes ($p<0.0001$), but more importantly in GRN than *C9orf72* patients ($p=0.016$, $R^2=0.85$) (figure 3A,B). Notably, one GRN patient had an extreme value (~ 600 pg/mL) in his terminal stage, few days before his death.

The mean yearly increase of 13.62 pg/mL in patients, corresponding to an ARC of +26.7%, was much higher than that in controls (+4%, $p<0.0001$). This rate was slightly higher in GRN (+29.3%) than in *C9orf72* carriers (+24.7%). Among *C9orf72* patients, the ARC differed according to the phenotypes, with a mean value of +37% in ALS, +21.7% in FTD and +8.3% in psychiatric presentations.

Importantly, pNfL progression over time was slower in *C9orf72* patients with slowly progressive disease ($p=0.05$, $R^2=0.95$) (figure 3C). Their ARC was only +2.5%, i.e. in the range of controls and markedly lower than that in *C9orf72* patients with a standard course ($p=0.05$).

Genotype-specific and age-specific cut-offs

We determined cut-off values discriminating patients from controls (table 3 and online supplemental figure A2). Given the distinct gene-specific trajectories, we separately determined thresholds for *C9orf72* and for GRN patients. A cut-off at 19.00 pg/mL yielded the best sensitivity/specificity trade-off to separate *C9orf72* patients from controls (83% and 88%, respectively). A higher threshold of 27.48 pg/mL differentiated GRN patients from controls, with 94% sensitivity and 97% specificity.

As age has a major impact on pNfL levels in controls and, to a lesser degree, in *C9orf72* carriers, we stratified the two genetic cohorts in distinct age classes. Cut-offs by decades are provided in table 3. They ranged from 9.74 pg/mL for *C9orf72* patients of <50 years to 27.71 for those ≥ 70 years, and from 15.70 pg/mL to 26.47 pg/mL for GRN patients of the same age classes. As expected, all cut-offs yielded better performances for GRN patients.

These cut-offs could be thereby employed in the analysis of pNfL in PS, suprathreshold values likely predicting proximity to disease onset.

pNfL levels in PS: two genes, two trajectories

The 85 PS included 48 *C9orf72* and 37 GRN carriers. Their median age at sampling (41.2 years) was similar in both genotypes (table 1). Their pNfL values were comparable to controls and remarkably lower than those of patients ($p<0.0001$) (figure 2A). *C9orf72* had higher pNfL levels (8.48 pg/mL) than GRN carriers (7.69 pg/mL, $p=0.004$). Levels in PS significantly increased with age at sampling ($p<0.0001$), as in controls. The correlation was much stronger in *C9orf72* ($r=0.651$, $p<0.0001$) than in GRN ($r=0.359$, $p=0.029$) (figure 4). To sum up, pNfLs were slightly higher and showed a more age-related trend during the presymptomatic phase of *C9orf72* disease.

Follow-up plasma samples over a mean interval of 3.0 ± 1.3 years were available for 43 *C9orf72* and 23 GRN PS (table 1). Levels slightly increased over time, with a mean ARC of +3.2% (+3.2% in *C9orf72* and +3.3% in GRN), similarly to controls ($p=0.703$).

High pNfL values in PS: prodromal stage or outliers?

Four *C9orf72* carriers, described in online supplemental table A1, moved to prodromal stage during their follow-up, one of whom developed ALS 6 years after baseline. All had elevated baseline and/or follow-up pNfL levels with respect to their age (as detailed in online supplemental appendix A2 and figure 4), and three had remarkable longitudinal trajectories, with higher ARC (mean: +7.3%, up +15% in one case) than in non-converting carriers (mean: +3.2%).

Notably, four other mutation carriers had elevated pNfL levels or ARC but did not develop any prodromal signs, at least during the time of their follow-up. One of them was a 44-year-old individual carrying the *C9orf72* expansion. He displayed higher pNfL levels than expected in his age class (17.17 pg/mL). The other three were GRN PS who had normal pNfL values at baseline but high ARC, from +19% to +62% during follow-up, though not reaching suprathreshold values for their age classes. So far, none displayed clinical changes at their last follow-up.

DISCUSSION

pNfLs hold promise to serve as efficient disease-tracking biomarkers in genetic forms of FTD and ALS.^{12 14 20 30} However, more insights about the dynamics of pNfL in the healthy and a thorough understanding of the differential progression in genetic

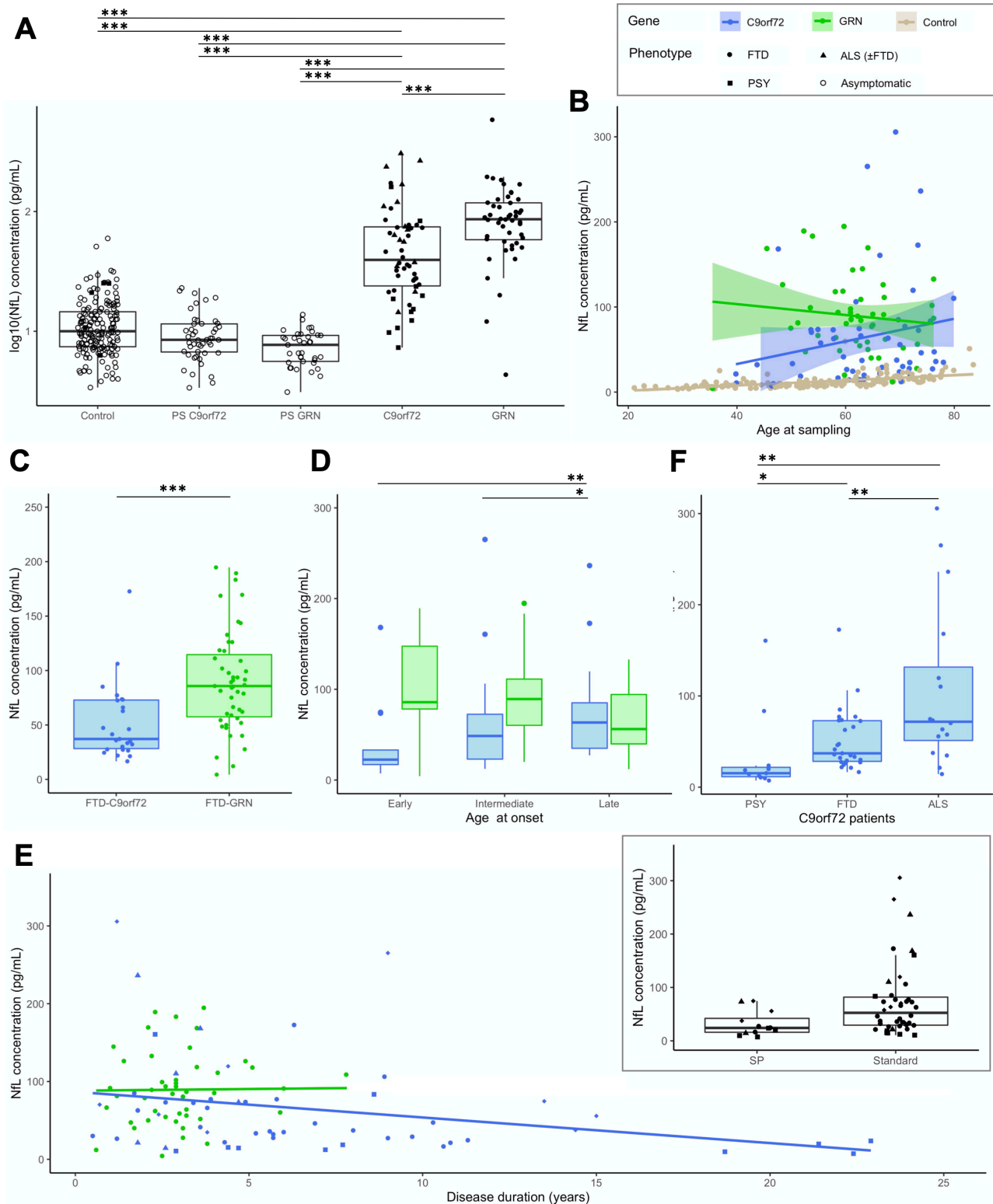


Figure 2 Baseline pNfL levels in patients. (A) pNfL levels in *C9orf72* and *GRN* patients compared with presymptomatic carriers and controls. (B) pNfL levels according to the age at sampling in *C9orf72* ($r=0.284$, $p=0.037$) and in *GRN* ($r=-0.123$, $p=0.406$) patients, with controls displayed for comparison. (C) Comparison of pNfL levels between *C9orf72* and *GRN* patients, restricting the analysis to those with FTD phenotype only. (D) Comparison of pNfL levels according to the age at onset, classified as early (before 50 years), intermediate (between 50 and 65 years) and late (after 65 years). Levels significantly differed in *C9orf72* patients, but not in *GRN* patients. (E) pNfL levels according to disease duration, evidencing a negative correlation in *C9orf72* patients ($r=-0.311$, $p=0.021$) but not in *GRN* patients ($r=0.088$, $p=0.552$). In the insert, *C9orf72* carriers with atypical, SP disease course are compared with patients with standard disease duration. (F) Comparison of pNfL levels according to clinical phenotype in *C9orf72* patients; patients with ALS were considered as a unique group, regardless of the presence of associated FTD. Asterisks indicate the significance of post hoc comparisons between the groups: * $p<0.05$, ** $p<0.01$, *** $p<0.001$. ALS, amyotrophic lateral sclerosis; FTD, frontotemporal dementia; NfL, neurofilament light chain; pNfL, plasma neurofilament light chain; PSY, psychiatric presentations; SP, slowly progressive.

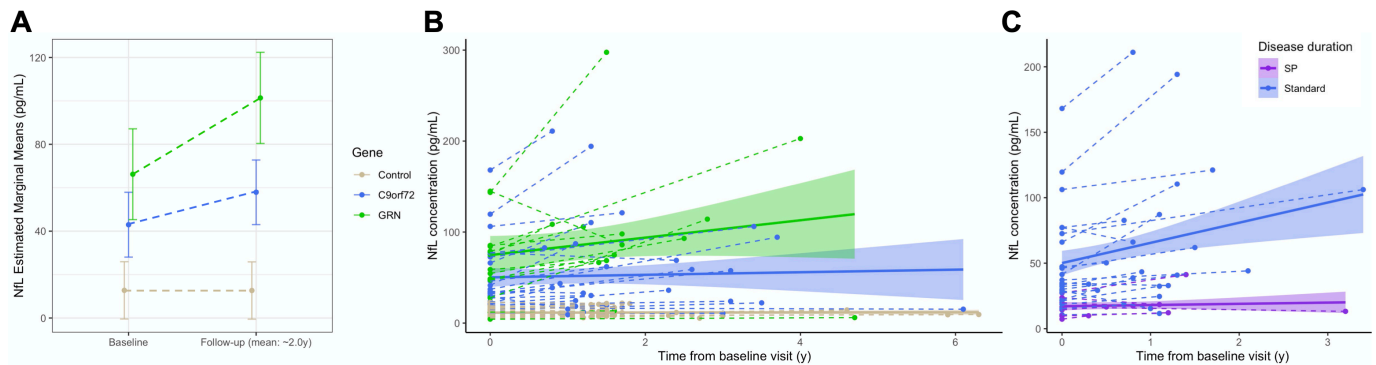


Figure 3 Longitudinal pNfL changes in patients and controls. (A) Mean baseline and follow-up pNfL levels in 44 patients and 36 controls with comparable demographic variables undergoing longitudinal sampling (mean follow-up: 2 years). There was greater increase in *C9orf72* and *GRN* patients compared with controls ($p < 0.0001$), and in *GRN* patients compared with *C9orf72* patients ($p = 0.016$). (B) Spaghetti plot representing pNfL changes from the first to the last observation in the same participants, at the individual (dashed lines) and group (continuous lines, CI 99%) levels. (C) Individual-level and group-level trajectories of SP *C9orf72* patients compared with those with standard disease course over two consecutive visits (mean follow-up: 1.2 years), showing a lesser increase in the former ($p = 0.05$). CI: confidence interval; NfL, neurofilament light chain; pNfL, plasma neurofilament light chain; SP, slowly progressive; y, years.

FTD/ALS are needed to implement pNfL dosage in clinical care and research practice, and to define appropriate endpoints in the forthcoming gene-tailored therapeutic trials.^{9 11 16 19} These critical points are addressed in this study, which analyses pNfL in one of the largest cohorts of FTD/ALS mutation carriers, followed over 2–3 years, thereby allowing definition of gene-specific changes and longitudinal trajectories for *C9orf72* and for *GRN* carriers, separately.

First, we provided detailed cross-sectional and longitudinal characterisation of age-related changes in controls, where NfL release is mainly due to physiological axonal turnover.¹¹ This is a fundamental prerequisite to appropriately interpret values in pathological conditions. Prior studies have addressed the impact of age on NfL, but most focused on elderly populations, during normal or pathological ageing.^{9 14 31–33} Here, we traced pNfL dynamics across the life span with a broad representation of age classes, from <30 to >70 years, providing greater information on early and mid-adulthood. pNfL levels progressively increase with age, from ~5 pg/mL in the youngest to ~18 pg/mL in the eldest individuals. This progression is quasi-linear up to 60 years and is followed by a steeper age-related trend in older subjects. Importantly, pNfL markedly increase throughout the sixth and seventh decades, the life period in which FTD and ALS usually

manifest. This is possibly due to less efficient protein turnover or a progressive ageing-related axonal loss. Alternatively, clinically silent neurological disorders may affect a subset of the oldest controls, in whom clinical proximity to other unrelated neurodegenerative conditions cannot be excluded. A similar low-amplitude progression was evidenced in another study focused on normal ageing,³³ supporting the robustness of our findings. These studies indicate that NfL levels must be cautiously interpreted in neurological diseases, relatively to reference values in age-matched controls. Thereby, we established thresholds by decades, taking into account the physiological pNfL increases throughout the life span. It has to be kept in mind, however, that these thresholds may change on different analytical conditions, thus encouraging joint efforts between centres to standardise dosing techniques and harmonise the interpretation of results.³⁴

Additionally, we determined reference values in controls for all age classes (table 2) and a mean expected ARC of about +4%, from longitudinal observations over a 3-year time course. This rate, concordant with other works,^{11 32 33 35} may serve as a landmark for clinical studies.

Overall, patients presented higher pNfL levels than controls and greater progression over time with an ARC of ~27%. In our study, an in-depth analysis depicts two distinct pNfL trajectories according to the genotype. *GRN* disease was associated with extremely high levels and progression rates, overshadowing the effect of ageing. The higher baseline levels in *GRN* compared with *C9orf72* patients, and the ARC of ~30%, could reflect the impressive neuroaxonal degeneration and frequent white matter changes in *GRN* disease.^{5 36 37} Lower levels in *C9orf72* patients may also be partly due to the clinical heterogeneity within this group, some patients presenting a less aggressive, slowly progressive course.

In *C9orf72* patients, pNfL levels were tightly associated with the aggressiveness of the phenotype. ALS and psychiatric presentations showed the highest and lowest values, respectively. This is concordant with prior studies in patients with ALS, displaying higher levels compared with other neurodegenerative conditions, possibly due to the large-calibre axonal degeneration characterising ALS.^{17 18 30 38} On the other hand, the patients with psychiatric presentations usually have longstanding disease course, without patent markers of neurodegeneration.²⁶ Accordingly, their pNfL levels were significantly lower

Table 3 Optimal cut-off values separating patients from controls

	pNfL value	AUC	Youden	Se	Sp
<i>C9orf72</i> patients versus controls					
Overall	19.00	0.93	0.71	0.83	0.88
<50 years	9.74	0.87	0.66	0.83	0.82
50.0–59.9 years	16.03	1	1	1	1
60.0–69.9 years	20.85	0.92	0.65	0.81	0.84
≥70 years	26.47	0.90	0.76	0.88	0.88
<i>GRN</i> patients versus controls					
Overall	27.48	0.97	0.91	0.94	0.97
<50 years	15.70	0.77	0.73	0.75	0.98
50.0–59.9 years	17.77	1	1	1	1
60.0–69.9 years	35.69	0.97	0.96	0.96	1
≥70 years	27.71	0.98	0.88	1	0.88

Values are indicated in pg/mL.

AUC, area under the curve; pNfL, plasma neurofilament light chain; Se, sensitivity; Sp, specificity.

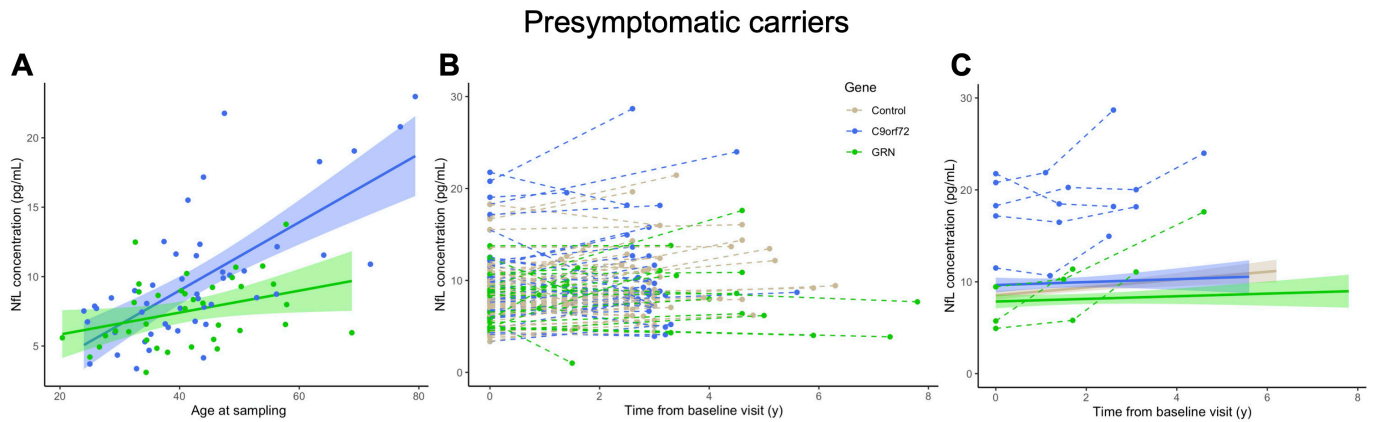


Figure 4 Baseline pNfL levels and longitudinal changes in presymptomatic carriers. (A) pNfL levels at baseline according to the age at sampling in *C9orf72* ($r=0.651$, $p<0.0001$) and in *GRN* carriers ($r=0.359$, $p=0.029$). (B) Spaghetti plot representing pNfL changes from the first to the last observations in 66 carriers and 58 controls with comparable demographic variables undergoing longitudinal sampling (mean follow-up: 3 years). (C) Longitudinal trajectories of pNfL levels in *C9orf72* and *GRN* carriers and controls (continuous lines, CI 99%), which were comparable at group level ($p=0.172$). Eight individuals (five *C9orf72* and three *GRN* carriers: dots and dashed lines) qualified as outliers, having remarkable baseline values and/or increases over time. Four of them were prodromal *C9orf72* carriers (see online supplemental table A1). CI: confidence interval; NfL, neurofilament light chain; pNfL, plasma neurofilament light chain; y, years.

than those of patients with FTD and ALS in our study and more similar to those of patients with primary psychiatric disorders. Prior findings highlighted the potential of NfL to differentiate bvFTD from psychiatric disorders.^{39 40} Our results go somehow further, indicating that NfL might not allow to distinguish atypical *C9orf72*-associated psychosis from patients with primary psychiatric disorders.

More importantly, this study suggests the ARC could be used to predict disease progression in *C9orf72* patients. It was impressively low in patients with slowly progressive phenotypes, displaying no detectable increases at 1 year, beyond what can be attributed to ageing. This strikingly contrasted with the annual ~25% increase in patients with typical disease course. These observations highlight the importance to repeat pNfL measurements, and the usefulness of the ARC in clinical and research settings as a prognostic index of progression in *C9orf72* patients, lower ARC predicting a longer, less aggressive course.

The differences we observed in the two genetic cohorts point out the importance of analysing each genotype independently also in presymptomatic/prodromal carriers.²⁰ A recent important study demonstrated the value of baseline NfL to predict phenocconversion.²¹ However, the cut-offs determined in two independent mixed genetic cohorts analysed in the latter study were not unequivocal, possibly because of demographic and/or genetic heterogeneity. Furthermore, the importance of repeated dosages during the presymptomatic stage has been already emphasised in genetic forms of Alzheimer disease.²⁹ We suggest the same attention should be paid to PS FTD/ALS mutation carriers, where a shift to higher ARC during follow-up dosages may unveil the emergence of pathological processes. In the overall PS group, the ARC was +3.2%, similar to controls, without differences between genotypes. Four *C9orf72* carriers, whose ARC was up to +15%, moved to the prodromal/symptomatic stage during follow-up, emphasising the major interest of repeated pNfL dosages for the prediction of phenocconversion. Notably, pNfL increased 3 years before clinical onset in one of them who developed ALS, in a similar timeframe than previously described converters.^{14 20 21}

More interestingly, four other PS (one *C9orf72* and three *GRN*) with high baseline pNfL and/or high ARC displayed no

clinical symptoms during follow-up. Similar proportions of ‘non-converting’ PS with high NfL levels have been reported by others.^{14 21} These individuals might be in an earlier preclinical stage than the former PS, before the emergence of prodromal symptoms, thus underlining the usefulness of long preclinical follow-ups. Accordingly, NfL levels increase early in the cascade of disease biomarkers in *GRN* PS, ~2 to 5 years before the mild behavioural/cognitive impairment stage.^{14 41} The integration of information stemming from pNfL dosage with that provided by biochemical, neuroimaging, cognitive biomarkers could refine our understanding of the disease trajectory and provide insights into the mechanisms associated with clinical conversion.

The overall pNfL trajectories during the entire disease course strikingly differed between the two genetic cohorts (figure 5). *GRN* carriers had low levels on average during the presymptomatic phase and displayed major and sustained increases after clinical onset. *C9orf72* carriers displayed higher pNfL values in the presymptomatic, and lower in the clinical phase, compared with the former. An association with age was evidenced throughout all *C9orf72*-disease, supporting a less abrupt transition between the preclinical and clinical phases. This suggests that disease course may extend throughout adulthood in *C9orf72* carriers and that progression biomarkers smoothly change during a long presymptomatic phase, in line with previous neuroimaging studies.^{24 42–44} Lastly, pNfL levels and change rates were rather heterogeneous in the clinical phase of *C9orf72* disease and were strongly influenced by the disease phenotype and progression pace. Notably, sustained increases were observed soon after disease onset in the large majority of patients and a few years before onset in prodromal carriers. On the other hand, patients with slow progression showed significantly lower levels even at several years from onset.

This study has some limitations. Quantitative measures of disease severity and neuroimaging data were not included, as standardised data was available only for a part of participants. However, other studies have already well demonstrated the association of NfL levels with cognitive decline and cerebral atrophy.^{14 16 21} For *C9orf72* carriers, the proposed cut-offs could be further refined according to phenotype and/or progression rate. Moreover, this study specifically focused on genetic FTD/

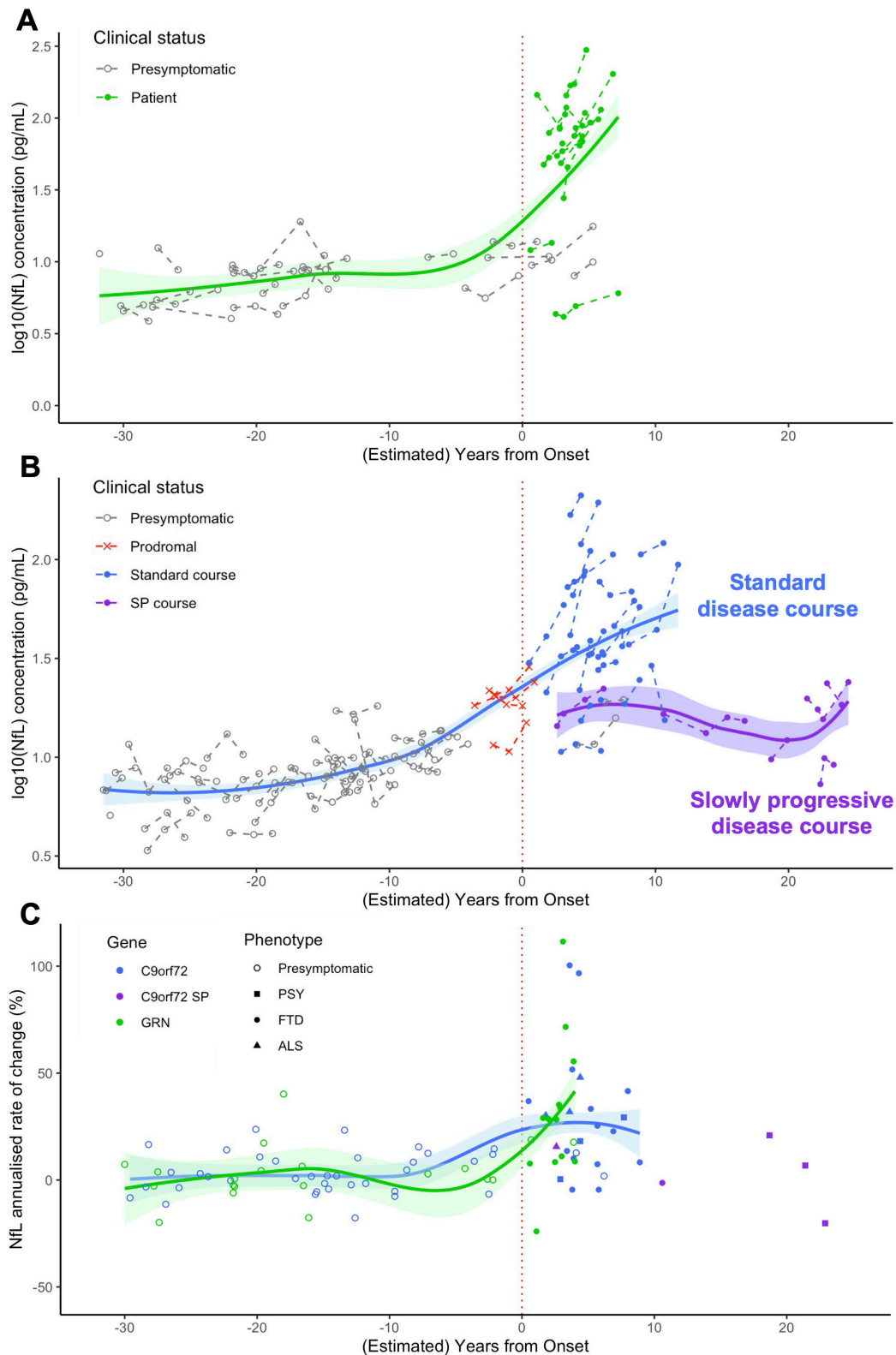


Figure 5 Modelling of pNfL trajectories and progression rates over the entire disease course, from presymptomatic phase to clinical phase, in *GRN* and *C9orf72* carriers. (A,B) pNfL levels at baseline and at follow-up visits in presymptomatic and symptomatic carriers of *GRN* (A) and *C9orf72* (B) mutations, at individual and group levels, according to their clinical status and their (estimated) distance to/from disease onset. (C) pNfL annualised rates of change (%) in presymptomatic and symptomatic *GRN* and *C9orf72* carriers according to their (estimated) distance to/from disease onset. Patients are classified according to their phenotype. Among *C9orf72* patients, those with SP disease course are presented in a different colour. On the x axis, the disease duration from onset is given for patients, and the estimated years to clinical onset is given for presymptomatic carriers. Estimated years to onset were calculated for each individual, taking into account the mean age of disease onset in his/her family. For prodromal *C9orf72* carriers, the age at their first subtle cognitive/behavioural and/or motor symptoms was considered. ALS, amyotrophic lateral sclerosis; FTD, frontotemporal dementia; NfL, neurofilament light chain; pNfL, plasma neurofilament light chain; PSY, psychiatric presentations; SP, slowly progressive.

ALS and the proposed thresholds should be used to predict clinical evolution in presymptomatic carriers only when the mutation status is known. They are not intended to be used in sporadic forms, or when other diseases are in the differential diagnosis. In the modelisation of pNfL trajectories, the estimation of the years to disease onset in presymptomatic carriers was performed taking into account the mean age at onset in their families, which is known to show an imperfect correlation with the individual's actual age at onset.⁵ Lastly, our findings should be replicated in other control populations, as well as in independent genetic cohorts, before employing references and thresholds in clinical practice. A standardised system for pNfL measurement would be highly recommended to reduce the variability across centres and harmonise the interpretation of the results.

Our study provides valuable information on pNfL dynamics under physiological conditions, and in *C9orf72* and *GRN* diseases, improving their interpretability as biomarkers in future studies and as potential prognostic indexes in clinical practice. In particular, the impact of age in the healthy and the specific pNfL trajectories in the two different genetic cohorts led us to propose age-specific and gene-specific thresholds and change rates. They allow partial filling of the gaps of knowledge currently existing in pNfL dynamics and may prove their usefulness to spot unusual values in at-risk subjects.

Author affiliations

¹Sorbonne Université, Paris Brain Institute - Institut du Cerveau - ICM, Inserm U1127, CNRS UMR 7225, AP-HP - Hôpital Pitié-Salpêtrière, Paris, France

²Reference Centre for Rare or Early Dementias, IM2A, Département de Neurologie, AP-HP - Hôpital Pitié-Salpêtrière, Paris, France

³Aramis Project Team, Inria Paris Research Centre, Paris, France

⁴Sorbonne Université, INSERM, Centre d'Immunologie et des Maladies Infectieuses-Paris (CIMI-Paris), Paris, France

⁵EPHE, PSL Research University, Paris, France

⁶Inserm U 1127, CNRS UMR 7225, Sorbonne Université, Paris Brain Institute—Institut du Cerveau (ICM), FRONTlab, Paris, France

⁷Centre of Excellence of Neurodegenerative Disease (CoEN), ICM, CIC Neurosciences, Département de Neurologie, AP-HP, Hôpital Pitié-Salpêtrière, Sorbonne Université, Paris, France

⁸UF de Neurogénétique Moléculaire et Cellulaire, Département de Génétique, AP-HP, Hôpitaux Universitaires La Pitié Salpêtrière-Charles Foix, Paris, France

⁹Univ Lille, Inserm U1171, CHU Lille, DistAlz, LiCEND, CNR-MAJ, Lille, France

¹⁰CMRR Service de Neurologie, CHU de Limoges, Limoges, France

¹¹CMRR Nouvelle Aquitaine, Institut des Maladies Neurodégénératives Clinique (IMNC), CHU de Bordeaux Hôpital Pellegrin, Bordeaux, France

¹²CMRR de l'Arc Alpin, POLE PRéNeLe, CHU Grenoble Alpes, Grenoble, France

¹³CHU Nantes, Inserm CIC04, Department of Neurology, Centre Mémoire de Ressources et Recherche, Nantes, France

¹⁴Department of Neurology, Toulouse University Hospital, Toulouse, France

¹⁵Toulouse Neuroimaging Centre (ToNIC), Inserm, UPS, University of Toulouse, Toulouse, France

¹⁶APHM, Timone, Service de Neurologie et Neuropsychologie, Hôpital Timone Adultes, Marseille, France

¹⁷Institut de Neurosciences des Systèmes (INS), Aix-Marseille University, Inserm, Marseille, France

¹⁸Department of Neurology and CNR-MAJ, Normandy Center for Genomic and Personalized Medicine, Normandie University, UNIROUEN, Inserm U1245 and Rouen University Hospital, Rouen, France

Acknowledgements We are grateful to the DNA and cell bank of the Institut du Cerveau (ICM) for the technical assistance (DNA and cell bank, ICM, Pitié-Salpêtrière hospital, Paris, France) and to Dr Foudil Lamari and Benoit Rucheton (DMU Biogem-Metabolic Biochemistry Department, Neurometabolic and Neurodegenerative Unit, APHP Sorbonne, Pitié-Salpêtrière hospital, Paris, France). The study was partially conducted with the support of the Centre d'Investigation Clinique Neurosciences (CIC 1422), Pitié-Salpêtrière Hospital, Paris.

Collaborators The French Research Network on FTD/FTD-ALS: Sophie Auriacombe (CHU Pellegrin, Bordeaux), Serge Belliard (CHU Rennes), Frédéric Blanc (Hôpitaux Civils, Strasbourg), Claire Boutoleau-Bretonnière (CHU Laennec, Nantes), Alexis Brice (Hôpital Pitié-Salpêtrière, Paris), Mathieu Ceccaldi (CHU La Timone, Marseille), Philippe Couratier (CHU Limoges), Mira Didic (CHU La Timone, Marseille), Bruno

Dubois (Hôpital Pitié-Salpêtrière, Paris), Charles Duyckaerts (Hôpital Pitié-Salpêtrière, Paris), Frédérique Etchary-Bouyx (CHU Angers), Maité Formaglio (CHU Lyon), Véronique Golfier (CHU Rennes), Didier Hannequin (CHU Charles Nicolle, Rouen), Lucette Lacomblez (Hôpital Pitié-Salpêtrière, Paris), Isabelle Le Ber (Hôpital Pitié-Salpêtrière, Paris), Bernard-François Michel (CH Sainte-Marguerite, Marseille), Jérémie Pariente (CHU Rangueil, Toulouse), Florence Pasquier (CHU Lille), Daisy Rinaldi (CHU Pitié-Salpêtrière, Paris), Mathilde Sauvée (CHU Grenoble Alpes), François Sellal (CH Colmar), Christel Thauvin-Robinet (CHU Dijon), Catherine Thomas-Anterion (CH Plein-Ciel, Lyon), and Martine Vercelletto (CHU Laennec, Nantes). PREVD-DEMALS & Predict-PGRN study groups: Elisabeth Auffray-Calvier (CHU Nantes), Eric Bardinet (ICM, Paris), Eve Benchetrit (Hôpital Pitié-Salpêtrière, Paris), Isabelle Berry (CHU Toulouse), Hugo Bertin (Hôpital Pitié-Salpêtrière, Paris), Anne Bertrand (Hôpital Pitié-Salpêtrière, Paris), Anne Bissery (Hôpital Pitié-Salpêtrière, Paris), Stéphanie Bombois (CHU Roger Salengro, Lille), Marie-Paule Boncoeur (CHU Limoges), Alexis Brice (ICM, Paris), Claire Boutoleau-Bretonnière (CHU Laennec, Nantes), Agnès Camuzat (ICM, Paris), Valérie Causse-Lemercier (Hôpital Pitié-Salpêtrière, Paris), Mathieu Chastan (CHU Charles Nicolle, Rouen), Yaohua Chen (CHU Roger Salengro, Lille), Marie Chupin (ICM, Paris), Olivier Colliot (ICM, Paris), Philippe Couratier (CHU Limoges), Xavier Delbeuck (CHU Roger Salengro, Lille), Christine Delmaire (CHU Roger Salengro, Lille), Vincent Deramecourt (CHU Roger Salengro, Lille), Mira Didic (CHU La Timone, Marseille), Aurélie Fankiewicz (Hôpital Pitié-Salpêtrière, Paris), Emmanuel Gerardin (CHU Charles Nicolle, Rouen), Nadine Girard (CHU La Timone, Marseille), Eric Guedj (CHU Marseille), Marie-Odile Habert (Hôpital Pitié-Salpêtrière, Paris), Didier Hannequin (CHU Charles Nicolle, Rouen), Aurélie Kas (Hôpital Pitié-Salpêtrière, Paris), Gregory Kuchinski (CHU Lille), Géraldine Lautrette (CHU Limoges), Isabelle Le Ber (Hôpital Pitié-Salpêtrière, Paris), Benjamin Le Toullec (ICM, Paris), Marie-Anne Mackowiak (CHU Roger Salengro, Lille), Olivier Martinaud (CHU Charles Nicolle, Rouen), Merry Masmanian (Hôpital Pitié-Salpêtrière, Paris), Jacques Monteil (CHU Limoges), Assi-Hervé Oya (Hôpital Pitié-Salpêtrière, Paris), Amandine Pallardy (CHU Nantes), Jérémie Pariente (CHU Rangueil, Toulouse), Florence Pasquier (CHU Roger Salengro, Lille), Grégory Petyt (CHU Roger Salengro, Lille), Pierre Payoux (CHU Toulouse), Daisy Rinaldi (Hôpital Pitié-Salpêtrière, Paris), Adeline Rollin-Sillaire (CHU Roger Salengro, Lille), Sabrina Sayah (Hôpital Pitié-Salpêtrière, Paris), and David Wallon (CHU Charles Nicolle Rouen).

Contributors Full access to all the data in the study and responsibility for the integrity of the data and the accuracy of the data analysis: DS. Study concepts and study design, literature research: DS and ILB. Laboratory analysis: DS and KD. Statistical analysis: DS and MH. Obtainment of funding and study supervision: ILB. Administrative, technical or material support: SF and ILB. Acquisition, analysis or interpretation of data; manuscript drafting or manuscript revision for important intellectual content; approval of final version of submitted manuscript: all authors.

Funding The research leading to these results received funding from the 'Investissements d'avenir' ANR-11-INBS-0011. This work was partially funded by the Programme Hospitalier de Recherche Clinique (PHRC) Predict-PGRN (to ILB, promotion by Assistance Publique—Hôpitaux de Paris), the PHRC FTL-D-exome (to ILB, promotion by Assistance Publique—Hôpitaux de Paris), by the ANR-PRTS PREVD-DEMALS project (to ILB, grant number ANR-14-CE15-0016-07, promotion by Assistance Publique—Hôpitaux de Paris) and the Fondation Vaincre Alzheimer (to ILB, grant number FR-17035).

Disclaimer The sponsors had no role in study design, data analysis or interpretation, writing or decision to submit the report for publication.

Competing interests Disclosure of interests unrelated to the present article: ILB served as a member of advisory board for Prevail Therapeutics and of the steering committee for Alector, and received research grants from ANR, DGOS, PHRC, ARSla Association, Fondation Plan Alzheimer outside of the present work.

Patient consent for publication Not required.

Ethics approval These clinical-genetic studies were approved by the Paris-Necker Hospital/AP-HP Ile-de-France VI ethics committees (CPP 68–15, ID RCB 2015-A00856-43). All participants or legal representatives gave informed consent.

Provenance and peer review Not commissioned; externally peer reviewed.

Data availability statement Data are available upon reasonable request. Data supporting the findings of this study are available from the corresponding author upon reasonable request.

Supplemental material This content has been supplied by the author(s). It has not been vetted by BMJ Publishing Group Limited (BMJ) and may not have been peer-reviewed. Any opinions or recommendations discussed are solely those of the author(s) and are not endorsed by BMJ. BMJ disclaims all liability and responsibility arising from any reliance placed on the content. Where the content includes any translated material, BMJ does not warrant the accuracy and reliability of the translations (including but not limited to local regulations, clinical guidelines, terminology, drug names and drug dosages), and is not responsible for any error and/or omissions arising from translation and adaptation or otherwise.

Open access This is an open access article distributed in accordance with the Creative Commons Attribution Non Commercial (CC BY-NC 4.0) license, which permits others to distribute, remix, adapt, build upon this work non-commercially, and license their derivative works on different terms, provided the original work is properly cited, appropriate credit is given, any changes made indicated, and the use is non-commercial. See: <http://creativecommons.org/licenses/by-nc/4.0/>.

ORCID iDs

Dario Saracino <http://orcid.org/0000-0002-4299-9743>

Karim Dorgham <http://orcid.org/0000-0001-9539-3203>

Raffaella Migliaccio <http://orcid.org/0000-0002-6960-8474>

Isabelle Le Ber <http://orcid.org/0000-0002-2508-5181>

REFERENCES

- Baker M, Mackenzie IR, Pickering-Brown SM, et al. Mutations in progranulin cause tau-negative frontotemporal dementia linked to chromosome 17. *Nature* 2006;442:916–9.
- Cruts M, Gijssels I, van der Zee J, et al. Null mutations in progranulin cause ubiquitin-positive frontotemporal dementia linked to chromosome 17q21. *Nature* 2006;442:920–4.
- DeJesus-Hernandez M, Mackenzie IR, Boeve BF, et al. Expanded GGGGCC hexanucleotide repeat in noncoding region of C9orf72 causes chromosome 9p-linked FTD and ALS. *Neuron* 2011;72:245–56.
- Renton AE, Majounie E, Waite A, et al. A hexanucleotide repeat expansion in C9orf72 is the cause of chromosome 9p21-linked ALS-FTD. *Neuron* 2011;72:257–68.
- Moore KM, Nicholas J, Grossman M, et al. Age at symptom onset and death and disease duration in genetic frontotemporal dementia: an international retrospective cohort study. *Lancet Neurol* 2020;19:145–56.
- Snowden JS, Rollinson S, Thompson JC, et al. Distinct clinical and pathological characteristics of frontotemporal dementia associated with C9orf72 mutations. *Brain* 2012;135:693–708.
- Khan BK, Yokoyama JS, Takada LT, et al. Atypical, slowly progressive behavioural variant frontotemporal dementia associated with C9ORF72 hexanucleotide expansion. *J Neurol Neurosurg Psychiatry* 2012;83:358–64.
- Valente ES, Caramelli P, Gambogi LB, et al. Phenocopy syndrome of behavioral variant frontotemporal dementia: a systematic review. *Alzheimers Res Ther* 2019;11:30.
- Khalil M, Teunissen CE, Otto M, et al. Neurofilaments as biomarkers in neurological disorders. *Nat Rev Neurol* 2018;14:577–89.
- Gaetani L, Blennow K, Calabresi P, et al. Neurofilament light chain as a biomarker in neurological disorders. *J Neurol Neurosurg Psychiatry* 2019;90:870–81.
- Bridel C, van Wieringen WN, Zetterberg H, et al. Diagnostic value of cerebrospinal fluid neurofilament light protein in neurology: a systematic review and meta-analysis. *JAMA Neurol* 2019;76:1035.
- Meeter LH, Dopper EG, Jiskoot LC, et al. Neurofilament light chain: a biomarker for genetic frontotemporal dementia. *Ann Clin Transl Neurol* 2016;3:623–36.
- Steinacker P, Anderl-Straub S, Diehl-Schmid J, et al. Serum neurofilament light chain in behavioral variant frontotemporal dementia. *Neurology* 2018;91:e1390–401.
- van der Ende EL, Meeter LH, Poos JM, et al. Serum neurofilament light chain in genetic frontotemporal dementia: a longitudinal, multicentre cohort study. *Lancet Neurol* 2019;18:1103–11.
- Benussi A, Karikari TK, Ashton N, et al. Diagnostic and prognostic value of serum NfL and p-Tau₈₁ in frontotemporal lobar degeneration. *J Neurol Neurosurg Psychiatry* 2020;91:960–7.
- Cajanus A, Katisko K, Kontkanen A, et al. Serum neurofilament light chain in FTL: association with C9orf72, clinical phenotype, and prognosis. *Ann Clin Transl Neurol* 2020;7:903–10.
- Steinacker P, Huss A, Mayer B, et al. Diagnostic and prognostic significance of neurofilament light chain NF-L, but not progranulin and S100B, in the course of amyotrophic lateral sclerosis: data from the German MND-net. *Amyotroph Lateral Scler Frontotemporal Degener* 2017;18:112–9.
- Verde F, Steinacker P, Weishaupt JH, et al. Neurofilament light chain in serum for the diagnosis of amyotrophic lateral sclerosis. *J Neurol Neurosurg Psychiatry* 2019;90:157–64.
- Benatar M, Zhang L, Wang L, et al. Validation of serum neurofilaments as prognostic and potential pharmacodynamic biomarkers for ALS. *Neurology* 2020;95:e59–69.
- Benatar M, Wu J, Lombardi V, et al. Neurofilaments in pre-symptomatic ALS and the impact of genotype. *Amyotroph Lateral Scler Frontotemporal Degener* 2019;20:538–48.
- Rojas JC, Wang P, Staffaroni AM, et al. Plasma neurofilament light for prediction of disease progression in familial frontotemporal lobar degeneration. *Neurology* 2021;96:e2296–312.
- Le Ber I, Guedj E, Gabelle A, et al. Demographic, neurological and behavioural characteristics and brain perfusion SPECT in frontal variant of frontotemporal dementia. *Brain* 2006;129:3051–65.
- Caroppo P, Habert M-O, Durrleman S, et al. Lateral temporal lobe: an early imaging marker of the presymptomatic GRN disease? *J Alzheimers Dis* 2015;47:751–9.
- Bertrand A, Wen J, Rinaldi D, et al. Early Cognitive, Structural, and Microstructural Changes in Presymptomatic C9orf72 Carriers Younger Than 40 Years. *JAMA Neurol* 2018;75:236.
- Kmetzsch V, Anquetil V, Saracino D, et al. Plasma microRNA signature in presymptomatic and symptomatic subjects with C9orf72-associated frontotemporal dementia and amyotrophic lateral sclerosis. *J Neurol Neurosurg Psychiatry* 2021;92:485–93.
- Devenney EM, Ahmed RM, Halliday G, et al. Psychiatric disorders in C9orf72 kindreds: study of 1,414 family members. *Neurology* 2018;91:e1498–507.
- Millecamps S, Boillée S, Le Ber I, et al. Phenotype difference between ALS patients with expanded repeats in C9ORF72 and patients with mutations in other ALS-related genes. *J Med Genet* 2012;49:258–63.
- Cammack AJ, Atassi N, Hyman T, et al. Prospective natural history study of C9orf72 ALS clinical characteristics and biomarkers. *Neurology* 2019;93:10.1212/WNL.0000000000008359.
- Preischo O, Schultz SA, Apel A, et al. Serum neurofilament dynamics predicts neurodegeneration and clinical progression in presymptomatic Alzheimer's disease. *Nat Med* 2019;25:277–83.
- Weydt P, Oeckl P, Huss A, et al. Neurofilament levels as biomarkers in asymptomatic and symptomatic familial amyotrophic lateral sclerosis. *Ann Neurol* 2016;79:152–8.
- Mattsson N, Andreasson U, Zetterberg H, et al. Association of plasma neurofilament light with neurodegeneration in patients with Alzheimer disease. *JAMA Neurol* 2017;74:557.
- Lleó A, Alcolea D, Martínez-Lage P, et al. Longitudinal cerebrospinal fluid biomarker trajectories along the Alzheimer's disease continuum in the BIOMARKAPD study. *Alzheimers Dement* 2019;15:742–53.
- Khalil M, Pirpamer L, Hofer E, et al. Serum neurofilament light levels in normal aging and their association with morphologic brain changes. *Nat Commun* 2020;11:812.
- Gray E, Oeckl P, Amador MDM, et al. A multi-center study of neurofilament assay reliability and inter-laboratory variability. *Amyotroph Lateral Scler Frontotemporal Degener* 2020;21:1–7.
- Mattsson N, Cullen NC, Andreasson U, et al. Association between longitudinal plasma neurofilament light and neurodegeneration in patients with Alzheimer disease. *JAMA Neurol* 2019;76:791.
- Caroppo P, Le Ber I, Camuzat A, et al. Extensive white matter involvement in patients with frontotemporal lobar degeneration: think progranulin. *JAMA Neurol* 2014;71:1562.
- Sudre CH, Bocchetta M, Heller C, et al. White matter hyperintensities in progranulin-associated frontotemporal dementia: a longitudinal GENFI study. *Neuroimage* 2019;24:102077.
- Feneberg E, Oeckl P, Steinacker P, et al. Multicenter evaluation of neurofilaments in early symptom onset amyotrophic lateral sclerosis. *Neurology* 2018;90:e22–30.
- Al Shweiki MHDR, Steinacker P, Oeckl P, et al. Neurofilament light chain as a blood biomarker to differentiate psychiatric disorders from behavioural variant frontotemporal dementia. *J Psychiatr Res* 2019;113:137–40.
- Fourier A, Formaglio M, Kaczorowski F, et al. A combination of total tau and neurofilaments discriminates between neurodegenerative and primary psychiatric disorders. *Eur J Neurol* 2020;27:1164–9.
- Panman JL, Venkatraghavan V, van der Ende EL, et al. Modelling the cascade of biomarker changes in GRN-related frontotemporal dementia. *J Neurol Neurosurg Psychiatry* 2021;92:494–501.
- Rohrer JD, Nicholas JM, Cash DM, et al. Presymptomatic cognitive and neuroanatomical changes in genetic frontotemporal dementia in the genetic frontotemporal dementia initiative (GENFI) study: a cross-sectional analysis. *Lancet Neurol* 2015;14:253–62.
- Lee SE, Sias AC, Mandelli ML, et al. Network degeneration and dysfunction in presymptomatic C9ORF72 expansion carriers. *Neuroimage* 2017;14:286–97.
- Le Blanc G, Jetté Pomerleau V, McCarthy J, et al. Faster Cortical Thinning and Surface Area Loss in Presymptomatic and Symptomatic C9orf72 Repeat Expansion Adult Carriers. *Ann Neurol* 2020;88:113–22.

SUPPLEMENTARY MATERIAL

Appendix A1. Selection of controls

Appendix A2. Identification of outliers

Table A1. Clinical descriptions of four presymptomatic *C9orf72* carriers in their prodromal phase

Table A2. Demographic data of 44 patients with longitudinal samplings compared with 36 controls

Table A3. Demographic data of 66 presymptomatic carriers with longitudinal samplings compared with 58 controls

Figure A1. Distribution of plasma NfL levels according to discrete age classes in patients

Figure A2. ROC curves and optimal cut-offs that discriminate patients from controls

Appendix A1. Selection of controls

A population of 165 neurologically healthy controls was recruited in the framework of research studies (PREV-DEMALS, Predict-PGRN, and RBM 02-59). All controls had normal neurological examination and cognitive scores. None of them had personal history of neurological diseases. Seventy-seven underwent at least one brain MRI scan, whose findings resulted unremarkable. Of the total population, 114 controls were clinically followed over a mean period of 3.0 ± 1.4 years; none developed neurological diseases in this time interval.

Appendix A2. Identification of outliers

After proper splitting of each population in discrete age classes, we looked for outliers, i.e., individuals with abnormally high plasma NfL (pNfL) levels, or abnormally fast progression, by applying the Tukey's rule ($>Q3 + kIQR$, where Q3 stands for third quartile, IQR for interquartile range and k a constant assuming the value of 1.5 for "minor" outliers and 3 for "major" outliers). When Tukey's rule was not applicable (too wide IQR) we considered as outliers the individuals with pNfL levels or progression above the 95th percentile for their category.

Table A1. Clinical descriptions of four presymptomatic *C9orf72* carriers in their prodromal phase.

Individuals	First evaluation	Follow-up
Case 1 Female 42 years	Baseline, 42 years: normal neurological examination, cognitive and behavioural scores. (pNfL value: 11.50 pg/mL).	1.5 years later, 44 years: normal examination. (pNfL value 10.67 pg/mL) 3 years after baseline, 45 years: attentional deficit, perseverations and social cognition deficit (faux-pas test 21/30). Upper and lower limbs brisk reflexes. (pNfL value: 14.95 pg/mL , ARC: +12%).
Case 2 Male 47 years	Baseline, 47 years: normal neurological examination, cognitive and behavioural scores. CDR@+NACC-FTLD: 0. (pNfL value: 21.76 pg/mL).	1.5 years later, 48 years: decreased reflexes. (pNfL value: 18.47 pg/mL) 3 years after baseline, 50 years: inappropriate familiarity, joviality and mild apathy. Decline on several cognitive tests (MDRS 130/144, faux-pas test 18/30). CDR@+NACC-FTLD: 0.5. Cramps and rare fasciculations at motor evaluation. (pNfL value: 18.48 pg/mL).
Case 3 Male 76 years	Baseline, 76 years: normal neurological examination, cognitive and behavioural scores. CDR@+NACC-FTLD: 0. (pNfL value: 20.79 pg/mL).	1.5 years later, 77 years: normal examination. (pNfL value: 21.87 pg/mL) 3 years after baseline, 79 years: fasciculations, cramps in LL, decreased UL and LL reflexes, attentional and working memory deficits (direct span: 6, reverse span: 4), FAB 16/18, WCST 15/20. CDR@+NACC-FTLD: 0.5. (pNfL value: 28.70 pg/mL , ARC: +15%).
Case 4 Female 64 years	Baseline, 64 years: Normal neurological examination, cognitive and behavioural scores. CDR@+NACC-FTLD: 0. (pNfL value: 18.30 pg/mL).	1.5 years later, 66 years: decreased reflexes (pNfL value: 20.02 pg/mL) 3 years after baseline, 67 years: emergence of executive dysfunction, deficit in mental flexibility and perseverations (WCST 9/20, MMSE 24/30, FAB 15/18). CDR@+NACC-FTLD: 0. Motor evaluation: cramps and fasciculations. (pNfL value: 23.99 pg/mL , ARC: +7%). 6 years after baseline, 70 years: spinal-onset ALS, EMG supported (amyotrophy, fasciculations, motor deficit in UL, left>right). Frontal cognitive decline (motor perseverations, emotional blunting, judgment impairment). (pNfL value : 30.40 pg/mL)

ARC: annualised rate of change; CDR@+NACC-FTLD: Clinical Dementia Rating Instrument plus National Alzheimer's Coordinating Center Behaviour and Language Domains for Frontotemporal Lobar Degeneration; FAB: frontal assessment battery; FBI: frontal behavioural inventory; LL: lower limbs; MDRS: Mattis Dementia Rating Scale; MMSE: mini mental state examination; pNfL: plasma neurofilament light chain; UL: upper limbs; WCST: Wisconsin card sorting test. Bolded values in table are abnormal values with respect to the individual's age class.

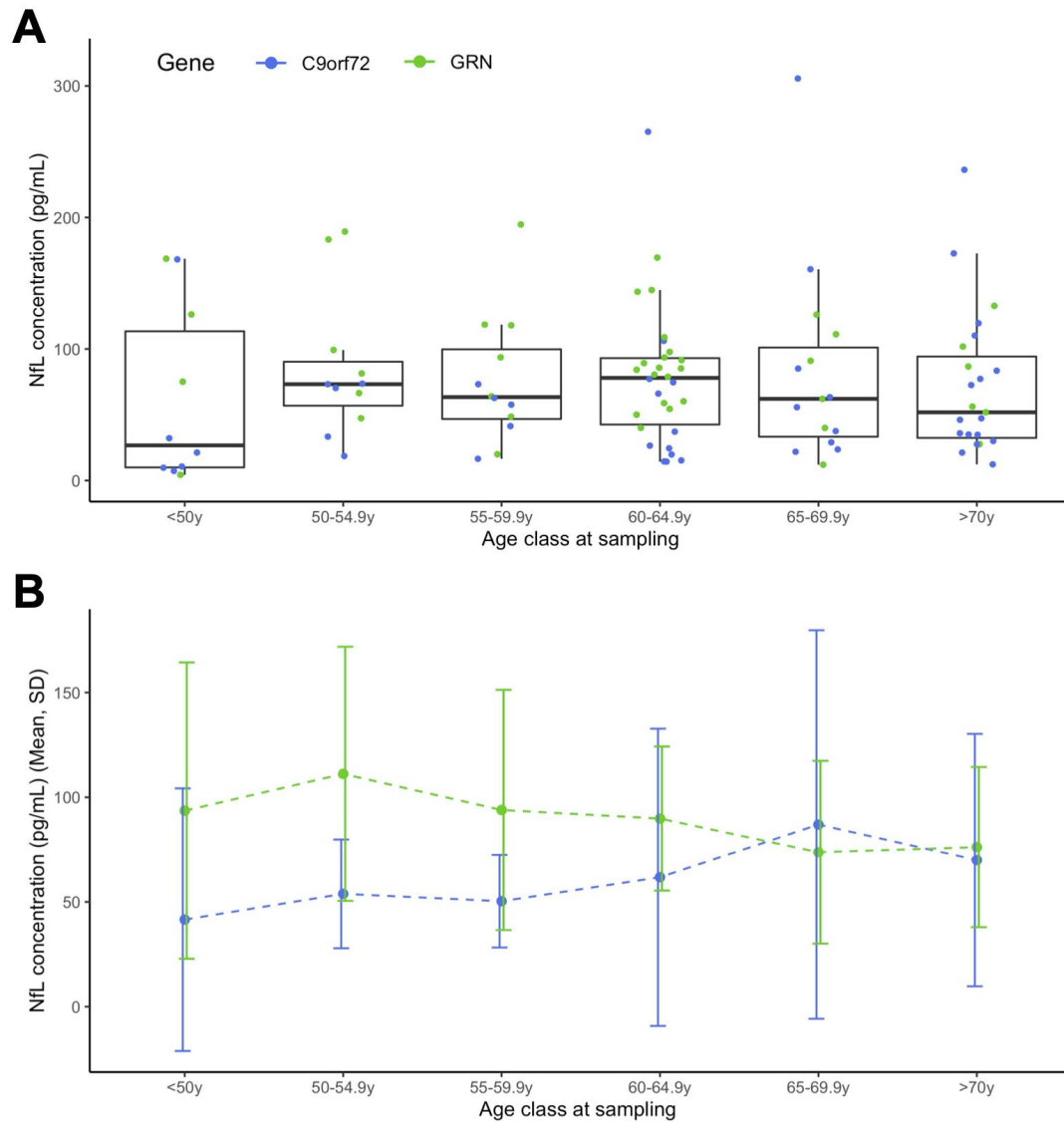
Table A2. Demographic data of 44 patients with longitudinal samplings compared with 36 controls.

	Controls	Patients		<i>p</i> -value
		<i>C9orf72</i>	<i>GRN</i>	
N=	36	29	15	-
Age at baseline sampling (years)	55.2 [47.8; 63.7]	62.8 [52.4; 67.2]		0.128
		63.0 [51.0; 70.2]	62.6 [58.9; 64.0]	0.304
Gender (F/M)	19 / 17	22 / 22		0.990
		15 / 14	7 / 8	0.917
Total follow-up duration (years)	1.5 [1.4; 1.9]	1.5 [1.2; 2.7]		0.438
		1.3 [1.1; 2.8]	1.6 [1.5; 2.5]	0.329

Table A3. Demographic data of 66 presymptomatic carriers with longitudinal samplings compared with 58 controls.

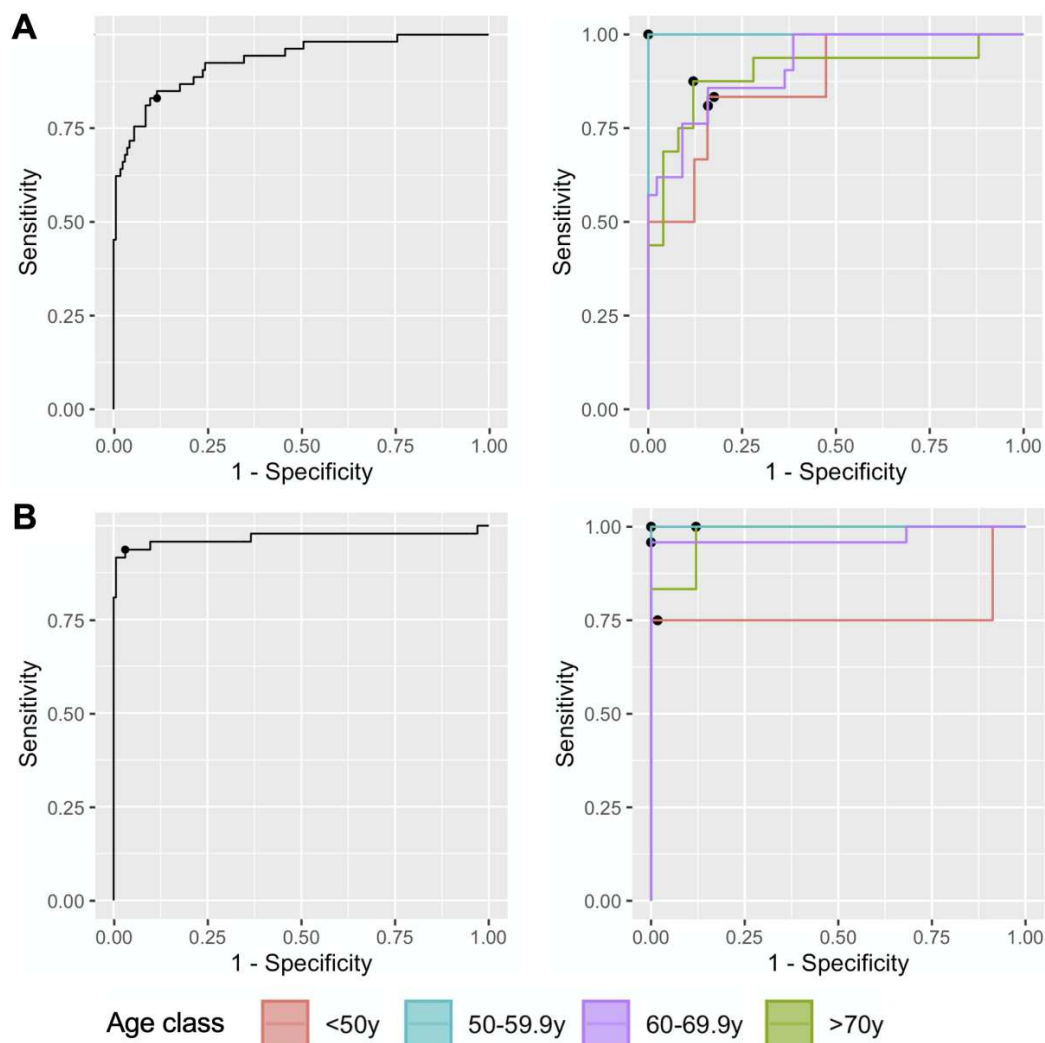
	Controls	Presymptomatic carriers		<i>p</i> -value
		<i>C9orf72</i>	<i>GRN</i>	
N=	58	43	23	-
Age at baseline sampling (years)	43.0 [34.4; 52.0]	41.2 [34.5; 47.3]		0.354
		42.6 [35.1; 47.3]	40.3 [33.2; 47.9]	0.624
Gender (F/M)	31 / 27	41 / 25		0.427
		27 / 16	14 / 9	0.878
Total follow-up duration (years)	2.9 [2.5; 3.1]	2.9 [2.5; 3.2]		0.956
		2.9 [2.5; 3.0]	3.3 [1.5; 4.6]	0.430

Figure A1. Distribution of plasma NfL levels according to discrete age classes in patients.



A: Dots represent individual values, box-plots show median values and quartiles, their whiskers extending to the lowest and highest values no further than $1.5 \times \text{IQR}$. B: Mean values and SD in each age class, according to the causative gene. No significant differences were found when comparing pNfL values between the age classes ($p=0.407$). IQR: interquartile range; pNfL: plasma neurofilament light chain; SD: standard deviation; y: years.

Figure A2. ROC curves and optimal cut-offs that discriminate patients from controls.



A: ROC curve for pNfL values in the population of *C9orf72* patients versus controls, with an AUC estimated at 0.93 on the left side, and individual ROC curves for each of the age-classes on the right side (for more details see Table 3). B: The same analysis for *GRN* patients, with an overall AUC estimated at 0.97. AUC: area under curve; pNfL: plasma neurofilament light chain; ROC: Receiver-operating characteristic; y: years.

4.3 Partie 3 – Profil évolutif du métabolisme cérébral chez les porteurs de mutations du gène *GRN* à la phase présymptomatique (article 4)

Article 4. Saracino D, Sellami S, Boniface H, Houot M, Péligrini-Issac M, Funkiewiez A, Rinaldi D, Locatelli M, Azuar C, Causse-Lemercier V, Jaillard A, Pasquier F, Chastan M, Wallon D, Hitzel A, Pariente J, Pallardy A, Boutoleau-Bretonnière C, Guedj E, Didic M, Migliaccio R, Predict-PGRN study group, Kas A, Habert MO, Le Ber I. Brain metabolic profile in presymptomatic GRN carriers throughout a 5-year follow-up (Soumis, Neurology).

Résumé

A côté des marqueurs biologiques, de nombreuses études ont cherché à identifier des marqueurs de neuroimagerie fiables. Les principaux résultats de ces études ont été présentés dans la partie de l'introduction abordant les marqueurs de la phase présymptomatique. Comme nous l'avons souligné, peu d'études ont évalué le métabolisme cérébral, et les rares études existantes ont porté sur de petites cohortes (Jacova et al., 2013), sans suivi longitudinal prolongé (Caroppo et al., 2015b), ou sur des cohortes hétérogènes mixant plusieurs formes génétiques (Mutsaerts et al., 2019).

Dans l'étude Predict-PGRN, nous avons évalué le métabolisme cérébral dans une cohorte de 80 individus à risque d'être porteurs de mutations du gène *GRN* ou porteurs au stade présymptomatique (article 4). La population a été recrutée à partir de 2010 dans 6 sites en France, et suivie pendant environ 5 ans. Le métabolisme cérébral a été évalué grâce au TEP-FDG, et cette évaluation a été combinée à une approche multimodale intégrant IRM structurelle, échelles cognitives et comportementales, dosage plasmatique des NfL. Ce protocole a été réalisé à la visite d'inclusion (t_0), après 20 (t_{20}) et 60 mois (t_{60}). Brièvement, sur les 80 individus constituant la cohorte initiale, 58 ont été inclus dans les analyses (27 porteurs et 31 contrôles), après application des critères d'exclusion. Quarante-deux sujets (20 porteurs et 22 contrôles) ont suivi le protocole complet, avec une durée moyenne de suivi de 57 ($\pm 6,9$) mois. Pour établir le stade d'évolution des participants, trois paramètres ont été considérés : la distance à l'âge estimé de la maladie, le score de l'échelle CDR+NACC FTLD (0 : préclinique ; 0,5 prodromal, ≥ 1 : symptomatique) et le dosage des NfL, dont nous avons montré précédemment qu'une augmentation était un bon marqueur de l'entrée dans le stade prodromal.

Les données d'imagerie TEP ont d'abord fait l'objet de comparaisons transversales à l'échelle de voxel entre porteurs et contrôles à chaque évaluation. L'analyse des changements longitudinaux a été réalisée avec deux approches complémentaires : test *T* appariés entre visites t_0 et t_{60} pour comparaison à l'échelle de voxel, et comparaison des cartes du pourcentage annualisé de changement (PET-PAC) entre porteurs et contrôles, calculées avec un pipeline dédié de la plateforme BrainVISA. Des modèles linéaires ont été utilisés pour tester l'association entre données métaboliques régionales et changements des autres biomarqueurs.

Un hypométabolisme du gyrus temporal supérieur et moyen gauche, incluant la région du sillon temporal supérieur, a été détecté chez les porteurs dès l'inclusion, 17 ($\pm 12,4$) ans en

moyenne avant le début attendu de la maladie. L'hypométabolisme était légèrement plus étendu dans cette même région, à t_{20} et t_{60} . L'étude de la progression longitudinale sur 5 ans a mis en évidence un déclin métabolique significatif au niveau du cortex temporal latéral supérieur/moyen et du pôle temporal à droite, ainsi que, dans une moindre mesure, du gyrus occipital supérieur gauche, du gyrus frontal supérieur droit et inférieur gauche chez les porteurs, en l'absence de toute progression significative chez les contrôles. En utilisant la méthode PET-PAC, nous avons identifié un profil de déclin presque superposable chez les porteurs, sans modification significative chez les contrôles. D'une façon intéressante, l'analyse volumétrique des IRM anatomiques ne retrouvait d'atrophie significative à aucune visite, ni de perte de volume plus importante chez les porteurs comparés aux contrôles au cours du suivi.

Sur la base de ces résultats, nous avons sélectionné les régions caractérisées par le déclin métabolique le plus significatif chez les porteurs, à savoir une région principale entre le gyrus temporal supérieur et moyen droit, une deuxième région incluant la partie supérieure du pôle temporal droit, et la région du gyrus occipital supérieur gauche. Les taux de changement métabolique, estimés à l'aide des cartes de PET-PAC, étaient significativement plus élevés chez les porteurs par rapport aux contrôles (par exemple, $-1,4\%$ par an *versus* $-0,2\%$ au niveau du gyrus temporal supérieur/moyen droit, $p=0,004$).

Nous avons utilisé les données métaboliques de la région temporale latérale droite pour les analyses suivantes, en particulier pour les comparaisons des données de métabolisme cérébral avec d'autres biomarqueurs. Nous avons fait ce choix compte tenu de la pertinence de cette région dans nos résultats, ainsi que dans des études d'imagerie structurale précédemment publiées (Moreno et al., 2013 ; Borrego-Ecija et al., 2021). Une fixation plus faible du glucose dans cette région était associée à une augmentation plus importante des taux de NfL chez les porteurs, non retrouvée chez les contrôles ($p=0,003$). D'une façon similaire, un déclin métabolique plus important était associé à une augmentation plus importante des NfL, cependant sans atteindre le seuil de significativité statistique ($p=0,093$). Finalement, nous avons proposé une modélisation simple de la séquence des changements des biomarqueurs au cours de la phase préclinique, en combinant les données métaboliques, les taux de NfL, l'âge et les années avant le début estimé de maladie.

Tous les individus porteurs sont restés au stade préclinique pendant toute la durée du suivi. Leurs scores cognitifs sont restés normaux, et leur score à la CDR+NACC FTLD à 0. Cependant, nous avons montré qu'une fixation plus faible du glucose dans la région du gyrus

temporal supérieur/moyen droit était associée à un déclin plus prononcé au sous-score du test des faux-pas « reconnaissance du personnage », et au score global de l'échelle de Mattis ($p=0,014$ pour les deux tests). Ceci suggère que les changements métaboliques dans cette région sont néanmoins prédictifs des subtiles modifications cognitives précliniques. L'association avec le test des faux-pas est particulièrement intéressante, compte tenu du rôle de la région du sillon temporal supérieur dans le comportement social, la reconnaissance des émotions et la prédiction des intentions d'autrui.

Pratiquement, dans le cadre de cette étude, j'ai réalisé l'ensemble des analyses d'imagerie structurelle (pré-traitement des images et analyses statistiques). J'ai également contribué, dans le cadre d'une collaboration avec l'équipe du Dr. Marie-Odile Habert (LIB, UPMC), à l'analyses des images TEP (incluant pré-traitement et analyses statistiques, en particulier pour l'étude longitudinale PET-PAC). Enfin, à partir des données TEP, j'ai contribué aux analyses de corrélation et regression avec les données de NFL et cognitives.

Brain metabolic profile in presymptomatic *GRN* carriers throughout a 5-year follow-up

Dario Saracino, MD,^{1,2,3,†} Leila Sellami, MD, MSc,^{1†} Hugo Boniface, MSc,^{4,5,6†} Marion Houot, MSc,^{1,2,7} Mélanie Péligrini-Issac, PhD,⁴ Aurélie Funkiewiez, PhD,^{1,2} Daisy Rinaldi, PhD,^{1,2} Maxime Locatelli, MSc^{1,4,5}; Carole Azuar, MD,² Valérie Causse-Lemercier, MD,⁸ Alice Jaillard, MD, PhD,⁹ Florence Pasquier, MD, PhD,¹⁰ Mathieu Chastan, MD,¹¹ David Wallon, MD, PhD,¹² Anne Hitzel, MD,¹³ Jérémie Pariente, MD, PhD,¹⁴ Amandine Pallardy, MD, PhD,¹⁵ Claire Boutoleau-Brettonnière, MD, PhD,¹⁶ Eric Guedj, MD, PhD,¹⁷ Mira Didic, MD, PhD,^{18,19} Raffaella Migliaccio, MD, PhD,^{1,2} Predict-PGRN study group, Aurélie Kas, MD, PhD,^{4,5,8} Marie-Odile Habert, MD, PhD^{4,5,8††} and Isabelle Le Ber, MD, PhD^{1,2††}

†These authors contributed equally to this work.

††These authors equally contributed as co-last authors.

Author affiliations:

1 Sorbonne Université, Paris Brain Institute – Institut du Cerveau – ICM, Inserm U1127, CNRS UMR 7225, AP-HP - Hôpital Pitié-Salpêtrière, Paris, France

2 IM2A, Reference Centre for Rare or Early-Onset Dementias, Département de Neurologie, AP-HP - Hôpital Pitié-Salpêtrière, Paris, France

3 Aramis Project Team, Inria Research Center of Paris, Paris, France

4 Sorbonne Université, CNRS, INSERM, Laboratoire d'Imagerie Biomédicale, LIB, F-75006 Paris, France

5 CATI, US52-UAR2031, CEA, ICM, SU, CNRS, INSERM, APHP, Ile de France, France

6 Université Paris-Saclay, CEA, CNRS, Neurospin, UMR9027 Baobab, Gif-sur-Yvette, France

7 Centre of Excellence of Neurodegenerative Disease (CoEN), AP-HP - Hôpital Pitié-Salpêtrière, Paris, France

8 Département de Médecine Nucléaire, AP-HP - Hôpital Pitié-Salpêtrière, Paris, France

9 Nuclear Medicine Department, CHU Lille, F-59000, Lille, France

10 Univ Lille, Inserm U1172, CHU Lille, DistAlz, LiCEND, CNR-MAJ, Lille, France

11 Department of Nuclear Medicine, Centre Henri Becquerel, Rouen University Hospital, Rouen, France

12 Normandie Univ, UNIROUEN, Inserm U1245 and CHU Rouen, Department of Neurology, CNR-MAJ, Normandy Center for Genomic and Personalized Medicine, CIC-CRB1404, F-76000, Rouen, France

13 Nuclear Medicine Department, Toulouse Purpan University Hospital, Toulouse, France

14 Department of Neurology and ToNIC, Toulouse NeuroImaging Centre, Inserm, UPS, Toulouse University Hospital, Toulouse, France

15 Nuclear Medicine Department, University Hospital of Nantes, Nantes, France

16 CHU Nantes, Inserm CIC04, Department of Neurology, Centre Mémoire de Ressources et Recherche, Nantes, France

17 Nuclear Medicine Department, Aix-Marseille University, APHM, CNRS, Centrale Marseille, Institut Fresnel, Timone Hospital, CERIMED, Marseille, France

18 APHM, Timone, Service de Neurologie et Neuropsychologie, APHM – Hôpital Timone Adultes, Marseille, France

19 Aix-Marseille Univ, INSERM, INS Institut de Neurosciences des Systèmes, Marseille, France

Correspondence to:

Dr Isabelle Le Ber, Institut du Cerveau Paris (ICM), AP-HP - Hôpital Pitié-Salpêtrière, Paris, France. Email: isabelle.leber@upmc.fr

Dr Marie Odile Habert, Laboratoire d'Imagerie Biomédicale (LIB), AP-HP - Hôpital Pitié-Salpêtrière, Paris, France. Email: marie-odile.habert@upmc.fr

Running title: Brain metabolism in preclinical *GRN* disease

Abbreviations: AD: Alzheimer disease; ASL = arterial spin labelling; bvFTD = behavioral variant of frontotemporal dementia; CDR+NACC FTLD = Clinical Dementia Rating plus National Alzheimer's Coordinating Center frontotemporal lobar degeneration; CV = coefficient of variation; EYO = expected years to onset; FDG = fluorodeoxyglucose; FTD = frontotemporal dementia; FWHM = full width at half maximum; GMA = grey matter atrophy GMA; HC = healthy controls; IQR = interquartile range; LMM = linear mixed models; MDRS = Mattis dementia rating scale; MNI = Montreal Neurological Institute; NfL = neurofilament light chain; PAC = percent annual changes; PPA = primary progressive aphasia; PS = presymptomatic; PS-*GRN*+ = presymptomatic *GRN* carriers; QC = quality control; ROI = region of interest; SD = standard deviation; SPM = Statistical Parametric Mapping; STS = superior temporal sulcus; VBM = voxel-based morphometry.

ABSTRACT

Background and Objectives. *GRN* mutations are a frequent cause of frontotemporal dementia (FTD). Monitoring disease progression in asymptomatic mutation carriers is a major challenge to deliver preventing therapies before clinical onset. This study aimed to assess the usefulness of fluorodeoxyglucose (FDG)-PET in identifying metabolic changes in presymptomatic *GRN* carriers (PS-*GRN*+), and to trace their longitudinal progression.

Methods. Eighty participants were longitudinally evaluated over 5 years in a prospective study focused on *GRN* disease (Predict-PGRN). They underwent cognitive/behavioral assessment, plasma neurofilament dosage, brain MRI and FDG-PET. Fifty-eight individuals (27 PS-*GRN*+ and 31 non-carriers) were included in the analyses. Voxel-wise comparisons of structural and metabolic imaging data between the two groups were performed for each time-point. Longitudinal PET changes were evaluated with voxel-wise comparisons and the metabolic percent annual changes method. The association of regional brain metabolism with plasma neurofilament and cognitive changes was analyzed.

Results. Cross-sectional comparisons between PS-*GRN*+ and controls found a significant hypometabolism in the superior temporal sulcus (STS) region (encompassing the middle and superior temporal gyri), around 15 years before the expected disease onset, without significant cortical atrophy. The longitudinal metabolic decline over the following 5 years peaked in the STS in carriers ($p < 0.001$), without significantly greater volume loss compared to controls. Their estimated annualized metabolic decrease (-1.37%) was higher than in controls (-0.21%, $p = 0.004$). Lower glucose uptake was associated with higher neurofilament increase ($p = 0.003$) and lower frontal cognitive scores ($p = 0.014$) in PS-*GRN*+

Discussion. This study detected brain metabolic changes in the preclinical phase, preceding structural and cognitive alterations, thus contributing to characterize the pathochronology of biomarkers in *GRN* disease. It supports an early impact of *GRN* mutations on a key hub in the STS area, before the spreading of neuronal dysfunction to other interconnected frontotemporal regions. Due to the STS involvement in the perception of facially communicated cues, and its selective activation by dynamic facial expressions, it is likely that its dysfunction contributes to social cognition deficits characterizing FTD. Overall, our study highlights brain metabolic changes as an early disease-tracking biomarker, and proposes annualized percent decrease as a metric to monitor therapeutic response in forthcoming trials.

KEYWORDS

Frontotemporal dementia; *GRN* (progranulin); PET; biomarker; presymptomatic.

DISCLOSURE

ILB served as a member of advisory board for Prevail Therapeutics, Denali, received consulting fees from Alector, and received research grants from Pfizer, ANR, DGOS, PHRC, ARSla Association, Fondation Plan Alzheimer outside of the present work. MOH received consulting fees from Blue Earth society, outside of the present work. The other authors report no disclosures relevant to the manuscript or outside of the present work.

INTRODUCTION

Frontotemporal dementias (FTD) are rare neurodegenerative diseases characterized by neuronal degeneration in frontal and temporal lobes. *GRN* mutations are among the most frequent causes of autosomal dominant FTD.^{1,2} The behavioral variant of FTD (bvFTD) is the main clinical phenotype of *GRN* mutation carriers, followed by primary progressive aphasia (PPA) and cortico-basal syndrome.³⁻⁵ Neuroimaging changes in *GRN* patients, apart from frontal involvement, include higher degree of asymmetry and greater extension to lateral temporal and parietal regions compared to other subtypes.⁶

Genetic neurodegenerative dementias valuably allow to evaluate preclinical changes in presymptomatic (PS) carriers, with biological, brain metabolic, functional and structural modifications occurring decades before symptoms onset.⁷⁻⁹ With the gene-tailored therapeutic advances and the perspective of early administering of preventive therapies, major efforts have been made to detect disease progression with wet and neuroimaging biomarkers in the context of national and international FTD research initiatives.⁸⁻¹² Elevated levels of neurofilament light chain (NfL) represent a valuable predictor of clinical proximity in PS carriers, their increase occurring ~2-5 years before the fully symptomatic disease in all genetic forms of FTD. NfL are less useful to track the pathology earlier, long before clinical conversion.¹³⁻¹⁶ Besides, the detection of early structural MRI changes in *GRN* carriers suggests that the underlying disease process starts several years before clinical onset.^{8,10} However, the limitation to translate neuroimaging changes identified at group-level into individual metrics, for clinical and therapeutic trials, is a major issue. The sequential chronology of biological, functional and structural biomarker alterations proper to the main genetic forms is another unresolved question.

In this regard, the lack of investigations assessing PET changes is an important gap in the discovery of PS neuroimaging markers. Brain metabolism decreases early in the cascade of changes in Alzheimer disease (AD), representing a promising marker in other degenerative dementias.^{7,17} So far, the knowledge on brain perfusion/metabolic changes during the PS stage of *GRN* disease is limited, not only by the scarce number of studies, mostly based on heterogeneous populations,¹⁸⁻²⁰ but also by the lack of longitudinal assessments to trace their propagation. In the present study, we investigated brain metabolism in a genetically homogeneous cohort of PS *GRN* carriers (PS-*GRN*+), and its longitudinal changes over 5 years. We assessed the potentiality of brain fluorodeoxyglucose (FDG)-PET in identifying preclinical

changes, tracking their sequential diffusion over time and predicting subsequent changes in fluid-based biomarkers and cognitive measures. Overall, this study aimed at better characterizing the biomarker pathochronology in *GRN* disease, and at fostering the usefulness of brain metabolism as a potential outcome measure in clinical and therapeutic trials.

METHODS

Study design and participants

Eighty individuals were enrolled in a prospective study (Predict-PGRN) between 2010 and 2018 from 6 French sites, and followed-up over ~5 years. All were first-degree relatives of *GRN* mutation carriers with 50% risk to carry a mutation. Their genetic status was established in the context of this research, as previously described.¹⁹ The investigators were blinded to the genetic status of the participants, as all participants were, except those wishing to undergo PS diagnostic testing.

Amongst the 80 participants, 21 were excluded from baseline analyses owing to imaging artefacts, unrelated MRI lesions or clinical symptoms (Figure 1, eMethods). One individual, harboring subtle signs at baseline and developing symptoms suggestive of clinical conversion during the study, was analyzed separately. So, a total of 58 asymptomatic participants, 27 PS-*GRN*⁺ and 31 non-carriers considered as healthy controls (HC), were included in baseline analyses (t_0). Fifty-four (26 PS-*GRN*⁺, 28 HC) of them were evaluated at the second visit ~20 months after inclusion (t_{20}). Forty-two of them (20 PS-*GRN*⁺, 22 HC) underwent the third visit (t_{60}). At each visit, all participants underwent the same clinical, neurological, behavioral, cognitive assessments, as well as standardized blood/plasma sampling, brain MRI and FDG-PET imaging protocols.

Standard Protocol Approvals, Registrations, and Patient Consents

This study (ClinicalTrials NCT04014673) was approved by ethics committee of AP-HP Ile-de-France VI. All participants provided written informed consent before their inclusion.

Clinical and behavioral assessments

A standardized semi-structured interview was conducted with informants (mainly spouses) by experimented examiners to identify relevant behavioral, personality, neuropsychiatric and functional changes. Behavioral symptoms were assessed at each visit using the Clinical Dementia Rating plus NACC FTLN (CDR+NACC FTLN) (global score, sum of boxes),²¹

Frontal Behavioral Inventory, Neuropsychiatric Inventory, Starkstein Apathy Scale.

Cognitive assessment

A standardized neuropsychological testing covering all major cognitive domains was performed by experienced neuropsychologists. Frontal executive functions were assessed with Frontal Assessment Battery, Wisconsin card sorting test, trail-making test, digit spans, and Hayling test. Social cognition was assessed with facial emotions recognition and faux-pas test.²² Participants also underwent Mini-Mental State Examination, Mattis dementia rating scale (MDRS), free and cued selective reminding test, fluency tasks, oral confrontation naming,²³ Rey's figure copy and recall, and praxis assessment.²⁴

Staging of the participants

Participants scoring 0 at the CDR+NACC FTLD were classified in preclinical stage, those scoring 0.5 in prodromal stage, and those scoring ≥ 1 were considered as fully symptomatic, as described.^{11,12} For some analyses, participants were stratified according to their proximity to clinical disease. We estimated the expected years to onset (EYO) in asymptomatic individuals by subtracting their age from the mean age at onset within the family, as in previous studies.^{8,19,25,26} Plasma NfL levels were used as marker of clinical proximity in PS-GRN+, as described above and in the literature.^{15,27}

MRI and PET acquisitions

A standardized imaging protocol was conducted in 6 French sites, consisting of high-resolution 3D T1-weighted MRI acquired with 3 or 1.5 Tesla scanners. MRI images were acquired with full brain coverage and isotropic voxels (TR=2300 ms; TE=4.18 ms; matrix=256 mm; slice thickness=1 mm). All centers used the same harmonized MRI sequences (CATI, <https://cati-neuroimaging.com>) to minimize center-related bias. Before the study, phantom acquisitions were performed to ensure the comparability of the results across centers.

FDG-PET scans were acquired in the same sites with a standardized protocol set up by the CATI.²⁸ Phantom acquisitions were performed before the study to measure the spatial resolution (full width at half maximum, FWHM) of each scanner. A dose of 2.5 MBq/Kg of ¹⁸fluorodeoxyglucose, between 125MBq and 250MBq per subject, was injected 30-45 minutes before a 15-minute scan. The participants remained in neuro-sensory rest, calm environment, eyes closed, at least 20 minutes after the injection.

MRI and PET preprocessing

All MRI and PET scans were centralized and quality-checked by the CATI. MRI volumes were segmented into probability maps, and spatially normalized to the Montreal Neurological Institute (MNI) space using Statistical Parametric Mapping software (SPM12), version v7487 (<http://www.fil.ion.ucl.ac.uk/spm>). PET images were corrected for partial volume effect, intensity normalized using pons from Pickatlas volume of interest as reference region and spatially normalized to MNI, then smoothed using an isotropic 8mm FWHM Gaussian kernel. Details about PET preprocessing are given in eMethods. A careful image quality control (QC) was performed for each step of the process.

To measure grey matter atrophy (GMA), MRI data processing for voxel-based morphometry (VBM) analyses was performed using the SPM toolbox CAT12 (<http://www.neuro.uni-jena.de/cat/>), including spatial registration, segmentation and bias correction for cross-sectional and longitudinal data. An additional region-of-interest (ROI)-based processing with FreeSurfer is detailed in eMethods.

FDG-PET analyses

Considering the challenges of FDG-PET longitudinal studies in PS mutation carriers and the likelihood of subtle metabolic changes, data were analyzed using different approaches to improve the robustness of the study.

Voxel-wise analyses

Cross-sectional voxel-wise comparisons between PS-GRN+ and HC were performed in SPM12, with a two-sample *T*-test on smoothed parametric images using an explicit mask. This mask was obtained from the mean of grey matter probability maps of each subject with a threshold of 0.4. A general linear model was applied with age, gender and centre as covariates. The uncorrected statistical threshold was set at $p < 0.001$, with a secondary cluster-extent threshold of 100 voxels. Longitudinal glucose metabolic changes in participants were assessed using SPM12 voxel-wise paired *T*-test, with two conditions (t_0 and t_{60}), using time interval as covariate. The primary cluster-defining threshold was $p = 0.001$, with the cluster-level extent threshold set at $p = 0.05$ for false discovery rate correction.

Metabolic percent annual changes (PAC) maps

The metabolic percent annual changes (PET-PAC) maps were obtained using an automated

pipeline developed with BrainVISA according to the previously reported method (eMethods).²⁹ These maps represent the voxel-wise calculation of percent metabolic change between t_0 and t_{60} expressed in percent annual change, according to the following formula:²⁹

$$\frac{(t_0 - t_{60})}{t_0} \times \frac{12}{\Delta months} \times 100$$

A voxel-by-voxel comparison of PET-PAC between PS-*GRN*+ and HC was then performed, after spatial normalization to MNI and smoothing with an isotropic 10 mm Gaussian kernel. Statistical comparisons were carried out with primary cluster-forming threshold set at $p=0.005$, and a secondary cluster-extent threshold of 1000.

ROI-based analyses

We extracted measures of glucose metabolism and longitudinal rate of change within the ROIs obtained from the thresholded SPM maps from voxel-wise analyses, after applying an additional cluster extent threshold of 400 voxels, to include only the most relevant clusters. These ROIs were overlaid on spatially normalized individual 3D T1-weighted MRI images and then applied to normalized co-registered PET images. The uptake value was referenced to the pons. For each ROI, we studied the association of glucose uptake values with NfL levels, cognitive and clinical measures, as described below. Using unsmoothed PET-PAC maps, the rate of annual metabolic change was calculated in each ROI, for PS-*GRN*+ and HC.

MRI analyses for GMA

The same test conditions were applied for cross-sectional voxel-wise comparisons of grey matter probability maps between PS-*GRN*+ and HC, and for longitudinal volume changes using two-sample *T*-tests and flexible factorial designs in SPM12. Age, gender, center and total intracranial volume were used as covariates in cross-sectional comparisons, whereas the t_0 - t_{60} time interval was included as covariate in longitudinal analyses.

NfL measurements

Blood samples were collected at each visit and centralized at the ICM biobank. Plasma NfL measurements were performed using Single Molecule Array (Quanterix, USA), as previously described,¹⁶ and detailed in eMethods. NfL dosages were interpreted with respect to reference values and expected rates of change previously established in controls and *GRN* carriers.^{15,16}

Statistical analyses

Statistical analyses were performed using R, version 4.0.5 (Vienna, Austria). A two-sided p -value <0.05 was considered significant. Demographic, clinical and cognitive characteristics between the groups were compared using Fisher's exact test for categorical variables, and Mann-Whitney-Wilcoxon or Kruskal-Wallis with Dunn's post-hoc test for continuous variables. Correlation analyses were performed with Spearman's test.

Linear mixed models (LMMs) were performed to study whether the evolution of ROI-based MRI volumes, NfL levels and behavioral/cognitive scores differed between PS-*GRN*⁺ and HC. In all LMMs, age at evaluation, gender, genetic group, time since first evaluation and interaction between the last two were used as fixed effects, and subject as random intercept effect. To investigate whether the evolution of NfL levels was impacted by baseline glucose uptake in selected ROIs or its longitudinal changes, we used the three-way interaction genetic group*time since t_0 *baseline uptake and all the lower interactions and main effects involved, and the three-way interaction genetic group*time since t_0 *annual metabolic change and all the lower interactions and main effects involved. To study the impact of baseline uptake on behavioral/cognitive scores in PS-*GRN*⁺ we used the two-way interaction time since t_0 *baseline uptake and the main effects involved. Details on each LMM are given in eMethods. Family distribution was set at either Poisson, Binomial or Bernoulli according to data generation mechanism. Multiple comparisons were handled with Benjamini-Hochberg correction.

Data availability

The data supporting the findings of this study are available from the corresponding author upon reasonable request.

RESULTS

Demographic and clinical characteristics

Characteristics of participants at baseline are displayed in Table 1; there were no differences between PS-*GRN*⁺ and HC. The PS-*GRN*⁺ group was at a mean distance of -17.4 ± 12.4 years of their own expected disease onset. Follow-up characteristics are in eTables 1,2. There were no differences between PS-*GRN*⁺ and HC at follow-up visits.

Brain metabolism throughout a 5-year follow-up

Cross-sectional comparisons

The cross-sectional comparison between PS-*GRN*⁺ and HC at baseline found a significant area of hypometabolism in the left temporal cortex, encompassing the superior and middle temporal gyrus, and the superior temporal sulcus (STS) (Figure 2A and eTable 3).

Cross-sectional analyses at t_{20} and t_{60} revealed slightly greater left temporal hypometabolism, with an additional cluster in the right medial prefrontal cortex at t_{60} (Figure 1B, eFigure 2). Notably, when restricting the baseline cross-sectional comparison to the 42 participants undergoing the entire follow-up, we identified a smaller hypometabolic cluster in the same temporal region (eFigure 3).

Statistical parametric maps of the subject at prodromal stage, analyzed separately from the PS-*GRN*⁺ group, showed clusters of hypometabolism in the right superior and middle temporal gyri at baseline and follow-up (eFigure 4).

Longitudinal changes

Longitudinal metabolic changes between t_0 and t_{60} in PS-*GRN*⁺ using SPM voxel-wise paired *T*-test demonstrated a pattern mainly involving the right temporal lobe (superior/middle temporal gyrus up to the temporal pole), the right superior frontal and precentral gyri, the left inferior frontal gyrus, and the left superior occipital gyrus (Figure 3). Overall, longitudinal metabolic changes were more significant in the right temporal lobe and in left occipital cortex; notably, the superior/middle temporal cluster was, by far, the largest and the most significant one (eTable 4). There was no significant longitudinal metabolic decline in HC.

The comparison of PET-PAC maps between PS-*GRN*⁺ and HC led to similar results, disclosing the same regions of greater annual metabolic decrease in carriers, notably in the right superior and middle temporal gyri, right temporal pole, right perirolandic cortex, and left superior occipital gyrus (Figure 4, eTable 5). No areas of greater percent annual decrease in HC compared to PS-*GRN*⁺ were found.

Three main ROIs were selected from voxel-wise comparisons, encompassing the right superior/middle temporal gyrus, the right temporal pole, and the left superior occipital gyrus. In these three areas, we estimated the annualized rate of metabolic change from PET-PAC maps in PS-*GRN*⁺ and HC, the latter representing the expected decrease under physiological

conditions. These rates significantly differed between the two groups in all ROIs, their mean values being equal to -1.37% (± 1.77) in PS-GRN+ versus -0.21% (± 1.04) in HC in right superior/middle temporal gyrus ($p=0.004$), -1.20% (± 1.22) versus -0.32% (± 1.44) in right temporal pole ($p=0.019$), and -1.25% (± 1.77) versus -0.05% (± 0.81) in left superior occipital gyrus ($p=0.002$). The annualized decreases tended to be more important with increasing age or closer proximity to disease onset in PS-GRN+, without any aging effects in HC (eFigure 5).

The right superior/middle temporal ROI was prioritized in subsequent ROI-based analyses given its relevance in both voxel-wise and PET-PAC results, and the strong supporting evidence of its critical involvement from previous studies.^{26,30}

Brain structural changes

There were no differences in brain volumes between PS-GRN+ and HC at baseline and all subsequent time points on VBM analyses nor on FreeSurfer analyses. In particular, there was no significant cortical atrophy in the left and right middle temporal gyri. Both carriers and controls exhibited diffuse clusters of volume loss between the t_0 and t_{60} time-points, but the comparisons between the two groups did not show any significant results. Additionally, we did not find any differences in the longitudinal volume change between PS-GRN+ and HC in the right middle/superior temporal ROIs with the FreeSurfer-based approach ($p=0.570$), or in any other ROIs.

Association of NfL levels with regional glucose metabolism in PS-GRN+

At baseline, median plasma NfL levels measured 7.45 pg/mL (interquartile range, IQR: 5.30 – 9.46) in PS-GRN+ and 8.80 pg/mL (IQR: 7.37 – 11.04) in HC ($p=0.210$). NfL levels increased over time ($p=0.036$) without differences between carriers and controls ($p=0.438$).

We analyzed the impact of baseline glucose metabolism in the right superior/middle temporal ROI on subsequent increase of plasma NfL levels during follow-up, which differed between PS-GRN+ and HC ($p=0.003$). Notably, among the PS-GRN+ the lower was the glucose uptake at t_0 , the higher the NfL increased during follow-up, with no such differences in HC (Figure 5A,B). When considering the longitudinal metabolic change in the same ROI, a similar tendency between PS-GRN+ and HC was found, without reaching statistical significance ($p=0.093$), with higher NfL increases among PS-GRN+ harboring greater metabolic loss.

Based on these findings, we attempted to assess the relevance of brain metabolic changes in relationship with participants' proximity to clinical onset, considering the information derived from NfL levels and individual age/EYO. We classified the PS-GRN+ based on their regional glucose metabolism and NfL values during follow-up. We dichotomized them in "PET-" and "PET+", the latter having 1) t_0 glucose uptake in the right superior/middle temporal ROI below mean -1 standard deviation (SD) value in HC, or 2) longitudinal decrease greater than mean +1SD decrease in HC. Similarly, they were classified as "NfL+" when 1) their plasma NfL values fell above the 95th percentile of their corresponding age-class, or 2) their annualized rate of change was higher than the mean +1SD of the expected increase, as previously established.¹⁶ Seven carriers were classified "PET-/NfL-", 11 "PET+/NfL-", and 2 "PET+/NfL+". No PS-GRN+ had NfL increases without altered glucose metabolism. Interestingly, the groups differed for their mean age ($p=0.021$), as PET-/NfL- were significantly younger (39 ± 8.7 years) than both PET+/NfL- (48 ± 6.4 , $p=0.032$) and PET+/NfL+ (61 ± 1.4 , $p=0.004$). The EYO also differed between PET-/NfL- and PET+/NfL+ ($p=0.012$), and between PET+/NfL- and PET+/NfL+ ($p=0.022$) (Figure 5C,D). Of note, no PS-GRN+ reached global CDR+NACC FTLD ≥ 0.5 . Similar distributions were found when considering the two other ROIs (eFigure 6).

Association of cognitive changes with regional glucose metabolism in PS-GRN+

Cognitive scores did not show any differences between PS-GRN+ and HC at baseline as well as during follow-up. At group-level, there was no significant change in cognitive scores between t_0 , t_{20} and t_{60} in PS-GRN+.

Interestingly, PS-GRN+ displaying the lowest glucose uptake at t_0 (10th percentile) in the right superior/middle temporal ROI presented the greatest decreases in two scores, the MDRS total score ($p=0.014$) and the character identification sub-score of the faux-pas test ($p=0.014$) (Figure 6). The metabolism in this same ROI had no impact on the score of faux-pas detection ($p=0.733$), overall facial recognition test ($p=0.898$), or any other cognitive tests.

DISCUSSION

This study investigated brain glucose metabolism in presymptomatic GRN carriers, and traced its longitudinal changes over a follow-up period of about 5 years. The main finding was the preclinical FDG-PET change in the temporal lobe, revealed more than 15 years before the expected age of onset, preceding brain atrophy and cognitive changes.

Methodologically, the study of FDG-PET progressive changes in PS genetic cohorts is challenging, due to intra- and inter-individual fluctuations of physiological brain glucose metabolism and the fact that metabolic changes at this early preclinical stage are expectedly subtle, which implies a complex optimization of the signal-to-noise ratio. In this study, we used a whole-brain voxel-wise approach without aprioristic assumptions regarding topographical localizations, and confirmed the results with PET-PAC method designed for the longitudinal assessment of voxel-wise FDG-PET changes, with the added value of providing a calculation of annualized rates of metabolic change.²⁹ The concordance of the results with the different longitudinal approaches validates their robustness, providing a solid basis to test the association of regional glucose metabolism with other biomarkers.

So far, only few studies have assessed brain metabolism or perfusion during the PS stages of genetic FTD with FDG-PET^{18,19} or Arterial Spin Labelling (ASL).²⁰ A surprisingly large pattern of frontotemporal and insular hypometabolism was detected in nine *GRN* carriers, probably impacted by a proportion of individuals at the prodromal/transitional phase.¹⁸ A multicenter GENFI ASL perfusion study identified decreased cerebral blood flow in frontal, temporal and parietal regions in a mixed genetic cohort, a profile largely driven by the *C9orf72* carriers.²⁰ The associations of brain metabolic/perfusion with markers of neurodegeneration, such as NfL and brain structural changes, or extensive cognitive biomarkers have not been explored in the previous studies. In this study, we investigated brain metabolism over time in a genetically homogeneous cohort of PS-*GRN*+, at an early preclinical stage (17.4±12.4 years before expected onset). The most significant cluster of glucose hypometabolism was detected in the STS region. This was also the region in which metabolism decreased the most in the longitudinal study. This is consistent with decreased cortical thickness in the superior and middle temporal gyri in older PS *GRN* carriers.^{26,30} Thus, there is converging evidence of an early impact of *GRN* mutations on the STS area (encompassing the middle and superior temporal gyri), before spreading to further interconnected frontal and temporal regions, as well as the contralateral hemisphere. The biological mechanisms underlying this selective regional vulnerability and its causal relationship with progranulin haploinsufficiency remain to be elucidated.

Interestingly, the STS region is a highly interconnected hub with a specific commitment to processing of audiovisual social information and communicative behavior.³¹ It is preferentially engaged in perceiving social interactions and in the representation of intentionality.^{32,33} The right STS region is particularly critical for the perception of salient facially communicated

cues, and selectively activated in response to dynamic facial expressions.^{34–36} Overall, the STS has been identified as playing a pivotal role in social perception processing by analyzing biological motion cues, such as body gesture, facial expressions, human voice and gaze direction, in order to decode and predict others' intentions.^{34–36} Anatomical and functional abnormalities of the STS have been widely studied in patients with autism spectrum disorders,³⁷ but have thus far received little attention in FTD. A recent study underscored the involvement of the right STS in reduced responses to dynamic facial emotions in bvFTD.³⁸ Our study suggests that these specialized functions are worth exploring during the PS stages of *GRN* disease. The association between glucose uptake in the right STS and the character identification score on the faux-pas test underscores subtle latent deficits in perception of intentionality. There was no significant overt decline in other social cognition scores, paralleling previous studies in PS *GRN* disease,³⁹ even in the late PS phase,^{40,41} which is likely attributable to the poor sensitivity of the standard tests. Indeed, recognition of static facial expressions may be not sensitive enough to capture subtle deficits in social perception processing. A testing based on dynamic social stimuli, such as recognition of biological motion cues of face morphs, could be more discriminative to detect mild social perception deficits associated with STS dysfunction in PS-*GRN*+

The hypometabolism in other cortical regions found in the present study could be interpreted in a network perspective. Significant metabolic decrease was found in the temporal pole, which is strongly associated with STS function in the identification of social traits and in the access to other people's identity, due to its key role in semantic memory. The synergistic activation of these regions in the same pathway has been evidenced by functional imaging studies.⁴² It is therefore conceivable that the spreading of the degenerative process could sequentially involve these two highly interconnected regions. How degenerative lesions propagate throughout cortical areas and neural systems is unknown. Emerging evidence suggests that proteinopathies may spread by “prion-like” seeding across disease-vulnerable networks, according to the concept of molecular nexopathy.^{43,44} Microstructural alterations mainly involving intra-hemispheric antero-posterior white matter tracts⁴⁵ and decreased connectivity between frontal and posterior associative regions⁴⁶ support a dissemination of the degenerative process along an anterior-posterior axis in preclinical *GRN* disease.

This multimodal study also provides elements supporting a sequential chronology of PS alterations in *GRN* disease. Prior studies evidenced that grey matter volume, white matter integrity, cognitive functions and NfL levels change in approximately the same time window,

becoming mostly detectable between 5 and 2 years before clinical conversion.^{10,40,41,47-49} Consistently, our MRI results showed no significant structural changes up to approximately 10 years before the expected disease onset, at the last evaluation in PS-*GRN*⁺. The short interval between the detection of structural/cognitive changes and clinical onset raises the critical issue of a very narrow window to initiate therapeutic interventions in the preclinical stage based on these markers. This emphasizes the need to identify more sensitive markers, tracing dynamic changes longer before phenoconversion. Our results evidence that metabolic alterations might occur more gradually, in the timeframe of ~15 years before disease onset. It supports a chronology of biomarker changes similar to that observed in genetic AD, brain hypometabolism being amongst the earliest detectable modifications, preceding structural changes.^{17,50} Moreover, our study evidenced that mean annualized rates of glucose metabolism decline in PS-*GRN*⁺ were in the same range as observed in preclinical AD,²⁹ and approximately seven-fold higher in PS-*GRN*⁺ (-1.4%) than in HC (-0.2%) in the STS. This supports the use of metabolic changes as an earlier detectable and more predictive biomarker than structural modifications. It fosters the implementation of annualized rates of change as a valuable metric to track preclinical disease progression, in combination with NfL levels, in particular in the perspective of therapeutic trials.

In our study, values of glucose uptake, and its longitudinal decrease, present a robust association with NfL increases during follow-up in carriers. This suggests that preclinical metabolic changes could predict subsequent structural damage, thus heralding the transition to the prodromal phase. To further investigate this hypothesis without aprioristic assumptions, we classified PS-*GRN*⁺ based on their detectable alterations in brain metabolism and NfL levels with respect to their age and EYO. This led to propose a schematic modelling where the youngest carriers, below 40 years of age, did not show any appreciable metabolic nor biological changes (Figure 5). Isolated metabolic changes without increased NfL were mostly found in older carriers, less distant from expected onset (aged 40-55 on average). Remarkably, the two carriers who had both increased NfL levels and more extensive metabolic changes were aged around 60, expectedly in closer proximity to phenoconversion, although none had obvious cognitive or behavioral changes. These age differences suggest a temporal sequence of biomarker changes during the PS phase, metabolic decrease occurring in the earliest preclinical stage, highlighting the added value of FDG-PET for carriers' stratification.

A first limitation of this study is the limited number of carriers undergoing the entire follow-up, even if our sample is relatively large for a genetic form of a rare disease, with longer follow-

up duration than previous studies. This is partly due to the criteria requiring a complete multimodal biomarker assessment to enter the study. Secondly, not all neuroimaging approaches have been employed here, but they were extensively explored in other works.^{10,41,47} The determination of EYO in PS-*GRN*⁺ was based on the mean age at onset in their families, a method commonly employed in other studies,^{8,25,26} but which does not necessarily reflect the individuals' actual age at onset. Therefore, we also used alternative ways to estimate clinical proximity, based on CDR+NACC FTL D scores,¹¹ and NfL levels.¹⁵ Finally, this study identified only two individuals expected to be close to onset and, consequently, does not allow to trace metabolic changes at the late presymptomatic and prodromal stages.

In summary, our study highlights the vulnerability of a selective hub, the STS region, in the *GRN*-associated degenerative process since its earliest stages, preceding the spreading of neuronal dysfunction to other interconnected areas. It contributes to define a topographic signature characterizing *GRN* disease and supports the usefulness of cerebral FDG-PET in tracing early disease progression in PS-*GRN*⁺, occurring in the same timeframe as in presymptomatic genetic AD, leading to consider brain metabolic changes as a valuable tool to monitor the response to therapeutic interventions during the preclinical phase.

ACKNOWLEDGEMENTS

We thank the DNA and cell bank of the ICM for the technical assistance, notably Philippe Martin-Hardy and Sylvie Forlani (DNA and cell bank, ICM), and Karim Dorgham from “Centre d'Immunologie et des Maladies Infectieuses” (CIMI), Pitié-Salpêtrière hospital, Paris. The study was conducted with the support of the “Centre d'Investigation Clinique Neurosciences” (CIC 1422), Pitié-Salpêtrière Hospital, Paris.

Appendix 1: Authors

Name	Location	Contribution
Dario Saracino, MD†	Hôpital Pitié-Salpêtrière, Paris, FR	Designed and conceptualized the study; analyzed and interpreted the data; drafted the manuscript for intellectual content
Leila Sellami, MD, MSc†	Hôpital Pitié-Salpêtrière, Paris, FR	Designed and conceptualized the study; analyzed and interpreted the data; drafted the manuscript for intellectual content
Hugo Boniface, MSc†	Laboratoire d'Imagerie Biomédicale, Paris, FR	Designed and conceptualized the study; analyzed and interpreted the data; drafted the manuscript for intellectual content
Marion Houot, MSc	Hôpital Pitié-Salpêtrière, Paris, FR	Analyzed the data
Mélanie Péligrini-Issac, PhD	Laboratoire d'Imagerie Biomédicale, Paris, FR	Analyzed the data; revised the manuscript for intellectual content
Aurélié Funkiewiez, PhD	Hôpital Pitié-Salpêtrière, Paris, FR	Major role in the acquisition of data; analyzed the data
Daisy Rinaldi, PhD	Hôpital Pitié-Salpêtrière, Paris, FR	Major role in the acquisition of data; revised the manuscript for intellectual content
Maxime Locatelli, PhD	Laboratoire d'Imagerie Biomédicale, Paris, FR	Analyzed the data; revised the manuscript for intellectual content
Carole Azuar, MD	Hôpital Pitié-Salpêtrière, Paris, FR	Revised the manuscript for intellectual content
Valérie Causse-Lemercier, MD	Hôpital Pitié-Salpêtrière, Paris, FR	Major role in the acquisition of data; revised the manuscript for intellectual content
Alice Jaillard, MD, PhD	Lille University Hospital, Lille, FR	Major role in the acquisition of data; revised the manuscript for intellectual content
Florence Pasquier, MD, PhD	Lille University Hospital, Lille, FR	Major role in the acquisition of data; revised the manuscript for intellectual content
Mathieu Chastan, MD	Rouen University Hospital, Rouen, FR	Major role in the acquisition of data; revised the manuscript for intellectual content

David Wallon, MD, PhD	Rouen University Hospital, Rouen, FR	Major role in the acquisition of data; revised the manuscript for intellectual content
Anne Hitzel, MD	Toulouse University Hospital, Toulouse, FR	Major role in the acquisition of data; revised the manuscript for intellectual content
Jérémie Pariente, MD, PhD	Toulouse University Hospital, Toulouse, FR	Major role in the acquisition of data; revised the manuscript for intellectual content
Amandine Pallardy, MD, PhD	Nantes University Hospital, Nantes, FR	Major role in the acquisition of data; revised the manuscript for intellectual content
Claire Boutoleau-Brettonnière, MD, PhD	Nantes University Hospital, Nantes, FR	Major role in the acquisition of data; revised the manuscript for intellectual content
Eric Guedj, MD, PhD	Aix-Marseille University Hospital, Marseille, FR	Major role in the acquisition of data; revised the manuscript for intellectual content
Mira Didic, MD, PhD	Aix-Marseille University Hospital, Marseille, FR	Major role in the acquisition of data; revised the manuscript for intellectual content
Raffaella Migliaccio, MD, PhD	Hôpital Pitié-Salpêtrière, Paris, FR	Analyzed and interpreted the data; revised the manuscript for intellectual content
Aurélie Kas, MD, PhD	Hôpital Pitié-Salpêtrière, Paris, FR	Interpreted the data; revised the manuscript for intellectual content
Marie-Odile Habert, MD, PhD††	Hôpital Pitié-Salpêtrière, Paris, FR	Designed and conceptualized the study; analyzed and interpreted the data; revised the manuscript for intellectual content
Isabelle Le Ber, MD, PhD††	Hôpital Pitié-Salpêtrière, Paris, FR	Designed and conceptualized the study; major role in the acquisition of data; analyzed and interpreted the data; drafted the manuscript for intellectual content

† These authors equally contributed to the work.

†† These authors equally contributed as co-last authors.

Appendix 2: Co-investigators

Name	Location	Role	Contribution
Eve Benchetrit, PhD	Hôpital Pitié-Salpêtrière, Paris, FR	Site investigator	Coordinated communication among sites
Hugo Bertin	Hôpital Pitié-Salpêtrière, Paris, FR	Site investigator	Coordinated neuroimaging among sites
Anne Bissery, MD	Hôpital Pitié-Salpêtrière, Paris, FR	Site investigator	Led communication among sites
Françoise Bodere, MD	Nantes University Hospital, Nantes, FR	Site investigator	Coordinated imaging for site
Stéphanie Bombois, MD, PhD	Lille University Hospital, Lille, FR	Site investigator	Coordinated communication among sites
Paola Caroppo, MD, PhD	Hôpital Pitié-Salpêtrière, Paris, FR	Site investigator	Coordinated communication among sites
Yaohua Chen	Lille University Hospital, Lille, FR	Site investigator	Coordinated imaging for site
Marie Chupin, PhD	Hôpital Pitié-Salpêtrière, Paris, FR	Site investigator	Coordinated neuroimaging among sites
Olivier Colliot, PhD	Hôpital Pitié-Salpêtrière, Paris, FR	Site investigator	Coordinated neuroimaging among sites
Xavier Delbeuck	Lille University Hospital, Lille, FR	Site investigator	Coordinated imaging for site
Vincent Deramecourt, MD, PhD	Lille University Hospital, Lille, FR	Site investigator	Coordinated communication among sites
Christine Delmaire, MD, PhD	Lille University Hospital, Lille, FR	Site investigator	Coordinated imaging for site
Emmanuel Gerardin, MD, PhD	Rouen University Hospital, Rouen, FR	Site investigator	Coordinated imaging for site

Pierrick Gouel, MD	Rouen University Hospital, Rouen, FR	Site investigator	Coordinated imaging for site
Claude Hossein- Foucher, MD (†)	Lille University Hospital, Lille, FR	Site investigator	Coordinated imaging for site
Didier Hannequin, MD, PhD	Rouen University Hospital, Rouen, FR	Site investigator	Coordinated communication among sites
Thibaud Lebouvier, MD, PhD	Lille University Hospital, Lille, FR	Site investigator	Coordinated communication among sites
Carine Lefort	Hôpital Pitié-Salpêtrière, Paris, FR	Site investigator	Coordinated communication among sites
Marie-Anne Mackowiak, MD, PhD	Lille University Hospital, Lille, FR	Site investigator	Coordinated imaging for site
Assi-Hervé Oya	Hôpital Pitié-Salpêtrière, Paris, FR	Site investigator	Led communication among sites
Pierre Payoux, MD, PhD	Toulouse University Hospital, Toulouse, FR	Site investigator	Coordinated imaging for site
Grégory Petyt, MD	Lille University Hospital, Lille, FR	Site investigator	Coordinated imaging for site
Adeline Rollin- Sillaire, MD, PhD	Lille University Hospital, Lille, FR	Site investigator	Coordinated imaging for site
Franck Semah, MD, PhD	Lille University Hospital, Lille, FR	Site investigator	Coordinated imaging for site
Pierre Vera, MD, PhD	Rouen University Hospital, Rouen, FR	Site investigator	Coordinated imaging for site
Martine Vercelletto, MD, PhD	Nantes University Hospital, Nantes, FR	Site investigator	Coordinated communication among sites

REFERENCES

1. Baker M, Mackenzie IR, Pickering-Brown SM, et al. Mutations in progranulin cause tau-negative frontotemporal dementia linked to chromosome 17. *Nature*. 2006;442(7105):916-919. doi:10.1038/nature05016
2. Cruts M, Gijselinck I, van der Zee J, et al. Null mutations in progranulin cause ubiquitin-positive frontotemporal dementia linked to chromosome 17q21. *Nature*. 2006;442(7105):920-924. doi:10.1038/nature05017
3. Le Ber I, Camuzat A, Hannequin D, et al. Phenotype variability in progranulin mutation carriers: a clinical, neuropsychological, imaging and genetic study. *Brain*. 2008;131(3):732-746. doi:10.1093/brain/awn012
4. Moore KM, Nicholas J, Grossman M, et al. Age at symptom onset and death and disease duration in genetic frontotemporal dementia: an international retrospective cohort study. *Lancet Neurol*. 2020;19(2):145-156. doi:10.1016/S1474-4422(19)30394-1
5. Saracino D, Ferrieux S, Noguès-Lassaille M, et al. Primary Progressive Aphasia Associated With GRN Mutations: New Insights Into the Non-amyloid Logopenic Variant. *Neurology*. 2021;97(1):e88-e102. doi:10.1212/WNL.00000000000012174
6. Whitwell JL, Weigand SD, Boeve BF, et al. Neuroimaging signatures of frontotemporal dementia genetics: C9ORF72, tau, progranulin and sporadics. *Brain*. 2012;135(3):794-806. doi:10.1093/brain/aws001
7. Bateman RJ, Xiong C, Benzinger TLS, et al. Clinical and Biomarker Changes in Dominantly Inherited Alzheimer's Disease. *N Engl J Med*. 2012;367(9):795-804. doi:10.1056/NEJMoa1202753
8. Rohrer JD, Nicholas JM, Cash DM, et al. Presymptomatic cognitive and neuroanatomical changes in genetic frontotemporal dementia in the Genetic Frontotemporal dementia Initiative (GENFI) study: a cross-sectional analysis. *Lancet Neurol*. 2015;14(3):253-262. doi:10.1016/S1474-4422(14)70324-2
9. Bertrand A, Wen J, Rinaldi D, et al. Early Cognitive, Structural, and Microstructural Changes in Presymptomatic C9orf72 Carriers Younger Than 40 Years. *JAMA Neurol*. 2018;75(2):236. doi:10.1001/jamaneurol.2017.4266
10. Jiskoot LC, Panman JL, Meeter LH, et al. Longitudinal multimodal MRI as prognostic and diagnostic biomarker in presymptomatic familial frontotemporal dementia. *Brain*. 2019;142(1):193-208. doi:10.1093/brain/awy288
11. Miyagawa T, Brushaber D, Syrjanen J, et al. Use of the CDR® plus NACC FTLD in mild FTLD: Data from the ARTFL/LEFFTDS consortium. *Alzheimers Dement*. 2020;16(1):79-90. doi:10.1016/j.jalz.2019.05.013
12. Benussi A, Alberici A, Samra K, et al. Conceptual framework for the definition of preclinical and prodromal frontotemporal dementia. *Alzheimers Dement*. Published online December 7, 2021. doi:10.1002/alz.12485

13. Meeter LH, Doppert EG, Jiskoot LC, et al. Neurofilament light chain: a biomarker for genetic frontotemporal dementia. *Ann Clin Transl Neurol.* 2016;3(8):623-636. doi:10.1002/acn3.325
14. van der Ende EL, Meeter LH, Poos JM, et al. Serum neurofilament light chain in genetic frontotemporal dementia: a longitudinal, multicentre cohort study. *Lancet Neurol.* 2019;18(12):1103-1111. doi:10.1016/S1474-4422(19)30354-0
15. Rojas JC, Wang P, Staffaroni AM, et al. Plasma Neurofilament Light for Prediction of Disease Progression in Familial Frontotemporal Lobar Degeneration. *Neurology.* 2021;96(18):e2296-e2312. doi:10.1212/WNL.0000000000011848
16. Saracino D, Dorgham K, Camuzat A, et al. Plasma NfL levels and longitudinal change rates in C9orf72 and GRN-associated diseases: from tailored references to clinical applications. *J Neurol Neurosurg Psychiatry.* 2021;92(12):1278-1288. doi:10.1136/jnnp-2021-326914
17. McDade E, Wang G, Gordon BA, et al. Longitudinal cognitive and biomarker changes in dominantly inherited Alzheimer disease. *Neurology.* 2018;91(14):e1295-e1306. doi:10.1212/WNL.0000000000006277
18. Jacova C, Hsiung GYR, Tawankanjanachot I, et al. Anterior brain glucose hypometabolism predates dementia in progranulin mutation carriers. *Neurology.* 2013;81(15):1322-1331. doi:10.1212/WNL.0b013e3182a8237e
19. Caroppo P, Habert MO, Durrleman S, et al. Lateral Temporal Lobe: An Early Imaging Marker of the Presymptomatic GRN Disease? *J Alzheimers Dis.* 2015;47(3):751-759. doi:10.3233/JAD-150270
20. Mutsaerts HJMM, Mirza SS, Petr J, et al. Cerebral perfusion changes in presymptomatic genetic frontotemporal dementia: a GENFI study. *Brain.* 2019;142(4):1108-1120. doi:10.1093/brain/awz039
21. Miyagawa T, Brushaber D, Syrjanen J, et al. Utility of the global CDR[®] plus NACC FTLD rating and development of scoring rules: Data from the ARTFL/LEFFTDS Consortium. *Alzheimer's Dement.* 2020;16(1):106-117. doi:10.1002/alz.12033
22. Funkiewiez A, Bertoux M, de Souza LC, Lévy R, Dubois B. The SEA (Social cognition and Emotional Assessment): a clinical neuropsychological tool for early diagnosis of frontal variant of frontotemporal lobar degeneration. *Neuropsychology.* 2012;26(1):81-90. doi:10.1037/a0025318
23. Merck C, Charnallet A, Auriacombe S, et al. La batterie d'évaluation des connaissances sémantiques du GRECO (BECS-GRECO) : validation et données normatives. *Revue de neuropsychologie.* 2011;3(4):235. doi:10.3917/rne.034.0235
24. Peigneux P, van der Linden M. Influence of ageing and educational level on the prevalence of body-part-as-objects in normal subjects. *J Clin Exp Neuropsychol.* 1999;21(4):547-552. doi:10.1076/jcen.21.4.547.881
25. Cash DM, Bocchetta M, Thomas DL, et al. Patterns of gray matter atrophy in genetic frontotemporal dementia: results from the GENFI study. *Neurobiol Aging.* 2018;62:191-

196. doi:10.1016/j.neurobiolaging.2017.10.008
26. Borrego-Écija S, Sala-Llonch R, van Swieten J, et al. Disease-related cortical thinning in presymptomatic granulin mutation carriers. *Neuroimage Clin.* 2021;29:102540. doi:10.1016/j.nicl.2020.102540
 27. van der Ende EL, Bron EE, Poos JM, et al. A data-driven disease progression model of fluid biomarkers in genetic frontotemporal dementia. *Brain.* Published online October 11, 2021. doi:10.1093/brain/awab382
 28. Habert MO, Marie S, Bertin H, et al. Optimization of brain PET imaging for a multicentre trial: the French CATI experience. *EJNMMI Phys.* 2016;3(1):6. doi:10.1186/s40658-016-0141-8
 29. Fouquet M, Desgranges B, Landeau B, et al. Longitudinal brain metabolic changes from amnesic mild cognitive impairment to Alzheimer's disease. *Brain.* 2009;132(8):2058-2067. doi:10.1093/brain/awp132
 30. Moreno F, Sala-Llonch R, Barandiaran M, et al. Distinctive age-related temporal cortical thinning in asymptomatic granulin gene mutation carriers. *Neurobiol Aging.* 2013;34(5):1462-1468. doi:10.1016/j.neurobiolaging.2012.11.005
 31. Ibañez A, Manes F. Contextual social cognition and the behavioral variant of frontotemporal dementia. *Neurology.* 2012;78(17):1354-1362. doi:10.1212/WNL.0b013e3182518375
 32. Saxe R, Xiao DK, Kovacs G, Perrett DI, Kanwisher N. A region of right posterior superior temporal sulcus responds to observed intentional actions. *Neuropsychologia.* 2004;42(11):1435-1446. doi:10.1016/j.neuropsychologia.2004.04.015
 33. Isik L, Koldewyn K, Beeler D, Kanwisher N. Perceiving social interactions in the posterior superior temporal sulcus. *Proc Natl Acad Sci U S A.* 2017;114(43):E9145-E9152. doi:10.1073/pnas.1714471114
 34. Belin P, Zatorre RJ, Lafaille P, Ahad P, Pike B. Voice-selective areas in human auditory cortex. *Nature.* 2000;403(6767):309-312.
 35. Engell AD, Haxby JV. Facial expression and gaze-direction in human superior temporal sulcus. *Neuropsychologia.* 2007;45(14):3234-3241. doi:10.1016/j.neuropsychologia.2007.06.022
 36. Sato W, Kochiyama T, Uono S, et al. Widespread and lateralized social brain activity for processing dynamic facial expressions. *Hum Brain Mapp.* 2019;40(13):3753-3768. doi:10.1002/hbm.24629
 37. Alaerts K, Woolley DG, Steyaert J, Di Martino A, Swinnen SP, Wenderoth N. Underconnectivity of the superior temporal sulcus predicts emotion recognition deficits in autism. *Soc Cogn Affect Neurosci.* 2014;9(10):1589-1600. doi:10.1093/scan/nst156
 38. Vandenbulcke M, Van de Vliet L, Sun J, et al. A paleo-neurologic investigation of the social brain hypothesis in frontotemporal dementia. *Cereb Cortex.* Published online March 7, 2022:bhac089. doi:10.1093/cercor/bhac089

39. Jiskoot LC, Panman JL, van Asseldonk L, et al. Longitudinal cognitive biomarkers predicting symptom onset in presymptomatic frontotemporal dementia. *J Neurol*. 2018;265(6):1381-1392. doi:10.1007/s00415-018-8850-7
40. Russell LL, Greaves CV, Bocchetta M, et al. Social cognition impairment in genetic frontotemporal dementia within the GENFI cohort. *Cortex*. 2020;133:384-398. doi:10.1016/j.cortex.2020.08.023
41. Panman JL, Venkatraghavan V, van der Ende EL, et al. Modelling the cascade of biomarker changes in GRN-related frontotemporal dementia. *J Neurol Neurosurg Psychiatry*. 2021;92(5):494-501. doi:10.1136/jnnp-2020-323541
42. Sellal F. Anatomical and neurophysiological basis of face recognition. *Rev Neurol (Paris)*. Published online December 1, 2021:S0035-3787(21)00764-5. doi:10.1016/j.neurol.2021.11.002
43. Warren JD, Rohrer JD, Schott JM, Fox NC, Hardy J, Rossor MN. Molecular nexopathies: a new paradigm of neurodegenerative disease. *Trends Neurosci*. 2013;36(10):561-569. doi:10.1016/j.tins.2013.06.007
44. Brettschneider J, Del Tredici K, Irwin DJ, et al. Sequential distribution of pTDP-43 pathology in behavioral variant frontotemporal dementia (bvFTD). *Acta Neuropathol*. 2014;127(3):423-439. doi:10.1007/s00401-013-1238-y
45. Borroni B, Alberici A, Premi E, et al. Brain magnetic resonance imaging structural changes in a pedigree of asymptomatic progranulin mutation carriers. *Rejuvenation Res*. 2008;11(3):585-595. doi:10.1089/rej.2007.0623
46. Premi E, Cauda F, Gasparotti R, et al. Multimodal fMRI Resting-State Functional Connectivity in Granulin Mutations: The Case of Fronto-Parietal Dementia. Zang YF, ed. *PLoS ONE*. 2014;9(9):e106500. doi:10.1371/journal.pone.0106500
47. Feis RA, Bouts MJRJ, de Vos F, et al. A multimodal MRI-based classification signature emerges just prior to symptom onset in frontotemporal dementia mutation carriers. *J Neurol Neurosurg Psychiatry*. 2019;90(11):1207-1214. doi:10.1136/jnnp-2019-320774
48. Staffaroni AM, Cobigo Y, Goh SYM, et al. Individualized atrophy scores predict dementia onset in familial frontotemporal lobar degeneration. *Alzheimers Dement*. 2020;16(1):37-48. doi:10.1016/j.jalz.2019.04.007
49. Bocchetta M, Todd EG, Peakman G, et al. Differential early subcortical involvement in genetic FTD within the GENFI cohort. *Neuroimage Clin*. 2021;30:102646. doi:10.1016/j.nicl.2021.102646
50. Gordon BA, Blazey TM, Su Y, et al. Spatial patterns of neuroimaging biomarker change in individuals from families with autosomal dominant Alzheimer's disease: a longitudinal study. *Lancet Neurol*. 2018;17(3):241-250. doi:10.1016/S1474-4422(18)30028-0

FIGURES

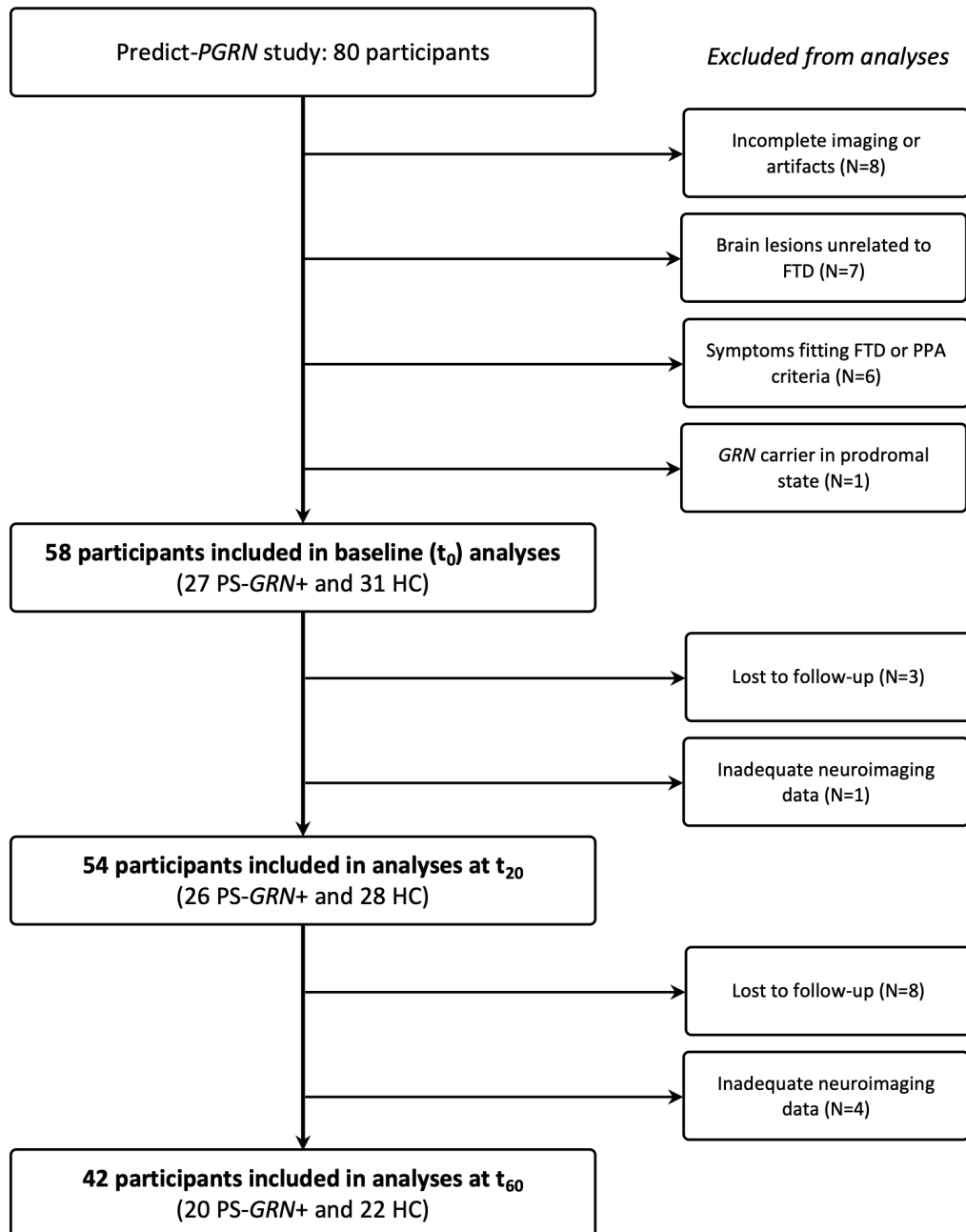


Figure 1. Flow-chart of participants included in the analyses over the three time points of the study. FTD: frontotemporal dementia; HC: healthy controls; PPA: primary progressive aphasia; PS-GRN+: presymptomatic GRN carriers.

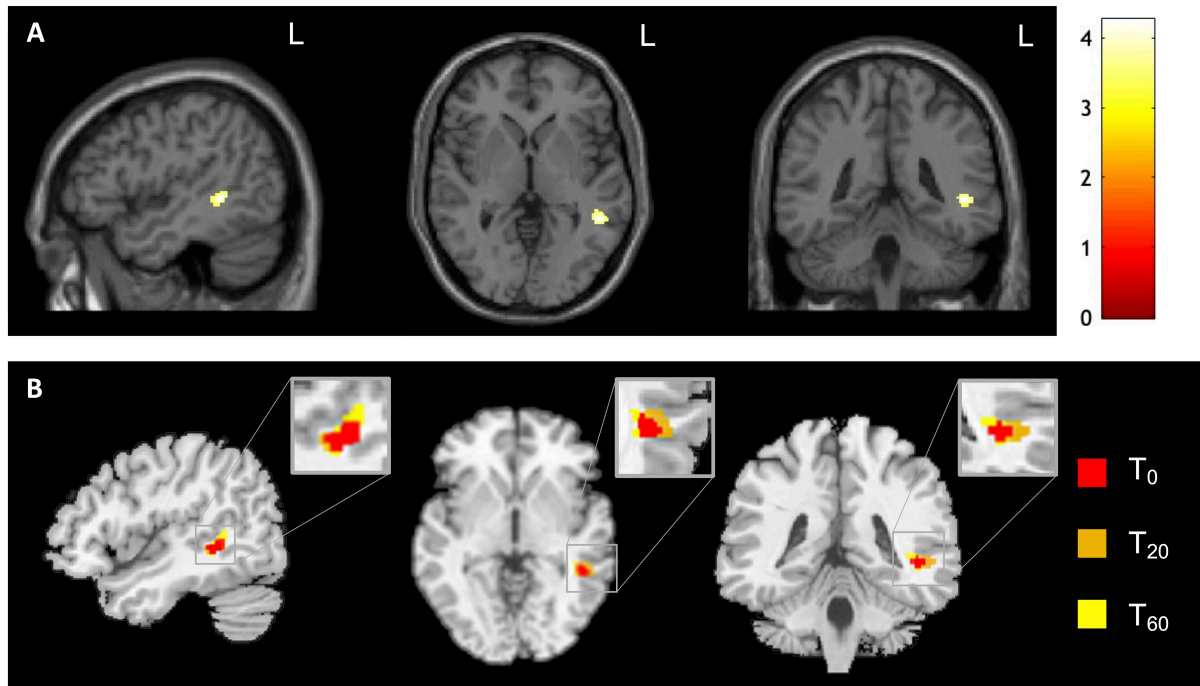


Figure 2. Cross-sectional comparison of brain metabolism between PS-GRN+ and HC. A: results of SPM voxel-wise comparisons at t_0 , using the contrast PS-GRN+ < HC. Statistical parametric maps are thresholded at $p < 0.001$, with a cluster-extent threshold at 100. Color bar refers to the T values. **B:** detail on the left middle temporal hypometabolic cluster over the three time points, each with its own color code. The results are visualized using xjView toolbox (<http://www.alivelearn.net/xjview>). HC: healthy controls; PS-GRN+: presymptomatic GRN carriers.

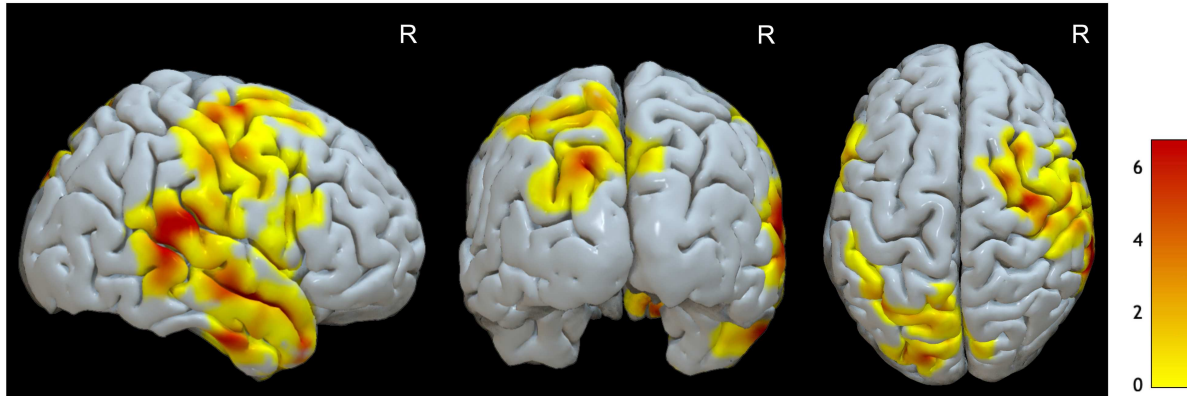


Figure 3. Longitudinal metabolic changes in PS-GRN+ over the entire follow-up, from voxel-wise comparison between t_0 and t_{60} . The primary cluster-forming threshold was $p=0.001$, with the extent threshold set at $p=0.05$ for false discovery rate. Results are displayed on the 3D brain template (lateral, posterior and axial views) realized with Surf Ice software (<https://www.nitrc.org/projects/surface/>). PS-GRN+: presymptomatic *GRN* carriers.

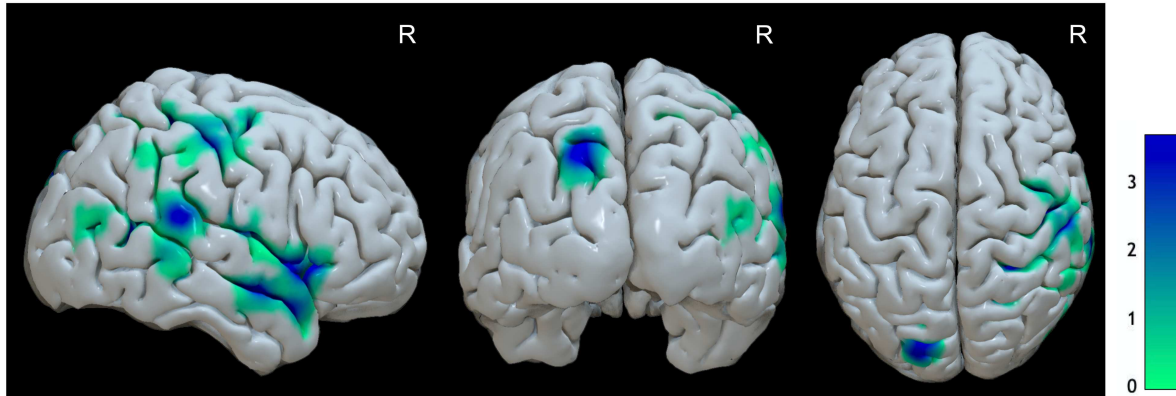


Figure 4. Clusters of greater longitudinal metabolic decrease in PS-GRN+ compared to controls, based on the analysis of PET-PAC maps calculated over the entire follow-up (from t_0 to t_{60}). Results were obtained with a primary cluster-forming threshold of $p=0.005$, and a secondary cluster extent threshold of 1000 voxels. Results are displayed on the 3D brain template (lateral, posterior and axial views) realized with Surf Ice software. PAC: percent annual changes. PS-GRN+: presymptomatic *GRN* carriers.

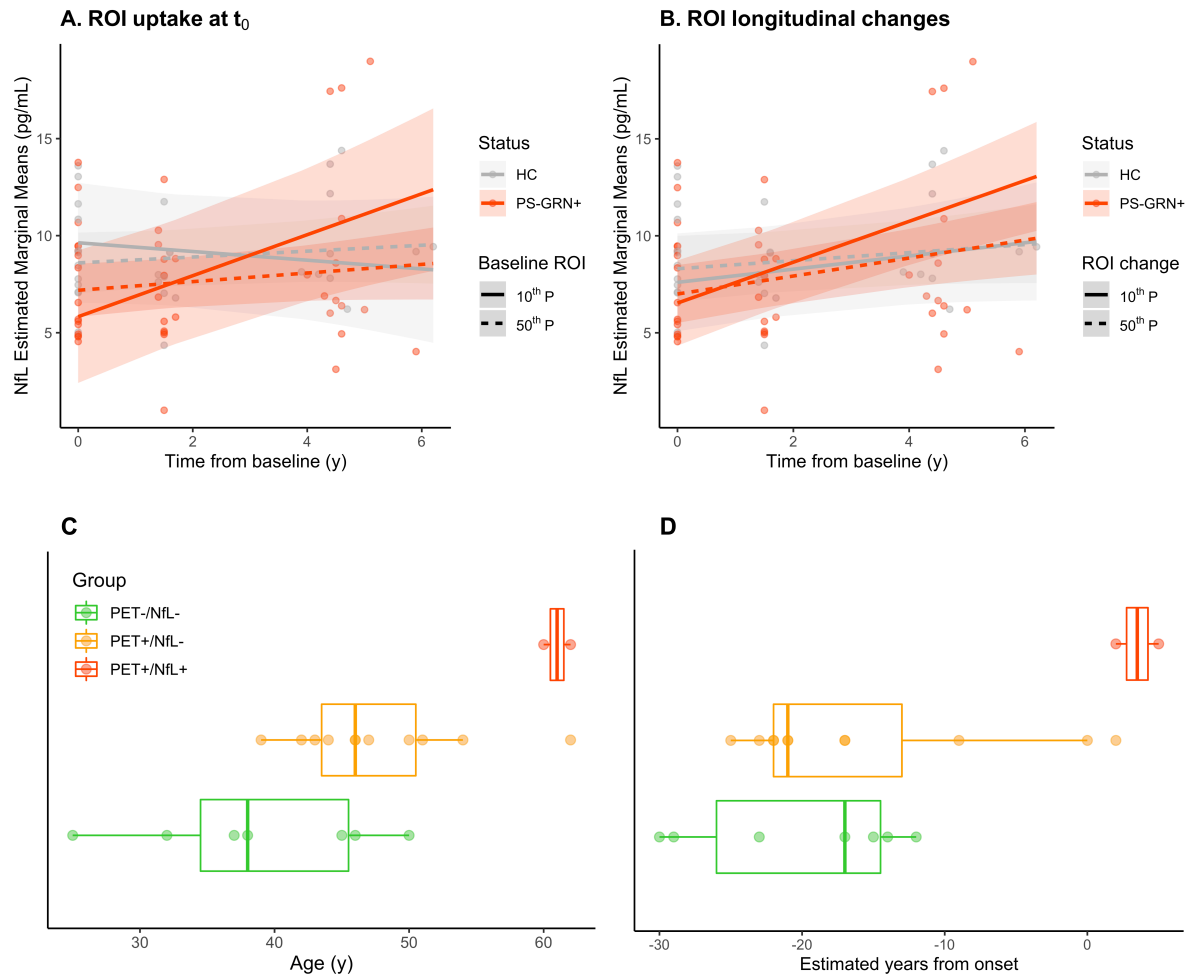


Figure 5. Association between glucose uptake in the right temporal superior/middle ROI and plasma NfL changes in participants undergoing the entire follow-up. A: the impact of baseline glucose uptake on NfL trajectory was different according to subject status ($p=0.003$). No impact of baseline ROI on NfL trajectory was found in HC, whereas in PS-GRN+ the lower the baseline ROI, the higher the NfL increase during follow-up. For comparison, the trend of plasma NfL increases in participants whose uptake was at the 10th and at the 50th percentile is shown. B: a similar tendency was observed with respect to metabolic decreases during the follow-up, though not reaching statistical significance ($p=0.093$). Among PS-GRN+, the greater the metabolic decrease over time, the higher the increases in NfL levels tended to be. C and D: modelization of metabolic and NfL changes in PS-GRN+, who have been classified based on low glucose uptake or accelerated decline with respect to reference parameters in HC (PET+) and higher NfL values or greater increases compared with age-matched HC (NfL+). Each individual is represented by a colored dot, plotted against subjects' age (C) and estimated years to disease onset (D). HC healthy controls; NfL: neurofilament light chain; PS-GRN+: presymptomatic GRN carriers; ROI: region of interest; y: years.

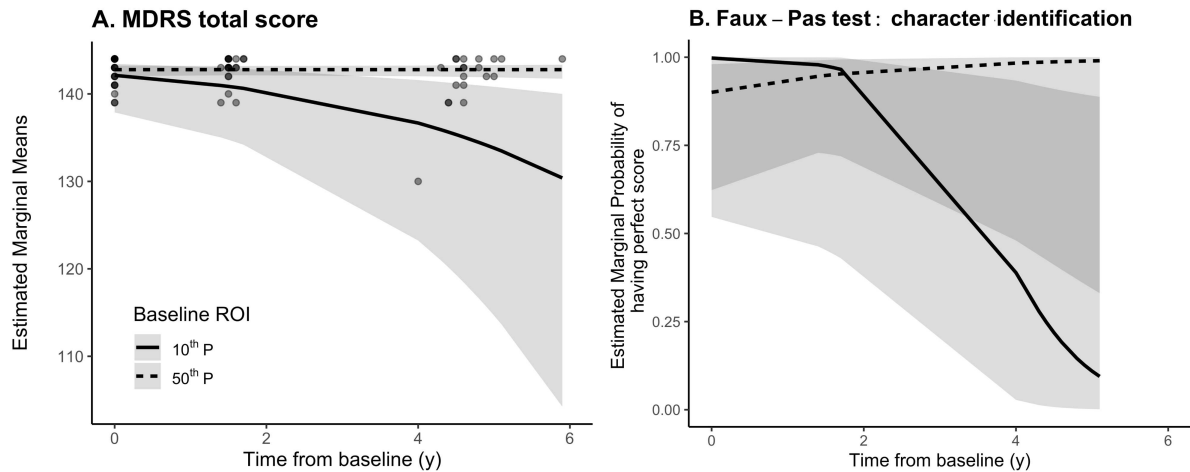


Figure 6. Impact of baseline glucose uptake in the right temporal superior/middle ROI on longitudinal changes of MDRS total score (A) and the character identification item of the faux-pas test (B). Among PS-*GRN*⁺ those who had the lowest glucose uptake at baseline showed the greatest decreases in these cognitive scores during follow-up (for both tests, $p=0.014$). For comparison, the trajectories of cognitive changes in PS-*GRN*⁺ whose uptake was at the 10th and at the 50th percentile are shown. MDRS: Mattis Dementia Rating Scale; PS-*GRN*⁺: presymptomatic *GRN* carriers; ROI: region of interest; y: years.

Table 1. Demographic and clinical characteristics of asymptomatic participants included in baseline (t₀) analyses.

	HC (n=31)	PS-GRN+ (n=27)	<i>p</i> -value
Demographics			
Age, years	45.4 (±14.4)	42.9 (±10.8)	0.78
Female, n (%)	18 (58%)	17 (63%)	0.91
Right-handed, n (%)	29 (93.5%)	25 (92.5%)	0.34
Education, years	14.5 (±2.6)	14.4 (±3.0)	0.81
Years from expected onset	-15.1 (±14.3)	-17.4 (±12.4)	0.60
Neuropsychological scores			
MMSE	28.9 (±1.2)	29.3 (±1.0)	0.26
MDRS	141.5 (±2.4)	141.5 (±3.9)	0.47
FCSRT			
Free recall	34.2 (±4.6)	34.9 (±5.5)	0.42
Total recall	47.2 (±1.1)	46.6 (±2.0)	0.29
Delayed free recall	13.4 (±1.8)	13.9 (±1.7)	0.38
Delayed total recall	16.0 (±0.0)	15.9 (±0.4)	0.14
FAB	17.3 (±1.0)	17.6 (±0.9)	0.15
WCST	19.2 (±1.4)	19.0 (±2.2)	0.99
Naming BECS GRECO	39.2 (±3.7)	39.5 (±1.0)	0.14
Fluency tasks			
Categories (animals)	35.7 (±9.8)	37.3 (±9.7)	0.58
Letter (P)	21.5 (±7.3)	25.0 (±6.0)	0.06
Mini-SEA			
Faux-pas test	26.0 (±3.9)	26.4 (±4.0)	0.71
Facial Emotion Recognition test	30.1 (±2.5)	30.3 (±2.5)	0.78

Data are n (%) or mean (±Standard Deviation). Statistical comparisons were performed with Fisher's exact test for categorical variables and Mann-Whitney-Wilcoxon test for numerical variables. BECS GRECO: Batterie d'Evaluation des Connaissances Sémantiques du GRECO; FAB: Frontal Assessment Battery; FCSRT: Free and Cued Selective Reminding Test; HC: healthy controls; MDRS: Mattis Dementia rating Scale; Mini-SEA: Social Cognition and Emotional Assessment, short form; MMSE: Mini-Mental State Examination; PS-GRN+: presymptomatic *GRN* carriers; WCST: Wisconsin Card Sorting Test.

SUPPLEMENTAL DATA

eMETHODS

Population included in baseline analyses

Amongst the 80 participants, eight were excluded from baseline analyses owing to imaging artefacts or incomplete neuroimaging data, six because of the discovery of lesions unrelated to FTD, and seven due to the presence of symptoms fitting FTD or PPA criteria at inclusion. One individual, who harbored subtle signs at baseline and developed frontal cognitive and behavioral changes suggestive of clinical conversion during the time span of the study (t_0 - t_{60}), is described below and was analyzed separately. So, a total of 58 asymptomatic participants who had both T1-weighted brain MRI and FDG-PET that passed quality control (QC) were included in the baseline analyses of this study. This cohort gathered 27 presymptomatic *GRN* carriers (PS-*GRN*+) and 31 non-carriers considered as a healthy control (HC) group.

Population studied in longitudinal analyses

Fifty-five of the 58 baseline participants were evaluated at the second visit, ~20 months after inclusion (t_{20}) (three withdrawals between t_0 and t_{20} due to participant's decision). One of them was excluded from the analyses because of neuroimaging motion artefacts. Fifty-four participants consisting of 26 PS-*GRN*+ and 28 HC were thus analyzed (mean delay between first and second visit: 19.0 ± 2.3 months).

Forty-six of them underwent the third visit (t_{60}) (eight withdrawals between t_{20} and t_{60} due to participant's decision). Four were excluded from analyses because of unsatisfactory neuroimaging QC. Forty-two participants were finally included in t_{60} analyses, consisting of 20 PS-*GRN*+ and 22 HC (mean delay between first and third visit: 56.8 ± 6.9 months).

Description of the transitional stage in a *GRN* carrier

One carrier presented subtle clinical signs at baseline visit, at age 36, consisting in forgetfulness and difficulties finding words. The Clinical Dementia Rating plus NACC FTLD (CDR+NACC FTLD) score was 0.5. The scores of Mini-Mental State Examination (MMSE, 30/30), Mattis dementia rating scale (MDRS, 135/144), Frontal Assessment Battery (FAB, 16/18) were normal.

Emotion recognition (26/35, cut-off 25/35) and faux-pas test scores were slightly altered (24/30, cut-off 25/30). During the following years, frontal cognitive and social cognition deficits slowly worsened until t_{60} (MMSE 28 and 24 at t_{20} and t_{60} respectively; MDRS 131, then 121/144; FAB 12, then 10/18; faux-pas 22, then 11/30; emotion recognition 27, then 20/35). Interview of his informant revealed increased sweet consumption at the second visit, these moderate eating changes persisting without other behavioral symptoms at t_{60} . Examination revealed mild upper limb rigidity and a dystonic posture of the left hand at t_{20} and at t_{60} . His changes did not strictly fit criteria for behavioral variant of frontotemporal dementia or corticobasal syndrome at t_{60} , but obvious frontal cognitive and social cognition deficits worsened over time supporting clinical progression. The CDR+NACC FTLD score was 1 at t_{60} . Plasma NfL levels increased from 4.1 pg/mL at t_0 to 6.0 pg/mL at t_{60} .

PET preprocessing

A correction for partial volume effects (PVE) was performed using symmetric geometric transfer matrix-derived region-based voxel-wise (RBV-sGTM) method¹ with a scanner-specific full width at half maximum (FWHM), using computed tissue masks from probability maps, co-registered to PET volume. PET corrected images were intensity normalized to take into account inter-individual variability, according to a reference region, namely the pons, yielding parametric images. Pons region was obtained from a Pickatlas volume of interest (<http://fmri.wfubmc.edu/software/pickatlas>). For voxel-wise analysis, a spatial normalisation to Montreal Neurological Institute (MNI) was applied to normalized PET data, by co-registering PET data to MRI and deformed to MNI using deformation field generated by MRI segmentation. The intensity normalized images were then smoothed using an isotropic 8 mm FWHM Gaussian kernel. A careful image QC process was carried out for each step of the process. All these steps were performed using an automated pipeline developed with BrainVISA software (<http://brainvisa.info/web/index.html>) (eFigure 1).

Cross-sectional and longitudinal MRI processing with FreeSurfer

A 3D T1-weighted MRI cross-sectional and longitudinal processing was performed with the FreeSurfer software version 6.0 (<http://surfer.nmr.mgh.harvard.edu/>), using the respective pipelines of the Clinica platform (www.clinica.run). Briefly, after segmentation and volume extraction of cortical and subcortical structures, longitudinal processing was conducted on the

images acquired at different time points for each subject. An unbiased (with respect to any time point) template volume was produced, and then, for each time point, used as an initialization (tailored to the subject) for the FreeSurfer cortical reconstruction process. The cerebral cortex was parceled into regions of interest (ROIs) using the Desikan-Killiany atlas, while the extraction of subcortical ROI volumes and the total intracranial volume (TIV) estimation were done with the aseg atlas.

Metabolic percent annual changes (PAC) maps processing

Follow-up MRI was co-registered to the baseline MRI, and a mean image was calculated. Next, baseline and follow-up PET images were co-registered to the baseline MRI, PVE-corrected using RBV-sGTM method, scaled with the mean pons uptake, and smoothed with an isotropic 4mm Gaussian kernel (eFigure 1). Individual PET-PAC maps were then calculated. The calculation was only made on voxels presents in both PET data.

Plasma Neurofilament light chain (NfL) measurements

Blood samples were collected at each visit for all participants and centralized at the ICM biobank. They were processed for plasma isolation, and plasma NfL measurements were performed using Single Molecule Array according to the manufacturer's instructions (Quanterix, USA), as previously described.² Samples were assessed at a 1:4 dilution in duplicate. NfL concentration was interpolated from standard curves. The median intra-assay coefficient of variation (CV) was 4.5% (range: 0.1-14.7%). Those with a CV $\geq 15\%$ were re-analyzed, or excluded from analyses.² NfL values in the study participants were interpreted with respect to values established in controls of different age-classes, and the expected annualized rates of change previously established in controls and in *GRN* mutation carriers.^{2,3}

Statistical analyses – Linear models

To study whether the evolution of MRI volumes in 87 ROIs derived from Desikan-Killiany and aseg atlases was different between PS-*GRN*⁺ and HC, linear mixed models (LMMs) were performed using each of the ROI volumes as dependent variable; age at first MRI evaluation, sex, genetic group, time since first evaluation (in years) and the interaction between the last two as fixed effects; and subject as random intercept effect. Benjamini-Hochberg correction was applied.

To investigate whether the evolution of NfL values was impacted by genetic group, baseline

glucose uptake in selected ROIs or its longitudinal changes, we implemented LMMs. A LMM was performed for each ROI using NfL levels as dependent variable. Fixed effects were age at first blood sample, sex, the three-way interaction genetic group*time since first blood sample (in years)*baseline uptake and all the lower interactions and main effects involved, and the three-way interaction genetic group*time since first blood sample (in years)*annual metabolic change and all the lower interactions and main effects involved. Subject was used as the random intercept effect. Benjamini-Hochberg correction was applied.

To study whether the evolution of behavioral/cognitive scores was different between PS-GRN+ and HC, and to study the impact of baseline glucose uptake in selected ROIs or its longitudinal changes on behavioral/cognitive scores in PS-GRN+ group, we performed Generalized Linear Mixed Models. For the first analysis who compared PS-GRN+ and HC. Fixed effects were age at first evaluation, sex and the two-way interaction time since first evaluation (in years)*genetic group and the main effects involved. For the second analysis, restricted to PS-GRN+, fixed effects were age at first evaluation, sex, the two-way interaction time since first evaluation (in years)*baseline uptake and the main effects involved, and the two-way interaction time since first evaluation (in years)*annual metabolic change and the main effects involved. For both analyses, all available behavioral/cognitive scores were investigated. Subject was used as the random intercept effect. Family distribution was set at either Poisson, Binomial or Bernouilli according to data generation mechanism. Benjamini-Hochberg correction was applied.

eREFERENCES

1. Greve DN, Salat DH, Bowen SL, et al. Different partial volume correction methods lead to different conclusions: An 18F-FDG-PET study of aging. *Neuroimage*. 2016;132:334–343.
2. Saracino D, Dorgham K, Camuzat A, et al. Plasma NfL levels and longitudinal change rates in C9orf72 and GRN-associated diseases: from tailored references to clinical applications. *J Neurol Neurosurg Psychiatry*. 2021;92:1278–1288.
3. Rojas JC, Wang P, Staffaroni AM, et al. Plasma Neurofilament Light for Prediction of Disease Progression in Familial Frontotemporal Lobar Degeneration. *Neurology*. 2021;96:e2296–e2312.

eTABLES

eTable 1. Characteristics of asymptomatic participants included in follow-up (t_{60}) analyses.

	HC (n=22)	PS-GRN+ (n=20)	<i>p</i> -value
Demographics			
Age at t_0 , years	46.6 (\pm 14.5)	41.3 (\pm 9.6)	0.28
Age at t_{60} , years	51.3 (\pm 14.5)	45.6 (\pm 9.4)	0.31
Female, n (%)	12 (54.5%)	13 (65.0%)	0.71
Right-handed, n (%)	20 (91%)	19 (95%)	0.99
Education, years	14.9 (\pm 2.9)	15.0 (\pm 2.1)	0.98
Years from expected onset (t_{60})	-9.7 (\pm 15.1)	-15.4 (\pm 10.5)	0.25
Follow-up duration, months (SD; range)	57.2 (\pm 7.9; 44-76)	56.5 (\pm 5.7; 43-72)	0.96

Data are n (%), or mean (\pm Standard Deviation). Statistical comparisons were performed with Fisher's exact test for categorial variables and Mann-Whitney-Wilcoxon test for numerical variables. HC: healthy controls; PS-GRN+: presymptomatic *GRN* carriers; SD: standard deviation.

eTable 2. Demographic and clinical characteristics of PS-GRN+ over follow-up.

	t₀ (n= 27)	t₂₀ (n= 26)	t₆₀ (n=20)	p-value
Demographics				
Age, years	42.9 (±10.8)	43.50 (±9.6)	46.0 (±9.4)	0.39
Female, n (%)	17 (63%)	17 (65%)	13 (65%)	0.98
Right-handed, n (%)	25 (92.5%)	25 (96%)	19 (95%)	0.85
Education, years	14.4 (±3.0)	14.8 (±2.3)	15.0 (±2.1)	0.87
Years from expected onset	-17.4 (±12.4)	-16.9 (±11.3)	-15.4 (±10.5)	0.68
Months since t ₀ (SD; range)	-	18.8 (±2.6; 12-25)	56.5 (±5.7; 43-72)	-
Neuropsychological scores				
MMSE	29.3 (±1.0)	29.6 (±0.8)	29.7 (±0.6)	0.27
MDRS	141.5 (±3.9)	142.7 (±1.5)	141.8 (±3.3)	0.46
FCSRT				
Free recall	34.9 (±5.5)	37.4 (±4.9)	38.3 (±3.9)	0.08
Total recall	46.6 (±2.0)	47.1 (±1.3)	47.3 (±1.0)	0.29
Delayed free recall	13.9 (±1.7)	14.2 (±1.6)	14.5 (±1.6)	0.41
Delayed total recall	15.9 (±0.4)	15.9 (±0.3)	16.0 (±0.2)	0.92
FAB	17.6 (±0.9)	17.9 (±0.3)	17.9 (±0.3)	0.20
WCST	19.0 (±2.2)	19.5 (±1.2)	19.7 (±0.7)	0.39
Naming BECS GRECO	39.5 (±1.0)	39.7 (±0.9)	39.6 (±0.7)	0.58
Fluency tasks				
Categories (animals)	37.3 (±9.7)	35.8 (±10.2)	39 (±10.1)	0.50
Letter (P)	25.0 (±6.0)	25.5 (±7.0)	27.2 (±6.8)	0.68
Mini-SEA				
Faux-pas test	26.4 (±4.0)	27.1 (±2.7)	26.9 (±3.5)	0.89
Facial Emotion Recognition test	30.3 (±2.5)	30.1 (±3.0)	30.8 (±2.4)	0.72

Data are n (%) or mean (±Standard Deviation). Statistical comparisons were performed with Fisher's exact test for categorial variables and Kruskal-Wallis test for numerical variables. BECS GRECO: Batterie d'Evaluation des Connaissances Sémantiques du GRECO; FAB: Frontal Assessment Battery; FCSRT: Free and Cued Selective Reminding Test; MDRS: Mattis Dementia rating Scale; Mini-SEA: Social Cognition and Emotional Assessment, short form; MMSE: Mini-Mental State Examination; PS-GRN+: presymptomatic GRN carriers; SD: standard deviation; WCST: Wisconsin Card Sorting Test.

eTable 3. Cross-sectional comparisons of brain metabolism between PS-GRN+ and HC at all time points.

Cluster-level p_{uncorr}	k_E	Peak-level p_{uncorr}	T	(Z)	MNI coordinates (x, y, z)			Region (AAL3.1)
					mm	mm	mm	
PS-GRN+ < HC at t_0								
0.165	141	<0.001	4.24	3.92	-48	-44	-2	Left middle temporal gyrus
PS-GRN+ < HC at t_{20}								
0.066	216	<0.001	4.29	3.94	-52	-44	-2	Left middle temporal gyrus
PS-GRN+ < HC at t_{60}								
0.055	267	<0.001	4.73	4.16	-44	-45	2	Left middle temporal gyrus
0.104	184	<0.001	4.40	3.92	16	33	32	Right superior frontal gyrus

The analysis was performed with SPM12 using a threshold of $p < 0.001$, uncorrected, and a cluster extent threshold of 100. Age, gender and center were used as covariates. No significant results were found when applying the contrast PS-GRN+ > HC at any of the time points. AAL: automatic anatomical labelling atlas; HC: healthy controls; K_E : extent coefficient; MNI: Montreal Neurological Institute; PS-GRN+: presymptomatic GRN carriers; T: value of T-test; (Z): value of Z test.

eTable 4. Clusters of longitudinal brain glucose metabolism decline in PS-GRN+ between t_0 and t_{60} .

Cluster-level				Peak-level				MNI coordinates (x,y,z)			Region (AAL3.1)	
p _{FWE-corr}	p _{FDR-corr}	k _E	p _{uncorr}	p _{FWE-corr}	p _{FDR-corr}	T	(Z)	p _{uncorr}	mm	mm	mm	
<0.001	<0.001	7072	<0.001	0.032	0.418	6.97	4.85	<0.001	66	-30	18	Right Superior Temporal Gyrus
				0.075	0.418	6.42	4.63	<0.001	68	-40	9	Right Middle Temporal Gyrus
				0.161	0.418	5.92	4.40	<0.001	42	16	-36	Right Temporal Pole (MTG)
<0.001	<0.001	2625	<0.001	0.164	0.418	5.91	4.40	<0.001	-24	-87	27	Left Superior Occipital Gyrus
				0.280	0.418	5.54	4.22	<0.001	-15	-86	39	
<0.001	0.001	1809	<0.001	0.055	0.418	6.61	4.71	<0.001	34	-8	64	Right Superior Frontal Gyrus
				0.348	0.418	5.39	4.15	<0.001	45	-20	63	Right Precentral Gyrus
0.001	0.021	1634	<0.001	0.466	0.453	5.16	4.03	<0.001	-51	32	-6	Left IFG (Orbital part)
				0.742	0.563	4.70	3.78	<0.001	-57	15	30	Left IFG (Triangular part)

The SPM paired t-test was performed using a primary cluster-forming threshold of $p=0.001$, with the extent threshold set at $p=0.05$ for FDR correction at cluster-level. Covariates were age, sex, center and time interval. Peak-level statistics and coordinates are displayed for completeness of information. AAL: automatic anatomical labelling atlas; FDR: false discovery rate; FWE: family-wise error; KE: extent coefficient; IFG: inferior frontal gyrus; MNI: Montreal Neurological Institute; MTG: middle temporal gyrus; PS-GRN+: presymptomatic *GRN* carriers; T: value of *T*-test; (Z): value of *Z* test.

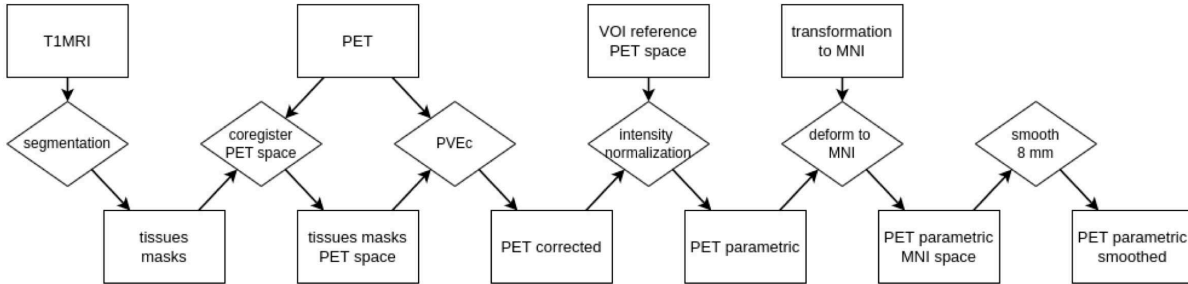
eTable 5. SPM comparison of PET-PAC maps calculated over the entire follow-up between PS-GRN+ and HC.

Cluster-level				Peak-level				MNI coordinates (x,y,z)			Region (AAL3.1)	
pFWE-corr	pFDR-corr	k _E	p _{uncorr}	pFWE-corr	pFDR-corr	T	(Z)	p _{uncorr}	mm	mm	mm	
0.221	0.708	5331	0.039	0.461	0.868	3.73	3.40	<0.001	46	-24	48	Right Postcentral Gyrus
				0.578	0.868	3.58	3.29	0.001	38	-16	54	Right Precentral Gyrus
0.253	0.708	4961	0.046	0.531	0.868	3.64	3.33	<0.001	57	-4	-16	Right Middle Temporal Gyrus
				0.665	0.868	3.48	3.21	0.001	48	14	-21	Right Temporal Pole (STG)
0.615	0.989	2395	0.150	0.741	0.868	3.38	3.13	0.001	64	-34	16	Right Superior Temporal Gyrus
				0.867	0.868	3.21	2.99	0.001	50	-57	10	Right Middle Temporal Gyrus
0.888	0.989	1014	0.343	0.477	0.868	3.70	3.39	<0.001	-16	-84	39	Left Superior Occipital Gyrus

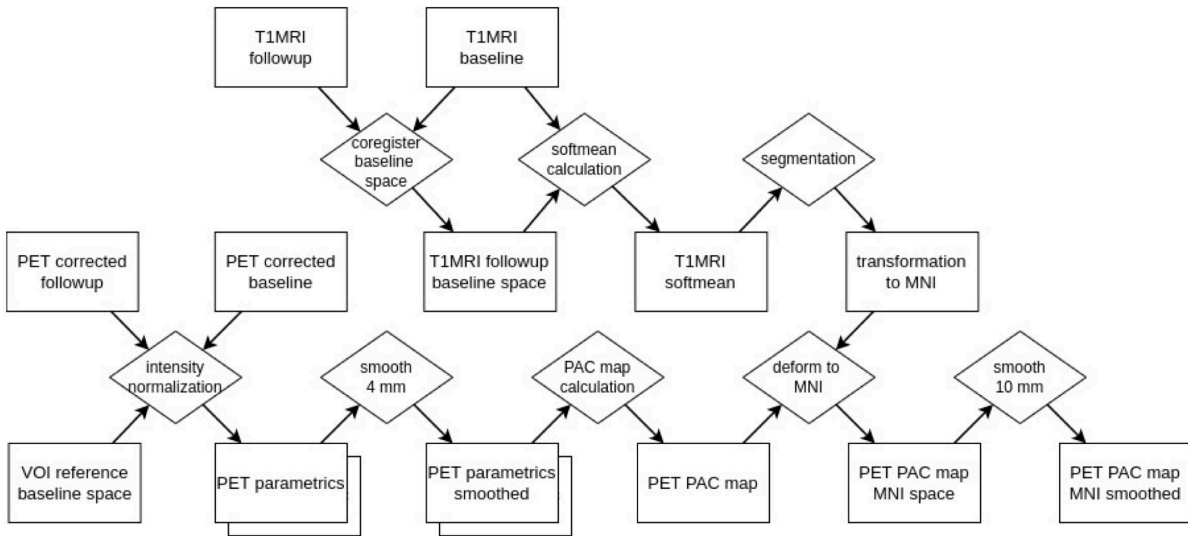
The analysis was performed with SPM12 using a primary cluster-forming threshold of $p=0.005$, and a secondary cluster extent threshold of 1000. AAL: automatic anatomical labelling atlas; FDR: false discovery rate; FWE: family-wise error; HC: healthy controls; K_E: extent coefficient; MNI: Montreal Neurological Institute; PS-GRN+: presymptomatic *GRN* carriers; STG: superior temporal gyrus; T: value of *T*-test; (Z): value of Z test.

eFIGURES

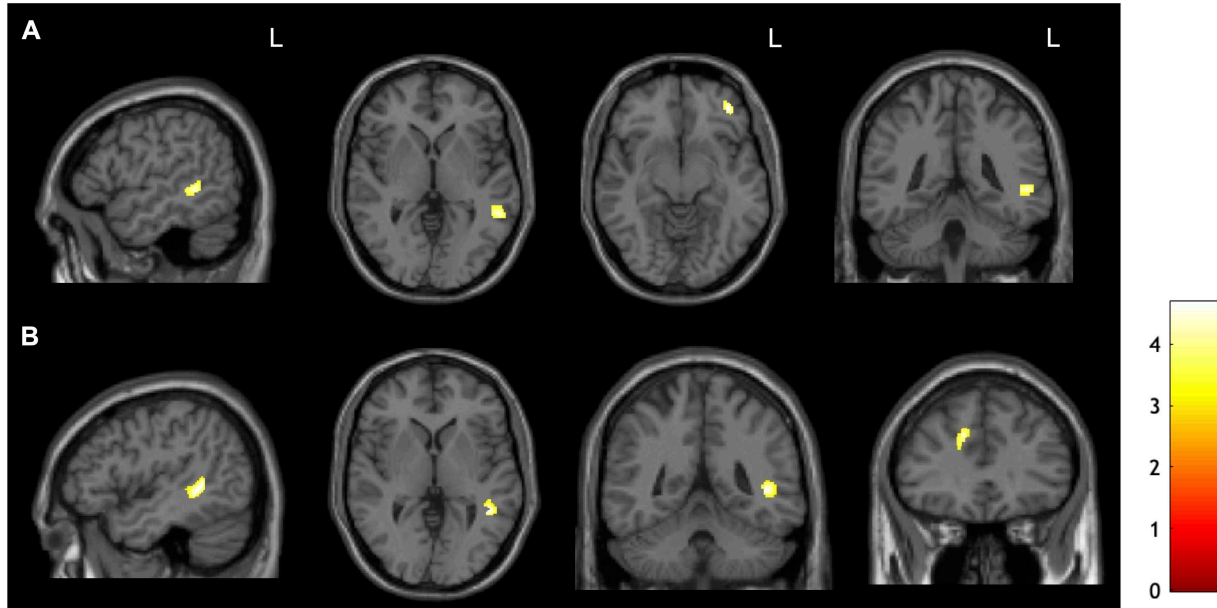
A – Cross-sectional PET preprocessing



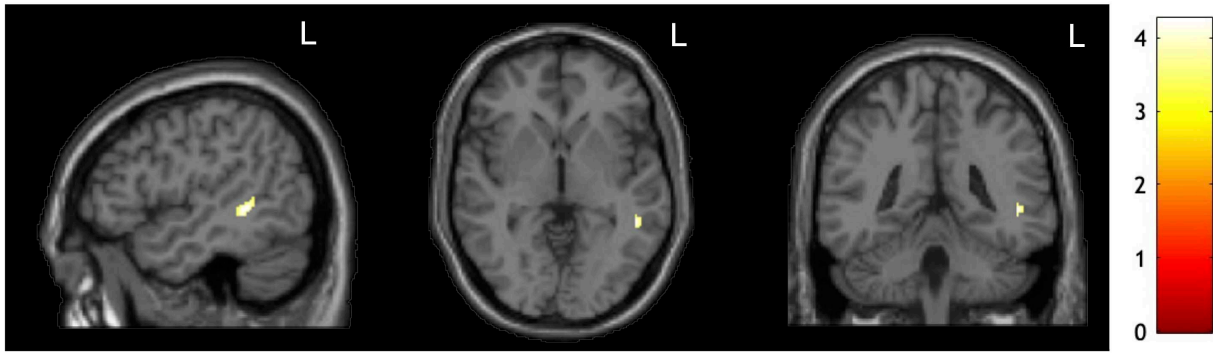
B – PET-PAC preprocessing



eFigure 1. Sequential steps for cross-sectional PET preprocessing (A), and longitudinal preprocessing with PET-PAC approach (B). All steps were performed using an automated pipeline developed with BrainVISA software (<http://brainvisa.info/web/index.html>). MNI: Montreal Neurological Institute; PAC: percent annual changes; PVEc: partial volume effect correction; VOI: volume of interest.

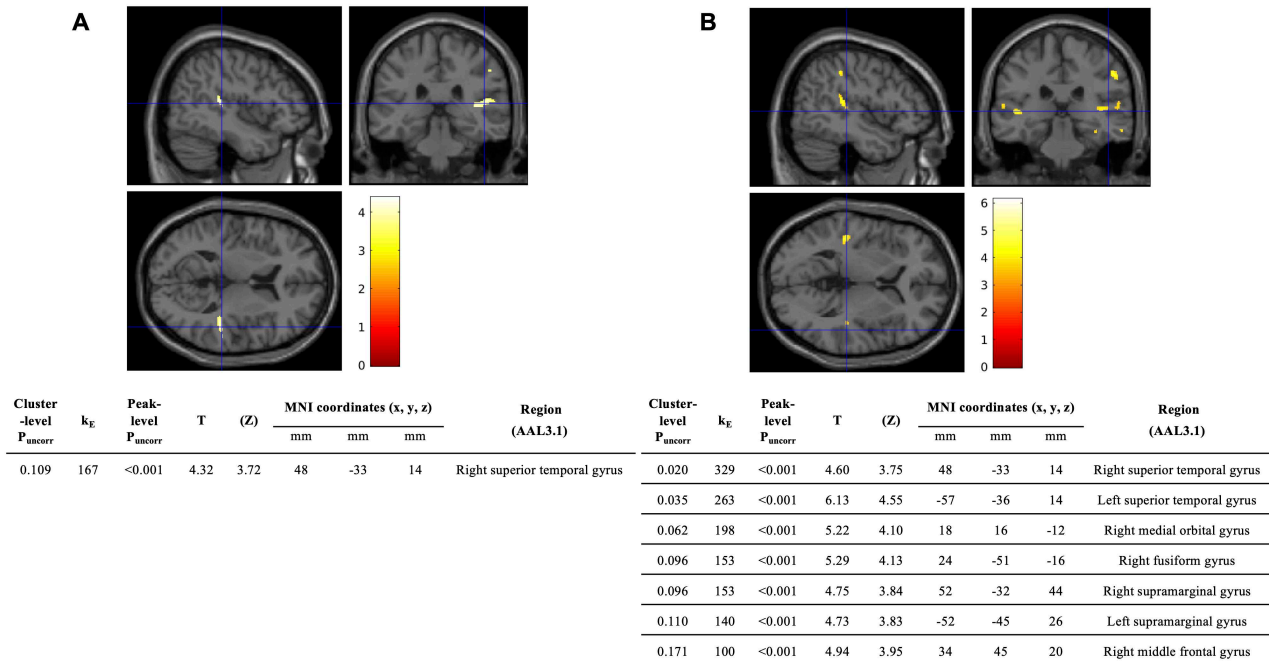


eFigure 2. Cross-sectional comparisons of brain metabolism between PS-GRN+ and HC at t_{20} (A) and t_{60} (B). The contrast PS-GRN+ < HC was applied. Statistical parametric maps are thresholded at $P < 0.001$, with a cluster-extent threshold at 100. Color bar refers to the T values. HC: healthy controls; PS-GRN+: presymptomatic *GRN* carriers.

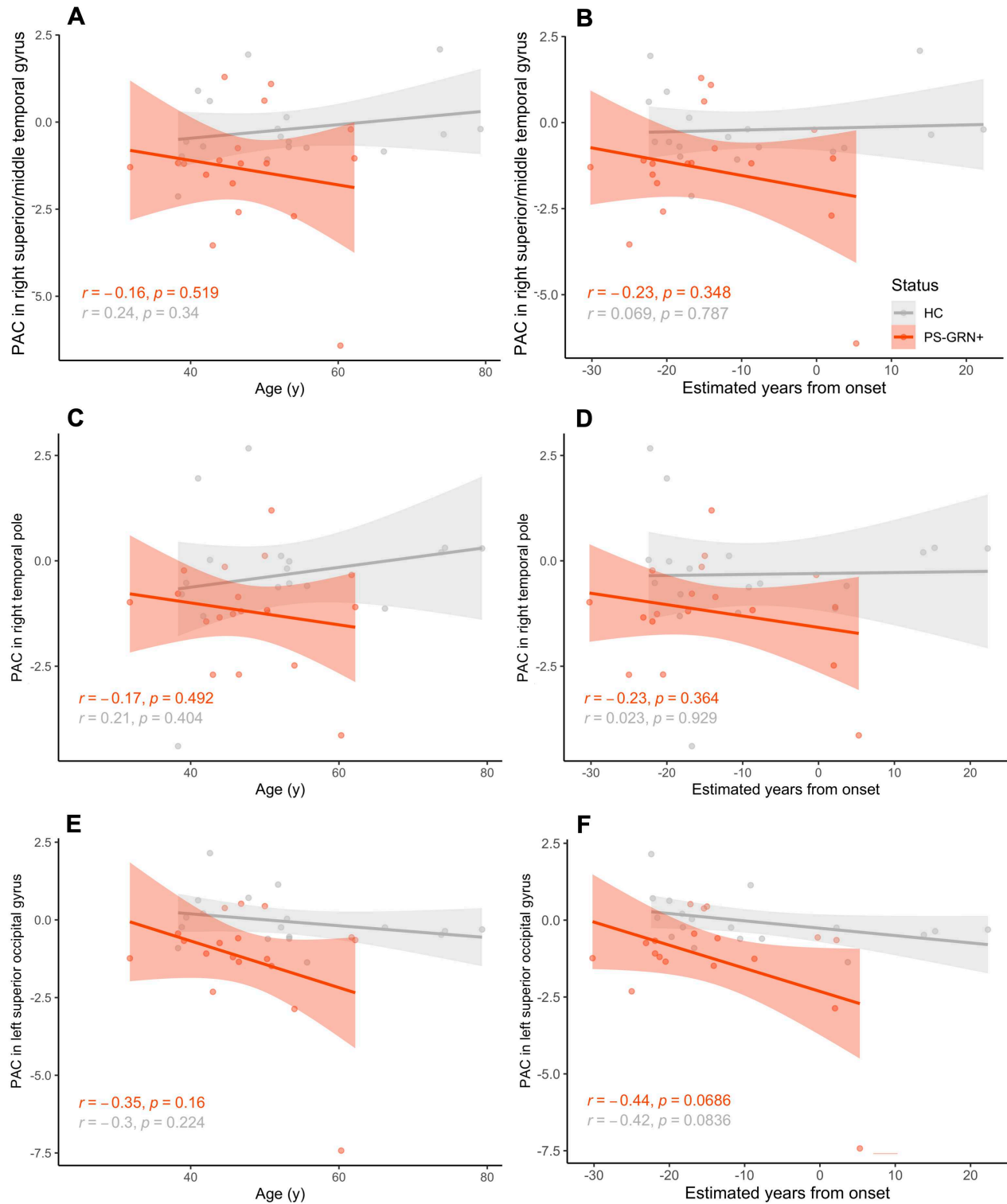


Cluster-level P_{uncorr}	k_E	Peak-level P_{uncorr}	T	(Z)	MNI coordinates (x, y, z)			Region (AAL3.1)
					mm	mm	mm	
0.268	81	<0.001	4.25	3.81	-48	-42	-2	Left middle temporal gyrus

eFigure 3. Cross-sectional comparison of brain metabolism at t_0 restricted to the 42 participants who underwent the entire follow-up. The contrast PS-GRN+ < HC was applied. Statistical parametric maps are thresholded at $P < 0.001$, with a cluster-extent threshold at 50. The results are coherent with what observed in the overall cohort of 58 individuals at t_0 , showing a cluster of hypometabolism in the left middle temporal gyrus. Color bar refers to the T values. AAL: automatic anatomical labelling atlas; HC: healthy controls; k_E : extent coefficient, MNI: Montreal Neurological Institute; PS-GRN+: presymptomatic GRN carriers; T: value of T -test; (Z): value of Z test.

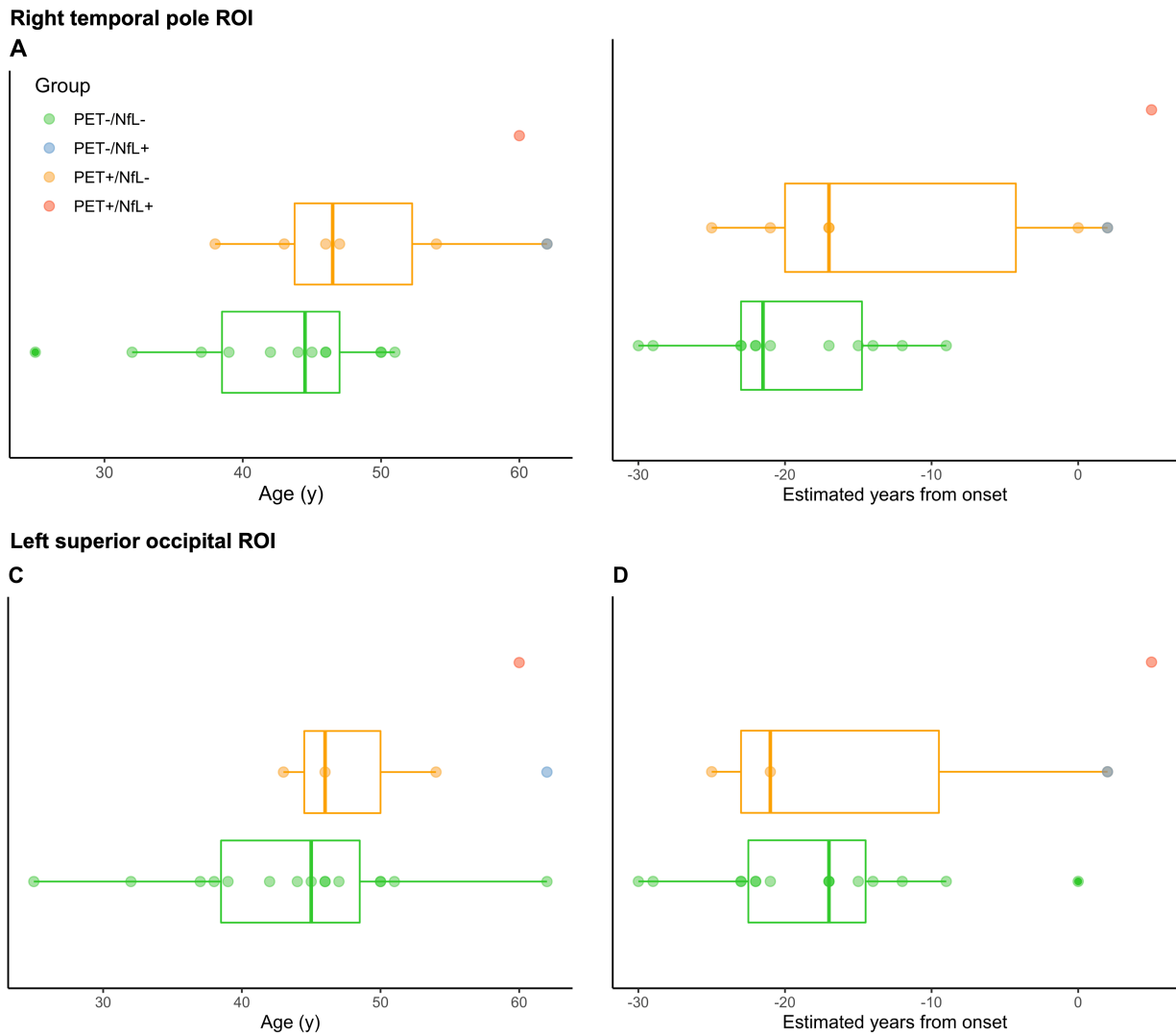


eFigure 4. Single-subject SPM analysis of the *GRN* carrier in the prodromal phase. Cross-sectional comparisons of brain metabolism *versus* age-matched controls are showed at t_0 (A) and at t_{60} (B), with their respective clusters of significant hypometabolism. Statistical parametric maps are thresholded at $p < 0.001$, with a cluster-extent threshold at 100. A comparable hypometabolic area in the lateral temporal lobe is present at baseline, with noticeable progression and spreading during follow-up. Color bars refer to the T values. AAL: automatic anatomical labelling atlas; k_E : extent coefficient, MNI: Montreal Neurological Institute; SPM: statistical parametric mapping; T : value of T -test; (Z): value of Z test.



eFigure 5. Individual PAC in the right superior/middle temporal gyrus (A,B), in the temporal pole (C,D) and in the left superior occipital gyrus (E,F). Values are plotted against participants'

age (A,C,E) and estimated years to onset (B,D,F). In PS-*GRN*⁺, annualized decreases tended to be slightly greater with advancing age and proximity to mean onset in the family. Results of the Spearman's correlations are shown for the two groups. HC: healthy controls; PAC: percent annual changes; PS-*GRN*⁺: presymptomatic carriers of *GRN* mutations; y: years.



eFigure 6. Modelization of metabolic and NfL changes in PS-GRN+ undergoing the entire follow-up based on the two other selected ROIs. The PET+ status has been defined with respect to reference parameters in HC in the right temporal pole ROI (A, B) and in the left superior occipital ROI (C, D). Higher NfL values or greater increases compared with age-matched HC defined the NfL+ status. Each individual is represented by a colored dot, plotted against subjects' age (A, C) and estimated years to disease onset (B, D). HC healthy controls; NfL: neurofilament light chain; PS-GRN+: presymptomatic *GRN* carriers; ROI: region of interest; y: years.

4.4 Partie 4 – Profil d’atrophie de la substance grise et modifications longitudinales chez les porteurs d’expansion *C9orf72* à la phase présymptomatique

Plusieurs études de neuroimagerie structurale ont démontré l’existence d’une atrophie cérébrale étendue chez les porteurs d’expansion du gène *C9orf72*, identifiable à l’échelle de groupe environ 25 ans avant le début supposé de la maladie (Rohrer et al., 2015 ; Lee et al., 2017b ; Bertrand et al., 2018 ; Bocchetta et al., 2021). Les connaissances actuelles sont beaucoup plus limitées en ce qui concerne l’évolution longitudinale de l’atrophie, les études précédentes n’ayant pas démontré de progression significative par rapport à ce qui est observé chez des individus non mutés. Ceci peut être dû à une sensibilité insuffisante pour la détection de changements subtils et/ou à des durées de suivi trop courtes (Panman et al., 2019) ou trop hétérogènes (Le Blanc et al., 2020). La dernière partie de ma thèse a été consacrée à l’analyse des altérations structurales et de leur évolution longitudinale au cours de la phase présymptomatique de la pathologie *C9orf72* dans la cohorte PREV-DEMALS (article en préparation).

Méthodes

L’étude prospective PREV-DEMALS est basée sur le suivi longitudinal de 114 individus concernés par la mutation *C9orf72* (22 patients, 92 apparentés de premier degré asymptomatiques), recrutés depuis 2015 dans quatre CHU français (Paris, Lille, Limoges, Rouen) et suivis pendant 3 ans. A chaque visite (à l’inclusion, à 18 et 36 mois) les participants ont bénéficié d’un protocole d’évaluation standardisé (décrit dans l’article de Bertrand et collaborateurs, 2018) incluant échelles cognitives et comportementales, imagerie structurale et métabolique, dosage plasmatique des NfL. Après application des critères d’exclusion, 88 participants asymptomatiques (46 porteurs et 42 contrôles) ont été inclus dans cette étude, et 80 d’entre eux (44 porteurs et 36 contrôles) ont complété le suivi.

Leurs caractéristiques sont brièvement récapitulées dans le Tableau 2. A l’échelle de groupe, les porteurs se situaient environ 19 ans avant l’âge de début estimé. Comme illustré dans l’article consacré à l’étude des trajectoires des NfL plasmatiques, cinq porteurs ont présenté, au cours du suivi, des valeurs de NfL et/ou des taux annualisés de changement nettement plus élevés que les valeurs de référence établies dans leur classe d’âge. Pour rappel,

quatre d'entre eux ont présenté des modifications comportementales, cognitives et/ou motrices subtiles qui, en accord avec les recommandations internationales, suggéraient l'entrée dans le stade prodromal (CDR+NACC FTLD = 0,5).

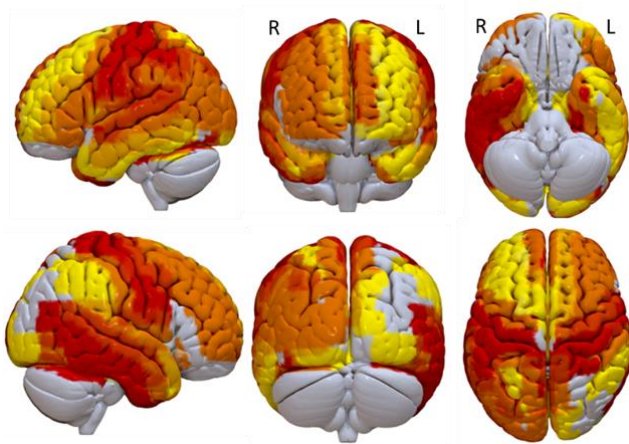
	Porteurs <i>C9orf72</i> +	Contrôles <i>C9orf72</i> -
Inclus à M₀ (N=)	46	42
Sexe (% F)	54,5 %	50 %
Age à M₀ (range)	41,5 (24 – 77)	46 (21 – 78)
Inclus à M ₁₈ (N=)	43	40
Inclus à M ₃₆ (N=)	44	36
Age à M ₃₆ (range)	44,9 (27 – 80)	47,9 (25 – 72)

Tableau 2. Caractéristiques des participants de la cohorte PREV-DEMALS inclus dans l'étude
M₀ : visite d'inclusion ; M₁₈ : visite de suivi à 18 mois ; M₃₆ : visite de suivi à 36 mois.

Dans cette étude, nous avons analysé les séquences d'IRM T1-pondérées, acquises avec des machines 3T avec un protocole standardisé entre les centres. Nous avons comparé les volumes cérébraux dans des régions d'intérêt discrètes entre porteurs et contrôles à l'inclusion et par rapport à leur évolution longitudinale. Deux approches de traitement d'image cross-sectionnel et longitudinal ont été utilisées en parallèle : l'une exploitant le logiciel FreeSurfer, l'autre SPM12 et son *toolbox* CAT12. Cette dernière approche, basée sur les principes de la VBM et le recalage anatomique dans l'atlas AAL3.1 récemment développé (Rolls et al., 2020), offre l'avantage d'une parcellisation plus exhaustive des structures sous-corticales par rapport au traitement standard de FreeSurfer. Après correction des volumes régionaux selon le volume intracrânien total, deux modèles linéaires à effets mixtes ont été utilisés pour chaque région, l'un comparant les différences entre porteurs et contrôles à l'inclusion (effets fixes : **statut génétique**, âge, sexe, centre ; effet aléatoire : famille), l'autre étudiant les différences de progression entre les deux groupes (effets fixes : statut génétique, âge à l'inclusion, temps de suivi, centre, **interaction statut génétique * temps de suivi** ; effets aléatoires : sujet, famille). Des modèles linéaires supplémentaires ont été réalisés pour des régions d'intérêt sélectionnées, afin de comparer les taux des porteurs selon leur proximité de la phénoconversion. La méthode de Benjamini-Hochberg a été utilisée pour la correction des comparaisons multiples.

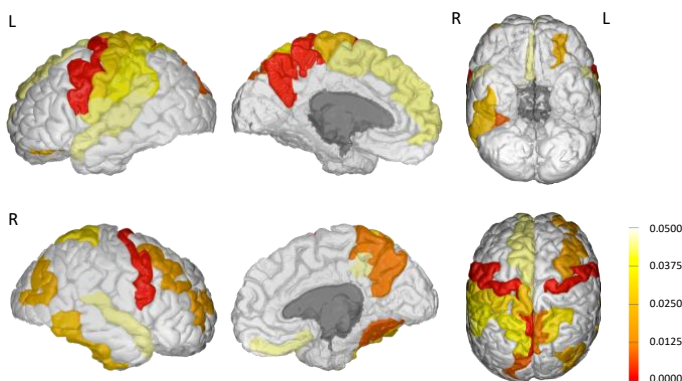
Résultats

Ces analyses révèlent un profil d'atrophie corticale étendu chez les porteurs de l'inclusion, concernant 48 des 120 régions corticales de l'atlas AAL3.1, étudiées avec la méthode de VBM (Figure 6), et 26 des 148 régions de l'atlas de Destrieux, étudiées avec la méthode de FreeSurfer (Figure 7). De manière concordante entre les deux approches, les régions dont les volumes étaient les plus significativement réduits chez les porteurs comprenaient les aires sensori-motrices primaires, les régions préfrontales médiales, les circonvolutions temporales latérales et le précuneus.



$p < 0,001^{***}$	$p < 0,01^{**}$	$p < 0,05^*$
Gyrus précentral G	Gyrus frontal supérieur D	Gyrus frontal supérieur G
Gyrus précentral D	Gyrus frontal moyen D	Gyrus frontal moyen G
Gyrus frontal méd sup G	Gyrus frontal inférieur G	Opércule rolandique G
Gyrus fusiforme D	Opércule rolandique D	Aire motrice supplémentaire G
Gyrus postcentral G	Cortex orbitofrontal latéral G	Aire motrice supplémentaire D
Gyrus postcentral D	Gyrus cingulaire moyen G	Gyrus frontal médial sup D
Gyrus pariétal inférieur G	Cunéus G	Insula D
Précuneus G	Gyrus occipital moyen G	Gyrus cingulaire moyen D
Gyrus temporal supérieur G	Gyrus supramarginal G	Hippocampe G
Gyrus temporal moyen G	Gyrus angulaire G	Parahippocampe D
Gyrus temporal inférieur G	Précuneus D	Amygdale D
	Gyrus temporal supérieur D	Cunéus D
	Pôle temporal supérieur D	Gyrus lingual G
	Gyrus temporal moyen G	Gyrus occipital inférieur D
		Gyrus pariétal supérieur G
		Gyrus supramarginal G
		Gyrus d'Heschl D
		Gyrus d'Heschl G
		Pôle temporal moyen G
		Pôle temporal moyen D
		Gyrus temporal inférieur G
		Gyrus cingulaire antérieur G
		Gyrus cingulaire antérieur D

Figure 6. Régions significativement atrophiées à la M₀ selon la méthode de CAT12
Dans la figure et dans le tableau, la couleur rouge indique une significativité à $p < 0,001$, orange à $p < 0,01$ et jaune à $p < 0,05$ (correction de Benjamini-Hochberg).



$p < 0,001^{***}$	$p < 0,01^{**}$	$p < 0,05^*$
Gyrus précentral G	Gyrus frontal moyen D	Gyrus & sillon paracentral G
Gyrus précentral D	Précuneus D	Gyrus & sillon subcentral G
Précuneus G	Gyrus fusiforme D	Gyrus frontal supérieur G
	Sillon temporal inférieur D	Gyrus rectus D
	Gyrus occipital supérieur G	Sillons orbitaux G
		Gyrus postcentral G
		Gyrus supramarginal G
		Gyrus pariétal supérieur G
		Gyrus pariétal supérieur D
		Sillon subpariétal D
		Sillon pariéto-occipital D
		Gyrus temporal supérieur G
		Sillon temporal supérieur G
		Planum temporale G
		Gyrus temporal supérieur D
		Gyrus temporal inférieur D
		Sillon occipito-temporal latéral G
		Gyrus occipital moyen D

Figure 7. Régions significativement atrophiées à la M₀ selon la méthode de FreeSurfer
La barre colorée représente la significativité statistique après correction de Benjamini-Hochberg.

A l'étage sous-cortical, une atteinte massive et bilatérale du thalamus était retrouvée chez les porteurs à l'inclusion, touchant 24 des 30 régions thalamiques explorées avec la méthode de VBM et labélisées selon l'atlas AAL3.1. Les noyaux les plus atteints, par ordre décroissant de significativité, étaient : le pulvinar dans toutes ses sous-divisiones, le noyau dorsomédian, ventral latéral, ventral postérieur latéral, latéral postérieur ($p < 0,001$) ; le noyau genouillé latéral et les noyaux intralaminaires ($p < 0,01$) ; et le noyau antéroventral ($p < 0,05$), de façon bilatérale.

Les analyses longitudinales sur les 3 ans de suivi ont mis en évidence une atrophie accélérée dans certaines régions chez les porteurs (sur la base de l'effet fixe d'interaction statut génétique * temps de suivi), plus importante que ce qui est attendu au regard du vieillissement normal chez les contrôles. Les résultats obtenus avec la méthode VBM se sont avérés significatifs dans trois régions : à savoir les deux putamen (gauche, $p = 0,003$; droit, $p = 0,022$) et l'insula gauche ($p = 0,008$) (Figure 8). Pour chacune de ces régions, nous avons calculé le taux annualisé de changement volumétrique qui était de 2 à 4 fois plus élevé chez les porteurs que chez les contrôles, mesurant respectivement -1,3 % *versus* -0,8 % au niveau du putamen gauche, -1,4 % *versus* -0,5 % au niveau du putamen droit, et -2,0 % *versus* -0,5 % au niveau de l'insula gauche. Aucune région ne présentait d'atrophie accélérée chez les porteurs avec la méthode de FreeSurfer.

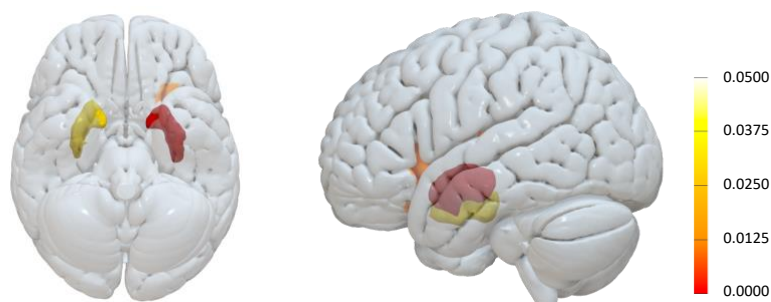


Figure 8. Régions présentant un déclin volumétrique accéléré chez les porteurs comparés aux contrôles durant le suivi

La barre colorée représente la significativité statistique après correction de Benjamini-Hochberg.

Pour aller plus loin, nous avons évalué si le taux de progression se modifiait dans chacune de ces régions au cours de la phase présymptomatique, en fonction de la proximité clinique. Nous avons stratifié les participants selon l'âge, distinguant phase présymptomatique

précoce (individus âgés de moins de 40 ans) et phase présymptomatique tardive (individus âgés plus de 40 ans). Cette analyse complémentaire a montré un effet significatif au niveau du putamen gauche ($p=0.003$) et du putamen droit ($p=0.008$). Le taux annualisé de changement chez les porteurs passait ainsi de -1,3 % à -2,3 % pour le putamen gauche, et de -1,0 % à -2,4 % pour le putamen droit (Figure 9).

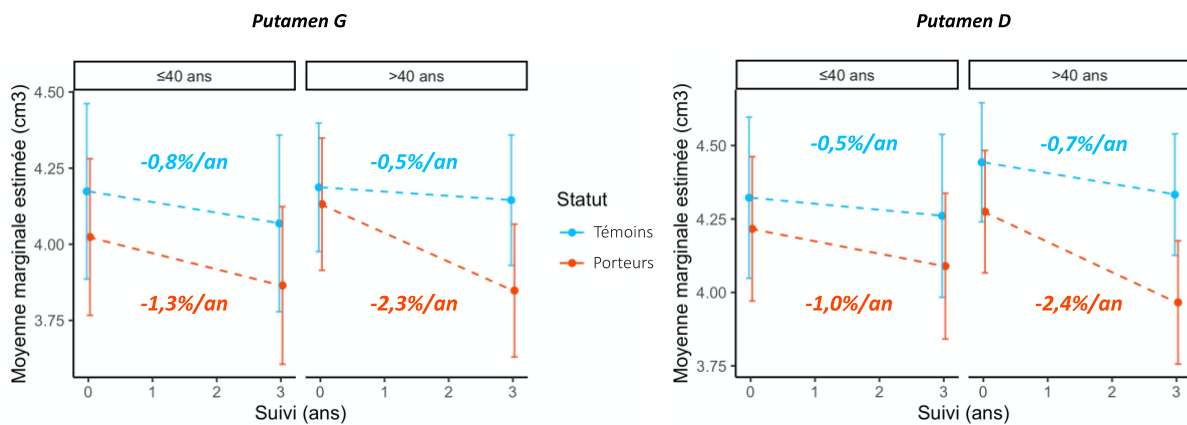


Figure 9. Comparaison de la progression longitudinale de l'atrophie des deux putamen entre porteurs à la phase présymptomatique précoce (≤ 40 ans) et tardive (> 40 ans)

Enfin nous avons analysé séparément les cinq individus porteurs d'expansion présentant une augmentation de leurs valeurs de NfL pendant le suivi, donc à proximité ou au stade prodromal. Bien que les comparaisons statistiques soient limitées par la taille réduite de ce sous-groupe, il existe une tendance vers une progression de l'atrophie plus importante dans certaines régions du cortex frontal, avec un effet plus prononcé au niveau du cortex précentral dans ce sous-groupe que chez les autres porteurs (taux annualisé de changement : -1,4 %, *versus* -0,8 % chez les autres porteurs et les contrôles).

Globalement, cette étude met en évidence un profil de déclin volumétrique cortico-sous-cortical accéléré durant la phase présymptomatique de la pathologie *C9orf72*. Le taux annualisé de changement dans trois régions, significativement différent entre porteurs et contrôles, pourrait servir de mesure au cours des essais thérapeutiques. Une atrophie accélérée des putamen n'est décelable que tardivement au cours de la phase présymptomatique, pouvant permettre une stratification des porteurs.

5. Discussion générale

Les connaissances dans le domaine des DLFT ont remarquablement progressé au cours des trois dernières décennies. Sur le plan clinique, la révision des critères permettant un diagnostic plus précis (Rascovsky et al., 2011 ; Gorno-Tempini et al., 2011) et la description de phénotypes atypiques dans le spectre des DLFT (Ulugut Erkoyun et al., 2020 ; Ducharme et al., 2020), mettent en évidence la grande hétérogénéité nosologique de ces syndromes. Sur le plan anatomopathologique, la vision uniciste des « tauopathies » a été remplacée par une classification complexe et articulée, suivant de près les avancées des connaissances sur les bases biologiques et moléculaires des DLFT (Lee et al., 2017a ; Forrest et al., 2018). Les connaissances génétiques se sont, elles aussi, considérablement améliorées, permettant maintenant d'identifier une cause génétique chez environ un quart à un tiers des patients (Pottier et al., 2016) et d'identifier les porteurs de mutation à la phase présymptomatique (dans un contexte de test présymptomatique), deux éléments fondamentaux à l'ère des premiers essais thérapeutiques ciblés (Desmarais et al., 2019). A ce stade, la connaissance approfondie de la phase présymptomatique représente un nouvel enjeu pour la communauté scientifique internationale. Des études de suivi longitudinal de porteurs de mutations sont menées dans le cadre de consortia ou d'initiatives nationales depuis quelques années, permettant de parvenir, récemment, à un consensus sur la définition des stades de la phase présymptomatique (Benussi et al., 2021 ; Benatar et al., 2022) et d'élaborer des premiers critères de recherche de « DFTc prodromale » (Barker et al., 2022). L'étude de la phase présymptomatique a aussi bénéficié d'avancées technologiques importantes dans le domaine de la neuroimagerie et des dosages biochimiques et moléculaires de haute sensibilité (Staffaroni et al., 2020b ; Swift et al., 2021b), permettant l'identification et la validation de biomarqueurs pour le suivi du processus pathologique et la réponse éventuelle à des traitements.

Cette thèse se positionne donc dans ce cadre dynamique, contribuant à faire avancer les connaissances concernant la caractérisation clinique, des biomarqueurs et de neuroimagerie des deux formes génétiques principales de DLFT, associées aux mutations des gènes *GRN* et *C9orf72*. La première partie des travaux réalisés (chapitre 4.1) est consacrée à l'étude de présentations cliniques rares et relativement mal caractérisées dans le contexte de ces deux causes génétiques, celles des aphasies primaires progressives. L'objectif est d'identifier les systèmes impliqués dans chaque forme, d'établir des corrélations phénotype-génotype et d'élargir les indications du diagnostic génétique. En effet, l'identification d'une mutation

causale *GRN* ou *C9orf72*, malgré les implications lourdes en termes de pronostic et de risque de récurrence, offre une possibilité concrète d'intervenir sur l'évolution de la maladie, ne serait-ce que par l'inclusion des patients et porteurs dans des protocoles thérapeutiques.

Dans le premier travail (article 1, Saracino et al., 2021a), nous avons analysé le profil clinique, langagier et d'imagerie dans la plus large cohorte de patients porteurs de mutations du gène *GRN* présentant un phénotype d'APP (« APP-*GRN* »). Le principal résultat de cette étude est que le vlAPP est le phénotype langagier le plus fréquent. Ce résultat peut sembler surprenant, puisque la majorité des vlAPP est associée à des lésions pathologiques de MA (Mesulam et al., 2008 ; Leyton et al., 2011). Néanmoins, depuis quelques années, plusieurs études pointent l'existence de formes logopéniques non amyloïdes (amyloïde-négatives) sur la base de la négativité des biomarqueurs de MA dans le LCR (Teichmann et al., 2013), du TEP-amyloïde (Josephs et al., 2014b), ou sur l'absence de lésion de MA sur les analyses anatomopathologiques (Kim et al., 2016). Ces formes représenteraient jusqu'à 20 % des cas, comme le montre une analyse basée sur les données *post mortem* de 99 patients avec vlAPP (Bergeron et al., 2018). Tous les patients de notre étude avaient des biomarqueurs non en faveur d'une MA, permettant de les classer parmi les APP logopéniques amyloïde-négatives. Finalement, notre étude contribue à améliorer les connaissances sur les variants logopéniques d'APP, mettant en évidence qu'une partie au moins des formes amyloïde-négatives sont associées à des mutations du gène *GRN*. Cette association est appuyée, dans notre étude, par les résultats des analyses d'imagerie structurale (de VBM et d'épaisseur corticale) montrant un profil d'atrophie principalement localisé au niveau de la partie postérieure du gyrus temporal moyen gauche, à proximité de la jonction temporo-pariétale, superposable à celui des patients avec une forme logopénique de MA. Le gyrus temporal moyen postérieur participe au circuit de la mémoire à court terme auditivo-verbale ou « boucle phonologique » (Buchsbbaum et D'Esposito, 2019), contribuant à la recherche des mots et à la production langagière (Choi et al., 2015). Cette région représente ainsi un nœud central du réseau du langage, dont le dysfonctionnement a été associé principalement à des troubles de la dénomination et de la répétition (Bonakdarpour et al., 2019), deux éléments caractérisant le vlAPP.

Enfin, le phénotype des vlAPP associés aux mutations *GRN* peut être un peu atypique, comme d'autres auteurs l'ont souligné (Rohrer et al., 2010b). Dans notre étude, la moitié des patients avec un vlAPP présentaient, en effet, des altérations additionnelles subtiles, identifiables en situation de test uniquement (patients vlAPP+), nous conduisant à proposer le

terme plus global de « spectre logopénique » pour désigner l'ensemble de ces présentations. A côté de cela, des éléments clairement logopéniques caractérisaient tous les patients avec une forme mixte d'APP (25 % de notre cohorte). Globalement, ces résultats encouragent donc la recherche de mutation du gène *GRN* (ou du dosage de la progranuline plasmatique) chez les patients présentant aussi bien un tableau d'APP logopénique classique que des formes plus atypiques ou mixtes, une fois écartée la présence d'une MA sous-jacente.

Les formes d'« APP-*C9orf72* » (article 2, Saracino et al., 2021b) sont, elles, caractérisées par deux éléments langagiers principaux: une apraxie de la parole, comme symptôme dominant chez les patients avec un phénotype de vfnAPP, et des troubles sémantiques, chez les patients présentant des formes sémantiques et mixtes d'APP. Sur la base des phénotypes rapportés et de leurs corrélats neuroanatomiques, nous avons pu montrer que les « APP-*C9orf72* » se caractérisent par une atteinte des composantes plus antérieures du réseau du langage, avec un tropisme particulier de l'atteinte structurelle pour le lobe temporal antérieur. Cela rapproche ces formes génétiques des formes d'APP associées à des mutations beaucoup plus rares, comme celles des gènes *MAPT* (Henz et al., 2015 ; Roncero et al., 2021), *TARDBP* (Caroppo et al., 2016 ; González-Sánchez et al., 2018 ; Mol et al., 2021) et *TBKI* (Caroppo et al., 2015a ; Hirsch-Reinshagen et al., 2019 ; Swift et al., 2021a) où des présentations sémantiques, en relation avec l'atteinte temporo-polaire, sont relativement habituelles. Ce profil contraste nettement avec l'atteinte prédominante des régions postérieures du réseau du langage décrite dans les « APP-*GRN* » avec présentation logopénique. Au total, ces études révèlent différents niveaux d'atteinte langagière et décrivent leurs corrélats neuroanatomiques dans les formes *GRN* et *C9orf72*. Le langage devrait être mieux exploré dans les études portant sur la phase présymptomatique, afin d'en capturer les premières altérations et parvenir, à terme, à une définition consensuelle d'« APP prodromale ».

Les perspectives thérapeutiques dans les formes *GRN* et *C9orf72* font de la connaissance de la progression de la maladie à la phase présymptomatique un défi majeur pour être en mesure de suivre la réponse aux thérapies préventives. Au cours des dernières années, plusieurs études ont exploré le potentiel de biomarqueurs fluidiques et de neuroimagerie comme outils de surveillance et/ou mesures de résultats (Rohrer et al., 2015 ; Staffaroni et al., 2020b ; van der Ende et al., 2021). Dans la deuxième partie de cette thèse (chapitres 4.2 – 4.4) nous avons cherché à établir des indicateurs basés sur des études longitudinales de neuroimagerie structurelle et métabolique pour tracer la progression de la maladie à l'échelle de groupe, mais

aussi individuelle, pour la pratique et la recherche clinique. Un point particulièrement délicat est celui de la stratification des porteurs à la phase présymptomatique en fonction de la proximité de la phénoconversion. Bien que l'approche basée sur le calcul de la distance à l'âge estimé de la maladie dans la famille ait été utilisée dans plusieurs études (Rohrer et al., 2015 ; Cash et al., 2018 ; Borrego-Ecjia et al., 2021), la forte variabilité intrafamiliale de l'âge de début dans ces formes génétiques en fait un indicateur imparfait. L'enthousiasme pour les NfL comme marqueurs prédictifs d'entrée dans le stade prodromal (van der Ende et al., 2019 ; Benatar et al., 2019 ; Rojas et al., 2021) a fait de leur dosage dans les biofluides une évaluation nécessaire dans toutes les études de la phase présymptomatique des DLFT. Néanmoins, leur utilisation pratique est actuellement limitée par des questions qui restent ouvertes autour de leurs trajectoires dans des conditions physiologiques et pathologiques, auxquelles nous avons cherché à répondre (article 3, Saracino et al., 2021c).

L'étude de l'impact de l'âge sur les taux des NfL chez l'adulte jeune puis tout au long de la vie chez des contrôles, c'est-à-dire dans des conditions physiologiques, apporte un premier résultat important. L'augmentation des NfL avec l'âge débute précocement, et augmente plus fortement après 60 ans. Cet effet confirme des études sur le vieillissement physiologique portant sur des populations plus âgées (Khalil et al., 2020), et peut être interprété comme une conséquence d'une perte axonale progressive, plus importante chez les sujets âgés, ou d'une modification des systèmes de dégradation et de turn-over protéique associée au vieillissement (Khalil et al., 2018). Cet effet peut aussi résulter de la présence de maladies neurologiques à l'état préclinique, non détectables au moment de l'évaluation, chez les individus les plus âgés. Notre étude montre néanmoins que les taux des NfL diffèrent selon les classes d'âge, et que l'âge doit donc être pris en compte dans l'interprétation de ces taux. Dans cette étude, nous proposons des valeurs de référence pour chaque classe d'âge basées sur nos résultats, et qui pourront être utilisées dans les études suivantes et les recherches futures. Nous soulignons néanmoins l'importance d'une standardisation des méthodes d'analyse et une harmonisation de l'interprétation des résultats, pour définir des valeurs de référence consensuelles.

Au-delà de ce premier facteur de variabilité, nous avons montré que plusieurs paramètres impactent les taux des NfL chez les patients, dont : la mutation causale, le phénotype clinique, l'âge de début et la rapidité de progression. Globalement, l'augmentation des NfL reflète la sévérité du processus lésionnel, comme en témoignent les niveaux plus élevés chez les patients atteints de SLA que chez ceux atteints de DFTc, et dans les formes *GRN*, marquées

par une évolution clinique agressive et des lésions fréquentes de la substance blanche (Ameur et al., 2016 ; Sudre et al., 2019 ; Moore et al., 2020a), que dans les formes *C9orf72*. Les formes atypiques associées au génotype *C9orf72* méritent une attention particulière. Les patients avec une présentation psychiatrique ont une augmentation tout à fait discrète, très comparable à celle observée chez des patients avec pathologie psychiatrique primaire (PPP). D'autres études ont montré l'utilité des NfL pour distinguer entre DFTc et PPP (Al Shweiki et al., 2019 ; Fourier et al., 2020). Notre étude complète ces résultats, soulignant que le dosage des NfL ne permet pas de discriminer les présentations psychiatriques des expansions *C9orf72* des PPP. De même, les patients avec une forme lentement progressive de DFTc ou SLA présentaient une augmentation beaucoup plus modérée que les patients présentant une durée de progression plus habituelle, et un taux annualisé de changement presque superposable aux contrôles non mutés. Ces résultats concordent avec l'atteinte structurelle qui est limitée dans ces formes particulières (Khan et al., 2012). Ils suggèrent que le taux annualisé de progression peut être utilisé comme outil prédictif de la rapidité d'évolution chez les porteurs d'expansion du gène *C9orf72*. L'analyse des NfL chez les porteurs présymptomatiques a, elle, révélé des trajectoires pathologiques avec une augmentation brutale des taux précédant de 3 ans les premiers changements cliniques chez quatre porteurs qui ont évolué vers la phénoconversion pendant leur suivi, confirmant ainsi les études précédentes sur ce sujet (van der Ende et al., 2019).

Au total, cette étude contribue à la modélisation de la trajectoire des NfL durant la phase présymptomatique et la phase clinique de la maladie, en fonction de la mutation causale. Les porteurs de mutations du gène *GRN* présentent des valeurs relativement stables durant la phase présymptomatique, et une augmentation particulièrement importante au stade clinique. Chez les porteurs d'expansion du gène *C9orf72*, la transition entre les deux phases est moins brusque, avec une augmentation modeste tout au long de la phase présymptomatique, et des trajectoires reflétant la sévérité de la progression au cours de la phase clinique. La contribution des NfL s'avère donc déterminante pour le suivi de la phase présymptomatique tardive, et les informations obtenues à partir de cette étude ont permis de définir des critères de stratification des porteurs par rapport à la proximité de la phénoconversion.

Dans la pathologie *GRN*, c'est aussi pendant les 5 années qui précèdent la phénoconversion qu'une progression significative de l'atrophie cérébrale devient détectable en imagerie structurelle, à l'échelle individuelle (Jiskoot et al., 2019). Si ces marqueurs sont utiles pour la prédiction de la transition vers la phénoconversion, ils ne permettent pas de suivre le

processus pendant la phase préclinique plus précoce, avant la survenue des dommages structurels neuronaux. L'étude longitudinale multimodale réalisée dans la cohorte Predict-PGRN (article 4) révèle que des changements du métabolisme cérébral sont détectables chez les porteurs présymptomatiques environ 15 ans avant l'âge estimé de début des symptômes, donc bien plus précocement que l'augmentation du taux de NfL et que les modifications structurelles. Cette chronologie est comparable à la séquence des changements des biomarqueurs observée dans les formes génétiques de MA. En effet, dans ces dernières, le déclin du métabolisme cortical (notamment au niveau du précuneus) est détectable en TEP-FDG environ 15 à 20 ans avant le début de la maladie, alors que l'atrophie hippocampique est détectée plus tardivement, seulement 3 à 5 ans avant la conversion clinique (Bateman et al., 2012 ; McDade et al., 2018). Dans notre étude, les résultats des analyses cross-sectionnelles et des analyses longitudinales convergent, mettant en évidence l'atteinte précoce du gyrus temporal supérieur et moyen, incluant le sillon temporal supérieur (STS), qui semble une région majeure dans la pathologie *GRN*. L'implication du STS dans la pathologie *GRN* est appuyé par une étude d'imagerie structurelle qui montre une atrophie corticale accélérée dans cette même région, chez les porteurs de mutations plus âgés, donc plus proches de la phénoconversion (Moreno et al., 2013 ; Borrego-Ecjia et al., 2021).

Le dysfonctionnement de la région du STS est particulièrement intéressant sur le plan des corrélats neuroanatomiques, car cette aire joue un rôle dans la cognition sociale et dans la communication non verbale (Isik et al., 2017). Le STS droit, qui présente le déclin métabolique le plus significatif dans notre étude, est impliqué dans la reconnaissance des expressions faciales dynamiques et le décodage des intentions d'autrui (Engell et al., 2007 ; Sato et al., 2019). Cette région a fait l'objet d'études de connectivité fonctionnelle chez les individus avec des troubles du spectre autistique, mettant en évidence une activité et une connectivité déficitaires (Alaerts et al., 2014). Nos résultats suggèrent que cette région neuroanatomique pourrait être impliquée aussi dans le déficit de la cognition sociale caractérisant la phase clinique des DFTc, et que des tests plus sensibles basés, à titre d'exemple, sur l'identification de stimuli sociaux dynamiques, pourraient être intéressants dans le suivi des porteurs à la phase présymptomatique.

Un dernier point fort de cette étude est la proposition d'une mesure quantitative, le taux annualisé de changement métabolique calculé avec la méthode PET-PAC, pour tracer la pathologie *GRN* dès la phase présymptomatique précoce. Dans la région du STS, ce taux est en moyenne 7 fois plus élevé chez les porteurs que chez les contrôles, et comparable aux valeurs

retrouvées chez des patients au stade prodromal de la MA (Fouquet et al., 2009). Ce paramètre quantitatif pourrait servir comme mesure d'évaluation dans les essais thérapeutiques ciblant le stade préclinique, en combinaison avec les taux des NfL. La modélisation simple de la progression à la phase présymptomatique que nous avons suggérée, se basant sur les données longitudinales du métabolisme dans la région du STS et les taux de NfL, supporte cette proposition. En effet, des modifications métaboliques isolées, sans élévation concomitante des taux de NfL, sont observées à un stade préclinique précoce, précédant une phase où les deux types de biomarqueurs sont altérés. Même si cette observation doit être confirmée par l'étude de cohortes plus larges, cela est en faveur d'un modèle en cascade, où les modifications métaboliques pourraient avoir un rôle prédictif de changements structuraux ultérieurs.

Une séquence temporelle différente semble caractériser la phase présymptomatique de la pathologie *C9orf72*. Des altérations structurelles cérébrales sont identifiables à un stade préclinique précoce, longtemps avant la phénoconversion, comme cela a déjà été mentionné (Lee et al., 2017b ; Bertrand et al., 2018 ; Panman et al., 2019). Cela conduit à s'intéresser de façon plus approfondie à la trajectoire d'évolution au cours de la phase présymptomatique en IRM structurelle, au moins dans certaines régions cérébrales d'intérêt. Nous avons donc analysé le profil régional de l'atrophie de la substance grise et ses modifications longitudinales dans la cohorte PREV-DEMALS, cohorte de suivi des porteurs présymptomatiques d'expansion *C9orf72*. Les comparaisons entre porteurs et contrôles à l'inclusion ont confirmé ce qui avait été mis en évidence dans des études volumétriques précédentes (Rohrer et al., 2015 ; Lee et al., 2017b ; Bertrand et al., 2018 ; Le Blanc et al., 2020 ; Bocchetta et al., 2021). Les résultats de notre étude enrichissent l'information à travers une « cartographie régionale » de l'atrophie, qui analyse des régions d'intérêt discrètes de taille plus restreinte. Il est intéressant de noter que, au-delà des aires dont l'implication est évidente dans les présentations cliniques de DFTc ou SLA, plusieurs autres régions corticales présentent des volumes significativement réduits, comme le cortex postcentral, le précuneus ou les aires associatives temporo-pariétales. Ce résultat peut être interprété dans une perspective de réseau, compte tenu de l'atteinte importante de nombreux noyaux du thalamus ayant une projection corticale, y compris ceux du groupe ventral postérieur, impliqués dans la somesthésie, et les pulvinar. Ces derniers, qui sont des relais importants médiant la communication entre aires préfrontales, limbiques et pariéto-occipitales (Zhang et al., 2008), méritent une attention particulière dans la pathologie *C9orf72*. Ils pourraient être l'une des régions les plus précocement atteintes dans le processus dégénératif, et l'une des premières à présenter les lésions spécifiques des expansions de *C9orf72*, les *foci*

d'ARN et les inclusions composées de protéines DPR, avant la présence d'inclusions TDP-43-positives, comme observé dans deux descriptions anatomopathologiques uniques (Vatsavayai et al., 2016).

L'apport principal de ce travail est la mise en évidence de régions spécifiques qui présentent une perte de volume plus rapide chez les porteurs comparés aux contrôles au cours des 3 années de suivi. Seules deux études ont exploré la progression de l'atrophie chez les porteurs d'expansion *C9orf72*. L'une, analysant 12 porteurs présymptomatiques suivis sur 2 ans, n'a pas retrouvé de différences par rapport aux contrôles (Panman et al., 2019). Une autre étude, basée sur l'analyse de l'épaisseur corticale, a montré un déclin plus rapide dans un groupe constitué de 54 porteurs à la phase clinique et 83 à la phase présymptomatique. Cependant, les analyses restreintes aux seuls porteurs présymptomatiques ne démontraient aucune différence significative par rapport aux contrôles (Le Blanc et al., 2020). Dans notre étude, la progression de l'atrophie à l'étage cortical n'est pas majeure. Elle concerne uniquement la région insulaire gauche, et a seulement été mise en évidence avec la méthode basée sur CAT12 (qui a aussi montré une sensibilité plus élevée pour révéler des différences de volume dans l'étude cross-sectionnelle). Le cortex insulaire fait partie du réseau de saillance qui est altéré précocement dans les DLFT (Seeley et al., 2010 ; Kumfor et Piguet, 2012). En particulier, l'insula gauche est une région particulièrement vulnérable dans les DLFT, une atrophie de sa partie antérieure étant associée à une apathie, à un déficit de la théorie de l'esprit et de la production langagière (Fathy et al., 2020). Ce résultat est cohérent avec une autre étude basée sur le TEP-FDG, révélant également un hypométabolisme insulaire chez les porteurs *C9orf72* à la phase présymptomatique (De Vocht et al., 2020). Des études complémentaires seront cependant nécessaires pour mieux définir la spécificité du retentissement insulaire dans la pathologie *C9orf72*, et ses associations avec les premiers changements cognitivo-comportementaux.

Notre étude montre aussi une progression significative de l'atrophie au niveau des deux putamen. Ces derniers, fonctionnellement associés avec les noyaux caudés au sein du « striatum dorsal » rentrent dans des boucles parallèles cortico-striato-pallido-thalamo-corticales impliquées dans le contrôle des mouvements, les fonctions exécutives, le contrôle des impulsions, la génération de comportements dirigés vers un but (Shipp, 2017). Dans la DFTc, l'atrophie putaminale a été associée à des comportements d'accumulation et de dépendance à l'environnement (Garibotto et al., 2011), ainsi qu'à l'anhédonie (Shaw et al., 2021). Une autre étude montre que le putamen est le noyau gris le plus significativement

atrophie chez les porteurs d'expansions *C9orf72* à la phase présymptomatique (Bocchetta et al., 2021). Notre étude apporte plus de précision, montrant que ce phénomène caractérise davantage la phase présymptomatique tardive, avec un taux annualisé de progression qui s'avère presque deux fois plus important chez les porteurs après 40 ans. La volumétrie des putamen apparaît ainsi un indicateur intéressant pour la prédiction de la phénoconversion, en particulier en combinaison avec d'autres biomarqueurs comme les NfL. L'un des obstacles à l'utilisation de la neuroimagerie structurale en tant que marqueur pour les essais thérapeutiques est lié à l'étendue de l'atteinte précoce au niveau cortical. Le suivi ciblé sur une structure cérébrale de volume plus limité, comme le striatum, représente une alternative possible contournant cette problématique. Nous poursuivons cette étude à la recherche de marqueurs de neuroimagerie qui soient communs aux différentes expressions cliniques de la maladie (pour un suivi de la progression en général) et de marqueurs précoces plus spécifiques qui soient prédictifs du phénotype au stade clinique.

Sur cette dernière question, le cortex précentral est l'une des régions présentant une tendance vers un déclin volumétrique plus important chez cinq porteurs de notre étude au stade prodromal. La progression dans cette région pourrait être mise en lien avec la présence de manifestations motrices subtiles chez trois de ces individus. Des études supplémentaires, intégrant, entre autres, volumétrie cérébrale et connectivité structurale, seront nécessaires pour établir la valeur pronostique du profil régional de progression à l'égard du phénotype de maladie à la phase clinique.

En conclusion, l'intégration des données de neuroimagerie et des NfL dans les cohortes de porteurs de mutations des gènes *GRN* et *C9orf72* met en évidence deux profils d'évolution nettement différents selon la forme génétique. Dans le cas des mutations *GRN*, bien qu'il existe des altérations fonctionnelles précoces, les altérations structurelles sont, elles, détectées tardivement à proximité de la phénoconversion, tout comme l'augmentation des NfL. Ce profil rend compte d'un processus pathologique agressif, d'évolution relativement rapide, peu avant l'entrée dans la phase clinique. Dans la pathologie *C9orf72*, les altérations structurelles cérébrales (et médullaires) sont présentes dès la phase préclinique précoce, témoignant d'une progression beaucoup plus lente jusqu'à la phase clinique, de façon concordante avec une élévation très progressive des NfL durant cette phase. Dans cette forme en effet, la mise en évidence d'une réduction volumétrique cortico-thalamique étendue, précoce et peu progressive, suggère un processus très lentement évolutif ou une éventuelle origine neurodéveloppementale

de ces altérations, comme certains auteurs l'ont évoqué (Lee et al., 2017b ; Bertrand et al., 2018). Cette hypothèse est appuyée par la détection d'anomalies qualitatives de la gyration corticale chez les porteurs d'expansion *C9orf72* (Caverzasi et al., 2019). Un lien entre anomalies neurodéveloppementales et neurodégénérescence a été établi dans certaines maladies génétiques comme la maladie de Huntington (Barnat et al., 2020). Des études complémentaires sur ce sujet sont nécessaires pour éclaircir les liens entre anomalies neurodéveloppementales, processus neurodégénératifs et leurs corrélats cliniques dans la pathologie *C9orf72*.

Ces premières études et celles de la littérature permettent de mieux définir les contours de la phénoconversion et du stade prodromal de la maladie. Elles illustrent néanmoins la difficulté à traduire des observations issues d'analyses de groupe à l'échelle individuelle pour disposer de métriques utilisables pour les évaluations cliniques et les essais thérapeutiques. Une autre difficulté est liée à l'absence de marqueurs spécifiques de lésions ne permettant pas, pour le moment, de définir la transition entre le stade « *no disease* » et le stade préclinique lésionnel. Il s'agit pourtant du stade le plus précoce et le plus intéressant dans la perspective du développement de thérapies à visée préventive. Pour aller plus loin, la recherche de marqueurs « lésion-spécifiques » est donc nécessaire à ce stade. Des approches multimodales, combinant différents biomarqueurs, pourront également être utiles pour mieux caractériser la cascade physiopathologique dans son ensemble, des phases les plus précoces, jusqu'à la définition du début lésionnel, et pour le suivi jusqu'à la phase symptomatique. À terme, les avancées issues de collaborations multidisciplinaires et de l'intégration de biomarqueurs multimodaux pourront permettre de mieux définir les phases précoces de la DLFT, y compris le stade prodromal, pour, éventuellement, adapter les critères actuels de diagnostic, proposer un diagnostic de précision et une prédiction de l'évolution à n'importe quel moment du continuum physiopathologique de la maladie.

Bibliographie

Adenzato M, Cavallo M, Enrici I. Theory of mind ability in the behavioural variant of frontotemporal dementia: an analysis of the neural, cognitive, and social levels. *Neuropsychologia*. 2010; 48: 2-12.

Agosta F, Ferraro PM, Riva N, Spinelli EG, Domi T, Carrera P, et al. Structural and functional brain signatures of C9orf72 in motor neuron disease. *Neurobiol. Aging*. 2017; 57: 206-219.

Ahmed RM, Latheef S, Bartley L, Irish M, Halliday GM, Kiernan MC, et al. Eating behavior in frontotemporal dementia: Peripheral hormones vs hypothalamic pathology. *Neurology*. 2015; 85: 1310-1317.

Ahmed RM, Irish M, Henning E, Dermody N, Bartley L, Kiernan MC, et al. Assessment of Eating Behavior Disturbance and Associated Neural Networks in Frontotemporal Dementia. *JAMA Neurol*. 2016; 73: 282-290.

Ahmed RM, Halliday G, Hodges JR. Hypothalamic symptoms of frontotemporal dementia disorders. *Handb. Clin. Neurol*. 2021; 182: 269-280.

Ahmed Z, Mackenzie IR, Hutton ML, Dickson DW. Progranulin in frontotemporal lobar degeneration and neuroinflammation. *J. Neuroinflammation*. 2007; 4: 7.

Ahmed Z, Sheng H, Xu YF, Lin WL, Innes AE, Gass J, et al. Accelerated lipofuscinosis and ubiquitination in granulin knockout mice suggest a role for progranulin in successful aging. *Am. J. Pathol*. 2010; 177: 311-324.

Ahmed Z, Bigio EH, Budka H, Dickson DW, Ferrer I, Ghetti B, et al. Globular glial tauopathies (GGT): consensus recommendations. *Acta Neuropathol*. 2013; 126: 537-544.

Al Shweiki MR, Steinacker P, Oeckl P, Hengerer B, Danek A, Fassbender K, et al. Neurofilament light chain as a blood biomarker to differentiate psychiatric disorders from behavioural variant frontotemporal dementia. *J. Psychiatr. Res*. 2019; 113: 137-140.

Al-Obeidi E, Al-Tahan S, Surampalli A, Goyal N, Wang AK, Hermann A, et al. Genotype-phenotype study in patients with valosin-containing protein mutations associated with multisystem proteinopathy. *Clin. Genet.* 2018; 93: 119-125.

Alaerts K, Woolley DG, Steyaert J, Di Martino A, Swinnen SP, Wenderoth N. Underconnectivity of the superior temporal sulcus predicts emotion recognition deficits in autism. *Soc. Cogn. Affect. Neurosci.* 2014; 9: 1589-1600.

Alberici A, Archetti S, Pilotto A, Premi E, Cosseddu M, Bianchetti A, et al. Results from a pilot study on amiodarone administration in monogenic frontotemporal dementia with granulin mutation. *Neurol. Sci.* 2014; 35: 1215-1259.

Alirezai Z, Pourhanifeh MH, Borran S, Nejati M, Mirzaei H, Hamblin MR. Neurofilament Light Chain as a Biomarker, and Correlation with Magnetic Resonance Imaging in Diagnosis of CNS-Related Disorders. *Mol. Neurobiol.* 2020; 57: 469-491.

Amador-Ortiz C, Lin, WL Ahmed Z, Personett D, Davies P, Duara R, et al. TDP-43 immunoreactivity in hippocampal sclerosis and Alzheimer's disease. *Ann. Neurol.* 2007; 61: 435-445.

Ameur F, Colliot O, Caroppo P, Ströer S, Dormont D, Brice A, et al. White matter lesions in FTL D: distinct phenotypes characterize GRN and C9ORF72 mutations. *Neurol. Genet.* 2016; 2: e47.

Armstrong MJ, Litvan I, Lang AE, Bak TH, Bhatia KP, Borroni B, et al. Criteria for the diagnosis of corticobasal degeneration. *Neurology* 2013; 80: 496-503.

Aron AR. The neural basis of inhibition in cognitive control. *Neuroscientist.* 2007; 13: 214-228.

Arrant AE, Filiano AJ, Unger DE, Young AH, Roberson ED. Restoring neuronal progranulin reverses deficits in a mouse model of frontotemporal dementia. *Brain.* 2017; 140: 1447-1465.

Arrant AE, Roth JR, Boyle NR, Kashyap SN, Hoffmann MQ, Murchison CF, et al. Impaired β -glucocerebrosidase activity and processing in frontotemporal dementia due to progranulin mutations. *Acta Neuropathol. Commun.* 2019; 7: 218.

Ashburner J, Friston KJ. Unified segmentation. *Neuroimage*. 2005; 26: 839-851.

Ashburner J. A fast diffeomorphic image registration algorithm. *Neuroimage*. 2007; 38: 95-113.

Ashburner J, Ridgway GR. Symmetric diffeomorphic modeling of longitudinal structural MRI. *Front. Neurosci*. 2013; 6: 197.

Azuar C, Saratxaga AA, Camus M, Funkiewiez A, Mauras T, Levy R, et al. The eating behavior inventory (EBI): A new clinical tool for the diagnosis of frontotemporal dementia. AAIC 2015 Podium Presentations: Thursday, July 23, 2015.

Baker M, Mackenzie IR, Pickering-Brown SM, Gass J, Rademakers R, Lindholm C, et al. Mutations in progranulin cause tau-negative frontotemporal dementia linked to chromosome 17. *Nature*. 2006; 442: 916-919.

Barbier M, Camuzat A, Houot M, Clot F, Caroppo P, Fournier C, et al. Factors influencing the age at onset in familial frontotemporal lobar dementia: Important weight of genetics. *Neurol. Genet*. 2017; 3: e203.

Barbier M, Camuzat A, El Hachimi K, Guegan J, Rinaldi D, Lattante S, et al. SLITRK2, an X-linked modifier of the age at onset in C9orf72 frontotemporal lobar degeneration. *Brain*. 2021; 144: 2798-2811.

Barker MS, Gottesman RT, Manoochehri M, Chapman S, Appleby BS, Brushaber D, et al. Proposed research criteria for prodromal behavioural variant frontotemporal dementia. *Brain*. 2022; 145: 1079-1097.

Barnat M, Capizzi M, Aparicio E, Boluda S, Wennagel D, Kacher R, et al. Huntington's disease alters human neurodevelopment. *Science*. 2020; 369: 787-793.

Barschke P, Oeckl P, Steinacker P, Al Shweiki MR, Weishaupt JH, Landwehrmeyer GB, et al. Different CSF protein profiles in amyotrophic lateral sclerosis and frontotemporal dementia with C9orf72 hexanucleotide repeat expansion. *J. Neurol. Neurosurg. Psychiatry*. 2020; 91: 503-511.

Bateman RJ, Xiong C, Benzinger TLS, Fagan AM, Goate A, Fox NC, et al. Clinical and Biomarker Changes in Dominantly Inherited Alzheimer's Disease. *N. Engl. J. Med.* 2012; 367: 795-804.

Beck J, Rohrer JD, Campbell T, Isaacs A, Morrison KE, Goodall EF, et al. A distinct clinical, neuropsychological and radiological phenotype is associated with progranulin gene mutations in a large UK series. *Brain.* 2008; 131: 706-720.

Beck J, Poulter M, Hensman D, Rohrer JD, Mahoney CJ, Adamson G, et al. Large C9orf72 hexanucleotide repeat expansions are seen in multiple neurodegenerative syndromes and are more frequent than expected in the UK population. *Am. J. Hum. Genet.* 2013; 92: 345-353.

Bede P, Siah WF, McKenna MC, Li Hi Shing S. Consideration of C9orf72-associated ALS-FTD as a neurodevelopmental disorder: insights from neuroimaging. *J. Neurol. Neurosurg. Psychiatry.* 2020; 91: 1138.

Beel S, Moisse M, Damme M, De Muynck L, Robberecht W, Van Den Bosch L, et al. Progranulin functions as a cathepsin D chaperone to stimulate axonal outgrowth in vivo. *Hum. Mol. Genet.* 2017; 26: 2850-2863.

Behler A, Knehr A, Finsel J, Kunz MS, Lang C, Müller K, et al. Eye movement alterations in presymptomatic C9orf72 expansion gene carriers. *J. Neurol.* 2021; 268: 3390-3399.

Belin P, Zatorre RJ, Lafaille P, Ahad P, Pike B. Voice-selective areas in human auditory cortex. *Nature.* 2000; 403: 309-312.

Benajiba L, Le Ber I, Camuzat A, Lacoste M, Thomas-Antérion C, Couratier P, et al. TARDBP mutations in motoneuron disease with frontotemporal lobar degeneration. *Ann. Neurol.* 2009; 65: 470-473.

Benatar M, Wu J. Presymptomatic studies in ALS: Rationale, challenges, and approach. *Neurology* 2012; 79: 1732-1739.

Benatar M, Wu J, Lombardi V, Jeromin A, Bowser R, Andersen PM, et al. Neurofilaments in pre-symptomatic ALS and the impact of genotype. *Amyotroph. Lateral Scler. Frontotemporal Degener.* 2019; 20: 538-548.

Benatar M, Zhang L, Wang L, Granit V, Statland J, Barohn R, et al. Validation of serum neurofilaments as prognostic and potential pharmacodynamic biomarkers for ALS. *Neurology*. 2020; 95: e59-e69.

Benatar M, Wu J, McHutchison C, Postuma RB, Boeve BF, Petersen R, et al. Preventing amyotrophic lateral sclerosis: insights from pre-symptomatic neurodegenerative diseases. *Brain*. 2022; 145: 27-44.

Benussi A, Karikari TK, Ashton N, Gazzina S, Premi E, Benussi L, et al. Diagnostic and prognostic value of serum NfL and p-Tau181 in frontotemporal lobar degeneration. *J. Neurol. Neurosurg. Psychiatry*. 2020; 91: 960-967.

Benussi A, Alberici A, Samra K, Russell LL, Greaves CV, Bocchetta M, et al. Conceptual framework for the definition of preclinical and prodromal frontotemporal dementia. *Alzheimers Dement*. 2021; doi: 10.1002/alz.12485.

Benussi L, Rossi G, Glionna M, Tonoli E, Piccoli E, Fostinelli S, et al. C9ORF72 hexanucleotide repeat number in frontotemporal lobar degeneration: A genotype-phenotype correlation study. *J. Alzheimers Dis*. 2014; 38: 799-808.

Bergeron D, Gorno-Tempini ML, Rabinovici GD, Santos-Santos MA, Seeley W, Miller BL, et al. Prevalence of amyloid- β pathology in distinct variants of primary progressive aphasia. *Ann. Neurol*. 2018; 84: 729-740.

Bertoux M, de Souza LC, Corlier F, Lamari F, Bottlaender M, Dubois B, et al. Two distinct amnesic profiles in behavioral variant frontotemporal dementia. *Biol. Psychiatry*. 2014; 75: 582-588.

Bertoux M, O'Callaghan C, Dubois B, Hornberger M. In two minds: executive functioning versus theory of mind in behavioural variant frontotemporal dementia. *J. Neurol. Neurosurg. Psychiatry*. 2016; 87: 231-234.

Bertoux M, Cassagnaud P, Lebouvier T, Lebert F, Sarazin M, Le Ber I, et al. Does amnesia specifically predict Alzheimer's pathology? A neuropathological study. *Neurobiol. Aging*. 2020; 95: 123-130.

Bertrand A, Wen J, Rinaldi D, Houot M, Sayah S, Camuzat A, et al. Early Cognitive, Structural, and Microstructural Changes in Presymptomatic C9orf72 Carriers Younger Than 40 Years. *JAMA Neurol.* 2018; 75: 236-245.

Biglan KM, Ross CA, Langbehn DR, Aylward EH, Stout JC, Queller S, et al. Motor abnormalities in premanifest persons with Huntington's disease: The PREDICT-HD study: Motor Abnormalities in Premanifest HD. *Mov. Disord.* 2009; 24: 1763-1772.

Bocchetta M, Gordon E, Cardoso MJ, Modat M, Ourselin S, Warren JD, et al. Thalamic atrophy in frontotemporal dementia - Not just a C9orf72 problem. *Neuroimage Clin.* 2018; 18: 675-681.

Bocchetta M, Iglesias JE, Neason M, Cash DM, Warren JD, Rohrer JD, et al. Thalamic nuclei in frontotemporal dementia: Mediodorsal nucleus involvement is universal but pulvinar atrophy is unique to C9orf72. *Hum. Brain Mapp.* 2020; 41: 1006-1016.

Bocchetta M, Todd EG, Peakman G, Cash DM, Convery RS, Russell LL, et al. Differential early subcortical involvement in genetic FTD within the GENFI cohort. *Neuroimage Clin.* 2021; 30: 102646.

Boeve B, Bove J, Brannelly P, Brushaber D, Coppola G, Dever R, et al. The longitudinal evaluation of familial frontotemporal dementia subjects protocol: Framework and methodology. *Alzheimers Dement.* 2020; 16: 22-36.

Boeve BF, Boylan KB, Graff-Radford N R, DeJesus-Hernandez M, Knopman D S, Pedraza O, et al. Characterization of frontotemporal dementia and/or amyotrophic lateral sclerosis associated with the GGGGCC repeat expansion in C9ORF72. *Brain.* 2012; 135: 765-783.

Boeve BF, Maraganore DM, Parisi JE, Ahlskog JE, Graff-Radford N, Caselli RJ, et al. Pathologic heterogeneity in clinically diagnosed corticobasal degeneration. *Neurology.* 1999; 53: 795-800.

Bonakdarpour B, Hurley RS, Wang AR, Ferreira HR, Basu A, Chatrathi A, et al. Perturbations of language network connectivity in primary progressive aphasia. *Cortex.* 2019; 121: 468-480.

Borrego-Écija S, Sala-Llonch R, van Swieten J, Borroni B, Moreno F, Masellis M, et al. Disease-related cortical thinning in presymptomatic granulin mutation carriers. *Neuroimage Clin.* 2021; 29: 102540.

Botha H, Duffy JR, Whitwell JL, Strand EA, Machulda MM, Schwarz CG et al. Classification and clinicoradiologic features of primary progressive aphasia (PPA) and apraxia of speech. *Cortex.* 2015; 69: 220-236.

Boxer AL, Gold M, Feldman H, Boeve BF, Dickinson SL-J, Fillit H, et al. New directions in clinical trials for frontotemporal lobar degeneration: Methods and outcome measures. *Alzheimers Dement.* 2020; 16: 131-143.

Boxer AL, Qureshi I, Ahljianian M, Grundman M, Golbe LI, Litvan I, et al. Safety of the tau-directed monoclonal antibody BIIB092 in progressive supranuclear palsy: a randomised, placebo-controlled, multiple ascending dose phase 1b trial. *Lancet Neurol.* 2019; 18: 549-558.

Braak H, Alafuzoff I, Arzberger T, Kretschmar H, Del Tredici K, et al. Staging of Alzheimer disease-associated neurofibrillary pathology using paraffin sections and immunocytochemistry. *Acta Neuropathol.* 2006; 112: 389-404.

Brettschneider J, Del Tredici K, Toledo JB, Robinson JL, Irwin DJ, Grossman M, et al. Stages of pTDP-43 pathology in amyotrophic lateral sclerosis. *Ann. Neurol.* 2013; 74: 20-38.

Brettschneider J, Del Tredici K, Irwin DJ, Grossman M, Robinson JL, Toledo JB, et al. Sequential distribution of pTDP-43 pathology in behavioral variant frontotemporal dementia (bvFTD). *Acta Neuropathol.* 2014; 127: 423-439.

Bridel C, van Wieringen WN, Zetterberg H, Tijms BM, Teunissen CE, the NFL Group, et al. Diagnostic value of cerebrospinal fluid neurofilament light protein in neurology: a systematic review and meta-analysis. *JAMA Neurol.* 2019; 76: 1035-1048.

Brooks BR, Miller RG, Swash M, Munsat TL, World Federation of Neurology Research Group on Motor Neuron Diseases. El Escorial revisited: revised criteria for the diagnosis of amyotrophic lateral sclerosis. *Amyotroph. Lateral Scler. Other Motor Neuron Disord.* 2000; 1: 293-299.

Brun A. Frontal lobe degeneration of non-Alzheimer type. I. Neuropathology. Arch. Gerontol. Geriatr. 1987; 6: 193-208.

Buchsbaum BR, D'Esposito M. A sensorimotor view of verbal working memory. Cortex. 2019; 112: 134-148.

Bunina TL. On intracellular inclusions in familial amyotrophic lateral sclerosis. Zh. Nevropatol. Psikiatr. Im. S S Korsakova. 1962; 62: 1293-1299.

Buratti E, Baralle FE. Characterization and functional implications of the RNA binding properties of nuclear factor TDP-43, a novel splicing regulator of CFTR exon 9. J. Biol. Chem. 2001; 276: 36337-36343.

Burgess P, Shallice T. The Hayling and Brixton Tests. Bury St Edmunds : Thames Valley Test Company. 1997.

Cajanus A, Katisko K, Kontkanen A, Jääskeläinen O, Hartikainen P, Haapasalo A, et al. Serum neurofilament light chain in FTL D: association with C9orf72, clinical phenotype, and prognosis. Ann. Clin. Transl. Neurol. 2020; 7: 903-910.

Calvo A, Moglia C, Canosa A, Cistaro A, Valentini C, Carrara G, et al. Amyotrophic lateral sclerosis/frontotemporal dementia with predominant manifestations of obsessive-compulsive disorder associated to GGGGCC expansion of the c9orf72 gene. J. Neurol. 2012; 259: 2723-2725.

Cammack AJ, Atassi N, Hyman T, van den Berg LH, Harms M, Baloh RH, et al. Prospective natural history study of C9orf72 ALS clinical characteristics and biomarkers. Neurology. 2019; 93: e1605-e1617.

Camuzat A, Barbier M, Saracino D, Houot M, Clot F, Rinaldi D, et al. Influence de la taille de l'expansion de la répétition GGGGCC du gène C9orf72 sur les caractéristiques cliniques des formes familiales de dégénérescences lobaires fronto-temporales. Poster présenté aux RFMASA 2021.

Carneiro F, Saracino D, Huin V, Clot F, Delorme C, Méneret A, et al. Isolated parkinsonism is an atypical presentation of GRN and C9orf72 gene mutations. Parkinsonism Relat. Disord. 2020; 80: 73-81.

Caroppo P, Le Ber I, Camuzat A, Clot F, Naccache L, Lamari F, et al. Extensive white matter involvement in patients with frontotemporal lobar degeneration: think progranulin. *JAMA Neurol.* 2014; 71: 1562-1566.

Caroppo P, Camuzat A, De Septenville A, Couratier P, Lacomblez L, Auriacombe S, et al. Semantic and nonfluent aphasic variants, secondarily associated with amyotrophic lateral sclerosis, are predominant frontotemporal lobar degeneration phenotypes in TBK1 carriers. *Alzheimer. Dement. (Amst).* 2015a; 1: 481-486.

Caroppo P, Habert MO, Durrleman S, Funkiewiez A, Perlberg V, Hahn V, et al. Lateral Temporal Lobe: An Early Imaging Marker of the Presymptomatic GRN Disease? *J. Alzheimers Dis.* 2015b; 47: 751-759.

Caroppo P, Camuzat A, Guillot-Noel L, Thomas-Antérion C, Couratier P, Wong TH, et al. Defining the spectrum of frontotemporal dementias associated with TARDBP mutations. *Neurol. Genet.* 2016; 2: e80.

Cash DM, Bocchetta M, Thomas DL, Dick KM, van Swieten JC, Borroni B, et al. Patterns of gray matter atrophy in genetic frontotemporal dementia: results from the GENFI study. *Neurobiol. Aging.* 2018; 62: 191-196.

Caso F, Agosta F, Magnani G, Galantucci S, Spinelli EG, Galimberti D, et al. Clinical and MRI correlates of disease progression in a case of nonfluent/agrammatic variant of primary progressive aphasia due to progranulin (GRN) Cys157LysfsX97 mutation. *J. Neurol. Sci.* 2014; 342: 167-172.

Caso F, Agosta F, Magnani G, Cardamone R, Borghesani V, Miller Z, et al. Temporal variant of frontotemporal dementia in C9orf72 repeat expansion carriers: two case studies. *Brain Imaging Behav.* 2020; 14: 336-345.

Caverzasi E, Battistella G, Chu SA, Rosen H, Zanto TP, Karydas A, et al. Gyrfication abnormalities in presymptomatic c9orf72 expansion carriers. *J. Neurol. Neurosurg. Psychiatry.* 2019; 90: 1005-1010.

Caviness VS Jr, Lange NT, Makris N, Herbert MR, Kennedy DN. MRI-based brain volumetrics: emergence of a developmental brain science. *Brain Dev.* 1999; 21: 289-295.

Cenik B, Sephton CF, Kutluk Cenik B, Herz J, Yu G. Progranulin: A proteolytically processed protein at the crossroads of inflammation and neurodegeneration. *J. Biol. Chem.* 2012; 287: 32298-32306.

Cerami C, Marcone A, Galimberti D, Villa C, Scarpini E, Cappa SF. From genotype to phenotype: two cases of genetic frontotemporal lobar degeneration with premorbid bipolar disorder. *J Alzheimers. Dis.* 2011; 27: 791-797.

Cerami C, Marcone A, Galimberti D, Zamboni Z, Fenoglio C, Serpente S, et al. Novel evidence of phenotypical variability in the hexanucleotide repeat expansion in chromosome 9. *J. Alzheimers Dis.* 2013; 35: 455-462.

Chamberlain SR, Sahakian BJ. The neuropsychiatry of impulsivity. *Curr. Opin. Psychiatry.* 2007; 20: 255-261.

Chan D, Anderson V, Pijnenburg Y, Whitwell J, Barnes J, Scahill R, et al. The clinical profile of right temporal lobe atrophy. *Brain.* 2009; 132: 1287-1298.

Chare L, Hodges JR, Leyton CE, McGinley C, Tan RH, Kril JJ, et al. New criteria for frontotemporal dementia syndromes: clinical and pathological diagnostic implications. *J. Neurol. Neurosurg. Psychiatry.* 2014; 85: 865-870.

Chausseot A, Le Ber I, Ait-El-Mkadem S, Camuzat A, de Septenville A, Bannwarth S, et al. Screening of CHCHD10 in a French cohort confirms the involvement of this gene in frontotemporal dementia with amyotrophic lateral sclerosis patients. *Neurobiol. Aging.* 2014; 35: 2884.e1-2884.e4.

Chen-Plotkin AS, Martinez-Lage M, Sleiman PMA, Hu W, Greene R, Wood EM, et al. Genetic and clinical features of progranulin-associated frontotemporal lobar degeneration. *Arch Neurol.* 2011; 68: 488-497.

Chiò A, Calvo A, Moglia C, Mazzini L, Mora G, PARALS study group. Phenotypic heterogeneity of amyotrophic lateral sclerosis: a population based study. *J. Neurol. Neurosurg. Psychiatry.* 2011; 82: 740-746.

Choi YH, Park HK, Paik NJ. Role of the posterior temporal lobe during language tasks: a virtual lesion study using repetitive transcranial magnetic stimulation. *Neuroreport.* 2015; 26: 314-319.

Chornenka K, Hirsch-Reinshagen V, Perez-Rosendahl M, Feldman H, Segal-Gidan F, Vinters HV, et al. Expanding the Phenotype of Frontotemporal Lobar Degeneration With FUS-Positive Pathology (FTLD-FUS). *J. Neuropathol. Exp. Neurol.* 2020; 79: 809-812.

Christidi F, Migliaccio R, Santamaría-García H, Santangelo G, Trojsi F. Social Cognition Dysfunctions in Neurodegenerative Diseases: Neuroanatomical Correlates and Clinical Implications. *Behav. Neurol.* 2018; 1849794.

Codjia P, Aygnac X, Mochel F, Mouzat K, Carra-Dalliere C, Castelnovo G, et al. Adult-Onset Leukoencephalopathy with Axonal Spheroids and Pigmented Glia: An MRI Study of 16 French Cases. *Am. J. Neuroradiol.* 2018; 39: 1657-1661.

Coppola C, Saracino D, Puoti G, Lus G, Dato C, Le Ber I, et al. A cluster of progranulin C157KfsX97 mutations in Southern Italy: clinical characterization and genetic correlations. *Neurobiol. Aging.* 2017; 49: 219.e5-219.e13.

Cordella C, Quimby M, Touroutoglou A, Brickhouse M, Dickerson BC, Green JR. Quantification of motor speech impairment and its anatomic basis in primary progressive aphasia. *Neurology.* 2019; 92: e1992-e2004.

Costa B, Manzoni C, Bernal-Quiros M, Kia DA, Aguilar M, Alvarez I, et al. C9orf72, age at onset, and ancestry help discriminate behavioral from language variants in FTLN cohorts. *Neurology.* 2020; 95: e3288-e3302.

Crary JF, Trojanowski JQ, Schneider JA, Abisambra JF, Abner EL, Alafuzoff I, et al. Primary age-related tauopathy (PART): a common pathology associated with human aging. *Acta Neuropathol* 2014; 128: 755-766.

Crockford C, Newton J, Lonergan K, Madden C, Mays I, O'Sullivan M, et al. Measuring reliable change in cognition using the Edinburgh Cognitive and Behavioural ALS Screen (ECAS). *Amyotroph. Lateral Scler. Front. Degener.* 2018; 19: 65-73.

Cruts M, Gijssels I, van der Zee J, Engelborghs S, Wils H, Pirici D, et al. Null mutations in progranulin cause ubiquitin-positive frontotemporal dementia linked to chromosome 17q21. *Nature.* 2006; 442: 920-924.

Cruts M, Gijselinck I, Van Langenhove T, van der Zee J, Van Broeckhoven C. Current insights into the C9orf72 repeat expansion diseases of the FTL/ALS spectrum. *Trends. Neurosci.* 2013; 36: 450-459.

Cruts M, Theuns J, Van Broeckhoven C. Locus-specific mutation databases for neurodegenerative brain diseases. *Hum. Mutat.* 2012; 33: 1340-1344.

Daniel R, He Z, Carmichael KP, Halper J. Cellular localization of gene expression for progranulin. *J. Histochem. Cytochem.* 2000; 48: 999-1009.

Day GS, Farb NA, Tang-Wai DF, Masellis M, Black SE, Freedman M, et al. Salience network resting-state activity: prediction of frontotemporal dementia progression. *JAMA Neurol.* 2013; 70: 1249-1253.

De Vocht J, Blommaert J, Devrome M, Radwan A, Van Weehaeghe D, De Schaepdryver M, et al. Use of Multimodal Imaging and Clinical Biomarkers in Presymptomatic Carriers of C9orf72 Repeat Expansion. *JAMA Neurol.* 2020; 77: 1008-1117.

De Vocht J, Stam D, Nicolini M, Lamaire N, Laroy M, Vande Casteele T, et al. Psychopathology in premanifest C9orf72 repeat expansion carriers. *J. Neurol. Neurosurg. Psychiatry.* 2022; 93: 565-567.

DeJesus-Hernandez M, Mackenzie IR, Boeve BF, Boxer AL, Baker M, Rutherford NJ, et al. Hexanucleotide Repeat in Noncoding Region of C9ORF72 Causes Chromosome 9pLinked FTD and ALS. *Neuron.* 2011; 72: 245-256.

Delbeuck X, Pollet M, Pasquier F, Bombois S, Moroni C. The Clinical Value of the Faux Pas Test for Diagnosing Behavioral-Variant Frontotemporal Dementia. *J. Geriatr. Psychiatry Neurol.* 2022; 35: 62-65.

Deloche G, Hannequin D. DO 80: Epreuve de dénomination orale d'image. ECPA (Editions du Centre de Psychologie Appliquée); 1997.

Deramecourt V, Lebert F, Debachy B, Mackowiak-Cordoliani MA, Bombois S, Kerdraon O, et al. Prediction of pathology in primary progressive language and speech disorders. *Neurology.* 2010; 74: 42-49.

Desikan RS, Ségonne F, Fischl B, Quinn BT, Dickerson BC, Blacker D, et al. An automated labeling system for subdividing the human cerebral cortex on MRI scans into gyral based regions of interest. *Neuroimage*. 2006; 31: 968-980.

Desmarais P, Rohrer JD, Nguyen QD, Herrmann N, Stuss DT, Lang AE, et al. Therapeutic trial design for frontotemporal dementia and related disorders. *J. Neurol. Neurosurg. Psychiatry*. 2019; 90: 412-423.

Destrieux C, Fischl B, Dale A, Halgren E. Automatic parcellation of human cortical gyri and sulci using standard anatomical nomenclature. *Neuroimage*. 2010; 53: 1-15.

Devenney E, Swinn T, Mioshi E, Hornberger M, Dawson KE, Mead S, et al. The behavioural variant frontotemporal dementia phenocopy syndrome is a distinct entity - evidence from a longitudinal study. *BMC Neurol*. 2018a; 18: 56.

Devenney EM, Ahmed RM, Halliday G, Piguet O, Kiernan MC, Hodges JR. Psychiatric disorders in C9orf72 kindreds: Study of 1,414 family members. *Neurology*. 2018b; 91: e1498-1507.

Dickson DW, Bergeron C, Chin SS, Duyckaerts C, Horoupian D, Ikeda K, et al. Office of Rare Diseases neuropathologic criteria for corticobasal degeneration. *J. Neuropathol. Exp. Neurol*. 2002; 61: 935-946.

Dickson DW, Hauw JJ, Agid Y, Litvan I. Progressive Supranuclear Palsy and Corticobasal Degeneration. In: Dickson DW, Weller RO, *Neurodegeneration: The Molecular Pathology of Dementia and Movement Disorders*. Wiley-Blackwell, Oxford. 2011: 393-403.

Dickson SS, Husain M. Are there distinct dimensions of apathy? The argument for reappraisal. *Cortex*. 2022; 149: 246-256.

Didic M, Aglieri V, Tramoni-Nègre E, Ronat L, Le Ber I, Ceccaldi M, et al. Progressive phonagnosia in a telephone operator carrying a C9orf72 expansion. *Cortex*. 2020; 132: 92-98.

Dubois B, Hampel H, Feldman HH, Scheltens P, Aisen P, Andrieu S, et al. Preclinical Alzheimer's disease: Definition, natural history, and diagnostic criteria. *Alzheimers Dement*. 2016; 12: 292-323.

Dubois B, Villain N, Frisoni GB, Rabinovici GD, Sabbagh M, Cappa S, et al. Clinical diagnosis of Alzheimer's disease: recommendations of the International Working Group. *Lancet Neurol.* 2021; 20: 484-496.

Ducharme S, Bajestan S, Dickerson BC, Voon V. Psychiatric Presentations of C9orf72 Mutation: What Are the Diagnostic Implications for Clinicians? *J. Neuropsychiatry Clin. Neurosci.* 2017; 29: 195-205.

Ducharme S, Pearl-Dowler L, Gossink F, McCarthy J, Lai J, Dickerson BC, et al. The frontotemporal dementia versus primary psychiatric disorder (FTD versus PPD) checklist: a bedside clinical tool to identify behavioral variant FTD in patients with late-onset behavioral changes. *J. Alzheimers Dis.* 2019; 67: 113-124.

Ducharme S, Dols A, Laforce R, Devenney E, Kumfor F, van den Stock J, et al. Recommendations to distinguish behavioural variant frontotemporal dementia from psychiatric disorders. *Brain.* 2020; 143: 1632-1650.

Edwards-Lee, Miller BL, Benson DF, Cummings JL, Russell GL, Boone K, et al. The temporal variant of frontotemporal dementia. *Brain.* 1997; 120: 1027-1040.

El Mendili M-M, Cohen-Adad J, Pelegriani-Issac M, Rossignol S, Morizot-Koutlidis R, Marchand-Pauvert V, et al. Multi-Parametric Spinal Cord MRI as Potential Progression Marker in Amyotrophic Lateral Sclerosis. *PLoS ONE.* 2014; 9: e95516.

Engell AD, Haxby JV. Facial expression and gaze-direction in human superior temporal sulcus. *Neuropsychologia.* 2007; 45: 3234-3241.

Fathy YY, Hoogers SE, Berendse HW, van der Werf YD, Visser PJ, de Jong FJ, et al. Differential insular cortex sub-regional atrophy in neurodegenerative diseases: a systematic review and meta-analysis. *Brain Imaging Behav.* 2020; 14: 2799-2816.

Feis RA, Bouts MJRJ, de Vos F, Schouten TM, Panman JL, Jiskoot LC, et al. A multimodal MRI-based classification signature emerges just prior to symptom onset in frontotemporal dementia mutation carriers. *J. Neurol. Neurosurg. Psychiatry.* 2019; 90: 1207-1214.

Feneberg E, Oeckl P, Steinacker P, Verde F, Barro C, Van Damme P, et al. Multicenter evaluation of neurofilaments in early symptom onset amyotrophic lateral sclerosis. *Neurology*. 2018; 90: e22-e30.

Ferrer I, Santpere G, van Leeuwen FW. Argyrophilic grain disease. *Brain*. 2008; 131: 1416-1432.

Fieldhouse JLP, Gossink FT, Feenstra TC, de Boer SCM, Lemstra AW, Prins ND, et al. Clinical Phenotypes of Behavioral Variant Frontotemporal Dementia by Age at Onset. *J. Alzheimers Dis*. 2021; 82: 381-390.

Fineberg NA, Chamberlain SR, Goudriaan AE, Stein DJ, Vanderschuren LJMJ, Gillan CM, et al. New developments in human neurocognition: Clinical, genetic, and brain imaging correlates of impulsivity and compulsivity. *CNS Spectrums*. 2014; 19: 69-89.

Finkel RS, Mercuri E, Darras BT, Connolly AM, Kuntz NL, Kirschner J, et al. Nusinersen versus Sham Control in Infantile-Onset Spinal Muscular Atrophy. *N. Engl. J. Med*. 2017; 377: 1723-1732.

Fischl B. FreeSurfer. *Neuroimage*. 2012; 62: 774-781.

Flanagan EP, Baker MC, Perkerson RB, Duffy JR, Strand EA, Whitwell JL, et al. Dominant frontotemporal dementia mutations in 140 cases of primary progressive aphasia and speech apraxia. *Demen. Geriatr. Cogn. Disord*. 2015; 39: 281-286.

Fletcher PD, Downey LE, Golden HL, Clark CN, Slattery CF, Paterson RW, et al. Pain and temperature processing in dementia: a clinical and neuroanatomical analysis. *Brain*. 2015a; 138: 3360-3372.

Fletcher PD, Downey LE, Golden HL, Clark CN, Slattery CF, Paterson RW, et al. Auditory hedonic phenotypes in dementia: A behavioural and neuroanatomical analysis. *Cortex*. 2015b; 67: 95-105.

Floris G, Borghero G, Cannas A, Di Stefano F, Murru MR, Corongiu D, et al. Bipolar affective disorder preceding frontotemporal dementia in a patient with C9ORF72 mutation: is there a genetic link between these two disorders? *J. Neurol*. 2013; 260: 1155-1157.

Forrest SL, Kril JJ, Stevens CH, Kwok JB, Hallupp M, Kim WS, et al. Retiring the term FTDP-17 as MAPT mutations are genetic forms of sporadic frontotemporal tauopathies. *Brain*. 2018; 141: 521-534.

Fouquet M, Desgranges B, Landeau B, Duchesnay E, Mézenge F, de la Sayette V, et al. Longitudinal brain metabolic changes from amnesic mild cognitive impairment to Alzheimer's disease. *Brain*. 2009; 132: 2058-2067.

Fourier A, Formaglio M, Kaczorowski F, Mollion H, Perret-Liaudet A, Sauvee M, et al. A combination of total tau and neurofilaments discriminates between neurodegenerative and primary psychiatric disorders. *Eur. J. Neurol*. 2020; 27: 1164-1169.

Fournier C, Barbier M, Camuzat A, Anquetil V, Lattante S, Clot F, et al. Relations between C9orf72 expansion size in blood, age at onset, age at collection and transmission across generations in patients and presymptomatic carriers. *Neurobiol. Aging*. 2019; 74: 234.e1-234.e8.

Franklin HD, Russell LL, Peakman G, Greaves CV, Bocchetta M, Nicholas J, et al. The Revised Self-Monitoring Scale detects early impairment of social cognition in genetic frontotemporal dementia within the GENFI cohort. *Alz. Res. Therapy*. 2021; 13: 127.

Freischmidt A, Wieland T, Richter B, Ruf W, Schaeffer V, Müller K, et al. Haploinsufficiency of TBK1 causes familial ALS and fronto-temporal dementia. *Nat. Neurosci*. 2015; 18: 631-636.

Funkiewiez A, Bertoux M, de Souza LC, Levy R, Dubois B. The SEA (Social cognition and Emotional Assessment): a clinical neuropsychological tool for early diagnosis of frontal variant of frontotemporal lobar degeneration. *Neuropsychology*. 2012; 26: 81-90.

Gaetani L, Blennow K, Calabresi P, Di Filippo M, Parnetti L, Zetterberg H, et al. Neurofilament light chain as a biomarker in neurological disorders. *J. Neurol. Neurosurg. Psychiatry*. 2019; 90: 870-881.

Gainotti G. Different patterns of famous people recognition disorders in patients with right and left anterior temporal lesions: a systematic review. *Neuropsychologia* 2007; 45: 1591-1607.

Galimberti D, Fenoglio C, Serpente M, Villa C, Bonsi R, Arighi A, et al. Autosomal dominant frontotemporal lobar degeneration due to the C9ORF72 hexanucleotide repeat expansion: late-onset psychotic clinical presentation. *Biol. Psychiatry*. 2013; 74: 384-391.

Galimberti D, Fumagalli GG, Fenoglio C, Cioffi SMG, Arighi A, Serpente M, et al. Progranulin plasma levels predict the presence of GRN mutations in asymptomatic subjects and do not correlate with brain atrophy: results from the GENFI study. *Neurobiol. Aging*. 2018; 62: 245.e9-245.e12.

Gallagher MD, Suh E, Grossman M, Elman L, McCluskey L, Van Swieten JC, et al. TMEM106B is a genetic modifier of frontotemporal lobar degeneration with C9orf72 hexanucleotide repeat expansions. *Acta Neuropathol*. 2014; 127: 407-418.

Ganguly J, Jog M. Tauopathy and Movement Disorders - Unveiling the Chameleons and Mimics. *Front. Neurol*. 2020; 11: 599384.

Garibotto V, Borroni B, Agosti C, Premi E, Alberici A, Eickhoff SB, et al. Subcortical and deep cortical atrophy in Frontotemporal Lobar Degeneration. *Neurobiol. Aging*. 2011; 32: 875-884.

Gasca-Salas C, Masellis M, Khoo E, Shah BB, Fisman D, Lang AE, et al. Characterization of Movement Disorder Phenomenology in Genetically Proven, Familial Frontotemporal Lobar Degeneration: A Systematic Review and Meta-Analysis. *PLoS One*. 2016; 11: e0153852.

Gazzina S, Grassi M, Premi E, Alberici A, Benussi A, Archetti S, et al. Structural brain splitting is a hallmark of Granulin-related frontotemporal dementia. *Neurobiol. Aging*. 2022; 114: 94-104.

Geevasinga N, Menon P, Nicholson GA, Ng K, Howells J, Kril JJ, et al. Cortical Function in Asymptomatic Carriers and Patients With C9orf72 Amyotrophic Lateral Sclerosis. *JAMA Neurol*. 2015; 72: 1268-1274.

Gellera C, Tiloca C, Del Bo R, Corrado L, Pensato V, Agostini J, et al. Ubiquilin 2 mutations in Italian patients with amyotrophic lateral sclerosis and frontotemporal dementia. *J. Neurol. Neurosurg. Psychiatry*. 2013; 84: 183-187.

Gelpi E, van der Zee J, Turon Estrada A, Van Broeckhoven C, Sanchez-Valle R. TARDBP mutation p.Ile383Val associated with semantic dementia and complex proteinopathy. *Neuropathol. Appl. Neurobiol.* 2014; 40: 225-230.

Gendron TF, C9ORF72 Neurofilament Study Group, Daugherty LM, Heckman MG, Diehl NN, Wu J, et al. Phosphorylated neurofilament heavy chain: A biomarker of survival for C9ORF72-associated amyotrophic lateral sclerosis. *Ann. Neurol.* 2017a; 82: 139-146.

Gendron TF, Chew J, Stankowski JN, Hayes LR, Zhang Y-J, Prudencio M, et al. Poly(GP) proteins are a useful pharmacodynamic marker for C9ORF72-associated amyotrophic lateral sclerosis. *Sci. Transl. Med.* 2017b; 9: eaai7866.

Ghetti B, Oblak AL, Boeve BF, Johnson KA, Dickerson BC, Goedert M. Invited review: frontotemporal dementia caused by microtubule-associated protein tau gene (MAPT) mutations: a chameleon for neuropathology and neuroimaging. *Neuropathol. Appl. Neurobiol.* 2015; 41: 24-46.

Ghidoni R, Stoppani E, Rossi G, Piccoli E, Albertini V, Paterlini A, et al. Optimal plasma progranulin cutoff value for predicting null progranulin mutations in neurodegenerative diseases: a multicenter italian study. *Neurodegen. Diseases.* 2012; 9: 121-127.

Giannini LAA, Peterson C, Ohm D, Xie SX, McMillan CT, Raskovsky K, et al. Frontotemporal lobar degeneration proteinopathies have disparate microscopic patterns of white and grey matter pathology. *Acta Neuropathol. Commun.* 2021; 9: 30.

Gil-Navarro S, Lladó A, Rami L, Castellví M, Bosch B, Bargalló N, et al. Neuroimaging and biochemical markers in the three variants of primary progressive aphasia. *Dement. Geriatr. Cogn. Disord.* 2013; 35: 106-117.

Godefroy O, Martinaud O, Narme P, Joseph PA, Mosca C, Lhommée E, et al. Dysexecutive disorders and their diagnosis: A position paper. *Cortex.* 2018; 109: 322-335.

Godefroy O. GREFEX. Fonctions exécutives et pathologies neurologiques et psychiatriques: Evaluation en pratique clinique. Marseille : Solal. 2008.

Goedert M, Spillantini MG, Potier MC, Ulrich J, Crowther RA. Cloning and sequencing of the cDNA encoding an isoform of microtubule-associated protein tau containing four tandem

repeats: differential expression of tau protein mRNAs in human brain. *EMBO J.* 1989; 8: 393-399.

Goedert M, Jakes R. Expression of separate isoforms of human tau protein: correlation with the tau pattern in brain and effects on tubulin polymerization. *EMBO J.* 1990; 9: 4225-4230.

Goldman JS, Farmer JM, Wood EM, Johnson JK, Boxer A, Neuhaus J, et al. Comparison of family histories in FTLN subtypes and related tauopathies. *Neurology.* 2005; 65: 1817-1819.

Goldman JS, Van Deerlin VM. Alzheimer's disease and frontotemporal dementia: the current state of genetics and genetic testing since the advent of next-generation sequencing. *Mol. Diagn. Ther.* 2018; 22: 505-513.

González-Sánchez M, Puertas-Martín V, Esteban-Pérez J, García-Redondo A, Borrego-Hernández D, Méndez-Guerrero A, et al. TARDBP mutation associated with semantic variant primary progressive aphasia, case report and review of the literature. *Neurocase.* 2018; 24: 301-305.

Gordon BA, Blazey TM, Su Y, Hari-Raj A, Dincer A, Flores S, et al. Spatial patterns of neuroimaging biomarker change in individuals from families with autosomal dominant Alzheimer's disease: a longitudinal study. *Lancet Neurol.* 2018; 17: 241-250.

Gordon PH, Delgadillo D, Piquard A, Bruneteau G, Pradat P-F, Salachas F, et al. The range and clinical impact of cognitive impairment in French patients with ALS: a cross-sectional study of neuropsychological test performance. *Amyotroph. Lateral Scler. Off. Publ. World Fed. Neurol. Res. Group Mot. Neuron Dis.* 2011; 12: 372-378.

Gorno-Tempini ML, Dronkers NF, Rankin KP, Ogar JM, Phengrasamy L, Rosen HJ, et al. Cognition and anatomy in three variants of primary progressive aphasia. *Ann Neurol.* 2004; 55: 335-346.

Gorno-Tempini ML, Brambati SM, Ginex V, Ogar J, Dronkers NF, Marcone A, et al. The logopenic/phonological variant of primary progressive aphasia. *Neurology.* 2008; 71: 1227-1234.

Gorno-Tempini ML, Hillis AE, Weintraub S, Kertesz A, Mendez M, Cappa SF, et al. Classification of primary progressive aphasia and its variants. *Neurology.* 2011; 76: 1006-1014.

Gossink F, Dols A, Stek ML, Scheltens P, Nijmeijer B, Cohn Hokke P, et al. Early life involvement in C9orf72 repeat expansion carriers. *J. Neurol. Neurosurg. Psychiatry*. 2022; 93: 93-100.

Graham AJ, Davies R, Xuereb J, Halliday G, Kril J, Creasey H, et al. Pathologically proven frontotemporal dementia presenting with severe amnesia. *Brain*. 2005; 128: 597-605.

Grasso M, Piscopo P, Confaloni A, Denti M. Circulating miRNAs as Biomarkers for Neurodegenerative Disorders. *Molecules* 2014; 19: 6891-6910.

Gray E, Oeckl P, Amador MDM, Andreasson U, An J, Blennow K, et al. A multi-center study of neurofilament assay reliability and inter-laboratory variability. *Amyotroph. Lateral Scler. Frontotemporal Degener.* 2020; 21: 452-458.

Gregory C, Lough S, Stone V, Erzinclioglu S, Martin L, Baron-Cohen S, et al. Theory of mind in patients with frontal variant frontotemporal dementia and Alzheimer's disease: theoretical and practical implications. *Brain*. 2002; 125: 752-764.

Greve DN, Salat DH, Bowen SL, Izquierdo-Garcia D, Schultz AP, Catana C, et al. Different partial volume correction methods lead to different conclusions: An (18)F-FDG-PET study of aging. *Neuroimage*. 2016; 132: 334-343.

Guerreiro R, Kara E, Le Ber I, Bras J, Rohrer JD, Taipa R, et al. Genetic Analysis of Inherited Leukodystrophies: Genotype-Phenotype Correlations in the CSF1R Gene. *JAMA Neurol*. 2013; 70: 875-882.

Gustafson L. Frontal lobe degeneration of non-Alzheimer type. II. Clinical picture and differential diagnosis. *Arch. Gerontol. Geriatr.* 1987; 6: 209-223.

Haapanen M, Katisko K, Hänninen T, Krüger J, Hartikainen P, Haapasalo A, et al. C9orf72 repeat expansion does not affect the phenotype in primary progressive aphasia. *J. Alzheimers Dis.* 2020; 78: 919-925.

Habert MO, Marie S, Bertin H, Reynal M, Martini JB, Diallo M, et al. Optimization of brain PET imaging for a multicentre trial: the French CATI experience. *EJNMMI Phys.* 2016; 3: 6.

Hardiman O, van den Berg LH, Kiernan MC. Clinical diagnosis and management of amyotrophic lateral sclerosis. *Nat. Rev. Neurol.* 2011; 7: 639-649.

Hardy CJ, Buckley AH, Downey LE, Lehmann M, Zimmerer VC, Varley RA, et al. The Language Profile of Behavioral Variant Frontotemporal Dementia. *J. Alzheimers Dis.* 2016; 50: 359-371.

Heller C, Foiani MS, Moore K, Convery R, Bocchetta M, Neason M, et al. Plasma glial fibrillary acidic protein is raised in progranulin-associated frontotemporal dementia. *J. Neurol. Neurosurg. Psychiatry.* 2020; 91: 263-70.

Hendrix SB, Mogg R, Wang SJ, Chakravarty A, Romero K, Dickson SP, et al. Perspectives on statistical strategies for the regulatory biomarker qualification process. *Biomark. Med.* 2021; 15: 669-684.

Henz S, Ackl N, Knels C, Rominger A, Flatz W, Teipel S, et al. A pair of siblings with a rare R5H-mutation in exon 1 of the MAPT-gene. *Fortschr. Neurol. Psychiatr.* 2015; 83: 397-401.

Hirsch-Reinshagen V, Alfaify OA, Hsiung GR, Pottier C, Baker M, Perkerson 3rd RB, et al. Clinicopathologic correlations in a family with a TBK1 mutation presenting as primary progressive aphasia and primary lateral sclerosis. *Amyotroph. Lateral Scler. Frontotemporal Degener.* 2019; 20: 568-575.

Hodges JR, RR Davies, JH Xuereb, Casey B, Broe M, Bak TH, et al. Clinicopathological correlates in frontotemporal dementia. *Ann. Neurol.* 2004; 56: 399-406.

Hogan DB, Jetté N, Fiest KM, Roberts JI, Pearson D, Smith EE, et al. The Prevalence and Incidence of Frontotemporal Dementia: A Systematic Review. *Can. J. Neurol. Sci.* 2016; 43: S96-S109.

Höglinger GU, Respondek G, Stamelou M, Kurz C, Josephs KA, Lang AE, et al. Clinical diagnosis of progressive supranuclear palsy: The movement disorder society criteria. *Mov. Disord.* 2017; 32: 853-864.

Holm AC. Neurodegenerative and psychiatric overlap in frontotemporal lobar degeneration: a case of familial frontotemporal dementia presenting with catatonia. *Int. Psychogeriatr.* 2014; 26: 345-347.

Hornberger M, Shelley BP, Kipps CM, Piguet O, Hodges JR. Can progressive and non-progressive behavioural variant frontotemporal dementia be distinguished at presentation? *J. Neurol. Neurosurg. Psychiatry*. 2009; 80: 591-593.

Hornberger M, Piguet O, Graham AJ, Nestor PJ, Hodges JR. How preserved is episodic memory in behavioral variant frontotemporal dementia? *Neurology*. 2010; 74: 472-479.

Hornberger M, Geng J, Hodges JR. Convergent grey and white matter evidence of orbitofrontal cortex changes related to disinhibition in behavioural variant frontotemporal dementia. *Brain*. 2011; 134: 2502-2512.

Howard D, Patterson K. The pyramids and palm trees test: A test of semantic access from words and pictures. Bury St Edmunds : Thames Valley Test Company. 1992.

Hsiung GY, DeJesus-Hernandez M, Feldman HH, Sengdy P, Bouchard-Kerr P, Dwosh E, et al. Clinical and pathological features of familial frontotemporal dementia caused by C9ORF72 mutation on chromosome 9p. *Brain*. 2012; 135: 709-722.

Hu WT, McMillan C, Libon D, Leight S, Forman M, Lee VM, et al. Multimodal predictors for Alzheimer disease in nonfluent primary progressive aphasia. *Neurology*. 2010; 75: 595-602.

Huin V, Barbier M, Bottani A, Lobrinus JA, Clot F, Lamari F, et al. Homozygous GRN mutations: new phenotypes and new insights into pathological and molecular mechanisms. *Brain*. 2020; 143: 303-319.

Hutton M, Lendon CL, Rizzu P, Baker M, Froelich S, Houlden H, et al. Association of missense and 50-splice-site mutations in tau with the inherited dementia FTDP-17. *Nature*. 1998; 393: 702-705.

Iacoangeli A, Al Khleifat A, Jones AR, Sproviero W, Shatunov A, Opie-Martin S, et al. C9orf72 intermediate expansions of 24–30 repeats are associated with ALS. *Acta Neuropathol. Commun*. 2019; 7: 115.

Ibañez A, Manes F. Contextual social cognition and the behavioral variant of frontotemporal dementia. *Neurology*. 2012; 78: 1354-1362.

Ibañez A, Yokoyama JS, Possin KL, Matallana D, Lopera F, Nitrini R, et al. The Multi-Partner Consortium to Expand Dementia Research in Latin America (ReDLat): Driving Multicentric Research and Implementation Science. *Front. Neurol.* 2021; 12: 631722.

Imbimbo BP, Ippati S, Watling M, Balducci C. A critical appraisal of tau-targeting therapies for primary and secondary tauopathies. *Alzheimers Dement.* 2021; doi: 10.1002/alz.12453.

Irwin DJ, McMillan CT, Brettschneider J, Libon DJ, Powers J, Rascovsky K, et al. Cognitive decline and reduced survival in C9orf72 expansion frontotemporal degeneration and amyotrophic lateral sclerosis. *J. Neurol. Neurosurg. Psychiatry.* 2013; 84: 163-169.

Irwin DJ, Cairns NJ, Grossman M, McMillan CT, Lee EB, Van Deerlin VM, et al. Frontotemporal lobar degeneration: defining phenotypic diversity through personalized medicine. *Acta Neuropathol.* 2015; 129: 469-491.

Isik L, Koldewyn K, Beeler D, Kanwisher N. Perceiving social interactions in the posterior superior temporal sulcus. *Proc. Natl. Acad. Sci. USA.* 2017; 114: E9145-E9152.

Ivanova MV, Hallowell B. A tutorial on aphasia test development in any language: Key substantive and psychometric considerations. *Aphasiology.* 2013; 27: 891-920.

Jabbari E, Holland N, Chelban V, Jones PS, Lamb R, Rawlinson C, et al. Diagnosis Across the Spectrum of Progressive Supranuclear Palsy and Corticobasal Syndrome. *JAMA Neurol.* 2020; 77: 377-387.

Jack CR, Bennett DA, Blennow K, Carrillo MC, Dunn B, Haeberlein SB, et al. NIA-AA Research Framework: Toward a biological definition of Alzheimer's disease. *Alzheimers Dement.* 2018; 14: 535-562.

Jackson JL, Finch NA, Baker MC, Kachergus JM, DeJesus-Hernandez M, Pereira K, et al. Elevated methylation levels, reduced expression levels, and frequent contractions in a clinical cohort of C9orf72 expansion carriers. *Mol. Neurodegener.* 2020; 15: 7.

Jacova C, Hsiung GYR, Tawankanjanachot I, Dinelle K, McCormick S, Gonzalez M, et al. Anterior brain glucose hypometabolism predates dementia in progranulin mutation carriers. *Neurology.* 2013; 81: 1322-1331.

Jarry C, Le Gall D, Allain P, Besnard J. Les phénomènes de dépendance à l'environnement : réflexions sur l'autonomie humaine à partir de la clinique neurologique. *Tétralogiques*. 2017; 22.

Jian J, Li G, Hettinghouse A, Liu C. Progranulin: A key player in autoimmune diseases. *Cytokine*. 2018; 101: 48-55.

Jiang J, Zhu Q, Gendron TF, Saberi S, McAlonis-Downes M, Seelman A, et al. Gain of toxicity from ALS/FTD-linked repeat expansions in C9ORF72 is alleviated by antisense oligonucleotides targeting GGGGCC-containing RNAs. *Neuron*. 2016; 90: 535-550.

Jiskoot LC, Panman JL, van Asseldonk L, Franzen S, Meeter LHH, Donker Kaat L, et al. Longitudinal cognitive biomarkers predicting symptom onset in presymptomatic frontotemporal dementia. *J. Neurol*. 2018; 265: 1381-1392.

Jiskoot LC, Panman JL, Meeter LH, Dopfer EGP, Donker Kaat L, Franzen S, et al. Longitudinal multimodal MRI as prognostic and diagnostic biomarker in presymptomatic familial frontotemporal dementia. *Brain*. 2019; 142: 193-208.

Josephs KA, Duffy JR, Strand EA, Whitwell JL, Layton KF, Parisi JE, et al. Clinicopathological and imaging correlates of progressive aphasia and apraxia of speech. *Brain*. 2006; 129: 1385-1398.

Josephs KA, Whitwell JL, Knopman DS, Boeve BF, Vemuri P, Senjem ML, et al. Two distinct subtypes of right temporal variant frontotemporal dementia. *Neurology*. 2009; 73: 1443-1450.

Josephs KA, Hodges JR, Snowden JS, Mackenzie IR, Neumann M, Mann DM, et al. Neuropathological background of phenotypical variability in frontotemporal dementia. *Acta Neuropathol* 2011; 122: 137-153.

Josephs KA, Murray ME, Whitwell JL, Parisi JE, Petrucelli L, Jack CR, et al. Staging TDP-43 pathology in Alzheimer's disease. *Acta Neuropathol*. 2014a; 127: 441-450.

Josephs KA, Duffy JR, Strand EA, Machulda MM, Vemuri P, Senjem ML. Progranulin-associated PiB-negative logopenic primary progressive aphasia. *J Neurol*. 2014b; 261: 604-614.

Joubert S, Felician O, Barbeau E, Ranjeva JP, Christophe M, Didic M, et al. The right temporal lobe variant of frontotemporal dementia: cognitive and neuroanatomical profile of three patients. *J. Neurol.* 2006; 253: 1447-1458.

Kaivorinne AL, Bode MK, Paavola L, Tuominen H, Kallio M, Renton AE, et al. Clinical Characteristics of C9ORF72-Linked Frontotemporal Lobar Degeneration. *Dement. Geriatr. Cogn. Dis. Extra.* 2013; 3: 251-262.

Kerklaan BJ, van Berckel BNM, Herholz K, Dols A, van der Flier WM, Scheltens P, et al. The added value of 18-fluorodeoxyglucose-positron emission tomography in the diagnosis of the behavioral variant of frontotemporal dementia. *Am. J. Alzheimers Dis. Other Demen.* 2014; 29: 607-613.

Kertesz A. Pick Complex: an integrative approach to frontotemporal dementia: primary progressive aphasia, corticobasal degeneration, and progressive supranuclear palsy. *Neurologist.* 2003; 9: 311-317.

Kertesz A, Ang LC, Jesso S, MacKinley J, Baker M, Brown P, et al. Psychosis and Hallucinations in FTD with C9ORF72 mutation: A detailed clinical cohort. *Cogn. Behav. Neurol.* 2013; 26: 146-154.

Khalil M, Teunissen CE, Otto M, Piehl F, Sormani MP, Gattringer T, et al. Neurofilaments as biomarkers in neurological disorders. *Nat. Rev. Neurol.* 2018; 14: 577-589.

Khalil M, Pirpamer L, Hofer E, Voortman MM, Barro C, Leppert D, et al. Serum neurofilament light levels in normal aging and their association with morphologic brain changes. *Nat. Commun.* 2020; 11: 812.

Khan BK, Yokoyama JS, Takada LT, Sha SJ, Rutherford NJ, Fong JC, et al. Atypical, slowly progressive behavioural variant frontotemporal dementia associated with C9ORF72 hexanucleotide expansion. *J. Neurol. Neurosurg. Psychiatry.* 2012; 83: 358-364.

Khoury R, Liu Y, Sheheryar Q, Grossberg GT. Pharmacotherapy for Frontotemporal Dementia. *CNS Drugs.* 2021; 35: 425-438.

Kim HJ, Kim NC, Wang Y-D, Scarborough EA, Moore J, Diaz Z, et al. Mutations in prion-like domains in hnRNPA2B1 and hnRNPA1 cause multisystem proteinopathy and ALS. *Nature*. 2013; 495: 467-473.

Kim G, Ahmadian SS, Peterson M, Parton Z, Memon R, Weintraub S, et al. Asymmetric pathology in primary progressive aphasia with progranulin mutations and TDP inclusions. *Neurology*. 2016; 86: 627-636.

Kim EJ, Kim YE, Jang JH, Cho EH, Na DL, Seo SW, et al. Analysis of frontotemporal dementia, amyotrophic lateral sclerosis, and other dementia-related genes in 107 Korean patients with frontotemporal dementia. *Neurobiol. Aging*. 2018; 72: 186.e1-186.e7.

Kmetzsch V, Anquetil V, Saracino D, Rinaldi D, Camuzat A, Gareau T, et al. Plasma microRNA signature in presymptomatic and symptomatic subjects with C9orf72-associated frontotemporal dementia and amyotrophic lateral sclerosis. *J. Neurol. Neurosurg. Psychiatry*. 2021; 92: 485-493.

Kok ZQ, Murley AG, Rittman T, Rowe J, Passamonti L. Co-Occurrence of Apathy and Impulsivity in Progressive Supranuclear Palsy. *Mov. Disord. Clin. Pract*. 2021; 8: 1225-1233.

Konno T, Yoshida K, Mizuno T, Kawarai T, Tada M, Nozaki H, et al. Clinical and genetic characterization of adult-onset leukoencephalopathy with axonal spheroids and pigmented glia associated with CSF1R mutation. *Eur. J. Neurol*. 2017; 24: 37-45.

Koppers M, Blokhuis AM, Westeneng HJ, Terpstra ML, Zundel CA, Vieira de Sá R, et al. C9orf72 ablation in mice does not cause motor neuron degeneration or motor deficits *Ann. Neurol*. 2015; 78: 426-438.

Kovacs GG, Ferrer I, Grinberg LT, Alafuzoff I, Attems J, Budka H, et al. Aging-related tau astroglial pathology (ARTAG): harmonized evaluation strategy. *Acta Neuropathol*. 2016; 131: 87-102.

Kreffft TA, Graff-Radford NR, Dickson DW, Baker M, Castellani RJ. Familial primary progressive aphasia. *Alzheimer Dis. Assoc. Disord*. 2003; 17: 106-112.

Krudop WA, Dols A, Kerssens CJ, Eikelenboom P, Prins ND, Möller C, et al. The pitfall of behavioral variant frontotemporal dementia mimics despite multidisciplinary application of the FTDC criteria. *J. Alzheimers Dis.* 2017; 60: 959-975.

Kumfor F, Piguet O. Disturbance of Emotion Processing in Frontotemporal Dementia: A Synthesis of Cognitive and Neuroimaging Findings. *Neuropsychol. Rev.* 2012; 22: 280-297.

Lagier-Tourenne C, Baughn M, Rigo F, Sun S, Liu P, Li H-R, et al. Targeted degradation of sense and antisense C9orf72 RNA foci as therapy for ALS and frontotemporal degeneration. *Proc. Natl. Acad. Sci. USA.* 2013; 110: E4530-4539.

Lambon Ralph MA, Lowe C, Rogers TT. Neural basis of category-specific semantic deficits for living things: evidence from semantic dementia, HSVE and a neural network model. *Brain.* 2007; 130: 1127-1137.

Landqvist Waldö M, Gustafson L, Passant U, Englund E. Psychotic symptoms in frontotemporal dementia: A diagnostic dilemma? *Int. Psychogeriatr.* 2015; 27: 531-539.

Langbehn D, Brinkman R, Falush D, Paulsen J, Hayden M, International Huntington's Disease Collaborative Group. A new model for prediction of the age of onset and penetrance for Huntington's disease based on CAG length. *Clin. Genet.* 2004; 65: 267-277.

Lattante S, Le Ber I, Galimberti D, Serpente M, Rivaud-Péchoux S, Camuzat A, et al. Defining the association of TMEM106B variants among frontotemporal lobar degeneration patients with GRN mutations and C9orf72 repeat expansions. *Neurobiol Aging.* 2014; 35: 2658.e1-2658.e5.

Le Ber I, Guedj E, Gabelle A, Verpillat P, Volteau M, Thomas-Antérion C, et al. Demographic, neurological and behavioural characteristics and brain perfusion SPECT in frontal variant of frontotemporal dementia. *Brain.* 2006; 129: 3051-3065.

Le Ber I, Camuzat A, Hannequin D, Pasquier F, Guedj E, Rovelet-Lecrux A, et al. Phenotype variability in progranulin mutation carriers: a clinical, neuropsychological, imaging and genetic study. *Brain.* 2008; 131: 732-746.

Le Ber I. Genetics of frontotemporal lobar degeneration: an up-date and diagnosis algorithm. *Rev. Neurol. (Paris).* 2013; 169: 811-819.

Le Ber I, Guillot-Noel L, Hannequin D, Lacomblez L, Golfier V, Puel M, et al. C9ORF72 repeat expansions in the frontotemporal dementias spectrum of diseases: a flowchart for genetic testing. *J. Alzheimers Dis.* 2013a; 34: 485-499.

Le Ber I, Camuzat A, Guerreiro R, Bouya-Ahmed K, Bras J, Nicolas G, et al. SQSTM1 Mutations in French Patients With Frontotemporal Dementia or Frontotemporal Dementia With Amyotrophic Lateral Sclerosis. *JAMA Neurol.* 2013b; 70: 1403-1410.

Le Blanc G, Jetté Pomerleau V, McCarthy J, Borroni B, van Swieten J, Galimberti D, et al. Faster Cortical Thinning and Surface Area Loss in Presymptomatic and Symptomatic C9orf72 Repeat Expansion Adult Carriers. *Ann. Neurol.* 2020; 88: 113-122.

Le Bouc R, Lenfant P, Delbeuck X, Ravasi L, Lebert F, Semah F, et al. My belief or yours? Differential theory of mind deficits in frontotemporal dementia and Alzheimer's disease. *Brain.* 2012; 135: 3026-3038.

Lee G, Leugers CJ. Tau and tauopathies. *Prog. Mol. Biol. Transl. Sci.* 2012; 107: 263-293.

Lee SE, Rabinovici GD, Mayo MC, Wilson SM, Seeley WW, DeArmond SJ et al. Clinicopathological correlations in corticobasal degeneration. *Ann. Neurol.* 2011; 70: 327-340.

Lee WC, Almeida S, Prudencio M, Caulfield TR, Zhang Y-J, Tay WM, et al. Targeted manipulation of the sortilin-progranulin axis rescues progranulin haploinsufficiency. *Hum. Mol. Genet.* 2014; 23: 1467-1478.

Lee JM, Wheeler VC, Chao MJ, Vonsattel JPG, Pinto RM, Lucente D, et al. Identification of Genetic Factors that Modify Clinical Onset of Huntington's Disease. *Cell.* 2015; 162: 516-526.

Lee EB, Porta S, Michael Baer G, Xu Y, Suh E, Kwong LK, et al. Expansion of the classification of FTLT-TDP: distinct pathology associated with rapidly progressive frontotemporal degeneration. *Acta Neuropathol.* 2017a; 134: 65-78.

Lee SE, Sias AC, Mandelli ML, Brown JA, Brown AB, Khazenzon AM, et al. Network degeneration and dysfunction in presymptomatic C9ORF72 expansion carriers. *Neuroimage Clin.* 2017b; 14: 286-297.

Lehmer C, Oeckl P, Weishaupt JH, Volk AE, Diehl-Schmid J, Schroeter ML, et al. Poly-GP in cerebrospinal fluid links C9orf72-associated dipeptide repeat expression to the asymptomatic phase of ALS/FTD. *EMBO Mol. Med.* 2017; 9: 859-868.

Leroy M, Bertoux M, Skrobala E, Mode E, Adnet-Bonte C, Le Ber I, et al. Characteristics and progression of patients with frontotemporal dementia in a regional memory clinic network. *Alzheimers Res. Ther.* 2021; 13: 19.

Levine TP, Daniels RD, Gatta AT, Wong LH, Hayes MJ. The product of C9orf72, a gene strongly implicated in neurodegeneration, is structurally related to DENN Rab-GEFs. *Bioinformatics.* 2013; 29: 499-503.

Levy R, Czernecki V. Apathy and the basal ganglia. *J. Neurol.* 2006; 253: VII54-61.

Levy R, Dubois B. Apathy and the Functional Anatomy of the Prefrontal Cortex-Basal Ganglia Circuits. *Cereb. Cortex.* 2006; 16: 916-928.

Leyton CE, Ballard KJ, Piguet O, Hodges JR. Phonologic errors as a clinical marker of the logopenic variant of PPA. *Neurology.* 2014; 82: 1620-1627.

Leyton CE, Villemagne VL, Savage S, Pike KE, Ballard KJ, Piguet O., et al. Subtypes of progressive aphasia: application of the international consensus criteria and validation using β -amyloid imaging. *Brain.* 2011; 134: 3030-3043.

Lillo P, Garcin B, Hornberger M, Bak TH, Hodges JR. Neurobehavioral features in frontotemporal dementia with amyotrophic lateral sclerosis. *Arch. Neurol.* 2010; 67: 826-830.

Litvan I, Agid Y, Calne D, Campbell G, Dubois B, Duvoisin RC, et al. Clinical research criteria for the diagnosis of progressive supranuclear palsy (Steele-Richardson-Olszewski syndrome): report of the NINDS-SPSP international workshop. *Neurology.* 1996; 47: 1-9.

Ljubenkova PA, Edwards L, Iaccarino L, La Joie R, Rojas JC, Koestler M, et al. Effect of the Histone Deacetylase Inhibitor FRM-0334 on Progranulin Levels in Patients With Progranulin Gene Haploinsufficiency: A Randomized Clinical Trial. *JAMA Netw. Open.* 2021; 4: e2125584.

Lleó A, Alcolea D, Martínez-Lage P, Scheltens P, Parnetti L, Poirier J, et al. Longitudinal cerebrospinal fluid biomarker trajectories along the Alzheimer's disease continuum in the BIOMARKAPD study. *Alzheimers Dement.* 2019; 15: 742-753.

Lomen-Hoerth C, Anderson T, Miller B. The overlap of amyotrophic lateral sclerosis and frontotemporal dementia. *Neurology.* 2002; 59: 1077-1079.

Lomen-Hoerth C, Murphy J, Langmore S, Kramer JH, Olney RK, Miller B. Are amyotrophic lateral sclerosis patients cognitively normal? *Neurology.* 2003; 60: 1094-1097.

Lulé DE, Müller H-P, Finsel J, Weydt P, Knehr A, Winroth I, et al. Deficits in verbal fluency in presymptomatic C9orf72 mutation gene carriers – A developmental disorder. *J. Neurol. Neurosurg. Psychiatry.* 2020; 91: 1195-1200.

Mackenzie IRA, Neumann M, Bigio EH, Cairns NJ, Alafuzoff I, Kril J, et al. Nomenclature and nosology for neuropathologic subtypes of frontotemporal lobar degeneration: an update. *Acta Neuropathol.* 2010; 119: 1-4.

Mackenzie IR, Neumann M, Baborie A, Sampathu DM, Du Plessis D, Jaros E, et al. A harmonized classification system for FTLTDP pathology. *Acta Neuropathol.* 2011a; 122: 111-113.

Mackenzie IR, Munoz DG, Kusaka H, Yokota O, Ishihara K, Roeber S, et al. Distinct pathological subtypes of FTLTDP-FUS. *Acta Neuropathol* 2011b; 121: 207-218.

Mackenzie IRA, Frick P, Neumann M. The neuropathology associated with repeat expansions in the C9ORF72 gene. *Acta Neuropathol.* 2014; 127: 347-357.

Mackenzie IR, Neumann M. Molecular neuropathology of frontotemporal dementia: insights into disease mechanisms from postmortem studies. *J. Neurochem.* 2016; 138: 54-70.

Mackenzie IR, Neumann M. Subcortical TDP-43 pathology patterns validate cortical FTLTDP subtypes and demonstrate unique aspects of C9orf72 mutation cases. *Acta Neuropathol.* 2020; 139: 83-98.

Macoir J, Légaré A, Lavoie M. Contribution of the Cognitive Approach to Language Assessment to the Differential Diagnosis of Primary Progressive Aphasia. *Brain Sci.* 2021; 11: 815.

Mahoney CJ, Beck J, Rohrer JD, Lashley T, Mok K, Shakespeare T, et al. Frontotemporal dementia with the C9ORF72 hexanucleotide repeat expansion: clinical, neuroanatomical and neuropathological features. *Brain* 2012; 135: 736-750.

Majounie E, Renton AE, Mok K, Dopper EG, Waite A, Rollinson S, et al. Frequency of the C9orf72 hexanucleotide repeat expansion in patients with amyotrophic lateral sclerosis and frontotemporal dementia: a cross-sectional study. *Lancet Neurol.* 2012; 11: 323-330.

Malpetti M, Jones PS, Tsvetanov KA, Rittman T, Swieten JC, Borroni B, et al. Apathy in presymptomatic genetic frontotemporal dementia predicts cognitive decline and is driven by structural brain changes. *Alzheimers Dement.* 2021a; 17: 969-83.

Malpetti M, Holland N, Jones PS, Ye R, Cope TE, Fryer TD, et al. Synaptic density in carriers of C9orf72 mutations: a [11 C]UCB-J PET study. *Ann. Clin. Transl. Neurol.* 2021b; 8: 1515-1523.

Marin RS. Differential Diagnosis and Classification of Apathy. *Am. J. Psychiatry.* 1990; 147: 22-30.

Marshall CR, Hardy CJD, Volkmer A, Russell LL, Bond RL, Fletcher PD, et al. Primary progressive aphasia: a clinical approach. *J. Neurol.* 2018; 265: 1474-1490.

Massimo L, Powers C, Moore P, Vesely L, Avants B, Libon GJ, et al. Neuroanatomy of apathy and disinhibition in frontotemporal lobar degeneration. *Dement. Geriatr. Cogn. Disord.* 2009; 27: 96-104.

Massimo L, Powers JP, Evans LK, McMillan CT, Rascovsky K, Eslinger P, et al. Apathy in Frontotemporal Degeneration: Neuroanatomical Evidence of Impaired Goal-directed Behavior. *Front. Hum. Neurosci.* 2015; 9: 611.

Mattsson N, Andreasson U, Zetterberg H, Blennow K, Alzheimer's Disease Neuroimaging Initiative. Association of Plasma Neurofilament Light With Neurodegeneration in Patients With Alzheimer Disease. *JAMA Neurol.* 2017; 74: 557-566.

Mattsson N, Cullen NC, Andreasson U, Zetterberg H, Blennow K. Association Between Longitudinal Plasma Neurofilament Light and Neurodegeneration in Patients With Alzheimer Disease. *JAMA Neurol.* 2019; 76: 791-799.

Mazaux J, Orgogozo J. HDAE (BDAE): Echelle d'évaluation de l'aphasie. Paris : ECPA (Editions du Centre de Psychologie Appliquée). 1982.

McDade E, Wang G, Gordon BA, Hassenstab J, Benzinger TLS, Buckles V, et al. Longitudinal cognitive and biomarker changes in dominantly inherited Alzheimer disease. *Neurology.* 2018; 91: e1295-e1306.

McGoldrick P, Zhang M, van Blitterswijk M, Sato C, Moreno D, Xiao S, et al. Unaffected mosaic C9orf72 case: RNA foci, dipeptide proteins, but upregulated C9orf72 expression. *Neurology* 2018; 90: e323-e331.

Meeter LH, Doppert EG, Jiskoot LC, Sanchez-Valle R, Graff C, Benussi L, et al. Neurofilament light chain: a biomarker for genetic frontotemporal dementia. *Ann. Clin. Transl. Neurol.* 2016; 3: 623-636.

Meeter LHH, Gendron TF, Sias AC, Jiskoot LC, Russo SP, Donker Kaat L, et al. Poly(GP), neurofilament and grey matter deficits in C9orf72 expansion carriers. *Ann. Clin. Transl. Neurol.* 2018; 5: 583-597.

Merck C, Charnallet A, Auriacombe S, Belliard S, Hahn-Barma V, Kremlin H, et al. La batterie d'évaluation des connaissances sémantiques du GRECO (BECS-GRECO): validation et données normatives. *Revue de Neuropsychologie.* 2011; 3: 235.

Mesulam MM. Slowly progressive aphasia without generalized dementia. *Ann. Neurol.* 1982; 11: 592-598.

Mesulam MM. Primary progressive aphasia. *Ann. Neurol.* 2001; 49: 425-432.

Mesulam MM, Grossman M, Hillis A, Kertesz A, Weintraub S. The core and halo of primary progressive aphasia and semantic dementia. *Ann. Neurol.* 2003; 54: S11-S14.

Mesulam M, Johnson N, Krefft TA, Gass JM, Cannon AD, Adamson JL, et al. Progranulin mutations in primary progressive aphasia: the PPA1 and PPA3 families. *Arch. Neurol.* 2007; 64: 43-47.

Mesulam M, Wicklund A, Johnson N, Rogalski E, Léger GC, Rademaker A, et al. Alzheimer and frontotemporal pathology in subsets of primary progressive aphasia. *Ann. Neurol.* 2008; 63: 709-719.

Mesulam MM, Weintraub S. Is it time to revisit the classification guidelines for primary progressive aphasia? *Neurology.* 2014; 82: 1108-1109.

Mesulam MM, Weintraub S, Rogalski EJ, Wieneke C, Geula C, Bigio EH. Asymmetry and heterogeneity of Alzheimer's and frontotemporal pathology in primary progressive aphasia. *Brain.* 2014; 137: 1176-1192.

Migliaccio R, Tanguy D, Bouzigues A, Sezer I, Dubois B, Le Ber I, et al. Cognitive and behavioural inhibition deficits in neurodegenerative dementias. *Cortex.* 2020; 131: 265-283.

Mignarri A, Battistini S, Tomai Pitinca ML, Monti L, Burrioni L, Ginanneschi F, et al. Double trouble? Progranulin mutation and C9ORF72 repeat expansion in a case of primary non-fluent aphasia. *J. Neurol. Sci.* 2014; 341: 176-178.

Millecamps S, Boillée S, Le Ber I, Seilhean D, Teyssou E, Giraudeau M, et al. Phenotype difference between ALS patients with expanded repeats in C9ORF72 and patients with mutations in other ALS-related genes. *J. Med. Genet.* 2012; 49: 258-263.

Miller DS, Robert P, Ereshefsky L, Adler L, Bateman D, Cummings J, et al. Diagnostic criteria for apathy in neurocognitive disorders. *Alzheimers. Dement.* 2021; 17: 1892-1904.

Miyagawa T, Brushaber D, Syrjanen J, Kremers W, Fields J, Forsberg LK, et al. Use of the CDR® plus NACC FTLD in mild FTLD: Data from the ARTFL/LEFFTDS consortium. *Alzheimers Dement.* 2020a; 16: 79-90.

Miyagawa T, Brushaber D, Syrjanen J, Kremers W, Fields J, Forsberg LK, et al. Utility of the global CDR® plus NACC FTLD rating and development of scoring rules: Data from the ARTFL/LEFFTDS Consortium. *Alzheimers Dement.* 2020b; 16: 106-117.

Mizielinska S, Lashley T, Norona FE, Clayton EL, Ridler CE, Fratta P, et al. C9orf72 frontotemporal lobar degeneration is characterised by frequent neuronal sense and antisense RNA foci. *Acta Neuropathol* 2013; 126: 845-857.

Mol MO, Nijmeijer SWR, van Rooij JGJ, van Spaendonk RML, Pijnenburg YAL, van der Lee SJ. Distinctive pattern of temporal atrophy in patients with frontotemporal dementia and the I383V variant in TARDBP. *J. Neurol. Neurosurg. Psychiatry*. 2021; 92: 787-789.

Montembeault M, Sayah S, Rinaldi D, Le Toullec B, Bertrand A, Funkiewiez A, et al. Cognitive inhibition impairments in presymptomatic C9orf72 carriers. *J. Neurol. Neurosurg. Psychiatry*. 2020; 91: 366-372.

Moore KM, Nicholas J, Grossman M, McMillan CT, Irwin DJ, Massimo L, et al. Age at symptom onset and death and disease duration in genetic frontotemporal dementia: an international retrospective cohort study. *Lancet. Neurol*. 2020a; 19: 145-156.

Moore K, Convery R, Bocchetta M, Neason M, Cash DM, Greaves C, et al. A modified Camel and Cactus Test detects presymptomatic semantic impairment in genetic frontotemporal dementia within the GENFI cohort. *Appl. Neuropsychol. Adult*. 2020b; 29: 112-119.

Moreno F, Sala-Llonch R, Barandiaran M, Sánchez-Valle R, Estanga A, Bartrés-Faz D, et al. Distinctive age-related temporal cortical thinning in asymptomatic granulin gene mutation carriers. *Neurobiol. Aging*. 2013; 34: 1462-1468.

Mutsaerts HJMM, Mirza SS, Petr J, Thomas DL, Cash DM, Bocchetta M, et al. Cerebral perfusion changes in presymptomatic genetic frontotemporal dementia: a GENFI study. *Brain* 2019; 142: 1108-1120.

Neary D, Snowden JS, Gustafson L, Passant U, Stuss D, Black S, et al. Frontotemporal lobar degeneration. A consensus on clinical diagnostic criteria. *Neurology*. 1998; 51: 1546-1554.

Nelson PT, Dickson DW, Trojanowski JQ, Jack CR, Boyle PA, Arfanakis K, et al. Limbic-predominant age-related TDP-43 encephalopathy (LATE): consensus working group report. *Brain*. 2019; 142: 1503-1527.

Nespolous J, Lecours A, Lafond D, Lemay MA, Puel M, Joannette Y, et al. Protocole Montréal-Toulouse d'examen linguistique de l'aphasie MT-86. Isbergues : Ortho Edition. 1992.

Neumann M, Sampathu DM, Kwong LK, Truax AC, Micsenyi MC, Chou TT, et al. Ubiquitinated TDP-43 in frontotemporal lobar degeneration and amyotrophic lateral sclerosis. *Science*. 2006; 314: 130–133.

Neumann M, Rademakers R, Roeber S, Baker M, Kretzschmar HA, Mackenzie IRA. A new subtype of frontotemporal lobar degeneration with FUS pathology. *Brain*. 2009; 132: 2922-2931.

Neumann M, Bentmann E, Dormann D, Jawaid A, DeJesus-Hernandez M, Ansorge O, et al. FET proteins TAF15 and EWS are selective markers that distinguish FTLD with FUS pathology from amyotrophic lateral sclerosis with FUS mutations. *Brain*. 2011; 134: 2595-2609.

Neumann M, Mackenzie IRA. Review: Neuropathology of non-tau frontotemporal lobar degeneration. *Neuropathol. Appl. Neurobiol*. 2019; 45: 19-40.

Nonaka T, Masuda-Suzukake M, Arai T, Hasegawa Y, Akatsu H, Obi T, et al. Prion-like properties of pathological TDP-43 aggregates from diseased brains. *Cell Rep*. 2013; 4: 124-134.

Nuytemans K, Bademci G, Kohli MM, Beecham GW, Wang L, Young JI, et al. C9ORF72 Intermediate Repeat Copies Are a Significant Risk Factor for Parkinson Disease. *Ann. Hum. Genet*. 2013; 77: 351-363.

Öijerstedt L, Chiang HH, Björkström J, Forsell C, Lilius L, Lindström AK, et al. Confirmation of high frequency of C9orf72 mutations in patients with frontotemporal dementia from Sweden. *Neurobiol. Aging*. 2019; 84: 241.e21-241.e25.

Olney NT, Spina S, Miller BL. Frontotemporal Dementia. *Neurol. Clin*. 2017; 35: 339-374.

Onyike CU, Diehl-Schmid J. The epidemiology of frontotemporal dementia. *Int. Rev. Psychiatry*. 2013; 25:130-137.

Panman JL, Jiskoot LC, Bouts MJRJ, Meeter LHH, van der Ende EL, Poos JM, et al. Gray and white matter changes in presymptomatic genetic frontotemporal dementia: a longitudinal MRI study. *Neurobiol. Aging*. 2019; 76: 115-124.

Panman JL, Venkatraghavan V, van der Ende EL, Steketee RME, Jiskoot LC, Poos JM, et al. Modelling the cascade of biomarker changes in GRN-related frontotemporal dementia. *J. Neurol. Neurosurg. Psychiatry*. 2021; 92: 494-501.

Papma JM, Jiskoot LC, Panman JL, Doppert EG, den Heijer T, Donker Kaat L, et al. Cognition and gray and white matter characteristics of presymptomatic C9orf72 repeat expansion. *Neurology*. 2017; 89: 1256-1264.

Paushter DH, Du H, Feng T, Hu F. The lysosomal function of progranulin, a guardian against neurodegeneration. *Acta Neuropathol*. 2018; 136: 1-17.

Peakman G, Russell LL, Convery RS, Nicholas JM, Van Swieten JC, Jiskoot LC, et al. Comparison of clinical rating scales in genetic frontotemporal dementia within the GENFI cohort. *J. Neurol. Neurosurg. Psychiatry*. 2022; 93: 158-168.

Peigneux P, van der Linden M. Influence of ageing and educational level on the prevalence of body-part-as-objects in normal subjects. *J Clin Exp Neuropsychol*. 1999; 21: 547-552.

Peplonska B, Berdyski M, Mandecka M, Barczak A, Kuzma-Kozakiewicz M, Barcikowska M, et al. TREM2 variants in neurodegenerative disorders in the Polish population. Homozygosity and compound heterozygosity in FTD patients. *Amyotroph. Lateral Scler. Frontotemporal Degener*. 2018; 19: 407-412.

Perrone F, Nguyen HP, Van Mossevelde S, Moisse M, Sieben A, Santens P, et al. Investigating the role of ALS genes CHCHD10 and TUBA4A in Belgian FTD-ALS spectrum patients. *Neurobiol. Aging*. 2017; 51: 177.e9-177.e16.

Petersen RC, Lopez O, Armstrong MJ, Getchius TSD, Ganguli M, Gloss D, et al. Practice guideline update summary: Mild cognitive impairment: Report of the Guideline Development, Dissemination, and Implementation Subcommittee of the American Academy of Neurology. *Neurology*. 2018; 90: 126-135.

Petkau TL, Leavitt BR. Progranulin in neurodegenerative disease. *Trends Neurosci*. 2014; 37: 388-398.

Pick A. Ueber die Beziehungen der senilen Hirnatrophie zur Aphasie. *Prager Medicinische Wochenschrift*. 1892; 17: 165-167.

Pickering-Brown S, Baker M, Bird T, Trojanowski J, Lee V, Morris H, et al. Evidence of a founder effect in families with frontotemporal dementia that harbor the tau + 16 splice mutation. *Am. J. Med. Genet.* 2004; 125: 79-82.

Pickering-Brown SM, Richardson AM, Snowden JS, McDonagh AM, Burns A, Braude W, et al. Inherited frontotemporal dementia in nine British families associated with intronic mutations in the tau gene. *Brain.* 2002; 125: 732-751.

Pickering-Brown SM, Rollinson S, Du Plessis D, Morrison KE, Varma A, Richardson AMT, et al. Frequency and clinical characteristics of progranulin mutation carriers in the Manchester frontotemporal lobar degeneration cohort: comparison with patients with MAPT and no known mutations. *Brain.* 2008; 131: 721-731.

Pickering-Brown SM. The complex aetiology of frontotemporal lobar degeneration. *Exp. Neurol.* 2007; 206: 1-10.

Piguet O, Petersén A, Yin Ka Lam B, Gabery S, Murphy K, Hodges JR. Eating and hypothalamus changes in behavioral-variant frontotemporal dementia. *Ann. Neurol.* 2011; 69: 312-319.

Poesen K, Van Damme P. Diagnostic and Prognostic Performance of Neurofilaments in ALS. *Front. Neurol.* 2019; 9: 1167.

Poos JM, Moore KM, Nicholas J, Russell LL, Peakman G, Convery RS, et al. Cognitive composites for genetic frontotemporal dementia: GENFI-Cog. *Alzheimers Res. Ther.* 2022; 14: 10.

Poos JM, Russell LL, Peakman G, Bocchetta M, Greaves CV, Jiskoot LC, et al. Impairment of episodic memory in genetic frontotemporal dementia: A GENFI study. *Alzheimers Dement. (Amst).* 2021; 13: e12185.

Popuri K, Beg MF, Lee H, Balachandar R, Wang L, Sossi V, et al. FDG-PET in presymptomatic C9orf72 mutation carriers. *Neuroimage Clin.* 2021; 31: 102687.

Pottier C, Bieniek KF, Finch N, van de Vorst M, Baker M, Perkersen R, et al. Whole-genome sequencing reveals important role for TBK1 and OPTN mutations in frontotemporal lobar degeneration without motor neuron disease. *Acta Neuropathol.* 2015; 130: 77-92.

Pottier C, Ravenscroft TA, Sanchez-Contreras M, Rademakers R. Genetics of FTL D: overview and what else we can expect from genetic studies. *J. Neurochem.* 2016; 138: 32-53.

Pottier C, Zhou X, Perkerson 3rd RB, Baker M, Jenkins GD, Serie DJ. Potential genetic modifiers of disease risk and age at onset in patients with frontotemporal lobar degeneration and GRN mutations: a genome-wide association study. *Lancet Neurol.* 2018; 17: 548-558.

Preische O, Schultz SA, Apel A, Kuhle J, Kaeser SA, Barro C, et al. Serum neurofilament dynamics predicts neurodegeneration and clinical progression in presymptomatic Alzheimer's disease. *Nat. Med.* 2019; 25: 277-283.

Premi E, Cauda F, Gasparotti R, Diano M, Archetti S, Padovani A, et al. Multimodal FMRI resting-state functional connectivity in granulin mutations: the case of fronto-parietal dementia. *PLoS One.* 2014; 9: e106500.

Querin G, Bede P, El Mendili MM, Li M, Pélégri ni-Issac M, Rinaldi D, et al. Presymptomatic spinal cord pathology in c9orf72 mutation carriers: A longitudinal neuroimaging study. *Ann. Neurol.* 2019; 86: 158-167.

Querin G, Biferi MG, Pradat PF. Biomarkers for C9orf7-ALS in Symptomatic and Pre-symptomatic Patients: State-of-the-art in the New Era of Clinical Trials. *J. Neuromuscul. Dis.* 2022; 9: 25-37.

Radakovic R., Abrahams S. Multidimensional apathy: Evidence from neurodegenerative disease. *Curr. Opin. Behav. Sci.* 2018; 22: 42-49.

Rademakers R, Baker M, Gass J, Adamson J, Huey ED, Momeni P, et al. Phenotypic variability associated with progranulin haploinsufficiency in patients with the common 1477C→T (Arg493X) mutation: an international initiative. *Lancet. Neurol.* 2007; 6: 857-868.

Rademakers R, Baker M, Nicholson AM, Rutherford NJ, Finch N, Soto-Ortolaza A, et al. Mutations in the colony stimulating factor 1 receptor (CSF1R) gene cause hereditary diffuse leukoencephalopathy with spheroids. *Nat. Genet.* 2012; 44: 200-205.

Rademakers R, Neumann M, Mackenzie IRA. Recent advances in the molecular basis of frontotemporal dementia. *Nat. Rev. Neurol.* 2012; 8: 423-434.

Ramos EM, Dokuru DR, Van Berlo V, Wojta K, Wang Q, Huang AY, et al. Genetic screen in a large series of patients with primary progressive aphasia. *Alzheimers Dement.* 2019; 15: 553-560.

Ramos EM, Dokuru DR, Van Berlo V, Wojta K, Wang Q, Huang AY, et al. Genetic screening of a large series of North American sporadic and familial frontotemporal dementia cases. *Alzheimers Dement.* 2020; 16: 118-130.

Rascovsky K, Hodges JR, Knopman D, Mendez MF, Kramer JH, Neuhaus J et al. Sensitivity of revised diagnostic criteria for the behavioural variant of frontotemporal dementia. *Brain.* 2011; 134: 2456-2477.

Rebeiz JJ, Kolodny EH, Richardson Jr EP. Corticodentatonigral degeneration with neuronal achromasia: a progressive disorder of late adult life. *Trans. Am. Neurol. Assoc.* 1967; 92: 23-26.

Renton AE, Majounie E, Waite A, Simón-Sánchez J, Rollinson S, Gibbs JR, et al. A hexanucleotide repeat expansion in C9ORF72 is the cause of chromosome 9p21-Linked ALS-FTD. *Neuron.* 2011; 72: 257-268.

Reuter M, Schmansky NJ, Rosas HD, Fischl B. Within-subject template estimation for unbiased longitudinal image analysis. *Neuroimage.* 2012; 61: 1402-1418.

Richards S, Aziz N, Bale S, Bick D, Das S, Gastier-Foster J, et al. Standards and guidelines for the interpretation of sequence variants: a joint consensus recommendation of the American College of Medical Genetics and Genomics and the Association for Molecular Pathology. *Genet. Med.* 2015; 17: 405-423.

Rissin DM, Kan CK, Campbell TG, Howes SC, Fournier DR, Song L, et al. Single-molecule enzyme-linked immunosorbent assay detects serum proteins at subfemtomolar concentrations. *Nat. Biotechnol.* 2010; 28: 595-599.

Robberecht W, Philips T. The changing scene of amyotrophic lateral sclerosis. *Nat. Rev. Neurosci.* 2013; 14: 248-264.

Robert P, Onyike CU, Leentjens AF, Dujardin K, Aalten P, Starkstein S, et al. Proposed diagnostic criteria for apathy in Alzheimer's disease and other neuropsychiatric disorders. *Eur. Psychiatry*. 2009; 24: 98-104.

Rogalski E, Cobia D, Martersteck A, Rademaker A, Wieneke C, Weintraub S, et al. Asymmetry of cortical decline in subtypes of primary progressive aphasia. *Neurology*. 2014; 83: 1184-1191.

Rogalski E, Sridhar J, Rader B, Martersteck A, Chen K, Cobia D, et al. Aphasie variant of Alzheimer disease: clinical, anatomic, and genetic features. *Neurology*. 2016; 87: 1337-1343.

Rohrer JD, Warren JD, Omar R, Mead S, Beck J, Revesz T. Parietal lobe deficits in frontotemporal lobar degeneration caused by a mutation in the progranulin gene. *Arch. Neurol*. 2008; 65: 506-513.

Rohrer JD, Rossor MN, Warren JD. Syndromes of nonfluent primary progressive aphasia: a clinical and neurolinguistic analysis. *Neurology*. 2010a; 75: 603-610.

Rohrer JD, Crutch SJ, Warrington EK, Warren JD. Progranulin-associated primary progressive aphasia: A distinct phenotype? *Neuropsychologia*. 2010b; 48: 288-297.

Rohrer JD, Ridgway GR, Crutch SJ, Hailstone J, Goll JC, Clarkson MJ, et al. Progressive logopenic/phonological aphasia: erosion of the language network. *Neuroimage*. 2010c; 49: 984-993.

Rohrer JD, Caso F, Mahoney C, Henry M, Rosen HJ, Rabinovici G, et al. Patterns of longitudinal brain atrophy in the logopenic variant of primary progressive aphasia. *Brain Lang*. 2013; 127: 121-126.

Rohrer JD, Nicholas JM, Cash DM, van Swieten J, Dopfer E, Jiskoot L, et al. Presymptomatic cognitive and neuroanatomical changes in genetic frontotemporal dementia in the Genetic Frontotemporal dementia Initiative (GENFI) study: a cross-sectional analysis. *Lancet Neurol*. 2015; 14: 253-262.

Rohrer JD, Woollacott IO, Dick KM, Brotherhood E, Gordon E, Fellows A, et al. Serum neurofilament light chain protein is a measure of disease intensity in frontotemporal dementia. *Neurology*. 2016; 87: 1329-1336.

Rojas JC, Wang P, Staffaroni AM, Heller C, Cobigo Y, Wolf A, et al. Plasma Neurofilament Light for Prediction of Disease Progression in Familial Frontotemporal Lobar Degeneration. *Neurology*. 2021; 96: e2296-e2312.

Rolls ET, Huang CC, Lin CP, Feng J, Joliot M. Automated anatomical labelling atlas 3. *Neuroimage*. 2020; 206: 116189.

Roncero C, Popov A, Chertkow H. Multiple high dose tDCS sessions produces perceived improvement and stabilisation in a person with a MAPT gene, presenting clinically as semantic variant primary progressive aphasia with severe cognitive impairment. *Brain Stimul*. 2021; 14: 358-360.

Rosen HJ, Gorno-Tempini ML, Goldman WP, Perry RJ, Schuff N, Weiner M, et al. Patterns of brain atrophy in frontotemporal dementia and semantic dementia. *Neurology*. 2002; 58:198-208.

Routier A, Habert MO, Bertrand A, Kas A, Sundqvist M, Mertz J, et al. Structural, Microstructural, and Metabolic Alterations in Primary Progressive Aphasia Variants. *Front. Neurol*. 2018; 9: 766.

Routier A, Burgos N, Díaz M, Bacci M, Bottani S, El-Rifai O, et al. Clinica: An Open-Source Software Platform for Reproducible Clinical Neuroscience Studies. *Front. Neuroinform*. 2021; 15: 689675.

Rubino E, Rainero I, Chiò A, Rogaeva E, Galimberti D, Fenoglio P, et al. SQSTM1 mutations in frontotemporal lobar degeneration and amyotrophic lateral sclerosis. *Neurology*. 2012; 79: 1556-1562.

Russell LL, Greaves CV, Bocchetta M, Nicholas J, Convery RS, Moore K, et al. Social cognition impairment in genetic frontotemporal dementia within the GENFI cohort. *Cortex*. 2020; 133: 384-398.

Ryan B, Baker A, Ilse C, Brickell KL, Kersten HM, Danesh-Meyer HV, et al. Diagnosing pre-clinical dementia: the NZ Genetic Frontotemporal Dementia Study (FTDGeNZ). *N Z Med. J*. 2018; 131: 88-91.

Saberi S, Stauffer JE, Schulte DJ, Ravits J. Neuropathology of Amyotrophic Lateral Sclerosis and Its Variants. *Neurol. Clin.* 2015; 33: 855-876.

Saint-Aubert L, Sagot S, Wallon D, Hannequin D, Payoux P, Nemmi F, et al. A case of logopenic primary progressive aphasia with C9ORF72 expansion and cortical florbetapir binding. *J. Alzheimers Dis.* 2014; 42: 413-420.

Samson D, Apperly IA, Humphreys GW. Error analyses reveal contrasting deficits in “theory of mind”: neuropsychological evidence from a 3-option false belief task. *Neuropsychologia.* 2007; 45: 2561-2569.

Santamaría-García H, Reyes P, García A, Baéz S, Martínez A, Santacruz JM, et al. First Symptoms and Neurocognitive Correlates of Behavioral Variant Frontotemporal Dementia. *J. Alzheimers Dis.* 2016; 54: 957-970.

Santos-Santos MA, Rabinovici GD, Iaccarino L, Ayakta N, Tammewar G, Lobach I, et al. Rates of amyloid imaging positivity in patients with primary progressive aphasia. *JAMA Neurol.* 2018; 75: 342-352.

Saracino D, Sellami L, Clot F, Camuzat A, Lamari F, Rucheton B, et al. The missense p.Trp7Arg mutation in GRN gene leads to progranulin haploinsufficiency. *Neurobiol. Aging.* 2020; 85: 154.e9-154.e11.

Saracino D, Ferrieux S, Noguès-Lassiaille M, Houot M, Funkiewiez A, Sellami L, et al. Primary Progressive Aphasia Associated With GRN Mutations: New Insights Into the Nonamyloid Logopenic Variant. *Neurology.* 2021a; 97: e88-e102.

Saracino D, Géraudie A, Remes AM, Ferrieux S, Noguès-Lassiaille M, Bottani S, et al. Primary progressive aphasias associated with C9orf72 expansions: Another side of the story. *Cortex* 2021b; 145: 145-159.

Saracino D, Dorgham K, Camuzat A, Rinaldi D, Rametti-Lacroux A, Houot M, et al. Plasma NfL levels and longitudinal change rates in C9orf72 and GRN-associated diseases: from tailored references to clinical applications. *J. Neurol. Neurosurg. Psychiatry.* 2021c; 92: 1278-1288.

Saracino D, Le Ber I. How can we define the presymptomatic C9orf72 disease in 2022? An overview on the current definitions of preclinical and prodromal phases. *Rev. Neurol. (Paris)*. 2022; In Press.

Sato W, Kochiyama T, Uono S, Sawada R, Kubota Y, Yoshimura S, et al. Widespread and lateralized social brain activity for processing dynamic facial expressions. *Hum. Brain Mapp.* 2019; 40: 3753-3768.

Saur D, Kreher BW, Schnell S, Kümmerer D, Kellmeyer P, Vry MS, et al. Ventral and dorsal pathways for language. *Proc Natl Acad Sci U S A.* 2008; 105: 18035-18040.

Saxe R, Xiao DK, Kovacs G, Perrett DI, Kanwisher N. A region of right posterior superior temporal sulcus responds to observed intentional actions. *Neuropsychologia.* 2004; 42: 1435-1446.

Schneider R, McKeever P, Kim T, Graff C, van Swieten JC, Karydas A, et al. Downregulation of exosomal miR-204-5p and miR-632 as a biomarker for FTD: a GENFI study. *J. Neurol. Neurosurg. Psychiatry.* 2018; 89: 851-858.

Schroeter ML, Pawelke S, Bisenius S, Kynast J, Schuemberg K, Polyakova M, et al. A Modified Reading the Mind in the Eyes Test Predicts Behavioral Variant Frontotemporal Dementia Better Than Executive Function Tests. *Front. Aging Neurosci.* 2018; 10: 11.

Seeley WW, Bauer AM, Miller BL, Gorno-Tempini ML, Kramer JH, Weiner M, et al. The natural history of temporal variant frontotemporal dementia. *Neurology.* 2005; 64: 1384-1390.

Seeley WW. Anterior insula degeneration in frontotemporal dementia. *Brain Struct. Funct.* 2010; 214: 465-475.

Selkoe DJ, Hardy J. The amyloid hypothesis of Alzheimer's disease at 25 years. *EMBO Mol. Med.* 2016; 8: 595-608.

Sellal F. Anatomical and neurophysiological basis of face recognition. *Rev. Neurol. (Paris)*. 2021; doi: 10.1016/j.neurol.2021.11.002.

Sellami L, St-Onge F, Poulin S, Laforce Jr R. Schizophrenia Phenotype Preceding Behavioral Variant Frontotemporal Dementia Related to C9orf72 Repeat Expansion. *Cogn. Behav. Neurol.* 2019; 32: 120-123.

Sellami L, Saracino D, Le Ber I. Genetic forms of frontotemporal lobar degeneration: Current diagnostic approach and new directions in therapeutic strategies. *Rev. Neurol. (Paris)*. 2020a; 176: 571-581.

Sellami L, Rucheton B, Ben Younes I, Camuzat A, Saracino D, Rinaldi D, et al. Plasma progranulin levels for frontotemporal dementia in clinical practice: a 10-year French experience. *Neurobiol. Aging*. 2020b; 91: 167.e1-167.e9.

Sellier C, Campanari ML, Corbier CJ, Gaucherot A, Kolb-Cheynel I, Oulad-Abdelghani M, et al. Loss of C9ORF72 impairs autophagy and synergizes with polyQ Ataxin-2 to induce motor neuron dysfunction and cell death. *EMBO J.* 2016; 35: 1276-1297.

Sergeant N, Delacourte A, Buée L. Tau protein as a differential biomarker of tauopathies. *Biochim. Biophys. Acta.* 2005; 1739: 179-197.

Sha SJ, Miller ZA, Min S, Zhou Y, Brown J, Mitic LL, et al. An 8-week, open-label, dose-finding study of nimodipine for the treatment of progranulin insufficiency from GRN gene mutations. *Alzheimers Dement. (NY)*. 2017; 3: 507-512.

Shaw SR, El-Omar H, Roquet D, Hodges JR, Piguet O, Ahmed RM, et al. Uncovering the prevalence and neural substrates of anhedonia in frontotemporal dementia. *Brain*. 2021; 144: 1551-1564.

She A, Kurtser I, Reis SA, Hennig K, Lai J, Lang A, et al. Selectivity and Kinetic Requirements of HDAC inhibitors as progranulin enhancers for treating frontotemporal dementia. *Cell. Chem. Biol.* 2017; 24: 892-906.

Sheelakumari R, Bineesh C, Varghese T, Kesavadas C, Verghese J, Mathuranath PS. Neuroanatomical correlates of apathy and disinhibition in behavioural variant frontotemporal dementia. *Brain Imaging Behav.* 2020; 14: 2004-2011.

Shewan CM, Kertesz A. Reliability and validity characteristics of the Western Aphasia Battery (WAB). *J. Speech Hear. Disord.* 1980; 45: 308-324.

Shinagawa S, Nakajima S, Plitman E, Graff-Guerrero A, Mimura M, Nakayama K, et al. Psychosis in frontotemporal dementia. *J. Alzheimers Dis.* 2014; 42: 485-499.

Shipp S. The functional logic of corticostriatal connections. *Brain Struct. Funct.* 2017; 222: 669-706.

Simón-Sánchez J, Dopper EG, Cohn-Hokke PE, Hukema RK, Nicolaou N, Seelaar H, et al. The clinical and pathological phenotype of C9ORF72 hexanucleotide repeat expansions. *Brain.* 2012; 135: 723-735.

Skibinski G, Parkinson NJ, Brown JM, Chakrabarti L, Lloyd SL, Hummerich H, et al. Mutations in the endosomal ESCRTIII-complex subunit CHMP2B in frontotemporal dementia. *Nat. Genet.* 2005; 37: 806-808.

Smallwood Shoukry RF, Clark MG, Floeter MK. Resting State Functional Connectivity Is Decreased Globally Across the C9orf72 Mutation Spectrum. *Front. Neurol.* 2020; 11: 598474.

Smith KR, Damiano J, Franceschetti S, Carpenter S, Canafoglia L, Morbin M, et al. Strikingly different clinicopathological phenotypes determined by progranulin-mutation dosage. *Am. J. Hum. Genet.* 2012; 90: 1102-1107.

Snowden JS, Adams J, Harris J, Thompson JC, Rollinson S, Richardson A, et al. Distinct clinical and pathological phenotypes in frontotemporal dementia associated with MAPT, PGRN and C9orf72 mutations. *Amyotroph. Lateral. Scler. Frontotemporal Degener.* 2015; 16: 497-505.

Snowden JS, Bathgate D, Varma A, Blackshaw A, Gibbons ZC, Neary D. Distinct behavioural profiles in frontotemporal dementia and semantic dementia. *J. Neurol. Neurosurg. Psychiatry.* 2001; 70: 323-332.

Snowden JS, Pickering-Brown SM, du Plessis D, Mackenzie IR, Varma A, Mann DM, et al. Progressive anomia revisited: focal degeneration associated with progranulin gene mutation. *Neurocase.* 2007; 13: 366-377.

Snowden JS, Pickering-Brown SM, Mackenzie IR, Richardson AMT, Varma A, Neary D, et al. Progranulin gene mutations associated with frontotemporal dementia and progressive non-fluent aphasia. *Brain.* 2006; 129: 3091-3102.

Snowden JS, Rollinson S, Thompson JC, Harris JM, Stopford CL, Richardson AM, et al. Distinct clinical and pathological characteristics of frontotemporal dementia associated with C9ORF72 mutations. *Brain*. 2012; 135: 693-708.

Spinelli EG, Mandelli ML, Miller ZA, Santos-Santos MA, Wilson SM, Agosta F, et al. Typical and atypical pathology in primary progressive aphasia variants. *Ann. Neurol*. 2017; 81: 430-443.

Staffaroni AM, Bajorek L, Casaletto KB, Cobigo Y, Goh SYM, Wolf A, et al. Assessment of executive function declines in presymptomatic and mildly symptomatic familial frontotemporal dementia: NIH-EXAMINER as a potential clinical trial endpoint. *Alzheimers Dement*. 2020a; 16: 11-21.

Staffaroni AM, Cobigo Y, Goh S-YM, Kornak J, Bajorek L, Chiang K, et al. Individualized atrophy scores predict dementia onset in familial frontotemporal lobar degeneration. *Alzheimers Dement*. 2020b; 16: 37-48.

Staffaroni AM, Goh S-YM, Cobigo Y, Ong E, Lee SE, Casaletto KB, et al. Rates of Brain Atrophy Across Disease Stages in Familial Frontotemporal Dementia Associated With MAPT, GRN, and C9orf72 Pathogenic Variants. *JAMA Netw. Open*. 2020c; 3: e2022847.

Steinacker P, Huss A, Mayer B, Grehl T, Grosskreutz J, Borck G, et al. Diagnostic and prognostic significance of neurofilament light chain NF-L, but not progranulin and S100B, in the course of amyotrophic lateral sclerosis: Data from the German MND-net. *Amyotroph. Lateral Scler. Frontotemporal Degener*. 2017; 18: 112-119.

Steinacker P, Anderl-Straub S, Diehl-Schmid J, Semler E, Uttner I, von Arnim CAF, et al. Serum neurofilament light chain in behavioral variant frontotemporal dementia. *Neurology*. 2018; 91: e1390-e1401.

Sudre CH, Bocchetta M, Heller C, Convery R, Neason M, Moore KM, et al. White matter hyperintensities in progranulin-associated frontotemporal dementia: A longitudinal GENFI study. *Neuroimage Clin*. 2019; 24: 102077.

Suhonen NM, Kaivorinne AL, Moilanen V, Bode M, Takalo R, Hänninen T, et al. Slowly progressive frontotemporal lobar degeneration caused by the C9ORF72 repeat expansion: a 20-year follow-up study. *Neurocase*. 2015; 21: 85-89.

Svetoni F, Frisone P, Paronetto MP. Role of FET proteins in neurodegenerative disorders. *RNA Biol*. 2016; 13: 1089-1102.

Swift IJ, Bocchetta M, Benotmane H, Woollacott I O C, Shafei R, Rohrer J D. Variable clinical phenotype in TBK1 mutations: Case report of a novel mutation causing primary progressive aphasia and review of the literature. *Neurobiol. Aging*. 2021a; 99: 100e9-100e15.

Swift IJ, Sogorb-Esteve A, Heller C, Synofzik M, Otto M, Graff C, et al. Fluid biomarkers in frontotemporal dementia: past, present and future. *J. Neurol. Neurosurg. Psychiatry*. 2021b; 92: 204-215.

Tabrizi SJ, Leavitt BR, Landwehrmeyer GB, Wild EJ, Saft C, Barker RA, et al. Targeting Huntingtin Expression in Patients with Huntington's Disease. *N. Engl. J. Med*. 2019; 380: 2307-2316.

Tábuas-Pereira M, Santana I, Almeida MR, Durães J, Lima M, Duro D, et al. Rare variants in TP73 in a frontotemporal dementia cohort link this gene with primary progressive aphasia phenotypes. *Eur. J. Neurol*. 2022; 29: 1524-1528.

Taga A, Maragakis NJ. Current and emerging ALS biomarkers: utility and potential in clinical trials. *Expert Rev. Neurother*. 2018; 18: 871-886.

Tan RH, Guennewig B, Dobson-Stone C, Kwok JBJ, Kril JJ, Kiernan MC, et al. The underacknowledged PPA-ALS: A unique clinicopathologic subtype with strong heritability. *Neurology*. 2019; 92: e1354-e1366.

Tanaka Y, Chambers JK, Matsuwaki T, Yamanouchi K, Nishihara M. Possible involvement of lysosomal dysfunction in pathological changes of the brain in aged progranulin-deficient mice. *Acta Neuropathol. Commun*. 2014; 2: 78.

Tang W, Lu Y, Tian QY, Zhang Y, Guo FJ, Liu GY, et al. The growth factor progranulin binds to TNF receptors and is therapeutic against inflammatory arthritis in mice. *Science*. 2011; 332: 478-484.

Tang D, Sheng J, Xu L, Yan C, Qi S. The C9orf72-SMCR8-WDR41 complex is a GAP for small GTPases. *Autophagy*. 2020; 16: 1542-1543.

Tavares TP, Mitchell DGV, Coleman KK, Coleman BL, Shoesmith CL, Butler CR, et al. Early symptoms in symptomatic and preclinical genetic frontotemporal lobar degeneration. *J. Neurol. Neurosurg. Psychiatry*. 2020; 91: 975-984.

Tayebi N, Lopez G, Do J, Sidransky E. Pro-cathepsin D, Prosaposin, and Progranulin: Lysosomal Networks in Parkinsonism. *Trends Mol. Med*. 2020; 26: 913-923.

Teichmann M, Kas A, Boutet C, Ferrieux S, Noguès M, Samri D, et al. Deciphering logopenic primary progressive aphasia: a clinical, imaging and biomarker investigation. *Brain*. 2013; 136: 3474-3488.

Tetreault AM, Phan T, Petersen KJ, Claassen DO, Neth BJ, Graff-Radford J, et al. Network Localization of Alien Limb in Patients with Corticobasal Syndrome. *Ann. Neurol*. 2020; 88: 1118-1131.

Tetzloff KA, Duffy JR, Clark HM, Utianski RL, Strand EA, Machulda MM, et al. Progressive agrammatic aphasia without apraxia of speech as a distinct syndrome. *Brain*. 2019; 142: 2466-2482.

The Lund and Manchester Groups. Clinical and neuropathological criteria for frontotemporal dementia. *J. Neurol. Neurosurg. Psychiatry*. 1994; 57: 416-418.

Thomas-Antérion C. Outils neuropsychologiques en pratique neurologique. *La Presse Médicale*. 2012; 41: 474-481.

Thompson SA, Patterson K, Hodges JR. Left/right asymmetry of atrophy in semantic dementia: behavioral-cognitive implications. *Neurology*. 2003; 61: 1196-1203.

Tran H, Moazami MP, Yang H, McKenna-Yasek D, Douthwright CL, Pinto C, et al. Suppression of mutant C9orf72 expression by a potent mixed backbone antisense oligonucleotide. *Nat. Med*. 2022; 28: 117-124.

Troakes C, Maekawa S, Wijesekera L, Rogelj B, Siklós L, Bell C, et al. An MND/ALS phenotype associated with C9orf72 repeat expansion: Abundant p62-positive, TDP-43-

negative inclusions in cerebral cortex, hippocampus and cerebellum but without associated cognitive decline. *Neuropathology* 2012; 32: 505-514.

Ulugut Erkoyun H, Groot C, Heilbron R, Nelissen A, van Rossum J, Jutten R. A clinical-radiological framework of the right temporal variant of frontotemporal dementia. *Brain*. 2020; 143: 2831-2843.

Ulugut H, Dijkstra AA, Scarioni M, Netherlands Brain Bank, Barkhof F, Scheltens P, et al. Right temporal variant frontotemporal dementia is pathologically heterogeneous: a case-series and a systematic review. *Acta Neuropathol. Commun.* 2021; 9: 131.

Valente ES, Caramelli P, Gambogi LB, Mariano LI, Guimarães HC, Teixeira AL, et al. Phenocopy syndrome of behavioral variant frontotemporal dementia: a systematic review. *Alzheimers Res. Ther.* 2019; 11: 30.

van Blitterswijk M, DeJesus-Hernandez M, Niemantsverdriet E, Murray ME, Heckman MG, Diehl NN, et al. Association between repeat sizes and clinical and pathological characteristics in carriers of C9ORF72 repeat expansions (Xpansize-72): a cross-sectional cohort study. *Lancet Neurol.* 2013; 12: 978-988.

van der Burgh HK, Westeneng H-J, Meier JM, van Es MA, Veldink JH, Hendrikse J, et al. Cross-sectional and longitudinal assessment of the upper cervical spinal cord in motor neuron disease. *Neuroimage Clin.* 2019; 24: 101984.

van der Ende EL, Meeter LH, Poos JM, Panman JL, Jiskoot LC, Doppert EGP, et al. Serum neurofilament light chain in genetic frontotemporal dementia: a longitudinal, multicentre cohort study. *Lancet Neurol.* 2019; 18: 1103-1111.

van der Ende EL, Xiao M, Xu D, Poos JM, Panman JL, Jiskoot LC, et al. Neuronal pentraxin 2: a synapse-derived CSF biomarker in genetic frontotemporal dementia. *J. Neurol. Neurosurg. Psychiatry.* 2020; 91: 612-621.

van der Ende EL, Bron EE, Poos JM, Jiskoot LC, Panman JL, Papma JM, et al. A data-driven disease progression model of fluid biomarkers in genetic frontotemporal dementia. *Brain*. 2021; doi: 10.1093/brain/awab382.

van der Zee J, Gijselinck I, Van Mossevelde S, Perrone F, Dillen L, Heeman B, et al. TBK1 Mutation Spectrum in an Extended European Patient Cohort with Frontotemporal Dementia and Amyotrophic Lateral Sclerosis. *Hum. Mutat.* 2017; 38: 297-309.

Van Langenhove T, van der Zee J, Gijselinck I, Engelborghs S, Vandenberghe R, Vandebulcke M, et al. Distinct clinical characteristics of C9orf72 expansion carriers compared with GRN, MAPT, and nonmutation carriers in a Flanders-Belgian FTLD cohort. *JAMA Neurol.* 2013; 70: 365-373.

Van Mossevelde S, van der Zee J, Gijselinck I, Engelborghs S, Sieben A, Van Langenhove T, et al. Clinical features of TBK1 carriers compared with C9orf72, GRN and non-mutation carriers in a Belgian cohort. *Brain.* 2016; 139: 452-467.

van Rooij J, Mol MO, Melhem S, van der Wal P, Arp P, Paron F, et al. Somatic TARDBP variants as a cause of semantic dementia. *Brain.* 2020; 143: 3827-3841.

van Swieten J, Spillantini MG. Hereditary frontotemporal dementia caused by tau gene mutations. *Brain Pathol.* 2007; 17: 63-73.

Vandebulcke M, Van de Vliet L, Sun J, Huang YA, Van Den Bossche MJA, Sunaert S, et al. A paleo-neurologic investigation of the social brain hypothesis in frontotemporal dementia. *Cereb. Cortex.* 2022; doi: 10.1093/cercor/bhac089.

Vatsavayai SC, Yoon SJ, Gardner RC, Gendron TF, Vargas JNS, Trujillo A, et al. Timing and significance of pathological features in C9orf72 expansion-associated frontotemporal dementia. *Brain* 2016; 139: 3202-3216.

Verde F, Del Tredici K, Braak H, Ludolph A. The multisystem degeneration amyotrophic lateral sclerosis - neuropathological staging and clinical translation. *Arch. Ital. Biol.* 2017; 155: 118-130.

Verde F, Steinacker P, Weishaupt JH, Kassubek J, Oeckl P, Halbgebauer S, et al. Neurofilament light chain in serum for the diagnosis of amyotrophic lateral sclerosis. *J. Neurol. Neurosurg. Psychiatry.* 2019; 90: 157-164.

Vinceti G, Olney N, Mandelli ML, Spina S, Hubbard HI, Santos-Santos MA, et al. Primary progressive aphasia and the FTD-MND spectrum disorders: clinical, pathological, and

neuroimaging correlates. *Amyotroph. Lateral Scler. Frontotemporal Degener.* 2019; 20: 146-158.

Warren JD, Rohrer JD, Schott JM, Fox NC, Hardy J, Rossor MN. Molecular nexopathies: a new paradigm of neurodegenerative disease. *Trends Neurosci.* 2013; 36: 561-569.

Watts GDJ, Wymer J, Kovach MJ, Mehta SG, Mumm S, Darvish D, et al. Inclusion body myopathy associated with Paget disease of bone and frontotemporal dementia is caused by mutant valosin-containing protein. *Nat. Genet.* 2004; 36: 377-381.

Waugh RE, Danielian LE, Shoukry RFS, Floeter MK. Longitudinal changes in network homogeneity in presymptomatic C9orf72 mutation carriers. *Neurobiol. Aging.* 2021; 99: 1-10.

Wear HJ, Wedderburn CJ, Mioshi E, Williams-Gray CH, Mason SL, Barker RA, et al. The Cambridge Behavioural Inventory revised. *Dement. Neuropsychol.* 2008; 2: 102-107.

Webster CP, Smith EF, Bauer CS, Moller A, Hautbergue GM, Ferraiuolo L, et al. The C9orf72 protein interacts with Rab1a and the ULK1 complex to regulate initiation of autophagy. *EMBO J.* 2016; 35: 1656-1676.

Wen J, Zhang H, Alexander DC, Durrleman S, Routier A, Rinaldi D, et al. Neurite density is reduced in the presymptomatic phase of C9orf72 disease. *J. Neurol. Neurosurg. Psychiatry.* 2018; 90: 387-394.

Weydt P, Oeckl P, Huss A, Müller K, Volk AE, Kuhle J, et al. Neurofilament levels as biomarkers in asymptomatic and symptomatic familial amyotrophic lateral sclerosis. *Ann. Neurol.* 2016; 79: 152-158.

Whitwell JL, Przybelski SA, Weigand SD, Ivnik RJ, Vemuri P, Gunter JL, et al. Distinct anatomical subtypes of the behavioural variant of frontotemporal dementia: a cluster analysis study. *Brain.* 2009; 132: 2932-2946.

Whitwell JL, Jack Jr CR, Boeve BF, Parisi JE, Ahlskog JE, Drubach DA, et al. Imaging correlates of pathology in corticobasal syndrome. *Neurology.* 2010; 75: 1879-1887.

Whitwell JL, Weigand SD, Boeve BF, Senjem ML, Gunter JL, DeJesus-Hernandez M, et al. Neuroimaging signatures of frontotemporal dementia genetics: C9ORF72, tau, progranulin and sporadics. *Brain*. 2012; 135: 794-806.

Whitwell JL, Duffy JR, Strand EA, Machulda MM, Senjem ML, Schwarz CG, et al. Clinical and neuroimaging biomarkers of amyloid-negative logopenic primary progressive aphasia. *Brain Lang*. 2015; 142: 45-53.

Wider C, Dachsel JC, Farrer MJ, Dickson DW, Tsuboi Y, Wszolek ZK. Elucidating the genetics and pathology of Perry syndrome. *J. Neurol. Sci*. 2010; 289: 149-154.

Wilke C, Haas E, Reetz K, Faber J, Garcia-Moreno H, Santana MM, et al. Neurofilaments in spinocerebellar ataxia type 3: blood biomarkers at the preataxic and ataxic stage in humans and mice. *EMBO Mol. Med*. 2020; 12: e11803.

Wilke C, Reich S, Swieten JC, Borroni B, Sanchez-Valle R, Moreno F, et al. Stratifying the Presymptomatic Phase of Genetic Frontotemporal Dementia by Serum NfL and pNfH: A Longitudinal Multicentre Study. *Ann. Neurol*. 2022; 91: 33-47.

Wilson KM, Katona E, Glaria I, Carcolé M, Swift IJ, Sogorb-Esteve A, et al. Development of a sensitive trial-ready poly(GP) CSF biomarker assay for C9orf72-associated frontotemporal dementia and amyotrophic lateral sclerosis. *J. Neurol. Neurosurg. Psychiatry*. 2022; doi: 10.1136/jnnp-2021-328710.

Wilson SM, Brambati SM, Henry RG, Handwerker DA, Agosta F, Miller BL, et al. The neural basis of surface dyslexia in semantic dementia. *Brain*. 2009; 132: 71-86.

Wood EM, Falcone D, Suh E, Irwin DJ, Chen-Plotkin AS, Lee EB, et al. Development and validation of pedigree classification criteria for frontotemporal lobar degeneration. *JAMA Neurol*. 2013; 70: 1411-1417.

Woollacott IOC, Nicholas JM, Heslegrave A, Heller C, Foiani MS, Dick KM, et al. Cerebrospinal fluid soluble TREM2 levels in frontotemporal dementia differ by genetic and pathological subgroup. *Alzheimers Res. Ther*. 2018; 10: 79.

Woollacott I, Nicholas J, Heller C, Foiani MS, Moore KM, Russell LL, et al. Cerebrospinal fluid YKL-40 and chitotriosidase levels in frontotemporal dementia. *Dement. Geriatr. Cogn. Disord.* 2020; 49: 56-76.

Xu W, Xu J. C9orf72 Dipeptide Repeats Cause Selective Neurodegeneration and Cell-Autonomous Excitotoxicity in *Drosophila* Glutamatergic Neurons. *J. Neurosci.* 2018; 38: 7741-7752.

Yeh TH, Liu HF, Li YW, Lu CS, Shih HY, Chiu CC, et al. C9orf72 is essential for neurodevelopment and motility mediated by Cyclin G1. *Exp. Neurol.* 2018; 304: 114-124.

Zamboni G, Huey ED, Krueger F, Nichelli PF, Grafman J. Apathy and disinhibition in frontotemporal dementia: Insights into their neural correlates. *Neurology.* 2008; 71: 736-742.

Zhang D, Snyder AZ, Fox MD, Sansbury MW, Shimony JS, Raichle ME. Intrinsic functional relations between human cerebral cortex and thalamus. *J. Neurophysiol.* 2008; 100: 1740-1748.

Zhang M, Ferrari R, Tartaglia MC, Keith J, Surace EI, Wolf U, et al. A C6orf10/LOC101929163 locus is associated with age of onset in C9orf72 carriers. *Brain.* 2018; 141: 2895-2907.

Annexe 1 – Critères diagnostiques

Tableau A1. Critères diagnostiques de DFTc (*adapté de Rascovsky et al., 2011*)

DFTc possible : ≥ 3 des critères A-F doivent être présents précocement (<3 ans de durée de maladie)		
Critères	Catégories	Exemples
A. Désinhibition comportementale	A.1 Comportement socialement inapproprié	Agressivité verbale ou physique, manque de pudeur, conduites sexuelles inappropriées ou criminelles
	A.2 Perte des convenances sociales	Rires inappropriés, remarques déplacées, manque de respect des limites, dégradation de l'hygiène corporelle
	A.3 Actions impulsives et irréfléchies	Jeu d'argent, conduite automobile dangereuse, vol d'objets, partage des informations personnelles ou confidentielles
B. Apathie ou inertie	B.1 Apathie	Manque d'envie de s'engager dans le travail, loisirs, activités sportives etc.
	B.2 Inertie comportementale	Perte de l'initiative dans les actions ou conversations, besoin d'un stimulus fort pour déclencher un comportement
C. Perte de sympathie ou empathie	C.1 Réponse diminuée aux besoins et émotions des autres	Indifférence aux états émotionnelles des autres, commentaires indélicats face aux souffrances d'autrui
	C.2 Diminution de l'intérêt social	Émoussement émotionnel, comportement détaché, déclin de l'engagement dans les activités sociales
D. Comportements persévératifs, stéréotypés ou compulsifs/ritualisés	D.1 Mouvements répétitifs simples	Applaudissements, frottements, raclements de gorge, mouvements des lèvres etc.
	D.2 Comportements complexes, compulsifs ou ritualisés	Rituels de nettoyage, allers-retours d'une pièce à une autre, rangement d'objets
	D.3 Stéréotypies langagières	Mots, phrases ou histoires entières répétées sans un but
E. Hyperoralité et changements alimentaires	E.1 Changement des préférences alimentaires	Préférence pour les aliments sucrés, rigidité sur certaines préférences alimentaires
	E.2 Alimentation compulsive	Ingestion d'aliments sans sentiment de satiété, consommation démesurée d'alcool et tabac
	E.3 Exploration orale	Succion, mastication ou exploration orale d'objets non comestibles
F. Profil neuropsychologique : déficits des fonctions exécutives avec préservation relative de la mémoire et des fonctions visuospatiales	F.1 Déficiences des fonctions exécutives, avec score pathologique dans au moins un test	Déficits d'attention, planification, fluences, contrôle inhibiteur, mémoire de travail ; persévérations, transgression des règles des épreuves
	F.2 Préservation relative de la mémoire	Mémoire verbale et non verbale préservée, notamment dans les épreuves qui ne nécessitent pas d'effort exécutif
	F.3 Préservation relative des fonctions visuospatiales	Orientation préservée, bonnes capacités à reproduire figures et formes complexes

DFTc probable : les 3 critères A-C doivent être présents

A. Critères de DFTc possible remplis

B. Évidence de déclin fonctionnel (rapporté par un informant et/ou objectivé dans des échelles)

C. Neuroimagerie compatible avec une DFTc

C.1 Atrophie frontale et/ou temporale antérieure à l'IRM ou au scanner

C.2 Hypoperfusion frontale et/ou temporale antérieure au SPECT ou hypométabolisme frontal et/ou temporal antérieur au TEP-FDG

DFTc avec pathologie DLFT définie : présence du critère A et d'un entre les critères B et C

A. Critères de DFTc possible ou probable remplis

B. Évidence de pathologie DLFT à l'examen *post mortem* ou à la biopsie

C. Présence d'une mutation causale connue

Critères d'exclusion pour DFTc : A et B doivent être toujours absents ; C peut être présent pour un diagnostic de DFTc possible, mais doit être absent pour un diagnostic de DFTc probable

A. Les déficits peuvent être expliqués par d'autres maladies neurologiques ou somatiques

B. Les troubles comportementaux peuvent être expliqués par un diagnostic psychiatrique

C. Les biomarqueurs sont fortement suggestifs pour une MA ou un autre processus neurodégénératif

Tableau A2. Critères diagnostiques des APP (adapté de Gorno-Tempini et al., 2011)

Critères d'inclusion et exclusion pour un diagnostic d'APP (adapté de Mesulam et al., 2001)	
Inclusion : les critères 1-3 doivent être présents	<ol style="list-style-type: none"> 1. La caractéristique clinique principale est un trouble du langage 2. Ces déficits sont la cause principale des difficultés dans les activités quotidiennes 3. L'aphasie est le déficit principal au début et dans les premières phases de la maladie
Exclusion : les critères 1-4 doivent être absents	<ol style="list-style-type: none"> 1. Les déficits sont mieux expliqués par une autre maladie neurologique ou somatique 2. Le trouble cognitif est mieux expliqué par un diagnostic psychiatrique 3. Déficit prédominant de la mémoire épisodique, visuelle et des fonctions visuo-perceptives 4. Déficit comportemental prédominant au début
Critères diagnostiques de vnfAPP	
Diagnostic clinique de vnfAPP	
≥ 1 des 2 critères principaux	<ol style="list-style-type: none"> 1. Agrammatisme dans la production langagière 2. Apraxie de la parole
≥ 2 des 3 critères de support	<ol style="list-style-type: none"> 1. Déficit de compréhension de phrases syntaxiquement complexes 2. Compréhension épargnée pour les mots isolés 3. Connaissances sémantiques épargnées
Diagnostic de vnfAPP avec le support de l'imagerie	
En plus des critères cliniques, ≥ 1 des 2 critères d'imagerie	<ol style="list-style-type: none"> 1. Atrophie prédominante dans les régions fronto-temporo-insulaires gauches à l'IRM 2. Hypoperfusion prédominante dans les régions fronto-temporo-insulaires gauches au SPECT ou hypométabolisme prédominant dans les régions fronto-temporo-insulaires gauches au TEP-FDG
Diagnostic de vnfAPP avec pathologie définie	
En plus des critères cliniques, ≥ 1 des 2 critères suivants	<ol style="list-style-type: none"> 1. Évidence anatomopathologique d'un processus neurodégénératif 2. Présence d'une mutation causale connue
Critères diagnostiques de vsAPP	
Diagnostic clinique de vsAPP	
Présence des 2 critères principaux	<ol style="list-style-type: none"> 1. Déficit de dénomination 2. Déficit de compréhension des mots isolés
≥ 3 des 4 critères de support	<ol style="list-style-type: none"> 1. Déficit des connaissances sémantiques (surtout pour les items de basse fréquence) 2. Dyslexie ou dysgraphie de surface 3. Répétition épargnée 4. Production langagière épargnée (absence d'agrammatisme et de troubles articulatoires)
Diagnostic de vsAPP avec le support de l'imagerie	
En plus des critères cliniques, ≥ 1 des 2 critères d'imagerie	<ol style="list-style-type: none"> 1. Atrophie prédominante dans les régions temporales antérieures à l'IRM 2. Hypoperfusion prédominante dans les régions temporales antérieures au SPECT ou hypométabolisme prédominant dans les régions temporales antérieures au TEP-FDG
Diagnostic de vsAPP avec pathologie définie	
En plus des critères cliniques, ≥ 1 des 2 critères suivants	<ol style="list-style-type: none"> 1. Évidence anatomopathologique d'un processus neurodégénératif 2. Présence d'une mutation causale connue

Critères diagnostiques de vlAPP

Diagnostic clinique de vlAPP

Présence des 2 critères principaux	<ol style="list-style-type: none">1. Difficultés à trouver les mots dans le langage spontané et les tâches de dénomination2. Déficit de répétition des phrases
------------------------------------	---

≥ 3 des 4 critères de support	<ol style="list-style-type: none">1. Erreurs phonologiques dans le langage spontané et en dénomination2. Compréhension des mots isolés et connaissances sémantiques épargnées3. Absence de troubles articulatoires4. Absence d'agrammatisme franc
------------------------------------	--

Diagnostic de vlAPP avec le support de l'imagerie

En plus des critères cliniques, ≥ 1 des 2 critères d'imagerie	<ol style="list-style-type: none">1. Atrophie prédominante dans les régions périsylvienes ou pariétales gauches à l'IRM2. Hypoperfusion prédominante dans les régions périsylvienes ou pariétales gauches au SPECT ou hypométabolisme prédominant dans les régions périsylvienes ou pariétales gauches au TEP-FDG
--	--

Diagnostic de vlAPP avec pathologie définie

En plus des critères cliniques, ≥ 1 des 2 critères suivants	<ol style="list-style-type: none">1. Évidence anatomopathologique d'un processus neurodégénératif2. Présence d'une mutation causale connue
--	---

Tableau A3. Critères diagnostiques de SLA (adapté de Hardiman et al., 2011)

Critères	SLA définie	SLA probable	SLA possible	Suspicion de SLA
El Escorial (1994)	Signes de neurone moteur supérieur et inférieur dans 3 régions	Signes de neurone moteur supérieur et inférieur dans ≥ 2 régions, avec des signes de neurone moteur supérieur rostraux aux signes de neurone moteur inférieur	Signes de neurone moteur supérieur et inférieur dans 1 région, signes de neurone moteur supérieur isolés dans ≥ 2 régions, ou signes de neurone moteur inférieur rostraux aux signes de neurone moteur supérieur	Signes de neurone moteur inférieur isolés, in ≥ 2 régions
Airlie House révisés (1998) incluant les critères d'Awaji-Shima (2008)	Signes cliniques et électrophysiologiques démontrant l'atteinte des neurones moteurs supérieurs et inférieurs dans la région bulbaire et ≥ 2 régions spinales, ou dans 3 régions spinales	Signes cliniques et électrophysiologiques démontrant l'atteinte des neurones moteurs supérieurs et inférieurs dans ≥ 2 régions spinales, avec des signes de neurone moteur supérieur rostraux aux signes de neurone moteur inférieur	Signes cliniques et électrophysiologiques démontrant l'atteinte des neurones moteurs supérieurs et inférieurs dans 1 seule région, ou signes de neurone moteur supérieur isolés dans ≥ 2 régions, ou signes de neurone moteur inférieur rostraux aux signes de neurone moteur supérieur	-

Annexe 2 – Les autres gènes de DLFT et SLA

Gène	Phénotypes associés	Références
<i>TARDBP</i>	DFTc, vnfAPP, vsAPP, SLA	Benajiba et al., 2009
<i>TBK1</i>	DFTc, vnfAPP, vsAPP, DFTvtd, SLA	Freischmidt et al., 2015
<i>CHMP2B</i>	DFTc, SLA	Skibinski et al., 2005
<i>TUBA4A</i>	DFTc, SLA	Perrone et al., 2017
<i>VCP</i>	DFTc, SLA, Maladie osseuse de Paget, Myopathie à corps d'inclusion	Watts et al., 2004
<i>SQSTM1</i>	DFTc, SLA, Maladie osseuse de Paget, Myopathie à corps d'inclusion	Rubino et al., 2012 Le Ber et al., 2013b
<i>hRNPA1</i> , <i>hRNPA2B1</i>	DFTc, SLA, Maladie osseuse de Paget, Myopathie à corps d'inclusion	Kim et al., 2013
<i>CSF1R</i>	DFTc, SCB, Leucoencéphalopathie de l'adulte avec sphéroïdes axonaux et glie pigmentée	Rademakers et al., 2012 Konno et al., 2017
<i>DCTN1</i>	DFTc, SLA, Syndrome de Perry	Wider et al., 2010
<i>CHCHD10</i>	DFTc, SLA, Myopathie mitochondriale, Troubles de l'audition	Chaussonnet et al., 2014
<i>TREM2</i>	DFTc, Syndrome de Nasu-Hakola	Peplonska et al., 2018
<i>UBQLN2</i>	SLA (±DFTc)	Gellera et al., 2013
<i>TP73</i>	SLA (±APP)	Tábuas-Pereira et al., 2022
<i>FUS/TLS</i> , <i>EWS</i> , <i>TAF15</i>	SLA (± DFTc)	Svetoni et al., 2016

Annexe 3 – Synopsis des protocoles Predict-PGRN et PREV-DEMALS

Predict-PGRN	PREV-DEMALS
Trois évaluations : inclusion, à 20 et 60 mois (durée du suivi : 5 ans)	Trois évaluations : inclusion, à 18 et 36 mois (durée du suivi : 3 ans)
Centres : Paris, Lille, Rouen, Marseille, Toulouse, Nantes/La-Roche-sur-Yon	Centres : Paris, Lille, Rouen, Limoges
A chaque évaluation :	
Examen neurologique	
<p>Bilan neuropsychologique MMS, échelle d'évaluation de la démence de Mattis, Batterie rapide d'efficacité frontale, empans, TMT, WCST, test de Hayling, test de reconnaissance des émotions faciales d'Ekman, test des faux-pas, test de cognition morale, RL/RI-16, test de copie et rappel de la figure de Rey, fluences catégorielles et phonologiques, test de dénomination du BECS-GRECO, BNT, batterie d'évaluation des praxies</p>	<p>Bilan neuropsychologique MMS, échelle d'évaluation de la démence de Mattis, Batterie rapide d'efficacité frontale, empans, TMT, WCST, test de Hayling, D-KEFS, DSST, test de reconnaissance des émotions faciales d'Ekman, test des faux-pas, test de cognition morale, RL/RI-16, test de copie et rappel de la figure de Benson, test des portes de Baddeley, fluences catégorielles et phonologiques, BNT, <i>Camel & Cactus test</i>, batterie d'évaluation des praxies, analyse de cubes de la VOSP</p>
<p>Échelles comportementales EDF, FBI, NPI, échelle de l'apathie de Starkstein</p>	<p>Échelles comportementales EDF, FBI, NPI, échelle de l'apathie de Starkstein</p>
<p>Échelles de sévérité de maladie e d'autonomie CDR+NACC FTLD, FRS, DAD</p>	<p>Échelles de sévérité de maladie e d'autonomie CDR+NACC FTLD, FRS, DAD</p>
<p>Échelles d'évaluation psychiatrique BDI-II, STAI</p>	<p>Échelles d'évaluation psychiatrique BDI-II, STAI</p>
<p>IRM cérébrale Séquences T1-pondérées 3D, T2-pondérées 2D et 3D, T2*-pondérées, FLAIR, DTI, GE-EPI pour IRM fonctionnelle de repos</p>	<p>IRM cérébrale Séquences T1-pondérées 3D, T2-pondérées 2D et 3D, T2*-pondérées, FLAIR, DTI, NODDI, GE-EPI pour IRM fonctionnelle de repos, ASL</p>
	<p>IRM médullaire Séquences T2, T2*, DTI</p>
<p>TEP cérébral au ¹⁸FDG</p>	<p>TEP cérébral au ¹⁸FDG</p>
<p>Prélèvements biologiques Plasma, ADN, ARN, lignées cellulaires</p>	<p>Prélèvements biologiques Plasma, ADN, ARN, lignées cellulaires</p>

ASL : *arterial spin labeling* ; BDI-II : Inventaire de dépression de Beck ; BECS-GRECO : Batterie d'évaluation des connaissances sémantiques du GRECO ; BNT : *Boston naming test* ; CDR+NACC FTLD : *Clinical Dementia Rating scale plus National Alzheimer's Disease Coordinating Center for Frontotemporal Lobar Degeneration* ; DAD : *disability assessment for dementia* ; D-KEFS : *Delis-Kaplan Executive Function System* ; DSST : *digit-symbol substitution test* ; DTI : *diffusion tensor imaging* ; EDF : échelle de dysfonctionnement frontal ; FBI : *frontal behavior inventory* ; FRS : *frontotemporal dementia rating scale* ; GE-EPI : *gradient-echo echo-planar*

imaging ; MMS : mini-mental state examination ; NODDI : neurite orientation dispersion and density imaging ; NPI : neuropsychiatric inventory ; RL/RI-16 : épreuve de rappel libre / rappel indicé à 16 items ; STAI : state-trait anxiety inventory ; TMT : trail making test ; VOSP : visual object and space perception battery ; WCST : Wisconsin card sorting test.

Annexe 4 – Méthodes d’analyse d’IRM structurelle

L’étude du profil d’atrophie de la substance grise a été réalisée avec deux approches complémentaires : l’analyse de l’épaisseur corticale et l’approche de VBM. Pour la première approche, le logiciel FreeSurfer version 6.0 (Fischl et al., 2012) a été utilisé par l’intermédiaire du pipeline dédié « *t1-freesurfer* » de la plateforme Clinica (Routier et al., 2021). Brièvement, ce pipeline englobe plusieurs outils du logiciel FreeSurfer, permettant la réalisation séquentielle de l’ablation des tissus non cérébraux, la transformation automatisée de Talairach, la segmentation de la substance grise et blanche sous-corticale, la normalisation de l’intensité, la tessellation de la limite substance blanche / substance grise corticale, la déformation des surfaces selon des gradients d’intensité, la coregistration à un atlas sphérique tenant compte de la géométrie corticale individuelle, la parcellisation du cortex en unités pour respecter l’organisation de gyri et des sillons, et finalement la computation de cartes de plusieurs mesures corticales (épaisseur, surface, volume), calculées à partir de la distance entre la limite substance blanche / substance grise et la limite substance grise / LCR mesurée à l’échelle de chaque vertex (Fischl et al., 2012). En plus d’une analyse statistique vertex-à-vertex réalisée à travers le pipeline « *statistics-surface* » de Clinica (Routier et al., 2021), les mesures corticales ont été recalées dans des atlas dédiés, à savoir celui de Desikan-Killiany (Desikan et al., 2006) et de Destrieux (Destrieux et al., 2010), pour permettre des analyses statistiques au niveau de région d’intérêt. Une adaptation du pipeline de traitement anatomique, « *t1-freesurfer-longitudinal* » a été adopté pour traiter une série d’images appartenant au même sujet mais espacées dans le temps. Ce pipeline inclut la création d’un modèle individuel pour permettre ensuite la segmentation, l’extraction des surfaces et la dérivation de mesures pour chacune des images (Reuter et al., 2012).

L’approche basée sur la VBM a été réalisée avec le logiciel SPM (*Statistical Parametric Mapping*) version 12 (<http://www.fil.ion.ucl.ac.uk/spm/software/spm12>), là encore par l’intermédiaire d’un pipeline de Clinica, « *t1-volume* » et ses différentes composantes (Routier et al., 2021). En synthèse, la procédure dite de Segmentation Unifiée effectue simultanément la segmentation des tissus, la correction des biais et la normalisation spatiale des images (Ashburner et Friston, 2005). Un modèle de groupe est créé à la suite utilisant le DARTEL, un algorithme pour la registration diffeomorphique d’image à partir des cartes de probabilité de substance grise dans l’espace natif (Ashburner, 2007). Ensuite, ces images sont recalées dans l’espace du MNI (*Montreal Neurological Institute*), permettant d’un côté des analyses de

comparaison à l'échelle de voxel, et de l'autre l'extraction de mesures de densité moyenne de substance grise dans des régions anatomiques obtenues à partir d'atlas différents dans le MNI, à savoir celui développé par Neuromorphometrics Inc. (Caviness et al., 1999) et l'AAL3 (Rolls et al., 2020). Afin de pouvoir réaliser des analyses par régions d'intérêt, un algorithme implémenté dans SPM permet d'obtenir des mesures volumétriques à partir des estimations de densité dans chaque région corticale et sous-corticale.

Pour certaines des analyses réalisées dans ces travaux de recherche, le *toolbox* CAT12 (*Computational Anatomy Toolbox*, <http://www.neuro.uni-jena.de/cat>), intégré dans SPM12, a remplacé le traitement standard par SPM12. Les avantages de CAT comprennent une meilleure correction des biais, une segmentation plus précise des structures sous-corticales, le calcul intégré des mesures de surface, et surtout un algorithme optimisé de traitement longitudinal, ce qui est le plus pertinent dans le cadre de certaines des études conduites. Dans ce prétraitement, CAT réaligne toutes les images appartenant à un même sujet avec des enregistrements rigides et applique des corrections de biais intra-sujet. Ensuite, chaque image est traitée individuellement, utilisant une transformation calculée à partir de la moyenne des images (Ashburner et Ridgway, 2012).

Table des illustrations

Figure 1. Classification des sous-types de DLFT-TDP.....	24
Figure 2. Représentation de la propagation de la pathologie TDP-43 dans la DFTc (I) et dans la SLA (II).....	26
Figure 3. Classification des tauopathies.....	29
Figure 4. Modèle conceptuel de la répartition en stades de la phase présymptomatique des DLFT génétiques.....	45
Figure 5. Critères de recherche proposés pour le trouble cognitif et / ou comportemental léger de la démence frontotemporale.....	47
Figure 6. Régions significativement atrophiées à la M ₀ selon la méthode de CAT12.....	227
Figure 7. Régions significativement atrophiées à la M ₀ selon la méthode de FreeSurfer.....	227
Figure 8. Régions présentant un déclin volumétrique accéléré chez les porteurs comparés aux contrôles durant le suivi.....	228
Figure 9. Comparaison de la progression longitudinale de l'atrophie des deux putamen entre porteurs à la phase présymptomatique précoce (≤ 40 ans) et tardive (> 40 ans).....	229

Table des tableaux

Tableau 1. Principaux biomarqueurs fluidiques étudiés dans les DLFT génétiques	50
Tableau 2. Caractéristiques des participants de la cohorte PREV-DEMALS inclus dans l'étude.....	226

Résumé

Les dégénérescences lobaires fronto-temporales (DLFT) sont la deuxième cause de démence de l'adulte après la maladie d'Alzheimer. Elles se caractérisent par une altération progressive des fonctions cognitives, des troubles comportementaux, du langage et/ou moteurs. Une cause génétique est retrouvée chez un quart à un tiers des patients, avec une implication majoritaire des gènes *GRN*, codant pour la protéine progranuline, et *C9orf72*. De par les avancées thérapeutiques, dans ces deux formes génétiques en particulier, l'étude de la phase présymptomatique constitue un enjeu majeur pour l'administration de traitements ciblés, dans le but de ralentir ou d'arrêter le processus lésionnel. Cette thèse vise à améliorer les connaissances autour de la caractérisation clinique et en neuroimagerie des DLFT associées aux mutations des gènes *GRN* et *C9orf72*.

La première partie est consacrée à l'étude d'une présentation clinique rare de DLFT génétique, les aphasies primaires progressives (APP), avec l'objectif d'identifier les systèmes impliqués dans les différents variants d'APP et d'élargir les indications du diagnostic génétique. L'un des résultats clés est que le variant logopénique est la forme la plus fréquente chez les patients porteurs de mutations du gène *GRN*. Nous avons mis en évidence un profil d'atteinte du réseau du langage différent selon la cause génétique et décrit les corrélats neuroanatomiques propres à chaque forme.

La seconde partie consiste en l'étude de la phase présymptomatique des mutations des gènes *GRN* et *C9orf72*, à l'aide de biomarqueurs biochimiques et de neuroimagerie. Nous avons caractérisé les taux de neurofilaments plasmatiques durant toute la durée de la maladie, de la phase présymptomatique à la phase clinique, en étudiant leurs principaux facteurs de variabilité dans des conditions physiologiques et pathologiques et en définissant des seuils pour la détection des porteurs proches de la phénoconversion. Ces informations ont permis une meilleure stratification des porteurs pour les études d'imagerie que nous avons menées à la suite. Dans les formes *GRN*, nous avons mis en évidence un dysfonctionnement métabolique précoce, notamment au niveau du gyrus temporal supérieur et moyen et du sillon temporal supérieur, précédant les altérations structurelles. Nous avons proposé un index quantitatif, le taux annualisé de changement métabolique, pour tracer la pathologie dès la phase présymptomatique précoce. Dans les formes *C9orf72*, des altérations structurelles sont identifiables à un stade préclinique bien plus précoce. Nous avons relevé une progression accélérée de l'atrophie au niveau de l'insula et des putamen, avec une perte de volume prédominante à la phase présymptomatique tardive pour ces derniers. Ces résultats suggèrent

que la volumétrie des putamen pourrait être un indicateur intéressant pour la prédiction de la phénoconversion, en combinaison avec d'autres biomarqueurs. Ces études contribuent à mieux définir les contours de la phénoconversion et du stade prodromal de la maladie et proposent des métriques utilisables pour les évaluations cliniques et les essais thérapeutiques.

Mots clés : Dégénérescences lobaires frontotemporales, démence frontotemporale, aphasie primaire progressive, progranuline, *GRN*, *C9orf72*, présymptomatique, prodromal, biomarqueur.

Clinical and neuroimaging characterization of genetic frontotemporal lobar degeneration at the clinical and presymptomatic phase

Abstract

Frontotemporal lobar degeneration (FTLD) is the second most common cause of adult-onset dementia after Alzheimer disease. It is characterized by a progressive alteration of cognitive functions, as well as behavioral, language and/or motor disorders. Between a quarter and a third of patients present an identifiable genetic cause, with mutations in *GRN* gene, coding for progranulin, and *C9orf72* gene displaying the highest frequency. The recent therapeutic advances, especially in these two genetic forms, made the study of the presymptomatic phase a major challenge, with the objective of slowing down or stopping the lesional process. This thesis aims to improve the existing knowledge on clinical and neuroimaging features of FTLD associated with *GRN* and *C9orf72* mutations.

The first part is devoted to the study of a rare clinical presentation of genetic FTLD, the primary progressive aphasia (PPA) phenotype, with the aim of identifying the neural systems involved in the different PPA variants and enlarging the indications for genetic testing. A key finding was that the logopenic variant is the most common form in patients with *GRN* mutations. We found a different pattern of language network impairment depending on the genetic cause and described the neuroanatomical correlates of each form.

The second part deals with the study of the presymptomatic phase of *GRN* and *C9orf72* gene mutations, using biochemical and neuroimaging biomarkers. We characterized plasma neurofilament levels throughout the overall disease course, from the presymptomatic to the clinical phase, investigating their main factors of variability under physiological and pathological conditions, and defining thresholds for the detection of carriers close to phenoconversion. This information allowed a better stratification of carriers for the subsequent neuroimaging studies. We demonstrated an early metabolic dysfunction, namely in the superior and middle temporal gyrus and the superior temporal sulcus, preceding structural alterations in *GRN* disease. We proposed a quantitative index, the annualized rate of metabolic change, to trace the pathology from the early presymptomatic phase. Structural alterations are identifiable at a much earlier preclinical stage in *C9orf72* disease. We found faster atrophy progression in the insula and putamen, with more significant volume loss in the late presymptomatic phase for the latter. These results suggest that putamen volumetry could be an interesting parameter for

the prediction of phenoconversion, in combination with other biomarkers. These studies help to better outline the phenoconversion and the prodromal disease stage, and provide metrics usable for clinical evaluations and therapeutic trials.

Keywords: Frontotemporal lobar degeneration, frontotemporal dementia, primary progressive aphasia, progranulin, *GRN*, *C9orf72*, presymptomatic, prodromal, biomarker.